kOMUNIKÁCIE
COMMUNICATIONS

A - OPERATION AND ECONOMICS

SINGLE EUROPEAN RAILWAY AREA AND THE PROBLEM OF RAIL INFRASTRUCTURE CHARGES – CASE STUDIES IN V4 COUNTRIES A208
A. Dolinayová , I. Dömény, J. Jansák, P. Šulko

VARIOUS APPROACHES PROPOSED FOR ELIMINATING DUPLICATE DATA IN A SYSTEM A223
R. Čerešňák, K. Matiaško, A. Dudáš

GDP EFFECT ON B2C E-COMMERCE TURNOVER AND NUMBER OF EXPRESS SHIPMENTS IN SELECTED EUROPEAN POST-COMMUNIST COUNTRIES A233
M. Novotná, D. Gottwald, L. Švadlenka

DELIVERY TIMES AND DELAY IN DELIVERY OF CONSIGNMENT UNDER THE CONDITIONS OF INTERNATIONAL CARRIAGE A248
J. Sosedová, Z. Otáhalová, A. Dávid, A. Galieriková

THE CASE STUDY OF INTERNATIONAL TRANSPORT BY THE FREIGHT FORWARDER IN FRANCE A256
I. Kubasáková, J. Kubáňová, P. Kollárová

IMPACT OF KEY MARKETING TOOLS ON GLOBAL CAR MARKET DEVELOPMENT A264
O. Savych, T. Shkoda

B - MECHANICAL ENGINEERING

NANOINDENTATION AS A METHOD FOR DETERMINING THE MECHANICAL PROPERTIES OF COLD SPRAY COATINGS B250
M. Makrenek

BRICKLAYING ROBOT LIFTING AND LEVELLING SYSTEM B257
P. Wos, R. Dindorf, J. Takosoglu

EMISSION OF SELECTED EXHAUST GAS COMPONENTS AND FUEL CONSUMPTION IN DIFFERENT DRIVING CYCLES B265
A. Kuranc, J. Caban, B. Šarkan, A. Dudziak, M. Stoma

NUMERICAL AND ANALYTICAL INVESTIGATION OF STABILITY OF THE REINFORCED PLATE B278
G. A. Manuylov, S. B. Kositsyn, I. E.Grudtsyna

EXPERIMENTAL RESEARCH OF THE COAGULATION PROCESS OF EXHAUST GASES UNDER THE INFLUENCE OF ULTRASOUND B288
A. S. Kadyrov, B. K. Sarsembekov, A. A. Ganyukov, Z. Z. Zhunusbekova, K. N. Alikarimov

EXPERIMENTAL ANALYSIS OF VERTICAL VIBRATIONS OF A RAILWAY BOGIE B299
M. Dumitriu, I. C. Cruceanu

EFFECT OF THE RME BIODIESEL ON THE DIESEL ENGINE FUEL CONSUMPTION AND EMISSION B308
D. Kurczyński

ESTIMATION OF WHEELS' NORMAL REACTION FORCES OF AUTOMOBILE IN STEADY-STATE CURVILINEAR MOTION B317
P. Fundowicz, H. Sar, M. Brukalski

PRACTICAL APPLICATION OF THE NEW APPROACH TO FMEA METHOD ACCORDING TO AIAG AND VDA REFERENCE MANUAL B325
D. Plinta, E. Golińska, L. Dulina

ELECTRO-HYDRAULIC PROPORTIONAL SYSTEM REAL TIME TRACKING CONTROL DEVELOPMENT BASED ON PULSE WIDTH MODULATION METHOD B336
E. E. Ibrahim, T. Elnady, M. S. Hassan, I. Saleh

INVESTIGATION OF THE IMPACT STRENGTH OF THE EPOXY-POLYESTER MATERIAL FOR USING IN AGGRESSIVE ENVIRONMENTS IN THE WATER TRANSPORT B346
S. Yakushchenko, M. Brailo, A. Buketov, A. Sapronova, O. Sapronov, A. Menou

C - ELECTRICAL ENGINEERING

SIMULATION VERIFICATION OF BALANCING SYSTEM BASED ON NUMBER OF CELLS C83
M. Šimčák, M. Danko

D - CIVIL ENGINEERING IN TRANSPORT

COMPARATIVE LIFE CYCLE ANALYSIS OF HYBRID AND CONVENTIONAL DRIVE VEHICLES IN VARIOUS DRIVING CONDITIONS D34
E. M. Szumska

E - MANAGEMENT SCIENCE AND INFORMATICS

OPTIMIZATION OF ENERGY MANAGEMENT IN A CITY BUS POWERED BY THE HYDROGEN FUEL CELLS E56
A. Małek, R. Taccani, D. Kasperek, J. Hunicz

TWO OBJECTIVE PUBLIC SERVICE SYSTEM DESIGN PROBLEM E68
J. Janáček, M. Kohání, D. Grygar, R. Fabricius

G - TRAVEL AND TOURISM STUDIES IN TRANSPORT DEVELOPMENT

FATHERS' PREDOMINANCE IN TRANSPORT ARRANGEMENTS FOR FAMILY TOURISM: E-CHAID-BASED PROFILING IN EAST ASIA G13
Y.-F. Lan, Ch.-J. Su

CREATIVE CITIES AND KNOWLEDGE MANAGEMENT APPROACH TO CULTURE-BASED URBAN REGENERATION IN SLOVAKIA: A MODEL G25
M. Tajtáková, M. Olejárová

INCREASED INTEREST IN MILITARY TOURISM ON SELECTED EXAMPLES FROM THE AREA OF NORTHERN AND NORTHEASTERN POLAND G38
A. Zienkiewicz, T. Podciborski, R. Kaźmierczak

Dear colleague,

Journal Communications - Scientific Letters of the University of Zilina are a well-established open-access scientific journal aimed primarily at the topics connected with the field of transport. The main transport-related areas covered include Civil engineering, Electrical engineering, Management and informatics, Mechanical engineering, Operation and economics, Safety and security, Travel and tourism studies. The full list of main topics and subtopics is available at: *http://komunikacie.uniza.sk/index.php/communications/topics*

Journal Communications - Scientific Letters of the University of Zilina are currently indexed by EBSCO and SCOPUS.

We would like to invite authors to submit their papers for consideration. We have an open-access policy and there are no publication, processing or other fees charged for published papers. Our journal operates a standard double-blind review procedure, the successful completion of which is a prerequisite for paper publication.

The journal is issued four times a year (in January, in April, in July and in October).

I would also like to offer you the opportunity of using already published articles from past issues as source of information for your research and publication activities. All papers are available at our webpage: *http://komunikacie.uniza.sk*, where you can browse through the individual volumes.

For any questions regarding the journal Communications - Scientific Letters of the University of Zilina please contact us at: *komunikacie@uniza.sk*

We look forward to future cooperation.

Sincerely

Branislav Hadzima
editor-in-chief

SINGLE EUROPEAN RAILWAY AREA AND THE PROBLEM OF RAIL INFRASTRUCTURE CHARGES - CASE STUDIES IN V4 COUNTRIES

Anna Dolinayová[1,*], Igor Dömény[1], Jan Jansák[2], Peter Šulko[3]

[1]University of Zilina, Zilina, Slovakia
[2]Integrated transport of the Central Bohemian Region, Prague, Czech Republic
[3]Railways of the Slovak Republic, Bratislava, Slovakia

*E-mail of corresponding author: anna.dolinayova@fpedas.uniza.sk

Resume

This paper deals with the charging system and rail infrastructure fees use in V4 countries. The goal was to find out how the charges differ in terms of the train type, weight and distance traveled on different track categories. The charging principle for minimum access packages and for the access and services supplied in service facilities was investigated. Due to different technical, technological and other conditions for the rail infrastructure capacity utilization, the modeled situation was compared to the real one. This research shows differences between individual countries, both in the charging system and in the price for the rail infrastructure use (the prices were recalculated to € and in the PPP-purchasing power parity). It is interesting that the differences are not only significant with regard to the category of track used and the train's weight (especially in the freight transport), but with regard to other factors, as well, in particular the type of train and price for the use of railway stations.

Available online: https://doi.org/10.26552/com.C.2021.4.A208-A222

Article info

Received 14 October 2020
Accepted 11 February 2021
Online 23 June 2021

Keywords:

access,
rail infrastructure,
total and unit fees,
passenger transport,
freight transport,
network statement

ISSN 1335-4205 (print version)
ISSN 2585-7878 (online version)

1 Introduction

The major aim of the European transport policy is to achieve sustainable transport. The European Green Deal described the aims in the same areas such as alternative fuels, multimodal transport, the Single European Sky etc. Transport accounts for a quarter of the EU's GHG (greenhouse gasses) emission. To achieve a climate-neutral EU by 2050 requires among other a shift to more sustainable transport such as rail and inland waterways [1]. The rail transport is still considered as one of the ecological modes of transport, especially the use of electric traction. "Rail is still the most efficient solution for carrying freight across medium-long distances and it should therefore become more competitive" [2]. However, carriers and passenger will use the rail transport services if they are good quality and at an affordable price, which means that the railway transport would be competitive and effective. The European Union adopted a number of directives and regulations to achieve this goal, which described in the railway packages, the main goal of the Fourth Railway Package is a single European railway area. This Package comprises two "pillars" which have been negotiated largely in parallel, "technical pillar" and "market pillar". One of the goals of the Fourth Railway Package is to liberalize the rail passenger market and to remove barriers for interoperability. The development of the railway infrastructure and improvement of quality of the rail passenger services are the key priorities in promotion of a sustainable transport and mobility system in Europe [3].

The rail infrastructure charges are one of the main conditions to achieving a single European railway area. The principles of the rail infrastructure charges are defined by legislative framework of the European Parliament, Council and Commission mainly in Directive 2012/34/EU of the European Parliament and of the Council of 21 November 2012 establishing a single European railway area. Chapter IV of this Directive is focused on charges for the use of railway infrastructure and allocation of the railway infrastructure capacity. Infrastructure managers must publish the content of network statement free of charge in electronic format on their webs in at least two official European Union languages [4]. Directive 2012/34/EU has been amended by Directive (EU) 2016/2370 but this amendment did not affect the charging scheme neither the infrastructure capacity allocation model (except for the timing of the capacity allocation process).

Although the Directive describes the general principles and sets-out the basic framework for the rail infrastructure charging, each EU country uses a different rail infrastructure charging system. As

This is an open access article distributed under the terms of the Creative Commons Attribution 4.0 International License (CC BY 4.0), which permits use, distribution, and reproduction in any medium, provided the original publication is properly cited. No use, distribution or reproduction is permitted which does not comply with these terms.

a result, any carrier wishing to use the infrastructure of one or more countries must become very familiar with the specific charging systems of each country. From the viewpoint of railway undertakings, this is a very lengthy process.

This study compares the rail infrastructure charges for the specific freight and passenger trains in the different track categories in V4 countries. The V4 countries were chosen because the V4 regional cooperation is also successfully developing in the current period, mainly in the sectoral policies, such as economy, digitalization, infrastructure and innovation. In addition, authors have dealt with several projects funded by the International Visegrad Fund. For the relevance of the comparison, authors have recalculated the prices in the individual countries according to purchasing power parities. The presented case studies were modeled since it is not possible to achieve exactly the same conditions in all the countries in practice.

2 Literature review

A number of papers that dealt with rail infrastructure costs from a different point of view were studied. The marginal maintenance costs of the rail infrastructure have been researched very often. Some authors researched this issue from the traffic point of view [5-8]. Calvo et al. researched the impact of the train type (short-distance trains, long-distance trains and freight trains) to maintenance and renewal costs [9]. Odolinski estimate the impact of axle loads on rail infrastructure maintenance costs [10]. Smith et al. estimated the relative marginal cost of different vehicles types running on the rail infrastructure [11].

Appropriate access charges are one of the conditions for guaranteeing fair competition in the rail sector [12]. Infrastructure managers in European Countries use different railway infrastructure tariff system principles to set the price for using a rail network such as marginal cost of a train running in the network, recovering the marginal costs plus a mark-up, recovering the full costs or recovering the full costs minus a State subsidy [13]. Nash researched the rail infrastructure charges in 23 European countries. He stated that a wide variety of both structure and level of charges existed [14].

Some authors researched the different factors or processes which influence rail infrastructure costs or charges. Some of these factors can be influenced by the rail infrastructure managers, some by the rail freight or passenger operators. The rail network capacity utilization can influence those infrastructure charges and simultaneous optimal rail infrastructure capacity utilization is necessary for terms of a liberalized access to the infrastructure [15]. The lower rail infrastructure charges can be achieved by using modern wagon types [16]. Ober et al. investigated rail infrastructure charges with respect to vehicles' characteristics [17]. Savelsberg and Talebian researched a proposed access charge regime aimed at motivating the operators to use longer train configurations [18].

In most articles, authors have examined the rail infrastructure charges or charging system in individual countries. Stendard et al. used an econometric approach to estimate the costs function and marginal costs in regional lines, which constitute the basis for the railway charges in Slovenia [19]. Trampish explained the financing system of the German railway sector, especially due to the control- and supervision duties of Bundesnetzagentur, which is under the new rail regulation law in charge of controlling the charging system of infrastructure managers [20]. Abramovic dealt with the calculating infrastructure charges and considered problems with the way in which this is dealt with in a case study in Croatia [21]. Alvarez-SanJaime et al. analyzed access charges for the use of the rail infrastructure and other factors to the introduction of on-track competition in High Speed Rail lines in Spain [22]. Talebian et al. studied a rail track access charging policy proposed by the Australian Rail Track Corporation, in which a discount on access charges is offered if above-rail operators employ the train with a particular length, which results in the efficient use of a train path [23]. Bugarinovic et al. developed a model for the access charges based on the analytic network process approach. Their model presents the objectives of the identified stakeholders through the established criteria from three different perspectives: the government influence, railway market environment, network use efficiency and used it in the Serbian Railways case study [24]. Crozet and Chassagne explain why, in terms of welfare and subject to some conditions, high rail access charges are economically justified. They have been estimating the market entry conditions for the high speed rail in France for a competitor [25]. Nikolova evaluated the pricing principles and approaches to charging infrastructure costs in Bulgaria [26].

As can be seen in this literature review, authors mainly investigated the rail infrastructure charges from two points of view: comparison of the principles and methods of rail infrastructure charges and description of the rail infrastructure charges in individual countries. Authors did not find scientific papers comparing the rail infrastructure charges in V4 countries (expect [27]). This issue is mentioned marginally in scientific papers dealing with the rail competition, for example in [28-30]. There are very few articles that compare the rail infrastructure charges for certain transportation in several countries.

3 Methodology

The rail infrastructure charging system is described in Network Statement (NS) in each of the EU countries. The NS have a uniform structure, most often with the

following chapters:

- general information
- access conditions
- infrastructure
- infrastructure capacity allocation
- services
- charges.

In this study, a basic formula for calculating the charges for minimum access packages was used. In the Slovak Republic the formula is [31]:

$$U_{mp} = \sum_{i=1}^{n} U_{1i} * V1_i + \sum_{i=1}^{n} U_{2i} * V1_i + \\ + \sum_{i=1}^{n} \frac{U_{3i} * V2_i}{1000} * k_e + \sum_{i=1}^{n} \frac{U_{4i} * V2}{1000}, \quad (1)$$

where:

U_{mp} charges for the minimum access packages,
U_{1i} maximum charges for ordering and allocating infrastructure capacity,
U_{2i} maximum charges for the traffic management and organization,
U_{3i} maximum charges for ensuring railway infrastructure serviceability,
U_{4i} maximum charge for use of the electrical supply equipment to supply traction current,
$V1_i$ train km performances in the *i*-tracks category,
$V2_i$ gross ton km performances in the *i*-tracks category,
k_e coefficient that takes into account the diesel trains running on electrified tracks.

Besides the minimum access charges described in Equation (1), the carriers must pay charges for the access and the services supplied in service facilities [31]:

- charges for access to passenger stations, its premises and facilities, including the facilities for travel related information
- charges for access to a location for ticketing services at passenger stations
- charges for access to train formation stations and train formation equipment, including the shunting facilities and to freight terminals solely operated by the Railways of the Slovak Republic - ZSR (Zeleznice Slovenskej Republiky / Railways of the Slovak Republic)
- charge for the access to storage tracks.

The Czech Republic use different rail infrastructure charging systems, which is focused in the three following formulas [32]:

$$C = K_1 + K_2 * D_t + K_3 * P_{dj}, \quad (2)$$

where:

C railway capacity allocation price,
K_1 rate for processing and planning of the timetable and allocating railway capacity,
K_2 rate for designing a train route,
K_3 daily rate for a train route allocation,
D_t distance of the allocated route between the departure and final points of the route on railway network,
P_{dj} number of days for which the route is allocated.

$$C_s = L * Z * K * P_x * S_1 * S_2, \quad (3)$$

where:

C_s costs of using the railway by one sub-train,
L length of the sub-train movement,
Z basic price per 1 train km,
K track category coefficient,
P_x product factor P_1 to P_5,
S_1, S_2 specific factors.

$$C_{PK} = \sum_{n=11}^{15} (Z_n^{pk} * m_{pk} * N_{zn}), \quad (4)$$

where:

C^{PK} the costs of using the access roads for passengers on a passenger train,
z_n^{pk} basic price for one scheduled stop of a passenger train for boarding and/or disembarking of passengers at railway stations and stops of category "n",
m_{pk} train weight for calculating the cost of using passenger access services on a passenger train,
N_{zn} the planned number of stops of a passenger train for boarding and / or disembarking passengers at "n" category railway stations and stops.

The minimum access package described in Equation (2) and (3) includes the costs of the allocation of rail capacity and the price of the infrastructure manager for the use of track by running the train. The price of using access roads for passengers on a passenger train (Equation (4)) is the price for services provided within the minimum scope and content of services and forms a separate component of the regulated price for the use of track by train [32].

The rail infrastructure charges (minimal access packages) in Hungary are based on charges for ensuring the train path, running of trains, use of catenary, use of station for the passenger and freight trains. Those charges are described using the following formulas by Network Statement MAV (Magyar Allamvasutak - Hungarian State Railways), 2020 [33]:

$$E_{vt} = P_{trkm} * S_{tkm}, \quad (5)$$

where:

E_{vt} ensuring the train path,
P_{trkm} performances in train km,
R_e rate of insurance per train km.

$$R = \sum_{i=1}^{n} P_{itkm} * R_{rtkm} + P_{grtkm} * R_{grtkm} + P_{tkm} * R_e, \quad (6)$$

where:

R running of trains,
P_{trkm} performances in train km in the *i*-line section category,
R_r running rate per train km,
P_{grtkm} performances in gross ton km in the *i*-line section category,
R_{grtkm} running rate per gross ton km,
R_e catenary use rate.

$$P_{St-PT} = \sum_{i=1}^{n} N_i^{PT} * R_i^{St} + \sum_{i=1}^{n} N_i^{PT-o/d} * R_i^{PT-o/d}, \quad (7)$$

where:

$P_{St\text{-}PT}$ station use charges for passenger trains,
N_i^{PT} number of factual passenger train stopping at stations in the i-station category,
R_i^{St} fee for use of stations for stopping the passenger trains,
$N_i^{PT\text{-}o/d}$ number of origin/destination stations by the passenger trains,
$R_i^{PT\text{-}o/d}$ fee for use of origin/destination stations by the passenger trains.

$$P_{St-FT} = \sum_{i=1}^{n} N_i^{FT} * R_i^{St-FT}, \quad (8)$$

where:

$P_{St\text{-}FT}$ charges for station use for freight trains,
N_i^{FT} number of factual freight train stoppings at stations in i-station category,
$R_i^{St\text{-}FT}$ fee for station use for stopping the freight trains.

Hungary has two infrastructure managers - MAV Zrt and GYSEV Zrt (Gyor-Sopron-Ebenfurth Railway). Both have the same charging principle described in Equations (5) - (8), only fees for individual charging are different.

The rail infrastructure charges in Poland are based on train and gross train km; unlike the Czech Republic and Hungary Poland does not take into account type of passenger and freight trains similar to Slovakia. The basic principle of charges by Annex 12 of Network Statement is described by the following Formula [34]:

$$Ch_{SF} = R_{MK} * (W_{TC} * P_{trkm} + S_{MPB} * W_w * P_{trkm}) + \\ + R_E * P_{trkm.} \quad (9)$$

where:

Ch_{SF} charges for using the railway infrastructure - standard fees,
R_{MK} average rate according to the train weight and railway line category,
W_{TC} rate factors according to the railway line category,
W_w rate factors according to total planned train gross weight,
R_E sub rate varying according to traction for trains and shunting operations based on electric traction,
P_{trkm} performances in train km.

Besides the charges described in Equation (9), the rail freight and passenger carriers must pay a handling fee for capacity allocation applications.

The fundamental principle of the rail infrastructure charges, under the minimal access packages, are described in the previous formulas. More detailed information, as well as fees are given in the individual NS on the website of each rail infrastructure manager.

The methodology for calculating the rail infrastructure charges in the V4 countries is based on the assumption that the transport process is carried out under the same conditions in all the countries (the same trainset, the same gross weight of locomotive and wagons, the use of railway stations and railway lines of the same category, etc.). This is the basic condition for a relevant comparison of the level of the rail infrastructure charges in each country.

As the rail infrastructure charges for the minimum access packages and railway access to services facilities fall into the category of regulated prices, infrastructure managers must publish them on their websites. Given that this is a number of prices depending on various factors, Table 1 provides an overview of prices for passenger trains for the 1st or the highest railway line category and also for the highest railway station category.

All the fees were recalculated to euros according to the official exchange rates and then those fees were recalculated according to the purchasing power parity (PPP) for individual countries. Table 2 shows the data used.

Calculation of the rail infrastructure charges was realized for the five alternatives:

- rail passenger transport:
  - express train (Ex) in the first or comparable railway line category - electrified
  - regional train in the second or comparable line category - non electrified
  - regional train in the third or comparable line category - non electrified
- rail freight transport:
  - through freight train in the first or comparable railway line category - electrified
  - container train in the first or comparable railway line category - electrified.

The calculation of the rail infrastructure charges was realized in the spreadsheet program MS Excel based on Equations (1) – (9) by use of prices from the Network statements of the V4 countries. More detailed information about the trains parameters and other factors are described in the next section. The total fees of the rail infrastructure charges were modelled due to distance to better present the differences.

4 Results - case studies in the V4 countries

The change in the rail infrastructure access fees was investigated with respect to various distances in different situations in the rail passenger and freight transport. The calculation is based on the NS and individual Annexes of NS, regarding relating to price or specific charging conditions for timetable 2020/2021. The rail infrastructure charges for minimum access packages and railway access to services facilities, were compared. Charges of additional and ancillary services were not taken into account because those charges are very different and depend on a number of different factors. In

Table 1 *Selected prices of the rail infrastructure charges for passenger trains*

country	capacity allocation		running of train		use of electrical supply equipment		station use charges	
	factor	price	factor	price/ coefficient	factor	price	factor	price
Slovakia	train km	0.0691/train km	train km	0.997/train km	gross ton km	0.000228/ gross ton km	number of stops -regional trains	0.510/1stop
			gross ton km	0.001102/ gross ton km			number of stops - long-distance trains (express train, intercity train …)	5.100/1 stop
Czech Republic	fixed rate (for time table)	64.947	train km (Z)	0.8214/train km	-	-	multiply number of stops and gross ton of train	0.0031
	distance	0.3056/km	product factor coefficient (P)	1				
	number of days	0.3820/day	gross ton km (S_1) -interval	0.94 (for interval 300 - 399)				
			using ETCS level 2 coefficient (S_2) - yes/no	1.0/0.95				
Hungary	train km	0.0232/train km	train km	1.1306/train km	train km	0.1768/train km	number of stops (origin/ destination station)	9.5637/1 stop
			gross ton km	0.0008/gross ton km			number of stops (other station)	6.6386/1 stop
Poland	fixed	22.7051	train km - average rates	1.7486/train km	train km	0.05/train km	-	-
			rate factors coefficient - gross weight	0.96 (for interval 300 - 360)				
			rate factors coefficient - gross weight - average line category	1.2191				

Note: All the prices are listed in € without VAT

Based on Network Statements of each country [31-34]

Table 2 *Data of exchange rates and PPP*

country	PPP	exchange rate as of 01.08.2020	
European Union	100	-	
Czech Republic	73.4	26.175	CZK per 1€
Hungary	64.5	344.95	HUF per 1€
Poland	59.5	4.4034	PLN per 1€
Slovakia	79.7	-	

Source: [35-36]

Table 3 *The passenger train parameters*

	type of locomotive	weight of locomotive HKV (t)	type of wagon	number of wagons	weight (t)	capacity (passengers)	total weight of trainset (t)
express train	193 (Siemens Vectron)	89	WRmz817	1	54	-	347.84
			Ampz143	1	49	58	
			Bdmpee233	3	44	80	
regional train	Diesel Multiple Unit 643	-	-	-	57	137	67.96
regional train	Diesel Multiple Unit 861	-	-	-	120	291	143.28

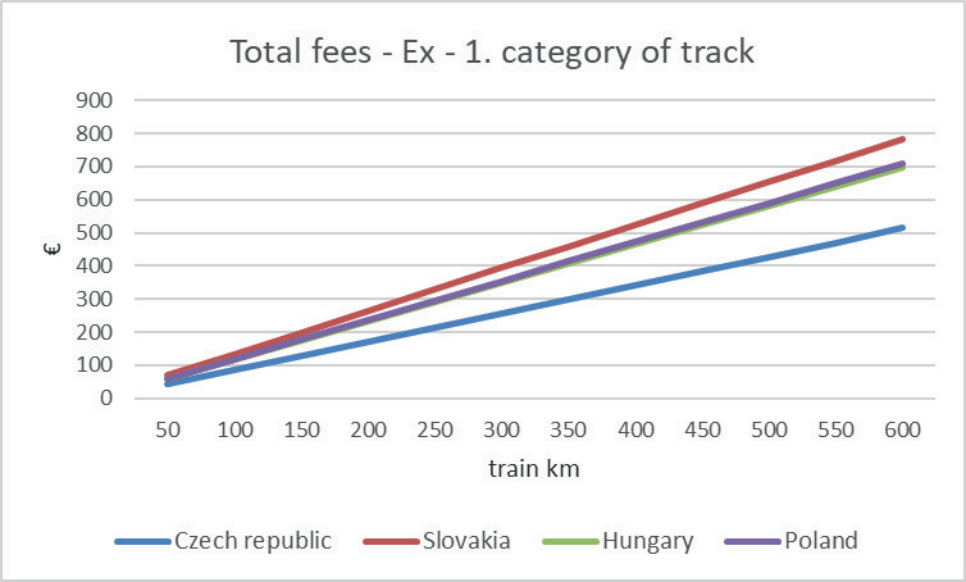


Figure 1 *Total fees of the rail infrastructure access for an express train in the first track category*

addition, the rates for these services are commercial and the resulting prices depend on the contract between the manager and the carrier.

4.1 The passenger transport

With regard to passenger transport the express train in the first or higher track category (by NS of individual countries) and regional trains (Re) on second and third or comparable track categories were taken into account. Table 3 shows train switching and other parameters needed for calculation of fees.

Calculation is based on these premises:

- type of train is the same in all the V4 countries although this is sometimes not realistically possible (e.g. due to the technical parameters of wagons, locomotives and trains)
- an express train stops every 50 km on average in the A or the first station category, a passenger train stops on average every 5 km in the second and third or comparable station category
- trains do not use the track for storage.

The results of the total and unit fees for an Express train in the first track category are shown in Figure 1 and Figure 2.

As can be seen in Figure 1, Slovakia has the highest fees for use of the railway infrastructure capacity. In Poland, compared to other V4 countries, the base rate, which depends on the train km, is almost twice as large (e.g. in the Czech Republic it is 21.50 CZK - € 0.8214 per train km, in Poland is 7.7 PLN - € 1.7486 per train km), but there is no charge for use of the electrical supply equipment to supply traction current of Poland Unit fees are the same for any train km in Poland. It is caused by the system of the rail infrastructure charges, which has no special price for access to services facilities in Poland. Differences between Slovakia and Hungary are not great, for example total fees for 200 train km in Slovakia is € 264 and in Hungary € 234. The Czech Republic has the lower fees (in the modeled conditions), approximately 30 % compared to Slovakia and Hungary.

The system of the rail infrastructure charges is the same for Regional trains and Express trains in all the V4 countries. The differences are only in prices, no V4 countries take into account market segmentation in the rail passenger transport. Figures 3 and 4 show results of the rail infrastructure charges, calculated for a regional

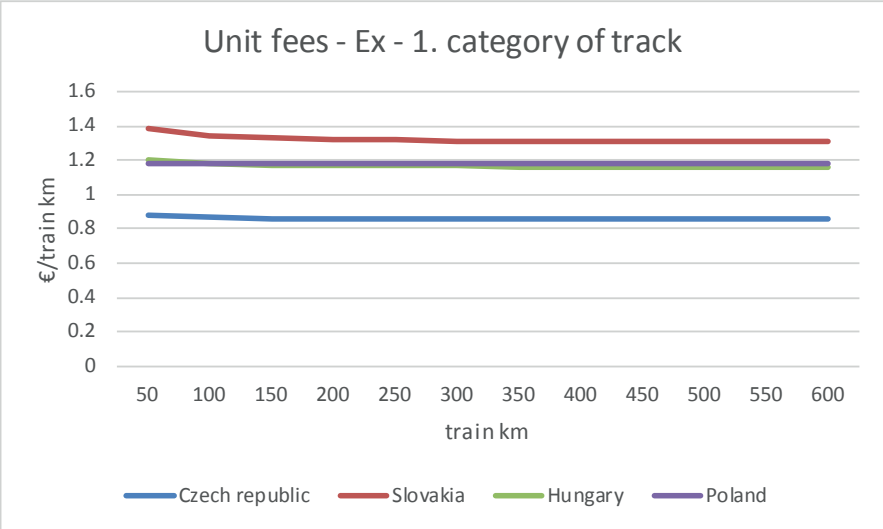


Figure 2 *Unit fees of the rail infrastructure access for an express train in the first track category*

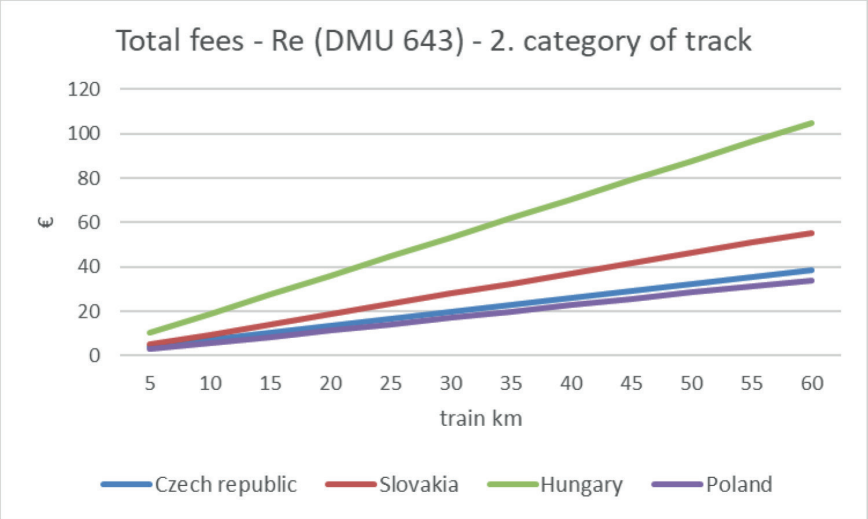


Figure 3 *Total fees for the rail infrastructure access for a regional train (DMU 643) in the second track category*

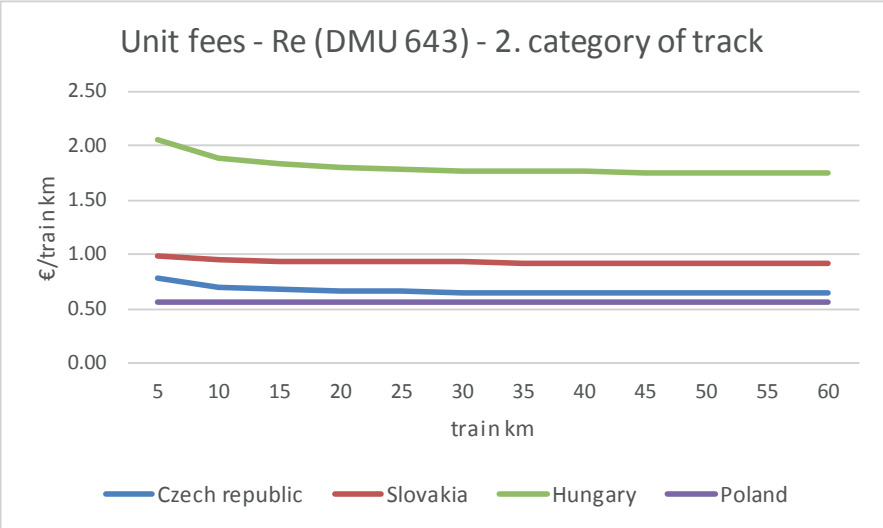


Figure 4 *Unit fees for the rail infrastructure access for a regional train (DMU 643) in the second track category*

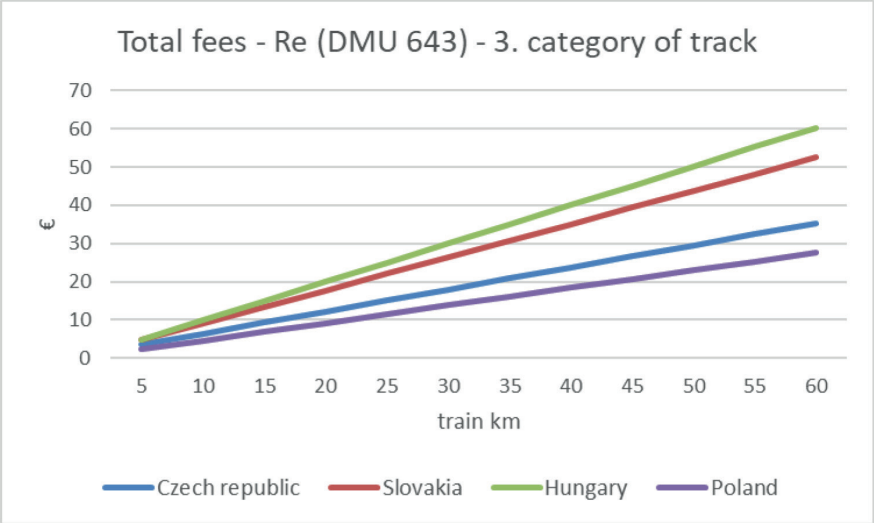


Figure 5 *Total fees of the rail infrastructure access for regional trains (DMU 643) in the third track category*

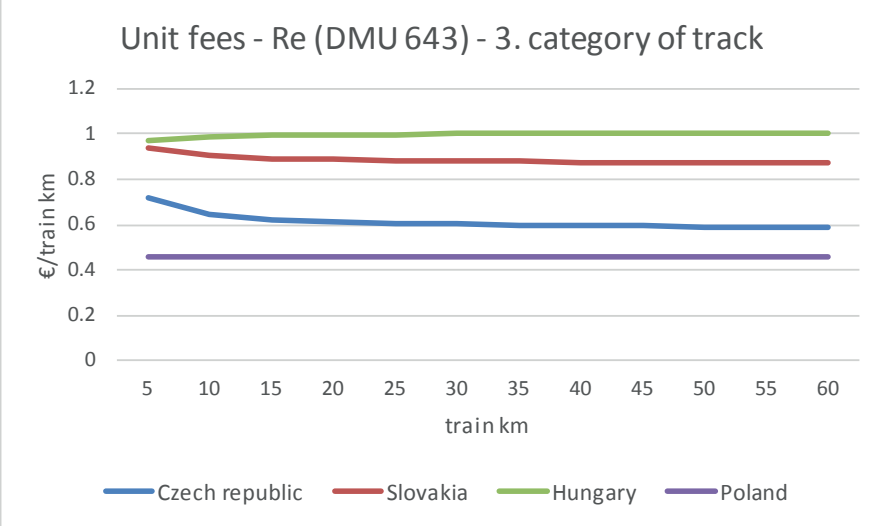


Figure 6 *Unit fees of the rail infrastructure access for regional trains (DMU 643) in the third track category*

train (train switching - DMU 643) in the second track category and Figures 5 and 6 show the results in the third track category.

When comparing Figures 3 and 5 one can see differences in the price level of the second and third track categories. While in the Czech Republic and Poland the total fees are approximately the same in the second track category (differences is only 4.425 € for 60 km distance), in the third track category difference is 7.735 € for 60 km distance. The total fees are very different in the second and third track categories in Hungary. If one compares Hungary (the highest total fees) to Poland (the lowest total fees), in the second category the difference is 70.958 €, but in the third it is only 32.586 €. In the case of passenger trains, which run over short distances, station charges were much more pronounced in the rail infrastructure charges. In Tables 4 and 5 the fees in the 2. and 3. track category are compared, divided into the minimum access packages (MAP) and access to services facilities (ASF).

In Poland, the fee for access to services' facilities is paid only for services, which are supplied (for example shunting) mainly for freight trains. Therefore, this fee is not listed in the Table 4 and 5 to make it comparable to other countries.

As can be seen in Tables 4 and 5, in the Czech Republic the price level for the minimum access packages is approximately the same for the second and third track categories, the price level for the third track category is approximately 58% lower compared to the second category in Hungary. Access to services facilities fees is also lower in the third track category.

Here is also investigated how the fees would change if the train shifting changed. Figures 7 and 8 show the results for Regional train (train switching - DMU 861) in the second track category.

Due to the fact that the change of train switching affects only the part of the fees that are dependent on the gross ton km, there is no significant differences

Table 4 *Total fees of the minimum access packages and access to services facilities in the 2. track category*

	Czech Republic		Slovakia		Hungary		Poland
train km	MAP	ASF	MAP	ASF	MAP	ASF	MAP
5	3.187	0.726	4.203	0.765	3.434	6.829	2.235
10	5.963	1.089	8.407	1.148	6.869	12.004	5.669
15	8.739	1.452	12.610	1.530	10.303	17.180	8.504
20	11.515	1.815	16.814	1.913	13.738	22.356	11.339
25	14.291	2.178	21.017	2.295	17.172	27.531	14.173
30	17.067	2.540	25.221	2.678	20.606	32.707	17.008
35	19.843	2.903	29.424	3.060	24.041	37883	19.843
40	22.619	3.266	33.628	3.443	27.475	43.059	22.677
45	25.395	3.629	37.831	3.826	30.910	48.234	25.512
50	28.172	3.992	42.035	4.208	34.344	53.410	28.347
55	30.948	4.355	46.238	4.591	37.779	58.586	31.181
60	33.724	4.718	50.442	4.973	41.213	63.761	34.016

Table 5 *Total fees of the minimum access packages and access to services facilities in the 3. track category*

	Czech Republic		Slovakia		Hungary		Poland
train km	MAP	ASF	MAP	ASF	MAP	ASF	MAP
5	3.010	0.581	3.973	0.733	1.443	3.414	2.303
10	5.609	0.871	7.945	1.100	2.886	7.004	4.606
15	8.207	1.161	11.918	1.466	4.329	10.594	6.909
20	10.806	1.452	15.891	1.833	5.772	14.185	9.212
25	13.405	1.742	19.864	2.200	7.215	17.775	11.515
30	16.004	2.032	23.836	2.566	8.658	21.365	13.818
35	18.603	2.323	27.809	2.933	10.101	24.955	16.121
40	21.201	2.613	31.782	3.300	11.544	28.545	18.424
45	23.800	2.903	35.755	3.666	12.987	32.135	20.727
50	26.399	3.194	39.727	4.033	14.430	35.725	23.030
55	28.98	3.484	43.700	4.399	15.873	39.315	25.333
60	31.97	3.774	47.673	4.766	17.316	42.905	27.586

between countries. For example, if we take into account the distance of 60 km, the difference in the fee between the Slovak Republic and Czech Republic is 16.69 € for DMU 861 and 16.97 for DMU 643. Comparing Figures 3 and 7, it can be seen that the differences between countries are minimal.

4.2 The freight transport

The comparison of the rail infrastructure charges for the freight transport is more complicated than for the passenger transport. This is because the final price can be affected by several different factors, such as the division of the freight transport into several different categories that have their own rates or coefficients affecting the final price (standard freight trains, combined transport trains, individual wagon consignments), different prices for different railway line categories or route ordering regime (up to annual timetable, ad-hoc). In addition, not all the infrastructure managers use the same freight transport distribution factors to calculate fees. Therefore, only 2 types of a freight train - through freight train (Figure 9 and 10) and container train (Figure 11 and 12) in the first track category, were compared.

Calculation is based on these premises:

- gross ton weight of a through freight train is 1,700 tons and container train 1,000 tons,
- both trains stop only in the originating and destination stations of a train,
- both originating and destination stations are the highest category,
- trains do not use track for storage,
- trains are planned in the annual timetable no ad-hoc (Hungary and Poland do not have a special price level for ordering and allocating infrastructure capacity for ad-hoc train).

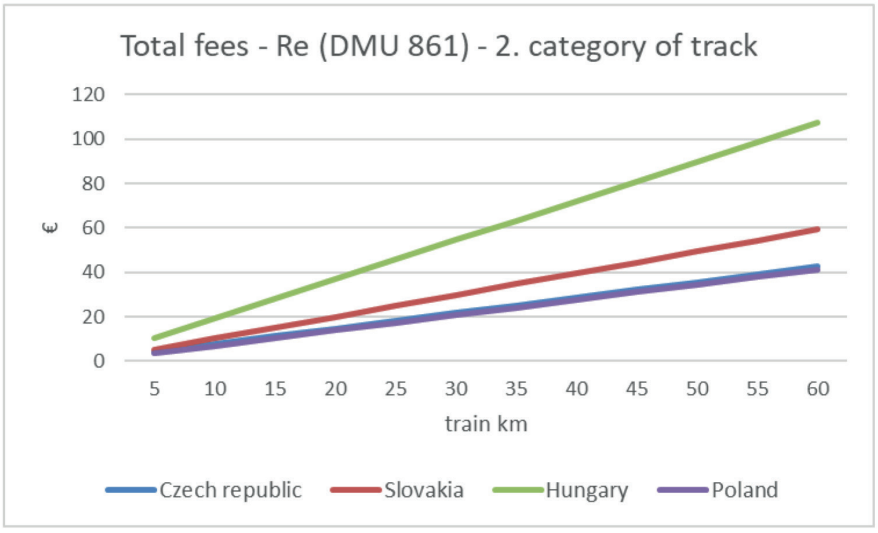


Figure 7 *Total fees for the rail infrastructure access for a Regional train (DMU 861) in the second track category*

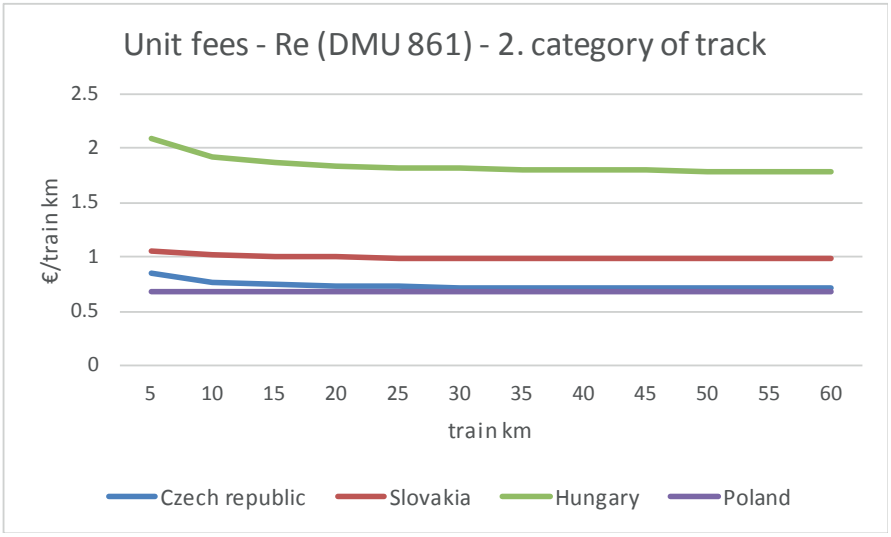


Figure 8 *Total fees for the rail infrastructure access for a regional train (DMU 861) in the second track category*

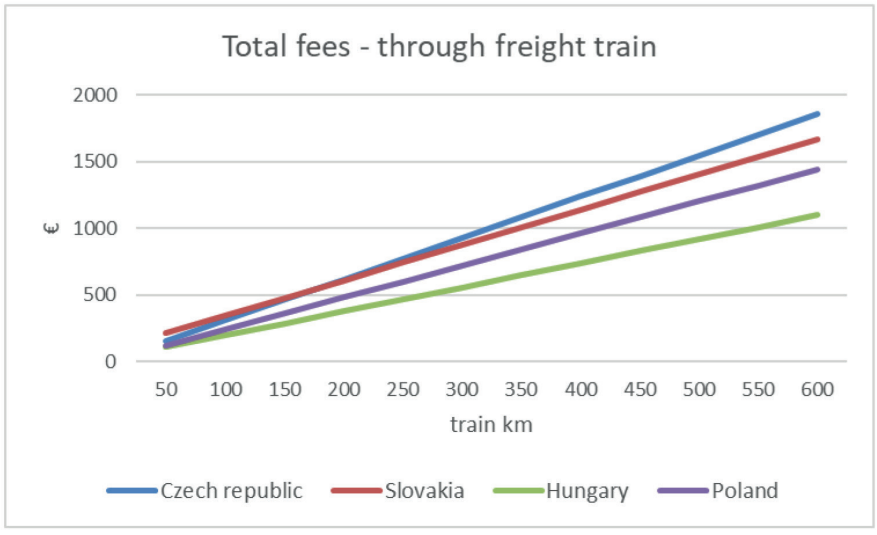


Figure 9 *Total fees for the rail infrastructure access for a through freight train in the first track category*

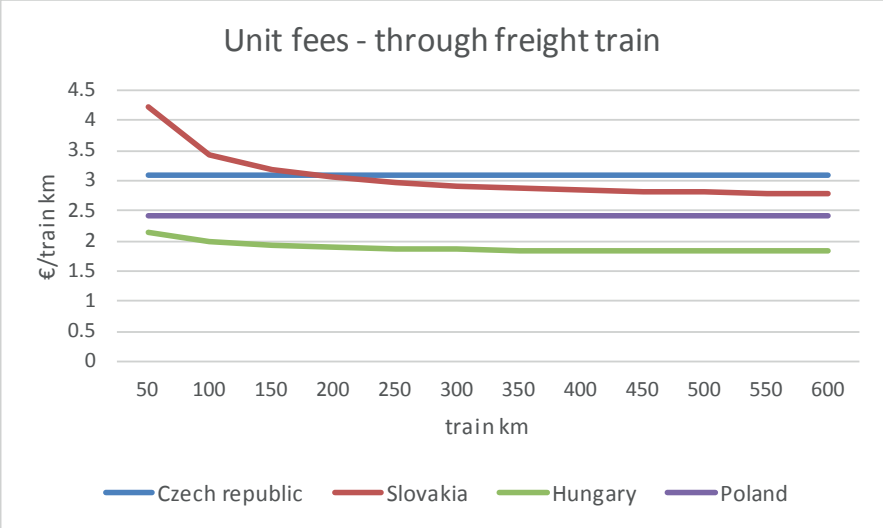


Figure 10 *Unit fees the for rail infrastructure access for a through freight train in the first track category*

Table 6 *Total fees of the minimum access packages and access to services facilities in the 1. track category for a through freight train*

gross ton of train	distance							
	200 km				500 km			
	Czech Republic	Slovakia	Hungary	Poland	Czech Republic	Slovakia	Hungary	Poland
300	169.109	312.649	236.762	194.928	422.16	662.95	565.48	590.84
600	242.880	376.249	267.054	215.506	606.58	821.96	641.21	653.55
900	349.585	439.850	297.345	286.173	873.36	980.96	716.94	849.98
1200	487.906	503.451	327.636	329.093	1 219.15	1 139.96	792.67	980.79
1500	556.408	567.051	357.928	374.701	1 390.40	1 298.96	868.39	1119.79
1800	689.460	630.652	388.219	422.681	1 723.03	1 457.96	944.12	1266.02
2100	752.692	694.252	418.510	468.793	1 881.11	1 616.96	1 019.85	1406.56
2400	887.061	757.853	448.802	329.093	2 217.04	1 775.97	1 095.58	1544.54
2700	951.611	821.454	479.093	557.804	2 378.41	1 934.97	1 171.31	1677.84
3000	1 145.261	885.054	509.385	597.406	2 862.54	2 093.97	1 247.04	1798.54

As can be seen in Figure 9 and 10, the highest rail infrastructure access fees are in the Czech Republic (from 220 km distance). But if one takes into account the through freight train with lower fees for the gross tons (e. g. 300 gross tons) fees in the Czech Republic would be the cheapest as can be seen in Table 6. That is caused by the rapid increase in specific factor S1 (formula (3)), which takes the train weight category into account. For the train's gross tons, 500 tons, S1 factor is 1.34, for 2,000 tons is 5.37. The Slovak Republic has the highest charges for access to a train formation station which can be seen in the unit costs.

The total fees for the container train were compared, because some infrastructure managers (in the Czech Republic and Poland) use a specific factor for this train and the total fees are lower compared to the through freight train.

Fees for a container train are the lowest in the Czech Republic because this country provide a direct discount on freight trains, which are operated as combined transport trains. This discount serves to support the development of this market segment and should therefore motivate carriers to use both the railway itself and use of various types of transport equipment, such as conventional containers, Innofreight container system etc. The infrastructure manager uses a product factor - P4 (formula (3)) for this discount, which has a rank of 0.65. However, this discount does not apply to the total fee for the Z rail infrastructure, but to a fee for the running trains' track use. The rail infrastructure manager in Slovakia does not take any freight train segmentation, rail infrastructure manager in Hungary uses different rates dependent on gross tons for standard freight train and other trains. In Slovakia,

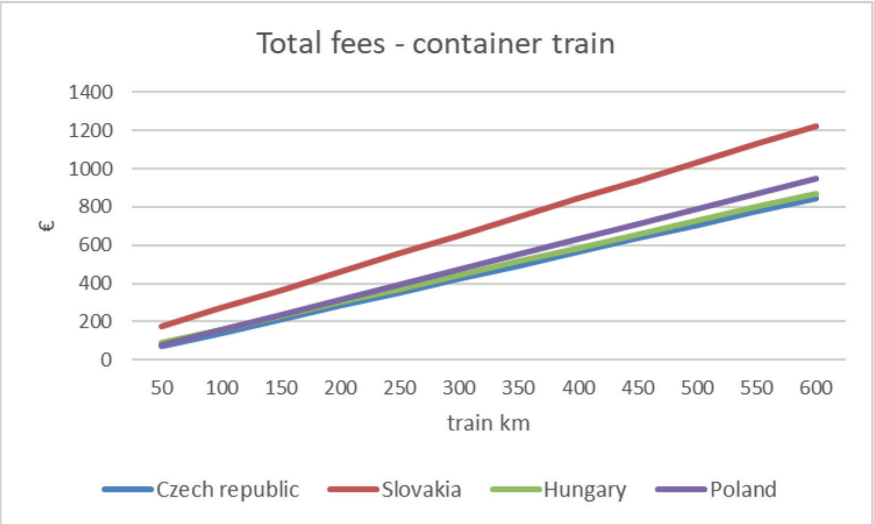


Figure 11 *Total fees for the rail infrastructure access for a container train in the first track category*

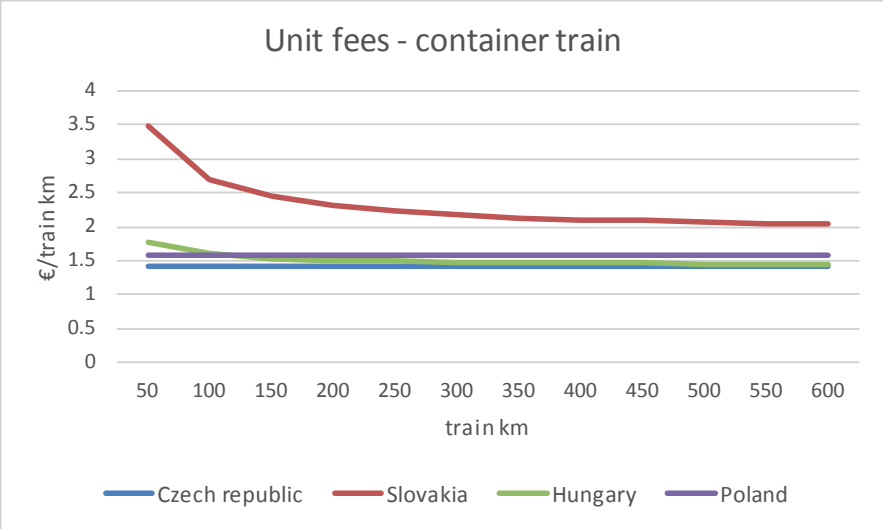


Figure 12 *Unit fees for the rail infrastructure access for a container train in the first track category*

the most expensive is access to train formation stations (more than three times that of Hungary) for that the unit fees are higher for 50 km distance and then fall rapidly.

5 Discussion

Charges for the railway infrastructure use are the important costs item of the rail passenger and freight carriers. Carriers must be able to calculate this fee in advance for a correct calculation of these costs to the product. In the case of international railway transport, the prices of the rail infrastructure services and mainly the system of rail infrastructure charges are different. Despite the fact that the train km and gross ton km are the main parameters which the fees depend on, the systems are very different.

Comparison of charges for use of the railway infrastructure, for different passenger and freight trains in different track categories, in the V4 countries, showed many interesting differences like:

- the cheapest fees for passenger train on the first track category are in the Czech Republic, the most expensive are in Slovakia;
- the results on the second and third track category are different, for example the fees for Passenger train in Slovakia is the cheaper than in Hungary;
- in the case of a freight train, there is a different situation in the Czech Republic compared to the other countries; the fees for the through train are the highest (approximately the same as in Poland), but for the container train are the cheapest.

This study and its results are limited by the premises of passenger and freight train introduced in sections 4.1 and 4.2, as well as by the current Network Statement of the rail infrastructure managers in the V4 countries. In practice, there may be a change in the

train set (for example, in the border's exchange station a locomotive can be changed), the number of train stops at the same distance is different, etc. Some countries change prices of individual rail infrastructure services every year (for the period of validity of the timetable) or change the system of rail infrastructure charges. However, for the purposes of the relevant comparison, not all the real factors (especially as far as the train parameters are concerned) can be taken into account, as the results would be distorted.

6 Conclusions

Achieving a single European railway area is a demanding and lengthy process. Besides the technical differences, there are many other differences, which complicate rendition of the rail passenger and freight services especially in international transport. One of these differences is the rail infrastructure charging system. Despite the fact that there is a common EU legal framework in the field of charges for the use of railway infrastructure, individual countries use different systems. The presented study shows that larger differences are for passenger trains.

In the case of passenger trains, it can be stated that in all the analyzed countries there is no difference in terms of rail infrastructure charges, whether it is an express train or a lower category train, such as a regional train. If the train category affects the price, then only assuming the use of different types of locomotive that have different weights, or whether the set uses dependent or independent traction, since in some countries (Slovakia, Hungary, Poland) the resulting price is less affected by charging the overhead contact line. However, it is necessary to mention that Slovakia adds the factor of train running independent traction on the line to the price, where an electric traction line is available at the same height, as a separate fee for locomotive dependent traction using this device. The final price in Slovakia, Czech Republic and Hungary is also affected by charging for use of the railway stations for passenger transport, which is a mandatory part of the rail infrastructure fees (as can be seen in tables 4 and 5). However, in the case of Slovakia, this part of the charge is a negligible amount of only a small amount of euros per train stop (in the case of regional train for distance 60 km, difference is 58.788 €). In this case, Hungary has the most expensive charge for use of the railway stations, which is, on average, € 7.03 per stop.

There are many factors that affect the fees of the rail infrastructure use regarding the freight transport. Among the V4 countries, the Czech Republic uses the most possible factors that may affect the final price for infrastructure in its charging system. Their system is based on product and specific factors, which allows the segmentation of the fees by type of train, using level of ETCS (European Train Control System) and other factors comparable to other countries. The development of fees with regard to distance, is also significantly affected by the train's weight. While charges for the through freight trains with a lower weight are the lowest in the Czech Republic, for trains with a higher weight (more than 1,700 gross tons) they are the lowest in Hungary and in the Czech Republic are the highest (as can be seen in table 6). The situation is completely different when comparing international transport trains. Due to the fact that the Czech Republic uses a product factor that favors these trains, the fees are significantly lower than in Slovakia. When those charges on other categories of tracks, under approximately comparable conditions, were analyzed, it turned out that the differences in the level of charges among these countries were the same.

The current different charging systems increase the requirements on the distribution processes of carriers, especially when planning the new transports or comparing the costs of alternative routes, for example, in the case of insufficient railway infrastructure capacity. However, the unification of charging systems (not rates) is not a technical or economic problem, but rather a political problem.

Acknowledgements

The paper was supported by the VEGA Agency, Grant No. 1/0379/20 "Socio-economics aspects of rail transport market services deregulation in the context of EU legal framework and sustainable mobility", at Faculty of Operations and Economics of Transport and Communication, University of Zilina, Slovakia.

References

[1] Sustainable transport. An official website of the European Union [online]. 2020. Available from: https://ec.europa.eu/transport/themes/sustainable_en

[2] Going climate - neutral by 2050. A strategic long-term vision for a prosperous, modern, competitive and climate - neutral EU economy. Luxembourg: Publications Office of the European Union, 2019.

[3] Directive (EU) 2016/2370 of the European Parliament and of the Council of 14 December 2016 amending Directive 2012/34/EU as regards the opening of the market for domestic passenger transport services by rail and the governance of the railway infrastructure [online]. Available from: https://eur-lex.europa.eu/legal-content/en/ALL/?uri=CELEX%3A32016L2370

[4] Directive 2012/34/EU DIRECTIVE 2012/34/EU of the European parliament and of the council of 21 November 2012 establishing a single European railway area [online]. Available from: https://eur-lex.europa.eu/legal-content/EN/ALL/?uri=celex%3A32012L0034

[5] JOHANSSON, P., NILSSON, J.-E. An economic analysis of track maintenance costs. *Transport Policy* [online]. 2004, **11**(3), p. 277-286. ISSN 0967-070X. Available from: https://doi.org/10.1016/j.tranpol.2003.12.002

[6] WHEAT, P., SMITH, A. S. J. Assessing the marginal infrastructure maintenance wear and tear costs for Britain's railway network. *Journal of Transport Economy and Policy*. 2008, **42**(2), p. 189-224. ISSN 0022-5258, eISSN 1754-5951.

[7] ANDERSSON, M. Marginal cost of railway infrastructure wear and tear for freight and passenger trains in Sweden. *European Transport - Transporti Europei*. 2011, **48**, p. 3-23. ISSN 1825-3997.

[8] ODOLINSKI, K., BOYSEN, H. E. Railway line capacity utilisation and its impact on maintenance costs. *Journal of Rail Transport Planning and Management* [online]. 2019, **9**, p. 22-33. ISSN 2210-9706. Available from: https://doi.org/10.1016/j.jrtpm.2018.12.001

[9] CALVO, F. J., DE ONA, J. DE ONA, R., LOPEZ, G., GARACH, L. A proposal for cost-related and market-oriented train running charges. *Transportation Planning and Technology* [online]. 2014, **37**(4), p. 354-372. ISSN 0308-1060, eISSN 1029-0354. Available from: https://doi.org/10.1080/03081060.2014.897127

[10] ODOLINSKI, K. Estimating the impact of traffic on rail infrastructure. *Journal of Transport Economics and Policy*. 2019, **53**, p. 258-274. ISSN 0022-5258, eISSN 1754-5951.

[11] SMITH, A., IWNICKI, S., KAUSHAL, A., ODOLINSKI, K., WHEAT, P. Estimating the relative cost of track damage mechanisms: combining economic and engineering approaches. *Proceedings of the Institution of Mechanical Engineers Part F-Journal of Rail and Rapid Transit* [online]. 2017, **231**(5), p. 620-636. ISSN 0954-4097, eISSN 2041-3017. Available from: https://doi.org/10.1177/0954409717698850

[12] ROTOLI, F., VALERI, E., RICCI, S., RIZZETTO, L. An analysis of the railway access charges regime in the Italian context. *Transport Policy* [online]. 2018, **64**, p. 20-28. ISSN 0967-070X, eISSN 1879-310X. Available from: https://doi.org/10.1016/j.tranpol.2018.01.006

[13] FRANKLIN, F., NEMTANU, F., TEIXEIRA, P. F. Rail infrastructure, ITS and access charges. *Research in Transportation Economics* [online]. 2013, **41**(1), p. 31-42. ISSN 0739-8859. Available from: https://doi.org/10.1016/j.retrec.2012.10.004

[14] NASH, C. Rail infrastructure charges in Europe. *Journal of Transport Economics and Policy*. 2005, **39**, p. 259-278. ISSN 0022-5258.

[15] GASPARIK, J., ABRAMOVIC, B., ZITRICKY, V. Research on dependences of railway infrastructure capacity. *Tehnicki Vjesnik-Technical Gazette* [online]. 2018, **25**(4), p. 1190-1195. ISSN 1330-3651, eISSN 1848-6339. Available from: https://doi.org/10.17559/TV-20160917192247

[16] MASEK, J., KENDRA, M., CAMAJ, J. Model of the transport capacity of the train and railway track based on used types of wagons. In: 20th International Scientific Conference Transport Means 2016: proceedings. 2016. p. 584-588.

[17] OBERG, J., ANDERSSON, E., GUNNARSSON, J. Track access charging with respect to vehicle characteristics. 2. ed. Repport LA-BAN 2007/31, Banverket, 2007.

[18] SAVELSBERGH, M., TALEBIAN, M. Cost allocation under competition: a new rail access charging policy. *Euro Journal on Transportation and Logistics* [online]. 2019, **8**(5), p. 511-534. ISSN 2192-4376. Available from: https://doi.org/10.1007/s13676-018-0133-z

[19] STENDARD, M., JAGRIC, T., ROSI, B. Estimating marginal infrastructure cost in new infrastructure charging model. *Tehnicki Vjesnik-Technical Gazette* [online]. 2018, 24(3), p. 829-836. ISSN 1330-3651, eISSN 1848-6339. Available from: https://doi.org/10.17559/TV-20160218095139

[20] TRAMPISCH, C. Track access charge control in the railway sector, its interaction with specific financing structures and the determination of incentives - the German infrastructure manager DB Netz AG. *Review of Network Economics* [online]. 2017, **16**(2), p. 177-186. ISSN 2194-5993, eISSN 1446-9022. Available from: https://doi.org/10.1515/rne-2018-0015

[21] ABRAMOVIC, B. Infrastructure access charges. In: *Sustainable rail transport* [online]. MARINOV, M. (ed.). 2016. ISBN 978-3-319-58642-7, eISBN 978-3-319-58643-4, p. 45-58. Available from: https://doi.org/10.1007/978-3-319-58643-4_4

[22] ALVAREZ-SANJAIME, O., CANTOS-SANCHEZ, P., MONER-COLONQUES, R., SEMPERE-MONERRIS, J. J. Rail access charges and internal competition in high speed trains. *Transport Policy* [online]. 2016, **49**, p. 184-195. ISSN 0967-070X, eISSN 1879-310X. Available from: https://doi.org/10.1016/j.tranpol.2016.04.006

[23] TALEBIAN, M., SAVELSBERGH, M., MOFFIET, C. A new rail access charging policy: Hunter Valley coal chain case study. *Transport Policy* [online]. 2016, **46**, p. 101-108. ISSN 0967-070X, eISSN 1879-310X. Available from: https://doi.org/10.1016/j.tranpol.2015.10.007

[24] BUGARINOVIC, M., DIMITRIJEVIC, B., BOSKOVIC, B. The missing component in rail charging modelingaccess charges principle selection. *International Transactions in Operational Research* [online]. 2015, **22**(5), p. 841-859. ISSN 0969-6016, eISSN 1475-3995. Available from: https://doi.org/10.1111/itor.12117

[25] CROZET, Y., CHASSAGNE, F. Rail access charges in France: beyond the opposition between competition and financing. *Research in Transportation Economics* [online]. 2013, **39**, p. 247-254. ISSN 0739-8859. Available from: https://doi.org/10.1016/j.retrec.2012.06.021

[26] NIKOLOVA, CH. User charges for the railway infrastructure in Bulgaria. *Transportation Research Part A-Policy and Practice* [online]. 2008, **42**(3), p. 487-502. ISSN 0965-8564. Available from: https://doi.org/10.1016/j.tra.2008.01.015

[27] DOLINAYOVA, A., CAMAJ, J. Rail infrastructure charges in the V4 countries. In: Road and Rail Infrastructure. In: 5th International Conference on Road and Rail Infrastructure CETRA 2018: proceedings. 2018. p. 917-923.

[28] KROL, M., TACZANOWSKI, J., JARECKI, S., KOLOS, A. Publicly-owned operators can also challenge incumbents. New cases of open-access passenger rail competition in Poland. *Journal of Rail Transport Planning and Management* [online]. 2019, **12**, 100150. ISSN 2210-9706, eISSN 2210-9714. Available from: https://doi.org/10.1016/j.jrtpm.2019.100150

[29] ERDOS, A. K. Enhancing the competitiveness of passenger railway markets. *Procedia Economics and Finance* [online]. 2014, **12**, p. 138-143. ISSN 2212-5671. Available from: https://doi.org/10.1016/S2212-5671(14)00329-3

[30] PITMAN, R., JANDOVA, M., KROL, M., NEKRASENKO, L., PALETA, T. The effectiveness of EC policies to move freight from road to rail: evidence from CEE grain markets. *Research in Transportation Business and Management* [online]. 2020, **37**, 100482. ISSN 2210-5395. Available from: https://doi.org/10.1016/j.rtbm.2020.100482

[31] Network statement for timetable 2019/2020 - ZSR [online]. Available from: https://www.zsr.sk/files/dopravcovia/zeleznicna-infrastruktura/podmienky-pouzivania-zel-infrastruktury/network-statement-2020/networkstatement_2019-2020_amendment_1.pdf

[32] Network statement on the nationwide and regional railways 2020 - SZDC [online]. Available from: https://www.spravazeleznic.cz/documents/ 50007830/51603092/ Network+Statement+2020_2amendment.pdf/209553bb-972a-4c40-9637-1392d1e00205

[33] Network Statement MAV, 2020. Online. Available at: https://www2.vpe.hu/eng/network-statement/network-statement-2019-2020

[34] Network statement PKP 2019/2020. Annex 12 Price list of of fees for using the 1435 mm track gauge railway infrastructure managed by PKP - Polskie Linie Kolejowe s.a. [online]. Available from: https://en.plksa.pl/files/public/user_upload/pdf/Reg_przydzielania_tras/ Regulamin_sieci_2019_2020/Zal_12_Reg19_20_v10_Pricelist1435.pdf

[35] Eurostat 2019. GDP - Purchasing power parities (PPPs), price level indices and real expenditures for ESA 2010 aggregates [online]. Available from: https://ec.europa.eu/eurostat/data/database

[36] ECB foreign exchange reference rates [online]. 2020. Available from: https://www.nbs.sk/en/statistics/exchange-rates/ecb-foreign-exchange-reference-rates

VARIOUS APPROACHES PROPOSED FOR ELIMINATING DUPLICATE DATA IN A SYSTEM

Roman Čerešňák[1,*], Karol Matiaško[1], Adam Dudáš[2]

[1]Department of Informatics, Faculty of Management Science and Informatics, University of Zilina, Zilina, Slovakia
[2]Department of Computer Science, Faculty of Natural Siences, Matej Bel University, Banska Bystrica, Slovakia

*E-mail of corresponding author: roman.ceresnak@fri.uniza.sk

Resume
The growth of big data processing market led to an increase in the overload of computation data centers, change of methods used in storing the data, communication between the computing units and computational time needed to process or edit the data. Methods of distributed or parallel data processing brought new problems related to computations with data which need to be examined. Unlike the conventional cloud services, a tight connection between the data and the computations is one of the main characteristics of the big data services. The computational tasks can be done only if relevant data are available. Three factors, which influence the speed and efficiency of data processing are - data duplicity, data integrity and data security. We are motivated to study the problems related to the growing time needed for data processing by optimizing these three factors in geographically distributed data centers.

Article info
Received 27 November 2020
Accepted 26 January 2021
Online 23 June 2021

Keywords:
duplication data,
distributed data processing,
software architecture

Available online: https://doi.org/10.26552/com.C.2021.4.A223-A232

ISSN 1335-4205 (print version)
ISSN 2585-7878 (online version)

This is an open access article distributed under the terms of the Creative Commons Attribution 4.0 International License (CC BY 4.0), which permits use, distribution, and reproduction in any medium, provided the original publication is properly cited. No use, distribution or reproduction is permitted which does not comply with these terms.

1 Introduction

Severe data change led not only to a change of database types, specifically to a data transfer from the relational databases to non-relational ones, but it caused a rapid development of technology known as distributed data processing. Google belongs to the first pioneers of this technology, which spreads its network in 13 data centers in 8 countries on four continents [1]. The potential of big data indicates great benefit in various industries since 2007 - whether in economical statistics, transport system management or behavior of transport unit analysis, in the medical field with the diagnosis of illnesses or in the computer science. The costs, related to the performance of computing operations, were growing with the popularity growth in relevant industries.

Hand in hand with the increasing use of distributed processing systems, the first problems were occurring related to distributed data processing. A considerable effort was made to reduce the issues related to the processes working with distributed data. A method of maximal duplicated segment and choice of storage nodes to distributed file fragments was created. System of duplication detection and fragmentation (DDFP) and method for deduplication - which virtually eliminates the duplicated data - were designed. Other than that, there were significant methods developed for the storing of data fragments and allocation of unique occurrences of the data file on nodes [2]. Suppression of duplicities in the systems was also examined in study [3], which deals with data processing by technologies like MapReduce, Spark and SQL queries.

Secondly, the network security became crucial component in the data processing and various fields and sectors of informatics. Regarding distributed data processing, the security is divided into variety of elements, such as Tool security, environment Hadoop, Flink, Samza, Spark [4] or many others. Critical parts of cloud security consist of the safety of the data storing in the cloud [5], monitoring, anomaly and threat detection [6] and last but not the least data audit [7]. The largest part of security is management of accesses and keys, sharing the access groups and last, but not the least, there is a problem of security of data itself.

Thirdly, the service quality (QoS) of big data tasks was not taken into account in already existing work. Similar to conventional cloud services, the big data applications exhibit a service level agreement (SLA) between a service provider and the applicants. The computational tasks are foremost determined according to where they are located and number of computation resources assigned to the task. The portable speed is another significant influence factor because the big data tasks are devoted to the data. The computational task cannot continue until the available data do not match each other. Existing studies regarding the computing clouds are generally, for example [8], mainly focused on

restriction of computational capacity while ignoring the limits of the system's portable speed.

Optimization of solutions, studied here, is related to data duplicity, data integrity and data security in the geographically distributed centers, to overcome the weak points related to the distributed data processing in a cloud envirnment. The servers are equipped by the limited storing and computational tools. Each data block has a demand for storage space. The goal is to minimalize the number of duplicities of the big data, reduce the number of accesses and increase data integrity. Main benefits of presented research can be summarized as follows:

- Based on the growing amount of data, it is necessary to control the data in the system; Not only that the speed of the data processing is increased, but the amount of storage space needed for the data is effectively reduced.
- Here is dealt with the minimization of the data access - the data centers - and thus the higher data security is ensured and the amount of restrictions is reduced.

The rest of the paper is arranged as follows. Part 2 summarizes the related work. This part is the crucial aspect of research direction compared to other researchers' approaches, who are dealing with the same research topics. Part 3 presents the system model. it is necessary to find out which architecture is more effective in eliminating duplicate data which enter the system during our research. Two architectures are introduced and the proposed methodology was tested experimentally. These experiments are described in part 4 and serve as verification of theoretical findings. Finally, conclusion of the presented research and experiments is provided in the part 5.

2 Related work

Many factors influence the current state of the distribution data processing. It is well known that data that comes to the system contains in any way the same duplicate data. This factor influence leads to an increase in the transformation process and of the course distribution process. The same data for multiple users are stored at the same time. This factor leads, with the replication factor equal to 3 for two users, to store data 6 times. This wasting memory and increasing server costs lead many researchers to develop methods, which decrease the duplicated data and save the operating costs. During this research, many papers that worked with the issue were studied.

The researchers in [9] created an approach based on the method known as Data deduplication. This data deduplication process is widely used in cloud storage to decrease storage space and upload bandwidth. However, only one copy of each file is stored, even if many users own such a file. By using, deduplication system, the progress of storage utilization and reliability is increased. Besides that, the dare of privacy for sensitive data also occurs when outsourced by users to the cloud. In this approach authors used new distributed deduplication systems with upper dependability. The data chunks are distributed from the corner to cornering multiple cloud servers. The well-being needs of information security and label soundness are refined by presenting a deterministic mystery sharing plan in circulated capacity frameworks. On the other hand, a deduplication technique can reduce the server-side storage cost and save the upload bandwidth at the user side.

In further research, authors came across a method of data mining and fuzzy logic, the aim of which is to eliminate duplication. In the paper [10], a practical and novel duplicate elimination system is presented, which exploits a fuzzy inference engine for handling the uncertainty involved in detecting fuzzy duplicates. The system's innovation is capturing an expert's knowledge in the form of natural language fuzzy rules and using these simple rules to clean the data efficiently. This, in turn, reduces the time required for the repetitive and time-consuming task of hard-coding for deduplication based on a scheme for each database.

The presented examination issue's objective was to dispense with duplication of information, which is the essential objective. Notwithstanding, it is understood that replication in numerous regions also guarantees the framework's unwavering quality during the exploration. To look after dependability, authors were compelled to address consistency with steadfast quality in lessening duplications. The specialists [11] considered the referenced viewpoint and they thought of the case that the deduplication framework improves capacity usage while reducing dependability. Besides that, the test of protection for touchy information likewise emerges when clients redistribute them to the cloud. Meaning to address the above security challenges, this paper makes the primary endeavor to formalize the idea of dispersed, dependable deduplication frameworks. The new disseminated deduplication frameworks were proposed with higher unwavering quality in which the information pieces are distributed over various cloud workers. The security prerequisites of information classification and label consistency are likewise accomplished by presenting a deterministic mystery sharing plan in appropriated capacity frameworks, rather than utilizing united encryption, as in past deduplication frameworks. Security examination shows that the proposed deduplication frameworks are secure, as far as the proposed security model's definitions. As confirmation of the idea, the proposed frameworks were actualized and it is indicated that the acquired overhead is restricted in practical conditions. Cloud companies from Amazon, Microsoft or Google, are among the areas that are gaining more and more popularity, which results in exploring duplicates even in a quiet environment. In their work [11], the researchers presented certain pitfalls

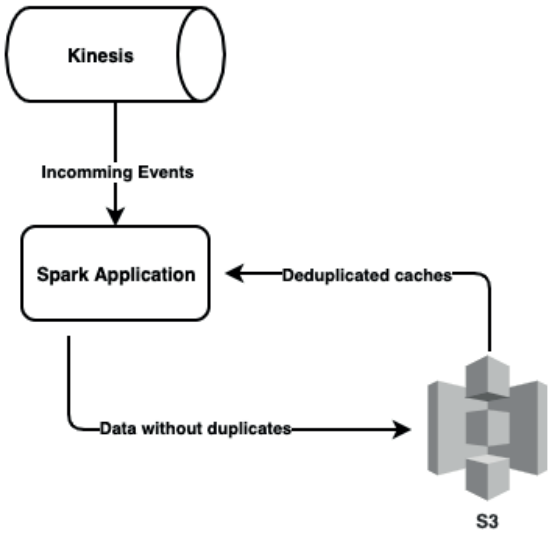


Figure 1 *Stream data processing*

that occur in cloud services. They also provided a solution at work that has developed a solution that includes data security and space efficiency in server storage and distributed content checksum storage systems. Here is adopted a method called interactive Message-Locked Encryption with Convergent Encryption (iMLEwCE). In this iMLEwCE, the data is encrypted firstly and then the ciphertext is again encrypted. Block-level deduplication is used to reduce the storage space. Encryption keys are generated in a consistent configuration of data dependency from the chunk data. The identical chunks will always encrypt to the same ciphertext. The hacker cannot deduce the keys configuration from the encrypted chunk data. Thus, the information is protected from the cloud server. This paper focuses on reducing the storage space and providing security in online cloud deduplication.

In paper [12], researchers defined their own proposed temporal architecture concerning element registration in the system. Whereas the data models depicted attributes and temporality definition, evolve, it is necessary to create a complex environment and possibilities for dealing with these changes and reflections to the temporal management layer. The temporal registration concept does it. Researchers developed a method that significantly decreases the duplication of data in a database, which led to reduced performance of used servers.

Another interesting idea was presented in [13], which deals with the granularity management of the temporal system proposes a data sharing model based on the reliability, sensitivity and precision of data providers. A new concept of the temporal benefit is introduced, which is consecutively evaluated in the experiment section. Optimization of the data flow by historical data aggregation and limitation of the data amount is a core part for the system decision making, whereas the time for data transferring is strictly limited.

A similar method, as one presented in [9], was shown in [2]. The process they took as the primary method and from which they relied on is called data deduplication. In their paper, the researchers saw the main challenge of identifying the maximum duplicate segment and selecting the storage nodes to distribute files. In this paper, researchers proposed Duplicate Detection and Fragment Placement (DDFP). This deduplication system virtually eliminates duplicate data and fragments placement that allocates individual data files on storage nodes. For repeated data, a reference point is used and unique data is stored on the storage node. The created approach increases the percentage of duplicate data detection. A fragment placement algorithm is used for placing fragments on different storage nodes. The T-coloring is used to select nodes, set T is used, which restricts the nodes at distance T from one another. The DDFP considerably achieves duplicate elimination and obtain a high level of security on data fragments by storing fragments of the data file using the T-coloring. This selects the nodes that are not adjacent, which prevents unauthorized access to data from other users.

As can be seen from previous research, the problem being solved in the current paper increasingly impacts efficiency of the algorithm and other factors, such as reliability, reducing server utilization and reducing the cost of storing data in the system.

3 Design and implementation of the real-time data catching method

In the rapidly developing world, the duplicated data are a big problem, which was examined in various studies. This paper's main objective was designing and implementing a method capable of catching the data in real-time, thus reducing the data duplicity to a minimum. The architecture, presented in Figure 1, is designed to fulfill this objective.

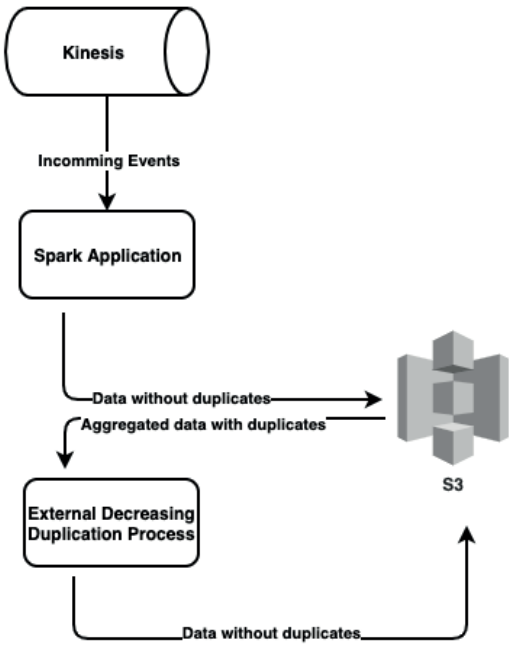


Figure 2 *Improved stream data processing*

3.1 One data storage

As presented in Figure 1, this architecture consists of three essential parts: Amazon Kinesis, Apache Spark and S3.

Naturally, while burning-through information from Kinesis, Spark provides data catching in any time period. This is accomplished with Kinesis checkpointing, which keeps up the putting away and balances time frame Kinesis stream in DynamoDB. On the off chance that Spark crashes in the middle of the Kinesis checkpointing, it always begins with calling of all the functions from the earliest starting point of the span. This implies that each operation can be processed or entered into system more than once, which can lead to creation of duplicates.

Apache Spark provides a component to avoid duplicates, which recoups information after the crashes and keeps the streams from handling documents called Spark checkpointing. The implicit Spark Streaming element should not be mistaken for the Kinesis checkpointing (which was referenced above). At the point when the Spark checkpointing is empowered, Spark stores metadata and handles RDDs to dependable, persevering capacity, e.g., HDFS. Another component of the Spark Streaming are the Write Ahead Logs (WALs). The WAL contains information obtained from Kinesis (or some other information stream). It is utilized for the state recuperation after the disappointments of the driver and the beneficiaries. Once implemented, the blend of checkpointing and WAL should be useful as a way of precision boosting of the system. As it may be, these highlights in Spark don't work effectively and cause execution corruption, mainly if more seasoned renditions are utilized. In this implementation, Spark 1.5.2 was used.

To maintain a necessary distance from each of these issues, it is chosen to utilize Kinesis checkpointing to update it at any rate, ensure and plan a different lightweight answer to limit the probability of duplicates. Two unique methodologies were designed; the second worked fundamentally better than the first one. Both methodologies are next described in some detail and it is clarified how authors came to that conclusion.

The system portrayed in Figure 2 did not make the data catching effective even though the duplicity recognition was possible. The architecture presented in the Figure 2 solves this problem with a different approach. It catches not only the data, which do not contain duplicity but exactly the data, which include deception. it was decided to use the Amazon S3 file storage, since it was necessary to effectively control parallel processes, parallel approach and useful incoming data expanding the in-memory database such as Redis or Memcached.

During the handling, the information was divided into the Spark stream. Each function got a particular ID dependent on the current timestamp and was set in a basin determined as a hash code of ID function. Here is an example of the information partitioning:

```
def createPair(fields: Map[String, String]):
(DateTimePartitionKey, Map[String, String]) = {
    val partitionKey = DateTimePartitionKey(
        fields(FlowField.EventId)
        fields(FlowField.EventHour),
        fields(FlowField.EventDate),
    )
    partitionKey -> fields
    }
```

To accomplish the non-problematic execution, it was expected to run the deduplication prepared concurently.

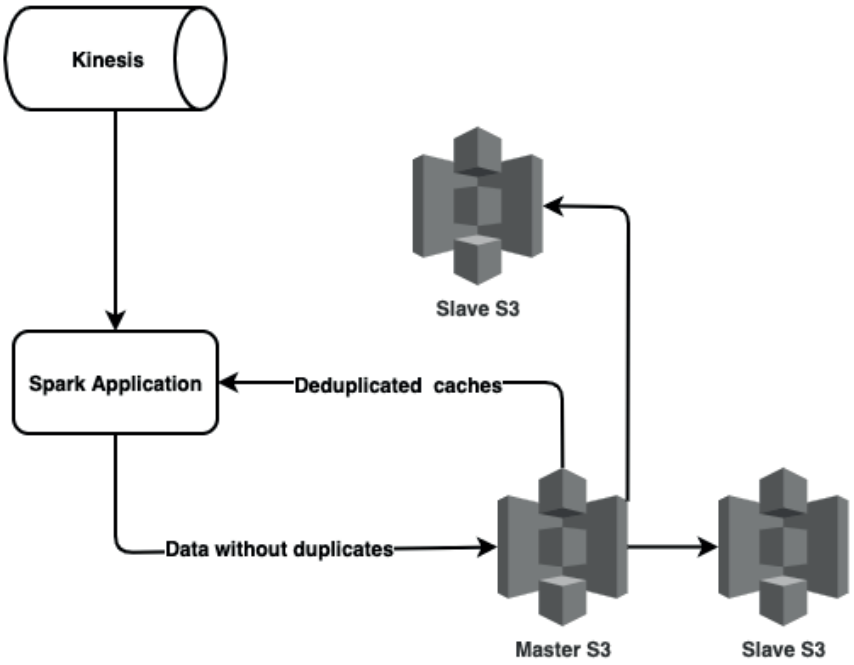


Figure 3 *Multiple data storage architecture*

Since the information, corresponding to the parceling plan depicted above was previously handled, the similar parallelism was used for deduplication. Consequently, it was expected to parcel the reserve put away in the S3 file system in a similar way the information in the stream was divided.

3.2 Multiple data storage

During the research, the second method, capable of working with the data, was also examined. As opposite to the first proposed method, the data is stored in several data storages. A new type of architecture was developed due to the multiple data storage spaces, which is portrayed in Figure 3.

To achieve the satisfying performance, it was necessary to start the deduplication processing in parallel. Since the data were already processed in parallel with the above-described division scheme, the same type of parallelism was used for the deduplication process. That is why it was necessary to divide the cache. The date in the file system S3 was stored by use of the method for splitting the data in the stream.

The division into sections was implemented with the hierarchical directory structure:

- The first level - batch creation data
- The second level - time (hour) of the batch creation
- The third level - the storing of cache files to a bucket

Having multiple cache files for each segment could become a problem caused by the high latency of reading operations in S3. Operation efficiency of S3, however, was sufficiently compelling and because of the achievement of remaining performance, the files were read in several threads. The same approach was also valid for writing the data to S3. The S3 File System was used since the parallel processing of the data was needed to secure the testing and real purposes for several Amazon instances. Amazon S3 File system allows several sources to access the data and read the information in them, which is one factor that played an essential role in the seletion of data storage.

For the consistency sake, both data and storages were endured in one exchange. This was conceivable, since both knowledge and reserves were put away in the S3 filesystem. During the group preparation, information and stores were kept in touch with the transitory catalogs. When a clump was handled, its substance was moved to the last area as a nuclear activity. In the event, when one of the move tasks fizzled, the entire stream was halted until the predictable state was reestablished physically.

The Cache itself is a straightforward information structure comprised of two sections. The first is an unchanging set, which containes information stacked from S3. The other one is a variable set, which was utilized for including new function IDs.

Thus, it was necessary to perform various intermediate steps, as they are portrayed in Figure 4 and to create a code capable of suppressing the duplicity. The source code is provided at the following address: https://github.com/romanceresnak/deduplication/blob/main/deduplication.java.

The function *getCache* needed to be called just once for each parcel key. In the other case, one can use an obsolete reserve since some new function IDs may be continued in an impermanent area. The simplest method to do this is to sort information by key. This should be possible during the repartitioning utilizing worked in the *repartitionAndSortWithinPartitions* Spark

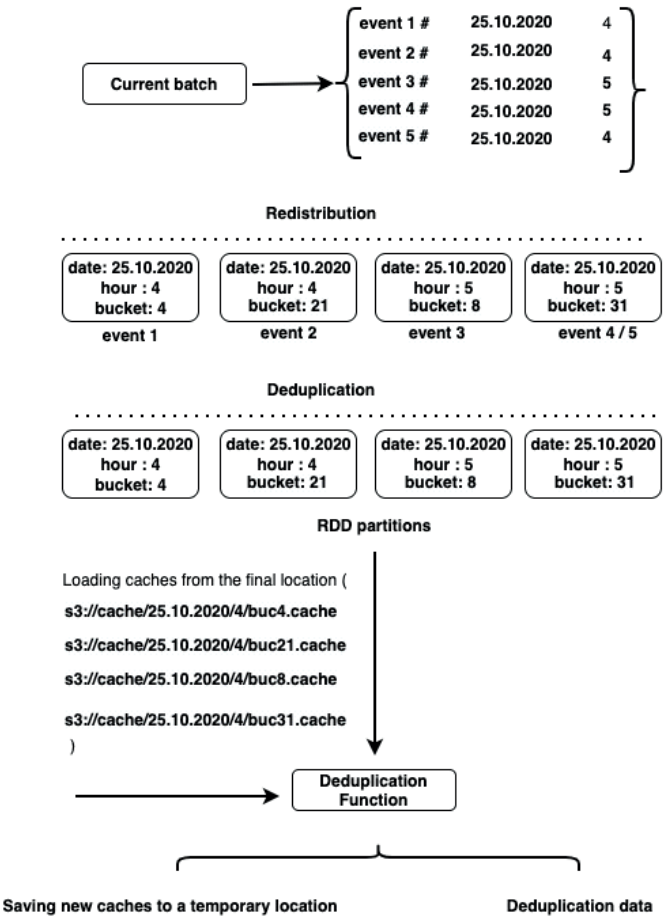


Figure 4 *Individual data processing steps*

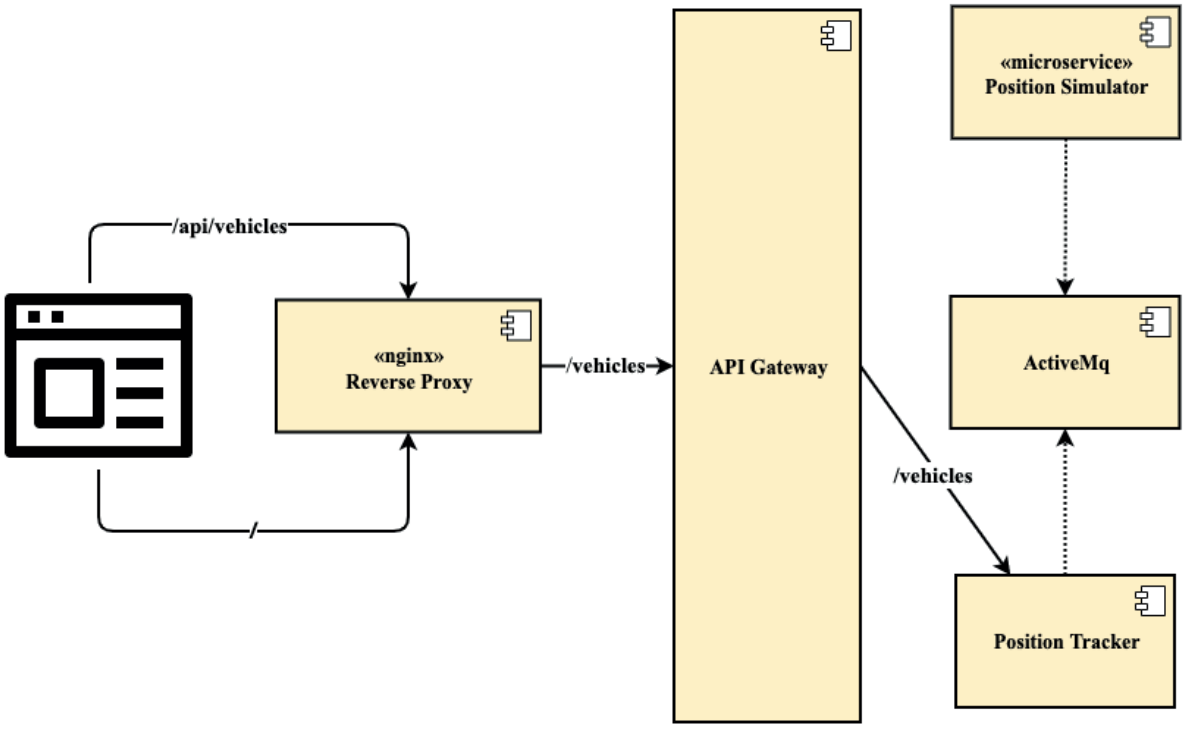


Figure 5 *Architecture of application*

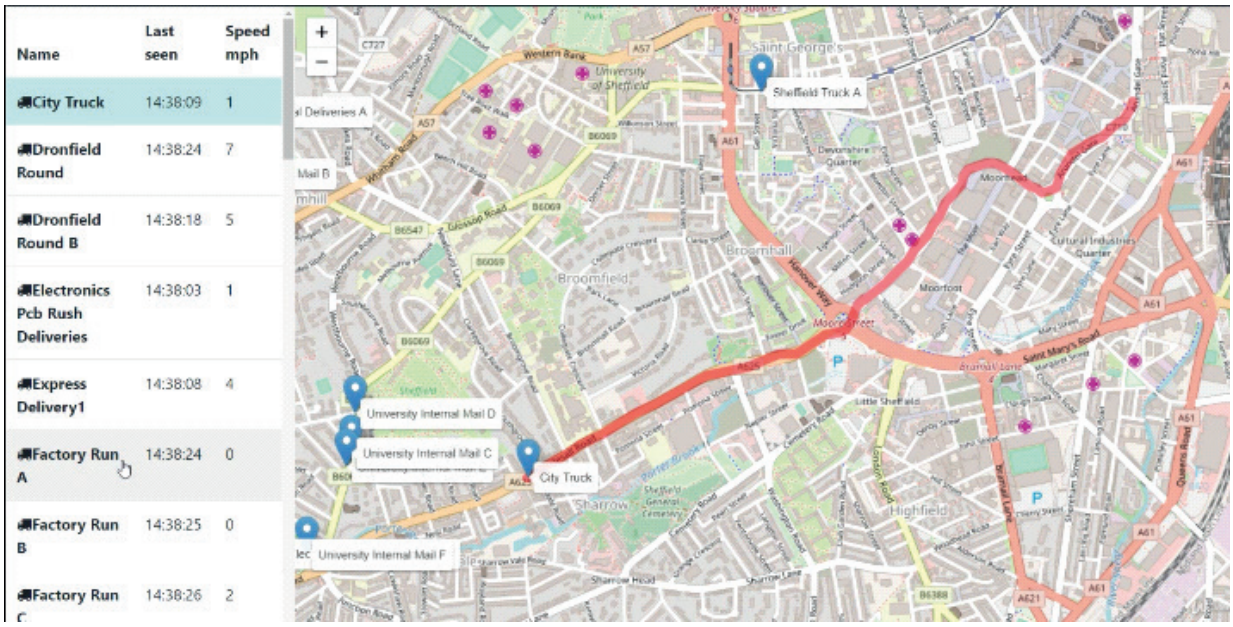


Figure 6 *Tracking car*

Table 1 *Server configuration*

technology	parameters
• EC2 instance	• cloud • a1.medium • vCPU: 1 • MeM(GiB): 2
• EMR cluster	• master: 1x • m3.xlarge • core: 2x • m4.4xlarge
• spark	• 1 r5.12xlarge master node • 19 r5.12xlarge core nodes • 8 TB total RAM • 960 total virtual CPUs • 170 executor instances • 5 virtual CPUs/executor • 37 GB memory/executor • parallelism equals 1,700

technique. At last, the deduplication part of work can be described as follows.

In this capacity, the data stream is mapped to a flood of sets where the principal component is a composite parcel key while the subsequent one contains the information. From that point forward, a changing work is applied to this stream, which permits to work with the RDDs and bunch time. At last, the *repartitionAndSortWithinPartitions* was considered on the RDD and the copies were channeled utilizing the pass-through storing system.

4 Experiments for the real-time data catching method

For experimental testing of proposed methods, an application, which monitors the GPS position of the delivery car, was created. That application is based on microservices and is shown in Figure 5.

Delivery routes can be the same at specific points, but based on this proposal, the duplicate data were captured and were not store it in the database. In the end, this approach allowed not only to reduce the amount of data in the system, which is shown in Figure 6, but also to lower the load of the server.

```
Host namenode
    HostName ec2-18-216-40-160.us-east 2.compute.
    amazonaws.com
    User ubuntu
    IdentityFile ~/.ssh/MyLab_Machine.pem

Host datanode1
    HostName ec2-18-220-65-115.us-east-2.compute.
    amazonaws.com
    User ubuntu
```

Table 2 *Results of GPS data recording in the interval of 1 hour*

configuration	one data storage (architecture A)	multiple data storage (architecture B)
RAM	1.2 TB	2 TB
CPU	5 GB	2 GB
FILES	1	50
transform time	85 seconds	90 seconds

Table 3 *Results of GPS data recording in the interval of 2 hours*

configuration	one data storage (architecture A)	multiple data storage (architecture B)
RAM	3.6 TB	4.8 TB
CPU	10 GB	4 GB
FILES	1	103
transform time	2 min and 32 s	2 min and 32 s

Table 4 *Results of GPS data recording in the interval of 3 hours*

configuration	one data storage (architecture A)	multiple data storage (architecture B)
RAM	5 TB	8 TB
CPU	8 GB	4 GB
FILES	1	158
transform time	7 min and 13	5 min and 25 s

```
    IdentityFile ~/.ssh/MyLab_Machine.pem
Host datanode2
    HostName ec2-52-15-229-142.us-east-2.compute.
    amazonaws.com
    User ubuntu
    IdentityFile ~/.ssh/MyLab_Machine.pem

Host datanode3
    HostName ec2-18-220-72-56.us-east-2.compute.
    amazonaws.com
    User ubuntu
    IdentityFile ~/.ssh/MyLab_Machine.pem
```

4.1 Results of experiment for the proposed methodology

Three types of data were used for experimental work. For the purpose of the experiments, the configuration shown in Table 1 was used. The application records the GPS positions at intervals of one, two and three hours. The recorded values are presented in Tables 2, 3 and 4, respectively.

The values that were measured during the data recording for the interval of one hour are presented in e Table 2. This data set contains 34 similar records. Three aspects were evaluated - RAM, CPU and number of files - which point to the fact, that with the same configuration, architecture A uses more CPU performance to watch the duplicated components, but it uses less RAM. It also clearly states that all the data are stored in a single file, as oppose to architecture B, which needs up to 50 files in order to work correctly and keep watch over the duplicated data.

Time is crucial. Based on measured values, finding of the duplicated values is faster while using architecture A. A large problem was recognized during the run of the process - it was not the inefficiency of architecture B, but the necessity to merge and manage the duplicated data in various files in parallel.

The values that were measured during the data recording for the interval of two hours are presented in Table 3. it was chosen to limit values, where the efficiency of duplicated data's processing is the same. The CPU load has doubled, which does not cause any significant problems in actual processing. During the experiments, the number of files increased, as well, which allowed effective searching, as oppose to architecture A, processing all the data in a single file – approach, which degrades with higher ammount of data.

Lastly, the values that were measured during the data recording for the interval of three hours are presented in Table 4. In this step, the efficiency of parallel processing with various files can be seen clearly. Even if the operations of file division and subsequently their connecting are time-consuming with the vast amount of the data, the parallel processing, clearly surpasses the efficiency of the processing of data in one file.

The results at the beginning hinted at the superiority of the architecture A. However, regarding the interval

of 2 hours, the efficiency was equal for both proposed architectures and architecture B proved its efficiency with the increasing ammount of data.

5 Conclusion

In the current, quickly developing world, the duplicity suppression has a significant influence on the velocity of system performance and the storing of the data to the data storages. The primary objective of many researchers in the area is examining the problem related to the duplicity suppression - user data searching in various data storages and the reduction of the systems needed for the processing of data by system. Finally, the duplicated data increases ammount of space needed in the data storages, which is, in the end, mirrored even in need of buying new hardware and expanding the data centers.

To make the process more effective and reduce computational costs, authors created the method dealing with the catching of the same data coming from several sources to the system. Specifically, the duplicated data are caught in the first phase of our proposed algorithm and by creating a reference to a particular source creating a link. The second phase of proposed algorithm is based on distributed data processing. After finishing the processing, the system always found a particular value, which means the algorithm must create a correct reference for the given value.

The experiments, performed for a test of the designed method confirmed this. The conventional opposite process of distributed data processing, which missed the duplicated value, this system effectively reduced the server overload. It reduced the time needed for the whole distribution of the data on several nodes. The second significant result, which is the data decrease in the nodes and the cost reduction, is related to the data node reduction.

The future research, dealing with the duplicity suppression, will be related to improvement of the designed method, not only the in cloud service Amazon, but in creating a general module in programming language golang, as well, which will help with implementation of parallelism. Authors also want to focus on more effective reference creation in the primary step in the control of duplicities entering the system. The research presented in this paper also points to the selected topics in the area of signal theory similar to research presented in [14].

Acknowledgement

This work was supported by Grant System of University of Zilina No. 1/2020 (8056).

References

[1] KAMAL, J., MURSHED, M., BUYYA, R. Workload-aware incremental repartitioning of shared-nothing distributed databases for scalable OLTP applications. *Future Generation Computer Systems* [online]. 2016, **56**(C), p. 421-435. ISSN 0167-739X. Available from: https://doi.org/10.1016/j.future.2015.09.024

[2] PATIL, J., BARVE, S. S. DDFP: Duplicate detection and fragment placement in deduplication system for security and storage space. In: 1st International Conference on Intelligent Systems and Information Management ICISIM 2017: proceedings [online]. 2017. Available from: https://doi.org/10.1109/ICISIM.2017.8122177

[3] DOLEV, S., FLORISSI, P., GUDES, E., SHARMA, S., SINGER, I. A survey on geographically distributed big-data processing using MapReduce. *IEEE Transactions on Big Data* [online]. 2017, **5**(1), p. 60-80. eISSN 2332-7790. Available from: https://doi.org/10.1109/TBDATA.2017.2723473

[4] GAI, K., QIU, M., ZHAO, H. Security-aware efficient mass distributed storage approach for cloud systems in big data. In 2nd IEEE International Conference on Big Data Security on Cloud IEEE BigDataSecurity 2016, 2nd IEEE International Conference on High Performance and Smart Computing IEEE HPSC 2016 and IEEE International Conference on Intelligent Data and Security IDS: proceedings [online]. Vol. 1. 2016. Available from: https://doi.org/10.1109/BigDataSecurity-HPSC-IDS.2016.68

[5] CAO, N., WANG, C., LI, M., REN, K., LOU, W. Privacy-preserving multi-keyword ranked search over encrypted cloud data. *IEEE Transactions on Parallel and Distributed Systems* [online]. 2014, **25**(1), p. 222-233. ISSN 1045-9219, eISSN 1558-2183. Available from: https://doi.org/10.1109/TPDS.2013.45

[6] KOTENKO, I., SAENKO, I., BRANITSKIY, A. Framework for mobile internet of things security monitoring based on big data processing and machine learning. *IEEE Access* [online]. 2018, **6**, p. 72714-72723. ISSN 2169-3536. Available from: https://doi.org/10.1109/ACCESS.2018.2881998

[7] DIAO, Z., WANG, Q., SU, N., ZHANG, Y. Study on data security policy based on cloud storage. In: 3rd IEEE International Conference on Big Data Security on Cloud BigDataSecurity 2017, 3rd IEEE International Conference on High Performance and Smart Computing HPSC 2017 and 2nd IEEE International Conference on Intelligent Data and Security: proceedings [online]. 2017. ISBN 978-1-5090-6296-6, p. 145-149. Available from: https://doi.org/10.1109/BigDataSecurity.2017.12

[8] RAO, L., LIU, X., XIE, L., LIU, W. Minimizing electricity cost: optimization of distributed internet data centers in a multi-electricity-market environment. In: IEEE INFOCOM 2010: proceedings [online]. 2010. Available from: https://doi.org/10.1109/INFCOM.2010.5461933

[9] JUNGHARE, S. A., MAHALLE, V. S. Overview of secure distributed de-duplication system with improved reliability. In: International Conference on Inventive Systems and Control ICISC 2017: proceedings [online]. 2017. Available from: https://doi.org/10.1109/ICISC.2017.8068613

[10] SHAHRI, H. H., BARFORUSH, A. A. Z. Data mining for removing fuzzy duplicates using fuzzy inference. In: Annual Conference of the North American Fuzzy Information Processing Society - NAFIPS 2004: proceedings [online]. 2004. ISBN 0-7803-8376-1. Available from: https://doi.org/10.1109/NAFIPS.2004.1336229

[11] LI, J., CHEN, X., HUANG, X., TANG, S., XIANG, Y., HASSAN, M. M., ALELAIWI, A. Secure distributed deduplication systems with improved reliability. *IEEE Transactions on Computers* [online]. 2015, **64**(12), p. 3569-3579. ISSN 0018-9340, eISSN 1557-9956. Available from: https://doi.org/10.1109/TC.2015.2401017

[12] KVET, M. KVET, M. Temporal database management: temporal registration. In: International Conference on Information and Digital Technologies IDT 2017: proceedings [online]. 2017. ISBN 978-1-5090-5688-0, p. 227-233. Available from: https://doi.org/10.1109/DT.2017.8024301

[13] KVET, M. Data distribution in ad-hoc transport network. In: International Conference on Information and Digital Technologies IDT 2019: proceedings [online]. 2019. ISBN 978-1-7281-1401-9, p. 275-282. Available from: https://doi.org/10.1109/DT.2019.8813437

[14] DOBRUCKY, B., HARGAS, L., MARCOKOVA, M., KONARIK, R., KONIAR, D. A LabVIEW implementation of digital waveform quadrature oscilator by virtual instrumentation. In: International Siberian Conference on Control and Communications SIBCON 2017: proceedings [online]. 2017. eISSN 2380-6516. Available from: https://doi.org/10.1109/SIBCON.2017.7998547

GDP EFFECT ON B2C E-COMMERCE TURNOVER AND NUMBER OF EXPRESS SHIPMENTS IN SELECTED EUROPEAN POST-COMMUNIST COUNTRIES

Michaela Novotná*, Dalibor Gottwald, Libor Švadlenka

Faculty of Transport Engineering, University of Pardubice, Pardubice, Czech Republic

*E-mail of corresponding author: michaela.novotna7@student.upce.cz

Resume

The impact of the e-economy has been observable in almost all the sectors of the national economies of the states in the last few years. The growing influence of this phenomenon is due to development of the Internet, which has already become a viable part of almost all the business activities including buying and selling. Therefore, it can be assumed that the area of e-commerce will have an increasing impact, not only on national economic development, but on the express mail market, as well. The content of the article is designed to provide a comprehensive view of the interdependence between the level of economic maturity (the GDP gross Domestic Product) per capita in the PPS (Purchase Power Standard) indicator), development of the e-commerce (indicator B2C (Business to Customer) e-commerce turnover) and the number of express deliveries. Identifying the influence between the aforementioned indicators, it will be possible to take certain measures to support the development of the e-commerce market.

Article info

Received 17 November 2020
Accepted 22 December 2020
Online 13 September 2021

Keywords:

e-commerce,
express deliveries,
GDP

Available online: https://doi.org/10.26552/com.C.2021.4.A233-A240

ISSN 1335-4205 (print version)
ISSN 2585-7878 (online version)

This is an open access article distributed under the terms of the Creative Commons Attribution 4.0 International License (CC BY 4.0), which permits use, distribution, and reproduction in any medium, provided the original publication is properly cited. No use, distribution or reproduction is permitted which does not comply with these terms.

1 Introduction and literature review

Different indicators are used in macroeconomics to measure the economic performance of a state. One of the most important indicators is the gross domestic product per capita in purchasing power standard (GDP per capita in the PPS). The GDP per capita in PPS is, according to the most common definition also given by Eurostat, defined as the market value of all the manufactured goods and services produced in a given economy, in this case the economy of a given state, over a certain period of time, using the factors of production available in the territory of the selected economy, while independent of the ownership of those factors, calculated per capita [1]. Development of the GDP per capita in PPS then depends on many factors. Transport and technical infrastructure, civic equipment and public spaces are among the most important [2]. The quality of infrastructure, especially in terms of its scope, coverage density, throughput, safety and other specific factors, influences the possibility of using production factors and thus the performance of the state economy.

In recent years there has been a dramatic increase in development of the e-commerce, which also stimulates the need to develop the logistics industry [3]. The infrastructure that enables the development of the e-commerce phenomenon is undoubtedly the Internet communication network. Its coverage averages 82.49% in the European countries [4]. The Internet enables both wholesale and retail businesses to reach a wider range of customers, move in the distribution network and optimize resources in overall. This means the necessary fulfillment of both, the supply, as well as the return, of the goods through the distribution chain, an important component of which are the postal and logistics service providers, who must adapt to this new market situation. The increasing volumes of goods to be delivered to customers were already highlighted by the European Commission in 2012, while pointing out the need to find new solutions in this area of business [5-6]. Some authors also write about the importance of focusing on stakeholders in the distribution chain [7]. The costliest component of this chain is the last mile where goods are delivered to the end customers [8]. At the same time, it is important to perceive the increasing customer demands, which no longer focus solely on the quality of the goods or their sellers, but increasingly these demands on the part of customers are directed to the postal providers as well [9]. The requirements relate to ensuring flexibility in time and place of delivery, the possibility of returning the delivered products with an option to make a complaint and/or to get a refund, finally, also, the variability of payment terms. Currently, the role of a customer is shifting [10]. A customer is now considered a co-creator of service innovation. At the same time, the customers demand shorter delivery time.

According to the authors, it is important, that the postal system looks for common features with other branches of the communications sector and identify possible interoperability [11].

The relationship between the turnover of the e-commerce and GDP per capita in PPS was investigated by many researchers [12]. The authors focused in particular on the legislative side of the matter, which prevents faster development of the e-commerce. They see problems not only in telecommunications infrastructure, but also in the adequacy of consumer rights protection [12]. Here it is worth mentioning that authors highlighted the Czech Republic and Ireland, as countries in which businesses have created the right conditions to connect online. During the research regarding the impact of the e-commerce on GDP, several obstacles were found influencing the development of the e-commerce. Therefore, the European countries were split up into several groups with similar characteristics [13]. Next author focused on three countries for which she examined the relationship of the e-commerce not only with GDP per capita in PPS, but also with the unemployment rate, as another indicator of economic development [14]. The increasing turnover of the e-commerce, which is growing by an average of 14.28% per year in the business to customer (B2C) model, puts enormous pressure on postal operators and the need for their rapid adaptation to increasing customer demands [4]. At this point, it should be noted that, there are other commonly used e-commerce models, among which the authors include business-to-business (B2B), customer-to-customer (C2C), customer-to-business (C2B) and the already mentioned B2C model, which this article deals with in particular [15]. Especially for the B2C sector in China, the last mile raises great concerns due to the rapid development of the e-commerce, with customers looking for delivery through express companies [16]. Some authors are looking into how to deliver a package the same day, using free public transport capacity [17]. Other authors go even further and propose a new concept of the city's railway transit system with stations equipped with freight platforms, which assumes a pre-known demand, but also works with customer's requests regarding delivery time [18]. Further research focuses on challenges and opportunities of urban logistics as a whole in order to prioritize allocation of resources to ensure quality of life of the population and meeting its needs [19]. Some other studies head in different direction and work with the option of returning the vehicle to a depot for new shipments before delivering already loaded shipments, even seeing possible improvements that can offer preventive returns to the depot [20]. These improvements include reduction in delivery times or more efficient use of a vehicle capacity.

The liberalization of the postal market has taken place gradually by 2012 [21]. Full liberalization of the postal services was completed in all the states by the beginning of 2013 including the last 13 countries that had an exemption. Countries such as the Czech Republic, Slovakia, Romania, under the EU Directive thus had longer time to remove the remaining barriers for the new logistics service providers and at the same time existing monopolists had time to implement the cost-cutting strategies and focus on parcel delivery and express parcel delivery, an area where the substantial competition had already flourished [21-22]. Year 2012 is also an important year for this sector, the operators entered the global monitoring system, which enabled improved shipments tracking. This system, which has gradually integrated all the countries, allowed for more than 20% increase in express shipment and proof of delivery timeliness in 90% of cases between 2014 and 2015 [23].

The objective of this article is to evaluate the existence of dependence of the economic development of the state, monitored by the macroeconomic indicator GDP per capita in PPS, on the year-over-year turnover of B2C e-commerce and the number of express mail shipped using the postal infrastructure. The regression and correlation analyses were used to achieve the objective of the article. The objective is divided into two sub-objectives that must be completed in order to achieve the main objective. The first step is to assess the existence of dependence of the GDP per capita in PPS in each state on the year-over-year turnover of the B2C e-commerce. The second sub-objective is to assess the existence of dependence of the GDP per capita in PPS in each state on the number of express items shipped.

2 Methodology

Data series are described in detail at the beginning of this section, followed by defined hypotheses the validity of which was tested using the selected mathematical and statistical methods, which are also described in detail.

2.1 Datasets

All the variables used, i.e. the GDP per capita in PPS, B2C e-commerce turnover and number of transported express shipments, were monitored in all the selected European countries between 2013 and 2017. Since some data was not available for some of the years or some of the states, only those states were chosen for which all the data for all the relevant years were available and subsequently tested to confirm or reject validity of hypotheses.

To compare the national economic performance through the GDP per capita, this variable was expressed in PPS (purchasing power standards), a common currency that eliminates differences between countries. The GDP data per capita in PPS was obtained from European Statistical Office documents [1]. „The value of the total output of goods and services produced by an economy, less intermediate consumption, plus net

taxes on products and imports. The GDP per capita is calculated as the ratio of GDP to the average population in a specific year", [1].

Another variable used is turnover of the B2C e-commerce. The data was obtained from the Ecommerce Foundation, which works with 19 national associations and more than 75,000 companies, including SAP, Asendia Management SAS and MultiSafepay. The E-commerce Foundation analyzes the B2C e-commerce market and focuses, in particular, to negotiate the better conditions for development of the e-commerce with European Union legislators [1].

The last variable is the number of transported express shipments. Data on the number of express shipments transported was extracted from Universal Postal Union documents [23]. Universal Postal Union brings together information from all national regulatory authorities of the Member States. These regulatory authorities provide Universal Postal Union with data on number of express shipments transported.

2.2 Characteristics of tested hypotheses and used mathematical and statistical methods

With reference to the objective, set out in the introduction of this article, the following hypotheses were established:

$H0_1$: Development of the GDP per capita in PPS indicator in a given state does not have a significant impact on development of the B2C e-commerce indicator in that state.

HA_1: Development of the GDP per capita in PPS in a given state has a significant impact on the development of the B2C e-commerce indicator in that state.

$H0_2$: Development of the GDP per capita in PPS indicator in a given state does not have a significant impact on development of the indicator of the number of express shipments transported in that state.

HA_2: Development of the GDP per capita in PPS indicator in a given state has a significant impact on development of the indicator of the number of express shipments transported in that state.

The validity of the presented hypotheses were verified for the Czech Republic, Bulgaria, Poland, Estonia and Romania.

2.3 Methods

To test validity of the hypotheses in relation to the defined objective of this article, first, it will be necessary to test the normality of the data for each variable.

One of the tests to verify the normality of data is the Kolmogorov-Smirnov test (K-S test):

$$D_n = \sup\left|F_n(x) - F(x)\right|, \tag{1}$$

where:

F_n - the empirical distribution function for n independent and identically distributed ordered observations Xi,

$\sup_x$ - supremum of the set of distance.

The zero hypothesis assumes that the tested data series correspond to the selected theoretical distribution, i.e. the normal distribution. A zero hypothesis is rejected if the critical boundary (D_{max}) of criterion D_n is exceeded. As a rule, zero hypothesis is rejected if the P-value < 0.05. Therefore, if the P-value < 0.05, it is unlikely that the data series follows the normal distribution.

After verifying the normality of the tested data and after the acceptance of zero hypothesis using the Kolmogorova-Smirnov test, the strength of the correlation of the monitored variable using the Pearson correlation coefficient was examined:

$$r = \frac{\sum(X - \bar{X})(Y - \bar{Y})}{\sqrt{\sum(X - \bar{X})^2 \sum(Y - \bar{Y})^2}}, \tag{2}$$

where:

$\bar{X}$ Mean of X variable,

$\bar{Y}$ Mean of Y variable.

The final determination of significance of correlation was established based on calculation of the P-value with significance level at 5%.

3 Results

Based on the methodology described above, the content of this section of the article is focused on presentation of results of the hypotheses validity testing, followed by the detailed examination of the monitored variables correlation.

3.1 Czech Republic

The Kolmogorov-Smirnov test was used to assess whether the monitored data series from Table 1 have the normal distribution. The test results for the Data Series of the Czech Republic are shown in Table 2.

Tests reveal that all the data series have a normal distribution. Table 3 shows the results of the Pearson correlation coefficient, resulting in a strong correlation

Table 1 *The Czech Republic - data series, [1, 4, 22]*

year	2013	2014	2015	2016	2017
GDP per capita in PPS (per person in EUR)	22400	23800	25300	25600	26900
e-commerce B2C turnover (EUR bn)	2210	2600	3150	3800	4470
transported express shipments	480077	488636	529281	563239	635237

Table 2 *Czech Republic - Kolmogorov-Smirnov test for data*

data series	D_n	p-value	D_{max}	test result
GDP per capita in PPS (per person in EUR)	0.2133	0.90999	0.565	H0 accepted
e-commerce B2C turnover (EUR bn)	0.1613	0.98133	0.565	H0 accepted
transported express shipments	0.3191	0.16461	0.565	H0 accepted

Table 3 *Czech Republic - Pearson correlation coefficient*

data series	Pearson's r	p-value	95% interval	test result
GDP per capita in PPS and e-commerce B2C turnover	0.9659	0.0075	0.5656 to 0.9978	HA_1 accepted
GDP per capita in PPS and express shipments	0.9311	0.0215	0.2736 to 0.9956	HA_2 accepted

between the GDP per capita in PPS and E-commerce B2C turnover, as well as between GDP per capita in PPS and the number of express shipments transported.

Bulgaria and Poland show the same results, which can be seen in the following sections of the article.

3.2 Bulgaria

The Kolmogorov-Smirnov test was used to assess whether the monitored data series from Table 4 had a normal distribution. The test results for Bulgaria's data series are shown in Table 5.

Testing shows that all the data series have a normal distribution. Table 6 shows the results of the Pearson correlation coefficient, revealing the strong dependence between the GDP per capita in PPS and E-commerce B2C turnover, as well as between the GDP per capita in PPS and the number of express shipments transported.

3.3 Poland

The Kolmogorov-Smirnov test was used to assess whether the monitored data series from Table 7 had a normal distribution. The test results for Poland's data series are shown in Table 8.

Testing shows that all the data series have normal distribution. Table 9 shows the results of the Pearson correlation coefficient, resulting in a strong dependence between the GDP per capita in PPS and E-commerce B2C turnover, as well as between the GDP per capita in PPS and the number of express shipments transported.

3.4 Estonia

The Kolmogorov-Smirnov test was used to assess whether the monitored data series from Table 10 have

Table 4 *Bulgaria - data series, [1, 4, 22]*

year	2013	2014	2015	2016	2017
GDP per capita in PPS (per person in EUR)	12 200	12 900	13 700	14 200	14 800
e-commerce B2C turnover (EUR bn)	199.43	250	330	419.4	488.6
transported express shipments	1002409	1109686	1236146	1318089	1289516

Table 5 *Bulgaria - Kolmogorov-Smirnov test*

data series	D_n	p-value	D_{max}	test result
GDP per capita in PPS (per person in EUR)	0.154	0.99622	0.565	H0 accepted
e-commerce B2C turnover (EUR bn)	0.1695	0.7887	0.565	H0 accepted
transported express shipments	0.233	0.16191	0.565	H0 accepted

Table 6 *Bulgaria - Pearson correlation coefficient*

data series	Pearson's r	p-value	95% interval	test result
GDP per capita in PPS and e-commerce B2C turnover	0.9896	0.0013	0.8459 to 0.9993	HA_1 accepted
GDP per capita in PPS and express shipments	0.9526	0.0123	0.4404 to 0.9970	HA_2 accepted

Table 7 *Data series in Poland, [1, 4, 22]*

year	2013	2014	2015	2016	2017
GDP per capita in PPS (per person in EUR)	17900	18600	19900	19900	20900
e-commerce B2C turnover (EUR bn)	1930	3450	4960	6280	8380
transported express shipments	136396000	194464000	214159000	264070000	307751000

Table 8 *Poland - Kolmogorov-Smirnov test*

data series	D_n	p-value	D_{max}	test result
GDP per capita in PPS (per person in EUR)	0.2509	0.78607	0.565	H0 accepted
e-commerce B2C turnover (EUR bn)	0.1328	0.99781	0.565	H0 accepted
transported express shipments	0.1557	0.2197	0.565	H0 accepted

Table 9 *Poland - Pearson correlation coefficient*

data series	Pearson's r	p-value	95% interval	test result
GDP per capita in PPS and e-commerce B2C turnover	0.9742	0.0049	0.6544 to 0.9984	HA_1 accepted
GDP per capita in PPS and express shipments	0.949	0.0137	0.4100 to 0.9967	HA_2 accepted

normal distribution. The test results of data series collected in Estonia are shown in Table 11.

Testing shows that all the data series have a normal distribution. Table 12 shows the Pearson correlation coefficients, revealing strong dependence between the GDP per capita in PPS and E-commerce B2C turnover, but the dependence between the GDP per capita in PPS and the number of express shipments transported is refuted. The Pearson coefficient even reaches negative values.

3.5 Romania

The Kolmogorov-Smirnov test was used to assess whether the monitored data series from Table 13 have normal distribution. The test results for the Romania data series are shown in Table 14.

Testing shows that all the data series have normal distribution. Table 15 shows the Pearson correlation coefficients, revealing strong dependence between the GDP per capita in PPS and E-commerce B2C turnover,

Table 10 *Estonia - Data series, [1, 4, 22]*

year	2013	2014	2015	2016	2017
GDP per capita in PPS (per person in EUR)	20200	21300	22000	22500	23600
e-commerce B2C turnover (EUR bn)	101	119	159	175	204
transported express shipments	1341503	909900	910000	1079846	1228902

Table 11 *Estonia - Kolmogorov-Smirnov test*

data series	D_n	p-value	D_{max}	test result
GDP per capita in PPS (per person in EUR)	0.125	0.99982	0.565	H0 accepted
e-commerce B2C turnover (EUR bn)	0.1826	0.94702	0.565	H0 accepted
transported express shipments	0.2311	0.45197	0.565	H0 accepted

Table 12 *Pearson correlation coefficient for Estonia*

data series	Pearson's r	p-value	95% interval	test result
GDP per capita in PPS and e-commerce B2C turnover	0.9833	0.0026	0.7624 to 0.9989	HA_1 accepted
GDP per capita in PPS and express shipments	-0.1101	0.8601	-0.9046 to 0.8553	$H0_2$ accepted

Table 13 *Romania - Data series, [1, 4, 22]*

year	2013	2014	2015	2016	2017
GDP per capita in PPS (per person in EUR)	14500	15200	16300	17400	18800
e-commerce B2C turnover (EUR bn)	1040	1200	1490	2050	2800
transported express shipments	4211266	3472404	3515399	38746320	4489918

Table 14 *Romania - Kolmogorov- Smirnov test*

data series	D_n	p-value	D_{max}	test result
GDP per capita in PPS (per person in EUR)	0.2918	0.8544	0.565	H0 accepted
e-commerce B2C turnover (EUR bn)	0.1859	0.9689	0.565	H0 accepted
transported express shipments	0.2568	0.5375	0.565	H0 accepted

Table 15 *Romania - Pearson correlation coefficient*

data series	Pearson's r	p-value	95% interval	test result
GDP per capita in PPS and e-commerce B2C turnover	0.9854	0.0021	0.7892 to 0.9991	HA_1 accepted
GDP per capita in PPS and express shipments	0.4454	0.4522	-0.7198 to 0.9532	$H0_2$ accepted

Table 16 *GDP per capita in PPS 2018, 2019, [1]*

GDP	Bulgaria	Czech Republic	Estonia	Romania	Poland
2018	15 500	27 900	24 700	19 800	21 400
2019	16 500	28 900	26 100	21 700	22 700

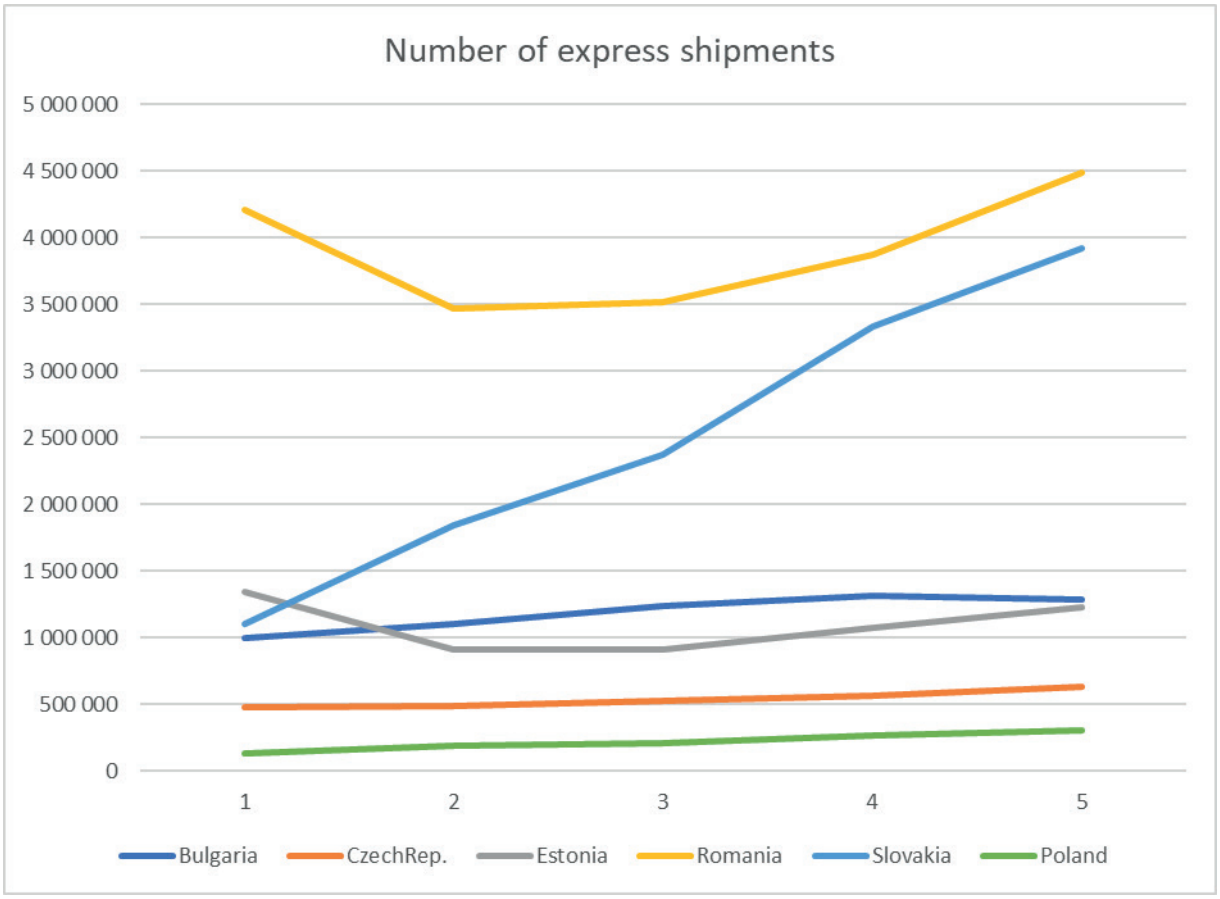


Figure 1 *Number of express shipments [23]*

but rejects the dependence between the GDP per capita in PPS and the number of express shipments transported.

4 Discussion and conclusion

The analysis of dependence between the GDP per capita in PPS and B2C e-commerce turnover, respectively between the GDP per capita in PPS and the number of express shipments transported, was established through the value of the correlation coefficient, respectively, the Pearson coefficient of serial correlation was used. Prior to the correlation analysis itself, the Kolmogorov-Smirnov data normality test was performed, which confirmed that the examined statistical selection had a normal probability distribution. Therefore, the Pearson coefficient of serial correlation could be used to determine the link between data series. The resulting values of the Pearson coefficient of serial correlation, verified by the significance testing, imply the existence of a strong dependence between all the variables for the Czech Republic, Bulgaria and Poland.

Dependency was not confirmed only between the GDP per capita in PPS and the number of express mail shipped in Estonia and Romania. This may be because, as can be seen in Figure 1, the data series of express shipments has an increasing trend for Estonia and Romania, same as other countries included in the studies, except for the year 2013. As the postal market was to be fully liberalized from 2013 on and this period marked a difficult transition for many countries, it is possible that the responsible authorities in Estonia and Romania did not proceed the same way as other countries when reporting the number of express mail transported, even though Estonia fully opened its market in 2009 [5]. The data series of express shipments was also obtained for Slovakia. Figure number 1 shows that Slovakia achieves higher value of number of express shipments than countries of similar size. However, the data series of E-commerce B2C turnover was not obtained for Slovakia, due to this fact Slovakia could not be included in the final group of analyzed countries.

A certain limit to this article is the unavailability of the data needed for other European countries, which is due to the inconsistent practice of European states in obtaining data based on which the comprehensive studies mapping the issue across the continent of Europe are carried out.

Based on the results presented in this article, it can be concluded that majority of tested hypotheses confirmed the impact of the GDP per capita in PPS on development of the B2C e-commerce turnover indicator during the considered time period as well as the impact of the GDP per capita in PPS on the number of express shipments transported during the same time period. Based on this fact, it is possible to ascertain that through the monitoring of the macroeconomic indicator GDP per capita in PPS, the prediction of the development of B2C e-commerce and the number of express shipments transported can be carried out.

Table 16 shows the GDP per capita in PPS in the group of analyzed countries in 2018 and 2019. In all the analyzed countries, there is a year-on-year increase in the value of the GDP per PPS in 2018 and 2019. Based on this fact and with reference to results of this article, it is possible to predict the growth of E-commerce B2C turnover in 2018 and 2019 as well.

The conclusions of the article opened space for further research to seek why the validity of the two sub-hypotheses had not been confirmed in Estonia and Romania.

Acknowledgements

The article was supported by student grant - SGS_2020_010.

References

[1] Purchasing power adjusted GDP per capita - Eurostat [online] [accessed 2019-12-15]. 2019 Available from: https://ec.europa.eu/eurostat/databrowser/view/sdg_10_10/default/table?lang=en

[2] Building act - Czech Republic [online] [accessed 2019-12-10]. 2006. Available from: https://businesscenter.podnikatel.cz/pravo/zakony/stavebni/#par2

[3] MOAGAR-POLADIAN, S., DUMITRESCU, G., TANASE, I. A. Retail e-commerce (e-tail) - evolution, characteristics and perspectives in China, the USA and Europe. *Global Economic Observer*. 2017, **5**(1), p. 167-178. ISSN 2343-9750.

[4] European ecommerce report - Ecommerce Foundation [online] [accessed 2019-12-13]. 2019. Available from: https://www.ecommercefoundation.org/shop/product/european-ecommerce-report-2019-176

[5] EU postal legislation, implementation and enforcement - European Commission [online] [accessed 2019-02-19]. 2012. Available from: https://ec.europa.eu/growth/sectors/postal-services/legislation_en

[6] MORGANTI, E., SEIDEL, S., BLANQUART, C., DABLANC, L., LENZ, B. The impact of e-commerce on final deliveries: alternative parcel delivery services in France and Germany. *Transportation Research Procedia* [online]. 2014, **4**, p. 178-190. ISSN 2352-1465. Available from: https://doi.org/10.1016/j.trpro.2014.11.014

[7] SOVIAR, J., VODAK, J. Value network as part of new trends in communication. *Communications - Scientific Letters of the University of Zilina* [online]. 2012, **14**(2), p. 70-75. ISSN 1335-4205, eISNN 2585-7878. Available from: http://komunikacie.uniza.sk/index.php/communications/article/view/749

[8] GAVAERS, R., VAN DE VOORDE, E., VANELSLANDER, T. Characteristics and typology of lastmile logistics from an innovation perspective in an urban context. In: *City distribution and urban freight transport: multiple perspectives*. MACHARIS, C., MELO, S. (eds.). Camberley Surrey: Edward Elgar Publishing Ltd., 2011. ISBN 978-085793274-7, p. 56-71.

[9] MICHALOWSKA, M., KOTYLAK, S., DANIELAK, W. Forming relationships on the e-commerce market as a basis to build loyalty and create value for the customer. Empirical findings. *Management - Poland* [online]. 2015, **19**(1), p. 57-72. ISSN 1429-9321. Available from: https://doi.org/10.1515/manment-2015-0005

[10] HOWELLS, J. Services and innovation and service innovation: new theoretical directions. *The handbook of innovation and services: a multi-disciplinary perspective*. Camberley Surrey: Edward Elgar Publishing Ltd., 2010. ISBN 978-184720504-9, p. 68-83.

[11] MADLENAKOVA, L., MADLENAK, R., DROZDZIEL, P., KURTEV, I. Layers and processes in the model of technological postal system. *Transport and Telecommunication* [online]. 2015, **16**(4), p. 353-360. ISNN 1407-6179. Available from: https://doi.org/10.1515/ttj-2015-0032

[12] BINCZAK, T., KACZMAREK, F., RYBACKI, J. Determinants of e-commerce turnover in Europe: consumer protection matters. *Gospodarka Narodowa*. 2018, **3**, p. 125-141, ISSN 0867-0005.

[13] BACH, M. P., DUMICIC, K., ZMUK, B., BARTOLIC, A., ZOROJA, J. Use of hierarchical clusters analysis in identification of obstacles to introduction of e-commerce in European countries. In: 42nd International Convention on Information and Communication Technology, Electronics and Microelectronics Mipro: proceedings. 2019. ISSN 1847-3946, p. 1535-1340.

[14] ZATONATSKA, T. Models for analysis of impact of the e-commerce on indicators of economic development of Ukraine, Poland and Austria. *Marketing and Management of Innovations* [online]. 2018, **2**, p. 44-53. ISSN 2218-4511, eISSN 2227-6718. Available from: http://doi.org/10.21272/mmi.2018.2-04

[15] CHEN, D.-N., JENG, B., LEE, W.-P., CHUANG, CH.-H. An agent-based model for consumer-to-business electronic commerce. *Expert Systems with Applications* [online]. 2008, **34**(1), p. 469-481. ISSN 0148-2963. Available from: https://doi.org/10.1016/j.eswa.2006.09.020

[16] SONG, L., MAO, B., WU, Z. Investigation of home delivery models and logistics services in China. *Transportation Research Record: Journal of the Transportation Research Board* [online]. 2019, **2673**(9), p. 11-22. ISNN 0361-1981. Available from: https://doi.org/10.1177/0361198119844453

[17] CHENG, G., GUO, D., SHI, J., QIN, Y. Planning city-wide package distribution using crowdsourced public transportation systems. *IEEE Access*. 2019, **7**, p. 1234-1246. ISSN 2169-3536.

[18] OZTURK, O., PATRICK, J. An optimization model for freight transport using urban rail transit. *European Journal of Operational Research* [online]. 2018, **267**(3), p. 1110-1121. ISNN 0377-2217. Available from: https://doi.org/10.1016/j.ejor.2017.12.010

[19] SAVELSBERGH, M., VAN WOENSEL, T. City logistics: challenges and opportunities. *Transportation Science* [online]. 2016, **50**(2), p. 579-590. ISNN 0041-1655. Available from: https://doi.org/10.1287/trsc.2016.0675

[20] ULMER, M. W., THOMAS, B. W., MATTFELD, D. C. Preemptive depot returns for dynamic same-dayday delivery. *EURO Journal on Transportation and Logistics* [online]. 2019, **8**(4), p. 327-361. ISNN 2192-4376. Available from: https://doi.org/10.1007/s13676-018-0124-0

[21] The liberalisation of European postal markets and the impact on employment and working conditions - Forba [online] [accessed 2020-04-31]. 2013. Available from: https://postkom.no/wp-content/uploads/2017/01/Postdirektivet-Utredning-FORBA-2013.pdf

[22] EU Directive 2008/6/EC of the European Parliament and of the Council [online] [accessed 2020-04-31]. 2008. Available from: https://eur-lex.europa.eu/legal-content/cs/TXT/?uri=CELEX%3A32008L0006

[23] Global or regional estimates - Universal Postal Union [online] [accessed 2019-12-13]. 2019. Available from: http://pls.upu.int/pls/ap/ssp_report.main?p_language=AN&p_choice=BROWSE

EVALUATION OF IMPACT OF THE OPERATIONAL AND TECHNICAL FACTORS ON DOWNTIME OF MUNICIPAL BUSES BASED ON A LINEAR REGRESSION MODEL

Joanna Rymarz[1,*], Anna Borucka[2], Andrzej Niewczas[3]

[1]Faculty of Mechanical Engineering, Lublin University of Technology, Lublin, Poland
[2]Faculty of Logistics and Management Security, Military University of Technology, Warsaw, Poland
[3]Motor Transport Institute, Warsaw, Poland

*E-mail of corresponding author: j.rymarz@pollub.pl

Resume
The objective of this study was to assess the effect of selected operational and technical factors on downtime of vehicles. The sample consisted of buses from a municipal transport company (Poland). Estimation of parameters of a linear regression model was performed. Month of failure (downtime event) and its type were used as predictors. Failures were divided into three categories: events related to the company's operations, including vehicle failures (1) and other (organizational) problems (2), as well as failures caused by external factors unrelated to the operations of the transport company (3). The downtime was found to be significantly associated with failure type and month of failure. A linear regression model of downtime with a reduced number of impact factors, taking into account two main failure types and two main periods of their occurrence during the year, was developed.

Article info
Received 18 September 2020
Accepted 16 March 2021
Online 16 September 2021

Keywords:
municipal buses,
downtime,
linear regression,
failure

Available online: https://doi.org/10.26552/com.C.2021.4.A241-A247

ISSN 1335-4205 (print version)
ISSN 2585-7878 (online version)

This is an open access article distributed under the terms of the Creative Commons Attribution 4.0 International License (CC BY 4.0), which permits use, distribution, and reproduction in any medium, provided the original publication is properly cited. No use, distribution or reproduction is permitted which does not comply with these terms.

1 Introduction

In public transport systems, vehicle failures and organizational shortcomings often substantially increase passenger waiting time. In this paper, disablement of a vehicle caused by technical or operational factors has been referred to with the umbrella term "failure". Vehicle failures are of concern to both drivers and fleet managers. In public transport systems, randomness of bus departure times and travel times has an influence on the quality of transport services [1]. In a situation when compliance with the timetable is the major requirement, the real travel time in the whole transport system is adjusted to a vehicle with the lowest operational speed. In the literature, this phenomenon is known as "bunching". Bunching forces passengers to arrive early at stations and to budget long travel time [2-5].

The literature describes several corrective strategies to reduce bus bunching. Hickman has proposed a stochastic model of vehicle operations based on recursive equations for expected values of headways and bus loads [6]. His strategy of improving transport services consists in holding operating buses along the service line, in order to regulate the system on an ongoing basis.

Daganzo and other authors have developed a mixed strategy in which passenger boarding and alighting can be limited to improve the regularity of headways [8-10]. Berrebi et. al. have studied the practical effects of implementation of these corrective strategies. They demonstrated that the "bus holding" system reduced bunching, thus also decreasing average passenger waiting time [2]. Adamski and Turnau have presented a transport system control strategy in which buses were sent at specific times to critical bus stops with high numbers of passengers [11]. However, it is worth mentioning that the "bus holding" method also had negative effects, such as disturbances in traffic flow and an increase in average waiting time [1, 12-18].

An important component of the "bus holding" strategy is prediction of fleet availability. One prediction method involves simulation of readiness based on a regression model developed with use of the retrospective data.

In this paper, a linear regression model is proposed, which links the bus downtime (not-ready time) with the month of the year in which a bus was stationary and type of downtime. A regression analysis of downtime was performed based on data obtained from the municipal transport company in Lublin, Poland. The main objective was to develop a regression model with a reduced number of factors, which could be used to effectively predict bus downtime and ensure continuity of system operation.

Table 1 *Descriptive statistics of the investigated buses*

vehicle make	indicator				
	vehicle type	number of objects (pcs)	average mileage per 1 vehicle M (km)	median mileage per 1 vehicle M_e (km)	standard deviation S_d (km)
1	single-decker	53	6041	6473	1699
2	single-decker	20	4414	5511	2671
3	articulated bus	27	4495	4519	926
4	articulated bus	28	4313	4972	2197
5	single-decker	22	3668	3523	1171
6	articulated bus	10	5966	6226	1448
7	single-decker	20	5062	5301	1507
8	articulated bus	30	5500	5593	873
9	single-decker	18	5014	5774	2504

2 Material and methods

Twenty one buses (8 different makes and models) were studied. The vehicles were between 10 and 16 years old. Observations were conducted in standard public transport conditions over 2 years of operation (2018-2019). The dates and times of bus arrival to and departure from the depot and the vehicle downtime were registered. Source documentation included the company's daily internal reports on the operational status of the fleet. The basic descriptive statistics of the buses are presented in Table 1.

The buses serviced standard routes in municipal traffic. The average monthly mileage was approximately 4637 km. The lowest average monthly mileage of 4313 km was recorded for a bus make 5 (Standard Deviation-SD 1711 km) and the highest mileage of 6041 km for a bus make 2 (SD 1699 km).

Fleet downtime data for the years 2018-2019 were analysed. The impact of two factors, month of failure and failure type, on the dependent variable (downtime) was considered.

Month of failure was analysed repeatedly in each year of observation and was thus an indicator of seasonality related to seasonal changes in weather and vehicle loads (number of passengers) over the year. In winter, many downtime events were caused by door freezing, failures of driver's cabin and passenger compartment heating and power outages. During the summertime, downtime was mainly due to high temperatures, i.e. engine overheating and lack of air conditioning in the vehicle.

The second factor that has been analysed was the failure type. Three types of most frequent failures (downtime events) were considered. Type A1 were failures related to a vehicle damage (e.g. broken/jammed door lock, fluid leakage, broken brakes, no ignition, engine overheating). Type A2 were organizational failures and other technical problems (e.g. a damaged wind shield, mirror, tyre). Some of these failures were related to weather conditions and some to the general status of the vehicles. Unfortunately, the data were not detailed enough to allow to discriminate which failure was caused by which factor. Type B were failures related to events outside the company's control (e.g. collision with another vehicle, freezing of the pneumatic system, vehicle trapped in the snow, a blocked route, an incident inside the vehicle).

3 Results

Downtime observation results were divided into "monthly" groups. The number of all the failures recorded in 2018-2019, broken down by month, is given in Table 2. Downtime data for the years 2018-2019, also broken down by month, are shown in Table 3. Monthly downtime duration is presented in Table 2. Figure 1 shows a box plot of downtime per month. As seen in the graph, median values of downtime are different for different months. The highest mean values were recorded in January, September, October and November. It is worth stressing that the number of failures is different for each month (Table 3). The largest number of failures occurred in March, however, the mean and median downtime values for this month were the lowest (Table 2), which means that the failures were short-term ones.

Significance of differences in downtime between months was assessed using the non-parametric Kruskal-Wallis test.

The Chi-squared statistic was $\chi^2 = 243.98$ and the p-value $< p < 0.0001$, which indicated that, at the significance level $\alpha = 0.05$, the null hypothesis of equality of means was rejected. This demonstrates that there were significant differences between at least two monthly downtime groups.

Another factor that was analysed was the type of failure. The observed failures were classified as one of the three categories (types), designated here as A1, A2, B. The largest group were type A2 failures, which occurred 1338 times in the whole study period.

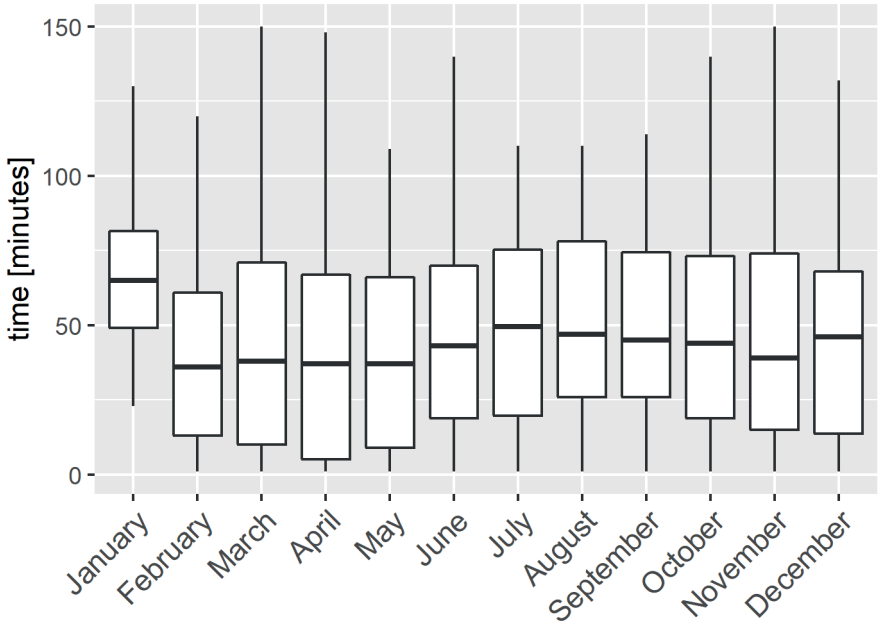


Figure 1 *The box plot of downtime in each month*

Table 2 *Descriptive statistics of bus downtime distribution in each month*

month	median M (minutes)	mean Me (minutes)	standard deviation S_d (minutes)
January	65	95.4	84.8
February	37	45.8	43.2
March	39	47.7	40.7
April	41	48.7	52.4
May	38	43.3	35.3
June	44	49.2	36.9
July	50	51.8	39.5
August	55.5	86.7	95.8
September	65	104	110.
October	62	101	106.
November	61	107	118.
December	48	53.4	51.7

Table 3 *Number of failures in each month in 2018-2019*

month	January	February	March	April	May	June
number of failures	332	339	369	305	227	228
month	July	August	September	October	November	December
number of failures	179	178	255	247	266	195

The number of type A1 failures was similar (1136 events). The lowest number of failures were the B type events (596 events). Descriptive statistics of downtime for each type of failure is presented in Table 4 and a box-plot of downtime versus failure type is shown in Figure 2.

As Figure 2 shows, downtime duration differed significantly depending on the type of failure. The longest downtimes (though the smallest in number) were caused by the B type failures, which were outside the company's control. The shortest stoppages were related to A1 type events associated with repair of subsystems (mechanisms) or scheduled maintenance of vehicles.

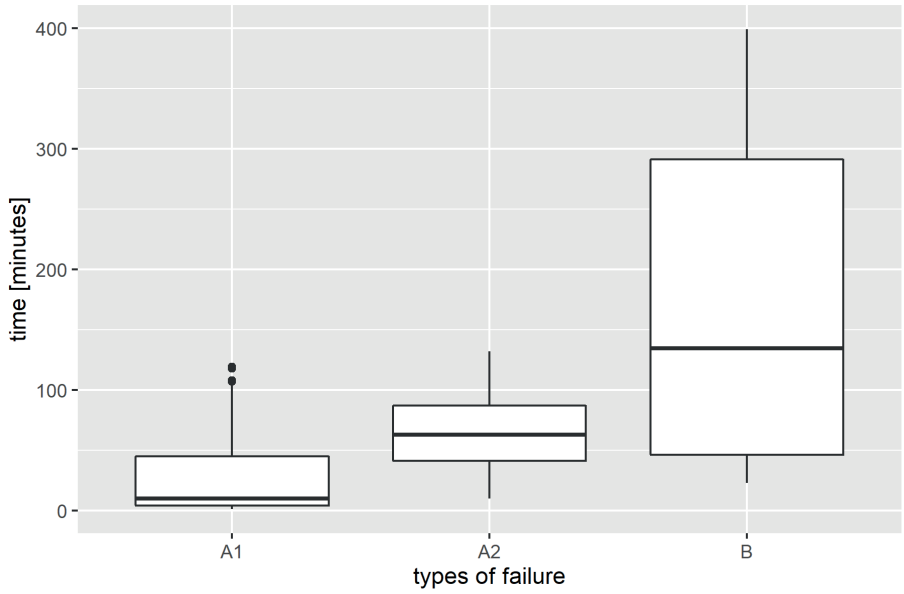


Figure 2 *The box plot of bus downtime versus type of failure*

Table 4 *Descriptive statistics of downtime distribution for different types of failures*

type of failure	median (minutes)	mean (minutes)	standard deviation (minutes)	min. (minutes)	max. (minutes)
A1	10	23.8	26	1	119
A2	63	64.1	27.1	10	132
B	134	167	124.	23	399

4 Linear regression model of downtime

Based on the bus downtime data discussed in Section 3, a multi-regression model describing the relationship of downtime duration with month and type of failure was developed. The general formula for the linear regression model is as follows:

$$y= \beta o+\beta_1 x_1+\beta_2 x_2+...+\beta_k x_k+\varepsilon, \quad (1)$$

where y is dependent variable, β_0 is intercept, x_k are independent variables, β_k are model parameters, ε is random parameter.

The regression coefficient β_k describes by how much the average value of the independent variable y will change if the value of the independent variable x_k changes by a unit, all the other independent variables being constant. The random component in the model reflects an incomplete fit to empirical data.

Due to the fact that the independent variables had a qualitative character and formed closed sets (24 months and 3 types of failures), they had to be recoded as binary variables. Then, each variable took either the value of 1 - when the phenomenon does occur or 0 - when it does not occur. Parameters of the regression function were estimated using the least-squares method after initial elimination of a selected variable in each of the studied category. Variables with extreme average values were selected: type A1 failure and the month of April. In this way, the effect of single-signedness of the remaining parameters with regards to the level of the omitted variable was obtained.

A statistical analysis was conducted to determine the structure of the linear regression model with binary variables, which resulted from the quantitative nature of the dependent variable and the qualitative character of the independent variables. The estimated model parameters are given in Table 5.

Four of the estimated parameters were statistically insignificant. The AIC (Akaike Information Criterion) = 34011 and corrected R^2 = 48 % indicate that the model does not fully explain the observed phenomena. This is also indicated by the residual distribution, which is different from the normal distribution (Lilliefors test statistics D = 0.088 and p-value < 0.001). Additionally, an analysis of the autocorrelation function (Figure 3) demonstrated significant dependencies not described by the model. This means that bus downtime is dependent on factors which have not been included in the model.

The regression equation is given by:

$$y= 18.4+36.1 *A2 + B*137.7 +29.6*January - 216 *February -13.6*March + 3.3*May + 1.8*July -3.8 *June + 23.1*August + 31.6*September + 30.0 *October + 32.1*November + 2.5*December+ \varepsilon. \quad (2)$$

Table 5 *Parameters of the linear regression model and evaluation of their significance*

parameter	estimate βk	std. err or $S(\beta_k)$	t value	p-value
β_0	18.4	3.379	5.432	< 0.001
failure A2	36.1	2.300	15.672	< 0.001
failure B	137.7	2.907	47.390	< 0.001
January	29.6	4.472	6.621	< 0.001
February	-21.6	4.453	-4.850	< 0.001
March	-13.6	4.357	-3.112	0.002
May	3.3	4.933	0.668	0.504
July	1.8	5.338	0.336	0.737
June	-3.8	4.930	-0.761	0.447
August	23.1	5.341	4.320	< 0.001
September	31.6	4.806	6.585	< 0.001
October	30.0	4.843	6.184	< 0.001
November	32.1	4.755	6.759	< 0.001
December	2.5	5.182	0.474	0.636

where Std. Err or $S(\beta_k)$ explains the accuracy of the parameter estimate (β_k). Indicates by how many units the assessment value (estimated) differs from the actual value of parameter β_k.

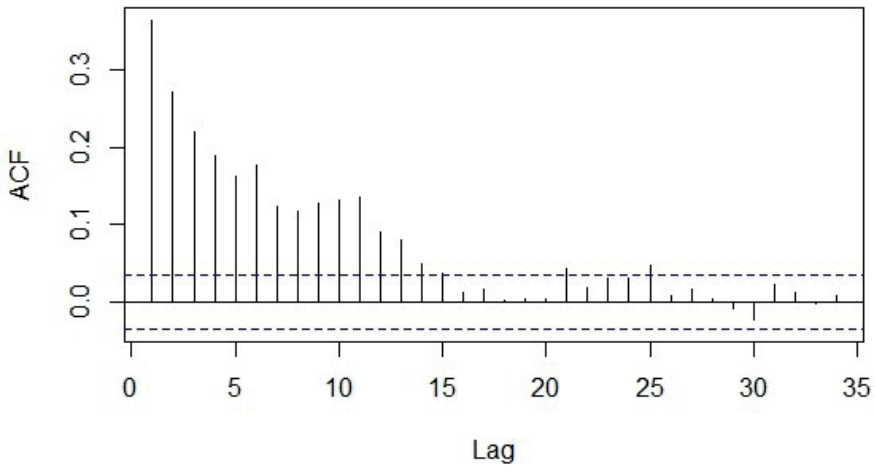


Figure 3 *Autocorrelation function of model residual*

The quality of fit of the regression model was evaluated using *AIC* (Figure 3). The value of *AIC* was found from the following equation:

$$AIC = -2 \ln L + 2k, \tag{3}$$

where k is the number of model parameters and L is the reliability function.

In accordance with the objective of the study, in the next stage of the calculations, the model was simplified. To limit the number of predictors, it was proposed that months with similar regression coefficients should be aggregated. Statistically similar months were grouped with Pairwise Wilcoxon Rank Sum Test, which is a non-parametric test with multi-testing correction\ used to compare pairs in groups. The null hypothesis for Pairwise Wilcoxon Rank Sum Test is that there are no differences between distributions, while the alternative hypothesis is that the differences are statistically significant. The test statistic is given by:

$$W = \sum_{i=1}^{N} [sgn(x_2 - x_1) \times R_i], \tag{4}$$

where *sgn* is the sign function, $R_i = \sum_j^k R_{ij}$, R_{ij} is the rank of observation, x_1, x_2 are study groups, N is sample size (number of study groups). Test results are presented in Table 6.

Based on the results, three groups of months were selected for which the downtime distributions were not significantly different. Additionally, the lack of significance of differences in each group was confirmed using the Kruskal-Wallis test. The first group of months (group I) included August, September, October and November. For this group, the chi-squared statistics $\chi^2 = 1.245$ and p-value = 0.742. The second group (group II) included February, March, April, May, June, July

Table 6 *Pairwise Wilcoxon Rank Sum Test*

	January	February	March	April	May	June	July	August	September	October	November
February	0.000										
March	0.000	0.623									
April	0.000	0.738	0.542								
May	0.000	0.795	0.481	0.990							
June	0.000	0.118	0.386	0.118	0.118						
July	0.000	0.040	0.166	0.046	0.046	0.576					
August	0.000	0.000	0.000	0.000	0.000	0.001	0.022				
September	0.036	0.000	0.000	0.000	0.000	0.000	0.000	0.340			
October	0.009	0.000	0.000	0.000	0.000	0.000	0.001	0.621	0.685		
November	0.004	0.000	0.000	0.000	0.000	0.000	0.004	0.711	0.576	0.991	
December	0.000	0.120	0.376	0.117	0.117	0.910	0.701	0.005	0.000	0.000	0.001

Table 7 *Parameters of the linear regression model*

parameter	estimate	std error	t value	p-value
(intercept)	12	1.815	6.634	< 0.001
failure A2	36.8	2.285	16.104	< 0.001
failure B	135.5	2.900	46.731	< 0.001
group I	36.2	2.297	15.772	< 0.001
group III	36.3	3.387	10.697	< 0.001

and December. For this group χ^2 = 10.878 and p-value = 0.092. The last group consisted of only one month, January, for which no goodness of fit with any other group was observed. The parameters of the estimated model are presented in Table 7.

The final form of the model was the following:

$$y = 12 + 36.8 * A2 + 135.5 * B + 36.2 * grI + 36.3 * gr\ III. \quad (5)$$

All the model parameters were statistically significant. Corrected R^2 = 48% and AIC = 34045.64. The values of the parameters describing the quality of the regression model did not differ significantly from the basic formula given by Equation (2). The reduction of the number of factors, achieved by their aggregation in the manner presented in this paper, did not reduce the quality of the initial regression model.

5 Summary

Based on a study of municipal bus operations, a linear multi-regression model of downtime, as a function of selected groups of months of the year and type of downtime event (failure), was developed.

This model allows to determine the impact of climate seasonality over the year and the effect of organizational and technical factors (type of failure) on bus downtime. The model also permits to predict the availability of a transportation system as part of the strategy of ensuring the continuity of transportation services, e.g. by introducing the «bus holding» control strategy.

From among the three types of downtime events, considered as independent variables, the model includes type B failures (events outside the company's control) as the dominant type and type A2 (operational and organizational) failures (which have four times less impact than type B events). Among the selected month groups, the reduced model presents the summer-autumn season, including August, September, October and November, as well as the winter season, which is represented by a single month - January. The effects of the two seasons on downtime duration are comparable and similar to the impact of A2 type failures.

Acknowledgement

The project/research was financed as part of the Lublin University of Technology's project- Regional Excellence Initiative, funded by the Polish Ministry of Science and Higher Education (contract no. 030/RID/2018/19).

References

[1] SAVSAR, M. Modeling and simulation of maintenance operations at Kuwait public transport company. *Kuwait Journal of Science* [online]. 2013, **40**(2), p. 115-129. ISSN 2307-4108, eISSN 2307-4116. Available from: https://journalskuwait.org/kjs/index.php/KJS/article/view/120

[2] BERREBI, S. J., WATKINS, K. E., LAVAL, J. A. A real-time bus dispatching policy to minimize passenger wait on a high frequency route. *Transportation Research Part B: Methodological* [online]. 2015, **81**(2), p. 377-389. ISSN 0191-2615. Available from: https://doi.org/10.1016/j.trb.2015.05.012

[3] BORUCKA, A, NIEWCZAS, A, HASILOVA, K. Forecasting the readiness of special vehicles using the semi-Markov model. *Eksploatacja i Niezawodnosc - Maintenance and Reliability* [online]. 2019, **21**(4), p. 662-669. ISSN 1507-2711. Available from: http://dx.doi.org/10.17531/ein.2019.4.16

[4] CABAN J., DROZDZIEL, P., KRZYWONOS, L., RYBICKA, I.,SARKAN, B., VRABEL, J. Statistical analyses of selected maintenance parameters of vehicles of road transport companies. *Advances in Science and Technology Research Journal* [online]. 2019, **13**(1), p. 1-13. ISSN 2299-8624. Available from: https://doi.org/10.12913/22998624/92106

[5] CHERNOYAROV, O. V., KUTOYANTS, Y. A., MARCOKOVA, M. On frequency estimation for partially observed system with small noises and observation equations. *Communications - Scientific Letters of the University of Zilina* [online]. 2018, **20**(1), p. 67-72. ISSN 1335-4205, eISSN 2585-7878. Available from: http://komunikacie.uniza.sk/index.php/communications/article/view/48

[6] HICKMAN, M. D. An analytic stochastic model for the transit vehicle holding problem. *Transportation Science* [online]. 2001, **35**(3), p. 215-237. ISSN 0041-1655, eISSN 1526-5447. Available from: https://doi.org/10.1287/trsc.35.3.215.10150

[7] LALANNE, C., MESBAH, M. Measures of association, comparisons of means and proportions for two samples or more. In: *Biostatistics and Computer-based Analysis of Health Data using Stata*. 1. ed. ISTE Press - Elsevier, 2016. ISBN 9781785481420, eISBN 9780081010846, p. 25-57.

[8] DAGANZO, C. F. A headway-based approach to eliminate bus bunching: Systematic analysis and comparisons. *Transportation Research Part B: Methodological* [online]. 2009, **43**, p. 913-921. ISSN 0191-2615. Available from: https://doi.org/10.1016/j.trb.2009.04.002

[9] EDWARD, K., BEATA, K., DARIUSZ, K., DARIUSZ, M. Survival function in the analysis of the factors influencing the reliability of water wells operation. *Water Resources Management* [online]. 2019, **33**(14), p. 4909-4921. ISSN 0920-4741, eISSN 1573-1650. Available from: https://doi.org/10.1007/s11269-019-02419-0

[10] MORALES, D., MUNOZ, J. C., GAZMURI, P. A stochastic model for bus injection in a public transport service. *Transportation Research Procedia* [online]. 2019, 38, p. 688-708. ISSN 2352-1465. Available from: https://doi.org/10.1016/j.trpro.2019.05.036

[11] ADAMSKI, A., TURNAU, A. Simulation support tool for real-time dispatching control in public transport. *Transportation Research Part A: Policy and Practice* [online]. 1998, **32**(2), p. 73-87. ISSN 0965-8564. Available from: https://doi.org/10.1016/S0965-8564(97)00019-0

[12] NIEWCZAS, A. MORAWSKI, L., DEBICKA, E. BORUCKA, A. Commercial vehicles incapacity risk analysis in the transport company. *Journal od KONBiN* [online]. 2019, **49**(4), p. 321-340. ISSN 2083-4608, eISSN 2083-4608. Available from: https://doi.org/10.2478/jok-2019-0089

[13] NIEWCZAS, A., MORAWSKI, L., DEBICKA, E., RYMARZ, J. Predicting costs of city buses' incapacity risk. *Journal of KONBiN* [online]. 2019, **49**(1) p. 425-448. ISSN 2083-4608, eISSN 2083-4608. Available from: https://doi.org/10.2478/jok-2019-0022

[14] NIEWCZAS, A., RYMARZ, J., DEBICKA, E. Stages of operating vehicles with respect to operational efficiency using city buses as an example. *Eksploatacja i Niezawodnosc - Maintenance and Reliability* [online]. 2019, **21**(1), p. 21-27. ISSN 1507-2711. Available from: http://dx.doi.org/10.17531/ein.2019.1.3

[15] RYMARZ, J., NIEWCZAS, A., STOKLOSA, J. Reliability evaluation of the city transport buses under actual conditions. *Transport and Telecommunication Journal* [online]. 2015, **16**(4), p. 259-266. ISSN 1407-6179, eISSN 1407-6179. Available from: https://doi.org/10.1515/ttj-2015-0023

[16] SANCHEZ, S. A. Optimizing performance-based mechanisms in road management: an agency theory approach. *European Journal of Transport and Infrastructure Research* [online]. 2015, **15**(4), p. 465-481. ISSN 1567-7141. Available from: https://doi.org/10.18757/ejtir.2015.15.4.3092

[17] ZAWIERZCHOWSKA, M. Evaluation of the quality of public transport services - selection of variables to be tested by the Delphic method. *Autobusy*. 2018, **19**(5), p. 18-21. ISSN 1509-5878, eISSN 2450-7725.

[18] ZHAO, F., ZENG, X. Optimization of transit route network, vehicle headways and timetables for large-scale transit networks. *European Journal of Operational Research* [online]. 2008, **186**(2), p. 841-855. ISSN 0377-2217. Available from: https://doi.org/10.1016/j.ejor.2007.02.005

DELIVERY TIMES AND DELAY IN DELIVERY OF CONSIGNMENT UNDER THE CONDITIONS OF INTERNATIONAL CARRIAGE

Jarmila Sosedová*, Zuzana Otáhalová, Andrej Dávid, Andrea Galieriková

Faculty of Operation and Economics of Transport and Communications, University of Zilina, Slovak Republic

*E-mail of corresponding author: jarmila.sosedova@fpedas.uniza.sk

Resume

Delivery time means a certain period in which the carrier is obliged to transport the consignment from one place to another. The delay occurs when the carrier does not deliver the consignment to the consignee within this period. The authors analyse individual legislative documents regulating the transport - legal conditions of international transport. In addition, they present the reasons for the delay in delivery of the consignment and point to the carrier's liability for non-fulfilment of the obligation to transport the consignment within the delivery period. By comparing the results, authors state that there is a diversity of regulations in the field of international transport, especially in the context of the multimodality development. Such a diversity in regulations causes inconsistencies in the transport market and therefore there is a need to harmonize unimodal transport systems.

Article info

Received 21 January 2021
Accepted 19 March 2021
Online 16 September 2021

Keywords:

delivery time,
carrier,
carriage of goods

Available online: https://doi.org/10.26552/com.C.2021.4.A248-A255

ISSN 1335-4205 (print version)
ISSN 2585-7878 (online version)

This is an open access article distributed under the terms of the Creative Commons Attribution 4.0 International License (CC BY 4.0), which permits use, distribution, and reproduction in any medium, provided the original publication is properly cited. No use, distribution or reproduction is permitted which does not comply with these terms.

1 Introduction

A delay in delivery of a consignment is related to a question of a delivery time. The delivery time means a certain time segment when a carrier is obliged to conduct a carriage and its related operations, i.e. to carry a consignment from one certain place (of shipment) to another certain place (of delivery, or destination). A time lag/delay happens when the carrier does not deliver the consignment to its recipient within this time segment, provided there are no obstacles to the delivery, which would release the carrier from liability for failure to meet the commitment to carry the consignment within the delivery time.

The reasons for a delay in delivery of the consignment may be both factual and legal. The factual reasons for a delay in delivery may lie in the impossibility to load or unload the consignment due to unsound technological transhipment equipment, a destruction of the consignment due to a breakdown, a theft of the consignment, a fire of a transport means, a freight explosion, etc.

The legal obstacles to a proper delivery of the consignment and a fulfilment of the contract of carriage mainly include a ban on export and import, or transit of the carried freight through a certain territory, a stoppage of carriage due to incomplete transport documentation, an infringement of provisions for the consignment carriage (mainly in the case of dangerous cargo carriage), a seizure of the freight by public authorities or an enforcement of a lien by the carrier, or another legal action of a third party towards the consignment (e.g. an execution based on a final judicial ruling towards the consignor or consignee of the consignment).

The following parts of the paper will deal with issues of a delay in delivery of a consignment and claims resulting from delay in delivery or non-observing the delivery time in individual (unimodal) transport systems [1].

2 Delivery time in international carriage of goods

Complaints about delays in the delivery of goods are one of the most common disputes in international transport between the consignor and the consignee. In order to be able to take adequate measures, both parties must be aware of their rights and obligations arising from the transport process [2].

The international carriage of goods by sea [3-6] is governed by various conventions such as the International Convention for the Unification of Certain Rules of Law Relating to Bills of Lading (Hague Rules) [7], Protocol to Amend the International Convention for the Unification of Certain Rules Relating to Bills of Lading 1924, (Hague - Visby Rules) 1968, 1979; [8] United Nations Convention on the Carriage of Goods by Sea, 1978 (Hamburg Rules) [9], United Nations Convention on Contracts for the International Carriage of Goods

(Wholly or Partly) by Sea, 2008 (Rotterdam Rules) [10]. Those rules established the minimum obligations, maximum immunities and the limit of carrier's liability and aims at creating one uniform law concerning the international carriage of goods by sea. Nevertheless, none of those attempts has been successful, instead, the present legal framework consists of a disordered array of international conventions designed to regulate the carriage of goods by sea, diverse regional/sub-regional agreements, national laws and standard term contracts. As a consequence, both the applied liability rules and the degree and extent of carrier's liability vary greatly from case to case and are unpredictable. Modern transport patterns and practices have been considerably affected by the growth of containerized transportation together with technological developments on the multimodal transferring systems [11-15]. In 1996, considering the absence of an updated maritime transport regime, the United Nations Commission on International Trade Law (UNCITRAL) proposed to include a review of modern practices and applicable law regimes in the international carriage of goods by sea in its work program with a view of establishing the need for uniform rules where such rules were lacking, so as to achieve greater uniformity of laws [16]. Accordingly, it assigned to the Secretariat the task of collecting information, ideas and opinions Reviews and analysis of the rules, instructions, conventions, etc. from governments and international organizations representing commercial sectors involved in the carriage of goods by sea. Increasingly, big liner shipping companies, some of which dominate the container shipments of ocean trade, are also expanding their services to offer transportation from door-to-door by involving other carriers to perform different modal stages of a multimodal transaction [14, 17-19]. The current liability framework reflects few developments that have taken place in terms of transport patterns, technology and markets. The international uniform regime has not been in force to govern liability for loss, damage or delay arising from multimodal transport.

2.1 Delivery time under the commercial code

Under the Contract of Carriage of Goods, pursuant to Article 610 of the Commercial Code - Act No. 513/1991 Coll. (the Commercial Code), a carrier is committed to a consignor to carry a package (a consignment) from a certain place (of shipment) to another certain place (of destination) and the consignor is committed to pay them a remuneration (a freightage) for this service. Under Article 617, the carrier is obliged to perform the carriage to the place of destination with diligent care within the agreed time, in other words without undue delay. Thus, if the time was not negotiated it is impossible for the carrier to store the freight into a warehouse and to start the carriage with a significant delay. For such a case the Commercial Code expressly defines that, when in doubts, the time starts to pass as of the day following the day when the consignment was accepted by the carrier. The amendment of the Commercial Code in Article 624 specifies that in the case of loss or damage of the consignment, the carrier is obliged to compensate the price of the consignment valid in time it was passed to them. In the case of damage or impairment of the consignment, the carrier is required to reimburse the difference between the price, which the consignment had at the moment of its acceptance by the carrier and the price, which the damaged or impaired consignment would have had at that time. The carrier is entitled to get the negotiated remuneration, or if not-negotiated the remuneration standard in time when the contract was concluded, considering the content of the carrier's commitment. The carrier becomes entitled to the freightage after the carriage to the place of destination is performed, if the contract does not determine another time as decisive. If the carrier cannot complete the carriage, due to facts they are not liable for, they are entitled to get an aliquot amount of the freightage, taking into account the carriage already performed. The legislation, however, does not mention any sanctions or a scope of claims of the consignor in the case of a delay in delivery.

The indemnification due to delay in delivery of the consignment would apply to damages of the consignment itself, as well as to damages directly related to the breach of commitments, accruing from the contract of carriage (Article 373 et seq. of the Commercial Code on the indemnification and breach of obligations resulting from a contractual relationship). In such a case, the burden of proof would lie on a plaintiff and a defendant - carrier would be entitled to invoke all the circumstances related to waiving their liability. The indemnification would include the actual damage, as well as loss of profit.

Under Article 629 of the Commercial Code, the implementing rules may differently regulate railway, air, road, inland water and sea transport, in terms of the origin of the contract, transport documents, exclusion of a package from carriage, acceptance of the consignment by the carrier and its dispatch to the consignee, scope of claims for the carrier and their fulfilment. This regulation, however, must not reduce the liability of the carrier in the case of the consignment damage.

2.2 Delivery time in international carriage by road under the CMR

The CMR (Convention Marchandise Routiere) - Convention on the Contract for the International Carriage of Goods by Road [20], in its Article 19 defines the delivery time as a time negotiated by parties; if it is not negotiated, then it is the time, which can be expected from a diligent carrier. In the case of a delay in delivery of the consignment there, of course, exists a consignor's/consignee's claim to get the indemnification occasioned

on the consignment itself, which was established in compliance with provisions of Article 23 of the CMR. In the case of exceeding the delivery time the eligible party also has a claim to the indemnification but only up to the amount of the freightage and provided that the eligible party proves the damage due to exceeding the delivery time and makes a claim within 21 days since the consignment dispatch. If exceeding the delivery time (e.g. of engineering components carriage) does not result in any damage (e.g. due to a sufficient stock capacity of carried goods at the consignee's site) and there happens no consignment damage, the eligible party will not be allowed to claim to compensation. The indemnification may consist of direct reimbursements, e.g. as a result of a production outage and indirect ones, provided they are provable and have a causal relationship with delay in delivery of the consignment. Those claims may refer to the reimbursement of a contractual penalty for the sub-customer, subsequent paid duty, loss of profit, claim due to price decrease or loss of market value of the consignment.

The consignor may claim a higher compensation, in compliance with Article 26 of the CMR, only if they together with the carrier negotiate the so-called particular interest in delivery of the consignment in the case of exceeding the delivery time and if the consignor pays a negotiated surcharge. In such a case the eligible party may claim to the indemnification due to delay in delivery of the consignment up to the amount quoted in the consignment note. These reimbursed damages will also include a purchase of destroyed or lost goods, loss of business, taxes and charges related to the freight and carriage, etc.

If a delay in delivery of the consignment arises due to an intentional act or negligence of the carrier equivalent to the intent, there will not be applied the maximum limit for the indemnification in the amount of the freight, but the carrier will be obliged to reimburse the incurred loss to the full extent. These consequences may mean a bankruptcy for the carrier since the damages caused intentionally or in gross negligence are not covered by insurance [21].

2.3 Delivery time in international carriage by rail under the COTIF/CIM

The COTIF (Convention relative aux transports internation aux ferroviaires) - Convention Concerning International Carriage by Rail [22], in its Appendix CIM related to international carriage of goods by rail, in Article 16, determines the delivery times for wagon and individual packages, although it takes the agreement between the consignor and the carrier as the basis for the delivery time determination. Under Article 23 of the CIM the carrier is liable for damage caused with exceeding the delivery time and they are waived this liability if the delivery time exceeding was caused by an eligible party, by order of an eligible party, due hidden defects of goods or circumstances, which could not have been avoided and whose consequences could not have been averted by the carrier. Article 23 Paragraph 3 also quotes situations when the carrier is waived the liability (carriage in open wagons, missing or faulty wrapping, natural ability of the goods to lose its properties, etc.).

To determine the extent of indemnities, the provision of Article 33 of the CIM is decisive - if the damage happens due to exceeding the delivery time, the carrier is obliged to pay the compensation, which represents no more than the four times the freightage. If the freight is completely lost, there is no compensation up to the four times of the freightage concurrently payable with the indemnity for loss of the consignment. In the case of partial loss of the freight, the indemnity reaches maximum four times of the freightage in proportion to the lost part of the consignment. In the case of the freight damage, which is not a consequence of exceeding the delivery time the indemnity is provided in parallel with the indemnity for the consignment damage. At the same time, however, Article 33 Paragraph 5 of the CIM establishes that the indemnity for exceeding the delivery time along with the indemnity for loss or damage of the consignment must not in any case be higher than the indemnity in the case of total loss of the freight.

In this context, it is necessary to highlight that the indemnity reaches 17 units of account (SDR, XDR) per each missing kilogram of gross weight of the consignment. At the same time, the COTIF assumes that if the delivery time is set by agreement, then there in this agreement it is possible to predict a different arrangement of the indemnity in connection with delay in delivery, as well. Provided the maximum delivery time, set in Article 16 Paragraph 2 of the CIM appendix, is exceeded, then the entitled party may request the indemnity negotiated with the carrier (i.e. a higher indemnity, too).

Under Article 35 of the CIM, in the case of exceeding the negotiated delivery time the consignor may enter into agreement with the carrier regarding the so-called indemnity, with quotation of interest in delivery of the freight, provided the consignor will record the calculated amount of their interest in the consignment note. Then, if a damage is occasioned due to exceeding the negotiated delivery time, this indemnity may be asked for up to the amount stated in the consignment note.

Under Article 36 of the CIM all the limitations of the carrier's liability will not be applied in the case of proving that the damage was caused with an act or negligence of the carrier, conducted either with intent to cause such a damage or with negligence and the knowledge of the carrier that such a damage could probably have happened (deliberate negligence).

2.4 Delivery time in international carriage by air under the Warsaw convention and Montreal protocol

This Convention for the Unification of Certain Rules for International Carriage by Air (1929, Warsaw Convention) [23], in its Article 19 defines that the carrier is liable for damage occasioned by delay in carriage of passengers, baggage or cargo by air. In the case of a delay, the limit of the carrier's liability is fixed at a sum of 250 francs per kilogram of the consignment's weight (for the purposes of the reimbursement calculation a franc means a monetary unit, which corresponds to 65.5 milligrams of gold of millesimal fineness nine hundred) [23].

In the case the consignor makes a special declaration of interest in delivery at destination and pays a supplementary sum at the moment when the consignment is handed over to the carrier, the carrier is obliged to indemnify the consignor the for a delay in delivery of the freight up to the amount negotiated. However, under Article 25 of the Warsaw Convention, the limit of liability mentioned above is not applicable in the case of proving that the damage resulted from an act or negligence of the carrier or their employees, done either with intent to cause such damage, or recklessly and with the knowledge that the damage would probably have resulted. At the same time, it is required to prove that the act, omission or negligence emerged or occurred within the scope of their employment. Furthermore, there is the condition that in the case of a delay in delivery of the consignment there must be a complaint against the carrier filed within 21 days from the date on which the baggage or cargo have been passed to the consignee.

The Convention for the Unification of Certain Rules for International Carriage by Air (1999, Montreal Protocol) in its Article 19 establishes the carrier's liability for damages occasioned by delay in carriage by air with the exception when the carrier proves that they and their employees and agents made all efforts and took all measures to avoid the damage or that it was impossible for them to take such measures. The liability of the carrier for a delay in delivery of the freight is limited with the sum of 19 units of account (SDR/XDR) per kilogram (under the legislation in force since 30. 12. 2009). Like the Warsaw Convention the Montreal Protocol allows for the consignor to make a special declaration of interest in delivery at destination and pay a supplementary sum at the time the freight is handed over for the carriage. In such a case the carrier is liable for the damage occasioned and is obliged to provide the compensation up to the designed amount. The value limit of the carrier's liability is not applicable in the case of proving that the damage happened due to an act or negligence of the carrier, their employees or agents, done either with intent to cause such damage, or recklessly and with the knowledge that the damage would probably have happened. In the case of a delay in delivery of the consignment the entitled party must file a complaint within 21 days from the date on which the baggage or freight have been passed to the consignee [24].

2.5 Delivery time by inland waterways under CMNI

The CMNI (Convention de Budapest relative au contract de transport de merchandises en navigation interieure) [25] - the Budapest Convention on the Contract for the Carriage of Goods by Inland Waterways in its Article 16 defines the liability of the carrier for a damage occasioned due to exceeding the delivery time, unless it is shown that the damage was due to circumstances, which a diligent carrier could not have prevented and the consequences of which he could not have averted. The delivery time, as indicated in Article 5, is the time limit agreed in the contract or, if there is no contractual agreement, it is the time limit, which could reasonably be required of a diligent carrier, taking into account the circumstances of the voyage and unhindered navigation [26].

Under Article 20 Paragraph 3 of the CMNI, the carrier's liability for the damage due to a delay in delivery shall not exceed the amount of the freightage. However, the full indemnification shall not exceed the amount, which would correspond to total loss of the freight based on the calculation done. The maximum limits of liability do not apply where the nature and higher value of the goods have been expressly specified in the transport document and the carrier has not refuted those specifications, or where the parties have expressly agreed to higher maximum limits of liability. Under Article 21 of the CMNI, the carrier loses the right for protection granted with the limited compensation, if it is proved that they themselves caused the damage by an act or negligence, either with the intent to cause such damage, or recklessly and with the knowledge that such damage would probably have resulted [26-27].

2.6 Delivery time in carriage by sea under the Hague, Hague-Visby, Hamburg and Rotterdam rules

Neither the Hague Rules [7] (International Convention for the Unification of Certain Rules of Law Relating to Bills of Lading), nor the Hague-Visby Rules (Protocol to Amend the International Convention for the Unification of Certain Rules of Law Relating to Bills of Lading) do directly deal with the question of the carrier's liability for a delay in delivery of the consignment. The indemnification is provided only in the case of damages of the freight itself, or damages related to the freight. Under the Hague Rules, the limited indemnities represent 100 pounds sterling per

package or unit, or a counter-value of this amount in another currency. Under the Hague-Visby Rules the limit of the carrier's liability is restricted with an amount of 2 units of account (SDR/XDR) provided the damage was not caused with negligence of the carrier intentionally or with the knowledge that such damage could probably have happened [7-10].

The Hamburg Rules (United Nations International Convention on the Carriage of Goods by Sea) in their Article 5 define that the carrier is liable for a delay in delivery if the occurrence, which caused the delay, took place while the goods were in their charge. Under the Hamburg Rules, the delay in delivery occurs when the goods have not been delivered at the port of discharge provided for in the contract of carriage by sea within the time expressly agreed upon or, in the absence of such an agreement, within the time, which it would be reasonable to require of a diligent carrier, having regard to the circumstances of the carriage. The liability of the carrier for a delay in delivery, according to provisions of Article 6 Paragraph 1, Subparagraph b) of the Hamburg Rules, is limited to an amount equivalent to two and a half times the freight payable for the goods delayed, but not exceeding the total freight payable under the contract of carriage of goods by sea. The aggregate liability of the carrier for damage of the freight and delay in delivery shall not exceed the amount, which would equal to the carrier's liability in the case of total loss of the freight. It is equivalent to two and a half times the units of account (SDR/XDR) per kilogram of gross weight, or 835 units of account per package or another freight/shipping unit. By agreement between the carrier and the consignor, limits of liability exceeding those quoted in the Hamburg Rules may be fixed [9, 28].

The Rotterdam Rules (United Nations Convention on Contracts for the International Carriage of Goods (Wholly or Partly) by Sea) [10] in their Article 21 define a delay as a moment when the freight is not delivered to the place of destination within the time expressly agreed upon. Under Article 60 of the Rotterdam Rules, the indemnity for loss or damage of the freight, due to a delay in delivery, is limited to an amount equivalent to two and a half times the freight payable for the goods lost or damaged. However, the full amount of indemnity must not exceed the amount, which would be payable in the case of total loss of freight. The carrier may ask for limitation of the liability in the case of intentional damages and negligence [29].

3 Discussion

The paper contains a thorough analysis of the law on the subject written primarily from the perspective of English law, but with reference to cases in other major developed countries. The main output focuses on international carriage measures, such as the Hague, Hague-Visby, Hamburg and Rotterdam Rules, the CMR, the COTIF/CIM, the Warsaw Convention and Montreal Protocol, CMNI and discusses the current developments towards uniformity. There are analysis of shippers' obligations, the obligations of the carrier and the rights and immunities of the carrier and there is a full coverage of the main issues in charterparties: transportation (including problems of Delivery time, delay in delivery). This paper seeks to examine, in a commercial context, the legal problems facing shipowners, charterers, shippers and receivers of goods and the solutions adopted by the courts and international conferences to those problems. Many of the legal principles involved are not restricted to shipping but serve the wider area of commercial law generally. The analysis shows that international rules present similarities in certain fields of international transport, however considerable differences exist (as each treaty was signed decades after the other) and to this respect the most important rules were compared with respect to the contract of carriage by the method of comparison. The dissimilarity of legislation is also shown and suggestions for further research in this area are given.

All the transport conventions contain a limitation of the compensation to be paid by a carrier. The Visby rules established the limitation per package at 666. 67 SDR, or 2 SDR per kg. The Hamburg rules raised the limit to 835 SDR per package or 2.5 SDR per kg. The 1980 Multimodal Convention (that has not entered into force yet) raised limit to 920 SDR per package and 2.75 per kg. The Rotterdam Rules in Article 59 adopt the limit of 875 SDR per package or unit and 3 SDR per kg. While the weight limits are still below those found in other modes, whether these new limits of liability are seen as better for cargo interests is, of course a different matter and will be evaluated by each cargo owner based on his or her claims history and experience. With comparison to unimodal modes, for instance the Budapest Convention on the Contract for the Carriage of Goods by Inland Waterway (CMNI) of 2001, establishing the liability of the carrier rate of 2 SDR per kilogram shipment or 666.67 SDR per package or any other unit load, or 1.500 SDR per container without the stored goods and further 25,000 SDR for goods stored in a container. The limit for transport of goods by air is almost nine times higher than the limit for maritime conveyances. However, the goods transported by air usually have a much higher value than their counterparts that are being shipped by sea [7-10]. Comparable Limits of Liability under Unimodal and Multimodal Regimes [20, 22-25] can be found in Table 1.

Containerization, the increasing complexity of modern supply chains, development of electronic documentation and the enhanced importance of security, have made carrier - shipper relations incredibly complex, while at the same time its driving governments towards a desire to harmonize the way in which global financial and trading rules are implemented. It is extremely important to the economic interests of all the

Table 1 *Comparable Limits of Liability under Unimodal and Multimodal Regimes*

regime	limit by weight	limit by item
sea carriage - Hague rules (Arts. IV(5) and IX) - Hague/Visby rules (Art. IV (5)) - Hamburg rules (Art. 6)	n/a 2.00 SDR/kg 2.50 SDR/kg	U.S. $500/pkg (= 346.21 SDR/pkg) 666.67 SDR/pkg 835 SDR/pkg,
ICC rules 1975 (rule 11(c))	30 Poincare francs/kg (~2 SDR/kg)	n/a
multimodal convention 1980 (Art. 18(1), (3).) - but if no sea leg	2.75 SDR/kg 8.33 SDR/kg	920 SDR/pkg
UNCTAD/ICC rules 1992 (rules 6.1 and 6.3) - but if no sea leg	2.00 SDR/kg 8.33 SDR/kg	666.67 SDR/pkg
Rotterdam rules 2009 (Art. 59)	3 SDR/kg	875 SDR/pkg
road carriage-CMR (Art. 23)	8.33 SDR/kg	n/a
rail carriage-CIM uniform rules (Arts. 7, 40 and 42)	17.00 SDR/kg	n/a
air carriage-Warsaw convention/ Montreal convention (Art. 22(2))	17.00 SDR/kg	n/a
inland water carriage - CMNI (Art. 20)	2 SDR/kg	666.67 SDR/pkg, 1500 + 25000 SDR/container

n/a (not available)
SDR (Special Drawing Rights)

trading nations that complicated supply chain functions seamlessly and equitably for all involved. To achieve such a goal, there must be not only the political will to sign and ratify improvements on existing carriage rules, but the widespread adoption of the contract terms as well, without exemptions being negotiated at the firm contract negotiation level.

The idea of the Rotterdam Rules is that it shall apply door-to-door mode, regardless of the mode of transport, as long as an international sea leg is involved. This broad scope of application of the Rotterdam Rules carries a risk of conflicts with unimodal transport conventions, which regulates carriage by air, road carriage, carriage by rail and carriage by inland water. Moreover, as the Rotterdam Rules only apply in the cases where damage is attributable to the marine sea leg, they are still not attractive from a cargo perspective, even though they have been more explicit in defining delay and have raised the limits of liability. For multimodal transport, there remains considerable confusion as to what will work best in the door-to door context and a trading environment focused on time-based competition where the consequences of cargo delay are a paramount consideration for a large portion of the moves [29-30].

4 Conclusion

The delivery time is usually negotiated in the contract of carriage between individual contracting parties, or it results from respective regulations or international treaties. European courts (mostly those of higher instances) have practiced appropriate periods of carriage (carriage times) several times, e.g. between Germany and Greece, Germany and Turkey, but these periods cannot be considered binding and applicable in all the cases.

The diversity of regulations in the area of international carriage of consignments through individual transport modes, mainly in context of the multimodality development, brings inconsistency and disharmony to the transport market. In conjunction with the anticipated and supported development of multimodal transport and a wider engagement in intermodal transport chains, the authors do recommend the unification of transport-legal conditions, not only with regard to delivery times in international carriage of goods and sanctions resulting from delay in delivery.

Acknowledgement

This work was supported by Project VEGA No. 1/0128/20: Research on the Economic Efficiency of Variant Transport Modes in the Car Transport in the Slovak Republic with Emphasis on Sustainability and Environmental Impact, Faculty of Operation and Economics of Transport and Communications: University of Zilina, 2020-2022.

References

[1] CULIK, K., KALASOVA, A., KUBIKOVA, S. Smart city - model of sustainable development of cities. In: 11th International Science-Technical Conference Automotive Safety: proceedings. 2018. p. 5.

[2] Traffic law e-newsletter [online]. 2007-2019. Available from: http://akmsv.cz/e-bulletin.

[3] FAGHFOURI, M. Overview of the UNCITRAL draft convention on contracts for the international carriage of goods wholly or partly by sea - IMMTA-News [online]. 2008. Available from: http://www.immta.org/uploads/IMMTANews-2008-1.pdf

[4] PAULAUSKAS, V., BENTZEN, K. Sea motorways as a part of the logistics chain. *Transport* [online]. 2008, 23(3), p. 202-207. ISSN 1648-4142, eISSN 1648-3480. Available from: https://doi.org/10.3846/1648-4142.2008.23.202-207

[5] LINGAITIENE, O. A mathematical model of selecting transport facilities for multimodal freight transportation. *Transport* [online]. 2008, 23(1), p. 10-15. ISSN 1648-4142, eISSN 1648-3480. Available from: https://doi.org/10.3846/1648-4142.2008.23.10-15.

[6] AFANDIZADEH, S., MOAYEDFAR, R. The feasibility study on creation of freight village in Hormozgan province. *Transport* [online]. 2008, 23(2), p. 167-171. ISSN 1648-4142, eISSN 1648-3480. Available from: https://doi.org/10.3846/1648-4142.2008.23.167-171.

[7] Hague rules. International convention for the unification of certain rules of law relating to bills of lading.

[8] Hague-Visby rules. Protocol to amend the international convention for the unification of certain rules of law relating to bills of lading.

[9] Hamburg rules. United Nations international convention on the carriage of goods by sea.

[10] Rotterdam rules. United Nations convention on contracts for the international carriage of goods (wholly or partly) by sea.

[11] TOLLI, A., LAVING, J. Container transport direct call - Logistic solution to container transport via Estonia. *Transport* [online]. 2007, 22(4), p. Ia-If. ISSN 1648-4142, eISSN 1648-3480. Available from: https://doi.org/10.1080/16484142.2007.9638149

[12] JARZEMSKIENE, I. The evolution of intermodal transport research and its development issues. *Transport* [online]. 2007, 22(4), p. 296-306. ISSN 1648-4142, eISSN 1648-3480. Available from: https://doi.org/10.3846/16484142.2007.9638145

[13] VASILIAUSKAS, A. V., BARYSIENE, J. An economic evaluation model of the logistic system based on container transportation. *Transport* [online]. 2008, p. 23(4), p. 311-315. ISSN 1648-4142, eISSN 1648-3480. Available from: https://doi.org/10.3846/1648-4142.2008.23.311-315

[14] JARZEMSKIENE, I., JARZEMSKIS, V. Allotment booking in intermodal transport. *Transport* [online]. 2009, 24(1), p. 37-41. ISSN 1648-4142, eISSN 1648-3480. Available from: https://doi.org/10.3846/1648-4142.2009.24.37-41

[15] LIU, W., XU, H., ZHAO, X. Agile service oriented shipping companies in the container terminal. *Transport* [online]. 2009, 24(2), p. 143-153. ISSN 1648-4142, eISSN 1648-3480. Available from: https://doi.org/10.3846/1648-4142.2009.24.143-153

[16] TETLEY, W. Reform of carriage of goods - the uncitral draft and Senate COGSA'99. *Tulane Maritime Law Journal*. 2003, 28(1), p. 1-44. ISSN 1048-3748.

[17] BURKOVSKIS, R. Efficiency of freight forwarder's participation in the process of transportation. *Transport* [online]. 2008, 23(3), p. 208-213. ISSN 1648-4142, eISSN 1648-3480. Available from: https://doi.org/10.3846/1648-4142.2008.23.208-213

[18] LINGAITIENE, O. A mathematical model of selecting transport facilities for multimodal freight transportation. *Transport* [online]. 2008, 23(1), p. 10-15. ISSN 1648-4142, eISSN 1648-3480. Available from: https://doi.org/10.3846/1648-4142.2008.23.10-15

[19] JARZEMSKIS, A., VASILIAUSKAS, A. V. Research on dry port concept as intermodal node. *Transport* [online]. 2007, 22(3), p. 207-213. ISSN 1648-4142, eISSN 1648-3480. Available from: https://doi.org/10.3846/16484142.2007.9638126

[20] CMR. Convention on the contract for the international carriage of goods by road.

[21] CULIK, K., KALASOVA, A., KUBIKOVA, S. Simulation as an instrument for research of driver-vehicle interaction. *MATEC Web of Conferences* [online]. 2017, 134, 00008. eISSN 2261-236X. Available from: https://doi.org/10.1051/matecconf/201713400008

[22] COTIF. Convention concerning international carriage by rail.

[23] Warsaw convention. Convention for the unification of certain rules relating to international carriage by air.

[24] Montreal convention. Convention for the unification of certain rules for international carriage by air.

[25] CMNI. Budapest convention on the contract for the carriage of goods by inland Waterways.

[26] JURKOVIC, M., DAVID, A. Technological and educational requirements for inland navigation simulator in the Danube region. *Nase More / Our Sea* [online]. 2015, 62(1), p. 13-19. ISSN 0469-6255, e-ISSN 1848-6320. Available from: https://doi.org/10.17818/NM.1.3.2015

[27] International maritime conventions. Prague: Czechoslovak Chamber of Commerce and Industry, 1981.

[28] JAGELCAK, A., DAVID, A. *Maritime transport and maritime containers*. Bytca: Druska Books as university textbook. 2014. ISBN 978- 80- 89646- 90-6.

[29] GROBARCIKOVA, A., SOSEDOVA, J. Carrier's liability under the international conventions for the carriage of goods by sea. *Transport Problems / Problemy Transportu*. 2014, 9(3), p. 75-82. ISSN 1896-0596, eISSN 2300-861X.

[30] SPARKA, F. *Jurisdiction and arbitration clauses in maritime transport documents*. Berlin: Springer-Verlag, 2010. ISSN 1614-2462.

THE CASE STUDY OF INTERNATIONAL TRANSPORT BY THE FREIGHT FORWARDER IN FRANCE

Iveta Kubasáková*, Jaroslava Kubáňová, Patrícia Kollárová

Department of Road and Urban Transport, Faculty of Operation and Economics of Transport and Communications, University of Zilina, Zilina, Slovak Republic

*E-mail of corresponding author: iveta.kubasakova@fpedas.uniza.sk

Resume

The article presents an analysis of the freight forwarder and carrier costs on transport in chosen country of Western Europe. Costs of transport point out to several existing problems in this part of Europe. The case study is given that deals about chosen transport in France. The article contains a review of transport routes during 2019, which were performed by an international forwarding company. These sessions were carried out in problematic areas in France. These are the transport of refrigerated and frozen perishable goods. The shipments are realized between logistics centres in France. The high problem is with carriers, with qualifications of their drivers, the number of drivers and seasonality of the goods. The article describes these problems as dependences of the forwarder´s costs on individual transport routes. The article deals about more solutions, which could be used in this part of Europe.

Article info

Received 26 January 2021
Accepted 24 March 2021
Online 20 September 2021

Keywords:

forwarder,
logistics,
chain,
costs,
carrier

Available online: https://doi.org/10.26552/com.C.2021.4.A256-A263

ISSN 1335-4205 (print version)
ISSN 2585-7878 (online version)

This is an open access article distributed under the terms of the Creative Commons Attribution 4.0 International License (CC BY 4.0), which permits use, distribution, and reproduction in any medium, provided the original publication is properly cited. No use, distribution or reproduction is permitted which does not comply with these terms.

1 Introduction

Forwarders companies are currently an integral part of the supply chain. A freight forwarder works with companies, importers and exporters, to make sure that the goods are transported in the safest, most efficient and cost-effective way. A freight forwarder works out the logistics and makes sure that all the basics are covered in the process of transporting goods from A to B. In order for the portfolio to be expanded in a targeted manner, the forwarder must also look for language-skilled employees and reduce the current employee turnover with appropriate tools. Due to the relatively strong competitive environment, it is necessary to take into account that the outgoing employee also takes the acquired contacts with him, which may in some cases deprive the employer of quality partnerships with carriers. It is important to build a strong corporate identity for employees and systematically reward their work, based on work results. It is important to note that for the most part, shipments are currently sold by people, despite an online platform where carriers can book them themselves.

As authors written in article [1], a grouping of shipments is performed to improve the logistics performance of the company. The food consignments are grouped from independent companies for one operator in order to eliminate the company´s CO_2 costs. The study presents a survey of dominant food flows and the models of supply chain optimization, to compare the food aggregation scenarios and their results, which can be generalized for further possible research in this area [1].

In another study, the authors described the possibilities of creating cooperating groups and how these groups should share the costs of this cooperating. They used the literature on networking, where the potential savings are modelled by cooperative play. Four business models in four different subgroups of leading companies were examined. They used a network model to determine a stable group in the calculation. The results are dependent on the selected model and it is possible to achieve different characteristics [2].

The solution is the cooperation of logistic companies, which is covered by an article with title Shipper collaboration, which solves the problem of freight transport and cooperation of individual forwarding companies in order to provide quality services at lower prices, streamlining cooperation between small and medium companies. Mathematically, Euclidean graph by a minimum costs set of constrained cycles was used. They formulated the lane covering problem, proposed several solution algorithms and conducted a computational study on the effectiveness of these methodologies [3].

The solution to the problem of transport of goods in France would also be possible by improving the quality of the rail transport, dealt with by authors in [4]. The solutions are adapted to the Spanish market,



Figure 1 *Location of places Dankerque and Reze on the map [GoogleMaps]*

but transport services can be used on the Paris-Orleans-Limoges- Toulouse (POLT) route in France, as well. Spain´s competitiveness depends on such projects [4].

Very important is study [5], which is one of the first analyses demonstrating the additional environmental costs that exist between mainland France and overseas France. Thus, the results demonstrate the importance of creating a specialized and regionalized database for the case of remote islands. That database would allow for professionals to have a precise environmental assessment, not on a national but on a regional scale. This document also provides a framework and guideline for policy decision-making in the overseas islands [5].

In the article [6] is presented a model that includes the freight transport supply and demand, as well as infrastructure quality and non-time-varying fixed effects related to the route, the exporting company, its strategy and the product. The results show that distance is a determining factor in the cost of transport, in spite of the infrastructure coverage and improvements in quality. At the same time, the analysis confirms that transport costs are more sensitive to the degree of competition on the route, the volume of freight on the route and the volume of goods shipped on the route by the exporting company, the configuration of the supply chain, the company strategy and the coverage and quality of transport infrastructure [6].

Despite the size of Europe, the costs market is relatively diverse. This is mainly due to different laws that have not yet been harmonized within the European Union. Despite the decline, France had the highest share of imports within the European Union during the period 2014 - 2018. That is exactly why the France domestic transport route was chosen.

2 The case study of chosen transport route in France

The analysed transport route is French domestic transport. This is a temperature-controlled transport between the logistics centres in the Nord Calais region and in the Loire region. The route leads specifically, as you can be seen in Figure 1. The distance between these points was set by the freight forwarder at 635 km. The transport was procured as one-way. The completed and validated CMR (Convention Marchandise Routière - Agreement on a contract of carriage in international road transport) consignment note required the carrier to enclose an invoice and a printed label showing the temperature in the vehicle´s cargo space during the transport.

The transport routes are analyzed in this section, from several points of view. This analysis also includes the success of the shipment tracking. Based on the results of the analysis, the measures are proposed that could contribute to improving the position of the forwarding company at the market as well as to greater transparency of the supply chain.

On this route, 39 different carriers carried goods and a total of 89 shipments took place between January 2019 and August 2019. Although it was a French domestic transport, the largest representation with a share of 36 % were polish carriers, followed by Lithuanian

carriers 21 % and Spanish with 15 %. Only one French carrier offered its services on this route.

The first transport on this route took place in January 2019. Due to the forwarder´s ability to acquire carriers on this route, the number of shipments that took place increased each month. This may also be due to an increase in the customer´s order, as the customer is a company, which deal with cultivation, storage and

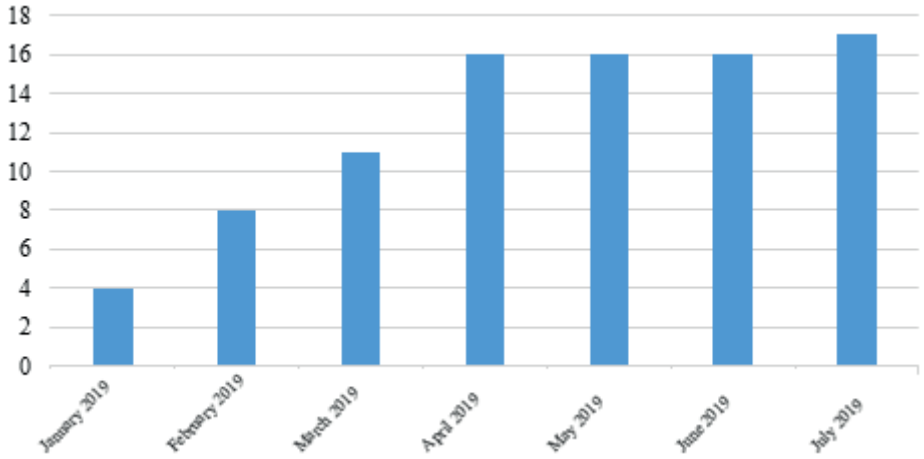


Figure 2 *The number of transports per month*

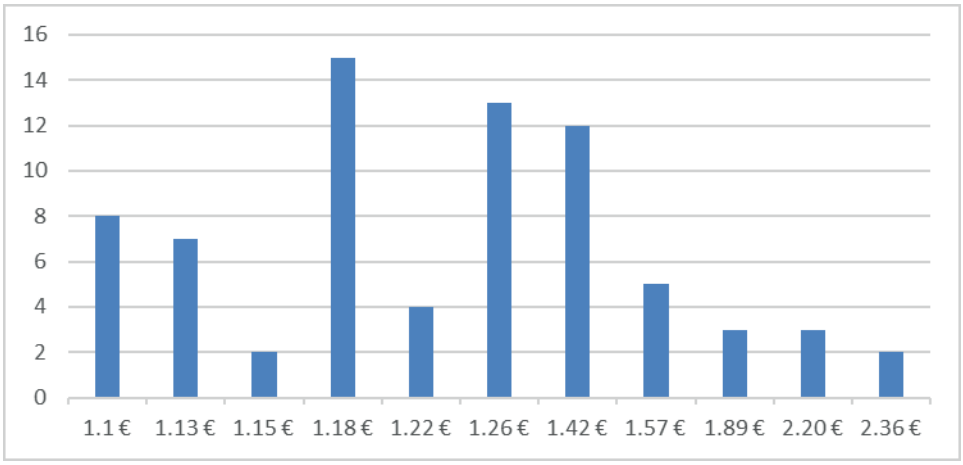


Figure 3 *Absolute price rates*



Figure 4 *Seasonality of prices*

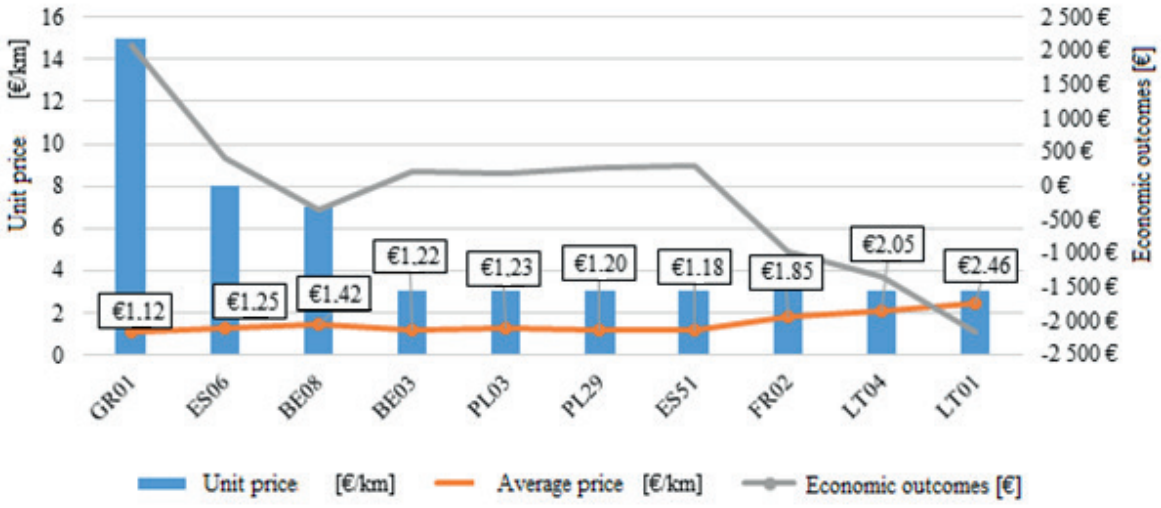


Figure 5 *Influence of the carrier´s price on the economic outcomes*

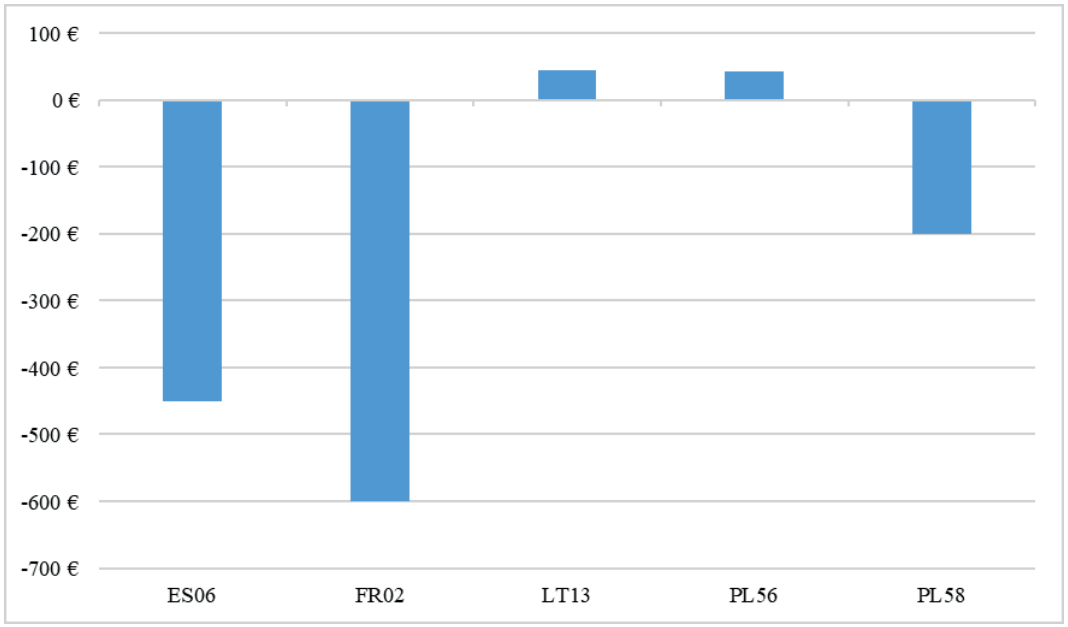


Figure 6 *Paid delays and provided discounts*

distribution of vegetables and fruits, for which the demand is rising in the summer months [7-9].

The data collection took place in early August, but as only one shipment was recorded in August, so this month was omitted from the statistics to avoid data distortions. The numbers of transports are presented in Figure 2.

Carriers offer the price as "ALL IN". The freight forwarder most often paid 1.18 € per kilometre to carriers. However, if there were low capacities on the market during the period, it was necessary to pay more than that was agreed with the customer to keep the customer. From January 2019, the price was the same, namely 1.34 €. The following graphs (in Figures 3, 4 and 5) show how this price affected the forwarder's profit or loss and whether the carriers were able and willing to travel below this price [10].

During January, February and June, the freight forwarder was able to benefit from the carrier´s prices. The largest loss was recorded during the month of May, when the forwarder had to invest € 3,200 in these transports from his own financial resources. This may be due to the low capacity of refrigerated semi-trailers in the area, which is presented in Figure 3 [11-13].

Due to the cooperation with Greek carriers in June 2019, the freight forwarder was able to produce a profit, despite the fact that the demand for refrigerated semi-trailers increased with the increased temperature during the summer months. In Figure 4 can be noticed that the customer did not change his price during the whole period and that he paid to the carrier 1.34 € per km. The market fluctuations reflected in prices of the carriers, therefore had to be taken over by the forwarder.

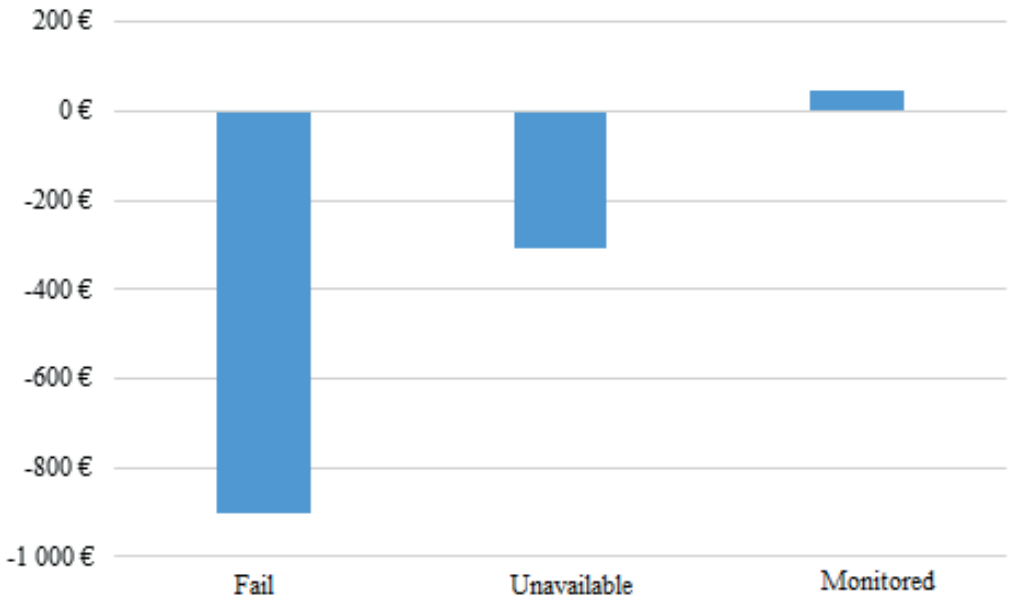


Figure 7 *Relationship between paid delays / provided discounts and traceability of the shipment*

The forwarder was on a loss on this route during the monitored period for EUR 4 390.

The loss or profit forwarding company is caused by the unit price of the carrier. The carrier is able to reduce the unit price by increasing the coefficients of fleet utilization, journey utilization and transport capacity utilization not only on a given transport route, but within the entire company. On the route that was monitored, the lowest price was offered by a Greek carrier, namely 1.12 € per km.

Among the analysed carriers, due to his optimal price and reliability he received the most shipments, namely 15 [14-15].

Figure 5 shows the effect of the carrier´s unit price on the number of received shipments and the loss or profit reported by the forwarder. The loss or profit of the forwarder is expressed as the difference between the carrier´s price and customer´s price.

In the event that the vehicle is delayed for loading/unloading for more than 2 hours, the customer pays for the delay, according to the pre-agreed conditions. One of them is to substantiate the movement of the vehicle from carrier´s GPS or from the tracking system of the forwarder [16-17].

The delays were charged by a total of three carriers on the given route, when there was a delay in loading or unloading of more than 2 hours. For delays within 24 hours, the customer paid a delay fee of EUR 200. The delays and provided discounts are in Figure 6.

The discount was provided by 2 carriers as a result of price negotiations, or the provision or a discount to the forwarder due to the previous provision of services at a lower level than expected (e.g. late arrival of the carrier for loading/unloading).

Connection to the forwarder´s tracking system can help reduce the customer delay fees paid to the carrier. It enables a faster reaction of the employee to the current situation and the movement of a vehicle and thus to be able to put pressure on the customer´s logistics centre in time for loading or unloading. This saves the customers costs and the carrier´s time.

The paid delays fees were paid for shipments whose status in the customer's tracking system reported either an error or unavailability. If the system reports an error, it can be cleared. Either the carrier has provided a vehicle registration number that is in the system but is not assigned to the transport or an employee in the system has assigned a vehicle registration number of the truck to the semi-trailer.

All the ten carriers, which transported the most consignments on the given route during the monitored period, also experienced errors or unavailability of tracking devices, which one can see in Figure 7.

The ten carriers were monitored, 50.98% were analysed from it. The system showed an error at 27.45% and an unavailability at 21.57%. Elimination of these discrepancies should be in the interests, not only of the forwarders, but of the carriers themselves, as well, as one can see in Figure 8. The correct setting of their fleet management software predestines them to provide services at a higher level and, at the same time, provides competitiveness within the forwarder´s portfolio.

Given the growing trend in the number of shipments ordered by the customer and the low number of involvement of domestic carrier, it is necessary for the freight forwarder to expand its portfolio to include carriers based in France. One of the factors that does not benefit carriers from abroad is cabotage. By Regulation (EC) no. 1072/2009 from 21 October 2009 on common rules for access to the international market for the carriage of goods by road, the carrier may transport no more than three consecutive cabotage operations within

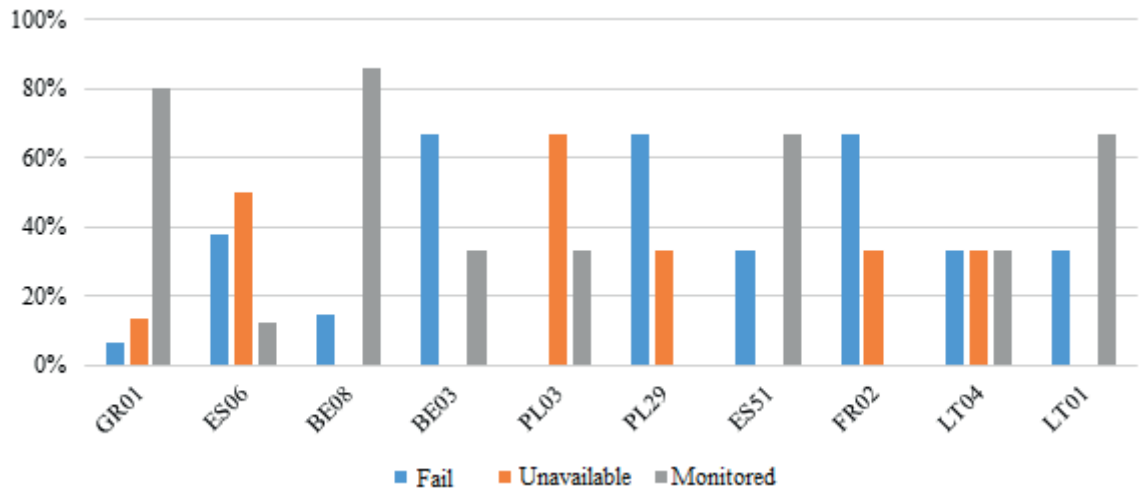


Figure 8 *Traceability of the shipment*

seven days from the last unloading in that member state during the importation. Insufficient knowledge of the legislation, as well as the associated sanctions, may deter carriers from doing it. In France, the fine for non-compliance with the conditions laid down, can amount to EUR 15 000 The freight forwarder should not only expand its portfolio to include French carriers, but also to others that offer their services in the region. A good example could be a long-term partnership with a Greek carrier that provides his services of the high quality on this transport route [18].

One of the problems is a delay of carriers on loading or unloading, which may be a negative factor in the future, due to which carriers will either demand a higher unit price for transport or refuse this transport. During the monitored period, the customer paid a delay of EUR 1,136.60 on the Lion Plage - Reze route. In this case, it is very important to communicate with the forwarder himself, to prevent an escalation of problems, to ensure the functionality of the internal information system, as well as to recalculate the capacities of loading platforms. Minimizing the costs of delays saves resources for the customer and the carrier reduces inefficient vehicle downtime. The forwarder, who is able to promptly solve problems that occur during the transport, increases his own credibility both with carriers and customers. He gains a competitive advantage in the form of lower unit prices from carriers and more shipments from customers.

3 Conclusions

The analysed route served us as a suitable example of how the costs market works in Western Europe and how seasonality can affect rates. This route also explains the principle of operation of the forwarding company towards the customer and the carrier, as well as some internal procedures.

It should be of interest for the forwarder itself to expand its own portfolio. Employees need to be trained to target potential partners. The freight forwards will be upgrading its services for facility of process, increasing flexibility, transparency and availability of services. It is a necessary process for the customer's satisfaction. The company's management has access to free capacities through important transport databases, such as TimoCom, where carriers publish the location of their free capacities and, among other things, telephone or e-mail contacts. Another suitable tool for searching for the new carriers are national databases, a suitable example being the Slovak database www.jiscd.sk. Although in some cases it does not provide the contact information for carriers, it is possible to search for it in another way. The participation of the forwarder in various fairs and conferences is also important, where he can come into personal contacts with carriers.

The forwarder also offers its services for one-time shipments. If one-time transport is properly valued, it is possible to make a profit on them, as the customer needs to transport the shipment and is often willing to pay extra for this service. These shipments are appreciated by the lower management, based on previous experience or a telephone survey among carriers. A more accurate method certainly is to use a dedicated software that can plan the route correctly according to the constraints of trucks, such as length and weight. As a result, the shipper can avoid errors caused by human factors, such as incorrect valuation of the transport due to a poorly chosen distance between the place of loading and unloading. However, the quality of one-time shipments can move the forwarder to the forefront of the customer's supply chain.

The aim of article was analysis of the chosen national and international carriers on transport in Western Europe by freight forwarder. The freight forwarder provides transport in Europe. The article presents the case study of chosen transport in France. This transport is an example of existing freight forwarder as working in Europe [19-21].

Acknowledgements

This paper was developed under the support of project: MSVVS SR - VEGA No. 1/0245/20 Poliak, M.: Identification of the impact of a change in transport related legislation on the competitiveness of carriers and carriage safety.

References

[1] PAN, S., BALLOT, E., FONTANE, F., HAKIMI, D. Environmental and economic issues arising from the pooling of SMEs' supply chains: case study of the food industry in western France. Flexible Services and Manufacturing Journal [online]. 2014, 26(1-2), p. 92-118. ISSN 1936-6582, eISSN 1936-6590. Available from: https://doi.org/10.1007/s10696-012-9162-3

[2] AUDY, J.-F., D'AMOURS, S., RONNQVIST, M. An empirical study on coalition formation and cost/savings allocation. International Journal od Production Economics [online]. 2012, 136(1), p. 13-27. ISSN 0925-5273. Available from: https://doi.org/10.1016/j.ijpe.2011.08.027

[3] ERGUN, O., KUYZU, G., SAVELSBERGH, M. Shipper collaboration. Computers and Operations Research [online]. 2007, 34(6), p. 1551-1560. ISSN 0305-0548. Available from: https://doi.org/10.1016/j.cor.2005.07.026

[4] DE ALARCON, R. F. Fundamental decisions for the transport of goods in Spain and with Europe / Decisiones fundamentales para el transporte de mercancias en Espana y con Europa (in Spanish). Revista de Obras Publicas. 2015, 162(3563), p. 43-50. ISSN 0034-8619, eISSN 1695-4408.

[5] AYAGAPIN, L., PRAENE, J. P. Environmental overcost of single family houses in insular context: a comparative LCA study of Reunion island and France. Sustainability [online]. 2020, 12(21), 8937. eISSN 2071-1050. Available from: https://doi.org/10.3390/su12218937

[6] CAMISON-HABA, S., CLEMENTE-ALMENDROS, J. A. A global model for the estimation of transport costs. Economic Research-Ekonomska Istrazivanja [online]. 2020, 33(1), p. 2075-2100. ISSN 1331-677X, eISSN 1848-9664. Available from: https://doi.org/10.1080/1331677X.2019.1584044

[7] ZAGORECKI, A., RISTVEJ, J., COMFORT, L. K., LOVECEK, T. Executive Dashboard Systems for Emergency Management. *Communications - Scientific Letters of the University of Zilina* [online]. 2012, **14**(2), p. 82-89. ISSN 1335-4205. ISSN 1335-4205, eISSN 2585-7878. Available from: http://komunikacie.uniza.sk/index.php/communications/article/view/751

[8] POLIAK, M., POLIAKOVA, A. Relation of social legislation in road transport on driver's work quality. In: Tools of Transport Telematics TST 2015: proceedings [online]. Vol. 531. Communications in Computer and Information Science. Cham: Springer, 2015. ISBN 978-3-319-24576-8, eISBN 978-3-319-24577-5, p. 300-310. Available from: https://doi.org/10.1007/978-3-319-24577-5_30

[9] Deloitte Intrastat guide 2018 - Deloitte [online]. Available from: https://www2.deloitte.com/be/en/pages/tax/articles/Deloitte-Intrastat-guide-Deloitte-Belgium-Tax.html

[10] CEMPIREK, V., GASPARIK, J., ZITRICKY, V., BLAHO, P. Control of modular conveyor and automated handling devices interconnection. *Advances in Science and Technology* [online]. 2018, **12**(3), p. 210-215. ISSN 2299-8624. Available from: https://doi.org/10.12913/22998624/94963

[11] European statistical recovery dashboard - Eurostat [online] [accessed 2020-02-17]. Available from: https://ec.europa.eu/eurostat/data/database

[12] A responsibility of the principals or user companies - Weblex [online]. Available from: https://www.weblex.fr/weblex-actualite/transport-entreprise-etrangere

[13] Mont Blanc Tunnel: Heavy Vehicle ETC - ATMB [online]. Available from: https://www.atmb.com/en/our-offers/mont-blanc-tunnel-cost-and-subscription/heavy-goods-vehicles-etc

[14] Royal Decree 1211/1990, of September 28, which approves the Regulation of the Law of Ordinance of Land Transport - Ministry of Transport, Tourism and Communications "BOE" [online]. Available from: https://www.boe.es/buscar/pdf/1990/BOE-A-1990-24442-consolidado.pdf

[15] HLATKA, M., STOPKA, O. STOPKOVA, M. Proposal of innovative flooring options for marine containers. *Nase More* [online]. 2018, **65**(4), p. 174-179. ISSN 0469-6255, e-ISSN1848-6320. Available from: https://doi.org/10.17818/NM/2018/4SI.2

[16] LOVECEK, T., RISTVEJ, J. Quantitative assessment parameters of the protection level of national strategic sites in the EU [online]. In: *Risk analysis VII: simulation and hazard mitigation*. Vol. 43. Southampton: WIT Press - WIT Transaction on Information and Communication Technologies; 2010. ISSN 1743-3517, ISBN 9781845644727, p. PI69-PI80. Available from: https://doi.org/10.2495/RISK100071

[17] Law 16/1987, of July 30, on the Regulation of Land Transport - Head of State "BOE" [online]. Available from: https://www.boe.es/buscar/pdf/1987/BOE-A-1987-17803-consolidado.pdf

[18] KAMPF, R., HLATKA, M., GROSS, P. Optimisation of distribution routes: a case study. *Communications - Scientific Letters of the University of Zilina* [online]. 2021, **23**(1), p. A62-A73. ISSN 1335-4205, eISSN 2585-7878. Available from: https://doi.org/10.26552/com.C.2021.1.A62-A73

[19] SIMAK, L., RISTVEJ, J. The present status of creating the security system of the Slovak Republic after entering the European Union. *Journal of Homeland Security and Emergency Management* [online]. 2009, **6**(1), 20. ISSN 1547-7355. Available from: https://doi.org/10.2202/1547-7355.1443

[20] DVORAK, Z., REHAK, D., DAVID, A., CEKEREVAC, Z. Qualitative approach to environmental risk assessment in transport. *International Journal of Environmental Research and Public Health* [online]. 2020, **17**(15), 5494. eISSN 1660-4601. Available from: https://doi.org/10.3390/ijerph17155494

[21] HARANTOVA, V., HAJNIK, A., KALASOVA, A. Comparison of the flow rate and speed of vehicles on a representative road section before and after the implementation of measures in connection with COVID-19. *Sustainability* [online]. 2020, **12**(17), 7216. eISSN 2071-1050. Available from: https://doi.org/10.3390/su12177216

IMPACT OF KEY MARKETING TOOLS ON GLOBAL CAR MARKET DEVELOPMENT

Oleksandr Savych[1], Tetiana Shkoda[2,*]

[1]Department of Marketing named after A. F. Pavlenko, Faculty of Marketing, Kyiv National Economic University named after Vadym Hetman, Kyiv, Ukraine
[2]Department of Department of Business Economics and Entrepreneurship, Faculty of Economics and Management, Kyiv National Economic University named after Vadym Hetman, Kyiv, Ukraine

*E-mail of corresponding author: tnshkoda@ukr.net

Resume
The purpose of the proposed study was to identify the functional patterns of influence of the marketing tools on sales of cars on the global market, to be able to predict sales volumes in the future, taking into account certain marketing tools that the company may use in a particular international market. For the purpose of this research the method of correlation-regression analysis is used to construct the corresponding economic and mathematical models of impact on the sales volumes of various instruments of product, price, promotion policy, etc. Using the models offered in the article, the feasibility of introducing certain measures can be determined, when entering new markets in order to increase car sales. Each instrument to which potential buyers are sensitive determines the effect of its use. Considering this effect, budgets can be set up for appropriate action.

Article info
Received 7 April 2021
Accepted 27 April 2021
Online 24 September 2021

Keywords:
impact,
marketing tools,
global car market,
modelling,
sales forecasting

Available online: https://doi.org/10.26552/com.C.2021.4.A264-A276

ISSN 1335-4205 (print version)
ISSN 2585-7878 (online version)

This is an open access article distributed under the terms of the Creative Commons Attribution 4.0 International License (CC BY 4.0), which permits use, distribution, and reproduction in any medium, provided the original publication is properly cited. No use, distribution or reproduction is permitted which does not comply with these terms.

1 Introduction

The modern global car market is characterized by a complex system of commercial relations, as well as the need to coordinate the activities and economic interests of a large number of businesses. Fluctuations in supply and demand in this market can provoke economic crises and can slow down the development of the world economy.

Entering any market is a great investment and risk, so businesses require the model for predicting success in specific markets using marketing parameters, which are relevant to this study.

In the process of studying the marketing activities of enterprises in the car market and the prospects for their effective operation, it is necessary to take into account the globalization processes [1-2], restrictions on access to natural resources and increase of their value [3-4], digitalization of society [5-6], intensification of competition [7-8] and government regulation [9-11], which are key factors influencing development of the automotive industry in the world. Besides that, since 2020 the world economy has largely been affected by the COVID-19 crisis [12] that has a great impact on the consumer's behavior worldwide; in general and on the global car market, in particular. In such circumstances, the way in which marketing can be used, has changed and shows similarities with its usage during the economic downturns [13]. The specifics of the COVID-19 crisis impact on marketing usage on the global car market is presented in the discussion section of this paper.

2 Literature review

Literature review covers two stages:

1. Review of the researches dedicated to the automotive industry development in various countries.
2. Specifics of marketing factors.

One of the modern conceptual models, proposed in current researches of the automotive industry in India, is a conceptual model by Goswani and Kumar [14], which captures interdependency of agility enablers and develops its underlying attributes. Some components such as cost management, product service or customer resource adaption are researched in this conceptual model, but not in the marketing context.

The other research on developing the key performance indicators for agile manufacturing, based on the data of the Indian auto component manufacturer, was made by Kumar Potdar and Routroy [7]. In this research the following marketing performance indicators were studied: capturing market environment, management of market volatility,

improvement in market share, entering new market, response time for customer orders and queries, quick response to market changes. EL-Khalil [15] considered the market only as an element of strategic flexibility in the research dedicated to the mediating effect of lean management on the relationship between flexibility implementation and operational metrics in US automotive manufacturing plants.

Cech and Januska [16] evaluated risk management maturity in the Czech Automotive Industry, placing the emphasis on competition in complex business environment and its riskiness for the car producers. The force field analysis of Indian automotive strategic sourcing risk management enablers and barriers was performed by Kumar Sharma, Singh and Matai [8]. This research considered such an important marketing factor as sharing information among partners in the automobile supply chain with the purpose to make the communication process clearer. The factor of marketing communication policy is also partially considered in the research of Demirbas, Wilkinson and Bennett [17]. They studied supplier relations impact within the UK automotive industry.

Dmytriiev et al. [18] devoted their study to forming the competitive strategy of an enterprise based on typologization of regional markets one example of the Ukrainian automotive industry. The marketing factor of regional coverage is emphasized in this paper.

The research of Chen [19] is devoted to analysis of the strategies of European, American, Japanese, Korean and Chinese car producers on the Chinese automobile market. The focus was made on differences in development of domestic and foreign car producers with attention to such marketing factors as: regional coverage, low price, breadth of the range, consumer preference for car compactness, preference given to producers located in the region.

Cooper [20] considered the drivers of success in the new-product development, paying attention to such marketing factors as building in voice-of-customer (like the factor of brand loyalty to previously owned car), adopting a global orientation for the project, a compelling value proposition (like the value of possessing factor), ecology (represented as a climate factor) and culture.

The analytical report of Deloitte [21] proves that such marketing factors as safety, connectivity, ecology (represented by the alternative engine solutions) and value of possessing (represented by unwilling to pay more than…) are still very important for consumers around the world.

In general, in the world, the new generation, i.e. young people under 35, choose a car according to 6 main sources of information, which are sorted by impact rating [22]:

1. Recommendations from family and friends.
2. Reviews on independent sites
3. News and articles in the media
4. Manufacturers' websites
5. Sellers in car dealerships
6. Social networks.

It is visible that in the top 6 information sources there is no advertising at all and trust in information of the car manufacturers (manufacturers' websites - 4th place and sellers in car dealerships - 5th place) is minimal. Therefore, automakers need to work harder to improve the brand loyalty, including improving the quality, reliability of the car and improving after-sales service to receive the final reward - the recommendations of people close to the consumer. In addition, it is necessary to actively work with independent sites and the media on effective PR activity.

The research dedicated to the concept of marketing efforts consolidation of car producers at the global car market [23] can be considered as the theoretical background of this paper. It includes the impact factors on strategic and tactical level. This research developed the concept in direction of the practical implication with the detailed analysis based on marketing factors important for the global car market. In addition, previous studies in this area [24] focused on modelling of global car market development under globalization impact, where the sales forecasting model is developed that can be useful for our research.

In order to identify the most effective marketing tools, the general list of explanatory variables proposed by Savych [25], the authors propose to supplement a set of features that characterize the needs and behavior of consumers in each part of the world, including product policy («Loyalty to the brand previously owned by the consumer», «Preference is given to manufacturers who are localized in the region», «The younger generation is the largest consumer in the share of all consumers», «Consumer advantage in the compactness of the car», «Safety», «Design», «Ecology/electric cars», «Breadth of assortment», «Brand premium», «Consumption level»), price policy («Cost of ownership», «Low price»), place policy («Personal sale», «Internet sales», «Region coverage»), promotion policy («Events», «Digital advertising», «Magazines», «Television», «Radio», «Recommendations from family and friends»), human resources policy («Motivation of sellers», «Qualification of sellers»).

Based on the analysis of literature sources, the authors proposed the following research hypotheses:

H_1: The model of forecasting car sales volume, considering marketing factors, can be used as a basis for conducting a study of various marketing tools impact on car sales volume.

H_2: The forecast volume of car sales in the world during 2007-2019 coincides with the actual figures.

H_3: The proposed set of marketing tools has a positive impact on the growth of car sales at the global market.

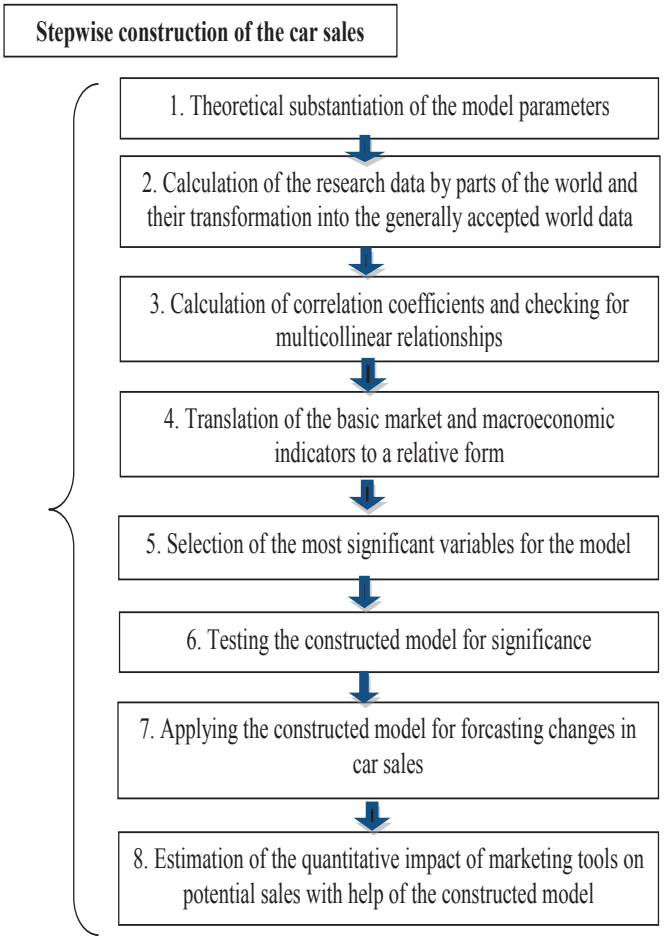


Figure 1 *Stepwise construction of the car sales forecasting model considering marketing parameters*

3 Methodology

Based on the performed literature review and to achieve the purpose of study, the authors propose to build appropriate economic and mathematical models of impact of the above mentioned tools of product, price, advertising policy etc. on sales volume.

To make the appropriate calculations and build the model of forecasting car sales considering the marketing parameters, Microsoft Excel software (package "Analysis of data") was used. The proposed stepwise construction of the car sales forecasting model, considering marketing parameters is presented on Figure 1.

For each of these features, according to the OICA statistics presented in [26] its affiliation to a certain part of the world (European Union, CIS, North American Free Trade Area (NAFTA), South America, Asia, Africa) - if any feature inherent in the needs of consumers in the region, it is opposed to «1» and «0» - otherwise.

Since for all the parts of the world the communication tool "Television" is marked as important (in all the records the value "1" is specified), for this indicator it is impossible to calculate correlation coefficients and determine the impact on the resulting variable, because in fact it becomes a constant. Accordingly, it will be excluded from the analysis.

For the rest of the indicators that characterize the needs and behavior of consumers in each part of the world, it is advisable to check for multicollinear relationships. Accordingly, in Table 1 and Table 2 their correlation matrix is presented.

As it can be seen from Table 1 and Table 2, a significant number of pairwise correlation coefficients are equal to one by modulo. This is due to the fact that such indicators in different parts of the world are either equally important or at the same time unimportant in determining the needs of residents in cars. Or, conversely, they have the opposite dependence, such as the characteristic "Cost of ownership" on the value of the correlation coefficient "-1" with many other factors.

Accordingly, in the case of including any of these factors in the model, all the variables that have a correlation relationship with it at the level of one by modulo, should be excluded from consideration. It is desirable to reject other variables that have a high level of pairwise correlation to avoid the manifestation of multicollinearity.

The fact that these features of the specifics of consumer behavior for each part of the world are constant tests of the study period 2006 - 2018, to a set of independent observations of these factors is 6 records - for several parts of the world (European Union, CIS, North American Free Trade Area (NAFTA), South America, Asia, Africa).

Therefore, in addition to these features that characterize the needs and specifics of consumer behavior in each part of the world, the model for forecasting car sales, considering marketing factors, must include basic market and macroeconomic indicators. In this case, the entire data sample will increase 13 times (by the number of years of observations). Moreover, the signs of the specifics of consumer behavior will be repeated for each year of observations for the relevant part of the world.

However, when combining information from different parts of the world, it should be borne in

Table 1 *Pairwise correlation coefficients between indicators that characterize the needs and behavior of consumers in the world*

Variables	Loyalty to the brand previously owned by the consumer	Preference is given to manufacturers who are localized in the region	The younger generation is the largest consumer	Consumer advantage in the compactness of the car	Safety	Design	Ecology/electric cars	Breadth of assortment	Brand premium	Consumption level	Cost of ownership
Loyalty to the brand previously owned by the consumer	1.000	1.000	1.000	0.707	1.000	0.333	1.000	0.707	0.000	0.000	-1.000
Preference is given to manufacturers who are localized in the region	1.000	1.000	1.000	0.707	1.000	0.333	1.000	0.707	0.000	0.000	-1.000
The younger generation is the largest consumer	1.000	1.000	1.000	0.707	1.000	0.333	1.000	0.707	0.000	0.000	-1.000
Consumer advantage in the compactness of the car	0.707	0.707	0.707	1.000	0.707	0.000	0.707	0.500	0.250	0.500	-0.707
Safety	1.000	1.000	1.000	0.707	1.000	0.333	1.000	0.707	0.000	0.000	-1.000
Design	0.333	0.333	0.333	0.000	0.333	1.000	0.333	0.707	0.707	-0.707	-0.333
Ecology/electric cars	1.000	1.000	1.000	0.707	1.000	0.333	1.000	0.707	0.000	0.000	-1.000
Breadth of assortment	0.707	0.707	0.707	0.500	0.707	0.707	0.707	1.000	0.500	-0.500	-0.707
Brand premium	0.000	0.000	0.000	0.250	0.000	0.707	0.000	0.500	1.000	-0.250	0.000
Consumption level	0.000	0.000	0.000	0.500	0.000	-0.707	0.000	-0.500	-0.250	1.000	0.000
Costs of ownership	-1.000	-1.000	-1.000	-0.707	-1.000	-0.333	-1.000	-0.707	0.000	0.000	1.000
Low price	-0.707	-0.707	-0.707	-0.250	-0.707	0.000	-0.707	-0.500	0.500	0.250	0.707
Personal sale	-0.707	-0.707	-0.707	-1.000	-0.707	0.000	-0.707	-0.500	-0.250	-0.500	0.707
Internet sales	1.000	1.000	1.000	0.707	1.000	0.333	1.000	0.707	0.000	0.000	-1.000
Region coverage	0.707	0.707	0.707	0.500	0.707	0.707	0.707	1.000	0.500	-0.500	-0.707
Events	-0.447	-0.447	-0.447	-0.316	-0.447	0.447	-0.447	0.316	0.632	-0.632	0.447
Digital advertising	0.707	0.707	0.707	0.500	0.707	0.707	0.707	1.000	0.500	-0.500	-0.707
Magazines	-0.707	-0.707	-0.707	-1.000	-0.707	0.000	-0.707	-0.500	-0.250	-0.500	0.707
Radio	-0.707	-0.707	-0.707	-1.000	-0.707	0.000	-0.707	-0.500	-0.250	-0.500	0.707
Recommendations from family and friends	-0.333	-0.333	-0.333	0.000	-0.333	0.333	-0.333	0.000	0.707	0.000	0.333
Motivation of sellers	-0.333	-0.333	-0.333	-0.707	-0.333	0.333	-0.333	0.000	0.000	-0.707	0.333
Qualification of sellers	0.447	0.447	0.447	0.316	0.447	0.447	0.447	0.632	0.316	-0.316	-0.447

Table 2 *Pairwise correlation coefficients between indicators that characterize the needs and behavior of consumers in the world (continuation of Table 1)*

Variables	Low price	Personal sale	Internet sales	Region coverage	Events	Digital advertising	Magazines	Radio	Recommendations from family and friends	Motivation of sellers	Qualification of sellers
Loyalty to the brand previously owned by the consumer	-0.707	-0.707	1.000	0.707	-0.447	0.707	-0.707	-0.707	-0.333	-0.333	0.447
Preference is given to manufacturers who are localized in the region	-0.707	-0.707	1.000	0.707	-0.447	0.707	-0.707	-0.707	-0.333	-0.333	0.447
The younger generation is the largest consumer	-0.707	-0.707	1.000	0.707	-0.447	0.707	-0.707	-0.707	-0.333	-0.333	0.447
Consumer advantage in the compactness of the car	-0.250	-1.000	0.707	0.500	-0.316	0.500	-1.000	-1.000	0.000	-0.707	0.316
Safety	-0.707	-0.707	1.000	0.707	-0.447	0.707	-0.707	-0.707	-0.333	-0.333	0.447
Design	0.000	0.000	0.333	0.707	0.447	0.707	0.000	0.000	0.333	0.333	0.447
Ecology/electric cars	-0.707	-0.707	1.000	0.707	-0.447	0.707	-0.707	-0.707	-0.333	-0.333	0.447
Breadth of assortment	-0.500	-0.500	0.707	1.000	0.316	1.000	-0.500	-0.500	0.000	0.000	0.632
Brand premium	0.500	-0.250	0.000	0.500	0.632	0.500	-0.250	-0.250	0.707	0.000	0.316
Consumption level	0.250	-0.500	0.000	-0.500	-0.632	-0.500	-0.500	-0.500	0.000	-0.707	-0.316
Costs of ownership	0.707	0.707	-1.000	-0.707	0.447	-0.707	0.707	0.707	0.333	0.333	-0.447
Low price	1.000	0.250	-0.707	-0.500	0.316	-0.500	0.250	0.250	0.707	0.000	-0.316
Personal sale	0.250	1.000	-0.707	-0.500	0.316	-0.500	1.000	1.000	0.000	0.707	-0.316
Internet sales	-0.707	-0.707	1.000	0.707	-0.447	0.707	-0.707	-0.707	-0.333	-0.333	0.447
Region coverage	-0.500	-0.500	0.707	1.000	0.316	1.000	-0.500	-0.500	0.000	0.000	0.632
Events	0.316	0.316	-0.447	0.316	1.000	0.316	0.316	0.316	0.447	0.447	0.200
Digital advertising	-0.500	-0.500	0.707	1.000	0.316	1.000	-0.500	-0.500	0.000	0.000	0.632
Magazines	0.250	1.000	-0.707	-0.500	0.316	-0.500	1.000	1.000	0.000	0.707	-0.316
Radio	0.250	1.000	-0.707	-0.500	0.316	-0.500	1.000	1.000	0.000	0.707	-0.316
Recommendations from family and friends	0.707	0.000	-0.333	0.000	0.447	0.000	0.000	0.000	1.000	-0.333	-0.447
Motivation of sellers	0.000	0.707	-0.333	0.000	0.447	0.000	0.707	0.707	-0.333	1.000	0.447
Qualification of sellers	-0.316	-0.316	0.447	0.632	0.200	0.632	-0.316	-0.316	-0.447	0.447	1.000

mind that economic, infrastructural, demographic and other characteristics are too different (some indicators may differ very much). If to include all these factors in absolute form, it will be lost the ability to build a regression model, which is most convenient for analyzing the degree of influence of individual factors on the resulting indicator (to optimize the parameters of such a model all its variables should be distributed according to normal law).

Accordingly, when building a model for forecasting car sales considering marketing factors, it is necessary to translate the basic market and macroeconomic indicators to a relative form. For this purpose, these variables are converted to relative increments for the year as a percentage of the ratio:

$$Z_i^t = \frac{X_i^t - X_i^{t-1}}{X_i^{t-1}} \cdot 100\%, \quad (1)$$

where X_i^t, X_i^{t-1} - the value of the i-th basic indicator in the t-th and previous years .

As it can be seen from Equation (1), a number of relative values of indicators will begin in 2007 (2006 serves as a basis for calculating the annual relative change). Therefore, the training sample for building a model for forecasting car sales considering marketing factors is reduced to the period from 2007 to 2018 for explanatory variables and from 2008 to 2017, for the resulting variable. Data on sales in 2019 are left to compare the result of the model calculation to the real data that were not taken into account in its construction.

From the list of the basic market and macroeconomic indicators, two factors are left out - “Inflation” and “Population expenditures, consumption”, because they are already presented in the original statistics in the form of annual relative percentage change (for them $Z_i^t = X_i^t$).

4 Results

To build a model for forecasting the car sales considering marketing factors, it was decided to add

Table 3 *Correlation of relative changes in car sales with the corresponding indicator*

Indicator	Correlation
Car Park, thousands units	0.024
Motorization, Quantity of cars per 1000 of population	0.178
Population, number of people	-0.061
Urbanization, %	0.128
Major Roads Length, km	0.128
Real fuel costs (average for gasoline and diesel fuel), USD	-0.008
GDP, USD	0.690
Inflation, %	-0.133
Unemployment, %	-0.308
Population expenditures, consumption, % of change	-0.003
Annual Average Sold Car Price, USD	-0.015
Average Fuel Consumption of Car Sold, liters per 100 km	-0.053
Average Costs of Sold Car Operation, USD	0.018
GDP per capita, USD	0.702
Car sales, units	0.197
Loyalty to the brand previously owned by the consumer	0.134
Preference is given to manufacturers who are localized in the region	0.134
The younger generation is the largest consumer	0.134
Consumer advantage in the compactness of the car	0.161
Safety	0.134
Design	0.075
Ecology/electric cars	0.134
Breadth of assortment	0.030
Brand premium	0.100
Consumption level	0.131
Costs of ownership	-0.134
Low price	0.069
Personal sale	-0.161
Internet sales	0.134
Region coverage	0.030
Events	-0.141
Digital advertising	0.030
Magazines	-0.161
Radio	-0.161
Recommendations from family and friends	0.062
Motivation of sellers	-0.120
Qualification of sellers	0.043

to analysis the indicator «GDP per capita» [27], which combines the two factors - «GDP» and «Population». In order to select the most significant explanatory variables for the model, their impact on the relative change in car sales next year (Table 3) was analyzed.

As it can be seen from Table 3, only two explanatory indicators have a significant impact on the dependent variable - "GDP" and "GDP per capita". Since there is a multicollinear relationship between them (direct dependence on each other and a correlation of 0.896), only one of them was left in the model - "GDP per capita", because it has a greater impact on the resulting variable and combines the two factors.

Other indicators have low values of correlation with the original variable, as it can be seen from Table 3. Therefore, the selection of the most significant of

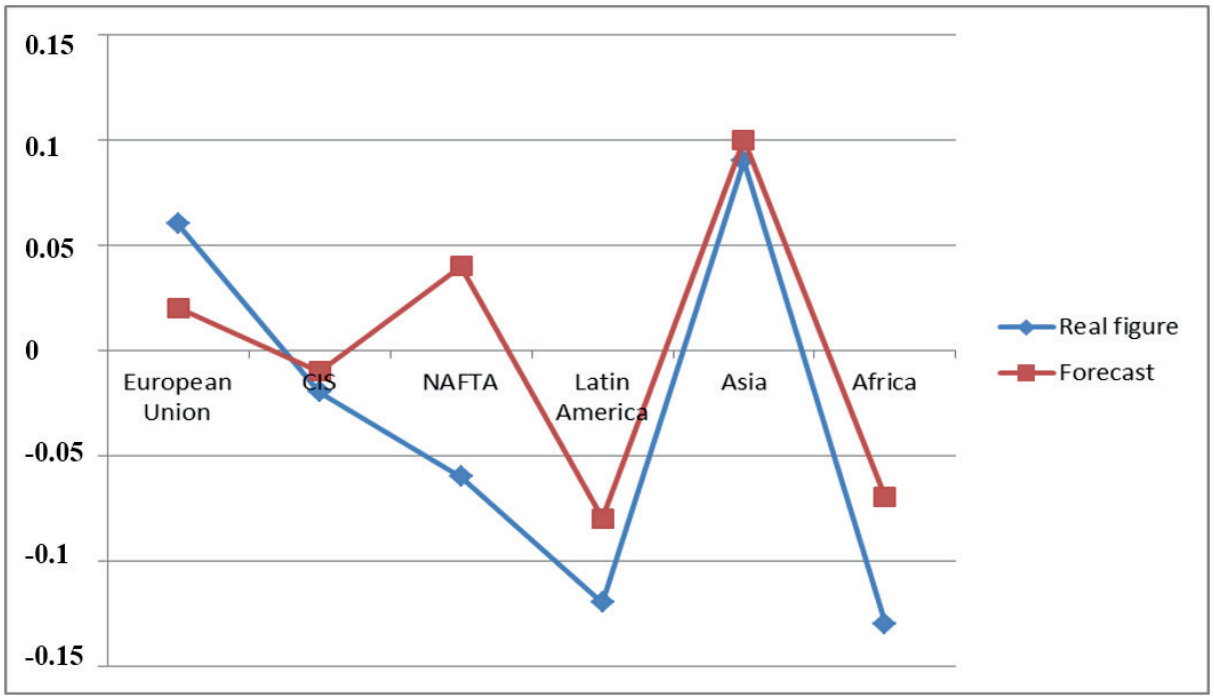


Figure 2 *Forecasting annual growth in car sales by parts of the world in 2018 according to Equation (2)*

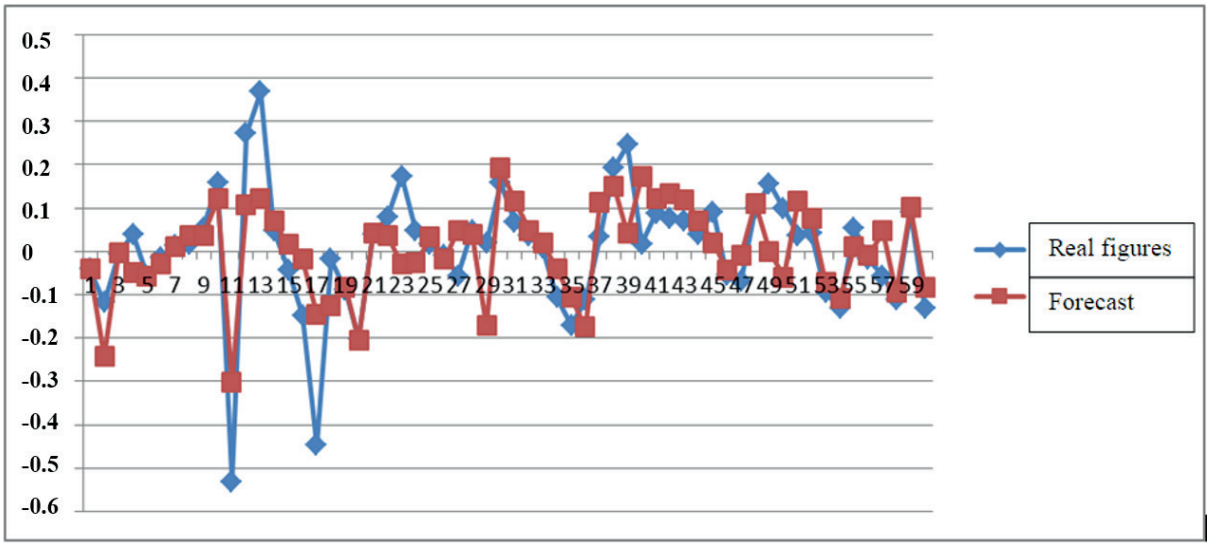


Figure 3 *Forecasting annual changes (in %) of car sales by parts of the world in the period from 2008 to 2019 according to Equation (2)*

them was made in the modelling process - the set of explanatory factors of the model was left, for which it would show the greatest accuracy in training and test data. Moreover, the coefficients of pairwise correlation between all the other relative variables (which are not presented in Table 3) were insignificant, so their combinations in the model could be anything. As a result of numerous experiments, with different composition of explanatory variables to the model of forecasting car sales considering marketing factors, it was decided to add such factors as «Inflation» and «Population expenditures, consumption» [27] to the indicator «GDP per capita". Finally, the model took the following form:

$$Y = 3.547 \cdot Z_1 - 0.459 \cdot Z_2 - 0.308 \cdot Z_3, \quad (2)$$

where

Y - annual growth in car sales, %;

Z_1 - annual change of GDP per capita, %;

Z_2 - inflation, %;

Z_3 - population expenditures, consumption, %.

Equation (2) proved to be the most effective of all the constructed with a coefficient of determination of 0.523 and an F-criterion of 18.6 at 51 degrees of freedom, that is the model is significant.

The forecast of changes in the car sales by parts of the world in 2018 relative to 2017 according to Equation (2) is shown in Figure 2.

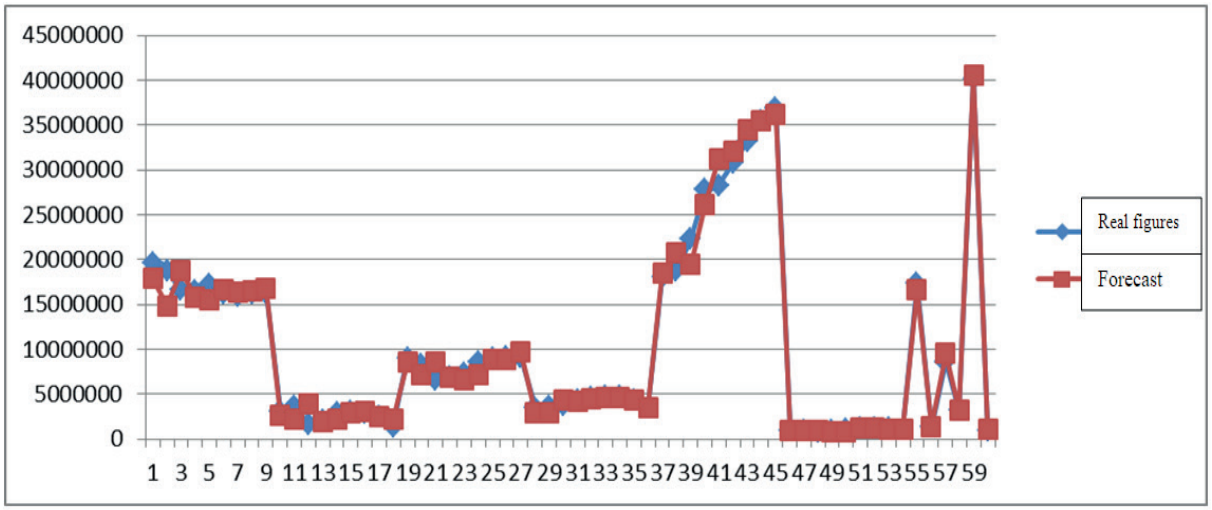


Figure 4 *Forecasting car sales by parts of the world in the period from 2008 to 2019 based on e Equation (2)*

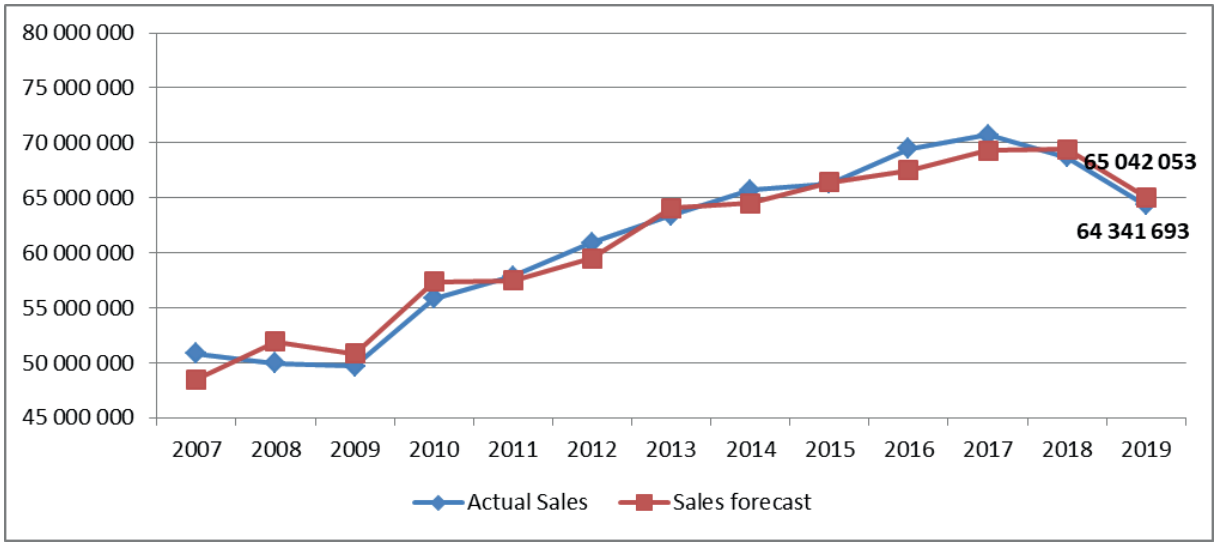


Figure 5 *Forecast and actual data on car sales in the world, 2007-2019 years*

It should be noted that Figure 2 shows the forecast on the test data of 2018, which were not used in selection of factors and optimization of Equation (2) parameters. As it can be seen from Figure 2, the model accurately predicts annual growth in car sales in almost all the parts of the world. Only for the countries of the North American Free Trade Area (NAFTA) a mistake was made in forecasting the dynamics of sales changes (in 2016 there was a decline [26], while the model predicted growth).

The forecast of changes in cars sales, according to Equation (2), for all parts of the world in the full studied time interval from 2008 to 2019 on the data of explanatory variables from 2007 to 2018, respectively, is shown in Figure 3.

When translating the relative changes in car sales projected by Equation (2). to the absolute values of sales in the period from 2008 to 2019, the graphical illustration in Figure 4 is obtained to compare the forecast to the real data.

As it can be seen from the obtained results, Equation (2) can be used as a basis for conducting a study of impact The hypothesis H_1 of this study is confirmed.

Therefore, the forecast data for the results of actual car sales in the world are presented in Figure 5. As it can be seen, the model is quite accurate, as it is possible to compare the actual data on car sales in the world in 2019 to the data of this model. The difference is only 1.01%, because according to our model, the projected sales are 65 042 053 cars, while the actual data [26] was 64 341 693 cars in 2019. So, the hypothesis H_2 of our study is also confirmed.

Firstly, the importance of «Loyalty to the brand previously owned by the consumer» should be analyzed to ensure the higher sales of cars. For this purpose, it was included in the list of explanatory variables of the model, resulting in the following dependence:

$$Y = 3.522 \cdot Z_1 - 0.419 \cdot Z_2 - 0.738 \cdot Z_3 + 0.021 \cdot Z_4, \quad (3)$$

where Z_4 - binary variable “Loyalty to the brand previously owned by the consumer”.

It should be noted that the indicators Y, Z_1, Z_2 and Z_3 in Equation (3) are the same as in Equation (2). This provides an opportunity to study the individual impact of the additionally added factor Z_4.

The coefficient of determination of Equation (3) remained almost unchanged at 0.529 and the F-criterion decreased slightly to 14.0, due to the decrease in the number of degrees of freedom to 50. However, the model remains significant. The addition of a new factor Z_4 did not change the effectiveness of the model on the training data, although the test prediction was a little more accurate, which can be concluded by comparing Figure 2 to Figure 5.

As it can be seen from the modelling results, the indicator "Loyalty to the brand previously owned by the consumer" was insignificant, which can be concluded, including the value of the coefficient 0.021 for the variable Z_4 in regression in Equation (3), as well as large, relative to this, the coefficient of the value of its standard error, which is equal to 0.026. However, the parameter 0.021 of Equation (3) of the factor Z_4 indicates that, on average, the manifestation of brand loyalty, which was previously owned by the consumer, increases the growth of car sales by 2.1%, which is quite a significant impact.

Therefore, in order to increase sales volume of its products to automotive concerns and their representative offices, it is advisable to implement a policy of maintaining loyalty to the brand, which was previously owned by the consumer.

Absolutely similar conclusions can be made about the characteristics "Preference is given to manufacturers who are localized in the region", "The younger generation is the largest consumer in the share of all consumers", "Safety", "Ecology/electric cars" and "Internet sales", after all, they repeat the value of the indicator "Loyalty to the brand previously owned by the consumer" (the coefficient of pair correlation with it is equal to +1, which can be seen from Table 3). That is, the intensification of marketing policy in the promotion of cars in each of these areas will increase sales by an average of 2.1%.

Instead, the price policy tool "Costs of ownership", associated with brand loyalty with a negative correlation of -1, while important for residents of the region reduces the demand for cars by an average of 1.9%, as it can be seen from the regression equation:

$$Y = 3.539 \cdot Z_1 - 0.279 \cdot Z_2 - 0.336 \cdot Z_3 - 0.019 \cdot Z_4, \quad (4)$$

where Z_4 - binary variable of the price policy tool "Costs of ownership".

Accordingly, in order to increase car sales, it is necessary to seek or reduce the costs of ownership, or work towards levelling the perception of this factor in the region.

Consumer advantage in the compactness of the car increases their sales by 1.1%, which can be seen from the function:

$$Y = 3.517 \cdot Z_1 - 0.445 \cdot Z_2 - 0.454 \cdot Z_3 + 0.011 \cdot Z_4, \quad (5)$$

where Z_4 - the product policy tool "Consumer advantage in the compactness of the car".

The product policy tool "Design" on average is able to reduce car sales by 0.5%, as it can be seen from the regression equation:

$$Y = 3.562 \cdot Z_1 - 0.449 \cdot Z_2 - 0.247 \cdot Z_3 - 0.005 \cdot Z_4, \quad (6)$$

where Z_4 - the tool of product policy "Design".

Most likely, the negative impact of consumer commitment to the design appearance of cars on their sales is associated with a corresponding increase in their price, which reduces the possibility of buying them.

Breadth of assortment, region coverage and digital advertising, on average, have the same positive impact on car sales at 0.8%, as can be seen from the model:

$$Y = 3.541 \cdot Z_1 - 0.473 \cdot Z_2 - 0.448 \cdot Z_3 + 0.008 \cdot Z_4, \quad (7)$$

where Z_4 - tools of product policy "Breadth of assortment", place policy "Region coverage" or promotion policy "Digital advertising".

Brand premium has a very significant negative impact on the level of car sales, which averages 2.6%, as can be seen from the equation of the forecast model:

$$Y = 3.666 \cdot Z_1 - 0.392 \cdot Z_2 - 0.175 \cdot Z_3 - 0.026 \cdot Z_4, \quad (8)$$

where Z_4 - the product policy tool "Brand premium".

From Equation (8) it can be concluded that the desire to buy premium cars significantly reduces their sales in the region as a whole, because such cars are usually more expensive and, accordingly, are bought less often and in smaller quantities. Thus, to increase car sales, it is possible to pursue a product policy aimed at reducing public perception of the benefits of brand premiums. Such research result satisfies the findings of Davvetas and Halkias [28], relationships of consumers with brands perceived as worldwide available are based on passionate feelings generated by brand competence.

Consumers' perception of the efficiency of cars has a positive effect on their sales. Thus, implementation of the product policy to accustom customers to economic cars can increase their sales by an average of 1.6%, which can be concluded from the value of the regression parameter at Z_4:

$$Y = 3.501 \cdot Z_1 - 0.526 \cdot Z_2 - 0.539 \cdot Z_3 + 0.016 \cdot Z_4, \quad (9)$$

where Z_4 - the product policy tool "Consumption level".

Regions with high sensitivity to the tool of price policy "Low price" are characterized by the low solvency of the population, due to which this factor shows a significant negative impact on car sales (at 3.6% of total sales decrease), as evidenced by the function:

$$Y = 3.715 \cdot Z_1 - 0.167 \cdot Z_2 - 0.091 \cdot Z_3 - 0.036 \cdot Z_4, \quad (10)$$

where Z_4 - the price policy tool "Low price".

That is, in those regions where the price is important, there are insignificant sales in quantity.

Introduction of such a place tool as "Personal sale", or the perception of media by population through "Radio" or "Magazines" can increase car sales by 1.2%, which can be concluded from the functional ratio:

$$Y = 3.571 \cdot Z_1 - 0.565 \cdot Z_2 - 0.377 \cdot Z_3 + 0.012 \cdot Z_4, \quad (11)$$

where Z_4 - binary variable of place tools "Personal sale", promotion tools "Radio" or "Magazines".

The importance of events highlighted by statistical data and expert assessments only for the countries of the former CIS cluster showed a negative impact of this promotion tool on car sales (- 3.1 %), which is due to the predominant decline in sales in the region during the study period, i.e. investment in the events are ineffective. The forecast model taking into account the binary variable of the promotion tool "Events" takes the following form:

$$Y = 3.532 \cdot Z_1 - 0.345 \cdot Z_2 - 0.379 \cdot Z_3 - 0.031 \cdot Z_4, \quad (12)$$

where Z_4 - the promotion tool "Events".

The importance of family and friends' recommendations reduces car sales by an average of 2%, as it can be seen from the equation:

$$Y = 3.631 \cdot Z_1 - 0.374 \cdot Z_2 - 0.145 \cdot Z_3 - 0.020 \cdot Z_4, \quad (13)$$

where Z_4 - the promotion tool "Recommendations from family and friends".

That is, the tastes of different consumers are different and recommendations from family and friends, in the authors' opinion, increase the time to make decisions about buying a car and reduce sales in a particular period of time, as the consumer hesitates and delays the purchase decision.

Increasing motivation of sellers contributes to the growth of car sales by an average of 0.8%, as it can be seen from the parameters of the model:

$$Y = 3.559 \cdot Z_1 - 0.515 \cdot Z_2 - 0.330 \cdot Z_3 + 0.008 \cdot Z_4, \quad (14)$$

where Z_4 - the human resources tool "Motivation of sellers".

Improving the qualification of sellers contributes to intensification of car sales by 1.6%, as can be seen from the equation:

$$Y = 3.527 \cdot Z_1 - 0.549 \cdot Z_2 - 0.563 \cdot Z_3 + 0.016 \cdot Z_4, \quad (15)$$

where Z_4 - the human resources tool "Qualification of sellers".

5 Discussions

The research limitations are in the studied period, which covers the 2007-2019 years period before the COVID-19 crisis and doesn't include the analysis of its impact on the global car market development. It is not recommended to include 2020 data on car sales into the constructed model of forecasting car sales, considering the marketing factors, because the situation in the car sales sector was considerably changed in 2020 because of the COVID-19 and the 2020 data will differ very much in comparison to the previous years. For example, in 2020 in comparison to 2019, the world car sales decreased -16.9% [26]. That is why the authors consider the possibility to expand this research in future taking into account some additional marketing factors arisen at the beginning of the pandemic period and construct the appropriate model that will include marketing factors typical for this period.

The Coronavirus crisis has dramatically changed the life priorities of consumers and accelerated shift from offline to online consumption [13]. Changes are also admitted by Donthu and Gustafsson study [29]: in the approach to work, business organization, business models and consumption. Some scientists [30] even consider the change of consumer behavior paradigm from consumer materialism to consumer spiritualism.

According to the McKinsey [31], the COVID-19 crisis has compelled about 95% of all German automotive-related companies to make their employees being temporarily laid off and receiving a substantial payment amount through the government. Globally, many auto-retail stores have remained closed for more than a month.

The leaders of the global automotive industry had profits decline by approximately $ 100 billion in 2020, which is equal to a roughly six-percentage-point decrease in comparison to 2018. It may take some years to recover. Based on this McKinsey research [31], the authors believe that such marketing factors as positive consumer preferences to digital sales interactions and on-demand mobility should be considered in the further studies of the marketing instruments impact on sales at the global car market.

Internet sales are one of the key marketing tools used by the car producers in their marketing policy to attract more consumers in pre-pandemic period, for which the car sales forecasting model, considering marketing factors, was created in this article. So, the authors should admit that in the post-pandemic period the impact of such marketing factor as Internet sales will increase as there is a great increase of online consumption under the influence of Coronavirus.

The other possible marketing factor for studying its impact on the global car market are the CSR (Corporate Social Responsibility) activities as the researchers got scientific findings [32] that the negative influence of

Table 4 *The impact level of marketing tools on car sales*

Tools	The impact level, %
Loyalty to the brand previously owned by the consumer	2.1
The younger generation is the largest consumer	2.1
Ecology/electric cars	2.1
Internet sales	2.1
Safety	2.1
Qualification of sellers	1.6
Consumption level	1.6
Personal sale	1.2
Radio	1.2
Magazines	1.2
Consumer advantage in the compactness of the car	1.1
Motivation of sellers	0.8
Breadth of assortment	0.8
Digital advertising	0.8
Region coverage	0.8
Design	-0.5
Costs of ownership	-1.9
Recommendations from family and friends	-2.0
Brand premium	-2.6
Low price	-3.6

recessions on the brand value can be limited by engaging in the CSR activities. That's why such marketing factors as the CSR activities is also recommended for including into further studies as one of the key modelling parameters.

6 Conclusions

The car sales forecasting model, created by the authors and estimation of the quantitative impact of marketing tools on potential sales can be used in the real marketing activities of car producers, as the model statistical error according to actual sales data in 2019 is only 1.01%. Therefore, the car producers, entering specific markets, can choose certain marketing tools in order to effectively use investments and marketing budgets according to Table 4. That is, the most effective actions can be: formation of consumer loyalty, focusing on the younger generation, production of eco- and electric cars, use of internet sales, production of safe cars, personnel qualifications and efficiency of the car, its low cost of operation. However, it should be borne in mind that these indicators may have different effects in different clusters of the world.

As it can be seen from the results, the basic model of forecasting car sales considering marketing factors in Equation (2) provides an effective instrument for studying the impact on sales of various marketing policy tools, which also confirms the hypothesis H_1 proposed by the authors. The performed calculations provide a basis for analysts and management of companies - manufacturers and sellers of cars to make rational decisions in the direction of forming a policy that can maximize car sales in different world markets. In particular, this applies to the proven hypothesis H_2, according to which the projected sales of cars in the world during 2007-2019 coincide with the actual figures (Figure 5).

In particular, using Equations (3) - (15) it is possible to determine the feasibility of introducing certain measures when entering new markets in order to increase car sales, which confirms the hypothesis H_3. For each instrument of product, price, place, promotion and human resources policy, it is possible to determine the effect specific to this region. Thus, different parts of the world are characterized by their own specific behavior of consumers and their reaction to the introduction of certain tools to promote the car brand. For each tool to which potential buyers are sensitive, the effect of its use is determined. Furthermore, taking into account this effect, it is possible to form budgets for carrying out the corresponding actions.

Thus, these models, according to the authors' opinion, allow determining the key factors influencing the volume of car sales in the forecast period, which, in turn, allows car producers to reasonably use the marketing budgets.

The impact of the COVID-19 crisis on the car sales at the global car market is recommended to be studied in

the further reasearch, paying attention to the additional marketing factors such as online consumption, online mobility and the CSR activities. Their impact has considerably increased during the pandemic period.

Reference

[1] STEENKAMP, J.-B. The uncertain future of globalization. Implications for global consumer culture and global brands. *International Marketing Review* [online]. 2019, **36**(4), p. 524-535 [accessed 2021-03-09]. ISSN 0265-1335. Available from: https://doi.org/10.1108/IMR-12-2018-0355

[2] WICAKSONO, P., PRIYADI, L., ERIZAPUTRI, S. Global production networks and social well-being: evidence from the Indonesian automobile industry. *International Journal of Business and Society* [online]. 2019, **20**(S1), p. 107-126 [accessed 2021-03-09]. ISSN 1511-6670. Available from: http://www.ijbs.unimas.my/images/repository/pdf/Vol20-S1-paper8.pdf

[3] VAN DER VOOREN, A., ALKEMADE, F., HEKKERT, M. P. Environmental performance and firm strategies in the Dutch automotive sector. *Transportation Research Part A: Policy and Practice* [online]. 2013, **54**, p. 111-126 [accessed 2021-03-09]. ISSN 0965-8564. Available from: https://doi.org/10.1016/j.tra.2013.07.005

[4] WESSELING, J. H., FARLA, J. C. M., HEKKERT, M. P. Exploring car manufacturers' responses to technology-forcing regulation: The case of California's ZEV mandate. *Environmental Innovation and Societal Transitions* [online]. 2015, **16**, p. 87-105 [accessed 2021-03-09]. ISSN 2210-4224. Available from: https://doi.org/10.1016/j.eist.2015.03.001

[5] IRAWATI, D. *Knowledge transfer in the automobile industry, global-local production networks*. London/New York: Routledge, 2013. ISBN 9780415704076.

[6] PAPOUSKOVA, K., TELECKY, M. CEJKA, J. Process efficiency analysis of selected automotive companies in Europe. *Communications - Scientific Letters of the University of Zilina* [online]. 2020, **22**(4), p. 20-27 [accessed 2021-03-14]. ISSN 1335-4205, eISSN 2585-7878. Available from: https://doi.org/10.26552/com.C.2020.4.20-27

[7] KUMAR POTDAR, P., ROUTROY, S. Performance analysis of agile manufacturing: a case study on an Indian auto component manufacturer. *Measuring Business Excellence* [online]. 2017, **21**(2), p.117-135 [accessed 2021-03-13]. ISSN 1368-3047. Available from: https://doi.org/10.1108/MBE-04-2016-0024

[8] KUMAR SHARMA, S., SINGH, R., MATAI, R. Force field analysis of Indian automotive strategic sourcing risk management enablers and barriers. *Measuring Business Excellence* [online]. 2018, **22**(3), p. 258-275 [accessed 2021-03-13]. ISSN 1368-3047. Available from: https://doi.org/10.1108/MBE-09-2017-0062

[9] KOTAK, B., KOTAK, Y. Review of European regulations and Germany's action to reduce automotive sector emissions. *European Transport* [online]. 2016, **61**, p. 1-19 [accessed 2021-03-12]. ISSN 1825-3997. Available from: http://www.istiee.unict.it/europeantransport/papers/N61/P07_61_08_2016.pdf

[10] MA, L., DU, Q., WU, T. Government intervention and automobile industry structure: theory and evidence from China. *Sustainability* [online]. 2019, **11**(17), p. 1-25 [accessed 2021-03-14]. ISSN 2071-1050. Available from: https://doi.org/10.3390/su11174721

[11] TYMOSHCHUK, M., TERLETSKA, V., FESHCHUR, R., SHYSHKOVSKYI, S., KOPYTKO, O. Model of partial economic balance of the automobile products of Ukraine. *Financial and Credit Activity: Problems of Theory and Practice* [online]. 2020, **3**(34), p. 196-206 [accessed 2021-03-10]. ISSN 306-4994, eISSN 2310-8770. Available from: https://doi.org/10.18371/fcaptp.v3i34.215509

[12] CAMPRA, M., ESPOSITO, P., BRESCIA, V. State of the art of COVID-19 and business, management and accounting. A bibliometrix analysis. *International Journal of Business and Management* [online]. 2021, **16**(1), p. 35-52 [accessed 2021-03-08]. ISSN 1833-3850, eISSN 1833-8119. Available from: https://doi.org/10.5539/ijbm.v16n1p35

[13] HOEKSTRA, J. C., LEEFLANG, P. S. H. Marketing in the era of COVID-19. *Italian Journal of Marketing* [online]. 2020, **2020**, p. 249-260 [accessed 2021-03-12]. ISSN 2662-3323, eISSN 2662-3331. Available from: https://doi.org/10.1007/s43039-020-00016-3

[14] GOSWANI, M., KUMAR, G. An investigation of agile manufacturing enablers in Indian automotive SMEs using structural equation model. *Measuring Business Excellence* [online]. 2018, **22**(3), p. 276-291 [accessed 2021-03-11]. ISSN 1368-3047. Available from: https://doi.org/10.1108/MBE-10-2017-0068

[15] EL-KHALIL, R. The mediating effect of lean management on the relationship between flexibility implementation and operational metrics in US automotive manufacturing plants. *Journal of Manufacturing Technology Management* [online]. 2018, **29**(8), p. 1741-1038X [accessed 2021-03-11]. ISSN 0148-2963. Available from: https://doi.org/10.1108/JMTM-04-2018-0108

[16] CECH, M., JANUSKA, M. Evaluation of risk management maturity in the Czech automotive industry: model and methodology. *Amfiteatru Economic* [online]. 2020, **22**(55), p. 824-845 [accessed 2021-03-08]. ISSN 1582-9146, eISSN 2247-9104. Available from: https://doi.org/10.24818/EA/2020/55/824

[17] DEMIRBAS, D., WILKINSON, L., BENNETT, D. Supplier relations impact within the UK automotive industry. *Benchmarking: An International Journal* [online]. 2018, **25**(8), p. 3143-3161 [accessed 2021-03-10]. ISSN 1463-5771. Available from: https://doi.org/10.1108/BIJ-07-2017-0172

[18] DMYTRIIEV, I., SHEVCHENKO, I., DMYTRIIEVA, O., DZHERELIUK, I., SEROHINA, T. Methodological and applied aspects of forming the competitive strategy of an enterprise based on typologization of regional markets (using the example of the automotive industry). *Financial and Credit Activity: Problems of Theory and Practice* [online]. 2020, **2**(33), p. 107-116 [accessed 2021-03-10]. ISSN 2306-4994, eISSN 2310-8770. Available from: https://doi.org/10.18371/fcaptp.v2i33.206563

[19] CHEN, J. The Chinese automobile market and the strategies of European, American, Japanese, Korean and Chinese auto makers. *International Relations and Diplomacy* [online]. 2017, **5**(5), p. 241-257 [accessed 2021-03-07]. ISSN 2328-2134. Available from: https://doi.org/10.17265/2328-2134/2017.05.001

[20] COOPER, R. G. The drivers of success in new-product development. *Industrial Marketing Management* [online]. 2018, **76**, p. 36-47 [accessed 2021-03-09]. ISSN 0019-8501. Available from: https://doi.org/10.1016/j.indmarman.2018.07.005

[21] Global automotive consumer study 2020 - Deloitte [online] [accessed 2021-03-14]. 2020. Available from: https://www2.deloitte.com/us/en/pages/manufacturing/articles/automotive-trends-millennials-consumer-study.html

[22] Global automotive consumer study 2014 - Deloitte [online] [accessed 2021-03-14]. 2014. Available from: https://www2.deloitte.com/content/dam/Deloitte/au/Documents/manufacturing/deloitte-au-mfg-2014-global-automotive-consumer-study-changing-nature-mobility-290914.pdf

[23] SAVYCH, O., SHKODA, T. The concept of marketing efforts consolidation at the global car market. In: 11th International Scientific Conference Business and Management 2020: selected papers [online] [accessed 2021-03-09]. Vilnius: Technika, 2020. ISBN 978-609-476-231-4, e-ISBN 978-609-476-230-7, p. 63-72. Available from: https://doi.org/10.3846/bm.2020.542

[24] SAVYCH, O., MOLCHANOVA, E. Modelling of global car market development under globalization impact. *Financial and Credit Activity: Problems of Theory and Practice* [online]. 2019, **3**(30), p. 273-282 [accessed 2021-03-10]. ISSN 2306-4994, ISSN 2310-8770. Available from: https://doi.org/10.18371/fcaptp.v3i30.179591

[25] SAVYCH, O. P. *Marketing on global car market* (in Ukrainian). The dissertation for getting a Doctor of Economics degree by specialty 08.00.04 - Economics and management of enterprises (by types of economics activities). Kyiv: SHEE "Kyiv National Economic University named after Vadym Hetman", 2018.

[26] Sales of new vehicles 2005-2020. Passengers Cars - International Organization of Motor Vehicle Manufacturers (OICA) [online] [accessed 2021-05-31]. 2020. Available from: http://www.oica.net/wp-content/uploads/pc_sales_2019.pdf

[27] GDP per capita - World Bank [online] [accessed 2021-03-14]. 2020. Available from: https://data.worldbank.org/indicator/NY.GDP.PCAP.CD

[28] DAVVETAS, V., HALKIAS, G. Global and local brand stereotypes: formation, content transfer and impact. *International Marketing Review* [online]. 2019, **36**(5), p. 675-701 [accessed 2021-03-09]. ISSN 0265-1335. Available from: https://doi.org/10.1108/IMR-01-2018-0017

[29] DONTHU, N., GUSTAFSSON, A. Effects of COVID-19 on business and research. *Journal of Business Research* [online]. 2020, **117**, p. 284-289 [accessed 2021-03-11]. ISSN 0148-2963. Available from: https://doi.org/10.1016/j.jbusres.2020.06.008

[30] MEHTA, S., SAXENA, T., PUROHIT, N. The new consumer behaviour paradigm amid COVID-19: permanent or transient? *Journal of Health Management* [online]. 2020, **22**(2), p. 291-301 [accessed 2021-03-14]. ISSN 0972-0634, eISSN 0973-0729. Available from: https://doi.org/10.1177/0972063420940834

[31] HOFSTATTER, T., KRAWINA, M., MUHLREITER, B., POHLER, S., TSCHIESNER, A. Reimagining the auto industry's future: it's now or never [online] [accessed 2021-03-14]. 2020. Available from: https://www.mckinsey.com/industries/automotive-and-assembly/our-insights/reimagining-the-auto-industrys-future-its-now-or-never

[32] BHATTACHARYA, A., GOOD, V., SARDASHTI, H. Doing good when times are bad: the impact of CSR on brands during recessions. *European Journal of Marketing* [online]. 2020, **54**(9), p. 2049-2077 [accessed 2021-03-07]. ISSN 0309-0566. Available from: https://doi.org/10.1108/EJM-01-2019-0088

UNIVERSITY
OF ŽILINA

In its over 65 years of successful existence, the University of Žilina (UNIZA) has become one of the top universities in Slovakia.



INAIR 2021

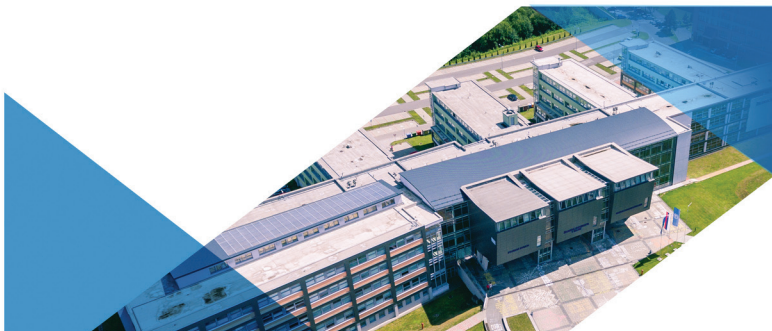
10th International Conference on Air Transport

CONFERENCE DESCRIPTION
INAIR 2021 represents a forum in which industry and academia meet to exchange their ideas, to share best practices and to set up common challenges. The interaction between researchers and industry representatives is significant in order to come up with innovative solutions for the challenges of the future in air transport.

CONFERENCE TOPICS OF INTEREST:
- Airport operation and design
- Airline operation
- Flight trainings
- afety and Security
- Air Traffic Management; air navigation services
- Human performance
- Air transportation governance, economics and policy
- Education and training
- UAVs: Development, Design, Protection and Regulation
- Aerospace engineering

VENUE & DATE
3. 11. – 4. 11. 2021
Malta
www.inair.uniza.sk

CONTACT:
UNIVERSITY OF ŽILINA
Air Transport Department
Faculty of Operation and Economics of Transport and Communications
Univerzitná 8215/1, 010 26 Žilina, Slovakia
e-mail: inair@fpedas.uniza.sk



NANOINDENTATION AS A METHOD FOR DETERMINING THE MECHANICAL PROPERTIES OF COLD SPRAY COATINGS

Medard Makrenek

Faculty of Management and Computer Modelling, Kielce, Poland

*E-mail of corresponding author: fizmm@tu.kielce.pl

Resume

The paper presents the methodology behind the statistical selection of input parameters using the example of spraying two cold-sprayed coatings. The Ti and Cr3C2-25(Ni20Cr)-Gr coatings were tested. Despite the large difference in the structure of these coatings, nanoindentation studies were carried out focusing on the nano hardness H and elastic modulus E. Based on the four input parameters and two output parameters, a 2-level factorial 2(k-p) experimental design was performed. The conducted analysis showed the significant influence of the spray distance on the H and E values in the case of the Ti coating. The input parameters of the spray distance and the type of carrier gas used turned out to be statistically significant in the case of the cermet coating. Taking into account the statistical analysis, the coatings were sprayed with modified values of the input parameters.

Article info

Received 22 October 2020
Accepted 11 January 2021
Online 23 June 2021

Keywords:

nanoindentation,
hardness,
elastic modulus,
cold spray,
2-level factorial statistics

Available online: https://doi.org/10.26552/com.C.2021.4.B250-B256

ISSN 1335-4205 (print version)
ISSN 2585-7878 (online version)

This is an open access article distributed under the terms of the Creative Commons Attribution 4.0 International License (CC BY 4.0), which permits use, distribution, and reproduction in any medium, provided the original publication is properly cited. No use, distribution or reproduction is permitted which does not comply with these terms.

1 Introduction

The basic functions of thermal spray coatings include different applications, e.g. wear-resistant and regenerating coatings [1-4]. Coatings with a thickness of a few to several mm make it possible to produce individual products, thus being classified as additive technologies [5]. Cold spraying is the latest generation of this technology and is now widely used in production engineering, as well as in implantology [6]. The basic properties connecting these coatings are the requirements related to the hardness H and elastic modulus E. In the article, $2^{(k-p)}$ optimization methods were tested for the selection of controlled parameters of the experiment to obtain high values of H and E of coatings applied with the SC technology. The problem of $2^{(k-p)}$ optimization is not often found in the literature on the CS superimposition technique. Two coatings with different microstructure were selected for the study. Nanoindentation tests were performed on these two coatings. The coatings were deposited by a cold spray process. For the tested compounds, this method ensures the absence of phase transitions during the coating application process. The material does not melt, thus minimising the influence of the process on properties of the resulting coating.

The titanium coating, applied by the cold spraying, takes over the properties of titanium. The coating is durable and resistant to various chemical and physical factors. Titanium has a low density but is stiff and resistant to corrosion. It is biologically compatible with human tissues and is neutral and harmless to them, which gives it further application possibilities. The other tested coating is made of the Cr_3C_2-25(Ni20Cr)-Gr composite powder [7]. This cermet is a good material for use in the production of machine parts or the aviation industry, improving wear parameters and reducing the impact of corrosion. The cold spray technology avoids the gradation of Cr_3C_2 carbides into soft $Cr_{23}C_6$ compounds and eliminates the influence of oxygen in the coating process [8]. The research focused on the hardness H and elastic modulus E. The parameter values, controlled by the researcher, should be indicated and their values determined so that the coating obtains its planned properties: hardness H, elastic modulus E. Values of the parameters controlled by the researcher should be indicated and their values determined so that the coating will reach its planned properties.

Nanoindentation research is an excellent tool for testing mechanical properties. This is due to the essence of the measurement technique's highly localized testing points. These tests are generally not destructive and, at the same time, enable the measurement of a diverse set of properties, including hardness and elastic modulus [9-11]. Modern testing devices enable quick measurement, which makes it possible to build maps containing from several to several dozen or even several hundred measurement points within several dozen minutes. Interpreting the results of nanoindentation requires taking various factors into account, such

as indentation spacing, strain rate effects and the indentation depth. Due to the load function of the indenter, a tester was used to measure the hardness and elastic modulus. A comprehensive approach to the problems of nanoindentation measurements is described in the work of Chromik et al. [12]. Nanoindentation research complements classical research [13].

Before qualifying the coating for technical applications, a tedious process of selecting technological (controlled) parameters was carried out. Controlled parameters are determined by the applied technique of cold spraying. In the discussed cold spraying, the controlled parameters include the temperature T, pressure p, distance d and speed of the gun V. The choice of these values determines the properties of the coating. In the present investigation, four input factors were considered as variables at two levels (low and high) to establish a 2-level factorial $2^{(k-p)}$ experimental design.

The aim of this work was to analyse the influence of input values on the output values and to modify them to obtain the best values of H and E.

2 Experimental and research

2.1 Design of experiment

Many conditions lead to different types of experimental design. It is advisable to create an experiment plan in which the main effects are not correlated with each other and, in some cases, are not correlated with interactions of the input quantities. In many cases, it can be assumed that the factors influencing the final result take only two values. Does a change in the factor value affect the final result and what is its share in the final result? The solution to this problem would be to change the input quantities values according to a complete plan, that is, to try all possible combinations of the values of the input quantities that make up the design of the experiment plan. Unfortunately, the number of necessary measurements (layouts) grows exponentially 2^n, where n is the number of input quantities. In order to test the influence of 4 input quantities, the necessary number of measurements is $2^4 = 16$. This is already a significant number of measurements. Use of the fractional designs makes it possible to reduce the number of measurements. When planning an experiment based on a $2^{(k-p)}$ fractional design, the number of input quantities to be tested, the number of plan designs and whether there is a division into blocks, should be taken into account. In addition to these basic considerations, it should also be considered whether the number of layouts would provide the required plan resolution and degree of entanglement for critical-order interactions at a given resolution.

Experiment planning allows two basic questions to be answered:

1. How should an optimal experience be planned?
2. How should the obtained research results be analysed?

In cold gas spraying processes, it is assumed that the coating property (output parameter) is related to the input factors of the spraying process by a mathematical relationship:

$$y = f(x_n), \tag{1}$$

where x_n refers to the input factors. It is important to plan the experiment with a minimum number of input factors so that the process of selecting the best output value is not complicated. It seems that the following linear function meets our expectations [14].

$$y = a_0 + a_1 x_1 + \cdots + a_n x_n, \tag{2}$$

where a_n is the linear regression coefficient and n is the number of input parameters.

In the first-order two-level programs, the input factors are normalized to two levels: upper (1) and lower (-1) and the central values are calculated as the arithmetic mean of the input factor. The significance of the coefficients was assessed with the use of ANOVA, F and P tests. The quality of the obtained results is presented in Pareto diagrams or profiles of approximated values and utility. The resulting coatings were tested for their mechanical properties by examining the nano hardness H and elastic modulus E. The research used a nano tester with a Berkovich diamond indenter (E - 1140 GPa, v_i - 0.07). The following input factors were selected for the Ti coating: temperature T [°C], pressure p [bar], distance of the spray head from the substrate d [mm] and the speed of the gun V [mm/s]. In the case of the composite coating, the following parameters were selected: graphite share u [%], gas [N_2, He], distance d [mm] and the head speed V [mm/s]. The new values of the input factors were estimated in proportion to coefficients of the linear Equation (2), determined for the nano hardness H and elastic modulus E. For example, the temperature value for the titanium coating is calculated as:

$$T_N = T_{-1} + (T_1 - T_{-1}) * a_{kN}, \tag{3}$$

$$a_{kN} = \frac{a_{kH} + a_{kE}}{\Sigma_i (a_{iH} + a_{iE})}, \tag{4}$$

where: T_N - new value of the input factor (T - temperature), a_{kH} and a_{kE} determined constants in linear equations for the nano hardness H and elastic modulus E.

2.2 Materials and processing

In this study, two coatings were made of Ti and Cr_3C_2-25(Ni20Cr)-Gr powders, which were applied by the cold spraying technology, using the Impact Innovations 5/8 system. The grain-size distribution of the powders

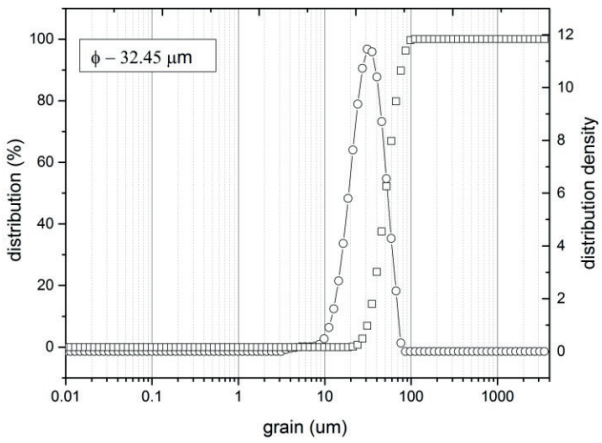


***Figure** 1 Grain size distributions of Ti. Titanium grain d_{10} = 32.06 µm, d_{50} = 51.41 µm, d_{90} = 75.07 µm*

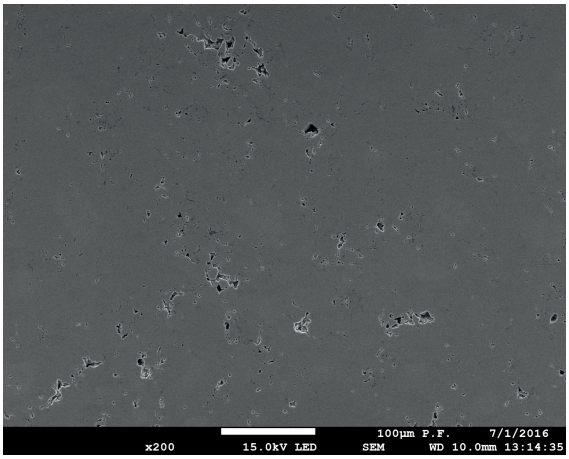


***Figure** 2 Microstructure of the titanium coating*

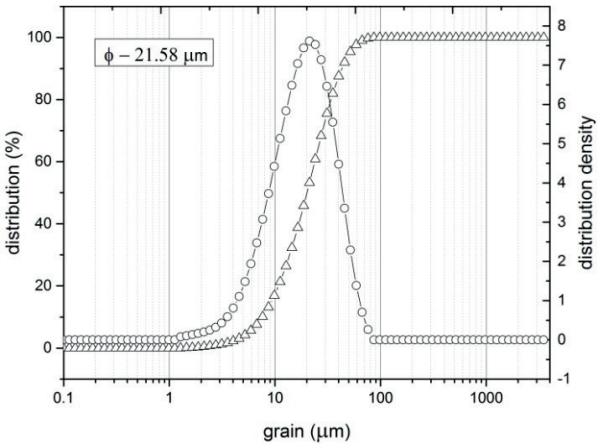


***Figure 3** Grain size distributions of Cr_3C_2-25(Ni20Cr)-Gr. Cermet grains d_{10} = 4.04 µm, d_{50} = 19.7 µm, d_{90} = 41.33 µm*

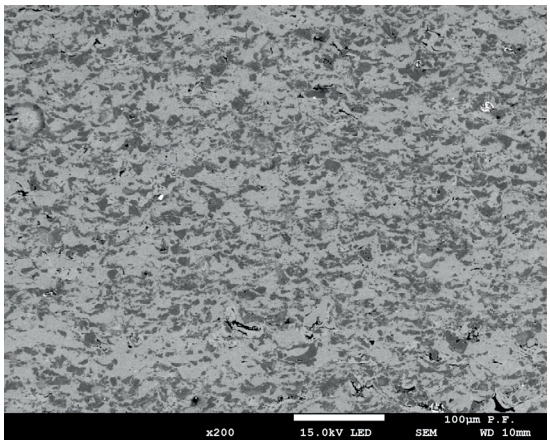


***Figure 4** Microstructure of the Cr_3C_2-25(Ni2OCr)-Gr coating*

was measured by a Malvern Mastersizer 3000 laser analyser. Substrate samples were made from a 7075 Al alloy with dimensions of 400 x 30 x 5 mm. Prior to the cold spraying, the substrate was grit-blasted. The cold-sprayed samples were deposited according to the parameters presented in Table 1 and Table 2. A scanning electron microscope (SEM - E-SEM FEI XL 30) was used to characterise the morphology of the obtained coatings. For the cross-section observations, coatings were embedded in a resin and polished using a diamond suspension. Hardness tests were performed on polished cross-sections of the sprayed coatings using a Nanovea tester with a Berkovich indenter, applying a load of 20 mN and a loading rate of 80 mN/min.

Titanium

The first coating is titanium powder, the second is Cr_3C_2-25(Ni20Cr) cermet. Figure 1 shows the particle size distribution of the powders based on which the tested coatings were formed. The dominant size of the titanium grains are grains of a diameter of 32.45 µm.

The distribution curve shows the asymmetry of the grain size distribution because d_{50} = 51.41 µm. In Figure 2 is shown a Ti coating applied using the cold spray technology. It is a single-component coating.

Cr_3C_2-25(Ni20Cr)-Gr

The distribution of the size of the studied grains and their distribution density asymmetry can be seen. The distribution density curve reaches its maximum for 21.58 µm and the d_{50} of the normal read is 19.7 µm.

Figure 4 shows a micrograph of the Cr_3C_2-25(Ni2OCr)-Gr coating micro structure. The photomicrograph clearly shows the brighter areas corresponding to Ni20Cr, while the darker areas reflect the places containing Cr_3C_2. These grains differ in hardness. The heterogeneity of the coating is significantly reflected in the values of the tested quantities H and E.

3 Experiments' design, results and discussion

In the tested titanium coating, the controlled parameters include the process temperature, gas pressure, distance from which the coating will be applied and the speed of the robot arm. The values of the control parameters influence the properties of the sprayed material. For the titanium coating, four values

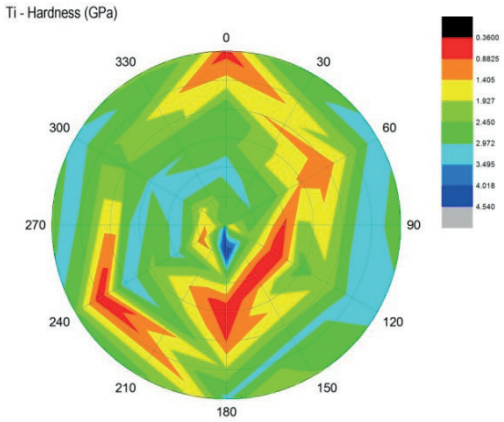


Figure 5 *Hardness map for the Ti coating obtained for the data from the second variant of the plan (Table 1)*

Table 1 *The DOE matrix for the Ti coatings deposition*

trial no.	input parameters				output parameters	
	T	p	d	V	H (GPa)	E (GPa)
1	700	30	30	300	2.5±0.2	102±9
2	800	30	30	500	2.6±0.2	95±7
3	700	45	30	500	2.3±0.3	102±12
4	800	45	30	300	2.9±0.1	151±6
5	700	30	50	500	3.0±0.1	163±7
6	800	30	50	300	2.9±0.2	163±8
7	700	45	50	300	3.0±0.1	176±7
8	800	45	50	500	3.1±0.1	151±10

were adopted from the following ranges: temperature T [°C] 700-800, pressure p [bar] 30-45, distance l [mm] 30-50 and head speed V [mm/s] 300-500.

The coatings were prepared as planned in Table 1 and then the hardness and elastic modulus were measured for each of them. Measurements were carried out on the cross-sections by performing the H and E tests. Further studies included mean values of the output parameters, which were analysed $2^{(k-p)}$. The H and E values from the measuring points formed hardness maps and elastic modulus maps, respectively. An example of a hardness map for the Ti coating obtained for the second configuration of input parameters from Table 1 is shown in Figure 5. In this figure, the dominant colour is about 2.6 GPa. Average and error values were calculated using the normal hardness distribution.

Table 1 shows the design of the experiment with the input parameter values for nano hardness H and E.

The collected results from Table 1 were analysed statistically using ANOVA and $2^{(k-p)}$. The coefficients of linear Equation (2) were calculated.

$$y = a_0 + \sum_{n=1}^{4} a_i x_i = a_0 + Tx_1 + px_2 + dx_3 + Vx_4, \quad (5)$$

where: y is output value, a_0 average value, a_i coefficients and x_i values of the input quantities.

For the Ti coating, the estimated nano hardness H value is given by the relationship:

$$H_{nano} = 2.787 + T * 0.0875 + p * 0.0375 + \\ + d * 0.125 - V * 0.0375. \quad (6)$$

Graphical presentation of the contribution of individual factors to the hardness of the coating is presented in Pareto diagram. In the cold gas spraying experiment, the distance has the greatest influence on hardness, while the temperature is slightly less influential.

The presented diagram shows the influence of the input quantities on the nano hardness of the coating. Statistical analyses showed that values of the input quantities had no significant influence on the nano painting value of the Ti coating. As can be seen from the Pareto diagram (Figure 6), the distance has the greatest influence on nano hardness, but it is not a statistically significant one (F = 8.75, p = 0.59). A similar analysis was performed by examining the elastic modulus and Figure 7 presents profiles of approximated values and utility. Similarly to the applied hardness, the distance has the greatest influence. In this case, the distance has a statistically significant effect (F = 14.58, p = 0.031).

The diagrams of Figure 7 emphasise the meaning of the input quantities values. The diagram of the utility of the distance differs the most from the level, thus it provides information about the significant influence of d on the value of the elastic modulus. The results of the above analysis reflect the coefficients in:

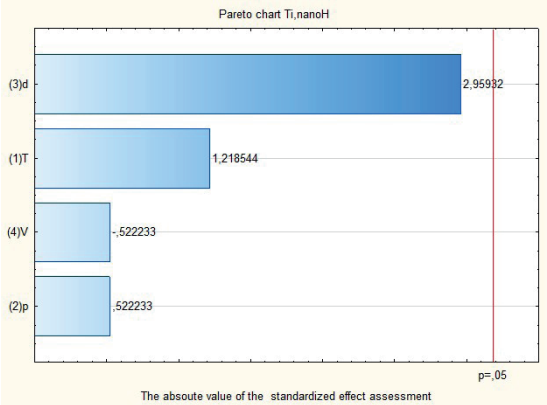


Figure 6 *The Pareto diagram for the Ti coating, nano hardness H*

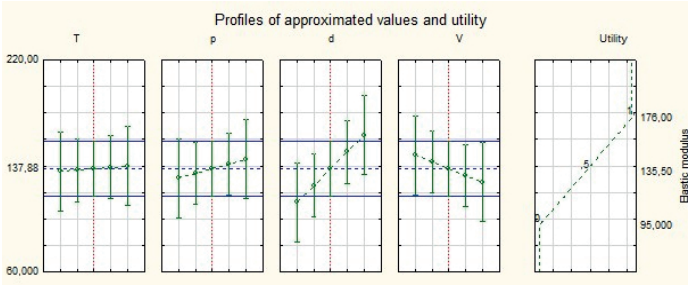


Figure 7 *Profiles of approximate values for the Ti coating including elastic modulus*

Table 2 *The DOE matrix for deposition of the Cr_3C_2-25(Ni20Cr)-Gr coatings*

trial no.	input parameters				output parameters	
	U	gas	d	V	H (GPa)	E (GPa)
1	5	N	20	200	5.1±0.4	190±15
2	15	N	20	400	5.4±0.3	188±25
3	5	He	20	400	5.2±0.5	181±19
4	15	He	20	200	5.1±0.3	130±28
5	5	N	40	400	4.6±0.6	142±15
6	15	N	40	200	5.0±0.4	116±12
7	5	He	40	200	4.1±0.5	123±19
8	15	He	40	400	3.6±0.6	143±21

$$E = 137.875 + T * 2.125 + p * 7.125 + \\ + d * 20.375 - V * 10.125. \quad (7)$$

Another input factor, influencing the output factor (E), is the speed of the spray head V. However, this effect is not statistically significant (F = 2.32, p = 0.22).

Optimisation tests for of the values cermet were carried out in a similar way, except that the input parameters were graphite by weight, gas, distance and speed of the robot arm.

The granulometry of the cermet grains is shown in Figure 3. The grains can be assigned a size of ϕ - 21.58 μm. A cermet micrograph is shown in Figure 4. Optimisation tests of the cermet coating were carried out according to the plan presented in Table 2. The last two columns of the table contain of the values mean values of nano hardness and elastic modulus calculated for 72 measurement impressions.

For the Cr_3C_2-25(Ni20Cr)-Gr coatings, the influence of individual input factors on the nano hardness H output factor is different. The type of gas used in the spraying process (F = 12.22, p = 0.030) and the distance (F = 28.17, p = 0.013) have a statistically significant influence on the nano hardness of the coating.

The equation estimating the value of nano hardness H takes the form:

$$H_{nano} = 6.912 - u * 0.062 - gas * 0.337 - \\ - d * 0.512 - V * 0.137. \quad (8)$$

A Pareto diagram (Figure 8) graphically shows influence of individual input factors on the nano hardness H of the Cr_3C_2-25(Ni20Cr)-Gr coating.

Figure 9 shows a polar map with distribution of the elastic modulus values for the cermet coating. The map was created based on 72 measurement points obtained in the first sample of the plan (Table 2).

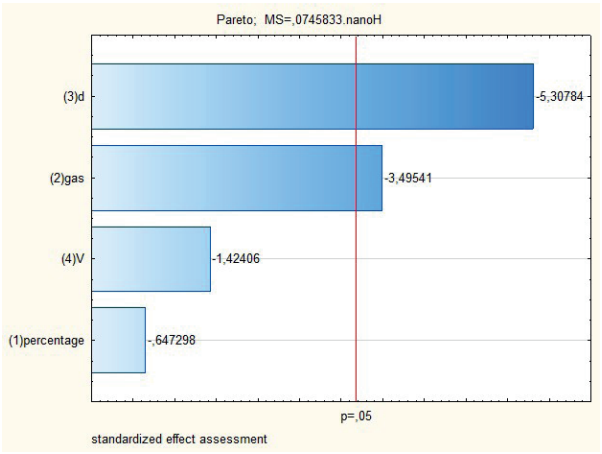


Figure 8 *Graphical presentation of influence of individual input factors on the nano hardness H of the cermet coating*

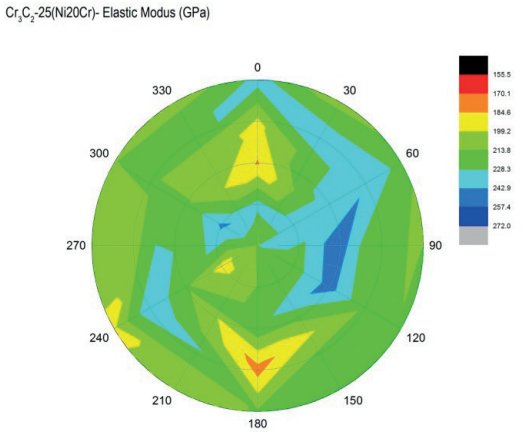


Figure 9 *Map of the elastic modulus E for the first coating of the Cr_3C_2-25(Ni20Cr)-Gr composite compound*

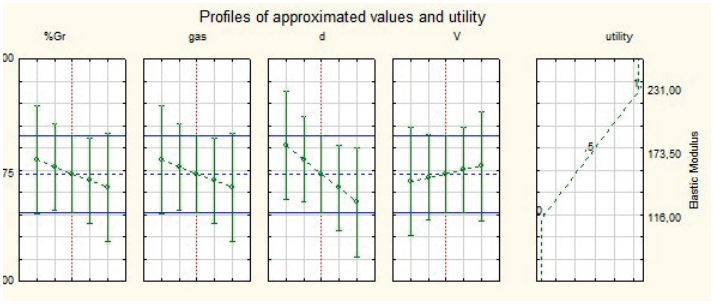


Figure 10 *Profiles of approximate values for the cermet coating including elastic modulus*

Table 3 *New input factors and corresponding output factors*

sample	new input factors				output	
Ti	T	p	d	V	H	E
	703	33	40	350	3.5±0.10	195±11
Cr_3C_2 - 25 (Ni20Cr)-Gr	u	gas	d	V	H	E
	7	78% N	29	224	5.4±0.2	235±11

The profiles of approximated values and utility of the elastic modulus E are shown in Figure 10. As in the case of nano hardness, the value of the elastic modulus is influenced the most by the distance d. In this case, the impact is significant (F = 5.6, p = 0.094).

Profiles of approximate values and utility emphasize the importance of the input values. The utility diagram d deviates the most from the level, thus it provides information about the significant influence of distance on the elastic modulus' value. The result of the above analysis is reflected in the coefficients in the equation, where the distance factor is equal to 25.75.

$$E = 943.5 - u * 12.5 - gas * 12.5 - \\ - d * 25.75 + V * 6.75. \tag{9}$$

An important element of the DOE is preparation of the optimal input parameters and verification of output parameters. Based on linear Equations (6) and (7), new values of the input factors for the titanium coating (T, p, d, V) were estimated. Equations (3) and (4) were used in the calculations. For example, the modified temperature in the Ti coating process is:

$$T_N = T_{-1} + (T_1 - T_{-1}) * a_{iN} = \\ 700 + \frac{(800 - 700) * 0.0875 + 2.125}{40.0235} \cong 703. \tag{10}$$

Calculations of the input factors for the cermet coating were performed in the same way. The calculation results are presented in Table 3.

The coatings formed from the new input factors have been tested for H and E. The results of these tests are contained in Table 3. The values of H and E for the resulting coatings are slightly greater than the values before the optimisation of input parameter values.

4 Conclusions

A factorial experimental design (DOE) was established for the principal cold spray process parameters, such as temperature, pressure, distance and speed when applying a titanium coating. In the

case of a cermet coating, the type of gas used, distance, velocities and percentage of graphite, were used. In the present investigation, the four input factors were considered as variables at two levels (low and high) to establish a 2-level factorial $2^{(k-p)}$ experimental design.

1. Based on the nanoindentation tests of the Ti coating and the correction of the input parameters, an increase in the value of H by 13 % and an increase in the value of E by 11 % in relation to the highest values of Table 1 were obtained.
2. Based on the nanoindentation tests of the Cr_3C_2-25(Ni20Cr)-Gr coating and corrections of the input parameters, an increase in the hardness value by 9 % and an increase in the E value by 23 % compared to the highest values in Table 2 were obtained.

It follows from the above that the cold gas spraying process is a complex process. For the Ti coating, the key input parameter is the distance of the spray head from the substrate (d) and for the cermet coating it is also d, as well as the used gas.

Acknowledgements

This work is supported by the National Science Centre, Poland (Project No. 2017/25/B/ST8/02228).

References

[1] PAWLOWSKI, L. *The science and engineering of thermal spray coatings*. 2. ed. Chichester: J. Willey & Sons Ltd, 2008. ISBN 0471490490.

[2] SCENDO, M., ZORAWSKI, W., STASZEWSKA, K., MAKRENEK, M., GORAL, A. Influence of surface pretreatment on the corrosion resistance of cold sprayed nickel coatings in acid chloride solution. *Journal of Materials Engineering and Performance* [online]. 2018, **27**(4), p. 1725-1737. ISSN 1059-9495. Available from: https://doi.org/10.1007/s11665-018-3298-6

[3] ZORAWSKI, W., MAKRENEK, M., GORAL, A. Mechanical properties and corrosion resistance of HVOF sprayed coatings using nanostructured carbide powders. *Archives of Metallurgy and Materials* [online]. 2016, **61**(4), p. 1839-1846. ISSN 1733-3490. Available from: https://doi.org/10.1515/amm-2016-0297

[4] OTMIANOWSKI, T., ANTOSZEWSKI, B., ZORAWSKI, W. Local laser treatment of tribological plasma sprayed coatings. In: 15th International Thermal Spray Conference: proceedings. 1998. p. 1333-1336.

[5] SILVA, F. S., CINCA, N., DOSTA, S., CANO, I. G., GUILEMANY, J. M., BENEDETTI, A. V. Cold gas spray coatings: basic principles, corrosion protection and applications. *Ecletica Química Journal* [online]. 2017, **42**, p. 9-32. ISSN 1678-4618. Available from: https://doi.org/10.26850/1678-4618eqj.v42.1.2017.p09-32

[6] MAKRENEK, M., BELKA, R., ZORAWSKI, W., KOWALSKI, SZ., SZTORC, M., GORAL, A. Physical and mechanical properties of hydroxyapatite plasma sprayed materials applied in implantology. *Medycyna Pracy* [online], 2018, **69**(6), p. 651-661. ISSN 0465-5893, eISSN 2353-1339. Available from: https://doi.org/10.13075/mp.5893.00725

[7] WOLFE, D. E., EDEN, T. J., POTTER, J. K., JAROH, A. P. Investigation and characterization of Cr3C2-based wear-resistant coatings applied by the cold spray process. *Journal of Thermal Spray Technology* [online]. 2006, **15**(3), p. 400-412. ISSN 1059-9630. Available from: https://doi.org/10.1361/105996306X124400

[8] MRDAK, M. Mechanical properties and microstructure of vacuum plasma sprayed Cr3C2-25(Ni20Cr) coatings. *Vojnotehnicki Glasnik / Military Technical Courier*. 2015, **63**(2), p. 47-63. ISSN 0042-8469, eISSN 2217-4753.

[9] PHARR, G. M., HARDING, D. S., OLIVER, W. C. Measurement of fracture toughness in thin films and small volumes using nanoindentation methods. In: *Mechanical properties and deformation behavior of materials having ultra-fine microstructures*. Nastasi, M. Parkin, D. M., Gleiter, H. (eds.). Dordrecht, the Netherlands: Kluwer Academic Publishers, 1993. ISBN 978-94-011-1765-4, p. 449-461.

[10] GORAL, A., ZORAWSKI, W., MAKRENEK, M. The effect of the standoff distance on the microstructure and mechanical properties of cold sprayed. *Surface and Coatings Technology* [online]. 2019, **361**, p. 9-18. ISSN 0257-8972. Available from: https://doi.org/10.1016/j.surfcoat.2019.01.006

[11] STEPIEN, A., SITARZ, M., LESNIAK, M. A Sustainable autoclaved material made of glass sand. *Buildings* [online]. 2019, **9**(11), 232. eISSN 2075-5309. Available from: https://doi.org/10.3390/buildings9110232

[12] CHROMIK, R. R., ZHANG, Y. Nanomechanical testing of third bodies. *Current Opinion in Solid State and Materials Science* [online]. 2018, **22**(4), p. 142-155. ISSN 1359-0286. Available from: https://doi.org/10.1016/j.cossms.2018.05.001

[13] HINTSALA, E. D., HANGEN, U., STAUFFER, D. High-throughput nanoindentation for statistical and spatial property determination. *JOM* [online]. 2018, **70**(4), p. 494-503. ISSN 1047-4838, eISSN 1543-1851. Available from: https://doi.org/10.1007/s11837-018-2752-0

[14] COOK, R. D. Detection of influential observations in linear regression. *Technometrics* [online]. 1977, **19**(1), p. 15-18. ISSN 0040-1706, eISSN 1537-2723. Available from: https://doi.org/10.1080/00401706.1977.10489493

BRICKLAYING ROBOT LIFTING AND LEVELLING SYSTEM

Piotr Wos*, Ryszard Dindorf, Jakub Takosoglu

Department of Manufacturing Engineering and Metrology,Faculty of Mechatronics and Mechanical Engineering, Kielce University of Technology, Kielce, Poland

*E-mail of corresponding author: wos@tu.kielce.pl

Resume

The article presents the concept of building and controlling a Bricklaying Robotic System (BRS). The research presents the design process and how to control a four-cylinder electro-hydraulic servo drive system. The article presents a mathematical model and optimizes the process of aligning the mobile support platform of the masonry robot. The lifting mechanism was presented and its kinematic analysis performed. The mathematical model of the hydraulic system was described. The control system, designed for the masonry robot lifting platform, includes position errors for a single drive axis and synchronization errors between the axes.

Article info

Received 17 September 2020
Accepted 26 January 2021
Online 23 June 2021

Keywords:

bricklaying robot,
electro-hydraulic servo drive,
levelling system

Available online: https://doi.org/10.26552/com.C.2021.4.B257-B264

ISSN 1335-4205 (print version)
ISSN 2585-7878 (online version)

This is an open access article distributed under the terms of the Creative Commons Attribution 4.0 International License (CC BY 4.0), which permits use, distribution, and reproduction in any medium, provided the original publication is properly cited. No use, distribution or reproduction is permitted which does not comply with these terms.

1 Introduction

The construction services market is a dynamically changing market in Europe, with a high indicator of sensitivity to economic fluctuations.The main limitations and problems associated with the traditional way of performing masonry work are: the low availability of qualified masonry brigades, timeliness and loyalty of executive resources towards the service recipient, maintaining constant accuracy and repeatability of masonry works and thus satisfactory, work pace related to efficiency, human work not supported by robotic tools. These factors cause difficulties with maintaining the schedule of works performed in accordance with the planned standard, which in the case of many investments, results in imposing financial penalties on the general contractor. The concept of a robotic masonry system for the construction services market brings a fundamental change in the specifics of the masonry services market through unique and innovative features of the system's functionality: fast masonry works in 24-hour operation - increasing the capacity of building recipients of technology, automating masonry - reducing the need for cheap employees, reducing the risk of losing contractors, reducing the cost of services, improving safety - fewer injuries and accidents, improving the accuracy of construction works and their repeatability.

Masonry works are one of the very early human craftsmanship. However, this discipline has not achieved a high degree of automation. A number of attempts were made to develop mobile construction works, the most advanced of which were the projects [1-2]. These studies date back to the early 90s of the 20th century, when the motivation for designers was to improve the efficiency and savings of building construction, mainly through the use of ability of machines to carry larger loads. These works, although very advanced, did not find full practical application because they were not flexible enough to adapt and respond to various situations occurring on the construction site. Thanks to introduction of digital technologies in architecture, research centers such as Harvard GSD, Carnegie Mellon and the University of Stuttgart have created research laboratories [3]. These centers have developed various technologies and prototype elements aimed at increasing the role of robots in construction works, in particular bricklaying. In addition, some commercial masonry works were developed, such as Hadrian and Semi Automated bricklaying robot SAM, which perform masonry processes. The common feature of these projects is that they have all tried to replace building materials with new materials that may be more suitable for the use of robots [4].

Contemporary works, intended for construction works, can be divided into several categories: remote controlled robots, which are controlled by a human using a remote control, where decisions are made by the operator based on the collected information, programmable construction machines in which the operator can choose from a function menu or teach a robot

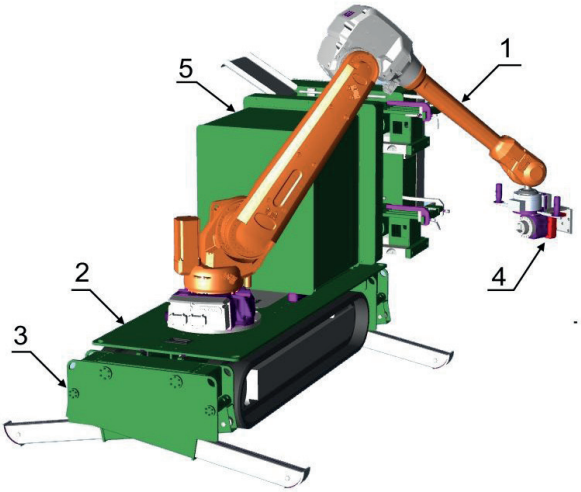


Figure1 *Model view Bricklaying Robotic System (BRS) 1 - basic robot (BR)with 6 DoF, 2 - mobile hydraulic module (MHM) 3 - support modules (SM), 4 - gripper, 5 - bricks feeder*

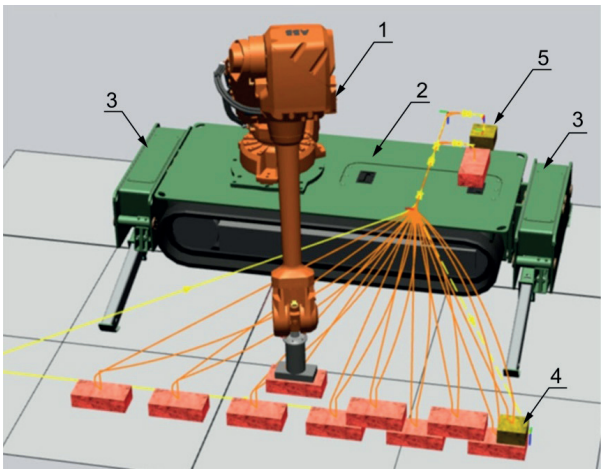


Figure 2 *Simulation tests of the bricklaying process: 1 - basic robot (BR) with 6 DoF, 2 - mobile hydraulic module (MHM) 3 - support modules (SM), 4 -.masonry wall, 5 - brick warehouse item*

to perform a new function, intelligent systems in which unmanned, fully automated construction machines perform tasks without direct human intervention. This category may also include the semi-automatic machines that are not completely unmanned and some level of human control is present.

Since the bricklaying is a repetitive process, it can easily be automated. To carry out the masonry process, the robot must detect and then take a brick from the warehouse. Then, the brick should be placed in the right position on a properly prepared base - mortar. During the capturing and laying bricks, the robot should avoid collisions with obstacles. For such a dynamic area as a construction site, obstacles detection requires the active motion planning techniques based on the real-time sensory data. In addition, the bricklaying machine must be "aware" of the progress of wall evolution. To introduce this technology during the masonry work, the following basic technical problems must be solved: robot movement along the erected wall, accurate reference of the robot working area axis relative to the entire wall (building), creating and programming complex interactions within the working area for the process collecting and laying of individual bricks, creating and programming interactions for the process of filling joints with mortar [5].

As a part of the research and development works, a design of the Bricklaying Robotic System (BRS) prototype was made (Figure 1), meeting the expectations of construction companies in the field of robotization of time-consuming and arduous manual construction works.

The Bricklaying Robotic System (BRS) consists of a basic robot (BR) (1) equipped with a gripper (4). Basic robot (BR) is placed on a Mobile Hydraulic Module (MHM) (2). The BRS is equipped with a lifting and positioning control system, as well as a control system for working movements of the basic robot. Concept of control system for levelling, as well as the system of indicators for measuring and controlling BRS work parameters, were developed. The BRS will have a feeder with a reservoir (5) for various building materials used during bricklaying, and a mortar feeder. Figure 2 shows the process of bricklaying simulation of the designed BRS prototype.

The designed BRS creates a wall 3.1 m high and 5.08 m long from one parking position.

2 Dynamic model of the MHM

Figure 3 shows the model of the Mobile Hydraulic Module (MHM). The Mobile Hydraulic Module is a support platform for further development of devices used in cooperating construction works, such as: construction manipulator, material warehouse or lifting platform. It is composed of a mobile platform, which ensures the movement of MHM and the two supporting modules (SM). Each of the supporting modules has extendable legs with a cross structure, which are lowered by means of two electro-hydraulic servo drives [6]. The main task of the platform is to move the BRS to the designated working area and then precisely raise the BRS to the desired height along with its levelling. Both of these tasks are significantly influenced by the dynamic behaviour of the mobile module itself and the mechanisms mounted on it.

Calculation diagram of the single supporting module (SM) consisting of the double-acting cylinder with one-sided piston rod and proportional directional control valve is presented in the Figure 4 [7]. The mass of the load M was placed centrally on a plane 2a wide and 2b long for simplicity.

For the module (MHM) (Figure 3) the following

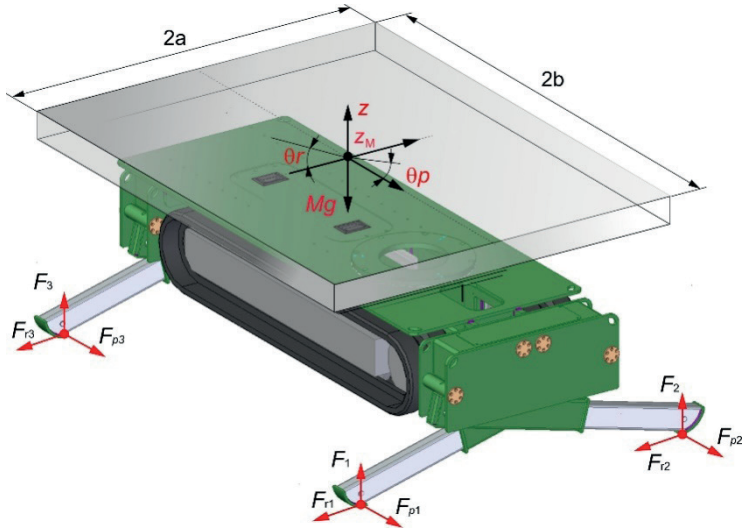


Figure 3 *Mobile Hydraulic Module (MHM)*

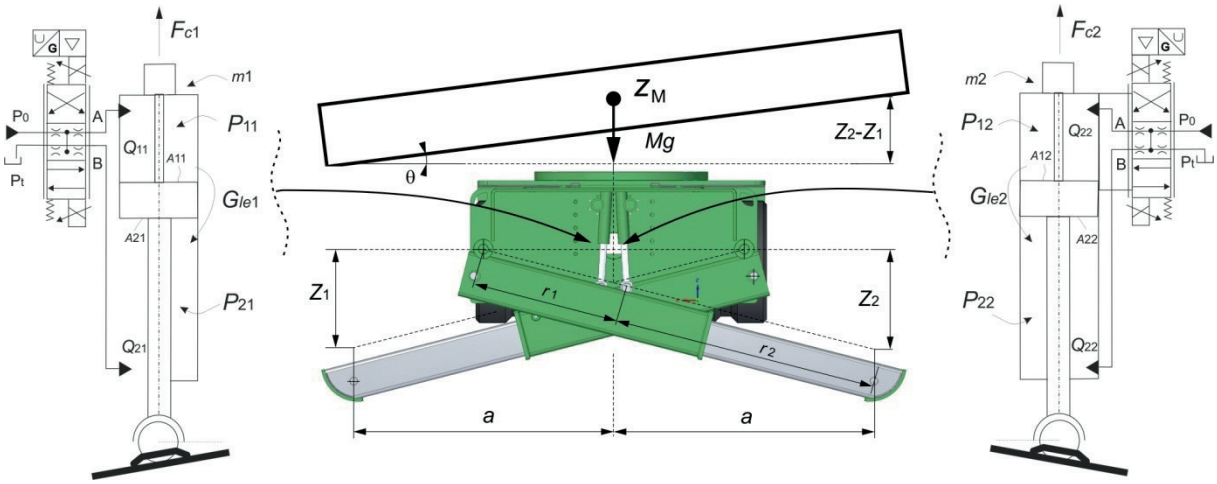


Figure 4 *Scheme of the support modules (SM) and the hydraulic cylinders: Q_{1i} - volumetric flow rate, C_{1i}, C_{2i} - fluid capacitances in the cylinder chambers, G_{lei} - coefficients of leakages in the cylinder, A_{1i}, A_{2i} - effective areas of cylinder's piston, p_{1i}, p_{2i} - pressure in individual cylinder's chambers, F_{ci} - reaction forces for electrohydraulic servo drives, m_i - the mass of the pistons, r_1, r_2 - mounting dimensions of the hydraulic cylinder and the support (legs), p_0 - supply pressure, p_T - pressure in the tank*

equations of motion along the direction of gravity and rotation around the axis X (r- roll) and Y (p- pitch) can be obtained:

$$\begin{aligned} M\ddot{z}_M &= \sum_{i=1}^{4} F_i + \sum_{i=1}^{4} F_{ri}\sin(\theta_r) + \sum_{i=1}^{4} F_{pi}\sin(\theta_p) - Mg \\ J_r\ddot{\theta}_r &= \sum_{i=1}^{4}((F_i + F_{ri}\sin(\theta_r))a_{ri} \\ J_p\ddot{\theta}_p &= \sum_{i=1}^{4}((F_i + F_{pi}\sin(\theta_p))b_{pi} \end{aligned} \quad , (1)$$

where: z_M- the coordinate determining the vertical position of the geometrical center of the platform, M - total mass of the load, g - gravitional constant, F_i, F_{ri}, F_{pi} - reaction forces for -mechanical supports (legs) for i = 1,2,...4, n = 4, a_{ri}, b_{pi} - arms' lengths for moments of forces, J_r, J_p - moments of inertia, θ_r,θ_p - angles of rotation. If one assumes that θ_r,θ_p are small, then $\sin(\theta_r) \approx 0$ and $\sin(\theta_p) \approx 0$.

Equations containing the mechanical and hydraulic variables for the single support module (SM) are described by (Figure 4):

$$\begin{aligned} F_i &= A_{1i}p_{1i} - A_{2i}p_{2i} \\ Q_{1i} &= A_{1i}\dot{z}_i + C_{1i}\dot{p}_{1i} + G_{lei}(p_{1i} - p_{2i}), i = 1,2,, \\ Q_{2i} &= A_{2i}\dot{z}_i - C_{2i}\dot{p}_{2i} + G_{lei}(p_{1i} - p_{2i}) \end{aligned} \quad (2)$$

where: Q_{1i} - volumetric flow rate, C_{1i}, C_{2i} - fluid capacitances in the cylinder chambers, G_{lei} - coefficients of leakages in the cylinder, A_{1i}, A_{2i}- effective areas of cylinder's piston, p_{1i}, p_{2i} - pressure in individual cylinder's chambers.

The hydraulic forces developed by the actuators are given by:

$$\begin{aligned} &[p_{1i}\cdot A_{1i} - p_{2i}\cdot A_{2i}] = \\ &\left[A_{1i}\cdot p_0 - A_{2i}\cdot p_T - \frac{A^3{}_{1i} + A^3{}_{2i}}{(K_1\cdot u + K_{0.1})^2}\cdot h_i^2\right], i = 1,2, \end{aligned} \quad (3)$$

where: u_i- control inputs, K_1, $K_{0.1}$ - constants factors, p_0 - supply pressure, p_T - pressure in the tank, which corresponds to the main and leakage valve flow paths.

The equation of motion of each hydraulic cylinder piston is:

$$m_i\ddot{z} = (P_{1i} - P_{2i})A_{2i} - b_i\dot{z} - F_{ci} \tag{4}$$

and the equations of motion of the support module (SM) are:

$$\begin{cases} F_1 + F_2 - Mg = M\ddot{z}_M \\ (F_1 + F_2)a = J\ddot{\theta} \end{cases}, \tag{5}$$

where: $x_M = (z_1 + z_2)/2, F_i = F_{ci}\dfrac{r_1}{(r_1 + r_2)}$ and $\theta = (z_1 - z_2)/2a$.

Due to the symmetrical shape of the MHM, it can be assumed that the center of gravity of the platform is in the middle. The system can be described by the formulas:

$$\begin{cases} M_L\ddot{z}_g = L_m G - mg \\ G = K_i(z_0 - z_i) + B_i(\dot{z}_0 - \dot{z}_i), i = 1,2,\cdots n, n = 4, \\ m\ddot{z}_L = F - G \end{cases} \tag{6}$$

where:

$G = [G_1, G_2, \cdots, G_n]^T$, is a vector of loading forces,

$z_q = [z_1, z_2, \cdots, z_n]^T$, is the platform displacement vector,

$z_h = [z_{h1}, z_{h2}, \cdots, z_{hn}]^T$, is the hydraulic cylinder displacement vector,

$L_m = \begin{bmatrix} 1 & 1 & \cdots & 1 \\ a_{r1} & a_{r2} & \cdots & a_{rn} \\ b_{p1} & b_{p2} & \cdots & b_{pn} \end{bmatrix}$, is an arm matrix with a fixed moment relative to the axis *r* (roll) and *p* (pitch),

$M = \begin{bmatrix} M \\ 0 \\ 0 \end{bmatrix}$, is a mass load matrix,

$F = MA \cdot \begin{bmatrix} A_{11} \cdot p_{11} - A_{21} \cdot p_{21} - m_1 g \\ A_{12} \cdot p_{12} - A_{22} \cdot p_{22} - m_1 g \\ A_{13} \cdot p_{13} - A_{23} \cdot p_{23} - m_1 g \\ \cdots \\ A_{1n} \cdot p_{1n} - A_{2n} \cdot p_{2n} - m_n g \end{bmatrix}$, is the matrix of forces generated by hydraulic cylinders, $MA = \dfrac{r_1}{(r_1 + r_2)}$ is a mechanical advantage.

$M_L = diag([M \;\; J_r \;\; J_p])L_{rp}^{-1}$, is the load inertia matrix,

where: $L_{rp} = \begin{bmatrix} 1 & a_{r1} & b_{p1} \\ 1 & a_{r2} & b_{p2} \\ \vdots & \vdots & \vdots \\ 1 & a_{rn} & b_{pn} \end{bmatrix}$,

$K_i = diag([k_1 \;\; k_2 \;\; \cdots \;\; k_n])$, is the contact stiffness matrix, $B_i = diag([b_1 \;\; b_2 \;\; \cdots \;\; b_n])$, is the contact viscous damping coefficient matrix.

3 Lifting process MHM

The process of extending the support module (SM) takes place in two stages: the extension of the module legs to the maximum elongation, followed by the MHM lifting process. The lifting process can be divided into three stages. The first stage occurs when the cross-drive cylinders quickly extend to the ground without load. After placing the legs on the ground, the second stage occurs, when the support cylinders synchronously extend to a certain height. This is followed by a levelling step when the MHM actuators move according to the horizontal slope relationship to complete the levelling. After thelevelling, the MHM platform is locked mechanically.

3.1 Synchronous movement

The problem of synchronization of many linear hydraulic cylinders arises in heavy, hydraulically controlled applications such as lifting devices, construction and agricultural machinery [8-9]. This problem is the most often solved by introducing an additional hydraulic resistance to each parallel actuator branch, adjusted manually or automatically. In the case of manually adjustable hydraulic resistance, this boils down to the use of a throttle valve and in the case of automatically adjustable hydraulic resistance, the use of a flow regulator. In both cases, the idea of solving the problem of motion synchronization boils down to creating additional pressure drops in the power supply branches of individual drives so that the pressure in the pump discharge line, determined from the equilibrium pressure equations arranged for the power branches of individual drives, is the same [10-12].

During the synchronization, the differential position errors between the hydraulic actuators converge to zero. The position error of *i*-th hydraulic actuator is defined as follows:

$$e_i(z) = z_i^d(t) - z_i(t), \tag{7}$$

where $z_i^d(t)$ is the desired generated length and $z_i(t)$ is the actual measured length of *i*-th hydraulic actuator.

The position error vector of four actuators is:

$$e(t) = [e_1(t), e_2(t), e_3(t), e_4(t)]^T. \tag{8}$$

If the ratio of the actual position of each hydraulic actuator at each sampling time is equal to that of all the other actuators, then the MHM moves in a synchronous manner. The synchronization goal is understood to be as follows:

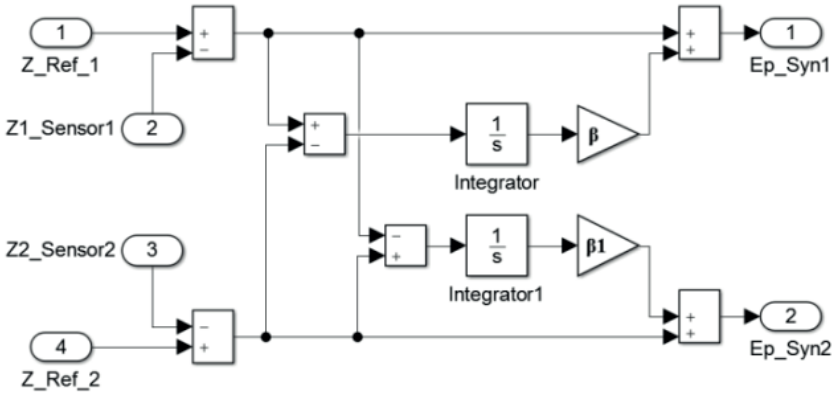


Figure 5 *Scheme of a subsystem of the synchronization controller in Matlab/Simulink*

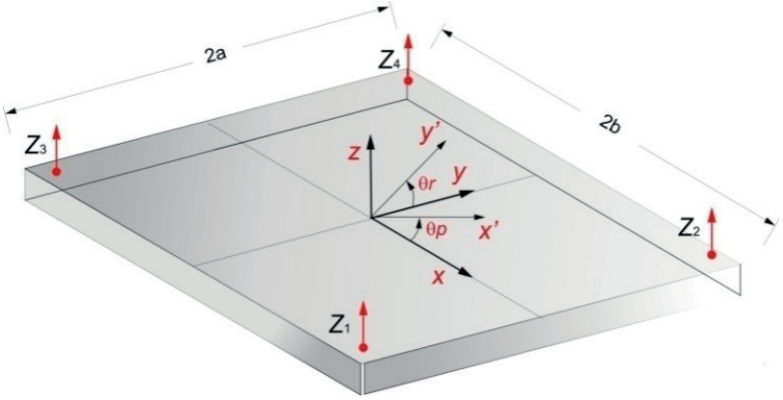


Figure 6 *Coordinate system for MHM*

$$e_1(t) = e_2(t) = e_3(t) = e_4(t). \tag{9}$$

Thus, the synchronization error is defined as:

$$\begin{cases} \varepsilon_1(t) = e_1(t) - e_2(t) \\ \varepsilon_2(t) = e_2(t) - e_3(t) \\ \varepsilon_3(t) = e_3(t) - e_4(t) \\ \varepsilon_4(t) = e_4(t) - e_1(t) \end{cases}. \tag{10}$$

The position control system is designed by combining the position error and synchronization error. Herein, in conceiving the cross-coupled controller (CCC), the cross-coupling error c_i includes the position error e_i and the synchronization error ε_i:

$$c_i(t) = e_i(t) + \beta_i \int_0^t \varepsilon_i(\omega) d\omega, \tag{11}$$

where β_i is the positive coupling parameter which, determines the weight of the synchronization error, wherein as β_i increases, the synchronization error ε_i decreases, ω is a parameter at a variable time, from $t = 0$ to t.

The position synchronization error looks for the difference between the position errors of many axes and is based on the synchronization function (12).

The block example diagram of the synchronization function designed in Matlab/Simulink is shown in Figure 5 [13].

3.2 Levelling

To obtain the relationship between the slope and displacement angles of hydraulic cylinders, it was assumed that the angle θ_p (pitch) is measured from the *X*-axis and the angle θ_r (roll) from the *Y*-axis in the direction of the *Z* axis. The purpose of levelling is to set the surface of the robot platform so that these angles are zero. The determined coordinate system is shown in Figure 6.

For this coordinate system, one can write the rotation matrices as:

$$\begin{aligned} R_x(\theta_r) &= \begin{bmatrix} 1 & 0 & 0 \\ 0 & \cos\theta_r & \sin\theta_r \\ 0 & -\sin\theta_r & \cos\theta_r \end{bmatrix}, \\ R_y(\theta_p) &= \begin{bmatrix} \cos\theta_p & 0 & \sin\theta_p \\ 0 & 1 & 0 \\ -\sin\theta_p & 0 & \cos\theta_p \end{bmatrix}. \end{aligned} \tag{12}$$

In fact, during the leveling process, the deviation in the platform level is small. With this assumption, one can determine the following relationships: $\cos\theta_r = \cos\theta_p = 1$ and $\sin\theta_r = \theta_r, \sin\theta_p = \theta_p$.

The equation for the coordinate transformation of a levelling plane is obtained as follows:

$$\begin{bmatrix} x' \\ y' \\ z' \end{bmatrix} = R_x(\theta_r) R_y(\theta_p) \begin{bmatrix} x \\ y \\ z \end{bmatrix}, \begin{bmatrix} x' \\ y' \\ z' \end{bmatrix} = \begin{bmatrix} 1 & 0 & \theta_p \\ 0 & 1 & \theta_r \\ -\theta_p & \theta_r & 1 \end{bmatrix} \begin{bmatrix} x \\ y \\ z \end{bmatrix}. \tag{13}$$

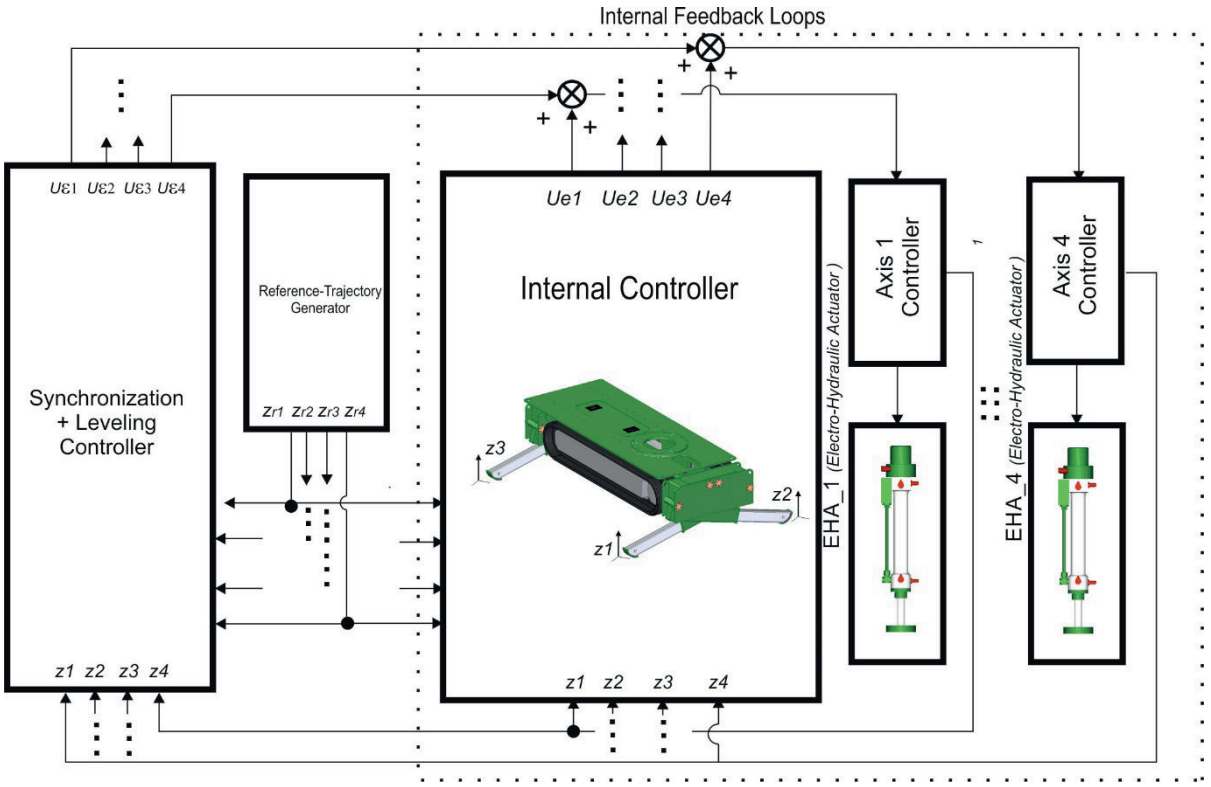


Figure 7 *The controller block diagram of the MHM with synchronization*

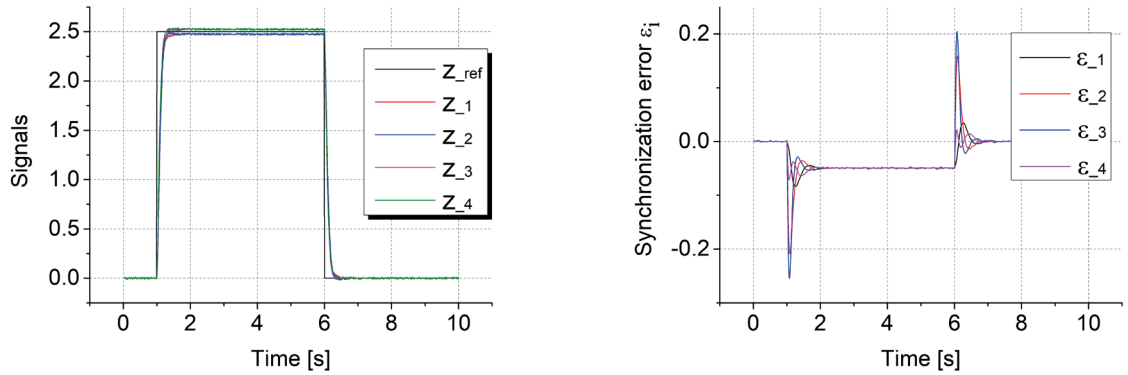


Figure 8 *Synchronization error* ε_i *for references rectangular input signals*

Table 1 *Simulation parameters*

simulation parameters	p_S (MPa)	M (kg)	A_{1i} (m²)	A_{2i} (m²)	$2a$ (mm)	$2b$ (mm)
values	16	1000	1.256 x10^{-3}	1.134 x10^{-3}	1568	2358

Each zero value of offsets z_1, z_2, z_3 and z_4 means the highest position in relation to the other legs of the supports.

$$\begin{cases} z_1 = 0, z_2 = 2a \cdot \theta_r, z_3 = -2b \cdot \theta_p, \\ z_4 = -2b \cdot \theta_p + 2a \cdot \theta_r, \\ z_1 = 2a \cdot \theta_r, z_2 = 0 \cdot \theta_r, z_3 = -2b \cdot \theta_p - 2a \cdot \theta_r, \\ z_4 = -2b \cdot \theta_p, \\ z_1 = 2b \cdot \theta_p, z_2 = 2b \cdot \theta_p + 2a \cdot \theta_r, z_3 = 0, \\ z_4 = 2a \cdot \theta_r, \\ z_1 = 2b \cdot \theta_p - 2a \cdot \theta_r, z_2 = 2b \cdot \theta_p, z_3 = -2a \cdot \theta_r, \\ z_4 = 0. \end{cases} \tag{14}$$

Figure 7 shows the control system diagram for the MHM with synchronization and levelling.

For the simulation purposes constant values of parameters were accepted and implemented (Table 1).

Figure 8 shows the diagrams of synchronization error ε_i for references rectangular input signals.

Figure 9 shows the diagrams of synchronization error ε_i for references sinusoidal input signals.

Graphs of angles θ_r (roll) and θ_p (pitch) are shown in Figure 10.

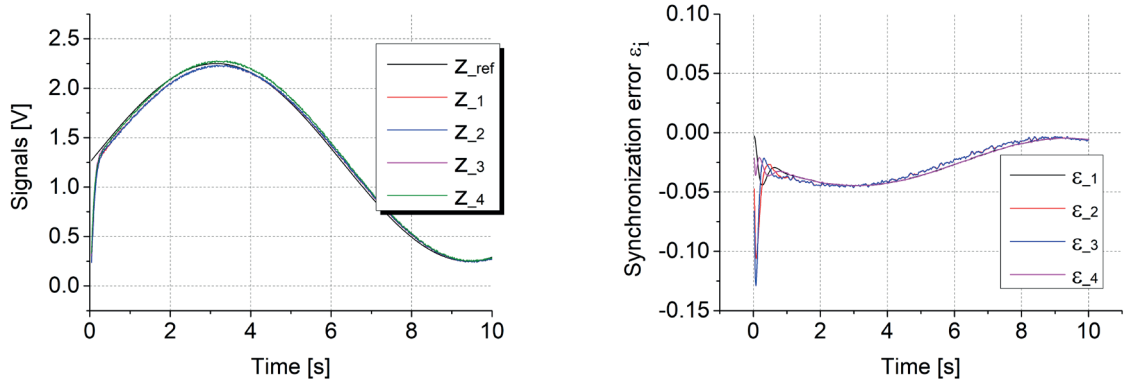


Figure 9 *Synchronization error* ε_i *for references sinusoidal input signals* z_{iref} *= 0.08 Hz*

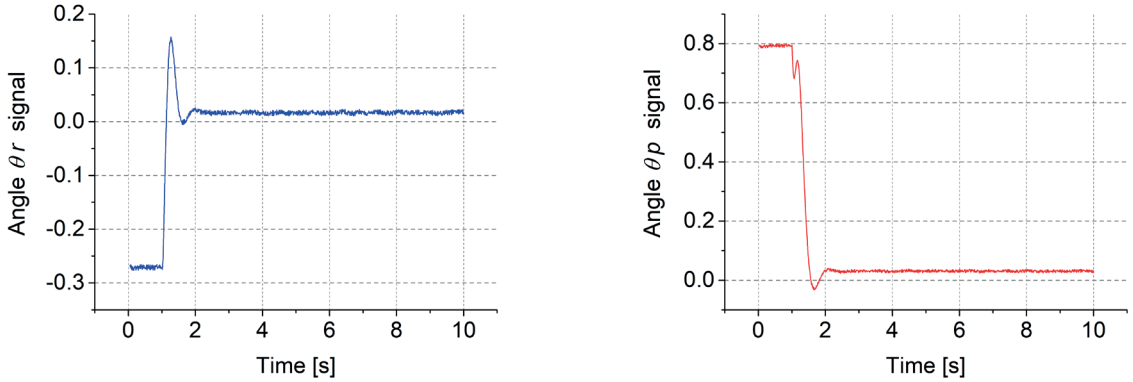


Figure 10 *Levelling angle signals:* θ_r *-roll and* θ_p *- pitch*

4 Summary

A technical solution was presented to the lifting and leveling system of the mobile hydraulic module (MHM) unit, where the electro-hydraulic control and drive systems were used. This assembly is used to displace, position and transport the Bricklaying Robotic System (BRS). A model of platform MHM dynamics was presented along with a model of hydraulic drives. A control system diagram was developed. Simulation tests were carried out to test the accepted scheme of the bricklaying robot. The presented MHM control system uses feedback from platform bracket position errors, synchronization errors and tilt angles.

Acknowledgment

This research was financially supported by The National Centre for Research and Development in Poland (Grant No. POIR.04.01.02-00-0045/18-00).

References

[1] AGUAIR, M. L., BEHDINAN, K. Design, prototyping, and programming of a bricklaying robot. *Journal of Student Science and Technology* [online]. 2015,**8**(3), p. 27-34. Available from: https://doi.org/10.13034/jsst.v8i3.92

[2] ANDRES, J., BOCK, T., GEBHART, F. First results of the development of the masonry robot system ROCCO. In: 11th International Symposium on Automation and Robotics in Construction ISARC: proceedings [online]. 1994. ISBN 9780444820440, p. 87-93. Available from:https://doi.org/10.1016/B978-0-444-82044-0.50016-3

[2] SPATH, I. D., SCHMIDT, I. J., ANDRES, D. I. J. Robot systems for residential building construction: integration and operation. In: 14th International Symposium on Automation and Robotics in Construction ISARC: proceedings [online]. 1997. p. 185-197. Available from:https://doi.org/10.22260/ISARC1997/0023

[3] HELM, V., ERCAN, S., GRAMAZIO, F., KOHLER, M. Mobile robotic fabrication on construction sites DimRob. In: IEEE/RSJ International Conference on Intelligent Robots and Systems IROS: proceedings [online]. IEEE, 2012. p. 4335-4341.Available from: https://doi.org/10.1109/IROS.2012.6385617

[5] ARDINY, H., WITWICKI, S., MONDADA, F., Are autonomous mobile robots able to take over construction? *International Journal of Robotics*. 2015, **4**(3), p. 10-21. ISSN 2008-7144.

[6] RADZYMINSKI, B., GOSZCZAK, J. Test stand for modelling hydraulically controlled continuously variable transmission, *The Archives of Automotive Engineering - Archiwum Motoryzacji* [online]. 2017, **78**(4), p. 63-77. eISSN 2084-476X.Available from: http://dx.doi.org/10.14669/AM.VOL78.ART5

[7] WOS, P., DINDORF, R. Nonlinear modeling and parameter identification for electro-hydraulic servo system. In: IEEE'2019 - 20th International Carpathian Control Conference: proceedings [online]. IEEE, 2019. p. 1-5. Available from: https://doi.org/10.1109/CarpathianCC.2019.8765947

[8] NING, S., WANG, S., Synchronization control to the hydraulic width system in hot rolling. In: IEEE2010 International Conference on Measuring Technology and Mechatronics Automation: proceedings. IEEE, 2010. p.710-713.

[9] SUN, D., Position synchronization of multiple motion axes with adaptive coupling control. *Automatica* [online]. 2003, **39**(6), p. 997-1005. ISSN 0005-1098. Available from: https://doi.org/10.1016/S0005-1098(03)00037-2

[10] DZIUBAK, T., SZCZEPANIAK, P. Model of the rate of flow of hydraulic fluid leaking through precision pairs in the electrohydraulic controller of an automatic transmission. *The Archives of Automotive Engineering - Archiwum Motoryzacji* [online]. 2017, **78**(4), p. 43-61. eISSN 2084-476X. Available from: https://doi.org/10.14669/AM.VOL78.ART3

[11] KASSEM, S., EL-DIN, T. S., HELDUSER, S., Motion synchronization enhancement of hydraulic servo cylinders for mould oscillation. *International Journal of Fluid Power*. 2012, **13**(1), p.51-60. ISSN 1439-9776, eISSN 2332-1180.

[12] LIU, Z., GAO, Q., YU, C., LI, X., GUAN, W., DENG, G., Collaborative synchronization digital control for double hydraulic cylinders. *Advances in Mechanical Engineering* [online]. 2014, **2014**(1), p. 1-18. Available from: https://doi.org/10.1155/2014/371403

[13] WOS, P, DINDORF, R. Synchronized trajectory tracking control of 3-DoF hydraulic translational parallel manipulator. In: *Mechatronics - ideas for industrial application*. *Advances in Intelligent Systems and Computing* [online]. Vol. 317. Cham: Springer, 2015. Available from: https://doi.org/10.1007/978-3-319-10990-9_24

EMISSION OF SELECTED EXHAUST GAS COMPONENTS AND FUEL CONSUMPTION IN DIFFERENT DRIVING CYCLES

Andrzej Kuranc[1,*], Jacek Caban[2], Branislav Šarkan[3], Agnieszka Dudziak[1], Monika Stoma[1]

[1]Department of Power Engineering and Transportation, Faculty of Production Engineering, University of Life Sciences in Lublin, Lublin, Poland
[2]Department of Automation, Faculty of Mechanical Engineering, Lublin University of Technology, Lublin, Poland
[3]Department of Road and Urban Transport, Faculty of Operation and Economics of Transport and Communications, University of Zilina, Zilina, Slovak Republic

*E-mail of corresponding author: andrzej.kuranc@up.lublin.pl

Resume
Road transport have significant impact on regional economic and social development, but one can also point out a number of its disadvantages, which include environmental pollution. The paper presents measurements of fumes exhaust emissions of a passenger car with a significant operational mileage. The tests were carried out in a laboratory on a chassis roller dynamometer using various driving cycles. To determine the exhaust emissions, data on the mass of air flowing through the intake manifold was used, among others. The work also describes an example of own driving cycle developed based on urban driving in Lublin, Poland.

Article info
Received 17 September 2020
Accepted 15 January 2021
Online 20 August 2021

Keywords:
exhaust emission,
internal combustion engine,
standardisation,
vehicle operation

Available online: https://doi.org/10.26552/com.C.2021.4.B265-B277

ISSN 1335-4205 (print version)
ISSN 2585-7878 (online version)

This is an open access article distributed under the terms of the Creative Commons Attribution 4.0 International License (CC BY 4.0), which permits use, distribution, and reproduction in any medium, provided the original publication is properly cited. No use, distribution or reproduction is permitted which does not comply with these terms.

1 Introduction

In addition to many positive aspects of the development in the automotive industry, one can also point out to a number of its disadvantages, which include environmental pollution. Scientists and legislators are working together to eliminate, or at least reduce, the environmental impact of vehicles. To reduce the problem of pollution from transport, the EU is introducing increasingly stringent emission standards, which should correspond to sustainable conditions of the environment during the operation of motor vehicles [1]. They are mainly concerned with the reduction of emissions of such components as: carbon monoxide, hydrocarbons, nitrogen oxides and solid particles. In Europe, Euro standards are used, which have been developed in a series of European Directives [2]. The first standard was the Euro 1 standard issued in 1993, while the latest one is Euro 6, which was introduced in 2014. The next stages of the Euro 6 standards - Euro 6B, 6C, 6D-TEMP and 6D - are increasingly raising the requirements for new engines [3]. Modern cars must emit significantly less harmful substances than vehicles from the 90s. To do that, manufacturers use, among others, AdBlue preparation, oxidation catalysts or particulate filters [4-5]. However, it turns out that the fight against one problem raises another. Recently, petrol engines are also equipped with GPF particulate filters. Unfortunately, by reducing the fuel consumption and CO_2 emissions, solutions have been introduced that have increased the amount of particulate matter emitted by petrol engines. Nowadays, there are more types of propulsions and fuels in road transport [6].

The average CO_2 emission of new cars sold in the European Union in 2018 was at the level of 120.5 g/km. From the beginning of 2020, 95% of cars sold in the European Union must meet the average maximum CO_2 emission limit of 95 g/km [7-8]. To reduce the fuel consumption and, consequently CO_2 emissions, manufacturers use the so-called downsizing or electric motors next to internal combustion ones. Downsizing is associated with use of a smaller-sized internal combustion engine, however, with similar performance parameters. That is possible mainly thanks to turbochargers or compressors [9-10]. In order to reduce emissions and effort to consume fewer non-renewable resources and use primarily raw materials of biological origin, the solution that has been used for many years is the use of alternative fuels [11-13], i.e. the use of an internal combustion engine as a dual-fuel engine [14-16]. Another solution is hybrid propulsion systems, consisting of a combustion unit and usually a supporting

electrical unit. The introduction of an electric unit allows for a temporary increase in the power of the vehicle's propulsion system while reducing fuel consumption (as well as carbon dioxide emissions).

The electric motor can support the internal combustion engine, or it can be the main one and the internal combustion engine works as a generator then. The 1997 Toyota Prius was the first car being produced on a large scale hybrid car. Other commonly available hybrid vehicles are: Honda CR-Z, Toyota Yaris, Chevrolet Volt and Opel Ampera. It is observed that the sale of electric cars is growing dynamically and the number of electric vehicles sold is doubling from year to year [17-18]. Despite the undoubted advantages concerning zero exhaust emissions at the place of use of a vehicle, or its movement dynamics, electric cars still have competition in terms of the carbon footprint. Vehicles with self-ignition engines powered by diesel fuel are again proving to be the cheapest in relation to electric vehicles, which are being charged from stations available in cities and on motorways [19]. Vehicle manufacturers, such as Mazda, are also joining the discussion, pointing out that the long distance driving can be associated with higher CO_2 emissions than using a diesel vehicle [20].

The Polish market is growing slower than in European neighboring countries [21]. There are still many proponents of combustion engine powered vehicles and it can be assumed that the electric engines will not so easily press the combustion ones out of the market. On the other hand, the increase in popularity of electric vehicles will reduce the demand for liquid fuels. This will affect their lower sales and lower revenues to the state budgets due to excise duty and that will certainly result in an increase in electricity charges.

Therefore, remaining with vehicles powered by internal combustion engines, it should be noted that many vehicles with a significant mileage, which is measured in hundreds of thousands of kilometers, are driven in Poland. The average age of a car on Polish roads in 2018 was about 14 years - according to data from the European Automobile Manufacturers Association (ACEA). The average vehicle age for European countries is 11 years. The oldest cars in the European Union run on the roads of Romania - the average age of passenger cars reaches 16 years [22]. For many vehicles with such a degree of operation, this is the time when the deficiencies of functioning fuel apparatus and exhaust after-treatment system occur [23-25].

2 Research objective

The purpose of the work was to determine the combustion ones exhaust emissions from a vehicle with a high mileage in relation to selected driving cycles, as well as based on the authors' own urban driving cycle, being a sample of traffic conditions in Lublin, Poland. The impact of the cycles on exhaust emissions and fuel consumption was assessed. The exhaust emissions tests were to assess the vehicle's technical condition in relation to emission standards for the given model.

3 Research methodology

Exhaust emission tests were carried out in the laboratory of the Department of Power Engineering and Transport Means of the University of Life Sciences in Lublin. A car equipped with a turbocharged diesel engine was tested. The vehicle participated in 4 driving cycles (3 were official cycles commonly used in vehicle testing and one was a cycle developed by the authors of the work, mapping the road conditions on a selected route in the center of Lublin). The cycles were carried out on MAHA MSR 500 single roller chassis dynamometer. The exhaust emissions tests were carried out using a simplified measurement procedure based on e use of the diagnostic tools MAHA MGT 5 gas analyzer and MAHA MPM 4 particulate emission meter. In addition, the VIAKEN diagnostic engine parameter reader/recorder and a smartphone with a GPS receiver equipped with an application for registering the distance travelled were used for the preparation of the tests.

3.1 Tested object

The object of the study was Volkswagen Golf A4 (Type 1J) manufactured in 2002 with a mileage of 312000 km (Figure 1). The vehicle was fitted with a 1.9 dm^3 direct-injection turbodiesel ASV engine of maximum torque 235 Nm at 1900 min^{-1} and maximum power output of 81 kW at 4150 min^{-1}, equipped with an exhaust gas recirculation system, variable turbine geometry (VTG) and oxidation reactor. The vehicle was adapted to comply with Euro 3 standard (Table 1). It also had a DLC connector enabling communication with OBD system and recording several data, such as engine's RPM and MAF (manifold air flow).

The technical condition of the vehicle and the engine in particular, was assumed as fair. At mileage of about 256000 km, the turbocharger was damaged. It became unsealed and the engine oil leaked into the exhaust system. Then the turbocharger was reconditioned and reinstalled. Taking into account the above mentioned situation it could be assumed that the technical condition of the catalyst was strained. The OBD system did not indicate any malfunctions and the owner of the vehicle declared that throughout the period of operation, maintenance activities had been performed on an ongoing basis and the replacement of engine oil, filters and timing components had been carried out in accordance with the recommended service schedule. At about 290000 km the exhaust braid became unsealed and then replaced. Before the driving cycle tests, dosing of the fuel injectors was checked and no deviations



Figure 1 *Tested vehicle at the test stand, source: authors*

Table 1 *Type approval emission limits for the tested vehicle, [2]*

curb mass	engine type	emission limit values, g×km^{-1}				valid from
		CO	HC	NOx	PM	
less than 2620 kg	compression ignition	0.64	0.06	0.50	0.05	01.01.2000

Table 2 *Chosen technical data of the research object*

no.	fuel consumption	directive 80/1268-1999/100 UE
1.	urban	6.5 dm^3/100 km
2.	suburban	4.0 dm^3/100 km
3.	average - combined	4.9 dm^3/100 km
4.	CO^2 emission	132 g/km
5.	emission standard	euro 3
6.	fuel	diesel fuel
7.	curb mass	1275 kg
8.	test mass	1360 kg
9.	engine model	ASV
10.	displacement	1896 cm^3
11.	cylinders	4 in line
12.	fuel injection	direct
13.	valves	8 v, SOHC
14.	maximum power	81 kW at 4150 rpm
15.	maximum torque	235 Nm at 1900 rpm
16.	gearbox	5 gears, manual
17.	drive	front wheel drive
18.	top speed	192 km/h
19.	acceleration time 0-100 km/h	11.3 s

beyond the tolerance range were found and the load tests on a chassis dynamometer showed performance results close to the values declared by the vehicle manufacturer.

Table 1 presents the type approval emission limits complied by the vehicle and the main important technical data of a vehicle are given in Table 2.

3.2 Equipment and its preparation

3.2.1 Emission measurements

For the purpose of exhaust gas study, the 5-component diagnostic gas analyser was used. Typically, such an analyser allows measurements of volumetric shares of four gaseous components such as: carbon monoxide CO, carbon dioxide CO_2, hydrocarbons HC and oxygen O_2. The used MAHA MGT5 is a "0" class by OIML (Organization Internationale de Metrologie Legale) analyser and it was additionally equipped with an electrochemical NOx concentration sensor. It was prepared to measure the rotational speed and engine oil temperature and also enabled communication with the vehicle's E-OBD module [26].

The MPM4 particulate emission meter is a device for measuring the mass concentration of particulates in a unit of exhaust gas volume. The measuring range extends from 0 to 700 mg/m^3 and the laser measuring system used in it allows detecting particles sizing from 0.1 µm to 10 µm [27]. The MPM4 was aligned with the exhaust gas analyser MGT5 and a PC.

The manufacturer of the chassis dynamometer, the analyser and particle meter also provided a possibility of their cooperation. The aforementioned instruments, including a PC and dedicated MAHA software, made up the exhaust gas composition measuring-and-recording system [28-29].

In order to determine the mass emission, information on the mass of exhaust gases or the mass of air supplying the engine was needed. For this purpose, the VIAKEN K+L diagnostic interface dedicated for VAG was used. The device allowed diagnostics of selected vehicle systems and registering chosen parameters of the vehicle's engine in driving conditions (e.g. rpm, MAF, MAP, injection dose, injection timing, etc.) [30-31].

3.2.2 Emission and fuel consumption calculations

As it was mentioned, the exhaust gas analyzer performs measurements of the volumetric shares of given fumes components. The shares, combined with information about the exhaust gas flow, can give information about the amount of a component emitted. Based on the combustion equation, described in [30], the coefficients for combustion products and their volumetric shares for each set of data recorded second by second were determined. Thanks to that, the volumetric shares of fumes components, other than measured, were determined and then transformed into the mass shares. On the other hand, the mass of fumes is the sum of the mass of the air and the fuel delivered to the combustion chamber and it can be determined by the intake manifold air flow (MAF) and the fuel injected dose. However, due to the equipment and methods used in the research, some assumptions and simplifications were required [28].

The fuel consumption can be found in two ways. The mass of the supplied fuel is 1/(λ*AFR) of the air mass. The composition of the exhaust gases can be used to determine the excess air ratio (λ) needed to calculate the fuel consumption. For the diesel fuel ($C_1H_{1.86}O_{0.005}$) and the combustion reaction for the stoichiometric mixture (λ = 1) the calculated air-fuel ratio (AFR) equals 14.46. In a compression-ignition engine, combustion is not stoichiometric (λ > 1), but it is comprehensive and total. Since, the diesel engine operates with a higher excess of air, the right value of λ can become known based on the fumes composition and Brettschneider's formula [32]. In this case the fuel consumption can be calculated as:

$$FC = \frac{MAF}{\lambda \cdot AFR}, \tag{1}$$

where:
FC - fuel consumption (g/s),
MAF - measured manifold air flow (g/s),
λ - air excess coefficient calculated by Brettschneider's formula (-),
AFR - air/fuel ratio for stoichiometric mixture (kg/kg).

Another way to evaluate the fuel consumption is based on the OBD data. Use of the OBD data, concerning the fuel injection dose and the engine's rotational speed (RPM), allows to estimate the amount of fuel being consumed. In the case of four cylinder four stroke engine, the calculation formula has the form:

$$FC = \frac{4 \cdot IQ \cdot RPM}{2 \cdot 60}, \tag{2}$$

where:
FC - fuel consumption (g/s),
IQ - fuel injection dose (g/cycle/injector),
RPM - engine's rotational speed (min^{-1}).

Equations (1) and (2) lead to results expressed in grams per cycle. To compare the results, they should be divided by the length of a given cycle in km. Dividing by the density of the diesel fuel (0.84 kg/dm^3) and multiplying by 100 leads to obtaining fuel consumption in dm^3 per 100 km.

3.2.3 Chassis dynamometer

Vehicle tests were carried out with MAHA's chassis dynamometer type MSR 500 (Figure 1). It was dedicated for vehicles with a wheel maximum power up to 250 kW. This was a single-roller stand with a drum diameter of 500 mm. The device could perform a continuous measurement of the driving force and rotational speed of the rollers driven by the vehicle wheels. At the same time, electronically controlled eddy-current brakes introduced additional load to the rollers to represent movement resistances, which are present in the road conditions [33].

Before starting the driving cycles, the load, that was to be applied by the test stand, had to be adjusted

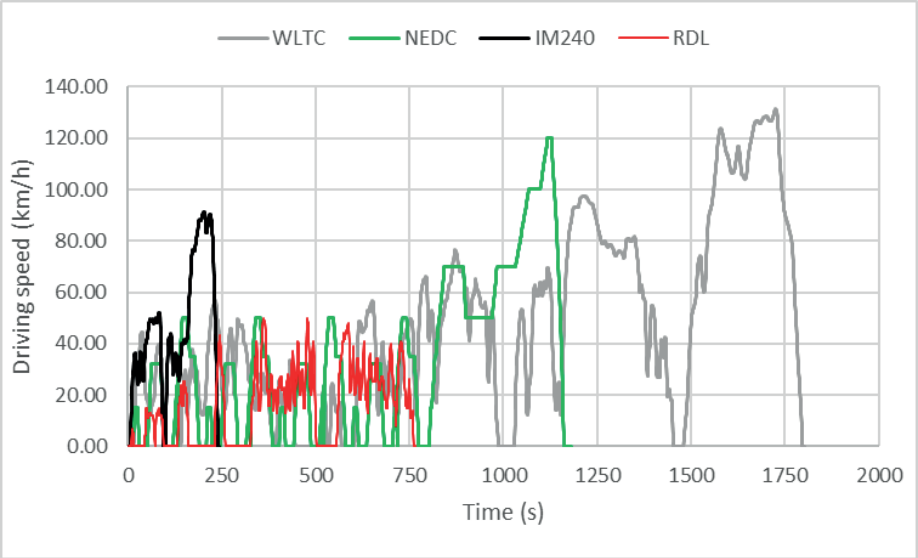


Figure 2 *Graphical comparison of utilised cycles*

Table 3 *Chosen parameters of utilized cycles*

cycle type	duration (s)	distance (m)	max speed (km/h)	aver. speed (km/h)
IM240	240	3100	91.2	47.3
NEDC	1180	11023	120	33.3
WLTC[1]	1800	23266	131.1	46.5
RDL[2]	762	3315	50.0	15.7

[1]WLTC - class 3b, [2]Real Drive Lublin, [2]

to the selected vehicle. For this purpose, the field measurements of accelerating were carried out on a flat, levelled road of a good quality asphalt surface. The tested vehicle was accelerated to a speed of approx. 115 km/h. Then the powertrain system was disconnected and the vehicle run decelerating freely. During the coast down the speed of the vehicle was being recorded. However, relating to the vehicle, test track, test speed, atmospheric conditions and measuring equipment, several requirements were to be met for carrying out the coast down tests. The tests were performed several times following the procedures described in other publications [34-36]. Based on that, it was possible to assess the mechanical condition of the vehicle, chassis settings, influence of used tires and aerodynamic properties of the vehicle's body [34].

The determined run-off times between successive speeds decreasing from 110 km/h, every 10 km/h were entered into the vehicle's data sheet in the software controlling the dynamometer. Thanks to that, the application could make the necessary calculations to determine the braking forces applied by the rollers to simulate the road movement resistances. After starting the procedure, the rollers propelled the vehicle wheels up to 110 km/h and the coast down test was performed applying the calculated resistance forces. The coasting times were measured simultaneously. During the adjustment process, the dynamometer mapped the way of loading in subsequent tests as to obtain times in accordance with previously determined in the road conditions.

3.2.4 Driving cycles

Frequently used driving cycles were selected for the studies. These were IM240, NEDC and WLTC Class 3b and one own RDL test (Real Drive Lublin) developed based on urban driving in the city of Lublin. The tests lasted from 240 to 1800 seconds and, due to the unification of the procedures, were carried out on a warm engine.

The first one - IM240 test is a schedule recommended by the US EPA for emission testing of in-use light duty vehicles in inspection & maintenance (I&M) programs. The test was formulated based on selected segments of the FTP-75 test cycle. The IM240 is a short, 240 second test representing a 3.1 km route with a maximum speed of 91.2 km/h and an average speed of 47.3 km/h [2].

The next cycle was NEDC. It used to be a reference cycle for homologating vehicles until the introduction of Euro 6 standard in Europe. It is made of an urban part called ECE, which is repeated four times and an extra-urban part, the EUDC [2]. That was the cycle used in the tested vehicle type approval procedure.

The WLTC cycles (including WLTC class 3b) are

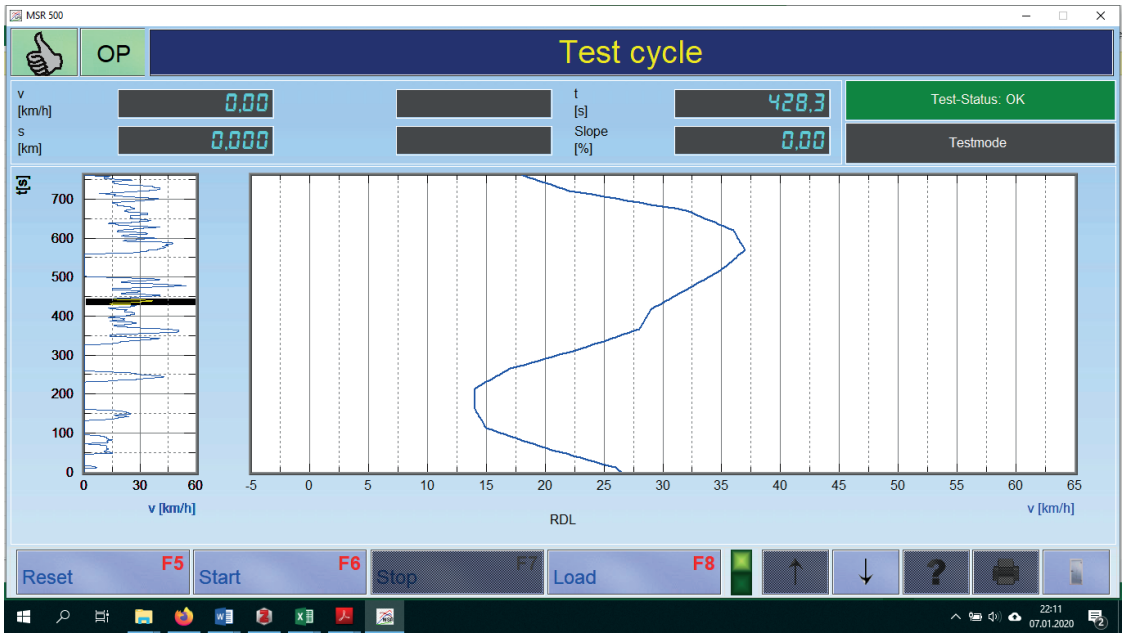


Figure 3 *Example of the speed pattern of a driving cycle*

part of the Worldwide harmonized Light vehicles Test Procedures (WLTP), published as UNECE Global technical regulation No 15. The WLTP replaces the European NEDC based procedure for type approval testing of light-duty vehicles [2, 37].

The fourth cycle was developed by the authors of the manuscript as a part of other research and was used as it represented an example of a real driving speed pattern obtained in the center of Lublin. The length of RDL was 3312 meters. The drive duration was 762 seconds and the average speed was 15.7 km/h. The route was driven twice with use of the same vehicle (VW Golf A4). The speed was recorded by a smartphone GPS receiver and VAG (Volkswagen Audi Group) interface connected by the vehicle's OBD (OnBoard Diagnosis) link connector. Then, the data was worked over and introduced into the dynamometer software.

The speed patterns of the used cycles are presented in Figure 2 and their basic data parameters are collected in Table 3. All the cycles differ according to duration, distance, maximum and average speed or stops and they also present different ways of driving.

The conduction of the tests consisted in controlling the vehicle positioned at the dynamometer in such a way that it realized the speed displayed on the screen of the stand computer. Figure 3 presents an exemplary test screen, according to which the car was to drive.

The study covered measurements and recording of the following parameters:

- volumetric shares of chosen gas components - CO carbon oxide, CO_2 carbon dioxide, O_2 oxygen, (%) and HC unburned hydrocarbons, NO_X nitrogen oxides, (ppm),
- λ air excess coefficient computed by the analyser,
- emission of particulate matter - PM (Particle Matter), ($mg \cdot m^{-3}$),
- engine rotational speed - RPM, (min^{-1}),
- engine oil temperature - T, (°C),
- manifold air flow - MAF (g/s),
- fuel dose (injection quantity/injector) - IQ (g/cycle)

The measurement results were recorded at frequency of 1 Hz. Next, the mass emission of the distinguished exhaust gas components was computed accordingly to the described earlier methodology.

4 Research results and analysis

As a result of measurements, the required parameters were recorded. Figure 4 presents an exemplary diagram (print screen) of the recorded values of volume shares of selected exhaust components, including solid particles, as a function of time for the last 250 seconds of the NEDC cycle.

4.1 Fuel consumption comparison for different cycles

The diagram (Figure 5) summarizes the fuel consumption in 4 different driving cycles with the manufacturer's data of the tested vehicle. Fuel consumption for each cycle was determined based on the emissions and simultaneously based on OBD (injection quantity) data. In three cases (NEDC, WLTC, RDL), when calculating the fuel consumption by the OBD data method, higher values were obtained than in the case of the first method. Only in the IM240 cycle the fuel consumption determined based on emissions turned out to be higher.

The measurement results for the NEDC cycle are similar to the manufacturer's data for the mixed driving

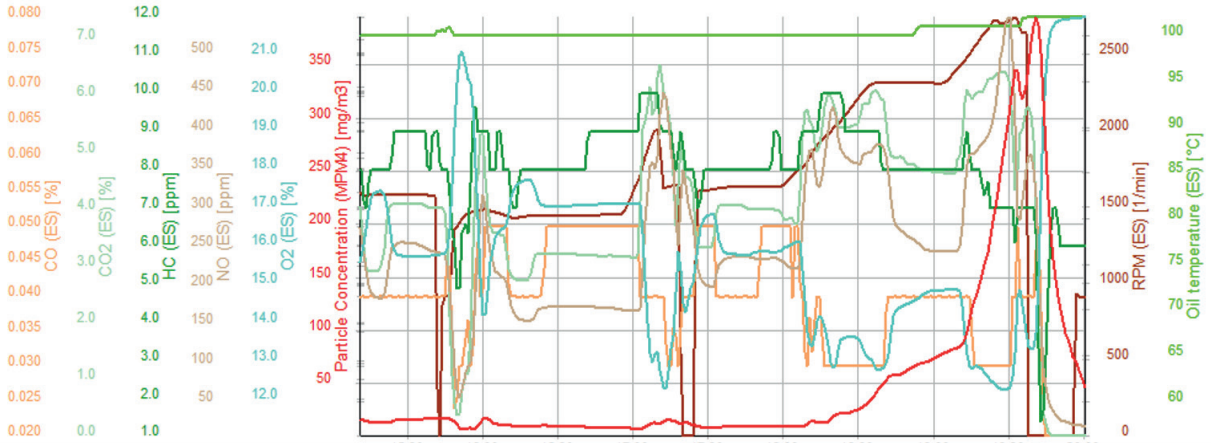


Figure 4 *Recorded emissions shares tested accordingly to NEDC*

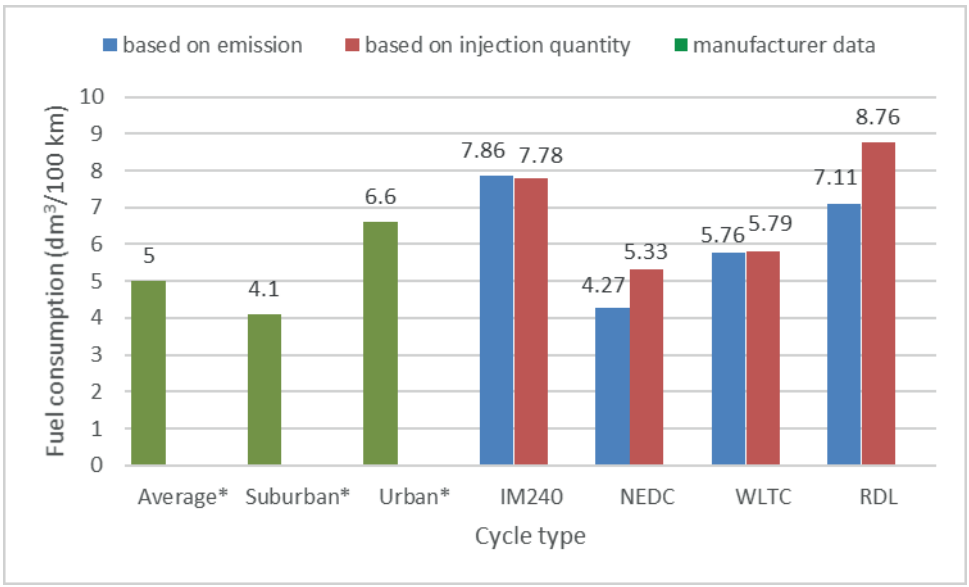


Figure 5 *Fuel consumption comparison for chosen cycles (*EU 99/100)*

patterns, while the results obtained for the WLTC (5.76 dm^3 and 5.79 dm^3) exceed the manufacturer's data. The average consumption for the WLTC cycle, which replaced the European NEDC test, is approx. 16% higher than it would appear from the vehicle manufacturer's data and approx. 18% and 9% higher than the values obtained in the NEDC tests for fuel consumption determined according to emissions and OBD, respectively. The higher fuel consumption in the WLTC cycle can be confirmed by various comparisons and the differences depending on the vehicle can reach values of up to 1.0 or 2.0 dm^3 per 100 km [38].

The authors' RDL driving test indicates even higher fuel consumption, but it is a cycle based solely on urban driving and therefore can be referred to the values indicated by the vehicle manufacturer for driving in such conditions (6.6 dm^3). Even in this comparison, the measurement result were 8% and 32% higher for emissions and OBD calculations, respectively. Similarly, the high consumption was observed for the IM240 cycle. Similar tendencies are observed in the real driving tests performed by other investigators [39-40].

4.2 Carbon dioxide emission

The tested vehicle was to emit 132 g/km of CO_2 during the type-approval test. This value was compared to emissions measured in four driving cycles. The results are presented in Figure 6. Of all the tests, CO_2 emissions closest to the values from the type-approval tests were found for the NEDC cycle measurement (Figure 6). For the WLTC cycle emissions were almost 22% higher than manufacturer's data (161 g/km in WLTC and 132 g/km by manufacturer). This result is confirmed by various tests and observations of independent centres [38, 41-42]. As might be expected, the CO_2 test results showed trends consistent with those obtained for the fuel consumption (Figure 5). In the case of the authors' RDL driving test, the emission was almost 40 g/km higher than according to the manufacturer's data.

That can find confirmation in numerous publications, the authors of which indicate the influence of the driving cycle speed profile for the energy demand of a vehicle and the resulting fuel consumption and CO_2 emissions [43-44]. Parameters, such as the average and maximum

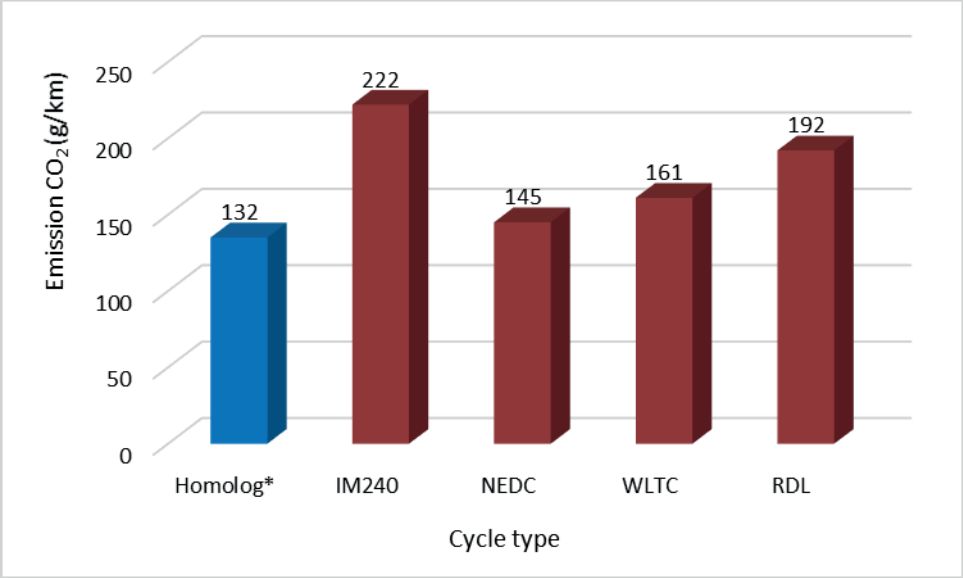


Figure 6 *Carbon dioxide emission comparison for chosen cycles*

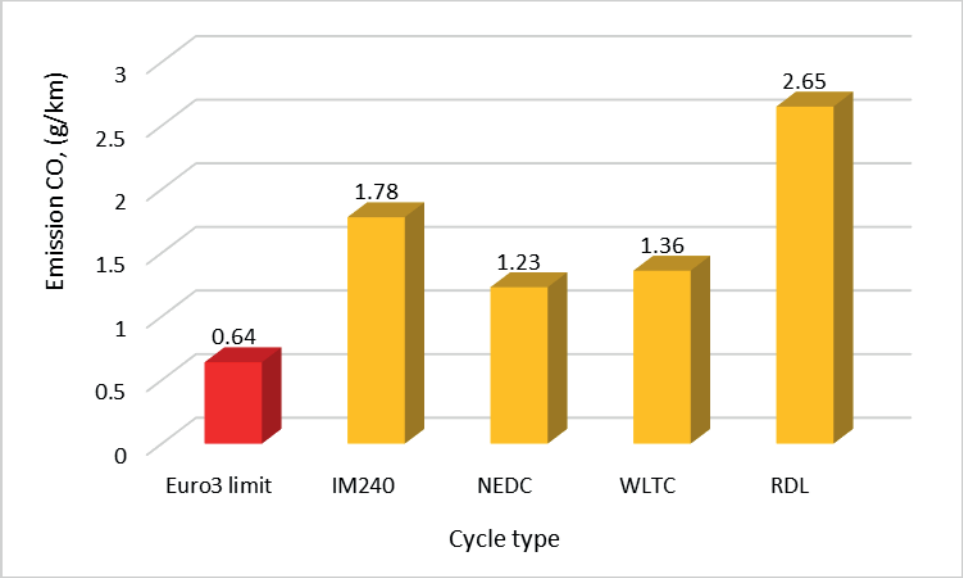


Figure 7 *Carbon monoxide emission comparison for chosen cycles*

speeds, the share and values of acceleration and deceleration in the speed profile, determine the energy demand of a vehicle necessary to drive the driving cycle. Thus, the cycle itself may cause changes in the energy and fuel consumption of the tested vehicle [45-47].

4.3 Carbon monoxide emission

According to the Euro 3 standard, a vehicle of this type can emit up to 0.64 g/km of carbon monoxide. However, for tests carried out on a given vehicle with a mileage of approximately 312000 km, the results were much higher (Figure 7).

The lowest value was obtained for the NEDC cycle (1.23 g/km), while the highest was the emission determined for the urban RDL cycle (2.65 g/km). This means that the measured values are 2 to 4 times higher than the normative data. Jaworski et al. in example of other vehicle presents problems in repeatability of the exhaust pollutant emission results [48]. However, the differences are not so significant as observed in presented in this case. Such situation may be caused rather by operational wear of the oxidation reactor, but may also be a result of malfunctions of fuel injectors or air inlet problems [49-50]. Analysing trends related to the CO emissions in individual tests, it can be concluded that the measured values show similarities to the results of the CO_2 emissions and fuel consumption measured based on the emissions.

4.4 Nitrogen oxides emission

According to the Euro 3 standard, the tested vehicle type could emit nitrogen oxides up to the level

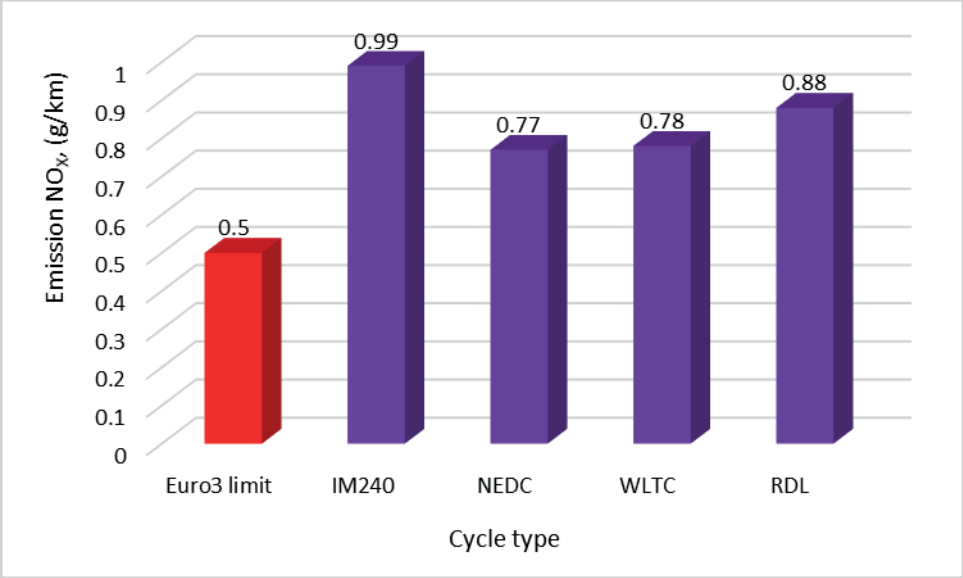


Figure 8 *Nitrogen oxides emission comparison for chosen cycles*

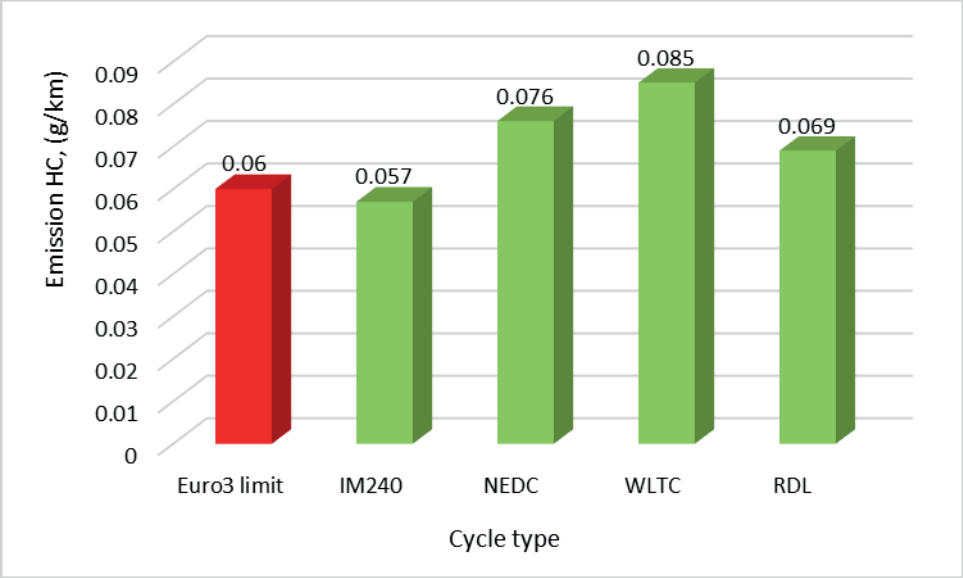


Figure 9 *Hydrocarbons emission comparison for chosen cycles*

of 0.5 g/km. All the results from the applied driving cycles were definitely higher than the permissible values. The emission of these components during the European NEDC test was 54% higher than the permissible limit according to Euro 3 (0.50 g/km - Euro 3 and 0.77 g/km - measurement according to NEDC). It can be assumed that these differences, like in the case of CO emissions, were caused by the wear of the catalytic converter or blocked EGR valve. Research of Huang at al. and other researchers confirms these assumptions [50-52]. Comparing emissions in the NEDC and WLTC cycles, a small difference (0.01 g/km more for WLTC) can be seen between them. Emission values of nitrogen oxides are shown in Figure 8, however, they are not as high in relation to the Euro 3 standard as the CO emissions.

4.5 Hydrocarbon emissions

Hydrocarbons are formed mainly as a result of incomplete combustion of fuel. They react quickly with oxygen and nitrogen compounds, which creates, among others peroxides and aldehydes.

According to the Euro 3 standard for diesel vehicles, the hydrocarbon emission should not exceed 0.06 g/km. In the case of the performed tests, such emission ranged from 0.045 g/km (RDL) to 0.085 g/km (WLTC and RDL) (Figure 9). Emissions from the NEDC test were 23% higher than emissions from the standard (0.06 g/km Euro 3 and 0.076 g/km NEDC), which may also suggest malfunctions of injectors or combustion problems combined with exhaust gas recirculation system [50]. Comparing the European NEDC test with

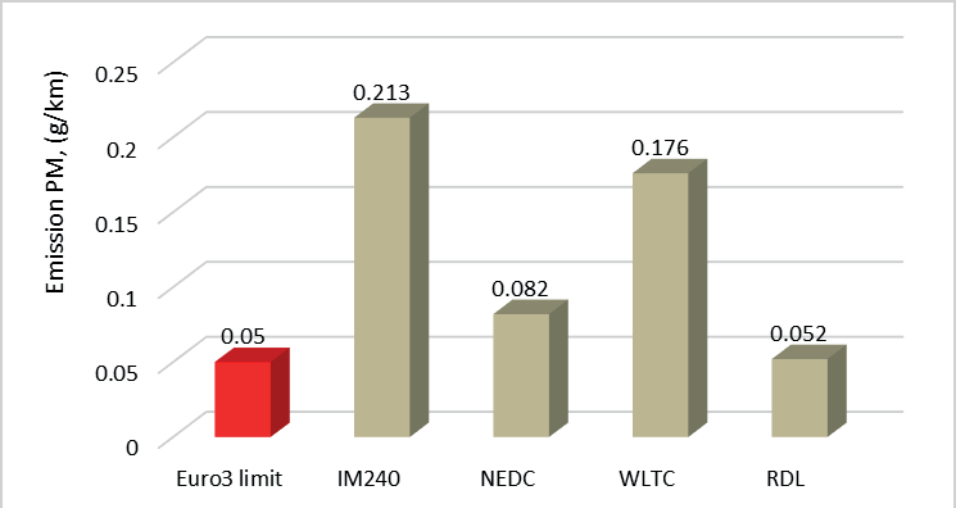


Figure 10 *Particle matter emission comparison for chosen cycles*

the new world WLTC test, it can be seen that emissions from the latter test were about 16 % higher. On the other hand, relatively low emission for the RDL cycle (0.045 g/km) was unexpected.

4.6 Particle matter emission

The PM (particle matter) are all the substances that leave the exhaust system in solid or liquid state. The high particulate emissions occur when the engine is started and its temperature is low. Increased PM emissions also occur with local oxygen deficiency, which can take place during a sharp increase of engine load and increase of fuel dose. Increased PM emissions may result from many irregularities. That can be caused by a malfunction of the oxidation catalytic converter, leaking injectors or problems with the intake and exhaust gas recirculation systems [49-50, 53].

Figure 10 shows the particulate emissions measured during the cycles. The particulate emission limit for the Euro 3 standard is 0.05 g/km. The results of all the tests exceeded the Euro 3 limit. However, there were two cycles that generated much higher values. These were IM240 and WLTC. In those cases, emissions exceeded the permissible limit of Euro 3 almost four times. The limit value was exceeded by 326 % and by 252 % for IM240 and WLTC, respectively. In the case of the NEDC test, emissions were "only" 64 % higher. In contrast, urban RDL generated the lowest amount of particles with a value of 0.052 g/km.

5 Conclusions

Based on the conducted research and evaluation of obtained results, the following conclusions can be drawn:

Fuel consumption and exhaust emissions show strong differentiation in relation to the driving cycles used in the tests.

The fuel consumption determined based on the exhaust gas emitted was, in three out of four cycles, at a lower level than calculated based on the injection injected quantity shown by the engine control unit. The highest values were found for the urban driving (RDL) at low speed and the lowest for the NEDC cycle.

The measurement results of exhaust emissions and fuel consumption for the WLTC harmonized driving test were significantly higher than for the NEDC test. This was probably due to greater speed variability in the WLTC cycle, which brings this cycle closer to the real driving conditions.

The results of emission of selected exhaust components in the analysed driving cycles in each case exceeded the values allowed by the Euro 3 standard (based on the NEDC cycle). In addition, it should be emphasized that the tests were carried out based on a vehicle that had been in operation for over 18 years, with a mileage exceeding 300000 km, which could be associated with the deficiencies of the exhaust after-treatment system.

Summing up, it should be emphasized that the exhaust emissions and fuel consumption, on the example of the tested vehicle, definitely exceed the norms. Only in the case of the NEDC cycle and two parameters, i.e. fuel consumption and carbon dioxide emissions, the values obtained were similar to those of the Euro 3 standard. However, it should be noted that the NEDC cycle was the basis for the approval tests of this vehicle. The emission of other components definitely exceeds the values specified in that standard. The reason for this may be age and thus the wear and tear of the vehicles' components.

It should be emphasized that these results apply only to this particular vehicle in a given technical condition and cannot be declared as general conclusions. However, the average car age in Poland is over fourteen years. That means that there is a serious probability of finding other vehicles in a similar technical condition that exceed the emission limits.

References

[1] TUCKI, K., MRUK, R., ORYNYCZ, O., BOTWINSKA, K., GOLA, A., BACZYK, A. Toxicity of exhaust fumes (CO, NOx) of the compression-ignition (diesel) engine with the use of simulation. *Sustainability* [online]. 2019, **11**, 2188. eISSN 2071-1050. Available from: https://doi.org/10.3390/su11082188

[2] Engine emission standards [online] [accessed 2020-01-19]. Available from: https://dieselnet.com/standards/#eu

[3] SUAREZ-BERTOA, R., VALVERDE, V., CLAIROTTE, M., PAVLOVIC, J., GIECHASKIEL, B., FRANCO, V., KREGAR, Z., ASTORGA, C. On-road emissions of passenger cars beyond the boundary conditions of the real-driving emissions test. *Environmental Research* [online]. 2019, **176**, 108572. ISSN 0013-9351. Available from: https://doi.org/10.1016/j.envres.2019.108572

[4] KURANC, A., WASILEWSKI, J.: Proecological trends in development of piston combustion engines. Diesel engines - new challenges 2010 (in Polish). Radom: Instytut Naukowo-Wydawniczy SPATIUM, 2010. p. 91-112. ISBN 978-83-928882-7-7

[5] SZPICA, D., CZABAN, J. The problems of investigations of vehicles equipped with diesel engines with FAP filter of solid particles in context of the EURO 5 standard / Problematyka badan pojazdow wyposazonych w silniki wysokoprezne z filtrami czastek stalych w kontekscie obowiazywania normy EURO 5 (in Polish). *Archiwum Motoryzacji*. 2009, **4**, p. 261-271. ISSN 1234-754X, eISSN 2084-476X.

[6] SKRUCANY, T., SEMANOVA, S., FIGLUS, T., SARKAN, B., GNAP, J. Energy intensity and GHG production of chosen propulsions used in road transport. *Communications-Scientific Letters of the University of Zilina* [online]. 2017, **19**(2), p. 3-9. ISSN 1335-4205, eISSN 2585-7878. Available from: http://komunikacie.uniza.sk/index.php/communications/article/view/174

[7] REGULATION (EU) 2019/631 OF THE EUROPEAN PARLIAMENT AND OF THE COUNCIL of 17 April 2019 - setting CO_2 emission performance standards for new passenger cars and for new light commercial vehicles and repealing Regulations (EC) No 443/2009 and (EU) No 510/2011.

[8] Exhaust emissions legislation in Europe [online] [accessed 2020-06-01]. Available from: http://vda.de

[9] SHAHED, S., BAUER, K. H. Parametric studies of the impact of turbocharging on gasoline engine downsizing. *SAE International Journal of Engines* [online]. 2009, **2**, p. 1347-1358. ISSN 1946-393, eISSN 1946-3944. Available from: https://doi.org/10.4271/2009-01-1472

[10] TURNER, J., POPPLEWELL, A., PATEL, R., JOHNSON, T., DARNTON, N., RICHARDSON, S., BREDDA, S., TUDOR, R., BITHELL, C., JACKSON, R. Ultra boost for economy: extending the limits of extreme engine downsizing. *SAE International Journal of Engines* [online]. 2014, **7**, p. 387-417. ISSN 1946-393, eISSN 1946-3944. Available from: https://doi.org/10.4271/2014-01-1185

[11] GARDYNSKI, L., KALDONEK, J. Research on lubrication properties of selected raw plant and animal materials. *Transport* [online]. 2020, **35**, p. 20-25. ISSN 1648-4142, eISSN 1648-3480. Available from: https://doi.org/10.3846/transport.2020.11961

[12] MAKAREVICIENE, V., MATIJOSIUS, J., PUKALSKAS, S., VEGNERIS, R., KAZANCEVA, I., KAZANCEV, K. The exploitation and environmental characteristics of diesel fuel containing rapeseed butyl esters. *Transport* [online]. 2013, **28**, p. 158-165. ISSN 1648-4142, eISSN 1648-3480. Available from: https://doi.org/10.3846/16484142.2013.801364

[13] ZDZIENNICKA, A., SZYMCZYK, K., JANCZUK, B., LONGWIC, R., SANDER, P. Surface, volumetric and wetting properties of oleic, linoleic and linolenic acids with regards to application of canola oil in diesel engines. *Applied Sciences* [online]. 2019, **9**(17), 3445. eISSN 2076-3417. Available from: https://doi.org/10.3390/app9173445

[14] LEBEDEVAS, S., PUKALSKAS, S., DAUKSYS, V., RIMKUS, A., MELAIKA, M., JONIKA, L. Research on fuel efficiency and emissions of converted diesel engine with conventional fuel injection system for operation on natural gas. *Energies* [online]. 2019, **12**, 2413. eISSN 1996-1073. Available from: https://doi.org/10.3390/en12122413

[15] LEBEDEVAS, S., PUKALSKAS, S., ZAGLINSKIS, J., MATIJOSIUS, J. Comparative investigations into energetic and ecological parameters of camelina-based biofuel used in the 1Z diesel engine. *Transport* [online]. 2012, **27**, p. 171-177. ISSN 1648-4142, eISSN 1648-3480. Available from: https://doi.org/10.3846/16484142.2012.694078

[16] MIKULSKI, M., BALAKRISHNAN, P. R., HUNICZ, J. Natural gas-diesel reactivity controlled compression ignition with negative valve overlap and in-cylinder fuel reforming. *Applied Energy* [online]. 2019, **254**, 113638. ISSN 0306-2619. Available from:10.1016/j.apenergy.2019.113638

[17] Electric car sales results in Europe (Q1 2019) / Wyniki sprzedazy samochodow elektrycznych w Europie (I kwartal 2019) - Electric cars / Samochody elektryczne (in Polish) [online] [accessed 2020-06-01]. Available from: https://elektrowoz.pl/auta/wyniki-sprzedazy-samochodow-elektrycznych-w-europie-i-kwartal-2019

[18] LUBCZANSKI, M. Electric cars with a new record / Samochody elektryczne z nowym rekordem (in Polish) [online] [accessed 2020-05-02]. Available from: https://e.autokult.pl/34559,sprzedaz-samochodow-elektrycznych-w-i-polroczu-2019-roku-auta-nowe-uzywane

[19] How much does driving an electric car really cost? „The trip has stopped paying off on the highways“ / Ile naprawde kosztuje jazda autem elektrycznym? “Podroz przestala sie oplacac na autostradach” (in Polish) [online] [accessed 2020-012-01]. Available from: http://forsal.pl/artykuly/1448077,samochod-elektryczny-zuzycie-energii-w-trasie-koszty-ladowania.html

[20] BERMAN, B. Mazda wrongly says long-range EVs are worse for CO_2 than diesel cars - Electrek [online] [accessed 2020-12-01]. Available from: https://electrek.co/2019/12/29/mazda-says-long-range-evs-are-worse-for-co2-than-diesel-cars

[21] SLIWA, M. Sale of electric cars in the world. Poland is far behind / Sprzedaz aut elektrycznych na swiecie. Polska daleko w tyle (in Polish) [online] [accessed 2020-06-01]. Available from: https://moto.rp.pl/tu-i-teraz/29120-sprzedaz-aut-elektrycznych-na-swiecie-polska-daleko-w-tyle

[22] The average age of cars in Poland and Europe / Sredni wiek samochodow w Polsce i w Europie (in Polish) [online] [accessed 2020-06-01]. Available from: https://tvn24bis.pl/article/url/978789

[23] KURANC, A. Emission of the fume‘s harmful components in the control tests upon the chosen population of vehicles / Emisja szkodliwych skladnikow spalin w badaniach kontrolnych wybranej populacji pojazdow samochodowych (in Polish). *Autobusy: technika, eksploatacja, systemy transportowe*. 2011, **12**(10), p. 282-290. ISSN 1509-5878, eISSN 2450-7725.

[24] LARISH, J. Population structure of cars and the results of periodical supervising for exhaust emissions carried out on the vehicle inspection station / Struktura populacji samochodow i wyniki badan emisji spalin wykonanych na stacji kontroli pojazdow ASO (in Polish). *Silniki Spalinowe* [online]. 2011, **50**(3). ISSN 0138-0346.

[25] SZPICA, D.: Coefficient of engine flexibility as a basis for the assessment of vehicle tractive performance. *Chinese Journal of Mechanical Engineering* [online]. 2019, **32**, 39. ISSN 1000-9345, eISSN 2192-8258. Available from: https://doi.org/10.1186/s10033-019-0352-8

[26] MAHA. Motor gas tester MGT 5 five-gas tester. Technical handbook. MAHA Maschinenbau Haldenwang GmbH & Co. 1999.

[27] MAHA. MPM4 - Particle Measurement Unit. Original Operating Instructions. MAHA Maschinenbau Haldenwang GmbH & Co. 2008.

[28] PIEKARSKI, W., KURANC, A. Exhaust emissions and fuel consumption in a chassis dynamometer load test in the aspect of modification of an engine controlling system. *Combustion Engines* [online]. 2017, **171**(4), p. 11-16. ISSN 2300-9896, eISSN 2658-1442. Available from: https://doi.org/10.19206/CE-2017-402

[29] ROCHA-HOYOS, J. C., ZAMBRANO, D., PORTILLA, A., ERAZO, G., TORRES, G., LLANES-CEDENO, E. Analysis of gases of the engine of a vehicle through static and dynamic tests / Analisis de gases del motor de un vehiculo a traves de pruebas estaticas y dinamicas (in Spaniah). *Ciencia Unemi* [online]. 2018, **11**(28), p. 97-108. ISSN 1390-4272, eISSN 1390-4272. Available from: http://ojs.unemi.edu.ec/index.php/cienciaunemi/article/view/711

[30] KURANC, A. Exhaust emission test performance with the use of the signal from air flow meter. *Eksploatacja i Niezawodnosc - Maintenance and Reliability* [online]. 2015, **17**(1), p. 129-134. ISSN 1507-2711. Available from: https://doi.org/10.17531/ein.2015.1.17

[31] Electronics for the automotive industry - Viaken / Elektronika dla motoryzacji - Viaken (in Polish) [online] [accessed 2020-05-02]. Available from: https://viaken.pl/pl/vag-usb-kkl-line-2-linie-k-we-wtyku-obd2.html

[32] Regulation No 83 of the Economic Commission for Europe of the United Nations (UN/ECE) - Uniform provisions concerning the approval of vehicles with regard to the emission of pollutants according to engine fuel requirements. Official Journal of the European Union. L 42/1. 2012.

[33] MAHA. MSR - Single Roller Dynamometer. Original operating instructions. 2011.

[34] KNEZ, M., JEREB, B., OBRECHT, M. Factors influencing the purchasing decisions of low emission cars: a study of Slovenia. *Transportation Research Part D: Transport and Environment* [online]. 2014, **30**, p. 53-61. ISSN 1361-9209. Available from: https://doi.org/10.1016/j.trd.2014.05.007

[35] SARKAN, B., SKRUCANY, T., SEMANOVA, S., MADLENAK, R., KURANC, A., SEJKOROVA, M., CABAN, J. Vehicle coast-down method as a tool for calculating total resistance for the purposes of type-approval fuel consumption. *Scientific Journal of Silesian University of Technology. Series Transport* [online]. 2018, **98**, p. 161-172. ISSN 0209-3324, eISSN 2450-1549. Available from: https://doi.org/10.20858/sjsutst.2018.98.15

[36] SARKAN, B., STOPKA, O., CHOVANCOVA, M., KURANC, A. Simulating real driving conditions on the single roller dynamometer: a case study in terms of the fuel consumption measurement. In: 11th International Science - Technical Conference Automotive Safety: proceedings [online]. 2018. p. 1-6. Available from: https://doi.org/10.1109/AUTOSAFE.2018.8373313

[37] Worldwide harmonized light vehicles test procedure. German association of the automotive industry (VDA) - WLTP [online] [accessed 2020-06-02]. Available from: http://vda.de

[38] KARCZMARZ, G. In WLTP cars consume about 1 liter/100 km more than the NEDC / W WLTP samochody zuzywaja okolo 1 litr/100 km wiecej niz wynikalo to z NEDC (in Polish) [online] [accessed 2020-01-20]. Available from: https://spidersweb.pl/autoblog/porownanie-wltp-vs-nedc

[39] JAWORSKI, A., KUSZEWSKI, H., LEJDA, K., USTRZYCKI, A., MADZIEL, M., LATALA, D. New procedure of examination of exhaust emission test from motor vehicles wit the use of road test / Nowa procedura przeprowadzania badan emisji spalin z pojazdow samochodowych z wykorzystaniem testow drogowych (in Polish). In: Scientific - Practical Conference Bus Construction and Passenger Transportation in Ukraine: proceedings. 2018. ISBN 966-941-140-8, p. 119-125.

[40] MERKISZ, J., PIELECHA, J., NOWAK, M. Exhaust emissions from vehicles in real traffic conditions on the example of Poznan agglomeration / Emisja zanieczyszczen z pojazdow w rzeczywistych warunkach ruchu na przykladzie aglomeracji poznanskiej (in Polish). *Postepy Nauki i Techniki* [online]. 2012, **15**, p. 103-115. ISSN 2080-4075.

[41] NEDC tested vs NEDC correlated - JATO [online] [accessed 2020-01-27]. Available from: https://www.jato.com/wp-content/uploads/2018/08/CO2-chart.jpeg

[42] Current legal framework: NEDC (New European Driving Cycle) [online] [accessed 2020-06-02]. Available from: http://vda.de

[43] FICE, M., SETLAK, R. Energy analysis of the real driving cycles / Analiza energetyczna rzeczywistych cykli jazdy (in Polish). *Zeszyty Problemowe - Maszyny Elektryczne* [online]. 2011, **2**(90), p. 99-103. ISSN 0239-3646, eISSN 2084-5618.

[44] PIELECHA, I., PIELECHA, J. Simulation analysis of electric vehicles energy consumption in driving tests. *Eksploatacja i Niezawodnosc - Maintenance and Reliability* [online]. 2019, **22**(1), p. 130-137. ISSN 1507-2711. Available from: https://doi.org/10.17531/ein.2020.1.15.

[45] KROPIWNICKI, J. Assessment of energy efficiency of motor vehicles with internal combustion engines / Ocena efektywnosci energetycznej pojazdow samochodowych z silnikami spalinowymi (in Polish). Gdansk: *Wydawnictwo Politechniki Gdanskiej*, 2011. ISBN 978-83-7348-357-6.

[46] MOCK, P., KUHLWEIN, J., TIETGE, U., FRANCO, V., BANDIVADEKAR, A., GERMAN, J. The WLTP: How a new test procedure for cars will affect fuel consumption values in the EU. In: International Council on Clean Transportation ICCT 2014: proceedings. 2014.

[47] UBYSZ, A. Energy conservation in motor vehicles / Poszanowanie energii w pojazdach samochodowych (in Polish). Gliwice: *Wydawnictwo Politechniki Slaskiej*, 2011.

[48] JAWORSKI, A., KUSZEWSKI, H., USTRZYCKI, A., BALAWENDER, K., LEJDA, K., WOS, P. Analysis of the repeatability of the exhaust pollutants emission research results for cold and hot starts under controlled driving cycle conditions. *Environmental Science and Pollution Research International* [online]. 2018, **25**(18), p. 17862-17877. ISSN 0944-1344, eISSN 1614-7499. Available from: https://doi.org/10.1007/s11356-018-1983-5

[49] RESITOGLU, I. A., ALTINISIK, K., KESKIN, A. The pollutant emissions from diesel-engine vehicles and exhaust aftertreatment systems. *Clean Technologies and Environmental Policy* [online]. 2015, **17**(1), p. 15-27. ISSN 1618-954X, eISSN 1618-9558. Available from: https://doi.org/10.1007/s10098-014-0793-9

[50] HUANG, Y., NG, E. C. Y., YAM, Y.-S., LEE, C. K. C., SURAWSKI, N. C., MOK, W.-C., ORGAN, B., ZHOU, J. L., CHAN, E. F. C. Impact of potential engine malfunctions on fuel consumption and gaseous emissions of a Euro VI diesel truck. *Energy Conversion and Management* [online]. 2019, **184**, p. 521-529. ISSN 0196-8904. Available from: https://doi.org/10.1016/j.enconman.2019.01.076

[51] TOMPKINS, B. T. SONG, H., JACOBS, T. J. Particulate matter emissions from late injection high EGR low temperature diesel combustion. In: Internal Combustion Engine Division Fall Technical Conference: proceedings [online]. 2011. ICEF2011-60067. ISBN 978-0-7918-4442-7, p. 373-381. Available from: https://doi.org/10.1115/ICEF2011-60067

[52] STEFANOPOULOU, A. G., KOLMANOVSKY, I. FREUDENBERG, J. S. Control of variable geometry turbocharged diesel engines for reduced emissions'. *IEEE Transactions on Control Systems Technology* [online]. 2000, **8**(4), p. 733-745. ISSN 1063-6536, eISSN 1558-0865. Available from: https://doi.org/10.1109/87.852917

[53] HUANG, C., LOU, D., HU, Z., FENG, Q., CHEN, Y., CHEN, C., TAN, P., YAO, D. A PEMS study of the emissions of gaseous pollutants and ultrafine particles from gasoline-and diesel-fueled vehicles. *Atmospheric Environment* [online]. 2013, **77**, p. 703-710. ISSN 1352-2310. Available from: https://doi.org/10.1016/j.atmosenv.2013.05.059

NUMERICAL AND ANALYTICAL INVESTIGATION OF STABILITY OF THE REINFORCED PLATE

Gaik A. Manuylov[1], Sergey B. Kositsyn[2], Irina E. Grudtsyna[2,*]

[1]Department of Structural Mechanics, Russian University of Transport (MIIT), Moscow, Russia
[2]Department of Theoretical Mechanics, Russian University of Transport (MIIT), Moscow, Russia

*E-mail of corresponding author: grudtsyna_ira90@mail.ru

Resume
The work is aimed at the construction of an algorithm for studying the equilibrium states of a reinforced plate near critical points, using the first (cubic terms) nonlinear terms of the potential energy expansion. Using geometrically nonlinear analysis of displacement, deformation and stress fields, the Eigenforms of buckling were calculated and bifurcation solutions and solutions for equilibrium curves with limit points were constructed depending on the initial imperfections.

Article info
Received 19 January 2021
Accepted 5 March 2021
Online 20 August 2021

Keywords:
geometrically nonlinear equilibrium equations,
bifurcation points,
limit points,
interaction of forms,
reinforced plate,
critical stresses

Available online: https://doi.org/10.26552/com.C.2021.4.B278-B287

ISSN 1335-4205 (print version)
ISSN 2585-7878 (online version)

This is an open access article distributed under the terms of the Creative Commons Attribution 4.0 International License (CC BY 4.0), which permits use, distribution, and reproduction in any medium, provided the original publication is properly cited. No use, distribution or reproduction is permitted which does not comply with these terms.

1 Introduction

Interest in the work of compressed reinforced plates appeared long ago, however, only starting with the work of Koiter and Kuiken [1], Koiter and Pignataro [2], van der Neut [3], Tvergaard [4], Hunt [5] and at a later time Manevich [6-8], systems of equilibrium equations were obtained taking into account geometric nonlinearity, which make it possible to analyze the bearing capacity of the mentioned plate either taking into account the total deflection, or taking into account the interaction of this deflection with local waveforms in the ribs or in the plate. Geometrically nonlinear equations for describing the loss of stability of the considered plates, taking into account the interaction of forms, were first presented by Koiter and Pignataro [2], Tvergaard focused his attention on study of plates with double critical loads for the total deflection and for wave formation in the plate [4].

In his work, important and general results were obtained for the calculation of reinforced plates of sufficiently large width and regular arrangement of ribs. For this, he isolated a regular T-shaped fragment, which was investigated in more detail; some of the results obtained by Tvergaard were used by Hunt [5] to construct the bifurcation surface of the homeoclinic bifurcation point corresponding to the catastrophe of the hyperbolic umbilic.

Tvergaard's studies were continued by authors of this work [9-11], who, using the FEM, numerically, studied the effect of initial imperfections on the bearing capacity of a reinforced plate in the case of multiple and multiple critical loads. In these works, it was found that, indeed, with simultaneous buckling in the total deflection and wave formation in platinum, in the case of coincidence of the critical loads, a double bifurcation is realized as a homeoclinic point of a hyperbolic umbilic. If buckling simultaneously occurs along the general deflection and wave formation in the ribs, then the double semi-symmetric point is an anticlinic bifurcation corresponding to the catastrophe of the elliptical umbilic [11]. Important results, using equations of the first and second geometrically nonlinear approximations (taking into account cubic and quartic terms in the expansion of potential energy), were obtained in the 80s by Manevich [7-8]. He was able to establish that, limiting himself to the first approximation (only cubic terms are taken into account), it is possible to obtain acceptable estimates of the bearing capacity of a compressed reinforced plate if the critical loads of the wave formation in its elements are close to or exceed the critical buckling load according to the general deflection scheme. If the waveform loads are significantly less than the critical load of the total deflection, then taking into account additional terms of the fourth order in decomposition of the potential energy makes it possible to increase the maximum load loss of the bearing capacity of the reinforced plate (on average) by 30-40%. However, taking into account quartic terms

significantly increases the computational complexity due to the need to determine the corrections of the second approximation to eigenforms. In this article, the authors limited themselves to taking into account only the cubic terms in the expansion of the fields of displacements, deformations and stresses, since in design practice such ratios of the geometric parameters of a reinforced plate are used, at which the critical loads of the wave formation in a plate or in the ribs are significantly higher than the critical load of the total deflection.

2 Semi-analitical solution

Here is considered consider a plate hinged at its ends, supported on one side by a regular set of thin rectangular ribs. The longitudinal edges are free. The plate is compressed by centrally applied forces. The plate material is infinitely elastic. This allows to investigate the stability of the reinforced plate by analyzing the equilibrium of one regular T-shaped fragment (by analogy with Tvergaard and Manevich) equidistant with the rest of the T-shaped fragments. Strains and Hooke's law are expressed as follows:

$$\varepsilon = L_1(U) + \frac{1}{2}L_2(U), \tag{1}$$

$$\sigma = H(\varepsilon), \tag{2}$$

where: L_1, H - is a linear operator,
L_2 -is a quadratic operator,
$L_2\ (U + V) = L_2\ (U) + 2\ L_{11}\ (U, V) + L_2\ (V)$, in this expression L_{11} - bilinear operator.

The total potential energy of the reinforced plate with the retention of terms no higher than the fourth order has the form:

$$\Pi_э = a_0 + \frac{1}{2}\sum_s a_s\left(1 - \frac{\lambda}{\lambda_s}\right)\xi_s^2 + \frac{1}{3}\sum_i\sum_j\sum_k \times \\ \times a_{ijk}\xi_i\xi_j\xi_k + \frac{1}{4}\sum_i\sum_j\sum_k\sum_l a_{ijkl}\xi_i\xi_j\xi_k\xi_l - \\ \sum_s a_s\xi_s\overline{\xi_s}\frac{\lambda}{\lambda_s}, \tag{3}$$

where: ξ - are normalized Eigenforms (the amplitude of the deviation of the Eigenmode relative to the plate thickness,
$\overline{\xi_s}$ - imperfections in the s-th form of buckling (s = 1, 2, … ..n).

Equilibrium equations are:

$$\left(\frac{\partial\Pi_э}{\partial\xi_1}\right) = 0; \left(\frac{\partial\Pi_э}{\partial\xi_2}\right) = 0; \ldots \left(\frac{\partial\Pi_э}{\partial\xi_s}\right) = 0, \tag{4}$$

$$a_s\left(1 - \frac{\lambda}{\lambda_s}\right)\xi_s + \sum_i\sum_j\sum_k a_{ijk}\xi_i\xi_j + \\ + \sum_i\sum_j\sum_k\sum_l a_{ijkl}\xi_i\xi_j\xi_k = \sum_s a_s\xi_s\overline{\xi_s}\frac{\lambda}{\lambda_s}. \tag{5}$$

If s = 2 (the total deflection (i = 1)) and the local form of wave formation (i = 2) are taken into account, then the potential energy, taking into account the interaction of these forms, will be written as follows:

$$\Pi_э = a_0 + \frac{1}{2}a_1\left(1 - \frac{\lambda}{\lambda_1}\right)\xi_1^2 + \frac{1}{2}a_2\left(1 - \frac{\lambda}{\lambda_2}\right)\xi_2^2 + \\ + \frac{1}{3}a_{111}\xi_1^3 + a_{122}\xi_1\xi_2^2 + \frac{1}{4}a_{1111}\xi_1^4 + \frac{1}{4}a_{2222}\xi_2^4 + \\ + \frac{1}{2}a_{1122}\xi_1^2\xi_2^2 - \frac{\lambda}{\lambda_1}a_1\overline{\xi_1}\xi_1\frac{\lambda}{\lambda_2}a_2\overline{\xi_2}\xi_2. \tag{6}$$

Accordingly, one obtains a simplified version of the equilibrium equations:

$$a_1\left(1 - \frac{\lambda}{\lambda_1}\right)\xi_1 + a_{111}\xi_1^2 + a_{122}\xi_2^2 + a_{1111}\xi_1^3 + \\ + a_{1122}\xi_1\xi_2^2 = \frac{\lambda}{\lambda_1}a_1\overline{\xi_1}, \tag{7}$$

$$a_2\left(1 - \frac{\lambda}{\lambda_2}\right)\xi_2 + 2a_{122}\xi_1\xi_2 + a_{122}\xi_1^2\xi_2 + \\ + a_{2222}\xi_2^3 = \frac{\lambda}{\lambda_2}a_2\overline{\xi_2}. \tag{8}$$

For the first nonlinear approximation equations, only the cubic terms are retained.

$$a_1\left(1 - \frac{\lambda}{\lambda_1}\right)\xi_1 + a_{111}\xi_1^2 + a_{122}\xi_2^2 = \frac{\lambda}{\lambda_1}a_1\overline{\xi_1}, \tag{9}$$

$$a_2\left(1 - \frac{\lambda}{\lambda_2}\right)\xi_2 + 2a_{122}\xi_1\xi_2 = \frac{\lambda}{\lambda_2}a_2\overline{\xi_2}. \tag{10}$$

If one divides each equation by coefficients a_1 and a_2, then one gets equations in the form given by Tvergaard [4] ($\lambda_1 = \lambda_2 = \lambda_c$)($\lambda_1 = \lambda_2 = \lambda_c$):

$$\left(1 - \frac{\lambda}{\lambda_1}\right)\xi_1 + d_1\xi_1^2 + d_2\xi_2^2 = \frac{\lambda}{\lambda_1}\overline{\xi_1}, \tag{11}$$

$$\left(1 - \frac{\lambda}{\lambda_1}\right)\xi_2 + d_3\xi_1\xi_2 = \frac{\lambda}{\lambda_2}\overline{\xi_2}, \tag{12}$$

where: $d_1 = \frac{a_{111}}{a_1}, d_2 = \frac{a_{122}}{a_1}, d_3 = \frac{2a_{122}}{a_2}$.

To determine the coefficients a_{ijk} and d_1, d_2 and d_3 it is necessary to calculate some definite integrals over the rectangular areas of the mentioned T-element of the reinforced plate. Expressions for these integrals: $a_1 = -\lambda_1\{\sigma^0 L_2(U^{(1)})\}$, $a_2 = -\lambda_2\{\sigma^0 L_2(U^{(2)})\}$, $a_{111} = \frac{3}{2}\{\sigma^1 L_2(U^{(1)})\}$ and $a_{112} = \{\sigma^1 L_2(U^{(2)})\} + + \{\sigma^2 L_{11}(U^{(1)}, U^{(2)})\}$ are given in the work of Tvergaard [4] and in a slightly modified form in the work of Manevich [8]. Equations (9) and (10) include the values of the critical parameters λ_1 and λ_2, which correspond to the general shape of bending and local wave formation in the plate or ribs. These quantities are found by solving a linear eigenvalue problem. Tvergaard solved a homogeneous boundary value problem for a system of biharmonic equations and eight boundary conditions for conjugation along the line of contact of the rib with the plate:

$$D\,\Delta\Delta w_c = \lambda_c N_X^0 w_{,xx}, \tag{13}$$

$$\frac{1}{Eh}\Delta\Delta F_C = 0\,. \tag{14}$$

These conditions express the relationship between the forces and displacements at the edges of the left-hand and right-hand parts of the plate in relation to the rib [8]. In this case, it is assumed that the total deflection develops along a curve close to a sinusoid corresponding to the buckling of the Eulerian rod. Eight unknown arbitrary constants are found from a system of homogeneous equations, the matrix of coefficients of which is given in the appendix to the work of Tvergaard [4]. Manevich solved the same problem variationally, using the Rayleigh ratio. By setting a different number of half-waves, he found the smallest value of the critical loads of wave formation in the plate or in the ribs.

In Equations (11) and (12), on the right-hand sides, there are values of the initial imperfections $\overline{\xi_1}$ and $\overline{\xi_2}$. They correspond to buckling shapes in terms of the total deflection and in terms of the shape of local wave formation. If both of these imperfections are nonzero, then the critical point is the limiting point. For a homogeneous bifurcation problem $\left(\overline{\xi_1} = \overline{\xi_2} = 0\right)$, the simplest solutions correspond to the case of multiple loads $(\lambda_1 = \lambda_2 = \lambda_c)$. Bifurcation solutions for simple loads $(\lambda_1 \neq \lambda_2)$ turn out to be somewhat more complicated. If the right-hand side of Equation (12) is zero and the right-hand side of Equation (11) has an imperfection $\left(\overline{\xi_1} \neq 0\right)$ proportional to the load parameter, then the bifurcation problem is implemented as a search for the critical value of the load at which a plate with a developing initial general deflection loses stability in the form of wave formation in the plate or in the ribs.

Let the solutions of the simplest problem for a double semi-symmetric bifurcation point be considered, corresponding to solutions of homogeneous equations of Tvergaard's type. For the general deflection and for the solution describing wave formation in the plate, the mentioned solutions can be written as follows:

$$\xi_1 = -\frac{1}{d_3}\left(1 - \frac{\lambda}{\lambda_c}\right), \tag{15}$$

$$\xi_2 = \mp\sqrt{\left(\frac{d_3 - d_1}{d_2 d_3^2}\right)}\left(1 - \frac{\lambda}{\lambda_c}\right) = \mp\xi_1\sqrt{\frac{d_3 - d_1}{d_2}}\,. \tag{16}$$

From the last relations it can be seen that the total deflection of the relative amplitude ξ_1 is an unconnected deformation. It depends on one coordinate only, while the wave formation with an amplitude ξ_2 is linearly related to the amplitude of the total deflection. If this amplitude ξ_1 is equal to zero, then the amplitude ξ_2 is also equal to zero. For the values of the coefficients of the equations calculated by Tvergaard d_1 = -0.0193, d_2 = 0.6731 and d_3 = 0.1138. The ratio between ξ_2 and ξ_1 is $\sqrt{\frac{d_3 - d_1}{d_2}} = 0.374$. Note that all the three coefficients d_1, d_2, and d_3 are negative, which is possible only with a homeoclinic bifurcation point (a variant of the catastrophe of a hyperbolic umbilic). This situation arises during wave formation in a plate. In the case of simple eigenvalues $(\lambda_1 \neq \lambda_2)$ the bifurcation solutions of the system of nonlinear equations with zero right-hand sides $\xi_1 = \xi_2 = 0$ turn out to be more complicated:

$$\xi_1 = -\frac{1}{d_3}\left(1 - \frac{\lambda}{\lambda_2}\right), \tag{17}$$

$$\xi_2 = \mp\frac{1}{d_3}\sqrt{\left(1 - \frac{\lambda}{\lambda_2}\right)\left(\begin{matrix}\frac{d_3}{d_2}\left(1 - \frac{\lambda}{\lambda_1}\right) - \\ -\frac{d_1}{d_2}\left(1 - \frac{\lambda}{\lambda_2}\right)\end{matrix}\right)} = \\ = \mp\xi_1\sqrt{\frac{d_3\left(1 - \frac{\lambda}{\lambda_1}\right)}{d_2\left(1 - \frac{\lambda}{\lambda_2}\right)} - \frac{d_1}{d_2}}. \tag{18}$$

Singular points (bifurcation points or limit points) appear on the equilibrium curves of the reinforced plate when the Hessian matrix degenerates in critical equilibrium $(\det H(\xi_1, \xi_2, \lambda) = 0)$. For Equations (11), (12) this matrix has the form:

$$H = \begin{bmatrix}\left(1 - \frac{\lambda}{\lambda_1}\right) + 2d_1\xi_1 & 2d_2\xi_2 \\ d_3\xi_2 & \left(1 - \frac{\lambda}{\lambda_2}\right) + d_3\xi_1\end{bmatrix}. \tag{19}$$

If a problem is considered in which the initial imperfection in the total deflection is specified $\left(\overline{\xi_1} \neq 0\right)$ and there is no initial wave formation $\left(\overline{\xi_2} = 0\right)$, then in this case the solution depends only on the coordinate $\xi_1(\xi_2 = 0)$ and the condition of equality to zero of the determinant $(\det H(\xi_1, \xi_2, \lambda) = 0)$ is reduced to the fulfillment of one of two relations:

$$h_{11} = \left(1 - \frac{\lambda}{\lambda_1}\right) + 2d_1\xi_1 = 0\,, \text{ or} \tag{20}$$

$$h_{22}\left(1 - \frac{\lambda}{\lambda_2}\right) + d_3\xi_1 = 0\,. \tag{21}$$

The most important condition is Equation (21). $(h_{22}(\lambda, d_3, \xi_1) = 0)$. In this case, the equilibrium Equation (12) $\left(\left(1 - \frac{\lambda}{\lambda_2}\right) + d_3\xi_1\right)\xi_2 = 0$ is fulfilled in two versions:

a) $\xi_2 = 0$, but $\left(\left(1 - \frac{\lambda}{\lambda_2}\right) + d_3\xi_1\right) \neq 0$.

Hence $(h_{22}(\lambda, d_3, \xi_1) \neq 0), \det H(\xi_1, \xi_2, \lambda) \neq 0)$, which corresponds to regular points on the equilibrium curve $\mu_1(\xi_1, \overline{\xi_1}), \left(\mu_1 = \frac{\lambda}{\lambda_1}\right)$.

b) $\xi_2 = 0$ and $\left(\left(1 - \frac{\lambda}{\lambda_2}\right) + d_3\xi_1\right) = 0$.

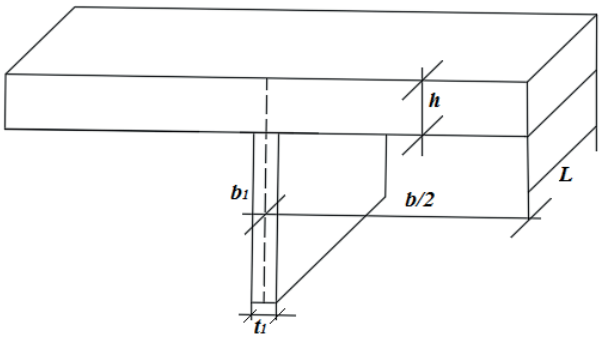


Figure 1 *Cross-section of a T-shaped fragment; here b - is the distance between the ribs in the axes, h - is the plate thickness, b_1 - is the rib height, t_1 - is the rib thickness, L - is the length of the reinforced plate, boundary conditions: hinged support along the short sides, along the longitudinal edges, fastening of the movable termination type*

Hence $h_{22}(\lambda, d_3, \xi_1) = 0, \det H(\xi_1, \xi_2, \lambda) = 0)$ and the corresponding point of the curve $\mu_1(\xi_1, \overline{\xi_1})$ is a point of singular equilibrium. Whether this point is a limit point or a bifurcation point depends on whether the value $\mu_1(\xi_1^{cr})$ is a local extremum or not. If the value $\mu_1(\xi_1^{cr})$ is not a local extremum, then the singular point is a bifurcation point (in this problem, symmetric and unstable).

c) $\xi_2 \neq 0, \left(\left(1 - \frac{\lambda}{\lambda_2}\right) + d_3\xi_1\right) = 0$ moreover $h_{22}(\lambda, d_3, \xi_1) = 0$.

However, $\det H(\xi_1, \xi_2, \lambda) = -2d_2 d_3 \xi_2^2 \neq 0$ and the corresponding equilibrium is regular. The greatest compression load is achieved here, since the post-bifurcation equilibrium turns out to be unstable. The values of the bifurcation load $\mu_1^{cr}\left(\mu_1 = \frac{\lambda}{\lambda_1}\right)$ are determined from the quadratic equation, compiled taking into account the relations:

$$h_{22}(\lambda, d_3, \xi_1) = 0, \xi_1 = -\frac{1 - k\mu_1}{d_3} = \frac{k\mu_1 - 1}{d_3}, \quad k = \frac{\lambda_2}{\lambda_1}, \tag{22}$$

$$\mu_1^2(k^2 d_1 - d_3 k) + \mu_1(d_3 + d_3 k - 2kd_1 - d_3^2\overline{\xi_1}) + d_1 - d_3 = 0. \tag{23}$$

In the problem solved by Tvergaard [4], the critical load is twofold (at the same time there is a general buckling and wave formation in the plate). By specifying a nonzero initial imperfection in the total deflection $\overline{\xi_1} \neq 0)$, it will be possible to plot the sensitivity curve of critical loads at the limiting points depending on the value of the initial deflection $\overline{\xi_1}$. Calculations according to Equation (23) for $k - 1$ give:

$$\begin{aligned} &\overline{\xi_1} = 0.2 \quad \mu_1^*(0,2) = 0.8476, \\ &\overline{\xi_1} = 0.5 \quad \mu_1^*(0,5) = 0.7703, \\ &\overline{\xi_1} = 1.0 \quad \mu_1^*(1,0) = 0.692. \end{aligned} \tag{24}$$

These results coincide with the values of ultimate loads with imperfections of the total deflection on the curves constructed by Tvergaard [4]. Consider the bifurcation problem in the presence of an initial imperfection in the form of a general deflection $(\overline{\xi_1} \neq 0)$. Its solution gives a critical waveform load in the relatively weak ribs of the reinforced plate (Figure 1). In the graphical form, results for this problem, with various initial imperfections, are presented in the work of Manevich ([8], ch. III, Figure 3.3). The investigated plate had the following dimensionless parameters:

$$\frac{b}{h} = 25, \frac{b_1}{t_1} = 20, \frac{t_1 b_1}{bh} = \frac{1}{5}, \frac{L}{b} = 5, k = \frac{\lambda_1}{\lambda_2} = 1.4852.$$

For the plate in Figure 1, the values of the coefficients of the Equations, (11) and (12): $d_1 = -0.009, d_2 = 1.024$ and $d_3 = 0.975$, taken from [8].

Note that this rib plate contains relatively weak elongated cantilever plates. Loss of stability by wave formation should be expected precisely in compressed ribs, and not in the plate. This is indicated by the signs of the coefficients $d_1 < 0$ (this is always), $d_2 > 0$ and $d_3 > 0$. If all the coefficients $d_i < 0$, then the wave formation should be expected in the plate. It is assumed that the relative amplitude of the initial total deflection is $\overline{\xi_1} = -0.5$. Substituting all the given data into Equation (23) one gets:

$$\mu^2 - 1.9927\mu + 0.67033 = 0. \tag{25}$$

The smallest root $\mu_1^{cr} = 0.428$ determines the load of the bifurcation of wave formation in the compressed ribs of the plate with an additional total deflection:

$$\xi_1 = -\frac{1 - k\mu_1}{d_3} = -0.3728. \tag{26}$$

This bifurcation is symmetrical and unstable, since in the presence of the initial additional wave formation in the edges $(\overline{\xi_2} \neq 0)$ loss of stability occurs at the limiting points. Note that in this case the equilibrium curve is spatial, since the load μ_1 depends on two coordinates ξ_1 and ξ_2.

The calculated value of the wave-forming load $\mu_1^{bif} = 0.428$ coincides with the critical point in table 3.5 in [8]. Having performed the similar calculations for other initial deflections, a curve is obtained of

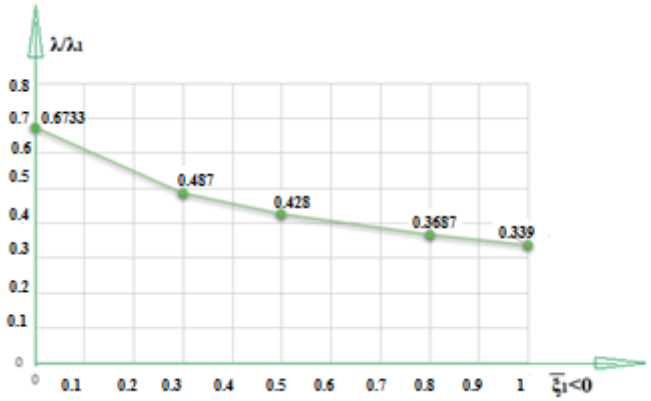


Figure 2 *Bifurcation curve*

dependence of the critical load for the wave formation bifurcation in the ribs (Figure 2) on value of the initial imperfection in a form of a general deflection.

From the graph in Figure 2 can be seen that the value of the critical load of wave formation in the ribs strongly decreases with an increase in the initial imperfection $\overline{\xi_1}$; when $\overline{\xi_1} = 1$, then the wave formation load is approximately twice smaller than the eigenvalue from the solution of the linear homogeneous problem $\left(\text{for } \overline{\xi_1} = 0, \lambda_2 = 0.6733\lambda_1, k = \frac{1}{0.6733} = 1.4852\right)$.

If in Equations (11) and (12) the right-hand sides are not equal to zero, then the problem arises of determining the coordinates of the limit point (ξ_1^*, ξ_2^*) and the value of the maximum load μ_1^*.

$$(1-\mu_1)\xi_1 + d_1\xi_1^2 + d_2\xi_2^2 = \mu_1\overline{\xi_1}, \tag{27}$$

$$(1-\mu_2)\xi_2 + d_3\xi_1\xi_2 = \mu_2\overline{\xi_2}. \tag{28}$$

From Equation (27) $\xi \neq 0$ is expressed as:

$$\xi_2 = \frac{k\mu_1\overline{\xi_2}}{1-k\mu_1+d_3\xi_1}. \tag{29}$$

Substituting the resulting expression into Equation (28) gives:

$$(1-\mu_1)\xi_1 + d_1\xi_1^2 + \\ + \frac{\left(k\mu_1\overline{\xi_2}\right)^2 d_2}{((1-k\mu_1)+d_3\xi_1)^2} = \mu_1\overline{\xi_1}. \tag{30}$$

As a result, freed from the denominator, to determine the coordinates of the equilibrium point ξ_1, (at a fixed value of the load μ_1) one obtains an equation of the fourth order with respect to ξ_1. After some transformations, it can be written as:

$$d_1d_3\xi_1^4 + \left[2d_1d_3(1-k\mu_1) + d_3^2(1-\mu_1)\right]\xi_1^3 + \\ + \left[2d_3(1-\mu_1)(1-k\mu_1) + d_1(1-k\mu_1)^2 - \right. \\ \left. - d_3^2\mu_1\overline{\xi_1}\right]\xi_1^2 + \left[(1-\mu_1)(1-k\mu_1)^2 - \right. \\ \left. - 2d_3(1-k\mu_1)\mu_1\overline{\xi_1}\right]\xi_1 + (k\mu_1)^2 d_2\xi\overline{\xi_2}^2 - \\ -(1-k\mu_1)^2\mu_1\overline{\xi_1} = 0. \tag{31}$$

The condition that the determinant of the Hessian matrix is equal to zero Is added to this equation:

$$\det H(\mu_1,\xi_1,\xi_2) = [(1-\mu_1) + 2d_1\xi_1]\times \\ \times[(1-k\mu_1) + d_3\xi_1] - 2d_2d_3\xi_2^2 = 0. \tag{32}$$

After excluding the coordinates ξ_2 from the corresponding expression, we will have:

$$\det H(\mu_1,\xi_1,\lambda) = (1-\mu_1) + 2d_1\xi_1(1-k\mu_1) + \\ + d_3\xi_1 - \frac{d_1d_3(k\mu_1)^2\overline{\xi}_2^2}{(1-k\mu_1+d_3\xi_1)^2} = 0. \tag{33}$$

As a result, one gets the two equations for variables μ_1 and ξ_1. However, their joint solution is quite difficult. Tvergaard was looking for limit points by directly constructing the equilibrium curve, while Manevich used algorithms for finding the extrema of a function of two variables.

The method of the step-by-step increase in the load, is used in this work, followed by solution of the equilibrium equation to approximately obtain the coordinates of the limiting point and the corresponding maximum load. As an example, the coordinates of the limiting point and the corresponding load are determined for the above stability problem of a reinforced plate with wave formation in the ribs. Substitution of numerical values into Equations (31), after some simplifications, leads to the following equation of the fourth order:

$$f(\xi_1) = -0.008773\xi_1^4 + 0.67376\xi_1^3 + 0.94993\xi_1^2 + \\ + 0.405\xi_1 + 0.0495 = 0. \tag{34}$$

With a fixed value of the force parameter $\mu_1 = 0.28$, one finds the minimal modulo negative root of this equation. For that is used a method of the non-singular extensions, proposed by Manuilov in 1971 [12].

$$\xi_1^{m+1} = \xi_1^m \pm \frac{\left|f(\xi_1^{(m)})\right|}{\sqrt{\left[f'^2(\xi_1^{(m)}) - f(\xi_1^{(m)})f''(\xi_1^{(m)})\right]}}. \tag{35}$$

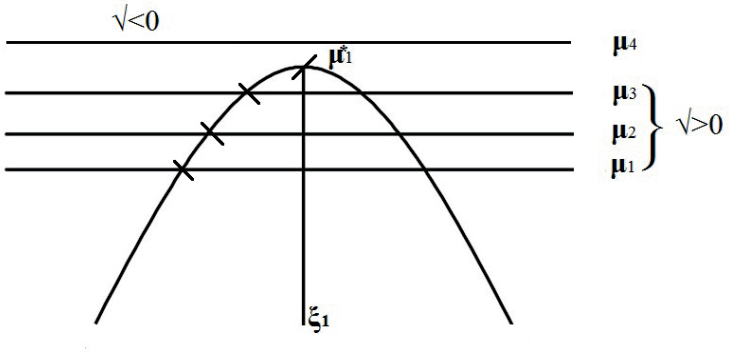


Figure 3 *"Hanging" extremum*

The iterative process of one-sided approximation to the nearest root of a power-law equation is based on local approximation of this equation by a hyperbola or an ellipse, depending on the sign of the curvature at the tangency point. A sufficient condition for one-sided convergence is that all the roots of the polynomial are real. The convergence of iterations to the nearest simple root of the power equation is asymptotically cubic.

If one moves along the equilibrium curve in sufficiently small steps along the load, then jumping over the limit point generates a "hanging" extremum (Figure 3). This will be indicated by the negative sign of the root expression in the denominator in Equation (35).

The solution of t equation (34) of the fourth order gives the desired negative root (closest to zero at $\mu_1 = 0.28$) equal to $\xi_1 = -0.21896$. The second coordinate of the equilibrium point is $\xi_2 = 0.10986$, according to Equation (29). However, the obtained equilibrium point is not the limiting one. Next, the value of μ_1 is increased to 0.3. A similar solution, using Equation (35), gives the equilibrium coordinates $\xi_1 = -0.2422$, $\xi_2 = 0.1399$. With the next value, equal to $\mu_1 = 0.325$, one obtains a negative root expression in the denominator in Equation (35), equal to -1.129·10^{-5}. For the slightly smaller values μ_1 of μ_1, a two-sided estimate: $0.32 < \mu_1^* < 0.325$ is obtained.

The corresponding approximate coordinates of the limit point: $\xi_1^* \simeq -0.3135, \xi_2^* \simeq -0.1998$.

For practical purposes, this is quite sufficient, although this result can be refined by subsequent calculations. The calculated coordinates of the limiting point are close to those shown in Figure 3.3 in the work of Manevich [8].

The relationship between the coefficients of Equations (11), (12) and the types of the wave formation (in the plate or in the ribs) is considered next. Hunt [5], investigating the problem of Tvergaard with a double critical load of the total deflection and wave formation in the plate, established the relationship between the derivatives of potential energy:

$$\Pi_3(\xi_1,\xi_2,\overline{\xi}_1,\overline{\xi}_2) = \frac{1}{6}V_{111}\xi_1^3 + \frac{1}{2}V_{122}\xi_2^2\xi_1 + \\ + \frac{1}{2}\mu_1(V_{11\mu}\xi_1^2 + V_{22\mu}\xi_2^2) + V_{1\overline{\xi}_1}\overline{\xi}_1\xi_1 + V_{2\overline{\xi}_2}\overline{\xi}_2\xi_2 \quad (36)$$

and the coefficients of the above equations d_i (i=1, 2, 3).

$$\frac{1}{6}V_{111} = -\frac{2}{3}d_1d_3; \frac{1}{2}V_{122} = -2d_2d_3; \frac{1}{2}V_{11} = -d_3, \quad (37)$$

$$\frac{1}{2}V_{22\mu} = -2d_2; V_{1\overline{\xi}_1} = 2d_3\mu_1; V_{2\overline{\xi}_2} = 4d_2k\mu_1. \quad (38)$$

In order for a double semi-symmetric bifurcation not to be monoclinic, the condition for the positiveness of the root expression T was established in [13]:

$$T = \frac{2V_{11\mu}}{V_{22\mu}} - \frac{V_{111}}{V_{122}} > 0, \text{ or} \quad (39)$$

$$T = \frac{-d_3}{-d_2} - \frac{d_1d_3}{d_2d_3} = \frac{d_3}{d_2} - \frac{d_1}{d_2} > 0. \quad (40)$$

The fulfillment of this condition shows that not one, but three new branches of equilibria in the form of straight lines pass through the double bifurcation point. The wave formation in the plate should be expected in the case of identical signs of the ratios $\frac{d_1}{d_2}$ and $\frac{d_3}{d_2}$. It will occur at the homeoclinic bifurcation point (hyperbolic umbilic). If the signs of the ratios $\frac{d_1}{d_2}$ and $\frac{d_3}{d_2}$ are different, then the wave formation will occur as a result of a local loss of stability of the ribs (anticlinic bifurcation point of the elliptical umbilic). For this reason, it was indicated above that if all the d_i are negative, then the local buckling corresponds to the wave formation in the plate. If $d_1 < 0$ (this is always) and $d_2d_3 > 0$, then the wave formation would occur in the edges of the reinforced plate. According to research of Manevich [8], this feature is also valid for multiple critical loads.

Note that signs of coefficients of Equations (11) and (12) significantly affect the interaction of the general deflection with the local wave formation. If this deflection was positive (all the $d_i < 0$), then its development provokes the wave formation in the plate, since it would receive additional compression.

On the contrary, the ribs in this case will be somewhat relieved by tensile stresses. If the total deflection is negative $(d_1 < 0, d_2 > 0, d_3 > 0)$ then, on the contrary, the plate will be unloaded and the ribs will be loaded with additional compression. This would cause the rippling in the ribs. The described interaction of the general deflection and the effects of

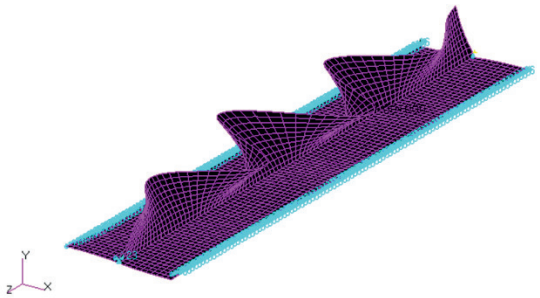


Figure 4 *First custom form*

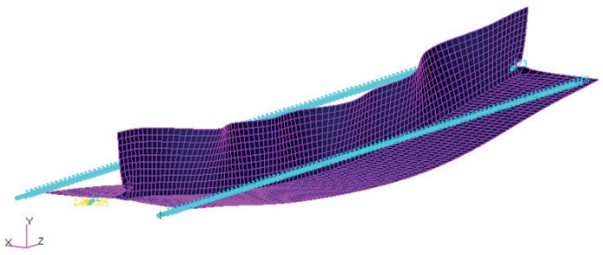


Figure 5 *Deformed equilibrium* (*at* $\overline{\xi_1} = 0$)

local wave formation is the main feature in behavior of a compressed reinforced plate.

When designing reinforced plates, the appropriate geometric parameters should be chosen so as to exclude the nonlinear interactions between the buckling shapes. For this, it is necessary that the critical loads of the wave formation are significantly higher than the critical loads of the general buckling. This problem requires a separate thorough investigation.

3 Numerical analysis of a T-shaped fragment of a reinforced plate

Algorithms for calculating the critical loads for a reinforced plate, obtaining singular points on equilibrium curves were considered earlier and the relationship between the signs of the coefficients of nonlinear equations and the type of possible wave formation was indicated. By limiting the consideration to one regular T-shaped fragment, one can draw conclusions about the nonlinear behavior of the entire structure containing their totality. A deep understanding of the stability problem, in which there is a question of the interaction of forms, is fully disclosed using the finite element modeling and numerical solutions, taking into account geometric nonlinearity.

In this part of the work, an analysis of the numerical solution using the MSC Software Patran - Nastran software package is presented. Finite elements of a shell type (3131 elements) are selected. The material was considered as absolutely elastic (E=196133.002MPa, μ = 0.3). Boundary conditions: hinged support along the short sides, along the long sides - floating terminations. The load is applied centrally. Geometric parameters were obtained from the relations of Manevich [8, Ch. III] for solving this class of problems h = 0.01 m, b = 0.25 m, t_1 = 0.005 m, b_1 = 0.1 m, L = 1.25 m. The results obtained are compared to the previously obtained results of the semi-analytical solution. The interaction of forms can be presented in two ways. The first option is the interaction of the general and local forms of plate buckling. It manifests itself when the deflection has a positive value. This option does not imply the possibility of the wave formation in the ribs, but only in the plate. The second option is the interaction of the general deflection with the local waveform of the ribs. This deformation is possible only if the deflection of a negative sign develops. The study of this behavior of the structure is reduced to solving the bifurcation problem of stability of a compressed T-shaped fragment. To take into account the local shape in modeling, the shell-type elements were used, which made it possible to consider this model as a set of plate-strips and take into account not only the membrane deformations of the plate, but the transverse deformations of the rib as well. When solving the linear stability problem, the calculation of critical loads for the first ten eigenforms was obtained. It is important to note that the first eight forms correspond to local forms of the wave formation, and only the ninth - to the form of the plate buckling, like an Eulerian rod $(\mathrm{E} = 196133.002\mathrm{Mpa}, \mu = 0.3)$. The first form has seven half-waves, which coincides with the result obtained in [11]. Figure 4 shows the first Eigenform from the linear solution.

Calculating the Euler's critical load, one gets the value $\mathrm{P_{cr}} = 2245803\mathrm{N}$. The result, calculated by the formula, gives an overestimated value of the critical load, since the scheme for calculating the plate as an Euler rack does not take into account the deformation of the plate elements of the bar. Research in a geometrically nonlinear setting without taking into account the initial imperfections $(\overline{\xi_1} = 0)$ made it possible to obtain a point of unstable bifurcation on the equilibrium curve, corresponding to the shape of the wave formation of the edge. The deformed equilibrium and equilibrium curve are shown in Figures 5 and 6, respectively. The critical load value was: $\mathrm{P_{cr}} = 1288934.01\mathrm{N}$.

Figure 5 shows that additional compressive stresses act in the zones adjacent to the free edge of the rib and cause the wave formation bifurcation at loads lower than those obtained from the linear calculation. This deformed state corresponds to equilibrium at the point of unstable bifurcation. The new branch, after passing the singular point, is falling and unstable.

In cases of the non-zero values of the initial imperfections in the total deflection, to construct the bifurcation curve (Figure 7), one sets the amplitudes of the initial deflections and calculates the critical loads. The results obtained $\left(\mu_1 = \frac{\lambda}{\lambda_1}\right)$ are in fairly good agreement with the results of the semi-analytical solution (Figure 2).

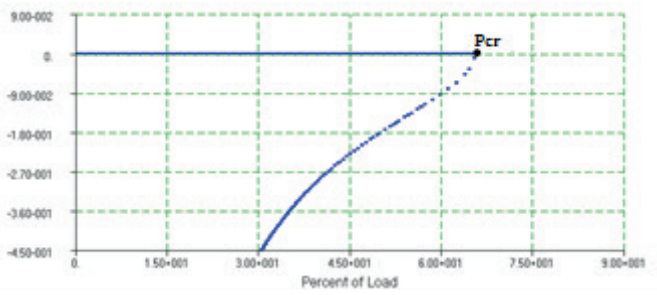


Figure 6 *Equilibrium curve (at* $\overline{\xi_1} = 0$ *)*

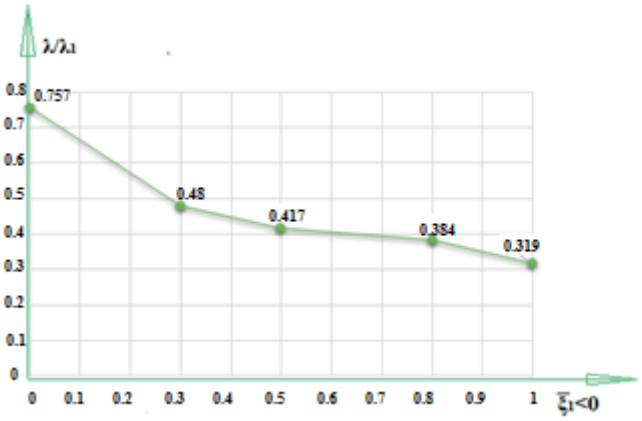


Figure 7 *Bifurcation curve*

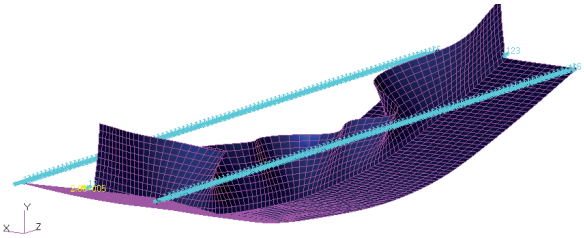


Figure 8 *Deformed equilibrium (at* $\overline{\xi_1} = -0.005\,m$*)*

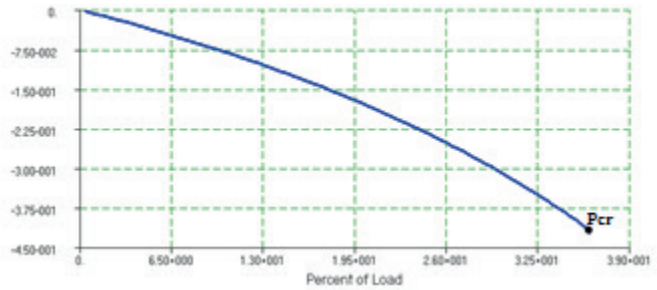


Figure 9 *Equilibrium curve (at* $\overline{\xi_1} = -0.005\,m$*)*

By setting the amplitude of the initial deflection $\overline{\xi_1} = 0.005$ m, one finds the critical load of wave formation $P_{cr} = 710026.8\text{N}$, and the value $\mu_1 = \frac{\lambda}{\lambda_1} = 0.417$, which is slightly less than $\mu_1^{bif} = 0.428$, obtained from the semi-analytical solution. The amount of deflection was $\xi_1 = -0.00427$ m, while using Equation (26) one got $\xi_1 = -0.003728$ m. The equilibrium curve and the initial deformed post-bifurcation equilibrium are shown in Figures 8 and 9, respectively.

The amplitudes of the rib deflections from the vertical plane are much larger in comparison to the similar deviations obtained in the problem without initial imperfection.

The load P_{cr} is maximum in the case when the initial imperfection is set in the total deflection $(\overline{\xi_1} = -0.5)$.

To get the limiting point on the equilibrium curve, it is necessary to specify imperfections in the local and general buckling shape. Setting the amplitudes $\overline{\xi_1} = 0.005$ m

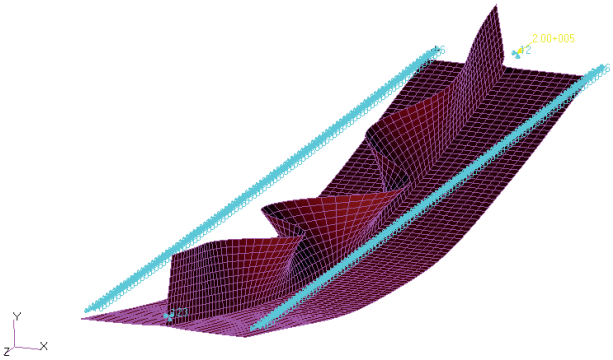


Figure 10 *Deformed equilibrium at the limit point* (*at* $\overline{\xi_1} = 0.005\,m,\ \overline{\xi_1} = 0.001\,m$)

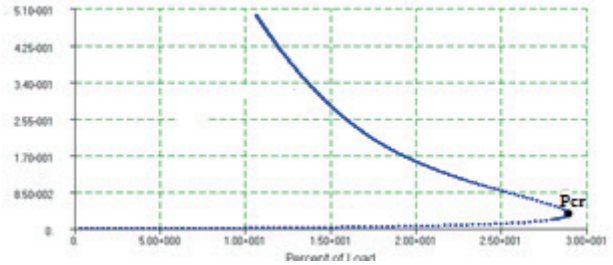


Figure 11 *Equilibrium curve* (*at* $\overline{\xi_1} = 0.005\,m,\ \overline{\xi_1} = 0.001\,m$)

and $\overline{\xi_1} = 0.001$ m, one finds the value of the critical load $\mathrm{P_{cr}} = 567021.126\mathrm{N}$ N, then $\mu_1^* = 0.33$, which quite well coincides with the upper estimate obtained from the semi-analytical solution $(0.32 < \mu_1^* < 0.325)$. The total deflection left: $\xi_1 = -0.00673$ m. The deformed balance is shown in Figure 10. The equilibrium curve is shown in Figure 11.

4 Conclusions

The article considers the solution of the nonlinear problem of the reinforced plate stability in the case of multiple and non-multiple critical loads. The most dangerous interaction of shapes is the mutual influence of local buckling of rectangular ribs with the shape of the general deflection. A detailed solution to this problem for the reinforced plates is given in [7]. The reduction in bearing capacity reached 60 %. The results of the semi-analytical and numerical solution of stability of the T-shaped fragment of the plate turned out to be quite close. The above equations are suitable for determining the coordinates of singular points on the curves of equilibrium and critical loads.

References

[1] KOITER, W. T., KUIKEN, G. D. C. The interaction between local buckling and overall buckling on the behavior of built -up columns. Delft Laboratory Report WTHD 23. 1971.

[2] KOITER, W. T., PIGNATARO, M. A. General theory for the interaction between local and overall buckling of stiffened panels. Delft WTHD Report 83. 1976, p 179-

[3] VAN DER NEUT, A. Mode interaction with a stiffened panel. In: *Buckling of structures* [online]. BUDIANSKY, B. (ed.). Berlin Heidelberg: Springer-Verlag, 1974. ISBN 978-3-642-50994-0, eISBN 978-3-642-50992-6, p. 117-132. Available from: https://doi.org/10.1007/978-3-642-50992-6

[4] TVERGAARD, V. Imperfection sensitivity of a wide integrally stiffened panel under compression. *International Journal of Solids and Structures* [online]. 1973, **9**(1), p. 177-192. ISSN 0020-7683. Available from: https://doi.org/10.1016/0020-7683(73)90040-1

[5] HUNT, G. W. Imperfection-sensitivity of semi-symmetric branching. *Proceedings of the Royal Society of London. A. Mathematical and Physical Sciences* [online]. 1977, **357**(1689), p. 193-211. ISSN 1364-5021, eISSN 1471-2946. Available from: https://doi.org/10.1098/rspa.1977.0163

[6] MANEVICH, A. To the theory of coupled buckling of reinforced thin-walled structures. 1982, **2**, p. 337-345. ISSN 0032-8235.

[7] MANEVICH, A. Interaction of buckling forms, compressed reinforced panels. *Structural Mechanics and Analysis of Constructions*. 1981, **5**, p. 24-29. ISSN 0039-2383.

[8] MANEVICH, A. *Nonlinear theory of stability of reinforced plates and shells taking into account the interaction of buckling forms*. Dnepropetrovsk, 1986.

[9] MANUYLOV, G., KOSITSYN, S., GRUDTSYNA, I. Numerical analysis critical equilibrium of flexible supported plate with allowance for influence initial geometrical imperfections. *Structural Mechanics and Analysis of Constructions*. 2020, **1**, p. 30-36. ISSN 0039-2383.

[10] MANUYLOV, G., KOSITSYN, S., GRUDTSYNA, I. Numerical analysis of stability of the stiffened plates subjected aliquant critical loads. *Structural Mechanics of Engineering Constructions and Buildings* [online]. 2020, **16**(1), p. 54-61. ISSN 1815-5235, eISSN 2587-8700. Available from: https://doi.org/10.22363/1815-5235-2020-16-1-54-61

[11] MANUYLOV, G., KOSITSYN, S., GRUDTSYNA, I. Influence of buckling forms interaction on stiffened plate bearing capacity. *International Journal for Computational Civil and Structural Engineering* [online]. 2020, **16**(2), p. 83-93. ISSN 2587-9618, eISSN 2587-0195. Available from: https://doi.org/10.22337/2587-9618-2020-16-2-83-93

[12] MANUYLOV, G. On the calculation of the roots of polynomials by the extension method. *Collection of MIIT Proceedings*. 1971, **371**, p. 133-147. ISSN 0208-3456.

[13] THOMPSON, J. M. T., TAN, J. K. Y., LIM, K. C. On the topological classification of postbuckling phenomena. *Journal of Structural Mechanics* [online]. 1978, **6**(4), p 383-414. ISSN 1539-7734, eISSN 1539-7742. Available from: https://doi.org/10.1080/03601217808907346

EXPERIMENTAL RESEARCH OF THE COAGULATION PROCESS OF EXHAUST GASES UNDER THE INFLUENCE OF ULTRASOUND

Adil Kadyrov, Bauyrzhan Sarsembekov, Aleksandr Ganyukov*, Zhanara Zhunusbekova, Kuanysh Alikarimov

Karaganda Technical University, Karaganda, Kazakhstan

*E-mail of corresponding author: ganukovktu@mail.ru

Resume

The authors propose the use of ultrasonic radiation to clean the exhaust gases of internal combustion engines of the solid particles. An experimental stand and research results are presented, proving the possibility and efficiency of using the process of ultrasonic cleaning of exhaust gases due to the process of the solid particles coagulation. The authors received a corresponding patent, the efficiency of which has been proven by results of the conducted research.

Article info

Received 22 February 2021
Accepted 8 March 2021
Online 27 August 2021

Keywords:

ultrasonic cleaning,
ultrasonic muffler,
exhaust gases,
experiment,
hydrodynamic coagulation,
orthokinetic coagulation

Available online: https://doi.org/10.26552/com.C.2021.4.B288-B298

ISSN 1335-4205 (print version)
ISSN 2585-7878 (online version)

This is an open access article distributed under the terms of the Creative Commons Attribution 4.0 International License (CC BY 4.0), which permits use, distribution, and reproduction in any medium, provided the original publication is properly cited. No use, distribution or reproduction is permitted which does not comply with these terms.

1 Introduction

One of the causes of air pollution is operation of a car engine. One of the main reasons for the excessive pollution by exhaust gases of our cities is the extremely low quality of automobile fuel. The exhaust gas consists of more than 170 harmful components, of which about 160 are hydrocarbon derivatives, which are the main causes of incomplete combustion of a fuel in an engine. The presence of harmful substances in the exhaust gases is ultimately determined by the type and condition of the fuel [1].

An increase in the concentration of exhaust gases leads to an increase in diseases of the cardiovascular system and lungs. Reducing the harmful emissions of exhaust gases from cars is an important task in solving the problem of environmental pollution [2].

The muffler is a part of the vehicle's exhaust system and is designed to reduce the noise level of a working internal combustion engine, reduce the temperature of exhaust gases and reduce the harmful emissions into the atmosphere. Reducing the harmful emissions in modern mufflers is carried out by installing systems for neutralizing and cleaning exhaust gases, operating on the methods of liquid, thermal, catalytic neutralization and particulate filters. Authors propose an ultrasonic method for cleaning the exhaust gases [3].

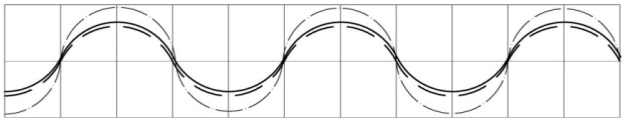
Currently, there are patents for ultrasonic cleaning of exhaust gases: when ultrasonic waves appear in a quarter-wave resonator, but without generating waves [4-6]. The article proves the advantage of cleaning exhaust gases using the design proposed in the patent [6].

In this research, the ultrasonic waves were generated by a generator. In addition, the process of cleaning the exhaust gases of a car differs in that the experimental muffler uses emitters of ultrasonic waves directed both in the transverse and longitudinal directions with respect to the exhaust gas flow.

2 Hypothesis and purpose of the research

The hypothesis is the assumed possibility of increasing the hydrodynamic coagulation of exhaust gases in the vehicle muffler under the action of ultrasonic waves. Coagulation refers to the adhesion and deposition of soot particles inside the muffler housing, which makes it possible to increase the efficiency of cleaning the exhaust gases from motor vehicles.

The aim of the research is to test the hypothesis of coagulation of soot particles under the action of ultrasonic exposure. To test the hypothesis, experimental modeling of the coagulation process was carried out on a specially designed stand and the physical essence of the process is described.



— — wave going from left to right
—— wave going from right to left
—·— the resulting wave

Figure 1 *Formation of standing waves*

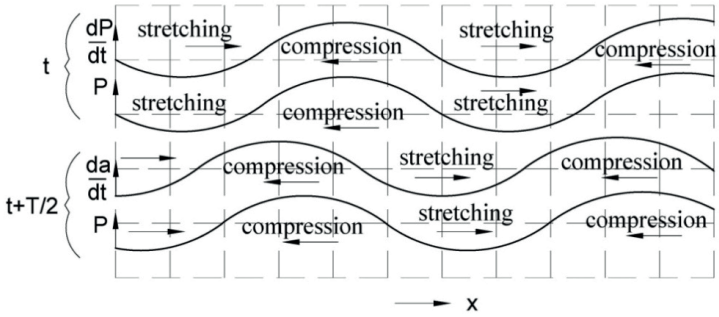


Figure 2 *Velocity distribution da/dt and pressures P in a standing sound wave*

3 The process of the gas particles coagulation under the action of ultrasound

Coagulation is accelerated when exposed to ultrasound, which has a dispersing effect on emulsions and liquid sols and has a coagulating effect on aerosols (smoke, fog, dust). This is due to the fact that only longitudinal waves causing compression are possible in gases. Shear waves cause deformation shears. In a longitudinal wave, the particles of the medium oscillate about their mean position in the direction parallel to the wave propagation [7].

The efficiency of the coagulation process increases when a standing wave occurs. Standing waves are a special case of interference. In that case, the two identical waves propagate in opposite directions. Figure 1 shows a diagram of the emergence of standing waves [7].

The resulting oscillation (Figure 1) has the same wavelength but does not move in space (standing wave) through each half of the wave (λ/2), there are no oscillations (nodes); the antinode points are located in the middle.

The pressure P in a standing wave is proportional to the displacement and contains nodes and antinodes. In this case, the position of the pressure nodes coincides with the position of the antinode nodes and vice versa (Figure 2). The pressure amplitude is twice this value for a single wave.

For the gas particles of different sizes, a certain vibration frequency occurs. At first, the particles follow the movement of the gas between the antinodes and the nodes, while sticking together and increasing in size. After that, the particles increase due to chaotic oscillations. The exhaust gas is composed of particles of different sizes. Depending on their size and vibration frequency, particles can follow sound vibrations and coagulate [8].

This process takes place at low vibration frequencies. With an increase in the vibration frequency, there is an optimal frequency segment at which the particles of different sizes have different amplitudes, collide with each other and coagulate. This kind of coagulation is called orthokinetic. As the frequency increases, coagulation becomes hydrodynamic and is carried out by friction. This process is described by the Bjerknes equations [9].

However, the frequency value is limited by the degree of participation of gas particles in oscillations and in cases with a standing wave they are related to the particle radius r and dynamic viscosity η.

The determining factor for the degree of participation of a particle in an oscillation is the quantity [9]:

$$Z = \frac{\rho r^2 f}{\eta}, \tag{1}$$

where:
Z - the particle magnification factor,
ρ - particle density [g/m^3],
r - particle radius [m],
f - frequency of gas oscillations under the action of ultrasound [kHz],
η - dynamic viscosity [Pa·s].

Denoting in Equation (1) the moment of inertia of the particle as $I = \rho r^2$, we get:

$$Z = \frac{If}{\eta}. \tag{2}$$

Namely, the participation of a particle in vibrations is the greater, the greater its moment of inertia and the frequency of ultrasonic vibrations and less with increasing viscosity. Equation (2) is further considered as a necessary condition for coagulation.

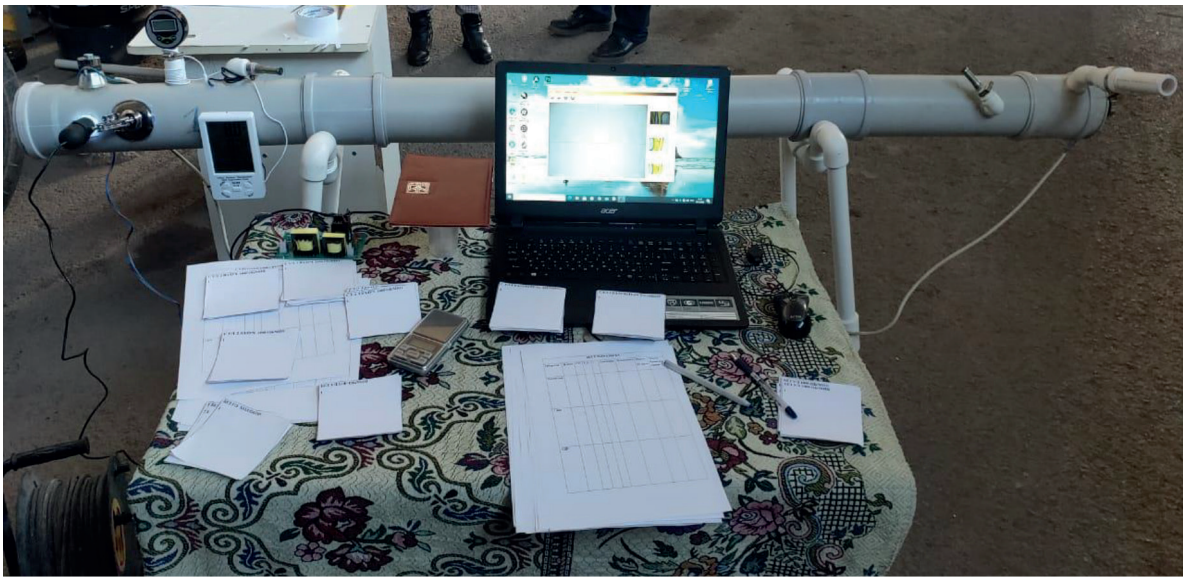
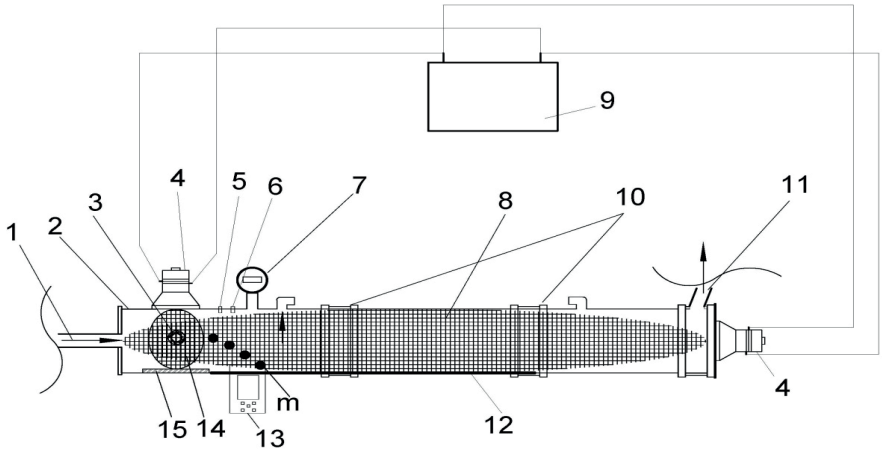


Figure 3 *Experimental ultrasonic muffler*



1- inlet pipe; 2 - the housing of the ultrasonic muffler; 3 - electron microscope MIKMED 2.0; 4 - ultrasonic emitter; 5 - temperature sensor; 6 - moisture meter; 7 - electronic pressure gauge; 8 - the area of influence of longitudinal ultrasonic waves; 9 - ultrasonic generator; 10 - pipe coupling; 11 - outlet branch pipe; 12 - the place of the soot collection; 13 - thermometer-hygrometer; 14 - the area of influence of the transverse ultrasonic waves; 15 - reflector

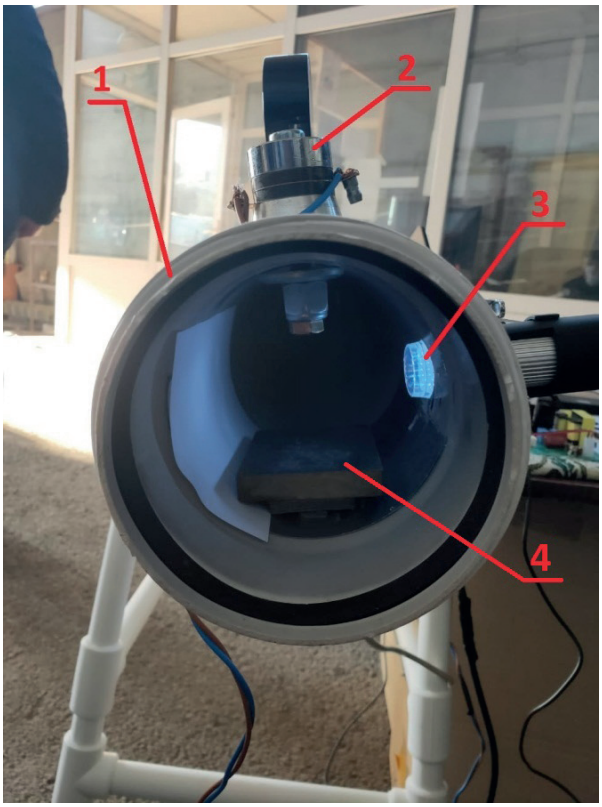
Figure 4 *Diagram of a universal ultrasonic muffler*

4 Experiment

The purpose of the experiment is to obtain dependencies that determine the parameters of coagulation: the mass of soot, the coagulation coefficient and its rate to achieve the set goals, a full-scale experiment was carried out on a developed laboratory full-size stand (Figures 3, 4 and 5). The exhaust gas contains toxins: CO (carbon monoxide) and CH (hydrocarbon). During the experiment, at the first stage, the degree of purification of the exhaust gas from hydrocarbon (CH) and carbon monoxide (CO) was determined. At the second stage, the graphs of the dependence of the mass of deposited soot on the length of the muffler L were established. During the processing, the coagulation coefficient was calculated.

The diagram of the experimental ultrasonic muffler is shown in Figure 4.

The experimental ultrasonic muffler (Figures 4 and 5) consists of a polypropylene pipe with a diameter of 110 mm and a length of 3 m. The ultrasonic equipment is installed in the muffler housing, consisting of an ultrasonic generator - *9*, two ultrasonic emitters - *4* and a reflector of ultrasonic waves - *15*; digital USB microscope Mikmed 2.0 - *3* with a magnification ratio of 20 to 200x with the possibility of photo and video recording at a resolution of 1920 × 1080 pixels; temperature sensor - *5* and hygrometer - *6*, transmitting information to the thermometer-hygrometer - *13*; electronic pressure gauge - *7*; reflector - *15*.



1- ultrasonic muffler body, 2 - ultrasonic emitter, 3 - digital USB microscope, 4 - reflector

Figure 5 *Internal design of an ultrasonic muffler*

To determine the qualitative and quantitative composition of the exhaust gas mixture, a Meta Autotest 01.03 gas analyzer was used. An ultrasonic generator manufactured by TOCOOL (China) was used. Input voltage AC 220 V, with emitter power - 50 W, ultrasonic wave generation frequency - 40 kHz. To investigate the internal processes of the ultrasonic muffler, a Mikmed 2.0 USB microscope was installed in the housing, designed for quality control and testing of industrial objects.

The experimental research was carried out as follows:

- tests were carried out without and with turning on the ultrasonic equipment for 5 minutes each;
- the lower part of the device along a semicircle was lined with five numbered sheets of paper 10 × 10 cm in size, with a total length of 50 cm, the mass of which was determined before and after testing with high-precision jewelry scales "MH-500";
- the research was carried out at an idle speed of the engine crankshaft (1000 rpm) and at 1250 rpm. Applied is Volkswagen Passat B3 1991, with engine capacity 1800 cc. see, fuel injection - mono-Motronic, engine power 90 kW, fuel grade - AI-92 gasoline.

The spent exhaust gas was supplied to the ultrasonic muffler through the inlet pipe *1* at a pressure that depends on the crankshaft speed. In the muffler, with the ultrasonic equipment turned on, the ultrasonic waves were applied to the exhaust gas in the transverse and longitudinal directions. In the sections, the ultrasonic intensification of coagulation processes and cleaning of exhaust gases took place due to the sedimentation of enlarged particles of exhaust gas at the place where the soot -*12* was collected. The cleaned exhaust gas was discharged through the outlet pipe -*11*.

During the operation of the ultrasonic muffler, the readings of the Meta Autotest 01.03 gas analyzer connected to the outlet pipe were taken. In addition the readings of the manometer, thermo-hygrometer were recorded and photos and video were recorded inside the ultrasonic muffler using a Mikmed 2.0 digital microscope, with the possibility of magnification from 20 to 200 x, at a maximum resolution of 1920 × 1080 pixels (photos are not shown due to the lack of clear images during the transfer). The gas analyzer data indicated the concentration of harmful substances (hydrocarbon (CH) and carbon monoxide (CO) contained in the exhaust gas. The data are presented in Tables 1, 2 and in the diagrams in Figures 6 and 7. After each test, the numbered paper with settled soot particles was carefully removed and weighed again. The net weight of the settled soot was determined by subtracting the weight of the paper from the weight of the carbon black paper. The position of the paper sheets in the ultrasonic muffler was used to calculate the settling distance of soot particles (Tables 3 - 6).

Table 1 *Concentration of CH and CO at 1000 rpm*

ultrasonic muffler operation	CH (ppm)	CO (%)
without ultrasound	50	1.2
with ultrasound (1 transverse emitter)	31	1.2
with ultrasound (2 emitters)	29	1.6
with ultrasound (1 longitudinal emitter)	27	1.2

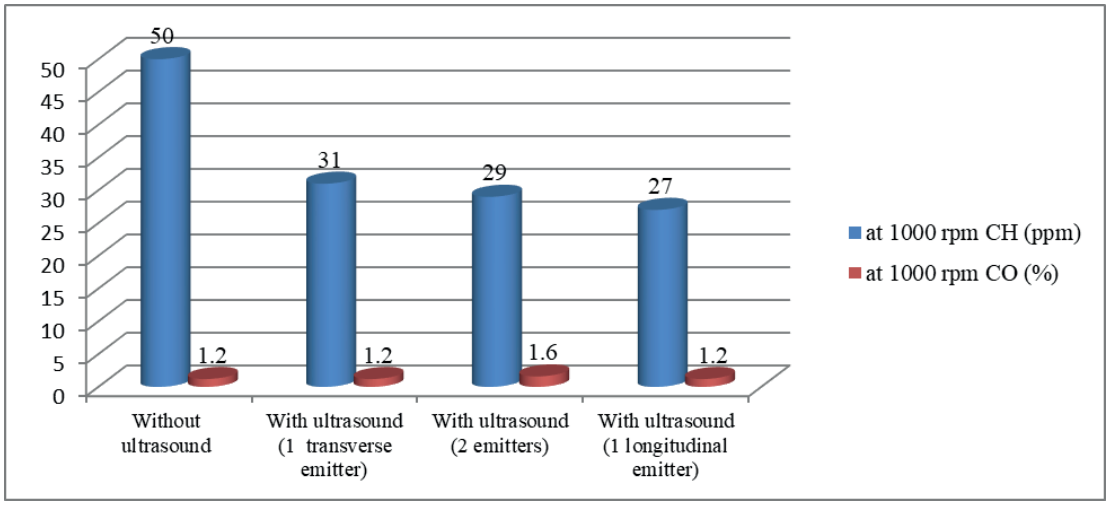


Figure 6 *Diagram of the CH and CO content in the exhaust gas at 1000 rpm of a crankshaft*

Table 2 *Concentration of CH and CO at 1250 rpm*

ultrasonic muffler operation	CH (ppm)	CO (%)
without ultrasound	27	0.62
with ultrasound (1 transverse emitter)	14	0.76
with ultrasound (2 emitters)	12	0.9

5 Experiment design, results and data processing

Previously, 5 repeated experiments were carried out. The coefficient of variation W is determined:

$$W = \frac{\sigma}{\overline{X}}, \tag{3}$$

where:
σ - the standard deviation,
$\overline{X}$ - the arithmetic mean of the results of five measurements (experiments).

The coefficient of variation was 0.07.

The minimum permissible value of repeated experiments with a confidence level of 90 % and a limiting relative experimental error of 9 % was determined [10].

The number of repeated experiments was determined from the expression:

$$n = \left(\frac{t_s W}{\varepsilon}\right)^2 = \left(\frac{2.13 \times 0.07}{0.09}\right) = 2.66 \approx 3, \tag{4}$$

where:
t_s - Student's coefficient, selected taking into account a given confidence level, from a specially compiled table of the distribution of the Student's values;
ε - limiting relative error of the experiment [11].

It was found that the number of repeated experiments is 3.

At the first stage of the experiment, the validity of the hypothesis about the possibility of cleaning the exhaust gases by ultrasound in a car muffler was proved. Tables 1 and 2 and diagrams (Figures 6 and 7) show the concentration of CH and CO in the muffler.

The longitudinal radiator is more efficient than the transverse one since the gas pressure from the collector and the pressure of sound waves are directed against each other, in this regard, the friction of particles increases, depending on the difference in velocities Δ V and dynamic viscosity η.

An increase in the number of revolutions increases the mass of deposited soot, which explains the difference in the diagrams shown in Figures 6 and 7. The bottom line is that with an increase in the mass of soot, the mass of the exhaust gas increases proportionally and the greater the number of engine revolutions. The hypothesis about the possibility of reducing the

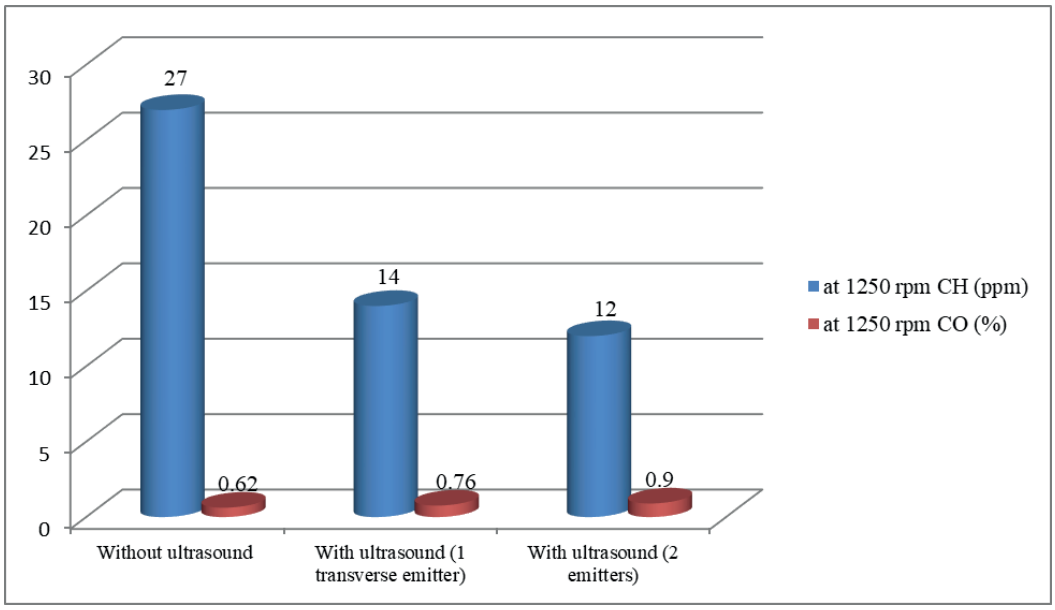


Figure 7 *Diagram of the CH and CO content in the exhaust gas at 1250 rpm of a crankshaft*

Table 3 *The mass of the settled soot at 1000 rpm without ultrasound*

time		thermometer reading	soot mass determination			
total time (min)	minute	t (°C)	distance (mm)	paper weight (g)	paper weight with soot (g)	net weight of settled soot (g)
5	1	10.5	100	0.75	1.00	0.25
	2	11.7	200	0.84	1.00	0.16
	3	12.3	300	0.84	0.95	0.11
	4	18.5	400	0.87	0.92	0.05
	5	20.3	500	0.84	0.94	0.10

Table 4 *The mass of the settled soot at 1000 rpm with ultrasound (2 emitters)*

time		thermometer reading	soot mass determination			
total time (min)	minute	t (°C)	distance (mm)	paper weight (g)	paper weight with soot (g)	net weight of settled soot (g)
5	1	16.1	100	0.74	1.08	0.34
	2	18.8	200	0.77	0.98	0.21
	3	23.0	300	0.74	0.88	0.14
	4	26.3	400	0.75	1.20	0.45
	5	29.2	500	0.72	1.10	0.38

Table 5 *The mass of the settled soot at 1000 rpm with ultrasound (1 transverse emitter)*

time		thermometer reading	soot mass determination			
total time (min)	minute	t (°C)	distance (mm)	paper weight (g)	paper weight with soot (g)	net weight of settled soot (g)
5	1	15.8	100	0.88	1.21	0.33
	2	19.3	200	0.88	1.15	0.27
	3	25.4	300	0.87	1.07	0.20
	4	27.8	400	0.86	1.02	0.16
	5	30.7	500	0.88	1.01	0.13

Table 6 *The mass of the settled soot at 1000 rpm with ultrasound (1 longitudinal emitter)*

time		thermometer reading	soot mass determination			
total time (min)	minute	t (°C)	distance (mm)	paper weight (g)	paper weight with soot (g)	net weight of settled soot (g)
5	1	18.6	100	0.78	1.46	0.37
	2	20.6	200	0.76	0.95	0.19
	3	23.2	300	0.79	0.91	0.12
	4	25.3	400	0.80	1.15	0.35
	5	27.2	500	0.78	1.04	0.26

Table 7 *Comparison of the mass of settled soot at 1000 rpm.*

distance (mm)	without ultrasound	with ultrasound (2 emitters)	with ultrasound (1 transverse emitter)	with ultrasound (1 longitudinal emitter)
100	0.25	0.34	0.33	0.37
200	0.16	0.21	0.27	0.19
300	0.11	0.14	0.2	0.12
400	0.05	0.45	0.16	0.35
500	0.1	0.38	0.13	0.26
Σ	0.67	1.52	1.09	1.29

Table 8 *Mass of settled soot at 1250 rpm without ultrasound*

time		thermometer reading	soot mass determination			
total time (min)	minute	t (°C)	distance (mm)	paper weight (g)	paper weight with soot (g)	net weight of settled soot (g)
5	1	23.9	100	0.8	1.50	0.70
	2	26.0	200	0.79	1.18	0.39
	3	29.2	300	0.76	0.88	0.12
	4	31.7	400	0.73	1.35	0.62
	5	33.0	500	0.74	1.05	0.31

Table 9 *Mass of settled soot at 1250 rpm with ultrasound (2 emitters)*

time		thermometer reading	soot mass determination			
total time (min)	minute	t (°C)	distance (mm)	paper weight (g)	paper weight with soot (g)	net weight of settled soot (g)
5	1	26.4	100	0.85	1.92	1.07
	2	28.8	200	0.77	1.86	1.09
	3	31.5	300	0.76	1.51	0.75
	4	33.3	400	0.78	1.62	0.84
	5	35.4	500	0.79	1.49	0.70

toxicity of exhaust gases in the ultrasonic muffler was confirmed. Moreover, the most effective cleaning of the exhaust gas of the hydrocarbon is when the emitter is operating in the longitudinal direction of gas movement since in this case the heaviest gas particles immediately begin to settle.

At the second stage of the experiment, the dependence of the settled soot mass on the sedimentation length L was investigated. Tables 3 to 11 give examples of the experimental results' recordings.

Tables 3, 4, 5 and 6 show the masses of settled soot without ultrasound, with two emitters, transverse and

Table 10 *Mass of settled soot at 1250 rpm with ultrasound (1 transverse emitter)*

time		thermometer reading	soot mass determination			
total time (min)	minute	t (°C)	distance (mm)	paper weight (g)	paper weight with soot (g)	net weight of settled soot (g)
	1	24.7	100	0.92	2.28	0.85
	2	27.3	200	0.88	1.79	0.91
5	3	29.4	300	0.86	1.78	0.92
	4	33.1	400	0.89	1.87	0.98
	5	38.0	500	0.96	1.63	0.67

Table 11 *Comparison of the mass of settled soot at 1250 rpm.*

distance (mm)	without ultrasound	with ultrasound (2 emitters)	with ultrasound (1 transverse emitter)
100	0.70	1.07	0.85
200	0.39	1.09	0.91
300	0.12	0.75	0.92
400	0.62	0.84	0.98
500	0.31	0.70	0.67
∑	2.14	4.45	4.33

longitudinal emitters at 1000 rpm. Determination of the net mass of the settled soot was made by subtracting the mass of the paper from the mass of the paper with soot. The results are summarized in Table 7. From that table follows that the operation of two emitters is the most effective and the longitudinal emitter is more conducive to large gas coagulation. Thus, the gas purification of the CH is the most effective with a longitudinal emitter, this is explained by the long path of the particles through the muffler and hence the long time of exposure to ultrasound. A change in the carbon monoxide (CO) reading indicates an increase in concentration due to exposure to ultrasonic waves. In this case, the length L, at which the CO molecules were to be deposited, is insufficient. The volatility of CO is higher than of the CH.

Tables 8, 9 and 10 show the gas coagulation data at 1250 rpm and Table 11 summarizes. Determination of the net mass of the settled soot was made by subtracting the mass of the paper from the mass of the paper with soot.

The conclusions from Table 11 are the same as before. However, it was found that the mass of coagulation increases significantly (2-2.5 times) with an increase in the engine speed. Figures 8 and 9 show experimental graphs of the dependence of the settled soot mass on the muffler's length L.

As follows from the graphs, there is a local maximum in the soot deposition at a distance of 400 mm from the exhaust pipe. This is quantitatively true for the stand, but the qualitative relationship will also be true for the polypropylene mufflers. Moreover, the highest deposition is provided by the two emitters and the longitudinal emitter is more efficient than the transverse one.

According to the tables, the following were determined:

- mass of the soot settled during the operation without ultrasound m_0, this mass corresponds to orthokinetic coagulation;
- the total mass of the soot under the action of ultrasound m_u;
- then the mass without the action of ultrasound m_0 was subtracted from the total mass m_u and the mass of the hydrodynamic coagulation soot m_g was determined [12]:

$$m_u - m_0 = m_s . \tag{5}$$

Tables 12 and 13 show the size data for orthokinetic and hydrodynamic coagulation. The data obtained made it possible to quantitatively determine the weight of hydrodynamic coagulation.

The coefficient of hydrodynamic coagulation was set in relation to the mass of orthokinetic coagulation, since the latter always takes place:

$$K_g = \frac{\sum m_g}{\sum m_0} . \tag{6}$$

The calculated values of the hydrodynamic coagulation coefficient are shown in Table 14.

According to the results of calculations from Table 14, it follows that hydrodynamic coagulation is the most effective under the influence of a longitudinal emitter, the maximum results were shown by the installation option with 2 emitters, since the intensity of ultrasound exposure was 2 times higher.

During the experiment, photo and video recordings were made inside the ultrasonic muffler using a Mikmed

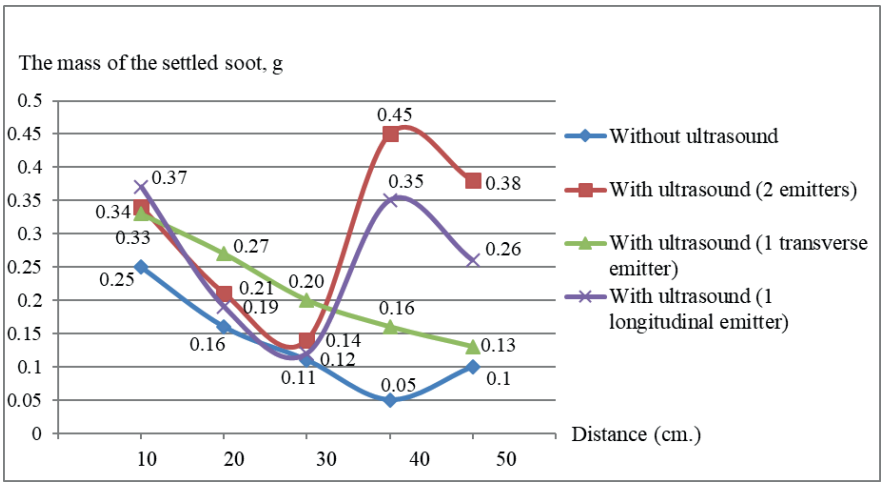


Figure 8 *Graph of dependence of the settled soot mass on the settling distance at 1000 rpm of the crankshaft*

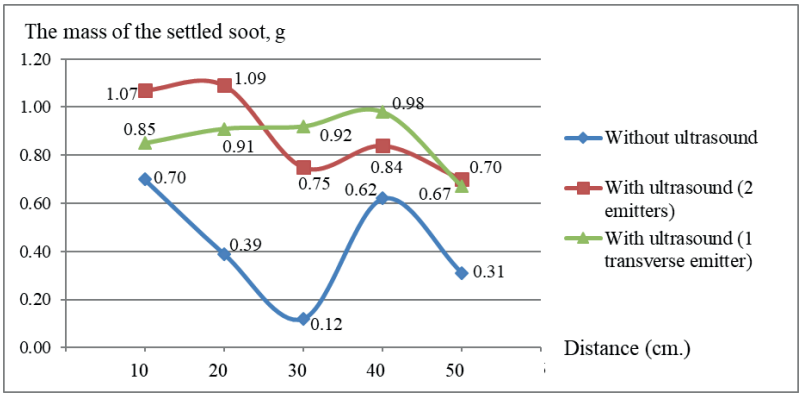


Figure 9 *Graph of dependence of the settled soot mass on the settling distance at 1250 rpm of the crankshaft*

Table 12 *Mass of soot from hydrodynamic coagulation at 1000 / 1250 rpm under the influence of 2 ultrasonic emitters*

	determination of the mass of soot		
distance (mm)	the mass of settled soot under the action ultrasound, m_u (g)	mass of settled soot without ultrasound (g) (action of orthokinetic coagulation), m_0	the mass of settled soot from the action of hydrodynamic coagulation, m_g (g)
100	0.34/1.07	0.25/0.70	0.9/0.37
200	0.21/1.09	0.16/0.39	0.05/0.7
300	0.14/0.75	0.11/0.12	0.03/0.63
400	0.45/0.84	0.05/0.62	0.4/0.22
500	0.38/0.70	0.10/0.31	0.28/0.39

Table 13 *Mass of soot from hydrodynamic coagulation at 1000 / 1250 rpm. under the influence of one transverse ultrasonic emitter*

	determination of the mass of soot		
distance (mm)	the mass of settled soot under the action ultrasound, m_u (g)	mass of settled soot without ultrasound (g) (action of orthokinetic coagulation), m_0	the mass of settled soot from the action of hydrodynamic coagulation, m_g (g)
100	0.33/0.85	0.25/0.70	0.08/0.15
200	0.27/0.91	0.16/0.39	0.11/0.52
300	0.20/0.92	0.11/0.12	0.09/0.8
400	0.16/0.98	0.05/0.62	0.11/0.36
500	0.13/0.67	0.10/0.31	0.03/0.36

Table 14 *The coefficient of hydrodynamic coagulation*

engine speed (rpm)	coagulation coefficient value, s^{-1}		
	under the influence of ultrasound (2 emitters)	under the influence of ultrasound (1 transverse emitter)	under the influence of ultrasound (1 longitudinal emitter)
1000/1250	1.27/1.08	0.62/1.26	0.93

2.0 digital microscope with the ability to magnify from 20 to 200x at a maximum resolution of 1920 × 1080 pixels without ultrasound and with ultrasound.

6 Conclusions

In order to reduce the transport emissions and purify the exhaust gases from vehicles, at minimum costs and maximum efficiency of this system, it is necessary to use the ultrasonic cleaning of exhaust gases, since the ultrasonic effect on aerosols makes it possible to enhance the phenomenon of the exhaust gas particles coagulation and contributes to their settling inside the muffler body in the form of carbon deposits. The proposed method of cleaning the exhaust gases, which is a result of the experiment, has shown its effectiveness and applicability in the field of transport.

The effectiveness of application of ultrasonic action on the exhaust gas of motor vehicles was proved in the course of the experiment and has a promising development in this direction of cleaning the aerosols of the harmful impurities by the proposed method. According to the results of the experiment, the concentration of the hydrocarbon decreased by more than twice - at 1000 rpm of the engine crankshaft from 50 ppm/min to 27 ppm/min and at 1250 rpm from 27 ppm/min to 12 ppm/min.

The total mass of the settled soot in the experimental device under the action of ultrasound exceeds the mass of the settled soot without ultrasound by more than 1.5 times. Hydrodynamic coagulation is superior to the orthokinetic cleaning in terms of efficiency. The longitudinal radiator is more efficient than the transverse radiator in the process of cleaning the exhaust gas from the hydrocarbon, since the coagulation takes place at a greater distance. In this experiment, the longitudinal emitter showed the maximum result for cleaning of the CH and in the process of the soot particles settling, a variant of an installation with two emitters. This fact indicates the need to use the two emitters in one design, longitudinal and transverse.

The article proves the hypothesis of reducing the harmful emissions through use of the ultrasonic mufflers, the design of which is proposed in the patent [6].

The conducted experimental studies are the basis for creating an engineering calculation method during the development of experimental samples of ultrasonic mufflers [13-14].

References

[1] KORABLEV, R. A., BELOKUROV, V. P., ZELIKOV, V. A., LIKHACHEV, D. V., RAZGONYAEVA, V. V., BOYKO, N. I. Environmental safety of vehicles. Voronezh, 2011.

[2] KADYROVA, I. A., MINDUBAEVA, F. A., GRJIBOVSKI, A. M. Prediction of outcomes after stroke: a systematic review (in Russian). *Human Ecology* [online]. 2015, **2015**(10), p. 55-64. ISSN 1728-0869. Available from: https://doi.org/10.33396/1728-0869-2015-10-55-64

[3] RIERA-FRANCO DE SARABIA, E., ELVIRA-SEGURA, L., GONZALEZ-GOMEZ, I., RODRIGUEZ-MAROTO, J. J., MUNOZ-BUENO, R., DORRONSORO-AREAL, J. L. Investigation of the influence of humidity on the ultrasonic agglomeration of submicron particles in diesel exhausts. *Ultrasonics* [online]. 2003, **41**(4), p. 277-281. ISSN 0041-624X. Available from: https://doi.org/10.1016/S0041-624X(02)00452-3

[4] Patent RU 2 364 736 C2 Method of cleaning exhaust gas from particles. Declared 12/20/2008, publ. 08/20/2009 Bul. No. 23.

[5] Patent RU 2 373 409 C2 Device for cleaning automobile exhaust gases from particles. Declared 06/10/2009, publ. 11/20/2009 Bul. No. 32.

[6] Patent RK No. 3194. Device for ultrasonic cleaning of exhaust gases. Declared 12/20/2017, publ. 10/02/2018.

[7] BALDEV, R., RAJENDRAN, V., PALANICHAMI, P. *Applications of ultrasound*. Moscow: Technosphere, 2006. ISBN 5-94836-088-1.

[8] DONG, S., LIPKENS, B., CAMERON, T. V. The effects of orthokinetic collision, acoustic wake and gravity on acoustic agglomeration of polydisperse aerosols. *Journal of Aerosol Science* [online]. 2006, **37**(4), p. 540-553. ISSN 0021-8502. Available from: https://doi.org/10.1016/j.jaerosci.2005.05.008

[9] BERGMAN, L. *Ultrasound and its application in science and technology*. Moscow: Publishing house of foreign literature, 1957.

[10] SHEROV, K. T., KHODZIBERGENOV, D. T., IBRAGIMOVA, Z. A., KHODZIBERGENOVA, U. D., ABDUKARIMOV, A., ESIRKEPOV, A. Some aspects of software in cutting tools designing and testing. *Russian Engineering Research* [online]. 2019, 39(9), p. 772-775. ISSN 1068-798X. Available from: https://doi.org/10.3103/S1068798X19090090

[11] YESSIRKEPOVA, A. B., SHEROV, K. T., MIKHAILOV, V. F., BUZAUOVA, T. M., MAZDUBAY, A. V., TASKARINA, A. Z. Research of ways of connecting reinforced bars in the production of reinforced concrete products. *Journal of Applied Engineering Science* [online]. 2020, **18**(3), p. 372-377. ISSN 1451-4117, eISSN 1821-3197. Available from: https://doi.org/10.5937/jaes18-24319

[12] IBATOV, M. K., KADYROV, A. S., PAK, I. A., KADYROVA, I. A., ASKAROV, B. S. Results of experimental studies of the operation of capacitive equipment for ultrasonic cleaning of exhaust gases of vehicles. *Ugol* [online]. 2020, **2**, p. 73-78. ISSN 0041-5790, eISSN 2412-8333. Available from: https://doi.org/10.18796 / 0041-5790-2020-2-73-78

[13] KADYROV, A., GANYUKOV, A., PAK, I., SULEYEV, B., BALABEKOVA, K. Theoretical and experimental study of operation of the tank equipment for ultrasonic purification of the internal combustion engine exhaust gases. *Communications - Scientific Letters of the University of Zilina* [online]. 2021, **23**(3), p. B219-B226. ISSN 1335-4205, eISSN 2585-7878. Available from: https://doi.org/10.26552/com.C.2021.3.B219-B226

[14] KADYROV A., ZHUNUSBEKOVA Z., GANYUKOV A., KADYROVA I., KUKESHEVA A. General characteristics for loading the working elements of drilling and milling machines when moving in the clay solution. *Communications - Scientific Letters of the University of Zilina* [online]. 2021, **23**(2), p. B97-B105. ISSN 1335-4205, eISSN 2585-7878. Available from: https://doi.org/10.26552/com.C.2021.2.B97-B105

EXPERIMENTAL ANALYSIS OF VERTICAL VIBRATIONS OF A RAILWAY BOGIE

Mădălina Dumitriu[1,*], Ioan Cristian Cruceanu[2]

[1]Department of Railway Vehicles, University Politehnica of Bucharest, Bucharest, Romania
[2]Doctoral School of Transport, University Politehnica of Bucharest, Bucharest, Romania

*E-mail of corresponding author: madalinadumitriu@yahoo.com

Resume
The paper presents a study of the vertical vibrations of a bogie of a passenger vehicle, based on the acceleration of the axles and the bogie frames, measured during the running at a constant velocity. To this purpose, the root mean square (RMS) acceleration is calculated for more measurement sequences at different velocities. In principle, the RMS acceleration increases along with the velocity and influence of the variability of the amplitude in the track defects upon the dispersion of the values in the RMS acceleration. Based on the spectral analysis of the measured acceleration, wheel defects and undulatory wear of the rolling surfaces of wheels and rail are highlighted.

Article info
Received 15 March 2021
Accepted 20 March 2021
Online 27 August 2021

Keywords:
vibrations,
railway bogie,
experimental analysis,
root mean square of acceleration,
spectral analysis

Available online: https://doi.org/10.26552/com.C.2021.4.B299-B307

ISSN 1335-4205 (print version)
ISSN 2585-7878 (online version)

This is an open access article distributed under the terms of the Creative Commons Attribution 4.0 International License (CC BY 4.0), which permits use, distribution, and reproduction in any medium, provided the original publication is properly cited. No use, distribution or reproduction is permitted which does not comply with these terms.

1 Introduction

While running, the railway vehicle is subjected to a permanent vibration regime, with adverse effects on the ride quality, ride comfort, integrity of the goods and traffic safety [1]. The vibrations of railway vehicles are mainly caused by the geometric deviations of the track and by irregularities of the rolling surfaces of the wheels and rails [2-8]. Due to its construction, the track features as a whole, on the one hand, many deviations from the ideal geometrical shape and, on the other hand, defects of the rolling surfaces of the rails. These two above, along with the constructive discontinuities of the rail, make up for the major causes of railway vehicle vibrations [9-14]. Wheel defects, such as eccentricity, oval, polygonal profile, corrugation, flat wheel, flattening or defects of rolling surfaces are also causes of railway vehicle vibrations [15-19].

The vibrations' issues of railway vehicles can be addressed either theoretically or experimentally. From the perspective of a theoretical study, based on the results of numerical simulations, the railway vehicle-track system must be represented by an equivalent mechanical model [20-22]. The railway vehicle is a complex oscillating system, which has specific vibration characteristics [23]. This makes it difficult to represent it through a model with a high degree of reliability, which accurately integrates all the factors that influence the vibration behaviour of a vehicle. However, the more complex the model, the closer the results would be to reality, but it would make it difficult to draw general conclusions about the vehicle vibration characteristics. Generally, the models for study of the railway vehicle vibrations are obtained through a simplified representation of the vehicle-track system, in which the most important factors that influence the vibration behaviour of ae vehicle are taken into account.

Although the numerical simulations are useful tools for evaluating the vibration behaviour of the railway vehicle from the design phase and then for investigations during the exploitation [24-25], a real estimate of vehicle vibration behaviour can be made only based on the experimental results obtained to circulation on a current track or on a test track. The experimental tests are expensive and require a high investment of time and effort, but the results reflect a real state even of the effects of uncontrollable variables that cannot be highlighted in a study based on numerical simulations [26].

Recent studies, based on the measured data or numerical simulations, have shown that the vehicle dynamic response is correlated with the track irregularities [10, 13, 27-29], which creates the premises of developing certain monitoring methods of track quality or the vehicle condition [30]. The correlation method has been used to highlight the connection between the lateral and vertical axle box acceleration and differently processed track geometry parameters,

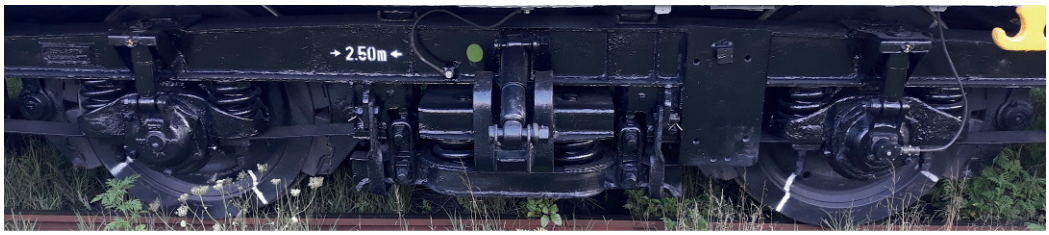


Figure 1 *Minden-Deutz bogie*

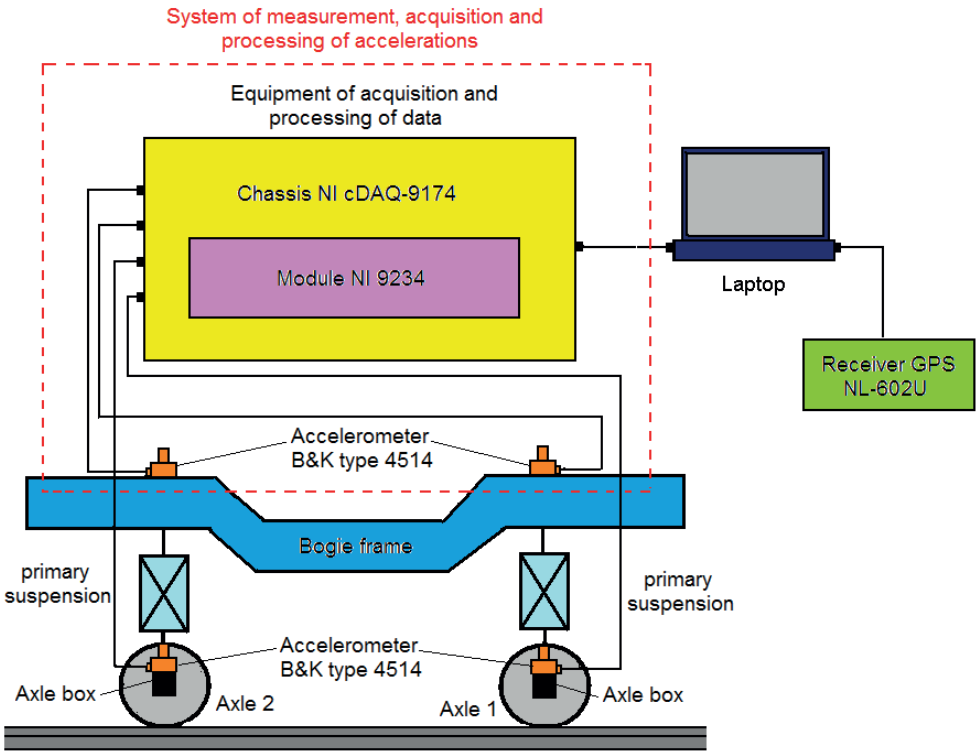


Figure 2 *Schematic representation of the measuring chain*

based on a measurement run on a straight track [10]. In addition, the correlation between the high-frequency vibrations of the axle box acceleration and the geometry of the rail welds has been used to develop an approach for the real-time health detection of rail welds [29]. The results of the numerical simulations were used for an analysis regarding the correlation between the dynamic response of a two-axle bogie and the track vertical irregularities, based on the Pearson correlation coefficient [13].

This paper presents an analysis of the vertical vibrations of a bogie in a rail passenger vehicle, based on the experimental results obtained by measurements done during the running on a current track, on a double-track section in alignment and vertical alignment. In fact, the RMS (root mean square) acceleration is looked at, measured in the axle boxes and on the bogie frame above the axles, for more measurement sequences at a constant velocity. In addition, the spectral analysis of the measured acceleration is done, which helps with e identification of a series of defects in the wheels and the rolling surfaces of the rail and wheels.

2 Measurements of the vertical acceleration of a bogie

The measurements were performed during the running on a current track, for which the maximum traffic velocity is 160 km/h, on a track section in alignment and vertical alignment. The vertical acceleration of the axles and bogie frames were measured for a passenger railway vehicle equipped with Minden-Deutz bogies (Figure 1). The maximum velocity of the vehicle is 140 km/h.

The measuring chain, used to measure the vertical acceleration of the axles and the bogie frames, is shown in Figure 2. It includes the components of the measurement, acquisition and processing system for the vertical acceleration, respectively, four 4514 Brüel & Kjær piezoelectric accelerometers and the set consisting of the NI cDAQ-9174 chassis for the data acquisition and the NI 9234 module for acquisition and synthesising the data from accelerometers. The NL-602U GPS receiver for monitoring and recording the vehicle velocity is also included in the measurement chain.



Figure 3 *Detail of mounting accelerometers on the bogie frame and the axle boxes*

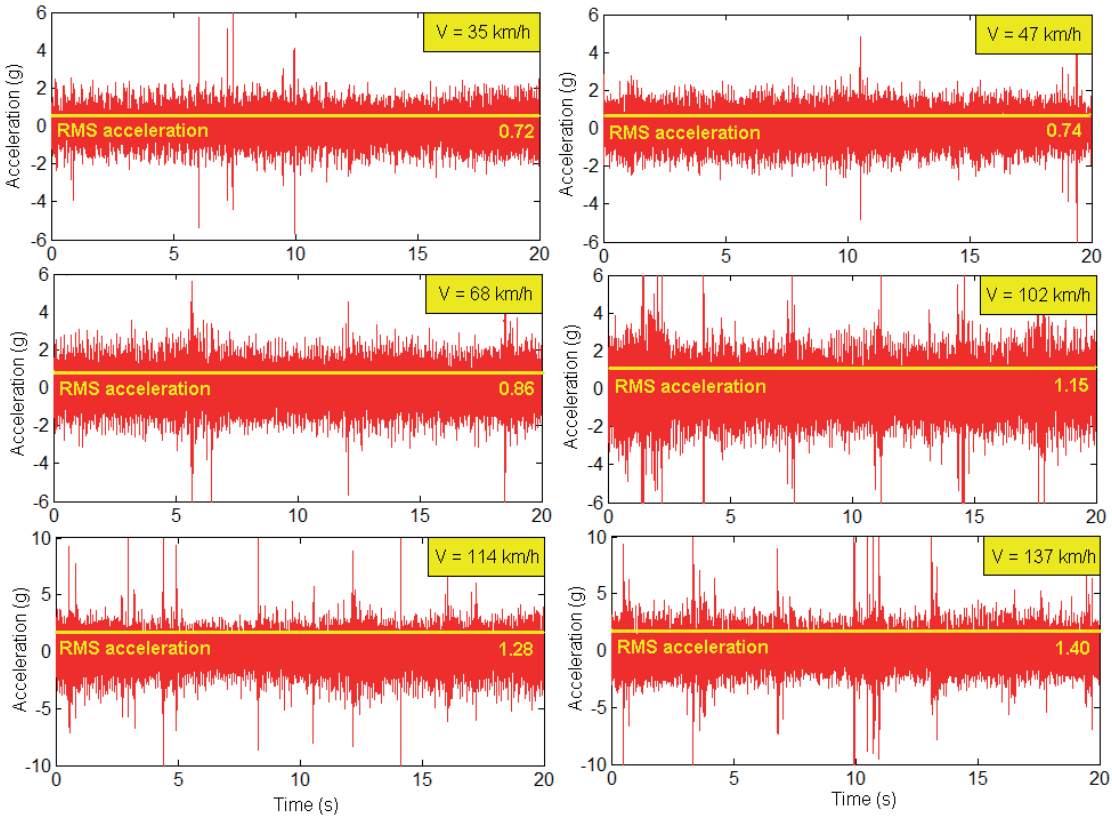


Figure 4 *Acceleration recorded on a measurement sequence at axle 1*

The accelerometers were mounted on a side of the bogie as follows: one accelerometer on each axle box and one accelerometer on the bogie frame against each axle (Figures 2 and 3) [30-31].

Recordings of acceleration were made at a constant velocity on a distance of circa 60 km direction of a traffic. The duration of a measurement sequence is 20 seconds, and the sampling frequency is 2048 Hz. The maximum velocity during the measurements was 137 km/h on direction 1 and 117 km/h on direction 2.

3 Analysis of experimental results

An analysis of the vibrations' characteristics of the axles and the bogie frame, based on the experimental results, is presented in this Section.

In Figures 4 and 5 are presented the accelerations, recorded on a time sequence at different velocities at axle 1 and at the bogie frame above axle 1, respectively. The RMS acceleration is also marked on the diagrams. In all the cases presented, it is observed that the RMS

accelerations, measured at the axle is circa twice higher than the one measured on the bogie frame. In addition, the results highlight the increase of the RMS acceleration with velocity.

The diagrams in Figure 6 show the spectra of the acceleration measured at the two axles and on the bogie frame for a measurement sequence at a velocity of 137 km/h, in the frequency range 1 - 200 Hz. The acceleration

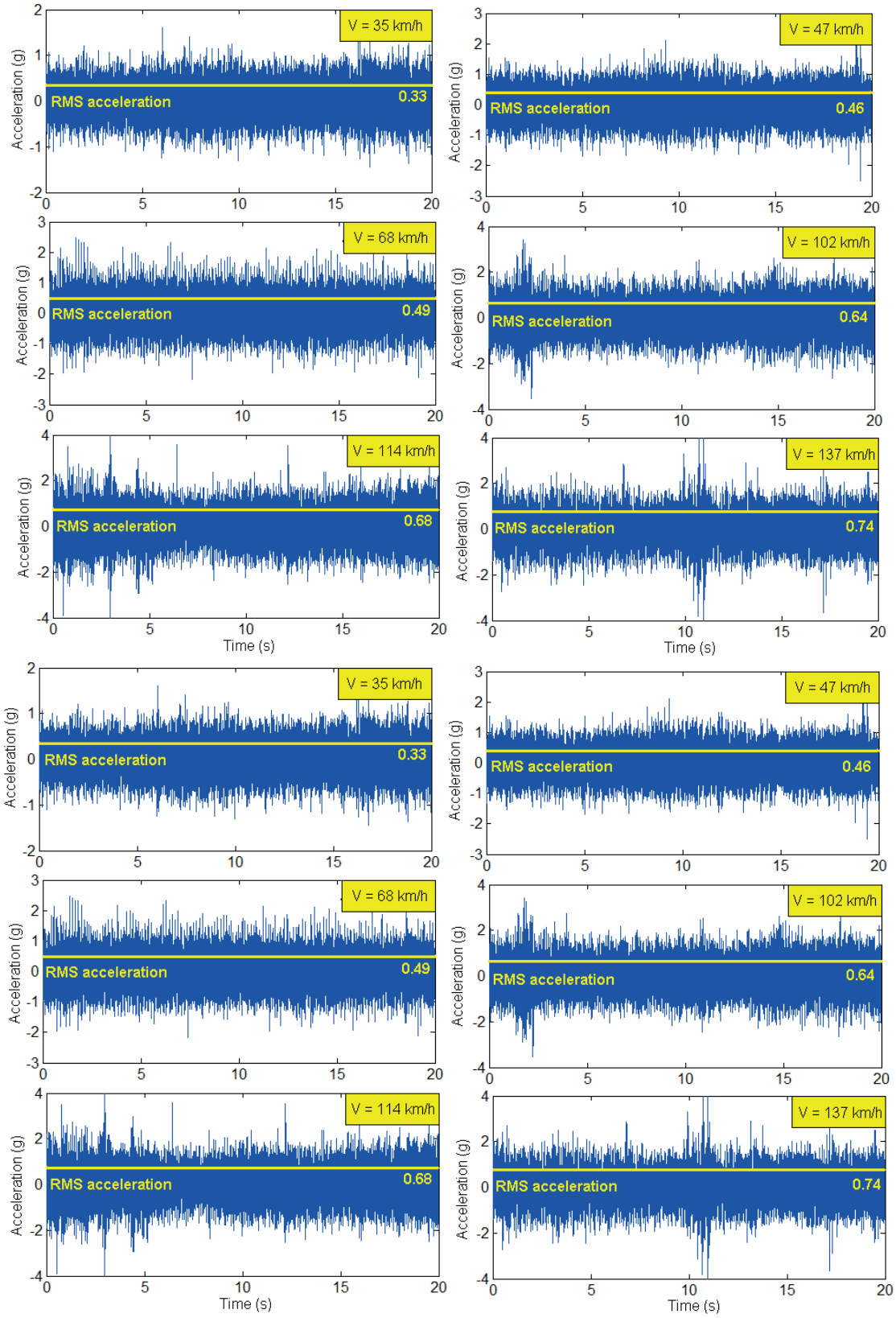


Figure 5 *Acceleration recorded on a measurement sequence at the bogie frame above axle 1*

spectra measured at the two axles show several peaks between 6.2 and 150 Hz, the frequency peak at 6.2 Hz corresponding to the resonant frequency of the bogie bounce. In this frequency range, several accentuated local peaks are observed, which are in arithmetic progression. The first peak corresponds to the frequency of 13.15 Hz and the other peaks have the following frequencies: 26.25, 39.45, 52.45, 65.85, 78.65, 91.9, 105.3 and 118.1 Hz. The first peak is due to y the eccentricity of the wheel, the second due to its ovality and the others due to the undulatory wear from the third order to the ninth order of the rolling surface of the wheel. Another peak occurs at 17.15 Hz, which corresponds to a wavelength of 2.2 m of irregularities of the rolling surface of the rail, signifying long-wave rail undulatory wear.

The spectra of the acceleration, measured on the bogie frame above the two axles, have a peak at frequency of 6.2 Hz, corresponding to the bounce frequency of the bogie. At frequencies higher than 10 Hz, the dominant peaks of the acceleration spectra are those corresponding to the rolling defects of the wheels or the undulatory wear of the rails listed above.

Figure 7 shows the RMS acceleration of the axles and the bogie frame for 29 measuring sequences at the constant velocity of 117 km/h. For axle 1, the RMS acceleration is dispersed between 1.12 g and 1.92 g, whereas for axle 2, the interval is 1.13 g - 2.04 g. In the case of the bogie frame, the RMS acceleration is 0.66 g - 0.92 g - above the axle 1 and 0.67 g - 0.97 g - above the axle 2. The dispersion of the measured acceleration is due to the variability in the amplitude of the defects along the track.

Figure 8 features the RMS acceleration of the axles and of the bogie frame for 20 measurement sequences at the constant velocity of 137 km/h. The influence of the defects' variability along the track on the bogies' vibrations is well visible here by having the RMS acceleration divided into two intervals. Corresponding to the measurement sequences 1-12, the RMS accelerations of the axles vary a little, as they are grouped between 1.27 g and 1.58 g. For the sequence 14, the RMS accelerations of the axles reach a maximum of 2.43 g - in axle 1 and 2.48 g - in axle 2. Further on, for the other measurement sequences, the RMS acceleration gradually decrease to 1.69 g - in axle 1 and to 1.72 g - in axle 2.

The RMS acceleration at the bogie frame has the same characteristics as the acceleration of the axles. Above the axle 1, the RMS acceleration is divided into two intervals, with 0.65 g - 0.75 g as a first interval, where the accelerations vary a little and another interval where the values decrease from 1.05 g to 0.79 g. Above the axle 2, the intervals of the RMS acceleration are 0.66 g - 0.84 g and 1.13 g - 0.83 g.

As shown earlier (see Figures 4 and 5) and in the diagrams in Figures 7 and 8, the RMS acceleration of the axles are noticed to be circa twice higher than the ones on the bogie frame. This is quite clear in the diagrams in Figure 9. Plus, the acceleration measured in the two axles is noticed to be unequal. Similarly, the acceleration for the bogie frame above the two axles is not equal, as well. The diagrams in Figure 10 show that the differences between the RMS acceleration of the two axles reach 0.17 g at the velocity of 117 km/h, whereas this difference for the bogie frame is 0.06 g at the most. At 137 km/h, the differences for the axles come to 0.13 g

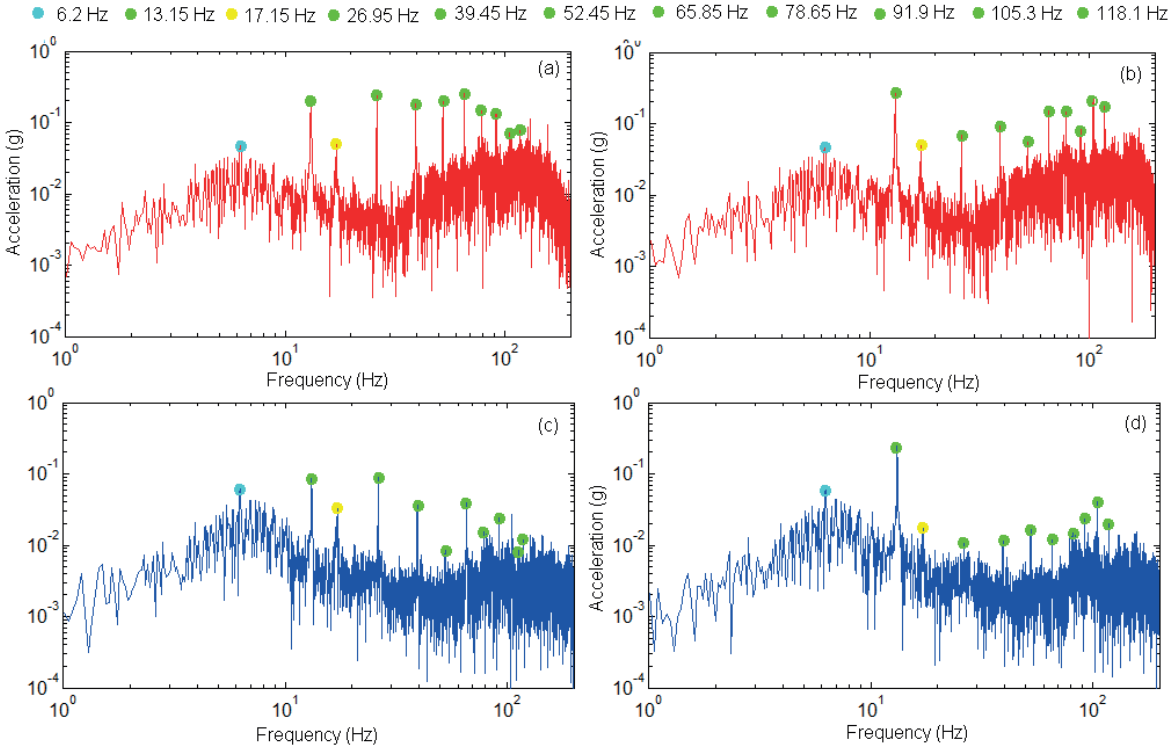


Figure 6 *Acceleration spectra measured at velocity of 137 km/h: (a) at axle 1; (b) at axle 2; (c) on the bogie frame above the axle 1; (d) on the bogie frame above the axle 2*

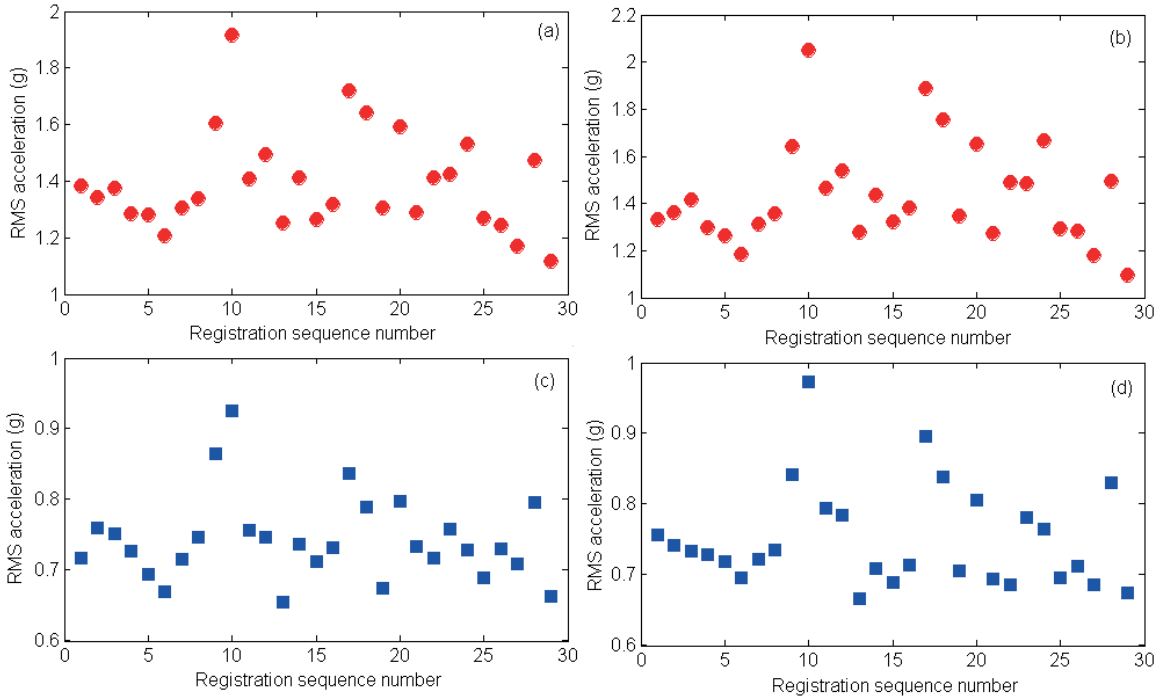


Figure 7 *The RMS acceleration at velocity of 117 km/h for 29 measurement sequences: (a) at axle 1; (b) at axle 2; (c) on the bogie frame above the axle 1; (d) on the bogie frame above the axle 2*

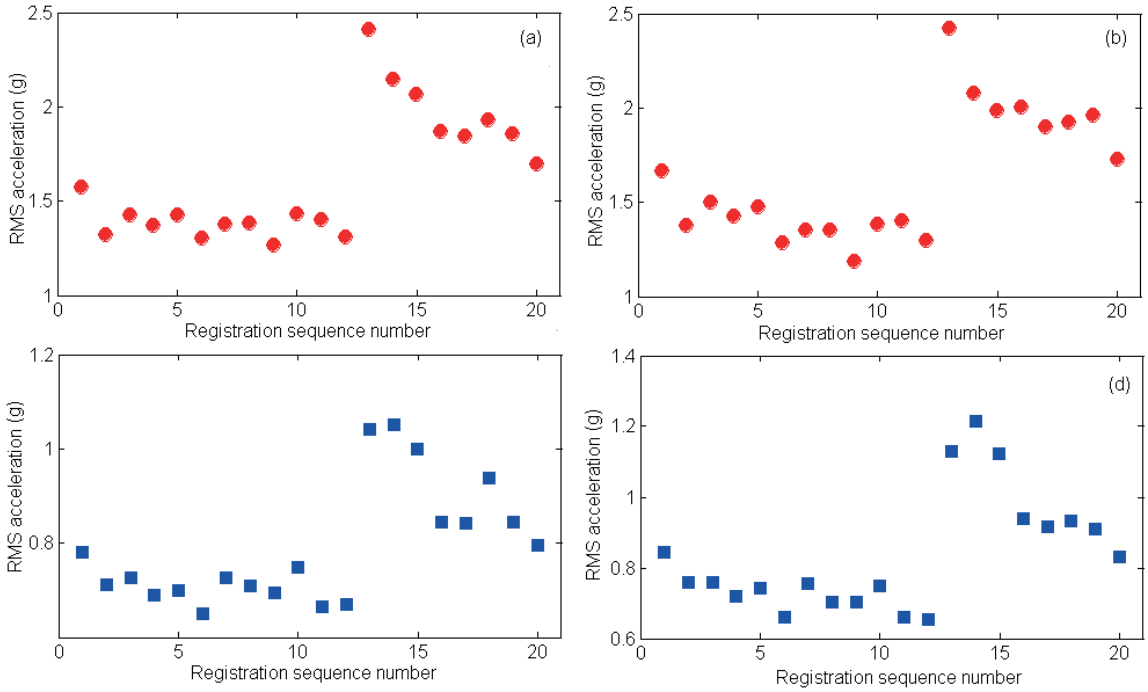


Figure 8 *The RMS acceleration at velocity of 137 km/h for 29 measurement sequences: (a) at axle 1; (b) at axle 2; (c) on the bogie frame above the axle 1; (d) on the bogie frame above the axle 2*

and for the RMS acceleration measured on the bogie frame, the value arrives at 0.17 g.

4 Conclusions

In this paper, the vertical vibrations of the axles and the bogie frame of a passenger vehicle were analysed. The analysis was based on the RMS acceleration for more measurement sequences at two constant velocities. The results showed the fact that the RMS acceleration are circa twice higher in the axles than in the bogie frame. In addition, the RMS acceleration has been proven to increase along with the velocity.

The analysis of the RMS acceleration for more measurement sequences at the same velocity has made visible the influence of the track defects on the

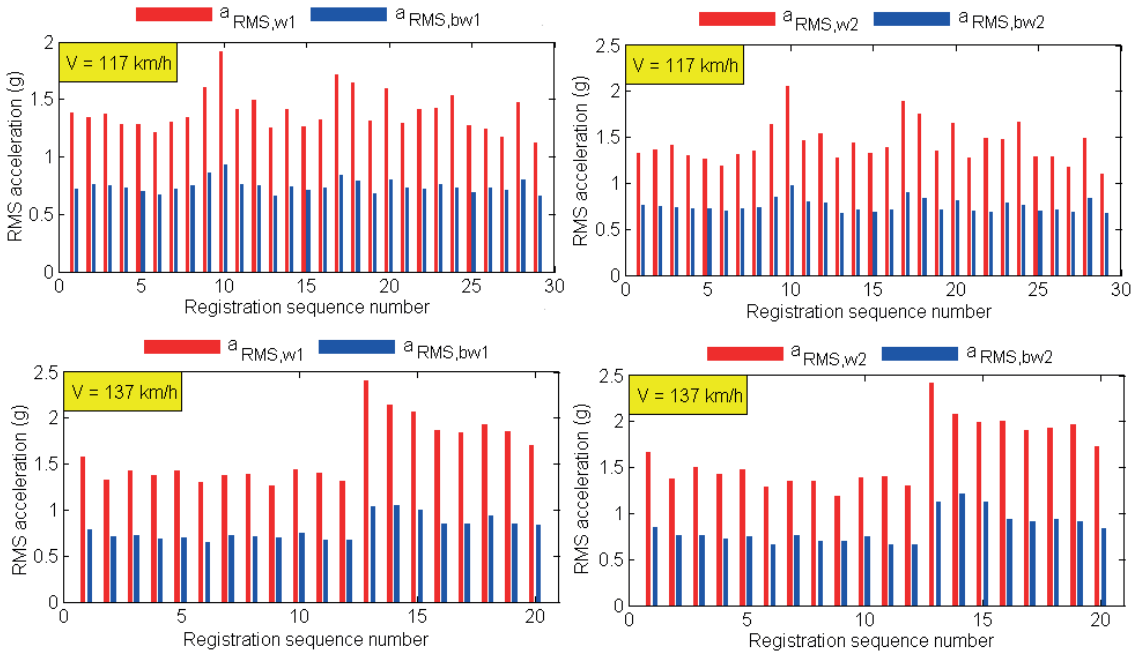


Figure 9 *The RMS acceleration: $a_{RMS,w1,2}$ - RMS acceleration of the axles; $a_{RMS,bw1,2}$ - RMS acceleration of the bogie frame above the axles 1 and 2*

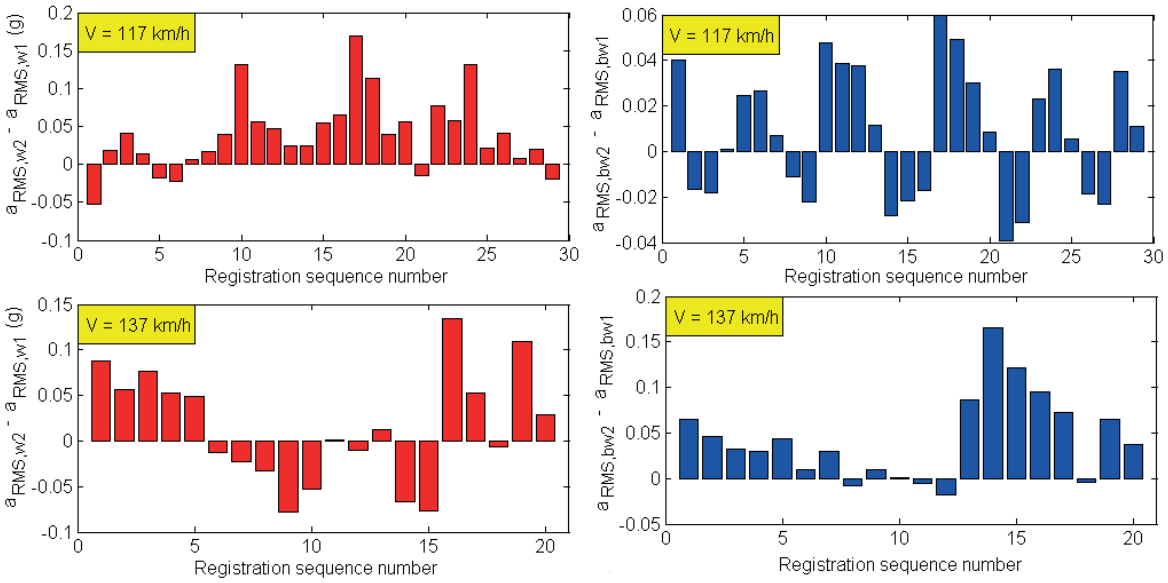


Figure 10 *The difference between the RMS acceleration: $a_{RMS,w1,2}$ - RMS acceleration of the axles; $a_{RMS,bw1,2}$ - RMS acceleration of the bogie frame above axles 1 and 2*

bogie vibrations. Due to the variability in the defects amplitude along the track, the RMS acceleration are not equal at the same velocity, as they are dispersed on interval of circa 0.03 g to 0.9 g.

Based on the spectral analysis of the measured accelerations, wheel defects were identified, namely, eccentricity and ovality and undulatory wear of the rolling surfaces of wheels and rail.

Future research may be aimed at analysis of correlation between the railway bogie vibrations and axles vibrations, based on the measured acceleration. The existence of a correlation between the accelerations measured on the axle boxes and the accelerations measured on the bogie frame may be the basis for development of a method for the condition monitoring of the vehicle primary suspension.

References

[1] SEBESAN, I., MAZILU, T. *Vibrations of the railway vehicles* (in Romanian). Bucharest: MatrixRom, 2010. ISBN 978-973-755-332-4.

[2] XU, L., ZHAI, W., GAO, J., MEACCI, M., CHEN, X. On effects of track random irregularities on random vibrations of vehicle-track interactions. *Probabilistic Engineering Mechanics* [online]. 2017, **50**, p. 25-35 [accessed 2021-03-15]. ISSN 0266-8920. Available from: https://doi.org/10.1016/j.probengmech.2017.10.002

[3] CHELI, F., CORRADI, R. On rail vehicle vibrations induced by track unevenness: analysis of the excitation mechanism. *Journal of Sound and Vibration* [online]. 2011, **330**, p. 3744-3765 [accessed 2021-03-15]. ISSN 0022-460X. Available from: https://doi.org/10.1016/j.jsv.2011.02.025

[4] YOUNG, T. H., LI, C. Y. Vertical vibration analysis of vehicle/imperfect track systems. *Vehicle System Dynamics* [online]. 2003, **40**(5), p. 329-349 [accessed 2021-03-15]. ISSN 0042-3114. Available from: https://doi.org/10.1076/vesd.40.5.329.17912

[5] DUMITRIU, M. Analysis of the dynamic response in the railway vehicles to the track vertical irregularities. Part I: the numerical analysis. *Journal of Engineering Science and Technology Review* [online]. 2015, **8**(4), p. 24-31 [accessed 2021-03-15]. ISSN 1791-2377. Available from: http://www.jestr.org/downloads/Volume8Issue4/fulltext8442015.pdf

[6] DUMITRIU, M. Analysis of the dynamic response in the railway vehicles to the track vertical irregularities. Part II: the numerical analysis. *Journal of Engineering Science and Technology Review* [online]. 2015, **8**(4), p. 32-39 [accessed 2021-03-15]. ISSN 1791-2377. Available from: http://www.jestr.org/downloads/Volume8Issue4/fulltext8452015.pdf

[7] DUMITRIU, M., SEBESAN, I. On the wheelset vibration due to the stochastic track vertical irregularities. *Applied Mechanics and Materials* [online]. 2015, **809-810**, p. 1037-1042 [accessed 2021-03-15]. ISSN 1662-7482. Available from: https://doi.org/10.4028/www.scientific.net/AMM.809-810.1037

[8] MAZILU, T. On the dynamic effects of wheel running on discretely supported rail. *Proceedings of the Romanian Academy, Series A: Mathematics, Physics, Technical Sciences, Information Science* [online]. 2009, **10**(3), p. 269-276 [accessed 2021-03-15]. ISSN 1454-9069. Available from: https://acad.ro/sectii2002/proceedings/doc2009-3/09-Mazilu.pdf

[9] MAZILU, T. Analysis of infinite structure response due to moving wheel in the presence of irregularities via Green's functions method. *Proceedings of the Romanian Academy, Series A: Mathematics, Physics, Technical Sciences, Information Science* [online]. 2009, **10**(2) p. 139-150 [accessed 2021-03-15]. ISSN 1454-9069. Available from: https://acad.ro/sectii2002/proceedings/doc2009-2/06-Mazilu.pdf

[10] AGH, C. Comparative analysis of axlebox acceleration in correlation with track geometry irregularities. *Acta Technica Jaurinensis* [online]. 2019, **12**(2), p. 161-177 [accessed 2021-03-15]. ISSN 2064-5228. Available from: https://doi.org/10.14513/actatechjaur.v12.n2.501

[11] XU, L., ZHAI, W., GAO, J. A probabilistic model for track random irregularities in vehicle/track coupled dynamics. *Applied Mathematical Modelling* [online]. 2017, **51**, p. 145-158 [accessed 2021-03-15]. ISSN 0307-904X. Available from: https://doi.org/10.1016/j.apm.2017.06.027

[12] POMBO, J., AMBROSIO, J. An alternative method to include track irregularities in railway vehicle dynamic analyses. *Nonlinear Dynamics* [online]. 2012, **68**, p. 161-176 [accessed 2021-03-15]. ISSN 1573-269X. Available from: https://doi.org/10.1007/s11071-011-0212-2

[13] DUMITRIU, M., FOLOGEA, D. Numerical analysis on the correlation between bogie dynamic response and vertical track irregularities. *UPB Scientific Bulletin, Series D: Mechanical Engineering* [online]. 2019, **81**(4), p. 99-110. ISSN 1454-2358. Available from: https://www.scientificbulletin.upb.ro/rev_docs_arhiva/rez1fd_907572.pdf

[14] DUMITRIU, M., CRUCEANU, I. C. Effect of vertical track irregularities on the vibration of railway bogie. *UPB Scientific Bulletin, Series D: Mechanical Engineering* [online]. 2019, **81**(1), p. 67-78. ISSN 1454-2358. Available from: https://www.scientificbulletin.upb.ro/rev_docs_arhiva/full866_449125.pdf

[15] SHAN, W., WU, P., WU, X., ZHANG, F., SHI, H. Effect of wheel polygonization on the axle box vibrating and bolt self-loosening of high-speed trains. *IOP Conference Series: Journal of Physics: Conference Series* [online]. 2019, **1213**, 052044. ISSN 1742-6596. Available from: https://doi.org/ 0.1088/1742-6596/1213/5/052044

[16] PENG, B., IWNICKI, S., SHACKLETONA, P., CROSBEE, D., ZHAO, Y. The influence of wheelset flexibility on polygonal wear of locomotive wheels. *Wear* [online]. 2019, **432-433**, 102917. ISSN 0043-1648. Available from: https://doi.org/10.1016/j.wear.2019.05.032

[17] MAZILU, T., DUMITRIU, M., TUDORACHE, C., SEBESAN, M. Wheel/rail interaction due to the polygonal wheel. *UPB Scientific Bulletin, Series D, Mechanical Engineering* [online]. 2011, **D**(3), p. 95-108. ISSN 1454-2358. Available from: https://www.scientificbulletin.upb.ro/rev_docs_arhiva/full81732.pdf

[18] MAZILU, T. A dynamic model for the impact between the wheel flat and rail. *UPB Scientific Bulletin Series D: Mechanical Engineering* [online]. 2007, **69**(2), p. 45-58. ISSN 1454-2358. Available from: https://www.scientificbulletin.upb.ro/rev_docs_arhiva/full58723.pdf

[19] MAZILU, T. Geometric model of a railway wheel with irregular contour. *Advances in Intelligent Systems and Computing* [online]. 2016, **356**, p. 155-166. ISSN 2194-5357. Available from: https://doi.org/10.1007/978-3-319-18296-4_13

[20] CLAUS, H., SCHIEHLEN, W. Modelling and simulation of railway bogie structural vibrations. *Vehicle System Dynamics* [online]. 1998, **28**, p. 538-552. ISSN 0042-3114. Available from: https://doi.org/10.1080/00423119808969585

[21] DUMITRIU, M. Modelling of railway vehicles for virtual homologation from dynamic behavior perspective. *Applied Mechanics and Materials* [online]. 2013, **371**, p. 647-651. ISSN 1662-7482. Available from: https://doi.org/10.4028/www.scientific.net/AMM.371.647

[22] EICKHOFF, B. M., EVANS, J. R., MINNIS, A. J. A review of modelling methods for railway vehicle suspension components. *Vehicle System Dynamics* [online]. 1995, **24**(6-7), p. 469-496. ISSN 0042-3114. Available from: https://doi.org/10.1080/00423119508969105

[23] DIANA, G., CHELI, F., COLLINA, A., CORRADI, R., MELZI, S. The development of a numerical model for railway vehicles comfort assessment through comparison with experimental measurements. *Vehicle System Dynamics* [online]. 2002, **38**(3) p. 165- 183. ISSN 0042-3114. Available from: https://doi.org/ 10.1076/vesd.38.3.165.8287

[24] EVANS, J., BERG, M. Challenges in simulation of rail vehicle dynamics. *Vehicle System Dynamics* [online]. 2009, **47**, p. 1023-1048. ISSN 0042-3114. Available from: https://doi.org/10.1080/00423110903071674

[25] SCHUPP, G. Simulation of railway vehicles: necessities and applications. *Mechanics based design of structures and machines* [online]. 2003, **31**(3), p. 297-314. ISSN 1539-7734. Available from: https://doi.org/10.1081/SME-120022852

[26] UIC 518 Leaflet. Testing and approval of railway vehicles from the point of view of their dynamic behaviour - safety - track fatigue - running behaviour. 2009

[27] KARIS, T., BERG, M., STICHEL, S., LI, M., THOMAS, D., DIRKS, B. Correlation of track irregularities and vehicle responses based on measured data. *Vehicle System Dynamics* [online]. 2018, **56**(6), p. 967-981. ISSN 0042-3114. Available from: https://doi.org/10.1080/00423114.2017.1403634

[28] KARIS, T., BERG, M., STICHEL, S. Analysing the correlation between vehicle responses and track irregularities using dynamic simulations and measurements. *Proceedings of the Institution of Mechanical Engineers, Part F: Journal of Rail Rapid Transit* [online]. 2020, **234**(2), p. 170-182. ISSN 0954-4097. Available from: https://doi.org/10.1177/0954409719840450

[29] BOYANG, A., WANG, P. J., XU, CHEN, R., CUI, D. Observation and simulation of axle box acceleration in the presence of rail weld in high-speed railway. *Applied Sciences* [online]. 2017, **7**, 1259. ISSN 2076-3417. Available from: https://doi.org/10.3390/app7121259

[30] DUMITRIU, M. Fault detection of damper in railway vehicle suspension based on the cross-correlation analysis of bogie accelerations. *Mechanics and Industry* [online]. 2019, **20**(1), 10. ISSN 2257-7777. Available from: https://doi.org/10.1051/meca/2018051

[31] DUMITRIU, M. RACANEL, I. R. Experimental verification of method to synthesize the track vertical irregularities. *Romanian Journal of Transport Infrastructure* [online]. 2018, **7**(2), p. 40-60. ISSN 2286-2218. Available from: https://doi.org/10.2478/rjti-2018-0011

EFFECT OF THE RME BIODIESEL ON THE DIESEL ENGINE FUEL CONSUMPTION AND EMISSION

Dariusz Kurczyński

Department of Automotive Vehicles and Transportation, Faculty of Mechatronics and Automotive Engineering, Kielce University of Technology, Kielce, Poland

*E-mail of corresponding author: kdarek@tu.kielce.pl

Resume

Road transport is the primary source of atmospheric air pollution, thus posing a threat to human health and life. The aim of the study was to determine the impact of fuel obtained from plants on the ecological properties of a compression ignition engine. The article reports the results of investigations into a modern engine with a Common Rail system, powered by the RME (rapeseed methyl esters) biodiesel and their blends with diesel. For comparison, the engine was also fuelled with conventional diesel oil without ester addition. When powering the engine with blends and pure biodiesel, brake specific fuel consumption increased. The concentrations of nitrogen oxides and carbon dioxide in the engine exhaust gas also slightly increased. At the same time, a clear reduction in average concentrations of carbon monoxide, hydrocarbons and particulates matter was obtained.

Article info

Received 17 September 2020
Accepted 10 March 2021
Online 27 August 2021

Keywords:

compression ignition engine,
emission,
alternative fuel,
biodiesel,
ecological safety

Available online: https://doi.org/10.26552/com.C.2021.4.B308-B316

ISSN 1335-4205 (print version)
ISSN 2585-7878 (online version)

This is an open access article distributed under the terms of the Creative Commons Attribution 4.0 International License (CC BY 4.0), which permits use, distribution, and reproduction in any medium, provided the original publication is properly cited. No use, distribution or reproduction is permitted which does not comply with these terms.

1 Introduction

Transport is a large source of harmful effects on the environment. It has a significant impact on people's health and lives. The main, noticeable example of the impact transport has on the environment are road accidents. Transport also causes the introduction of various types of chemical compounds and elements harmful to human health into the Earth's atmosphere. Their main contributors are the exhaust gases emitted by engines used in most means of transport. The road transport sector in 2017 was the largest source of total NO_X emissions and the second largest source of soot, CO emissions and an important source of $PM_{2.5}$ and Pb emissions [1]. According to data from the European Environment Agency, the road transport in the European Union in 2017 was responsible for emissions of: 39% nitrogen oxides, 28% carbon black, 19% carbon monoxide, 11% $PM_{2.5}$ particles, 11% PM_{10} particles and 8% non-methane volatile organic compounds. In addition, transport in the European Union accounts for around 25% of all the greenhouse gas emissions [2-3]. Estimates presented in [1] indicate that in the European Union countries, premature deaths related to exposure to $PM_{2.5}$, NO_2 and O_3, in 2016 amounted to 374000, 68000 and 14000 respectively. The $PM_{2.5}$ particles are the pollutants with the greatest impact on people's lives.

Transport is an energy-consuming sector of the economy. At present, the demand for energy in transport is met mainly by using fossil fuels, which are non-renewable energy sources. Combustion creates harmful compounds and carbon dioxide, which is the basic greenhouse gas that contributes to climate change. Renewable fuels, obtained from organic matter, can be a source of energy that reduces CO_2 and other harmful components of flue gas released into the atmosphere [4-8]. Fatty acid esters are biofuels that can be used in a pure form or as an additive to diesel fuel. They have similar properties to diesel fuel. They can be obtained from various raw materials [9-11]. Esters produced from vegetable oils are well recognized [12-17]. Inedible plants are currently being sought for ester production [18-19]. Such a raw material for obtaining fuels should not affect food prices. Research is also being carried out on development of new technologies for obtaining biofuels, including esters from algae [20-23]. Another important raw material for production of esters [24-27] may be organic waste from agriculture, the agri-food industry and food processing. Using them to produce fuels can also be a way to get rid of waste that is difficult to manage. For the production of esters, waste cooking oil can also be used [28-31]. Uddin et al. produced esters from oil from used coffee [32].

The use of esters to power compression ignition engines is the subject of numerous studies assessing their impact on emission of harmful exhaust components and carbon dioxide. Ozcanli et al. studied B100 methyl castor oil esters and their blends with diesel fuel: B5,

Table 1 *Basic physicochemical properties of commercial diesel fuel DF and rapeseed methyl esters RME [36-37]*

parameter	unit	diesel fuel	biodiesel RME
fatty acid methyl ester (FAME) contents	-	<0.05 % (V/V)	97.9 % (m/m)
density at a temperature of 15 °C	kg/m^3	833.4	883.1
kinematics viscosity at a temperature of 40 °C	mm^2/s	2.596	4.55
cetane number	-	51.0	51.3
cloud point	°C	-10	-6
cold filter plugging point	°C	-29	-22
ignition point	°C	63.5	above 111
sulphur (S) content	mg/kg	8.3	6.4
water content	mg/kg	84	180
particulate contents	mg/kg	7.3	18
10% distillation residue coking residue	% (m/m)	0.01	0.21
testing for corrosive action on copper (3 hours at 50 °C)	assessment	class 1	class 1

B10, B25 and B50 [33]. The measurements were carried out for a three-cylinder, naturally aspirated compression ignition engine with direct fuel injection. For pure esters and blends of esters and diesel oil, a reduction in CO and CO_2 concentrations was obtained compared to diesel fuel. At the same time, NO_x concentrations for B100, B5, B10, B25 and B50 were higher than for diesel. Raheman and Ghadge carried out tests using mahua oil (B100) methyl esters and its blends with diesel fuel B20, B40, B60 and B80 to supply the CI engine [34]. A single-cylinder diesel engine, operating at constant speed under varying loads, was used for the tests. The authors showed that the increase in the content of esters in the blend with diesel fuel resulted in a decrease in CO emissions and smoke opacity. The growing share of biodiesel in the tested fuels slightly increased the NO_x concentrations in comparison to the pure diesel oil. Ozener et al. studied biodiesel from soybean oil and its blends with diesel fuel: B10, B20, B50. The measurements were carried out for a single-cylinder, naturally aspirated compression ignition engine, operating at different rotational speeds of the crankshaft, at maximum load [35]. By supplying the engine with biodiesel and its blends, compared to diesel, reduced CO, HC and smoke opacity and increased CO_2 and NO_x concentrations. Raman et al. conducted tests of rapeseed oil methyl esters and their blends with diesel fuel: B25, B50 and B75 and for comparison pure diesel oil [12]. The tests were carried out for a stationary, single-cylinder diesel engine operating at a constant crankshaft rotational speed and variable load. They achieved a reduction in HC, CO emissions and an increase in NO_x and smoke opacity for fuels: B25, B50, B75 and B100 compared to DF.

In contrast to the above-presented analyses, the studies of RME rapeseed methyl esters and their blends with diesel fuel, presented in this work, were carried out using a modern compression ignition engine, with the Common Rail power supply system and electronically controlled electromagnetic injectors. This engine is typically used to power passenger cars. It is a construction designed in accordance with the direction of development of piston internal combustion engines called “downsizing”. The purpose of this study was to determine the effect of use of the RME biodiesel and its blends with diesel fuel: B20, B40, B60 and B80 on the ecological indicators of the tested engine.

2 The tested fuels

The tests were conducted with the engine being fed either with rapeseed methyl esters (RME) and with commercial diesel oil containing no plant oil esters. The rapeseed methyl esters (RME) constitute a renewable fuel of plant origin. The RMEs are obtained in the process of transesterification of rape oil triglycerides with methanol. The requirements imposed on esters intended for feeding self-ignition engines are specified in standard PN-EN 14214. The second fuel was the diesel fuel. It is a mixture of hydrocarbons obtained via various petroleum processing routes. The requirements for diesel fuel intended for feeding compressed ignition engines are specified in standard PN-EN 590. In the diesel oil purchased for performing the tests, there were no FAME esters. As compared to diesel oil, the RMEs are distinguished by higher density and viscosity, higher water and solid impurity contents, higher turbidity and cold filter blocking temperature, as well as a higher oxygen content in the elementary fuel composition, among other characteristics. Selected properties of the diesel fuel and the RME are presented in Table 1.

3 Experimental setup

Experimental tests were carried out on an engine test bed stand built in the Heat Engine Laboratory at the Kielce University of Technology. The test stand

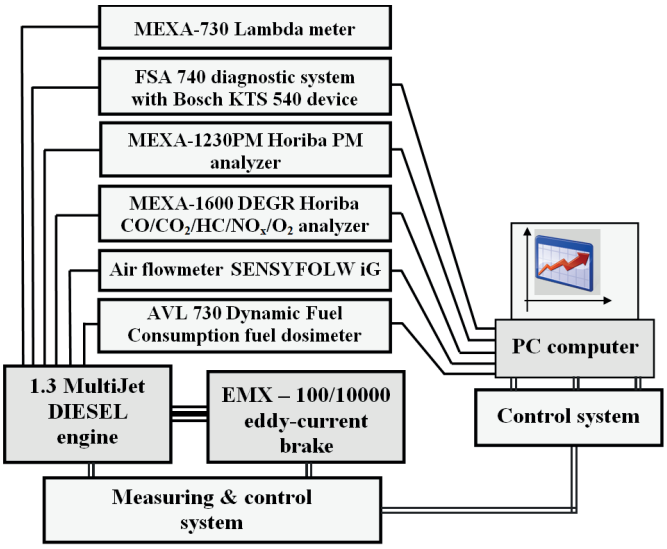


Figure 1 *A block diagram of the dynamometer test stand*

Table 2 *Basic metrological parameters of the test stand*

measured parameter	measuring ranges	accuracy	measurement resolution
rotational speed	0 - 10000 rpm	≤ 1 rpm	1 rpm
torque	0 - 240 Nm	1% of full scale	0.001 Nm
fuel consumption	0 - 150 kg/h	0.12% of measured value	0.001 g/s
air consumption	0 - 2000 kg/h	0.2% of measured value	0.001 kg/h

Table 3 *Metrological parameters of exhaust gas analyzers*

measured component	measuring ranges min/max	repeatability	measurement resolution
CO	0-100/3000 ppm	± 1% of full scale	0.1 ppm
CO_2	0-1/16%	± 1% of full scale	0.01%
THC	0-100/20000 ppm	± 1% of full scale	0.1 ppm
NO_x	0-100/5000 ppm	± 1% of full scale	0.1 ppm
O_2	0-10/25%	± 1% of full scale	0.01%
PM	0-300 mg/m^3	± 1% of full scale	0.01 mg/m^3

consisted of: a Fiat 1.3 MultiJet compression ignition engine, an eddy-current brake type EMX - 100/10 000, a control cubicle with a control system by AUTOMEX, a PC with software to control the test stand during the testing and to archive the test results. The fuel consumption measurement on the testing stand was done by the gravimetric method with an AVL 730 Dynamic Fuel Consumption fuel dosimeter. The air consumption during the testing was measured using an FMT500-IG (SENSYFOL iG) air flowmeter. The test stand control cubicle consists of: an AMX 202 brake power panel, an AMX 211 engine-brake assembly control module, an AMX212 PMO measuring module to measure the most important parameters describing the engine operation conditions (the crankshaft rotational speed and the torque) and a temperature and pressure measurement panel. Furthermore, the test stand was equipped with a FSA 740 diagnostic system complete with a Bosch KTS 540. The block diagram of the engine test stand on which the tests were performed is shown in Figure 1. Basic metrological parameters of the research stand are summarised in Table 2.

The test stand included also a MEXA-1600 DEGR combustion gas analyzer and a MEXA-1230PM particulate matter analyzer. The MEXA-1600DEGR analyzer is designed for the continuous real-time measuring of the concentrations of five internal combustion engine exhaust gas components, namely: carbon monoxide (CO), carbon dioxide (CO_2), hydrocarbons (THC), nitrogen oxides (NO_x) and oxygen (O_2). Moreover, this analyzer enables the assessment of the exhaust gas recirculation rate by the measurement of EGR-CO_2. All the subassemblies, needed for carrying out measurements, such as analyzer modules, a gas sampling and sample preparation system, an incorporated industrial-type computer and gas and electric connections, are all housed

Table 4 *Basic technical specification of the FIAT 1.3 Multijet*

parameter	unit	value
cylinder arrangement	-	in-line
number of cylinders	-	4
injection type	-	direct, multi-stage fuel injection
cylinder operation order	-	1 - 3 - 4 - 2
compression ratio, ε	-	17.6
cylinder bore, D	m	$69.6 \cdot 10^{-3}$
piston stroke, S	m	$82 \cdot 10^{-3}$
engine cubic capacity, V_{ss}	m^3	$1.251 \cdot 10^{-3}$
engine rated power, P	kW	66
rotational speed at rated power, n_P	rpm	4000
maximum engine torque, T	Nm	200
maximum torque rotational speed, n_T	rpm	1750
idling rotational speed	rpm	850±20

in a single cubicle. The computer software enables the control of the analyzer subassemblies, including the gas sampling and sample preparation system and the calibration gas connection system for performing calibrations. Moreover, it performs the collection of data and its archiving, editing and transmitting. The MEXA-1230PM analyzer is designed for the continuous real-time measurements of the particulate matter (PM) concentrations in the exhaust gas of compression ignition engine. The analyzer enables the separate and simultaneous measurement of the two particulate matter components: the Soluble Organic Fraction (SOF) and the Soot. It is able to sample exhaust gas either directly from the exhaust system or after it has been diluted in the measuring tunnel. The measurement of the Soot is done by measuring the quantity of electric charge transferred by soot particles charged in the electric field. The Soluble Organic Fraction (SOF) is measured using two FID detectors as the difference of their signals for the exhaust gas tested, at temperatures of 47 ºC and 191 ºC. Metrological parameters of the analysers used in the tests are shown in Table 3. The exhaust gases paths of these analysers comply with the requirements of ISO-8178.

The Fiat 1.3 MultiJet engine has been designed based on an engines development direction, aimed at designing engines with smaller geometrical dimensions and smaller mass, while maintaining or improving their ecological and energy indices. The basic technical specification of this engine is given in Table 4. The engine block is cast of cast iron and has an aluminium support plate and in-cast cast iron main bearing bushes. This provides the required rigidity of the engine with limited dimensions. The timing gear system uses two distribution shafts. The engine head incorporates four valves per cylinder: two inlet valves and two exhaust valves. This solution has been adopted to increase the cylinder filling ratio. The tested engine was equipped with a variable-geometry vane turbocompressor and a cooler for air delivered to the cylinders. The engine was furnished with an exhaust gas recirculation system with an exhaust gas cooling capability. The engine under investigation is equipped with the Common Rail MJD 6JF fuel feed system with electromagnetic injectors. The fuel injection process is electronically controlled. The feed system of the Fiat 1.3 Multijet engine allowed the fuel dose injected to the cylinder during one cycle to be divided into a maximum of three parts.

4 Research methodology

Engine tests were carried out to determine the exhaust gas composition and fuel consumption of the FIAT 1.3 Multijet engine, powered successively by blends of diesel oil and RME esters with an increasing volume of RME in the blends. The tests were conducted on the following RME and DF blends: B20, B40, B60 and B80. In addition, the engine was also powered by pure RME esters and, for comparison, diesel fuel that contains no esters. The tests were carried out at a constant crankshaft rotational speed of 3000 rpm. The engine load was changed from the smallest to the largest set value. Measurements were taken for the following torque values: 10, 20, 40, 60, 80,100, 120, 140, 160 and 180 Nm. At each measuring point, the results were recorded after establishing the speed-load and thermal conditions of engine operation. At the same time, the hourly fuel consumption, torque, effective power, hourly air consumption, excess air coefficient were measured as well as concentrations of the basic exhaust components: carbon monoxide CO, carbon dioxide CO_2, nitrogen oxides NO_x, total hydrocarbons THC, particulates matter PM and oxygen O_2. These concentrations were measured continuously under established engine operating conditions for approximately 60 seconds at a sampling rate of ten measurements per second. The quantity of the PM particles in exhaust gases was also measured. This measurement was also carried out for about 60

seconds with a sampling rate of one measurement per second. Measurements of gaseous exhaust components and particulates were taken simultaneously. The results of the exhaust gas composition measurements presented in the graphs are the averaged values at individual measurement points.

5 Results and discussions

The basic indicator, measured during the tests of the work of the FIAT 1.3 Multijet engine fuelled with: RME, B20, B40, B60, B80 and DF, was its hourly fuel consumption FC. The engine was operated at a constant crankshaft speed and variable loads. The results of these measurements are shown in Figure 2. Fuel consumption increased with the increase of the RME share in the blends with DF. The highest fuel consumption was obtained for the RME. The average increase in fuel consumption for B20, B40, B60, B80 and RME fuels in relation to DF was: 6.6, 6.8, 8.6, 12.7 and 13.2%, respectively. The increase in fuel consumption is a result of the lower calorific value of esters containing oxygen in their elemental composition. Brake specific fuel consumption BSFC was determined by dividing the values of hourly consumption by engine's power. The calculated BSFC values for the tested fuels are shown in Figure 3. Similar BSFC changes were obtained for B20, B40, B60, B80 and RME fuels in relation to DF, as in the case of FC. Other researchers also obtained an increase in BSFC when engines were run on esters or their blends with diesel oil compared to diesel oil [12, 17, 38].

The main objective of this study was to determine the impact of the increased participation of RME in blends with DF and to assess the effect of using the pure RME on concentrations of the basic measured components in the engine exhaust. Figure 4 compares the concentrations of the carbon monoxide in the engine exhaust gases when fuelled by: B20, B40, B60, B80, RME and DF. For all the blends tested and for biodiesel B100, concentrations of CO in the exhaust gases were reduced, as compared to diesel. The average CO reduction for B20, B40, B60, B80, RME compared to DF was 13.4, 13.7, 17.1, 21.2 and 27.4%, respectively. This is the result of the oxygen content of the elementary composition of biodiesel, which promotes the firing of fuel and oxidation of CO to CO_2. Many publications indicate CO reductions in exhaust gases when using biodiesels obtained from various raw materials [39-42].

The results of measurements of carbon dioxide concentrations in the exhaust gases of engines powered by the B20, B40, B60, B80, RME and DF are shown in Figure 5. When supplying the engine with blends and pure RME biodiesel, an average increase in CO_2 concentrations in the exhaust gas was obtained by about 2.0% - 5.7%. A slight increase in CO_2 concentrations in exhaust gases may be the result of increased fuel consumption and better CO-burning for CO_2. Other researchers also show an increase in carbon dioxide emission using esters to power engines [35, 43-44].

The results of various studies presented in the literature indicate an increase in nitrogen oxide concentrations using different biodiesels to power compression ignition engines [45-48]. This article also

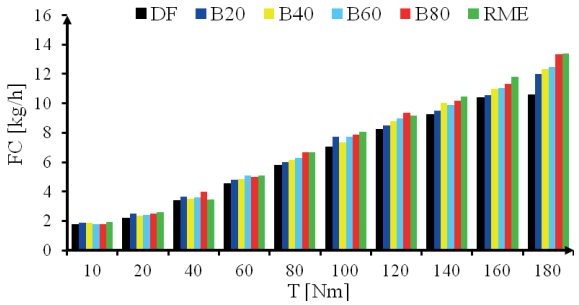


Figure 2 *Engine fuel consumpion as a function of its load, when fuelled: DF, B20, B40, B60, B80, RME*

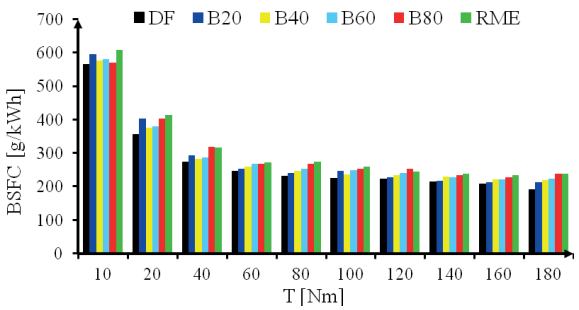


Figure 3 *Brake specific fuel consumption of the engine as a function of its load, when fuelled: DF, B20, B40, B60, B80, RME*

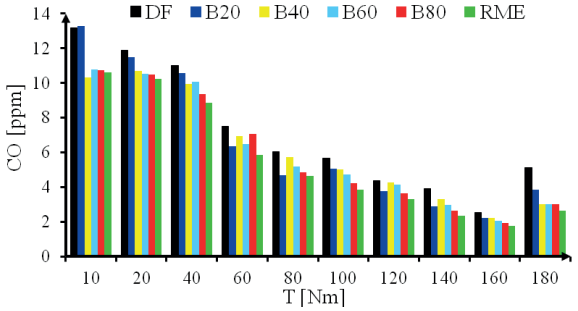


Figure 4 *Variation of the CO concentrations in engine exhaust gas as a function of its load, when fuelled: DF, B20, B40, B60, B80, RME*

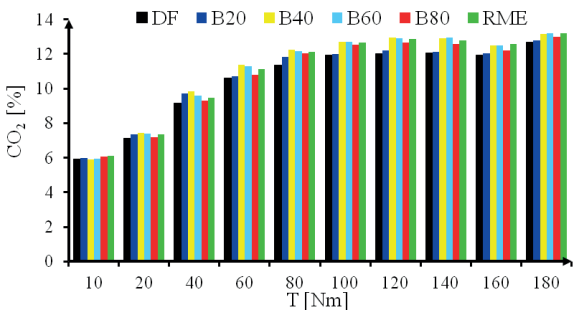


Figure 5 *Variation of the CO_2 concentrations in engine exhaust gas as a function of its load, when fuelled: DF, B20, B40, B60, B80, RME*

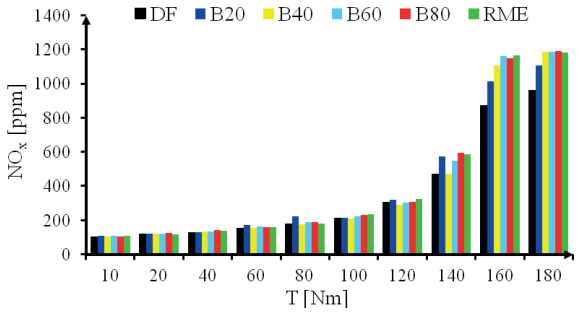


Figure 6 *Variation of the NO_x concentrations in engine exhaust gas as a function of its load, when fuelled: DF, B20, B40, B60, B80, RME*

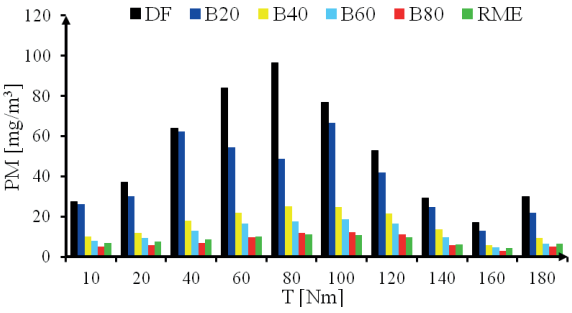


Figure 8 *Variation of the PM concentrations in engine exhaust gas as a function of its load, when fuelled: DF, B20, B40, B60, B80, RME*

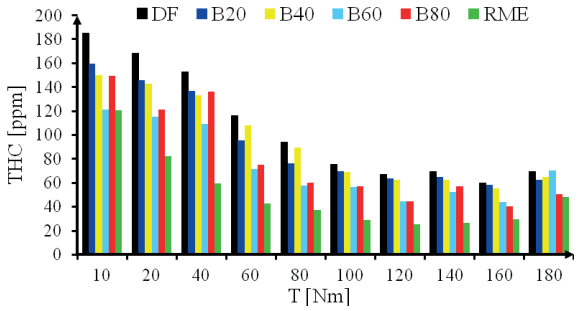


Figure 7 *Variation of the THC concentrations in engine exhaust gas as a function of its load, when fuelled: DF, B20, B40, B60, B80, RME*

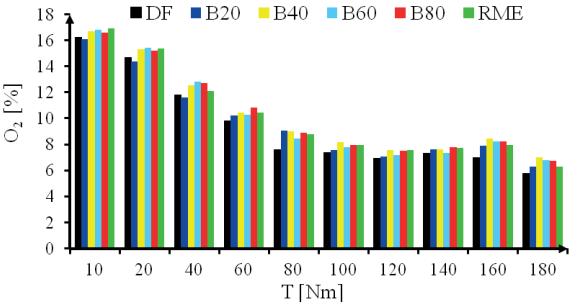


Figure 9 *Variation of the O_2 concentrations in engine exhaust gas as a function of its load, when fuelled: DF, B20, B40, B60, B80, RME*

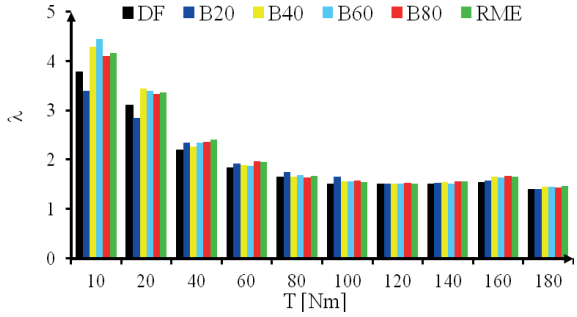


Figure 10 *Values of the excess air ratio λ as a function of engine load, when fuelled: DF, B20, B40, B60, B80, RME*

presents the results of studies that resulted in an increase in NO_x concentrations when supplying the CI engine with common rail power supply system, with RME and DF blends and pure RME. The NO_x concentrations for test fuels are shown in Figure 6. Powering by B20, B40, B60, B80 and RME fuels increases average NO_x concentrations as compared to diesel reaching 11.9, 7.5, 11.5, 13.1 and 13.4%, respectively. The increase in NO_x emissions using esters is a result of the higher temperatures when burning them, compared to the combustion of diesel fuel.

Figure 7 shows the results of measuring the THC concentrations when supplying the engine with tested fuels. The average THC reduction for B20, B40, B60, B80, RME compared to DF was 10.6, 9.9, 28.1, 26.7 and 53.8%, respectively. There was also a clear reduction of the PM concentrations in the exhaust gases of the engine fuelled with RME and blends of RME and DF. Results of the PM measurements for the engine supplied with tested fuels are shown in Figure 8. The average reduction in PM concentrations for B20, B40, B60, B80 and RME fuels was from 21.1% to even 84.3%. Merkisz et al. also showed a large reduction in the concentration of solid particles in the exhaust gas of a ZS engine with a Common Rail supply system fuelled by RME esters and blends of B20 and B50 [49]. Lemaire et al. showed that the carbon black arising from the combustion of diesel oil with the addition of RME esters oxidizes faster [50]. The reduction in both THC and PM concentrations in the exhaust gas is a result of the higher oxygen content and higher temperatures when burning B20, B40, B60, B80 and RME fuels. Figure 9 presents the results of measurements of the oxygen concentrations in the exhaust gases of an engine powered by tested fuels. For B20, B40, B60, B80 and RME fuels, average O_2 concentrations in flue gas were higher about 5.3% to 10.9%, compared to DF. This is also reflected in the measurements of the excess air coefficient, which are shown in Figure 10. They are higher for B20, B40, B60, B80 and RME fuels compared to diesel.

6 Conclusions

Based on the research carried out on the FIAT 1.3 Multijet SDE 90 HP engine, operating at variable loads and a constant speed of the crankshaft, fed with RME esters and their blends with diesel oil, the following conclusions can be drawn:

- By powering the engine with B20, B40, B60, B80 and RME fuels, an increase in hourly fuel consumption and brake specific fuel consumption was obtained. The increase in RME's share in DF resulted in an increase in FC and BSFC.
- Carbon monoxide concentrations in the exhaust gas, when the engine was fuelled with B20, B40, B60, B80 and RME fuels, were lower compared to diesel fuel. Along with the increase in the amount of esters in the blend with diesel oil, lower concentrations of CO were obtained. The lowest CO values were for pure biodiesel.
- Carbon dioxide concentrations were slightly higher when fuelling the engine with B20, B40, B60, B80 and RME fuels. The highest increase was obtained for B40 fuel - 5.7%, the smallest for B20 fuel - 2.0%.
- By powering the engine with fuels: B20, B40, B60, B80 and RME, the concentrations of nitrogen oxides in the exhaust gas increased in comparison to the diesel fuel. The biggest increase was obtained when the engine was powered by the RME biofuel.
- For the engine fuelled with B20, B40, B60, B80 and RME, the hydrocarbon concentrations in the exhaust gas are significantly reduced. By powering the engine with pure RME esters, this reduction was, for the conducted tests, over 50% on average.
- The concentrations of particulate matter were significantly lower when feeding the engine with esters and their blends with diesel fuel. For B80 and RME fuels, the average PM concentrations reductions for the study were over 80%.
- When the engine was fuelled with B20, B40, B60, B80 and RME fuels, the fuel-air mixture composition showed higher excess air ratios than those measured for diesel.
- Oxygen concentrations in the exhaust gas were higher when the engine was fuelled by blends of RME and DF and pure RME.

References

[1] Air quality in Europe - 2019 report. EEA Report [online]. 2019, 10. ISBN 978-92-9480-088-6, ISSN 1977-8449. Available from: https://www.eea.europa.eu/publications/air-quality-in-europe-2019

[2] Towards clean and smart mobility, transport and environment in Europe - EEA Signals [online]. 2016. ISBN 978-92-9213-739-7, ISSN 2443-7662. Available from: https://www.eea.europa.eu/publications/signals-2016

[3] AJANOVIC, A., HAAS, R. Technological, ecological and economic perspectives for alternative automotive technologies up to 2050. In: 2012 IEEE 3rd International Conference on Sustainable Energy Technologies ICSET: proceedings. 2012**. ISBN** 978-1-4577-1869-4, **p.** 129 - 134.

[4] DEMIRBAS, A. Characterization of biodiesel fuels. *Energy Sources, Part A: Recovery, Utilization and Environmental Effects* [online]. 2009, **31**(11), p. 889-896. ISSN 1556-7230. Available from: https://www.tandfonline.com/doi/abs/10.1080/15567030801904202

[5] KLIMIUK, E., PAWLOWSKA, M., POKOJ, T. *Biofuels. Technologies for sustainable development.* Warsaw: Polish Scientific Publishers PWN, 2012. ISBN 9788301171704.

[6] RIMKUS, A., ZAGLINSKIS, J., STRAVINSKAS, S., RAPALIS, P., MATIJOSIUS, J., BERECZKY, A. Research on the combustion, energy and emission parameters of various concentration blends of hydrotreated vegetable oil biofuel and diesel fuel in a compression-ignition engine. *Energies* [online]. 2019, **12**(15), p.1-18. ISSN 1996-1073. Available from: https://www.mdpi.com/1996-1073/12/15/2978

[7] KURCZYNSKI, D., LAGOWSKI, P. Performance indices of a common rail-system CI engine powered by diesel oil and biofuel blends. *Journal of the Energy Institute* [online]. 2019, **92**(6), p. 1897-1913. ISSN 1743-9671. Available from: https://doi.org/10.1016/j.joei.2018.11.004

[8] GHAZALI, W. N. M., MAMAT, R., MASAJUKI, H. H., NAJAFI, G. Effects of biodiesel from different feedstocks on engine performance and emissions: a review. *Renewable and Sustainable Energy Reviews* [online]. 2015, **51**, p. 585-602. ISSN 1364-0321. Available from: https://doi.org/10.1016/j.rser.2015.06.031

[9] TAMILSELVAN, P., NALLUSAMY, N., RAJKUMAR, S. A comprehensive review on performance, combustion and emission characteristics of biodiesel fuelled diesel engines. *Renewable and Sustainable Energy Reviews* [online]. 2017, **79**, p. 1134-1159. ISSN 1364-0321. Available from: https://doi.org/10.1016/j.rser.2017.05.176

[10] AMBAT, I., SRIVASTAVA, V., SILLANPAA, M. Recent advancement in biodiesel production methodologies using various feedstock: a review. *Renewable and Sustainable Energy Reviews* [online]. 2018, **90**, p. 356-369. ISSN 1364-0321. Available from: https://doi.org/10.1016/j.rser.2018.03.069

[11] KNOTHE, G., RAZON, L. F. Biodiesel fuels. *Progress in Energy and Combustion Science* [online]. 2017, **58**, p. 36-59. ISSN 0360-1285. Available from: https://doi.org/10.1016/j.pecs.2016.08.001

[12] RAMAN, L. A., DEEPANRAJ, B., RAJAKUMAR, S., SIVASUBRAMANIAN, V. Experimental investigation on performance, combustion and emission analysis of a direct injection diesel engine fuelled with rapeseed oil biodiesel. *Fuel* [online]. 2019, **246**, p. 69-74. ISSN 0016-2361. Available from: https://doi.org/10.1016/j.fuel.2019.02.106

[13] MANIGANDAN, S., GUNASEKAR, P., DEVIPRIYA, J., NITHYA, S. Emission and injection characteristics of corn biodiesel blends in diesel engine. *Fuel* [online]. 2019, **235**, p. 723-735. ISSN 0016-2361. Available from: https://doi.org/10.1016/j.fuel.2018.08.071

[14] GOGA, G., CHAUHAN, B. S., MAHLA, S. K., CHO, H. M. Performance and emission characteristics of diesel engine fueled with rice bran biodiesel and n-butanol. *Energy Reports* [online]. 2019, **5**, p. 78-83. ISSN 2352-4847. Available from: https://doi.org/10.1016/j.egyr.2018.12.002

[15] VELJKOVIC, V. B., BIBERDZIC, M. O., BANKOVIC-ILIC, I. B., DJALOVIC, I. G., TASIC, M. B., NJEZIC, Z. B., STAMENKOVIC, O. S. Biodiesel production from corn oil: a review. *Renewable and Sustainable Energy Reviews* [online]. 2018, **91**, p. 531-548. ISSN 1364-0321. Available from: https://doi.org/10.1016/j.rser.2018.04.024

[16] ISSARIYAKUL, T., DALAI, A. K. Biodiesel from vegetable oils. *Renewable and Sustainable Energy Reviews* [online]. 2014, **31**, p. 446-471. ISSN 1364-0321. Available from: https://doi.org/10.1016/j.rser.2013.11.001

[17] ILKILIC, C. The effect of sunflower oil methyl ester and diesel fuel blend on the performance of a diesel engine. *Energy Sources Part A: Recovery, Utilization and Environmental Effects* [online]. 2008, **30**(19), p. 1761-1770. ISSN 1556-7230. Available from: https://doi.org/10.1080/15567030701268443

[18] YADAV, A. K., KHAN, M. E., DUBEY, A. M., PAL, A. Performance and emission characteristics of a transportation diesel engine operated with non-edible vegetable oils biodiesel. *Case Studies in Thermal Engineering* [online]. 2016, **8**, p. 236-244. ISSN 2214-157X. Available from: https://doi.org/10.1016/j.csite.2016.08.001

[19] BALAT, M. Potential alternatives to edible oils for biodiesel production - a review of current work. *Energy Conversion and Management* [online]. 2011, **52**(2), p. 1479-1492. ISSN 0196-8904. Available from: https://doi.org/10.1016/j.enconman.2010.10.011

[20] AKUBUDE, V. C., NWAIGWE, K. N., DINTWA, E. Production of biodiesel from microalgae via nanocatalyzed transesterification process: a review. *Materials Science for Energy Technologies* [online]. 2019, **2**(2), p. 216-225. ISSN 2589-2991. Available from: https://doi.org/10.1016/j.mset.2018.12.006

[21] SUN, J., XIONG, X., WANG, M., DU, H., LI, J., ZHOU, D., ZUO, J. Microalgae biodiesel production in China: a preliminary economic analysis. *Renewable and Sustainable Energy Reviews* [online]. 2019, **104**, p. 296-306. ISSN 1364-0321. Available from: https://doi.org/10.1016/j.rser.2019.01.021

[22] CHEN, J., LI, J., DONG, W., ZHANG, X., TYAGI, R. D., DROGUI, P., SURAMPALLI, R. Y. The potential of microalgae in biodiesel production. *Renewable and Sustainable Energy Reviews* [online]. 2018, **90**, p. 336-346. ISSN 1364-0321. Available from: https://doi.org/10.1016/j.rser.2018.03.073

[23] RAJAK, U., NASHINE, P., VERMA, T. N. Assessment of diesel engine performance using spirulina microalgae biodiesel. *Energy* [online]. 2019, **166**, p. 1025-1036. ISSN 0360-5442. Available from: https://doi.org/10.1016/j.energy.2018.10.098

[24] CUNHA, A. JR., FEDDERN, V., DE PRA, M. C., HIGARASHI, M. M., DE ABREU, P. G., COLDEBELLA, A. Synthesis and characterization of ethylic biodiesel from animal fat wastes. *Fuel* [online]. 2013, **105**, p. 228-234. ISSN 0016-2361. Available from: https://doi.org/10.1016/j.fuel.2012.06.020

[25] KIRUBAKARAN, M., ARUL MOZHI SELVAN, V. A comprehensive review of low cost biodiesel production from waste chicken fat. *Renewable and Sustainable Energy Reviews* [online]. 2018, **82**(1), p. 390-401. ISSN 1364-0321. Available from: https://doi.org/10.1016/j.rser.2017.09.039

[26] BANKOVIC-ILIC, I. B., STOJKOVIC, I. J., STAMENKOVIC, O. S., VELJKOVIC, V. B., HUNG YUNG-TSE Waste animal fats as feedstocks for biodiesel production. *Renewable and Sustainable Energy Reviews* [online]. 2014, **32**, p. 238-254. ISSN 1364-0321. Available from: https://doi.org/10.1016/j.rser.2014.01.038

[27] ADEWALE, P., DUMONT, M.-J., NGADI, M. Recent trends of biodiesel production from animal fat wastes and associated production techniques. *Renewable and Sustainable Energy Reviews* [online]. 2015, **45**, p. 574-588. ISSN 1364-0321. Available from: https://doi.org/10.1016/j.rser.2015.02.039

[28] ABED, K. A., El MORSI, A. K., SAYED, M. M., El SHAIB, A. A., GAD, M. S. Effect of waste cooking-oil biodiesel on performance and exhaust emissions of a diesel engine. *Egyptian Journal of Petroleum* [online]. 2018, **27**(4), p. 985-989. ISSN 1110-0621. Available from: https://doi.org/10.1016/j.ejpe.2018.02.008

[29] SAHAR, SADAF, S., IQBAL, J., ULLAH, I., BHATTI, H. N., NOUREN, S., HABIB-UR-REHMAN, NISAR, J., IQBAL, M. Biodiesel production from waste cooking oil: an efficient technique to convert waste into biodiesel. *Sustainable Cities and Society* [online]. 2018, **41**, p. 220-226. ISSN 2210-6707. Available from: https://doi.org/10.1016/j.scs.2018.05.037

[30] BORAH, M. J., DAS, A., DAS, V., BHUYAN, N., DEKA, D. Transesterification of waste cooking oil for biodiesel production catalyzed by Zn substituted waste egg shell derived CaO nanocatalyst. *Fuel* [online]. 2019, **242**, p. 345-354. ISSN 0016-2361. Available from: https://doi.org/10.1016/j.fuel.2019.01.060

[31] FONSECA, M. J., TELEKEN, J. G., DE CINQUE ALMEIDA, V., DA SILVA, C. Biodiesel from waste frying oils: Methods of production and purification. *Energy Conversion and Management* [online]. 2019, **184**, p. 205-218. ISSN 0196-8904. Available from: https://doi.org/10.1016/j.enconman.2019.01.061

[32] UDDIN, M. N., TECHATO, K., RASUL, M. G., HASSAN, N. M. S., MOFIJUR, M. Waste coffee oil: A promising source for biodiesel production. *Energy Procedia* [online]. 2019, **160**, p. 677-682. ISSN 1876-6102. Available from: https://doi.org/10.1016/j.egypro.2019.02.221

[33] OZCANLI, M., SERIN, H., SARIBIYIK, O. Y., AYDIN, K., SERIN, S. Performance and emission studies of castrol bean (Ricinus communis) oil biodiesel and its blends with diesel fuel. *Energy Sources, Part A: Recovery, Utilization and Environmental Effects* [online]. 2012, **34**(19), p. 1808-1814. ISSN 1556-7230. Available from: https://doi.org/10.1080/15567036.2010.545800

[34] RAHEMAN, H., GHADGE, S. V. Performance of compression ignition engine with mahua (Madhuca indica) biodiesel. *Fuel* [online]. 2007, **86**(16), p. 2568-2573. ISSN 0016-2361. Available from: https://doi.org/10.1016/j.fuel.2007.02.019

[35] OZENER, O., YUKSEK, L., ERGENC, A. T., OZKAN, M. Effects of soybean biodiesel on a DI diesel engine performance, emission and combustion characteristics. *Fuel* [online]. 2014, **115**, p. 875-883. ISSN 0016-2361. Available from: https://doi.org/10.1016/j.fuel.2012.10.081

[36] Laboratory statement No. S/14541/0/01/2013: diesel oil.

[37] Quality certificate No. 12112368 for the product biodiesel.

[38] CAN, O., OZTURK, E., YUCESU, H. S. Combustion and exhaust emissions of canola biodiesel blends in a single cylinder DI diesel engine. *Renewable Energy* [online]. 2017, **109**, p. 73-82. ISSN 0960-1481. Available from: https://doi.org/10.1016/j.renene.2017.03.017

[39] CHAUHAN, B. S., KUMAR, N., CHO, H. M. A study on the performance and emission of a diesel engine fueled with Jathropa biodiesel oil and its blends. *Energy* [online]. 2012, **37**(1), p. 616-622. ISSN 0360-5442. Available from: https://doi.org/10.1016/j.energy.2011.10.043

[40] LIN, Y. C., HSU, K. H., CHEN, C. B. Experimental investigation of the performance and emissions of a heavy-duty diesel engine fueled with waste cooking oil biodiesel/ultra-low sulfur diesel blends. *Energy* [online]. 2011, **36**(1), p. 241-248. ISSN 0360-5442. Available from: https://doi.org/10.1016/j.energy.2010.10.045

[41] RAO, Y. V. H., VIOLETI, R. S., RAJU, A. V. S., REDDY, P. N. The effect of cottonseed oil methyl ester on the performance and exhaust emissions of a diesel engine. *International Journal Ambient Energy* [online]. 2010, **31**(4), p. 203-210. ISSN 2162-8246. Available from: https://doi.org/10.1080/01430750.2010.9675813

[42] KARABEKTAS, M. The effects of turbocharger on the performance and exhaust emissions of a diesel engine fueled with biodiesel. *Renewable Energy* [online]. 2009, **34**(4), p. 989-993. ISSN 0960-1481. Available from: https://doi.org/10.1016/j.renene.2008.08.010

[43] CELIKTEN, I., MUTLU, E., SOLMAZ, H. Variation of performance and emission characteristics of a diesel engine fueled with diesel, rapeseed oil and hazelnut oil methyl ester blends. *Renewable Energy* [online]. 2012, **48**, p. 122-126. ISSN 0960-1481. Available from: https://doi.org/10.1016/j.renene.2012.04.040

[44] ALDHAIDHAWI, M., CHIRIAC, R., BADESCU, V. Ignition delay, combustion and emission characteristics of Diesel engine fueled with rapeseed biodiesel - a literature review. *Renewable and Sustainable Energy Review* [online]. 2017, **73**, p. 178-186. ISSN 1364-0321. Available from: https://doi.org/10.1016/j.rser.2017.01.129

[45] NWAFOR, O. Emission characteristcs of diesel engine operating on rapeseed methyl ester. *Renewable Energy* [online]. 2004, **29**(1), p. 119-129. ISSN 0960-1481. Available from: https://doi.org/10.1016/S0960-1481(03)00133-2

[46] CHEN, H., XIE, B., MA, J., CHEN, Y. NOx emission of biodiesel compared to diesel: higher or lower? *Applied Thermal Engineering* [online]. 2018, **137**, p. 584-593. ISSN 1359-4311. Available from: https://doi.org/10.1016/j.applthermaleng.2018.04.022

[47] MOFIJUR, M., MASJUKI, H. H., KALAM, M. A., ATABANI, A. E. Evaluation of biodiesel blending, engine performance and emissions characteristics of Jatropha curcas methyl ester: Malaysian Perspective. *Energy* [online]. 2013, **55**, p. 879-887. ISSN 0360-5442. Available from: https://doi.org/10.1016/j.energy.2013.02.059

[48] GODIGANUR, S., MURTHY, C. H. S., REDDY, R. P. 6GBTA 5-9, G2-1 cummins engine performance and emission tests using methyl esters mahua (Madhuca indica) oil /diesel blends. *Renewable Energy* [online]. 2009, **34**(10), p. 2172-2177. ISSN 0960-1481. Available from: https://doi.org/10.1016/j.renene.2008.12.035

[49] MERKISZ, J., KOZAK, M., PIELECHA, J., ANDRZEJEWSKI, M. The influence of application of different diesel fuel-RME blends on PM emissions from a diesel engine. *Combustion Engines* [online]. 2012, **148**(1), p. 35-39. ISSN 2300-9896, eISSN 2658-1442. Available from: http://www.combustion-engines.eu/The-influence-of-application-of-different-diesel-fuel-RME-blends-on-PM-emissions,117049,0,2.html

[50] LEMAIRE, R., BEJAOUI, S., THERSSEN, E. Study of soot formation during the combustion of diesel rapeseed methyl ester and their surrogates in turbulent spray flames. *Fuel* [online]. 2013, **107**, p. 147-161. ISSN 0016-2361. Available from: https://doi.org/10.1016/j.fuel.2012.12.072

ESTIMATION OF WHEELS' NORMAL REACTION FORCES OF AUTOMOBILE IN STEADY-STATE CURVILINEAR MOTION

Piotr Fundowicz*, Hubert Sar, Mateusz Brukalski

Institute of Vehicles and Construction Machinery Engineering, Warsaw University of Technology, Warsaw, Poland

*E-mail of corresponding author: piotr.fundowicz@pw.edu.pl

Resume

Computer simulation seems to be one of the cheapest and relatively fast methods of investigating vehicle motion. Thereby, it may be important in the case of calculations for the reconstruction of traffic incidents. In particular, that may be important to answer the following question: How wheels' normal reaction forces differ during the cornering of a vehicle?

In this article, the authors presented how the normal reaction forces vary in the case of roll motion of a vehicle body. Suitable mathematical equations are presented. Furthermore, the measurements of the height of the centre of gravity were performed, which was necessary to obtain the normal reaction forces while vehicle body rolls. The authors decided to apply dimensionless coefficients, which represented the properties of a front and rear suspension. Additionally, dimensionless parameters were applied to consider the impact of asymmetrical distribution of vehicle load on normal reaction forces of wheels on a road surface.

Article info

Received 17 September 2020
Accepted 3 February 2021
Online 27 August 2021

Keywords:

vehicles,
safety,
traffic accidents reconstruction,
normal reaction forces,
vehicle motion modelling,
road tests,
curvilinear motion

Available online: https://doi.org/10.26552/com.C.2021.4.B317-B324

ISSN 1335-4205 (print version)
ISSN 2585-7878 (online version)

This is an open access article distributed under the terms of the Creative Commons Attribution 4.0 International License (CC BY 4.0), which permits use, distribution, and reproduction in any medium, provided the original publication is properly cited. No use, distribution or reproduction is permitted which does not comply with these terms.

1 Introduction

Automotive safety depends on many factors related to a vehicle, driver and space surrounding them. If one discusses problems connected with vehicles, one can apply different mathematical apparatus to describe vehicle's motion, for example the Lozia's model [1]. Considering surrounding, one usually has different weather conditions or different road surfaces being in contact with tyres [2]. Considering a driver, one can see the analysis of a driver's behaviour [3].

Knowledge of estimation of the changeability of wheels' normal reaction forces on the road surface cannot be skipped in some circumstances. It takes place, if one wants to simulate vehicle's curvilinear motion more precisely. Very often it cannot be skipped even for the steady-state conditions. To be able to observe this issue, one must know some basic parameters of a vehicle, for example mass of a vehicle, location of the centre of mass, including the height of the centre of gravity above road surface. One of traffic incidents, for which the changeability of normal reaction forces is necessary, is rollover of automobile.

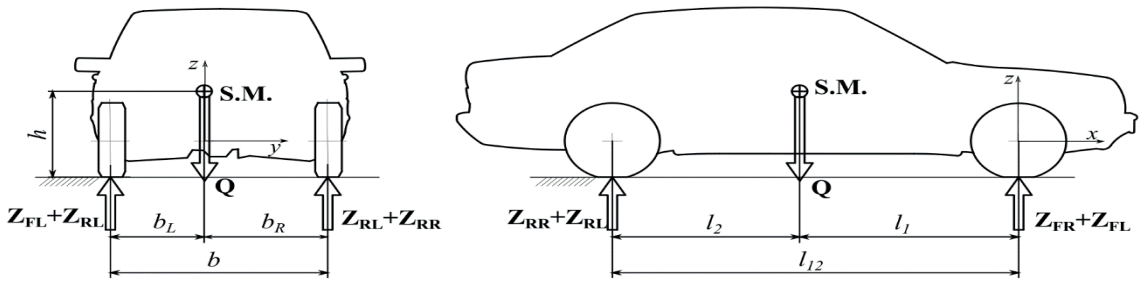
As for the use of vertical response modelling, this can be found for example in [4] and [5]. The double-track vehicle model is used there, including the roll motion of a vehicle's body, thus influencing normal reaction forces. Those forces also depend on suspension properties such as stiffness and damping. Next paper [6] shows similar approach, but with considering the risk analysis of a rollover road incident. The rollover accident is more probable for automobiles with high centre of mass. It was very interestingly discussed in work [7], where the special pressure was put on steering and braking system to prevent the rollover. Application of the normal forces prediction for the planar model of a vehicle was discussed in [8]. The normal forces have the influence both on longitudinal and lateral forces between the tyre and a road, according to proposed tyres characteristics. Of course, it is possible to measure the normal reaction forces during the road tests. To perform it, special force sensors mounted on a special tyre rim are applied as presented in paper [9].

2 Methodology applied in the research

2.1 Position of the centre of mass relative to the vehicle's axis and relative to the longitudinal plane

In general case, position of the vehicle's centre of mass describes its distance from the front and rear axles, distance from longitudinal median plane (*x0z*) and height above the ground - Figure 1. Symbol *S.M.* means the centre of mass.

The dimensionless values L_1, L_2 and H, describing the mass distribution in the vehicle were introduced for the analyses. It allowed for comparison of suspension's properties of vehicles with different dimensions:



Q, Z_{FR}, Z_{FL}, Z_{RR}, Z_{RL} - vertical forces (described in text)
S.M. - the centre of mass

Figure 1 *Location of the centre of mass Z_{FR}, Z_{FL} [N] - front axle vertical reaction forces, respectively under right, left wheel, Z_{RR}, Z_{RL} [N] - rear axle vertical reaction forces, respectively under right, left wheel, Q [N] - weight of a vehicle, S.M. - centre of mass of a vehicle, b_L [m] - distance between the left wheel and centre of mass in the y axis direction, b_R [m] - distance between the right wheel and centre of mass in the y axis direction, l_{12} [m] - wheelbase, l_1, l_2 [m] - distances of the centre of mass respectively from the front and rear axle of a vehicle, measured in the direction of x axis, h [m] - height, at which the centre of mass is located (in relation to ground), b [m] - wheels track, wheels track b was assumed as equal for the front and rear axle*

- L_1, L_2 [-] - position of the vehicle's centre of mass relative to the axle normalized to the wheelbase:

$$L_1 = \frac{l_1}{l_{12}},\ L_2 = \frac{l_2}{l_{12}}, \tag{1}$$

where:
l_1, l_2 - distances of the centre of mass from the front and rear axle of the vehicle, measured in longitudinal direction, l_{12} - wheelbase,
- H [-] - location of the vehicle's centre of mass above the ground, normalized to the wheelbase:

$$H = \frac{h}{l_{12}}, \tag{2}$$

where:
h - height, at which the centre of mass is located.

The condition of the vehicle is described by the acceleration values in the longitudinal (a_x) and lateral (a_y) directions. Later in the text, they are replaced by dimensionless coefficients:

- -braking intensity:

$$\gamma_x = \frac{a_x}{g}, \tag{3}$$

where:
$g\left[\frac{m}{s^2}\right]$ - gravitational acceleration,

- steer intensity:

$$\gamma_y = \frac{a_y}{g}. \tag{4}$$

Static equations are presented below:

$$Z_{FR} + Z_{FL} + Z_{RR} + Z_{RL} = m \cdot g, \tag{5}$$

$$Z_{FR} + Z_{FL} = m \cdot g \cdot (L_2 + H \cdot \gamma_x), \tag{6}$$

$$Z_{FR} + Z_{RR} = m \cdot g \cdot \left(B_L + \frac{H}{B} \cdot \gamma_y\right), \tag{7}$$

where:
indices: F, R - front and rear axle, R, L - right and left wheels, respectively,
m [kg] - mass of a vehicle,
Z [N] - vertical forces between the wheels and pavement,
B [-] -wheels track normalized to the wheelbase:

$$B = \frac{b}{l_{12}}. \tag{8}$$

B_L, B_R (optionally) - position of the vehicle's centre of mass relative to the axle normalized to the wheels' track:

$$B_L = \frac{b_L}{b},\ B_R = \frac{b_R}{b}. \tag{9}$$

If a vehicle moves on a plane, then the relationship between deflections (ζ) of a suspension of individual wheels (assuming the same wheels track b) of the front and rear axle) is satisfied:

$$\zeta_{FR} - \zeta_{FL} = \zeta_{RR} - \zeta_{RL}, \tag{10}$$

where:
ζ_{FR}, ζ_{FL} [m] - deflection of the front axle suspension of respectively right and left wheel,
ζ_{RR}, ζ_{RL} [m] - deflection of the rear axle suspension of respectively right and left wheel.

Normal reaction forces of individual wheels on the surface are associated with suspension deflections and torsion of both front and rear anti-roll bar (if a vehicle is equipped with them):

- respectively front right, front left normal reaction force:

$$Z_{FR,FL} = k_F \cdot \zeta_{FR,FL} \mp \frac{2 \cdot M_{sF}}{b}, \tag{11}$$

- respectively rear right, rear left normal reaction force:

$$Z_{RR,RL} = k_R \cdot \zeta_{RR,RL} \mp \frac{2 \cdot M_{sR}}{b}, \tag{12}$$

where:

$k_F\left[\frac{N}{m}\right]$ - coefficient of vertical stiffness of the left-hand or the right-hand side of front suspension,

$k_R\left[\frac{N}{m}\right]$ - coefficient of vertical stiffness of the left-hand or the right-hand side of rear suspension,
M_{sF} [Nm] - torsional torque of the front axle antiroll bar,
M_{sR} [Nm] - torsional torque of the rear axle antiroll bar.

It can be assumed that the torques resulting from functioning of the anti-roll bars (M_{sF}, M_{sR}), which increase the angular stiffness of the suspension, are proportional to the roll angle φ of the lateral inclination of vehicle body, associated with asymmetrical deflection of the suspension:

$$M_{sF} = k_{sF} \cdot \varphi = k_{sF} \cdot \frac{\zeta_{FR} - \zeta_{FL}}{b}, \tag{13}$$

$$M_{sR} = k_{sR} \cdot \varphi = k_{sR} \cdot \frac{\zeta_{RR} - \zeta_{RL}}{b}, \tag{14}$$

where:
k_{sF}, k_{sR} - proportionality constants.

Considering the above relationships from Equations (11) and (12), the suspension deflections can be determined as:

$$\zeta_{FR,FL} = \frac{Z_{FR,FL} \cdot k_F - (Z_{FR} + Z_{FL}) \cdot S_F}{k_F^2 - 2 \cdot k_F \cdot S_F}, \tag{15}$$

$$\zeta_{RR,RL} = \frac{Z_{RR,RL} \cdot k_F - (Z_{RR} + Z_{RL}) \cdot S_R}{k_R^2 - 2 \cdot k_R \cdot S_R}, \tag{16}$$

where:
$S_{F,R}$ - supporting variables:

$$S_{F,R} = \frac{2 \cdot k_{sF,sR}}{b^2}. \tag{17}$$

After substituting Equations (15) and (16) into Equation (10), the following equation is obtained:

$$Z_{FR} \cdot K_R - Z_{FL} \cdot K_R - Z_{RR} \cdot K_F + Z_{RL} \cdot K_F = 0, \tag{18}$$

where:
$K_{F,R}$ - supporting variables:

$$K_{F,R} = k_{F,R} - 2 \cdot S_{F,R} = k_{F,R} - \frac{4 \cdot k_{sF,sR}}{b^2}. \tag{19}$$

Together with Equations (5)-(7), the system of equations is created:

$$\begin{bmatrix} 1 & 1 & 1 & 1 \\ 1 & 0 & 1 & 0 \\ 1 & 1 & 0 & 0 \\ K_R & -K_F & -K_R & K_F \end{bmatrix} \cdot \begin{bmatrix} Z_{FR} \\ Z_{RR} \\ Z_{FL} \\ Z_{RL} \end{bmatrix} = m \cdot g \cdot \begin{bmatrix} 1 \\ L_2 + H \cdot \gamma_x \\ B_L + \frac{H}{B} \cdot \gamma_y \\ 0 \end{bmatrix}, \tag{20}$$

whose solution are the values of normal reaction forces of individual wheels on the surface.

In the static state, when the vehicle is positioned on a horizontal plane, expressions describing the wheel loads are as follows:

$$Z_{FR} = m \cdot g\left(\frac{L_2 + H \cdot \gamma_x + T_F}{2} + R_F \cdot \gamma_y\right), \tag{21}$$

$$Z_{FL} = m \cdot g\left(\frac{L_2 + H \cdot \gamma_x - T_F}{2} - R_F \cdot \gamma_y\right), \tag{22}$$

$$Z_{RR} = m \cdot g\left(\frac{L_1 - H \cdot \gamma_x + T_R}{2} + R_R \cdot \gamma_y\right), \tag{23}$$

$$Z_{RL} = m \cdot g\left(\frac{L_1 - H \cdot \gamma_x - T_R}{2} - R_R \cdot \gamma_y\right), \tag{24}$$

where:
$R_{F,R}$ [-] - parameters describing the suspension:

$$R_{F,R} = \frac{K_{F,R}}{K_F + K_R} \cdot \frac{H}{B}, \tag{25}$$

$T_{F,R}$ [-] - parameters describing a vehicle's asymmetrical load distribution:

$$T_{F,R} = \frac{2 \cdot K_{F,R}}{K_F + K_R} \cdot (B_L - 0.5). \tag{26}$$

If one assumes that $\gamma_x = 0$ and $\gamma_y = 0$, Equations (21) - (24) are simplified to the form presented below:

$$Z_{FR} = m \cdot g\left(\frac{L_2 + T_F}{2}\right), \tag{27}$$

$$Z_{FL} = m \cdot g\left(\frac{L_2 - T_F}{2}\right), \tag{28}$$

$$Z_{RR} = m \cdot g\left(\frac{L_1 + T_R}{2}\right), \tag{29}$$

$$Z_{RL} = m \cdot g\left(\frac{L_1 - T_R}{2}\right), \tag{30}$$

or equivalent matrix form:

$$\begin{bmatrix} 0 & 1 & 1 & 0 \\ 0 & 1 & -1 & 0 \\ 1 & 0 & 0 & 1 \\ 1 & 0 & 0 & -1 \end{bmatrix} \cdot \begin{bmatrix} L_1 \\ L_2 \\ T_F \\ T_R \end{bmatrix} = \frac{2}{Q} \cdot \begin{bmatrix} Z_{FR} \\ Z_{FL} \\ Z_{RR} \\ Z_{RL} \end{bmatrix}. \tag{31}$$

The object of research was Hyundai Veloster (2010). In the expressions describing the wheels loads, parameters describing the suspension (R_F, R_R) and parameters describing the load distribution of the vehicle (L_1, L_2, H, T_F, T_R) appear. The trial measurements were carried out in the Institute of Vehicles of Warsaw University of Technology to determine these parameters for selected vehicle. The position of the centre of mass was determined by well-known method - by measuring the wheels' normal loads of a vehicle standing on a plane and then once again measuring them after lifting one of the axles - Figure 2.

As a result of measurements for the unloaded vehicle (Hyundai Veloster (2010)), the following properties were obtained:

2.2 Vehicle positioned horizontally

If the normal reaction forces are estimated or measured separately for each wheel of a vehicle and if one also knows the vehicle's wheelbase $l_{12} = 2.650\,m$ and vehicle's width $B = 1.560\,m$, from the above equation the following parameters can be determined: L_1, L_2 - describing the distance of the vehicle's centre of mass and its axle and T_F, T_R - describing the distance of the centre of mass from the vehicle's symmetry plane (asymmetrical load).

For measured normal reaction forces:
Z_{FR} = 3408 N, Z_{FL} = 3817 N, Z_{RR} = 2570 N, Z_{RL} = 2482 N
it was calculated:
L_1 = 0.411, L_2 = 0.588, T_F = -33.3·10^{-3}, T_R = 7.2·10^{-3}.

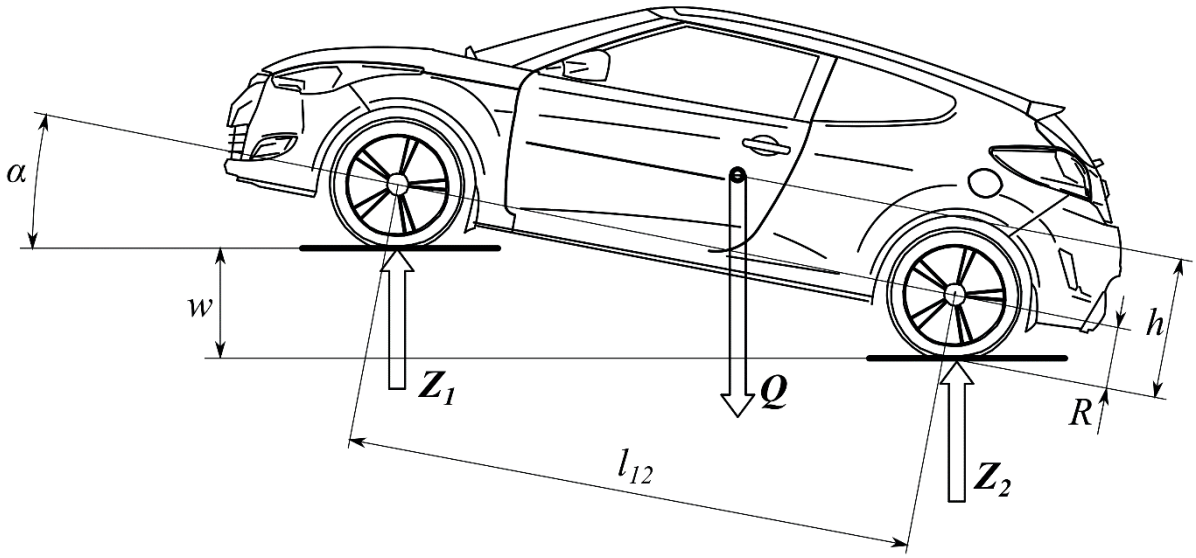
Next, the height of the centre of mass of the vehicle was obtained. It was performed in two different ways, firstly lifting the front and rear axle.

2.3 Height of the centre of mass relative to the pavement

The location of the centre of mass above the road surface (height of the centre of mass) was determined by the well-known method [10] through lifting one of the vehicle's axles to a known height and measuring the axle load on the surface - see Figure 2.

When the rear axle of the vehicle is raised, the front axle is weighed. The location of the centre of mass is described by the following formula (applied based on [10]):

$$h = \frac{Z_1 \cdot l_{12} - Q \cdot L_2}{Q \cdot tg\alpha} + R\,, \tag{32}$$



a)



b)



c)

Figure 2 *Method of measuring the position of the centre of mass above the pavement plane: a - measurement scheme, b - measurement of the front axle loads when raised to a height of about 0.9 m, c - measurement of the rear axle loads when raised to a height of about 0.6 m*

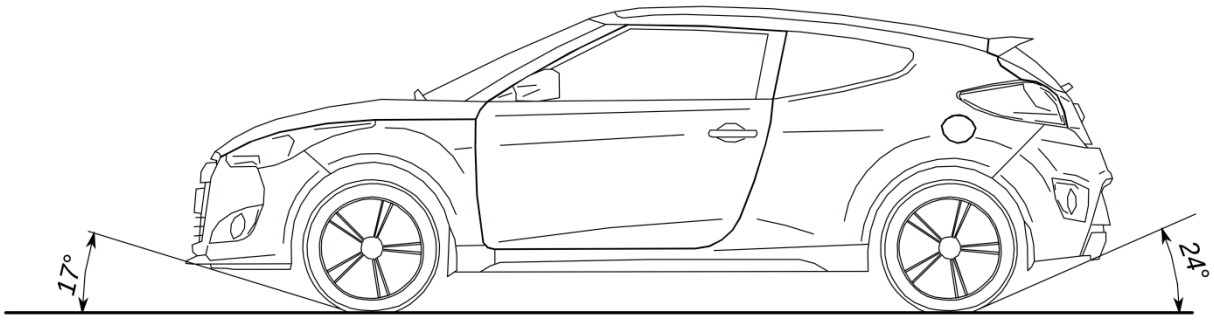


Figure 3 *Approach angle and departure angle of researched vehicle*

where:
Z_1 [N] - the sum of the front axle normal reaction forces on left and right wheel,
Q [N] - weight of a vehicle,
α [rad] - angle by which the vehicle was lifted:

$$\sin\alpha = \frac{w}{l_{12}}, \tag{33}$$

l_{12} = 2.650 m - vehicle's wheelbase,
R = 0.3 m - vehicle tyre's radius during tests.

When lifting the front axle of the vehicle, the rear axle is weighed and the centre of mass position is described by the formula, which is analogous to Equation (32):

$$h = \frac{Z_2 \cdot l_{12} - Q \cdot l_1}{Q \cdot \tan\alpha} + R, \tag{34}$$

where:
Z_2 [N] - the sum of the rear axle normal reaction forces on left and right wheel.

Due to the relatively large front ground clearance (approach angle α = 17°) in relation to the rear (departure angle β = 24°), the height of the rear part of the vehicle was limited by the possibility of collision of the front bumper with the road surface - see Figure 3.

The results obtained during the tests:

- lifted front axle of the vehicle:

For the height w = 0.70 m, the rear axle normal reaction force was measured:
Z_2 = 5393 N.

Angle between the pavement and a vehicle was:

$$\alpha = \arcsin\frac{w}{l_{12}} = \arcsin\frac{0.70m}{2.650m} = 0.267\,\text{rad}.$$

From obtained values of Z_2 and α height of the centre of gravity of a vehicle was calculated below.

$$h = \frac{Z_2 \cdot l_{12} - Q \cdot l_1}{Q \cdot \tan\alpha} + R = \frac{5393N \cdot 2.650m - 12277N \cdot 1.09m}{12277N \cdot \tan 0.267} + 0.30m = 0.57m.$$

For other values of height w, the following results were obtained:

w = 0.80 m,	Z_2 = 5468 N,	h = 0.58 m,
w = 0.90 m,	Z_2 = 5507 N,	h = 0.57 m.

In analogy to the calculations accompanying the lifting of the front axle, below are presented the results of calculations of the height of the centre of gravity for the rear axle lifted.

- lifted rear axle of the vehicle:

w = 0.47 m,	Z_1 = 7467 N,	h = 0.60 m,
w = 0.53 m,	Z_1 = 7493 N,	h = 0.59 m,
w = 0.57 m,	Z_1 = 7510 N,	h = 0.59 m,
w = 0.60 m,	Z_1 = 7513 N,	h = 0.57 m.

The result of measurements is the average of the upper presented values and equals as depicted below:
h = 0.58 m.

2.4 Parameters describing the effect of stabilizers on wheels' loads

The force F_y (see Figure 4) acting on the vehicle in the transverse direction, applied at the height H_y, creates a torque that corresponds to the lateral inertial (centrifugal) force:

$$F_b = F_y \cdot \frac{H_y}{h}, \tag{35}$$

h [m] - the height at which the vehicle's centre of mass is located.

Subsequent measurements were aimed at determining the values of parameters R_F and R_R. For this purpose, the vehicle was loaded with lateral force applied at known height and wheels' normal reaction forces were measured - Figure 4.

This force, in turn, corresponds to the lateral acceleration of the vehicle:

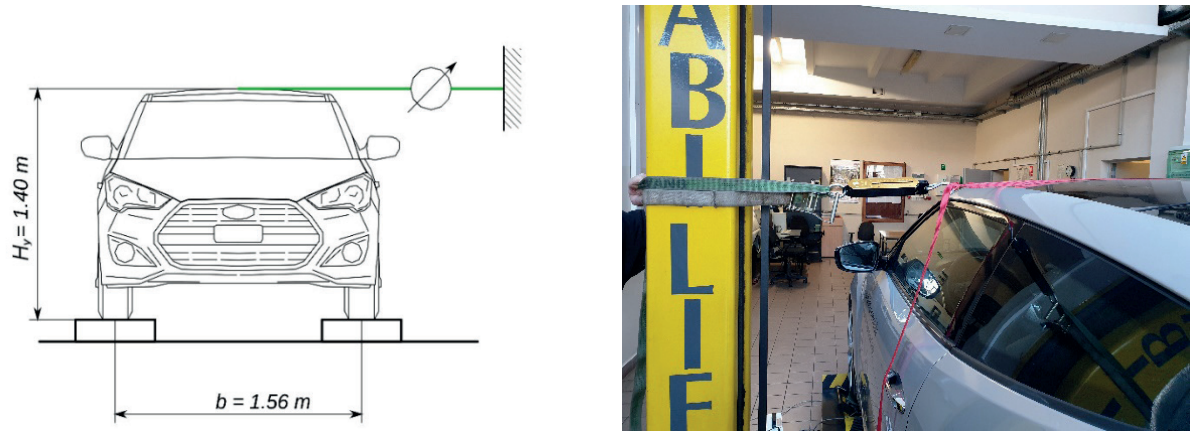
$$a_y = \frac{F_b}{m} = \frac{F_b}{Q} \cdot g, \tag{36}$$

or dimensionless indicator:

$$\gamma_y = \frac{a_y}{g} = \frac{F_y}{Q} \cdot \frac{H_y}{h}, \tag{37}$$

During the measurements, force was applied near the connection of the "B" pillar with the roof of the vehicle and equalled:
F_y = 245 N,

at the height of its roof:
H_y = 1.4 m.



a) b)

Figure 4 *Determination of the R_F and R_R parameters*

It corresponds to dimensionless coefficient:

$$\gamma_y = \frac{245N}{12277N} \cdot \frac{1.4m}{0.59m} = 46.6 \cdot 10^{-3}. \tag{38}$$

From equations describing the wheels loads on the surface, in the absence of longitudinal acceleration (γ_x = 0), the parameters R_F and R_R, describing the effect of the stabilizers (front and rear torsion beam) on normal reaction forces, can be determined:

- calculated based on normal reaction forces of the right wheels:

$$R_F = \frac{1}{\gamma_y} \cdot \left(\frac{Z_{FR}}{Q} - \frac{L_2 + T_F}{2} \right), \tag{39}$$

$$R_R = \frac{1}{\gamma_y} \cdot \left(\frac{Z_{RR}}{Q} - \frac{L_1 + T_R}{2} \right), \tag{40}$$

- calculated based on the load of the left wheels:

$$R_F = \frac{-1}{\gamma_y} \cdot \left(\frac{Z_{FL}}{Q} - \frac{L_2 - T_F}{2} \right), \tag{41}$$

$$R_R = \frac{-1}{\gamma_y} \cdot \left(\frac{Z_{RL}}{Q} - \frac{L_1 - T_R}{2} \right). \tag{42}$$

After including the data measured during the tests: Z_{FR} = 3309 N, Z_{FL} = 3919 N, Z_{RR} = 2472 N, Z_{RL} = 2590 N, it was given:
- based on right wheels normal reaction forces:
R_F = -0.168, R_R = -0.184,
- based on left wheels normal reaction forces:
R_F = -0.166, R_R = -0.194.

The difference between the results obtained from calculations based on the right and left wheels of the vehicle are due to the measurement errors, but because they are small (for R_F - 0.6%, for R_R - 5.0%), the average values were used as the test result:
R_F = -0.160, R_R = -0.189.

The forces that were applied to the vehicle's body during the measurements were relatively small, compared to the forces that can act on the vehicle when driving along a curvilinear track. When cornering, the transverse mass forces act as a result of the inertia of the vehicle's body, while during the laboratory tests - a concentrated force was applied at a selected point of the body. Applying a force, comparable to that which can occur under the normal driving conditions, could damage the vehicle body.

2.5 Influence of the passenger's weight on the vehicle's centre of mass displacement

Since during the reconstruction of traffic incident it makes no sense to analyse the movement of the unloaded vehicle, calculations were made to answer how loading a vehicle by a driver or a passenger influences the wheels' load. Figure 5 shows the position of the driver inside the passenger's compartment.

If the centre of mass of the unloaded vehicle with the mass m_p is in the position described with coordinates x_0, y_0, h_0, then after loading it with the mass m_1 of the passenger with the centre of mass in x_1, y_1, h_1 points, the centre of mass of the laden vehicle will be at the point described by the coordinates:

$$x = \frac{m_p \cdot x_0 + m_1 \cdot x_1}{m_p + m_1}, \tag{43}$$

$$y = \frac{m_p \cdot y_0 + m_1 \cdot y_1}{m_p + m_1}, \tag{44}$$

$$h = \frac{m_p \cdot h_0 + m_1 \cdot h_1}{m_p + m_1}. \tag{45}$$

The vehicle's mass during the test was:
m_P = 12285 N / 9.81 m/s^2 = 1252 kg.

2.5.1 Only a driver inside the vehicle

Assuming the coordinates describing the location of a driver inside a vehicle, it will be:
x_K = 1.42 m, y_K = 0.36 m, h_K = 0.59 m,
placing a driver with mass:
m_K = 85 kg

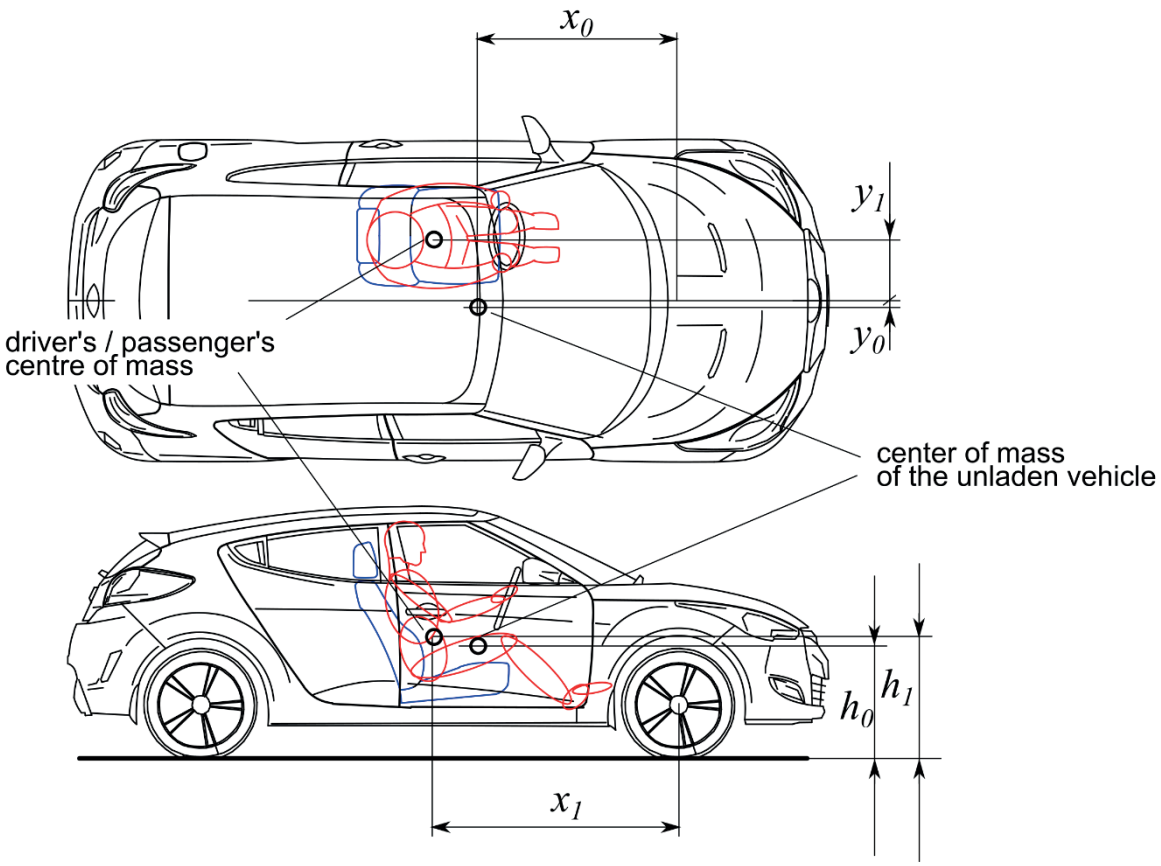


Figure 5 *Position of the driver inside the passenger's compartment*

results in displacement of the centre mass of the vehicle to new coordinates:

$$x = \frac{1252kg \cdot 0.412 \cdot 2.650m + 85kg \cdot 1.42m}{1252kg + 85kg} = 1.11m\,,$$

$$y = \frac{1252kg \cdot 0.02m + 85kg \cdot 0.36m}{1252kg + 85kg} = 0.040m\,,$$

$$h = \frac{1252kg \cdot 0.02m \cdot 2.650m + 85kg \cdot 059m}{1252kg + 85kg} = 0.60m\,,$$

where:
y [m] - position relative to the longitudinal axis of the vehicle (positive direction - left),
x [m] - position relative to the front axle of the vehicle (positive direction - backwards),
h [m] - location relative to the road surface.

Placing the driver inside the vehicle does not significantly change the location of the centre of mass.

$$L_1 = \frac{1.11m}{2.650m} = 0.419\,.$$

2.5.2 Driver and passenger on the front seats

$$x = \frac{\begin{array}{c}1252kg \cdot 0.412 \cdot 2.650m + 85kg \cdot \\ \cdot 1.42m \cdot 85kg \cdot 1.42m\end{array}}{1252kg + 85kg + 85kg + 85kg + 85kg} = 1.13m\,,$$

$$y = \frac{1252kg \cdot 0.02m}{1252kg + 85kg + 85kg} = 0.018m\,,$$

$$h = \frac{\begin{array}{c}1252kg \cdot 0.226 \cdot 2.650m + \\ + 85kg \cdot 0.59m + 85kg \cdot 0.59m\end{array}}{1252kg + 85kg + 85kg} = 0.60m\,,$$

$$L_1 = \frac{1.13m}{2.650m} = 0.426\,.$$

2.5.3 Driver and passenger on the front seats, two passengers on the rear seats

$$x = \frac{\begin{array}{c}1252kg \cdot 0.412 \cdot 2.650m + 170kg \cdot \\ \cdot 1.42m \cdot 170kg \cdot 2.035m\end{array}}{1252kg + 85kg + 85kg + 85kg + 85kg} = 1.23m\,,$$

$$y = \frac{1252kg \cdot 0.02m}{1252kg + 85kg + 85kg + 85kg + 85kg} = 0.016m\,,$$

$$h = \frac{\begin{array}{c}1252kg \cdot 0.226 \cdot 2.650m + \\ + 170kg \cdot 0.59m + 170kg \cdot 0.59m\end{array}}{1252kg + 85kg + 85kg + 85kg + 85kg} = 0.60m\,,$$

$$L_1 = \frac{1.23m}{2.650m} = 0.464\,.$$

Concluding obtained results, it is worth noting that even in the case of a relatively light passenger car, which

was tested, with the weight of the driver and passengers loaded, in all the cases considered, the centre of mass of the loaded vehicle did not move significantly:

- in the longitudinal direction - 0.02 to 0.04 m,
- in the transverse direction - no more than 0.04 m,
- vertically - up to about 0.02 m.

3 Conclusion

Information about distribution of normal reaction forces between the left and right wheels may be important in the case of vehicle's motion modelling - development of active safety systems, accidents' reconstruction. Between the road surface and a tyre normal reaction forces arise. However, the tangential transverse and longitudinal forces arise as well, which are transmitted between the tyre and pavement, are dependent on these normal forces. So, to properly describe a vehicle's motion in roll, pitch or yaw direction, the authors showed the method of a vehicle's research, which allows for obtaining properties related to the stiffness of the front and rear axle. Mentioned properties of suspension are dimensionless. Thus, it is possible to compare the automobiles, which differ in dimensions. Similarly, the dimensionless parameters were applied for description of asymmetrical load of a vehicle, as well. Of course, presented method can be applied by automotive experts even if the normal forces between the wheels and road are unknown. In this case, they should be estimated after an assumption of a mass distributed between the front and rear axles and additionally between the left-hand and the right-hand sides of a car. Another assumption may refer to location of passengers inside the passengers' compartment, which was also exemplarily presented in this paper.

Conducted experiments were performed only for one vehicle and to confirm the results, it should be repeated for many automobiles.

References

[1] LOZIA, Z. Rollover thresholds of the biaxial truck during motion on an even road. *Vehicle System Dynamics* [online]. 1998, **29**(sup1), p. 735-740 [accessed 2020-01-26]. ISSN 0042-3114, eISSN 1744-5159. Available from: https://doi.org/10.1080/00423119808969601

[2] POKORSKI, J., SAR, H., RENSKI, A. Influence of exploitation conditions on anti-skid properties of tyres. *Transport* [online]. 2019, **34**(4), p. 415-424 [accessed 2020-01-26]. ISSN 1648-4142, eISSN 1648-3480. Available from: https://doi.org/10.3846/transport.2019.10426

[3] JURECKI, R. S., STANCZYK, T. L., JASKIEWICZ, M. J.. Driver's reaction time in a simulated, complex road incident. *Transport* [online]. 2017, **32**(1), p. 44-54 [accessed 2020-01-26]. ISSN 1648-4142, eISSN 1648-3480. Available from: https://doi.org/10.3846/16484142.2014.913535

[4] LI, H., ZHAO, Y., LIN, F. ZHU, M. Nonlinear dynamics modelling and rollover control of an off-road vehicle with mechanical elastic wheel. *Journal of the Brazilian Society of Mechanical Sciences and Engineering* [online]. 2018, **40**(2), p. 1-17 [accessed 2020-01-26]. ISSN 1678-5878, eISSN 1806-3691. Available from: https://doi.org/10.1007/s40430-018-1009-8

[5] MASHADI, B. MOSTAGHIMI, H. Vehicle lift-off modelling and a new rollover detection criterion. *Vehicle System Dynamics* [online]. 2017, **55**(5), p. 704-724 [accessed 2020-01-26]. ISSN 0042-3114, eISSN: 1744-5159. Available from: https://doi.org/10.1080/00423114.2016.1278076

[6] SELLAMI, Y., IMINE, H., BOUBEZOUL, A. CADIOU, J.-C. Rollover risk prediction of heavy vehicles by reliability index and empirical modelling. *Vehicle System Dynamics* [online]. 2018, **56**(3), p. 385-405 [accessed 2020-01-26]. ISSN 0042-3114, eISSN 1744-5159. Available from: https://doi.org/10.1080/00423114.2017.1381980

[7] GHAZALI, M., DURALI, M. SALARIEH, H. Path-following in model predictive rollover prevention using front steering and braking. *Vehicle System Dynamics* [online]. 2017, **55**(1), p. 121-148 [accessed 2020-01-26]. ISSN 0042-3114, eISSN 1744-5159. Available from: https://doi.org/10.1080/00423114.2016.1246741

[8] MA, Z., ZHANG, Y., YANG, J. Velocity and normal tyre force estimation for heavy trucks based on vehicle dynamic simulation considering the road slope angle. *Vehicle System Dynamics* [online]. 2016, **54**(2), p. 137-167 [accessed 2020-01-26]. ISSN 0042-3114, eISSN 1744-5159. Available from: https://doi.org/10.1080/00423114.2015.1122817

[9] DOUMIATI, M., VICTORINO, A., CHARARA, A., LECHNER, D. Lateral load transfer and normal forces estimation for vehicle safety: experimental test. *Vehicle System Dynamics* [online]. 2009, **47**(12), p. 1511-1533 [accessed 2020-01-26]. ISSN 0042-3114, eISSN 1744-5159. Available from: https://doi.org/10.1080/00423110802673091

[10] ARCZYNSKI, S. *Mechanics of automobile's motion / Mechanika ruchu samochodu* (in Polish). Warszawa: Wydawnictwa Naukowo-Techniczne, 1993. ISBN 8320414881.

PRACTICAL APPLICATION OF THE NEW APPROACH TO FMEA METHOD ACCORDING TO AIAG AND VDA REFERENCE MANUAL

Dariusz Plinta*, Ewa Golinska, Ľuboslav Dulina

Department of Industrial Engineering, Faculty of Mechanical Engineering, University of Bielsko-Biala, Bielsko-Biala, Poland

*E-mail of corresponding author: dplinta@ath.bielsko.pl

Resume

System requirements in the automotive industry are constantly evolving and being improved. Currently, the entire supply chain, related to the automotive industry, is subject to the fourth amendment to the technical automotive standard - IATF 16949: 2016 Quality management systems - Detailed requirements for the use of ISO 9001: 2015 in serial production and production of spare parts in the automotive industry. In IATF standard, there are advices called reference manuals that provide important guidance on the quality system in this industry - one of them is the FMEA manual. The new guidelines in this regard, developed jointly by AIAG and VDA, entered into force in June 2019. Presentation of the most important changes introduced, as well as presentation of a practical example of the conducted analysis is the purpose of the article.

Article info

Received 18 January 2021
Accepted 19 March 2021
Online 27 August 2021

Keywords:

automotive industry,
risk analysis,
actions priority,
AIAG&VDA

Available online: https://doi.org/10.26552/com.C.2021.4.B325-B335

ISSN 1335-4205 (print version)
ISSN 2585-7878 (online version)

This is an open access article distributed under the terms of the Creative Commons Attribution 4.0 International License (CC BY 4.0), which permits use, distribution, and reproduction in any medium, provided the original publication is properly cited. No use, distribution or reproduction is permitted which does not comply with these terms.

1 Introduction

System quality management according to used standards has been used in organizations for over 30 years. During that time, those standards, primarily ISO 9000 series standards, have gained tremendous popularity and have also standardized business language around the world. In Poland, interest in certification of management systems appeared in the 1990s and is constantly popular. The popularity of certification for compliance with requirements of the ISO 9001 standard has become particularly important after Poland's accession to the European Union [1-2]. The first norm related to quality was developed in 1986 by International Organization for Standardisation (ISO) - it was the ISO 8402 norm Quality. Terminology. Over the years, standardized requirements in quality areas have evolved and in 2015 we saw the fourth revision of the ISO 9001 standard.

Quality management plays a special role in production management processes in the automotive industry. In this innovative industry, quality standards, based on the ISO 9000 series standards, are used. The best-known quality management standard in the automotive industry is QS, which is based on the now outdated ISO 9001: 1994 standard, extended by additional industry requirements, 9000 (Quality System Requirements). This standard was created in 1994 on the initiative of the so-called The Big Three of the US automotive industry - Chrysler Corporation, Ford Motor Company and General Motors Corporation. The emergence of this standard was a response to the lack of a standard adapted to requirements of the automotive industry. The above-mentioned car manufacturers jointly recognized that certified quality systems in accordance with requirements of the ISO 9000 series of standards allowed too much freedom for organizations applying them and there was a need to implement a uniform standard that would place higher requirements on suppliers and co-operators of the automotive industry. (Critics of ISO 9001 claim that the standard is too general and therefore useless for specific industries. Moreover, its usage may lead to abandoning creative thinking, inhibiting this way quality development [3-5]. They pointed out, among others, the lack of requirements regarding continuous improvement, application of problem-solving methods, approval of individual stages of project work or strategic quality planning. Votes of criticism in the abovementioned areas have been appearing consistently for years, regardless of any subsequent amendment to the standard.) Such behaviour of the automotive market leaders, ultimately responsible for product quality, was focused on providing supply facilities of the expected quality and was aimed at minimizing the nuisance of multiple assessments of current and potential suppliers and consequently meeting the expectations of the final customer [6-9].

The QS 9000 standard developed into ISO TS 16949

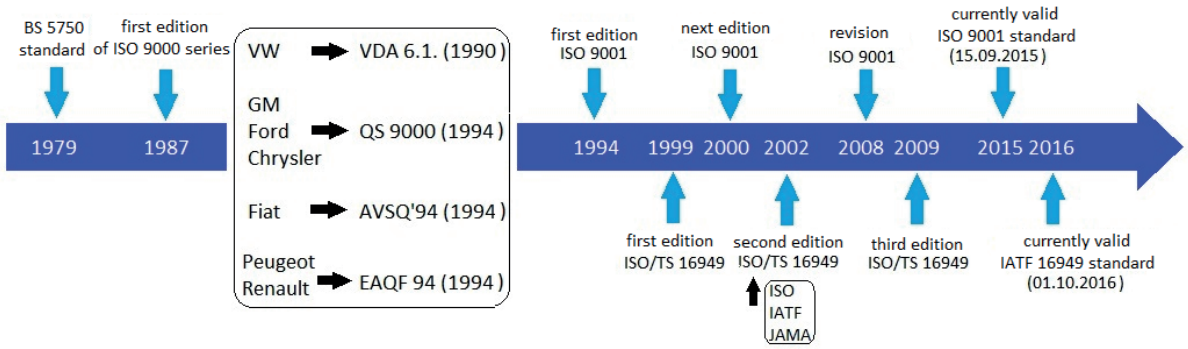


Figure 1 *Evolution of the ISO 9000 series standards and quality systems in the automotive industry, based on [13]*

standard; the design of the standard was approved in 1999. This standard contains a set of requirements that includes, in addition to the requirements of the previously mentioned Big Three (QS 9000), the requirements of the quality systems of the Italian, French and German automotive industry, as well [4], which were born in the process of evolution of quality improvement programs. The most popular of them, which are the sources of today's technical specification IATF 16949, are the following:

- QS 9000 - quality systems requirements of the Big Three of the American car industry (Quality System Requirements, Third Edition, March 1998).
- AVSQ'94 ANFIA - quality systems requirements of the Italian car industry (Valutazione Sistemi Qualita, Edizione 3, Febbraio 1995 + Addendum QS 9000 all' AVSQ, Edizione Marzo 1997).
- EAQF 94 - quality systems requirements of the French car industry (Evaluation Qualite Fournisseur, 1994 Edition plus QS 9000 Appendix to EAQF March 1997 Edition).
- VDA 6.1 - quality systems requirements of the German car industry (Qualitatsmanagement in der Automobilindustrie - QM - Systemaudit 4. vollstandig uberarbeitete Auflage 1998).

The above-mentioned standards, i. e. EAQF (France), VDA 6.1 (Germany), AVSQ (Italy), are recognized in the automotive market, although their universality is disproportionate to the QS 9000 (USA) standard (VDA 6.1 standard is also a commonly used norm for quality management, particularly in Europe, including Poland). However, a smaller number of certifications in the field of these systems or a smaller number of OEMs (Original Equipment Manufacturers) who put these systems as the required basis for management systems, in no way diminish the role, they played in the process of qualifying suppliers or shaping the IATF 16949 global standard [10-11].

It may seem that the QS 9000 standard is only slightly different from the ISO 9001 standard. However, this is not the case, also because in its content, QS 9000 repeatedly refers to the so-called manuals. Knowledge of these manuals is key in this standard and there is a need to include this information in the quality system. Although the QS 9000 standard ceased to be required in December 2006, the related manuals are constantly updated and recalled by many car manufacturers and certification body auditors as manuals with guidelines for meeting the IATF 16949 requirements.

As a part of the QS 9000 standard and today IATF 16949, a manufacturer can use the following manuals:

- APQP - Advanced Product Quality Planning and Control Plan.
- PPAP - Production Part Approval Process.
- SPC - Statistical Process Control.
- MSA - Measurement System Assessment.
- FMEA - Failure Mode and Effects Analysis.
- QSA - Quality System Assessment.

The present elaboration refers to analysing the changes in the area of the requirements included in the reference manuals. Two reference manuals have been analysed for this purpose - the manuals according to AIAG (*Automotive Industry Action Group*) and VDA (from German: *Verband der Automobilindustrie)* requirements, as well as their integration in form of a common, first edition of the FMEA manual [12].

The second edition of ISO / TS 16949: 2002 was developed in 2002 in cooperation of three organizations:

- ISO - International Organization for Standardization.
- IATF - International Automotive Task Force.
- JAMA - Japan Automobile Manufacturers Association.

Technical specifications in the automotive industry, just like the ISO 9000 series standards, are constantly evolving (Figure 1). Currently, the entire supply chain related to the automotive industry (not only suppliers, but also sub-suppliers, even when only a small part of their production is intended for the automotive industry) is obliged to apply the fourth amendment to the technical automotive standard IATF 16949 from 2016 - IATF 16949: 2016 Quality management systems - Detailed requirements for the use of ISO 9001: 2015 in series production and the production of spare parts in the automotive industry. Until today, it is the basic, though voluntary, standard in the automotive industry.

The reason for its issue was issuing the new ISO 9001: 2015 standards, which are the system basis for this technical specification. IATF 16949: 2016 is an automotive standard that is based on the structure

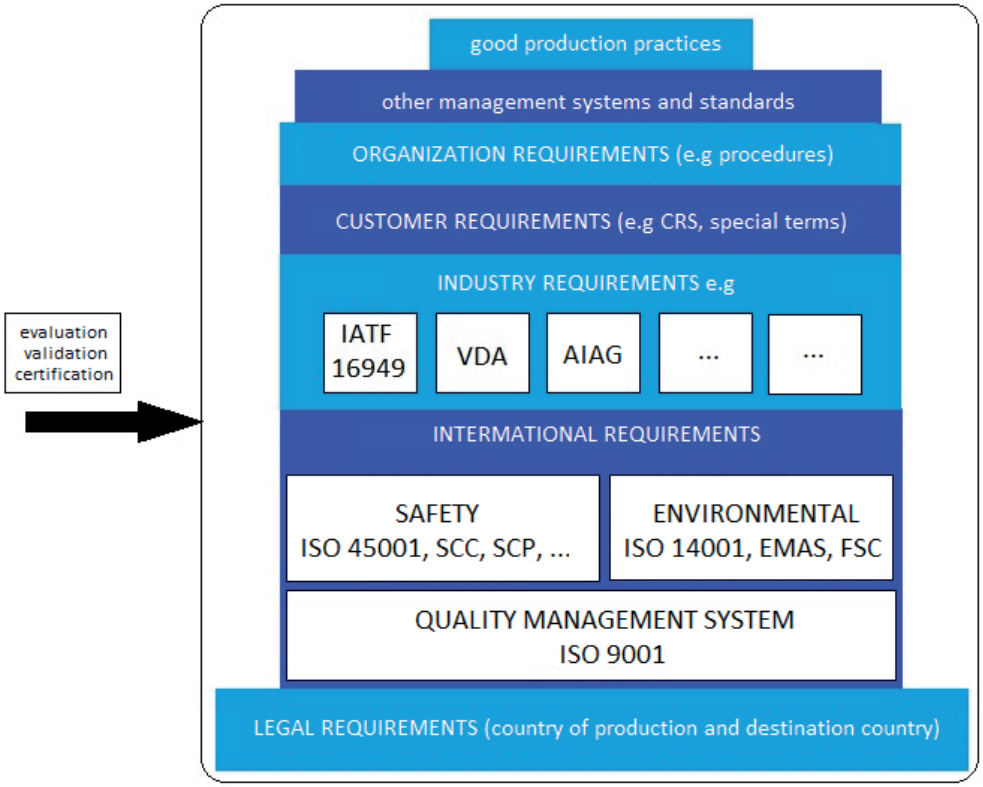


Figure 2 *A model of current requirements towards car manufacturers*

and requirements of ISO 9001: 2015, supplemented with specific technical issues specific to the automotive industry (mainly obligatory system documentation, i. e. procedures, instructions and records and requirements in the field of statistical process control or risk analyses).

Summarizing, IATF 16949 can be described as a compromise among car manufacturers. Therefore, it does not take into account all the requirements of each manufacturer, but only emphasizes the fulfilment of individual customer requirements. That is why a customer and his requirements determine the shape of the quality management system implemented in the company. This applies, for example, to the need or lack of need to use QS 9000 standard manuals. A simplified model of requirements for today's car manufacturers is shown in Figure 2.

The IATF 16949 standard has gained international significance - primarily due to its dynamically growing coverage, involving suppliers around the world. Currently, more than twenty years after the technical specification was introduced for the first time on the automotive market, it is widely recognized and absolutely required in North America and is increasingly common in Europe, South America, Australia and Asia. It should also be remembered that the group of enterprises that have implemented and require the IATF 16949 standard from their suppliers is growing. It is also significant that a company that builds the quality system according to IATF 16949 must require its subcontractors to meet the requirements of this standard, which, in turn, significantly expands the circle of companies interested in it.

However, compliance with restrictive requirements resulting from the IATF 16949 standard is often not sufficient for entrepreneurs in the logistics chain of the automotive industry. It is worth noting that organization-specific sets of requirements (CSR - Customer Specific Requirements) have emerged that extend the standard requirements. Due to the multitude of individual customer requirements, the set of the requirements placed on automotive suppliers is not limited (A part of the CSR requirements is described in the so- called Manuals - briefly mentioned in the introduction to this paper). The main requirements of the CSR include the FMEA analysis presented later in the article.

2 FMEA in the automotive industry

FMEA is a commonly applied, obligatory method in the automotive industry, therefore a unified approach to conducting this analysis seems necessary, but - as practice shows - this approach differs in different organizations and is usually carried out according with the CSR requirements.

Historically, the FMEA (Failure Mode, Effects and Criticality Analysis) method was born in the 1950s for the needs of the arms industry and received the greatest publicity when NASA used it in the Apollo space program. The next milestone in development of this approach was the first application of FMEA (Nowadays FMEA is used as an equivalent to FMECA. Both, Mode and Effects Analysis (FMEA) and Failure

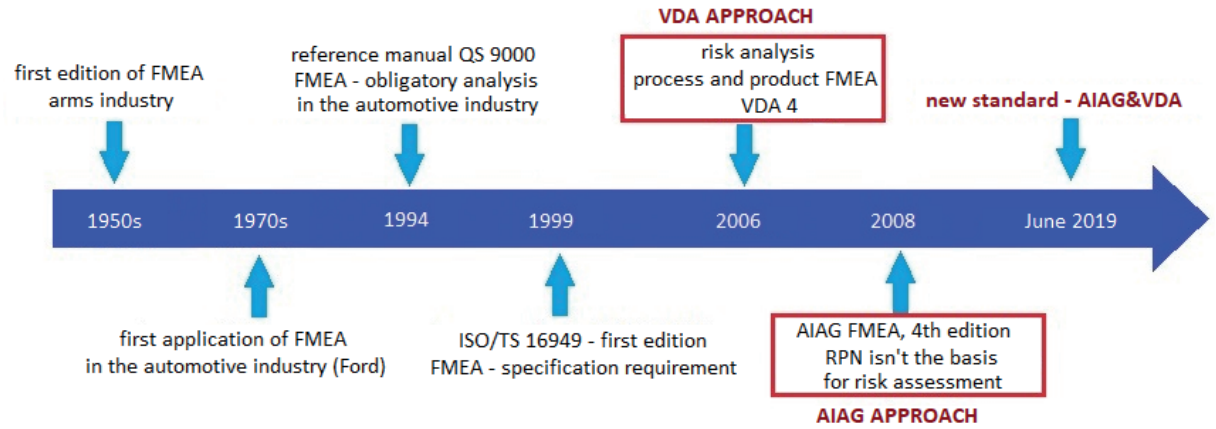


Figure 3 *Evolution of the approach to FMEA*

Modes, Effects and Criticality Analysis (FMECA) are methodologies designed to identify potential failure modes for a product or process, to assess the risk associated with those failure modes, to rank the issues in terms of importance and to identify and carry out corrective actions to address the most serious problems in the automotive industry by the Ford Motor Company (after the so-called Pinto scandal) and the analysis included meeting the requirements in terms of the car safety and compliance with legal requirements [14-16]. The FMEA became an obligatory analysis in the automotive industry only in 1994 (reference manual QS 9000). In addition, the first automotive standard (ISO / TS 16949 from 1999) maintained the obligation to conduct the FMEA analyses. Further on, the FMEA approach has had two important elaborations - from the VDA standard and the AIAG standard (Figure 3).

Since then, the AIAG has developed its requirements dedicated to automotive manufacturers in the United States (the last revision was the fourth edition of the 2008 manual) and VDA issued the VDA 4 standard, which showed a risk analysis from the point of view of the German car market (latest edition - second amended, updated in June 2012). The consequence of this was often the need to use a different approach to FMEA analysis in one organization, when it implemented projects for companies requiring opposite approaches (e. g. for Ford and VW - each of these clients expected to document the analysis in accordance with their requirements; Ford according to AIAG FMEA, whereas VW according to VDA 4), which led to chaos. Currently, a new standard has been released for conducting the FMEA analysis, which was based on a consensus regarding different expectations of AIAG and VDA as to the shape of FMEA. The changes in the manual can be considered revolutionary - for example, in relation to the resignation from the RPN (Risk Priority Number) indicator, however, looking from a wider perspective it can be safely stated that the guidelines of the new manual follow good practices in running the FMEA in organizations. A detailed description of differences and their summary in relation to both the AIAG and VDA requirements, can be found in Annex F of the FMEA Handbuch manual published jointly by AIAG & VDA in June 2019. The manual is a result of three years of cooperation between the OEMs and first-order suppliers belonging to AIAG and VDA and it replaces the AIAG FMEA edition 4, as well as VDA volume 4 FMEA Product and process manuals [16].

Discussing the detailed differences between standards is not within the scope of this study and will not be cited because of its extensiveness. Later in the paper, only the new FMEA procedure and a practical application of the approach are presented. The main purpose is to present a way of the risk assessment in accordance with the new demands and comparing it to results of the traditionally conducted FMEA, which were based on assessing the RPN.

3 The FMEA procedure according to coherent AIAG&VDA requirements

The new AIAG&VDA FMEA method is described in 7 steps, which are elaborated in detail and presented on examples in Section 4 of the present paper. The steps in order are the following:

- Step 1 - Planning and preparation
- Step 2 - Structure analysis
- Step 3 - Functional analysis
- Step 4 - Failure analysis
- Step 5 - Risk analysis
- Step 6 - Optimization
- Step 7 - Documenting results.

Irrespective of the fact whether the FMEA relates to the product (DFMEA - design FMEA) or a process (PFMEA - process FMEA,) the procedure is realized in analogical steps - the first 3 steps relate to system analysis, the following 3 steps are connected with failure analysis and limiting risk and the step number 7 is communicating the risk in an organization [12]. The main difference regarding the conducted analyses is the difference in the elements analysed during the method application - DFMEA analyses the features, functions and product requirements and in the case of PFMEA the analysis relates to operations included in the process.

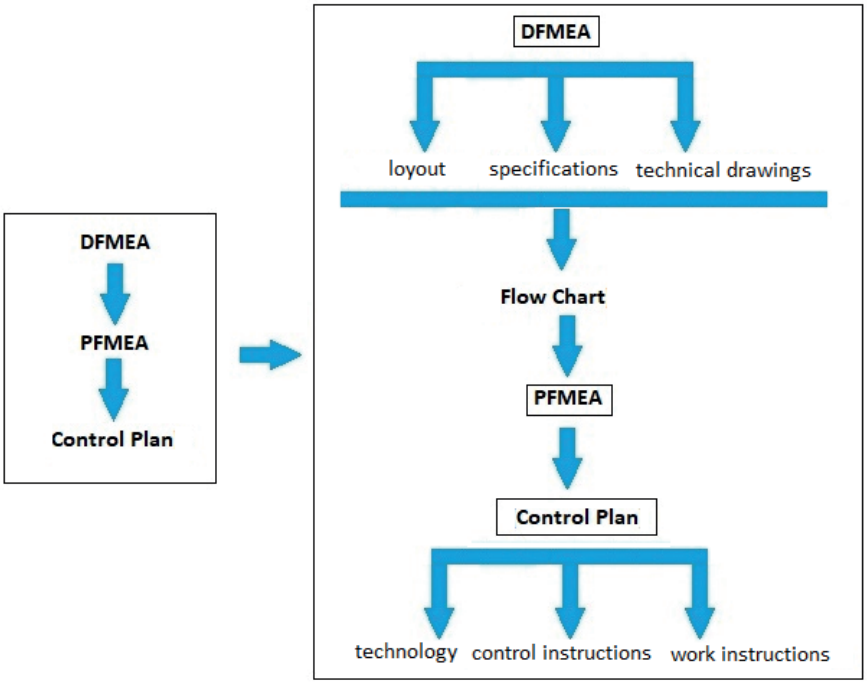


Figure 4 *Connections of DFMEA, PFMEA and other documents in an organization*

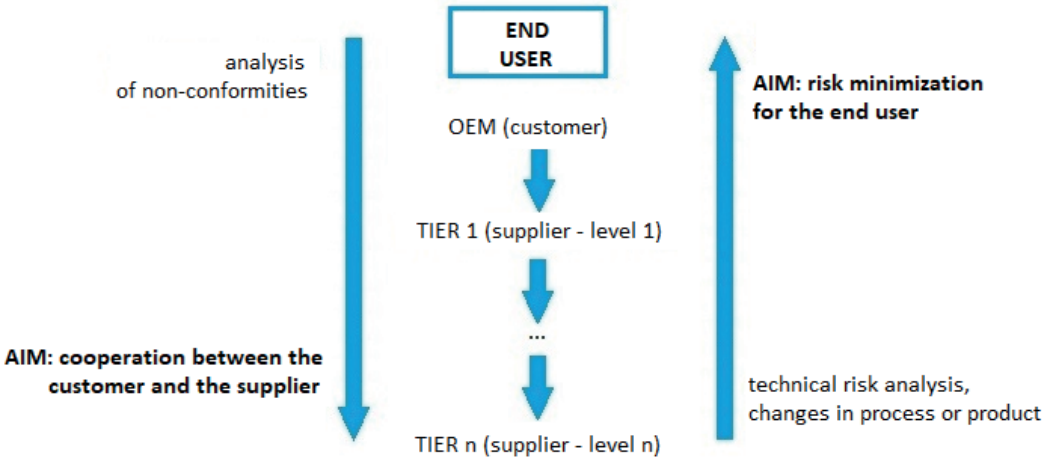


Figure 5 *Cooperation in creating FMEA in supply chain in the automotive industry (TIER - direct supplier for OEM, TIER 2 - second supplier in the logistics chain, etc.*

Accordingly, the FMEA sheets for design and process will be different. In the first case, the resulting sheet will be a combination of all the FMEA sheets for individual functions specified for the product, whereas in the second case it will include the FMEA sheets for all the operations of the analysed process.

Important changes in the new approach to FMEA concern step 5, where the commonly known RPN (Risk Priority Number) was replaced by AP (Action Priority). According to the guidelines, the AP is estimated on three levels: AP H - a high priority, AP M - medium priority, AP L - low priority of action; however, actions must be performed only in the case of AP H. Action priority was developed during the preparation of the new AIAG manual and presented in form of tables from which it is possible to read the action priority for risk reduction both for DFMEA and PFMEA. The AP, similarly, to RPN, is a combination of assessments related to the non-compliance significance, occurrence and detectability, however, the detail of the assessment proposed in the tables developed in the new manual significantly reduces the subjectivity of the expert assessment, which considerably affects improvement activities in the organization.

In production practice, the input document is the DFMEA and only then, on its basis, the PFMEA is created (according to Figure 4). Since October 2013, the FMEA rank has increased due to an update of Rules for achieving and maintaining IATF recognition [17]. The amendment introduced a point about connections between the Control Plans and FMEA and effective implementation of the changes introduced in the above documents - changes in FMEA should be reflected in Control Plans (Figure 4). Adding requirements in the

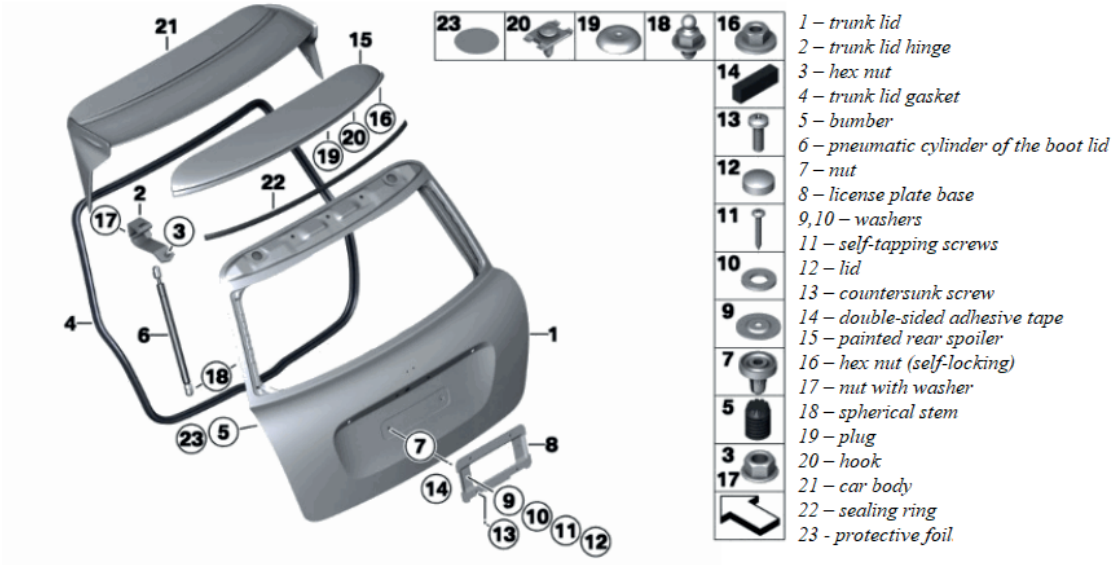


Figure 6 *A fragment of the workstation instruction related to operations conducted at workstation 9.8., source: authors on the basis of materials from production practice*

area of risk management to Rules for achieving and maintaining the IATF recognition is consistent with one of the basic principles of quality management - continuous improvement.

It should also be remembered that FMEA analyses are carried out at various levels in the supply chain in the automotive industry. First of all, from the OEM level, and from the point of view of different suppliers, as well. Until recently (before the introduction of the new approach to FMEA), multi-level assessment (from the point of view of the final, external and internal customer at every stage of this chain) were only good manufacturing practice. At present, they are already included in the new FMEA procedure and require close cooperation between organizations in the supply chain (Figure 5).

4 PFMEA for the assembly process of a spoiler in a passenger car - problem statement and a fragment of analysis

The process FMEA is aimed at analysing potential (or real) failures in the processes of production, assembly, logistics, etc. so as to manufacture products in accordance with the design intentions and meeting all the requirements of interested parties. The failures analysed in PFMEA are different from those analysed in DFMEA. By means of the FMEA, processes occurring in an enterprise are analysed taking into account (potential or actual) non-conformities that may arise due to process variability. Thanks to the PFMEA analyses, it is possible to prioritize preventive (corrective) actions and - if necessary - to improve control activities in an enterprise.

The process FMEA is carried out mainly before production starts, to prevent the occurrence of non-compliances associated with product manufacture, as well as the consequences of those defects. In the production practice, PFMEA is, however, conducted at cyclical intervals and constitutes the so-called Live document - during the course of the project, in which information on internal and external complaints, information from customers, information on process changes is supplemented. The FMEA sheet presents how the project is evaluated and constitutes a company's knowledge base.

The research was carried out at an automotive industry enterprise on the passenger car assembly line and concerned the workstation at which a car spoiler is mounted. The process of installing the spoiler at this workstation includes three basic variants - installing the spoiler in the classic, city and sport versions. Models that are not equipped with a spoiler are also produced. In production practice, individual parts, listed in workstation instructions, are provided in a coded version, enabling for their unambiguous identification (RFID codes). Figure 6 shows a fragment of the instruction for the analysed workstation. The document specifies a proper conduct of the installer at this workstation related to installing the license plate base and the spoiler.

All steps of the PFMEA analysis were carried out respectively.

1st Step - Planning and preparation.

At this stage, the project was identified, including its boundaries. According to the 5T method, the goal (Target) and project schedule (Timing) were developed, a team was appointed (Team), the tasks were distributed (Tasks) and quality management tools were selected to be applied in the project (Tools).

PFMEA was conducted for an existing process of spoiler mounting on workstation 9.8. In determining

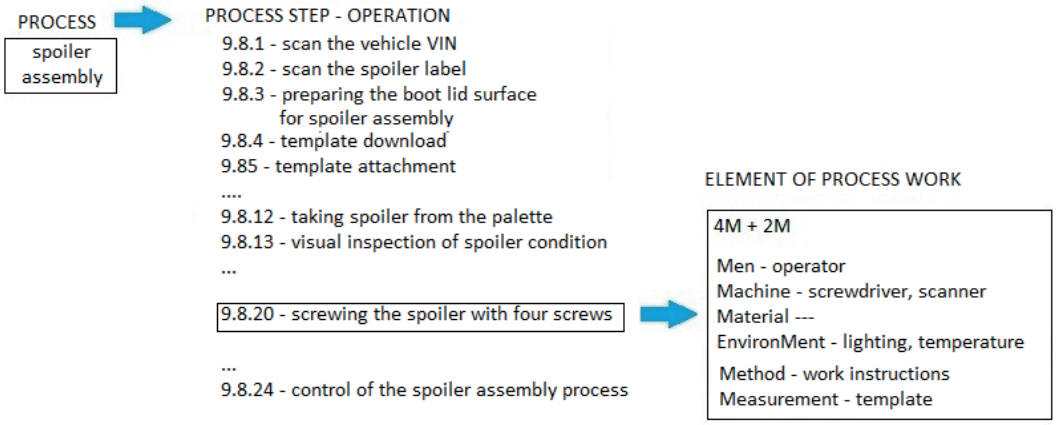


Figure 7 *A fragment of a structure tree for the analysed process*

the scope of the analysis, the team takes into account previous PFMEAs that have already been performed. It also takes into account the DFMEAs that have been received from suppliers. The requirements of all the interested parties were considered, with particular emphasis on legal requirements. At this point, it is worth noting that mounting a spoiler does not affect operation safety of the vehicle or pose a threat to the driver or passengers of the car, but it is a threat to other road users. That is why the assembly at this workstation is provided with safety characteristics (SC).

2nd Step - Structure analysis.

In this step, the team developed a process structure analysis using a structure tree. The new release of PFMEA also allows process diagram analysis in this step. Due to the documentation used in the company, the team could use ready-made flow diagrams (spoiler assembly process, workstation 9.8, activities 9.8.1-9.8.24); however, this solution is only seemingly easier. As production practice shows, the analyses carried out on defect trees effectively limit the possibility of overlooking a failure in the process [16, 18-19]. By using the structure tree analysis, the team organized the hierarchy of system components and illustrated relationships by means of structural connections. Thanks to such activities it was possible to understand the relationship between process elements, operations and process work elements (Figure 7).

The analysis presented in Figure 7 was carried out for all the operations related to this process and concerned all the elements of this process, which constitute the lowest level in this flow. The categories included by the team are not only standard 4M (man, machine, material, environment). In addition, when analysing work process elements, the team included two additional categories (method, measurement).

3rd Step - Functional analysis.

At this stage, the key is to link the requirements or process characteristics with the functions. The team did not identify characteristics other than those resulting from the DFMEA. Safety characteristics appear in the spoiler assembly process, so, in order to ensure that these characteristics are achieved through the process, they should be monitored. A fitter uses a template to measure the size of the gap after installing the spoiler. The durability of the connection is also verified (assessment of the supply of double-sided tape used in the process), as well as the tightening of the bolts fixing the spoiler (torque read by the IT system connected to the screwdriver).

4th Step - Failure analysis.

The main goal of this stage is to develop a failure chain by the team, i. e. the relationship between:

- A failure that occurred in the analysed element - determination of the FM (Failure Mode) in the sheet FMEA.
- The reason for this failure - FC (Failure Cause) designation in the FMEA sheet.
- The result of this failure - FE (Failure Effect) designation in the FMEA sheet.

Figure 8 shows a fragment of the team's work during step 4.

The most important guidelines that the team followed when analysing failures were:

- For FM - each fault was analysed separately, the possibility of detecting the fault during the inspections/tests was analysed.
- For FC - the causes of failures were analysed from the two levels perspective: the direct cause of the fault and the source fault, the reasons were considered in categories 4M + 2M using the Ishikawa diagram.
- For FE - the failures' results were analysed from the perspective of the internal and external customer (i. e. the user of the product), including the legal consequences.

5th Step - Risk assessment and analysis.

Step 5 is a basis for the process optimization. In the first stage, the team measures which preventive controls

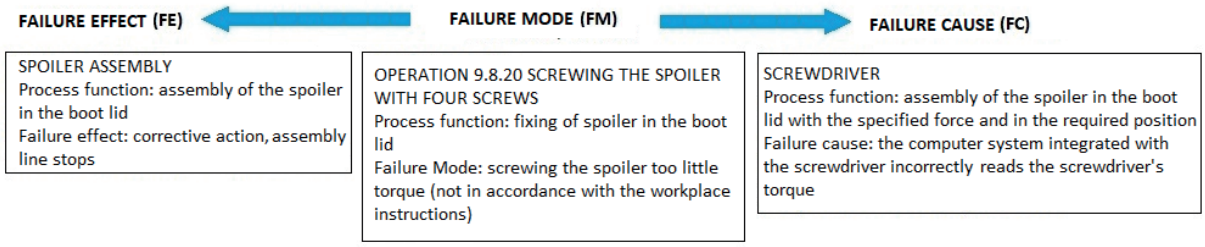


Figure 8 *An exemplary failure chain*

Table 1 *Risk assessment - AP activities prioritization according to guidelines from the new AIAG and VDA manuals (excerpt); AP assessment for the analysed case in bold in the table, based on [12]*

AP activities prioritization						
significance	S	occurrence	O	detection	D	AP
very high effect	9-10	very high	8-10	very low - low	7-10	H
				moderate	5-6	H
				high	2-4	H
				very high	1	H
		high	6-7	very low - low	7-10	H
				moderate	5-6	H
				high	2-4	H
				very high	1	H
		moderate	4-5	very low - low	7-10	H
				moderate	5-6	H
				high	2-4	H
				very high	1	M
		low	2-3	very low - low	7-10	H
				moderate	5-6	M
				high	2-4	L
				very high	1	L
		very low	1	very high - very low	1-10	L

(PC) and detecting controls (DC) are currently used in the process. For the presented example, for the needs of the article, the team identified: template-dependent spoiler position (PC), workstation instruction (PC), visual control (DC), control at the end of the analysed line section (DC) and random control (DC).

At a later stage, the team analysed independent risk factors for all the failure chains identified in step 4. As in previous approaches to FMEA, three criteria were considered: significance of the failure effect (S), occurrence of the failure cause (O) and detectability the failure or its cause (D). During the risk assessment, ready-made, very precisely prepared lists, indicating the level of all the criteria, were used. For example, by analysing the failure chain shown in Figure 8, according to the AIAG + VDA manual, the criterion significance was assessed at a moderate level (S = 8), because the manual determines the impact at level 8 when for an internal customer "a failure can cause deviations in the primary process, deterioration in the speed of the production line, a need to hire extra workforce." The team considered this failure not only in the context of its impact on its own production facility but looked at the problem from a wider perspective. Analysing the impact of this incompatibility on the final user, S = 10 and thus reaches the maximum in the analysed method. The manual describes failure significance determined at level 10 as follows: "the failure affects the safety of ae vehicle and/or other vehicles, the health of the driver and /or passengers or other road users, including pedestrians".

The other two criteria were assessed similarly. When assessing the occurrence (O), the following were taken into account: the type of control in the process (behavioural or technical - according to the manual), preventive control (preventive control partially effective in preventing the failure causes), the level of incidents per 1000 vehicles was rated as 1 / 500. Hence, reading from the Table 1, O = 6, which is high. In assessing detection (D), the team considered two areas: the maturity of the detection method (the control method has not been confirmed as effective and reliable) and the detection capability (human or manual control); hence D was estimated at level 8.

Table 2 *FMEA form - part 1; According to guidelines from the new AIAG and VDA manuals; the case analysed in the paper, based on [12]*

failure analysis - step 4				risk analysis - step 5					
FE	S	FM	FC	PC	O	DC	D	AP	SC
the need to conduct corrective action, assembly line standstills	8	screwing the spoiler with too little torque	the computer system incorrectly read the torque of the screwdriver	workstation instruction, the template of the spoiler's position	6	visual control, random check, end of line control	8	H	Δ
the product influences the safety of other road users	10	screwing the spoiler too little torque	the computer system incorrectly read the torque of the screwdriver	workstation instruction, the template of the spoiler's position	6	visual control, random check, end of line control	8	H	Δ

For the analysed failure chain S = 10, O = 6, D = 8. Based on that estimation, the team was able to proceed to prioritising AP activities and determined the highest priority for review and action (H), according to Table 1.

At this stage, the first part of the PFMEA form is also created. The fragment described in the article is presented in Table 2.

6th Step - Optimization

The main purpose of this stage was to identify the actions necessary to reduce the risk, including determining the scope of responsibility, deadlines for introducing actions and assessing their effectiveness, as well as re-assessing the risk after the actions are introduced. In both cases presented in the article, AP was estimated at a high level (priority H). In such a situation, taking action is obligatory. If the AP is estimated at level M or L, the FMEA only recommends taking action.

In this step, the team decided to take corrective actions. As the root cause of the problem, an unprotected computer program was identified that verified the torque at which the screwdriver fastened the bolts securing the spoiler to the boot lid. The cause has been eliminated and changes were documented. Although in the case presented in the paper the implemented actions did not affect the AP PFMEA result itself - priority is still at level H, the team managed to improve the process.

7th Step - Documenting results.

The last step of the analysis was to prepare an FMEA report and to communicate the results within the organization.

5 Comparing the analyses' results carried out under the old and new approach

While discussing the changes in the approach of risk assessment according to different approaches, it is important to analyse briefly the evolution of e approaches to the risk assessment in the automotive industry (Figure 9).

The initial indications for the FMEA analyses clearly informed the organization about the level of risk that should be accepted by it (RPN range 1 - 100, first column in Figure 9). Above this level, the risk associated with the analysed process, design, structure was unacceptable and it was absolutely necessary to take actions aimed at minimizing this risk. The next stage (column 2 in Figure 9) took into account the individual risk appetite of the organization. Each enterprise established its own, acceptable risk level above which it took corrective or preventive actions. The last stage of the risk analyses based on the FMEA method with the use of RPN (column 3 in Figure 9) took into account not only the individual approach to the acceptable risk level, but the organizational context, as well. In this situation, the risk area appeared, which was conditionally acceptable for the organization (depending on the favourable or not influences of the environment, as well as the analysis of the organization's own capabilities).

In the company presented in the study, the FMEA evolved in accordance with the presented diagram. In the final phase of the analyses carried out with use of the RPN, the following values were established for the measures: RPN at the level of 1 - 80 was an acceptable risk, up to 300 - conditionally acceptable risk and above 300 - unacceptable risk.

When assessing the risk associated with the process (presented and analysed in Section 4 of this study), according to the new and the old approach (in the old approach for O and D, the same results were obtained):

- Assessment of occurrence (O) included: type of control in the process (behavioural or technical - according to the manual), preventive controls (preventive controls partially effective in preventing the causes of error), the level of incidents was assessed as 1 / 500. Therefore - reading from the table, O = 6 that is moderate.
- Detection (D) was assessed - the team looked at two

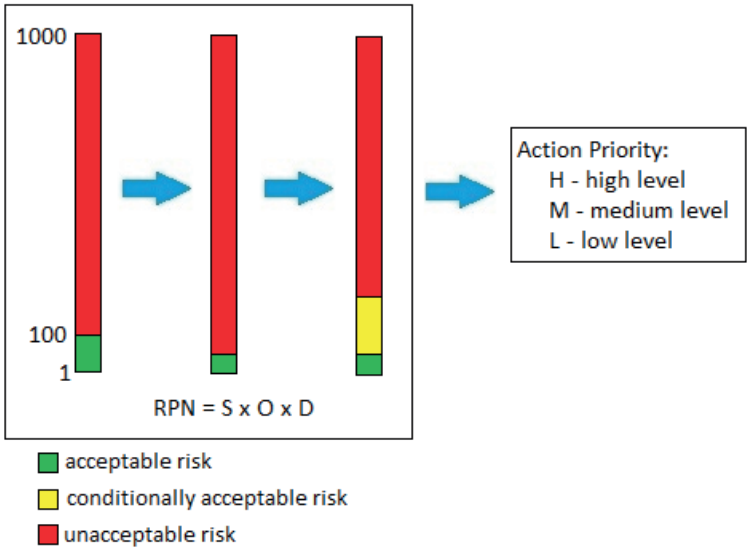


Figure 9 *Evolution of risk analysis in the automotive industry*

areas: the maturity of the detection method (the control method has not been proven effective and reliable) and ability to detect (human or hand-held inspection); therefore, D was estimated at 8.

- The severity (S) of the non-compliance was assessed. In the new approach, the assessment team considered this inconsistency not only in terms of its impact on its own production facility, but also looked at the problem more broadly.

The impact of non-compliance on the end user is S = 10, so it reaches its maximum with the analysed method. The manual book in the column Severity of error in assessment 10 has the following description: The error affects the operational safety of a vehicle and / or other vehicles, the health of the driver and / or passengers or other road users, including pedestrians (critical characteristics).

On the other hand, according to the old approach, in relation to the analysis of the severity of non-compliance, considerations were made only in the intra-organizational system, therefore S = 6. An error may cause deviations in the basic process, deterioration of the speed of the production line, the need to employ additional labour.

The following results were obtained:

- RPN estimated according to the old method was RPN = 288 (O = 6, D = 8, S = 6, RPN = 288) - the level of risk was conditionally acceptable. This means that with a favourable organizational context, the enterprise was not procedurally obliged to take actions to minimize the risk associated with the process.
- AP estimated according to the new method received the highest priority of actions (O = 6, D = 8, S = 10, AP at H level). This means that the organization is obliged to take actions with the identified risk.

The presented comparison illustrates the beneficial changes in the FMEA analyses, which, with the new approach developed by AIAG & VDA, consider a broader perspective of the risk assessment related to the organization's operations.

6 Conclusions

The emergence of the new FMEA handbook, developed thanks to the joint efforts of AIAG and VDA, has systematized good practice in risk analysis related to both the process and the product. Thanks to the precisely developed and described procedure for estimating the criteria affecting the risk: S, O, D, as well as the approach to AP estimation, the new method results in the greater repeatability of the assessment performed by various teams of experts. As a result, there is hope that companies from the automotive industry will stop perceiving the FMEA as an uncomfortable requirement of the standard that they must meet, but as a method generating value for the enterprise. It should be remembered that everything that has been or can be identified under the FMEA procedure constitutes its value and also significantly affects the effectiveness of the decision-making process.

Furthermore, properly conducted FMEA forms a strong basis for preparing the efficient control plans and it is a document, which can charge or release the responsibility of one of the parties in the logistics chain for the design and / or product.

The biggest problem in the correct application of the achievements, developed by the representatives of AIAG and VDA, is the time-consuming nature of the procedure, especially at the stage of implementing changes. Another disadvantage of the approach is the difficult access to knowledge - textbooks and training courses in this field are also payable and the participation of a competent consultant is expensive.

References

[1] KOBYLINSKA, U. Evolution or revolution? The new ISO 9001:2015 standard. *Economics and Management* [online]. 2014, **6**(1), p. 205-219. ISSN 2080-9646. Available from: http://dx.doi.org/10.12846/j.em.2014.01.12

[2] BURDUK, A., WIECEK, D., ZAJACKO, I., JURDZIAK, L., BLAZEJ, R.: Analysis and risk assessment of the supply of copper ore in the belt conveyor system in an underground mine. *Acta Montanistica Slovaca*. 2020, **25**(2), p. 236-249. eISSN 1339-3103.

[3] GUERRERO-CUSUMANO, J. L., SELEN W. J. A comparison of international quality standards: divergence and agreement. *Business Process Management Journal* [online]. 1997, **3**(3), p. 205-217. ISSN 1463-7154. Available from: https://doi.org/10.1108/14637159710192239

[4] BAGHBANI, M., IRANZADEH, S.,BAGHERZADEH, M. Investigating the relationship between RPN parameters in fuzzy PFMEA and OEE in a sugar factory. *Journal of Loss Prevention in the Process Industries* [online]. 2019, **60**, p. 221-232. ISSN 0950-4230. Available from: https://doi.org/10.1016/j.jlp.2019.05.003

[5] YIWU, J., IHSIAO, H. Food quality and safety risk diagnosis in the food cold chain through failure mode and effect analysis. *Food Control* [online]. 2021, **120**, 107501. ISSN 0956-7135. Available from: https://doi.org/10.1016/j.foodcont.2020.107501

[6] NIERZWICKI, W. *Quality management - selected issues* / *Zarzadzanie jakoscia - wybrane zagadnienia* (in Polish). Gdansk: Osrodek Doradztwa i Doskonalenia Kadr, 1999. ISBN 83-71871-92-9.

[7] TATARCHENKO, Y., LYFAR, V., TATARCHENKO, H. Information model of system of support of decision making during management of it companies. *Applied Computer Science* [online]. 2020, **16**(1), p. 85-94. ISSN 1895-3735, eISSN 2353-6977. Available from: https://doi.org/10.23743/acs-2020-07

[8] DANILCZUK, W., GOLA, A. Computer-aided material demand planning using ERP systems and business intelligence technology. *Applied Computer Science* [online]. 2020, **16**(3), p. 42-55. ISSN 1895-3735, eISSN 2353-6977. Available from: https://doi.org/10.23743/acs-2020-20.

[9] SWIC, A., GOLA, A. Economic analysis of casing parts production in a flexible manufacturing system. *Actual Problems of Economics*. 2013, **141**(3), p. 526-533. ISSN 1993-6788.

[10] LUCZAK, J. *Quality management system for suppliers in the automotive industry - assessment of the significance of requirements* / *System zarzadzania jakoscia dostawcow w branzy motoryzacyjnej - ocena istotnosci wymagan* (in Polish). Habilitation thesis. Poznan: Wydawnictwo Akademii Ekonomicznej, 2008. ISBN 978-83-7417-372-8.

[11] ALBAHLI, S. A deep ensemble learning method for effort-aware Just-In-Time defect prediction. *Applied Computer Science* [online]. 2020, **16**(3), p. 5-15. ISSN 1895-3735, eISSN 2353-6977. Available from: https://doi.org/10.23743/acs-2020-17

[12] AIAG and VDA FMEA Handbook. Design FMEA and process FMEA. Supplemental FMEA for monitoring and system response. 1. ed. USA: AIAG and VDA, 2019.

[13] LYSAK, D. Technical specification ISO / TS 16949 / Specyfikacja techniczna ISO / TS 16949 (in Polish). *Problemy Jakosci*. 2013, **45**(10), p. 21-27. ISSN 0137-8651.

[14] LIPENG, W., FANG, Y., FANG, W., ZIJUN, L. FMEA-CM based quantitative risk assessment for process industries - a case study of coal-to-methanol plant in China. *Process Safety and Environmental Protection* [online]. 2021, **149**, p. 299-311. ISSN 0957-5820. Available from: https://doi.org/10.1016/j.psep.2020.10.052

[15] CHANG, CH.-H., KONTOVAS, CH., YU, Q., YANG, Z. Risk assessment of the operations of maritime autonomous surface ships. *Reliability Engineering and System Safety* [online]. 2021, **207**, 10732. ISSN 0951-8320. Available from: https://doi.org/10.1016/j.ress.2020.107324

[16] GREBER, T. Webinar materials: New FMEA / Materialy webinar: Nowe FMEA (in Polish) [online] [accessed 2021-15-01]. Proqual Management Institute, 2019. Available from: https://fmea.com.pl/nowe-wymagania-aiag-i-vda-w-zakresie-fmea-definiowanie-wad-i-skutkow/

[17] Rules for achieving and maintaining IATF recognition - IATF [online] [accessed 2021-15-01]. 5th edition frequently asked question (FAQ). IATF publications - FAQ 1,2,3,4 - 2017, FAQ 5,6 - 2019. Available from: www.iatfglobaloversight.org

[18] KRAJCOVIC, M., GRZNAR, P. FUSKO, M. SKOKAN, R. Intelligent logistics for intelligent production systems. *Communications - Scientific Letters of the University of Zilina* [online]. 2018, **20**(4), p. 16-23. ISSN 1335-4205, eISSN 2328-5923. Available from: https://doi.org/10.26552/com.C.2018.4.16-23

[19] PACAIOVA, H., GLATZ, J. Maintenance management system. *MM Science Journal* [online]. 2015, p. 665-669. ISSN 1803-1269, eISSN 1805-0476. Available from: https://doi.org/10.17973/MMSJ.2015_10_201532

ELECTRO-HYDRAULIC PROPORTIONAL SYSTEM REAL TIME TRACKING CONTROL DEVELOPMENT BASED ON PULSE WIDTH MODULATION METHOD

Ezz Eldin Ibrahim*, Tarek Elnady, Mohamed Saffaa Hassan, Ibrahim Saleh

Military Technical College, Cairo, Egypt

*E-mail of corresponding author: ezzbos@gmail.com

Resume

The presented work was directed to develop the dynamic performance of an electro-hydraulic proportional system (EHPS). A mathematical model of the EHPS is presented using electro- hydraulic proportional valve (EHPV) by Matlab-Simulink, which facilitates the simulation of the hydraulic behavior inside the main control unit. Experimental work is done and the closed loop system is designed using the linear variable displacement transducer sensor (LVDT). The controller of the system is an Arduino uno, which is considered as a processor of the system. The model is validated by the experimental system. The study also presents a real time tracking control method, based on pulse width modulation, by controlling the speed of the actuator to achieve the position tracking with minimum error and low transient time, by applying the constant input signal 50 mm the transient time was 0.9 seconds and the error 1.8 %.

Article info

Received 17 February 2021
Accepted 15 April 2021
Online 17 September 2021

Keywords:

hydraulic control,
proportional valve,
electro hydraulic proportional system,
PWM control method,
position tracking control

Available online: https://doi.org/10.26552/com.C.2021.4.B336-B345

ISSN 1335-4205 (print version)
ISSN 2585-7878 (online version)

This is an open access article distributed under the terms of the Creative Commons Attribution 4.0 International License (CC BY 4.0), which permits use, distribution, and reproduction in any medium, provided the original publication is properly cited. No use, distribution or reproduction is permitted which does not comply with these terms.

1 Introduction

The proportional valve is a valve, which produces a proportional output to an electronic control input, or a valve that operates by proportional solenoids instead of on-off solenoids.

It can be classified to three types; pressure control valves, flow control valves and directional control valves.

The pressure control valves are designed mainly to control the pressure while the proportional flow control valves are designed mainly to control the flow rate and the proportional directional valve is used to control both the flow direction and the flow rate.

Many studies have dealt with the proportional valve investigations. Vaughan and Gamble [1] presented a nonlinear dynamic model of a high-speed direct acting solenoid valve, the model accurately predicted both the dynamic and steady state response of the valve to voltage inputs. Simulated voltage, current and displacement results were presented, which agreed well with experimental results.

Chen et al. [2] proposed an adaptive self-tuning controller to enable a hydraulic proportional valve to achieve accurate tracking control.

The performance of the closed-loop system was very robust as the system response remained the same under various operating conditions.

Rahman et al. [3] began the first step of converting a conventional on-off solenoid into the a proportional one. They studied the dynamic behavior of a conventional solenoid by letting the simulation depending on the linear magnetic principle, by using the simulation package SIMNON. A comparison was done between the results from simulation model and experimental work.

Niksefat and Sepehri [4] studied the development and experimental evaluation of a hydraulic force controller, using the nonlinear Quantitative Feedback Theory (QFT) design method. The designed controller was implemented on an industrial hydraulic actuator equipped with a low-cost proportional valve.

Elmer and Gamble [5] presented a generic non-linear dynamic model of a direct-acting electro-hydraulic proportional solenoid valve. The model accurately and reliably predicted both the dynamic and steady state responses of the valve to voltage inputs. Simulated results were presented, which agreed well with experimental ones.

Dasgupta and Watton [6] studied dynamics of a proportional controlled piloted relief valve through the bond-graph simulation technique. The simulation results were also verified by the experimental results.

Chen et al. [7] studied the nonlinear model of a variable displacement axial piston pump (VDAPP) with a three-way electro-hydraulic proportional valve (EHPV), which controlled the swash plate actuators. The time response for the swash plate angle was analyzed theoretically by the simulation model, as well as experimentally and a favorable model-following

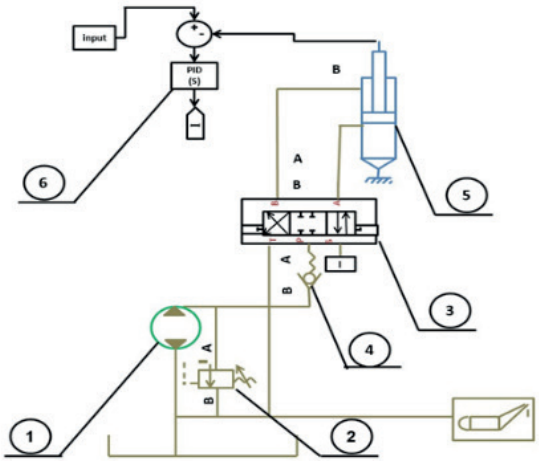


Figure 1 *The EHPS hydraulic circuit*

characteristics was achieved. The proposed neural controller, which conducts the nonlinear control in VDAPP, enhanced adaptability and robustness and improved the performance of the control system.

Liu et al. [8] studied an optimization of a throttle poppet valve based on hydraulic feedback principle to use it in machines. The study can be used as a guideline for design of various sizes of proportional valves.

Amirante et al. [9] designed a new methodology of spool surfaces of 4/3 proportional directional valve.

It was based on redesign of both the compensation profile and spool lateral surfaces to reduce the flow forces acting on it.

The proposed methodology achieved lower actuation forces compared to the commercial configuration.

Acuna-Bravo et al. [10] presented application of a model-based control structure called Embedded Model Control (EMC).

The position tracking of the spool presented a better result by using the EMC compared to those using an industrial manufacturer.

2 Model description

The system shown in Figure 1 consists of hydraulic pump (1), which feed the electro hydraulic proportional valve (EHPV) (3), through the pressure relieve valve (2).

The one-way valve (4) prevents the flow to return, while the pump is in no operation mode.

The EHPV controls the output hydraulic feed delivered to the hydraulic actuator (5) to allow the hydraulic actuator tracking the required input position by the PID controller (proportional integral derivative controller) (6).

3 Mathematical model

The proposed system modelling is mathematically done by Matlab-Simulink and the system components configuration are selected as the same as the experimental ones.

3.1 Hydraulic pump

The type of the hydraulic pump used in the electro-hydraulic system is a fixed displacement gear pump, which operates at nominal speed of 600 rpm and maximum output flow rate of 6.05 liter/min.

The pump is driven by an AC electric motor that operates at 220 Volts, 50 Hz and 1.5 Kw.

3.2 Relief valve

The relief valve is used to control the pressure in the hydraulic systems to protect its individual elements, pipes and hoses from the over-pressure problems; it is adjusted at a pressure of 60 bar.

3.3 Proportional directional valve

The 4/3 electro-hydraulic proportional directional valve, Figure 2, is a Hydraulic Ring manufactured as type NG6. It has maximum operating pressure of 315 bar, its valve spool has zero overlap and its motion is controlled by the two electrical proportional solenoids.

3.4 Hydraulic actuator

The hydraulic actuator used in this study is a double acting steel, with a cam for operating the limit switch.

It has a diameter of 32/22 mm, area ratio 1.6:1 and max pressure of 160 bar.

Figure 3 illustrates the flow through the proportional valve, were (P) is the valve pressure port, (T) is the valve return to the tank, (A) and (B) are the valve outputs to

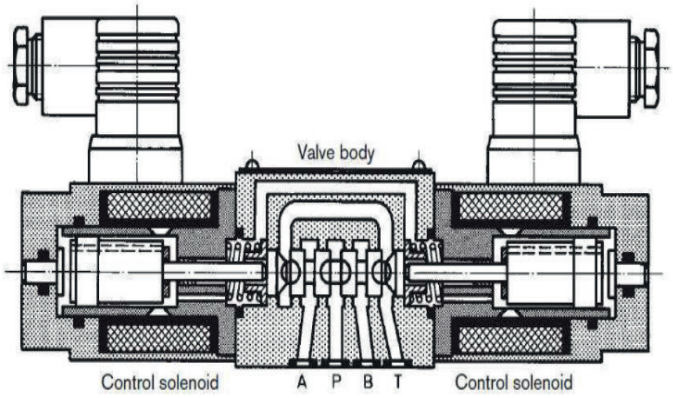


Figure 2 *Typical electrohydraulic proportional valve*

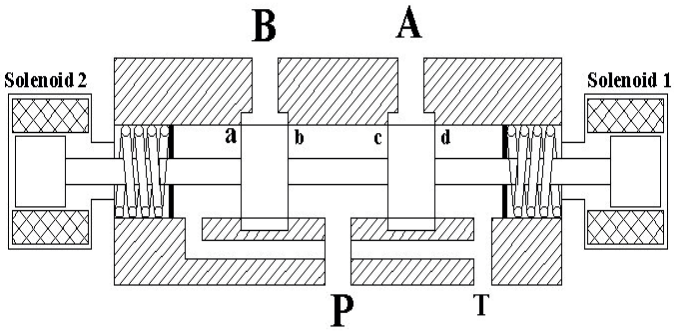


Figure 3 *Proportional directional valve Internal orifices*

the actuator; while a, b, c and d are the areas where the flow is subjected through the valve.

3.5 Model equations

The *Q*-*P* mathematical relation of the pump has been found as following:

$$Q_p = Q_{th} - (7 \times 10^{-13} P_p), \tag{1}$$

where:
Q_{th}: maximum theoretical flow rate of the gear pump = 6.05 liter/min,
P_P: pump output pressure.

The equation of poppet motion of the relief valve is:

$$m_p \frac{d^2 z}{dt^2} + f_r \frac{dz}{dt} + k_r (z + z_0) = p \cdot A_p + F_{seat}, \tag{2}$$

$$F_{seat} = K \cdot z_0. \tag{3}$$

The flow rate equation is:

$$Q_{rv} = C_d A \sqrt{\frac{2(P - P_t)}{\rho}}. \tag{4}$$

Equation of motion of the valve spool is:

$$F_s = m_s \frac{d^2 x}{dt^2} + f_s \frac{dx}{dt} + kx, \tag{5}$$

where: m_s = mass of spool + 0.5 (mass of the return spring) = 0.021 Kg,
mass of spool = 19.58 Kg [measured],
mass of spring = 1.972 Kg [measured],
f_s = 50: 100 N.s/m,
k = 24500 N/m [measured experimentally].

Flow rate equations through the proportional valve are:

$$Q_a = C_d A_a(x) \sqrt{\frac{2(P_B - P_s)}{\rho}}, \tag{6}$$

$$Q_b = C_d A_b(x) \sqrt{\frac{2(P_s - P_B)}{\rho}}, \tag{7}$$

$$Q_c = C_d A_c(x) \sqrt{\frac{2(P_s - P_A)}{\rho}}, \tag{8}$$

$$Q_d = C_d A_d(x) \sqrt{\frac{2(P_A - P_t)}{\rho}}. \tag{9}$$

Continuity equations through the hydraulic actuator are:

$$Q_{AR} - a\frac{dy}{dt} - Q_i - Q_e - \frac{(V_R + ay)}{B}\frac{dp_R}{dt} = 0, \tag{10}$$

$$A\frac{dy}{dt} + Q_i - Q_{psB} - \frac{(V_{ps} - Ay)}{B}\frac{dp_R}{dt} = 0. \tag{11}$$

Actuator's equation of motion is:

$$a \cdot p_R - A \cdot p_{ps} = m_c \frac{d^2 y}{dt^2} + f_c \frac{dy}{dt} + F. \tag{12}$$

These equations are modelled in Matlab-Simulink

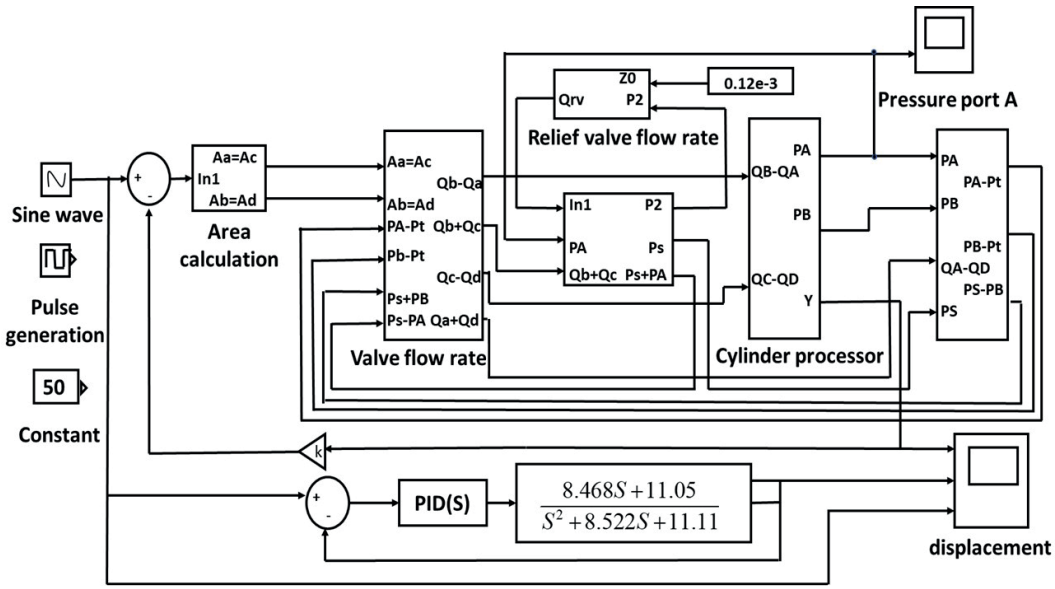


Figure 4 *The EHPS mathematical model code*

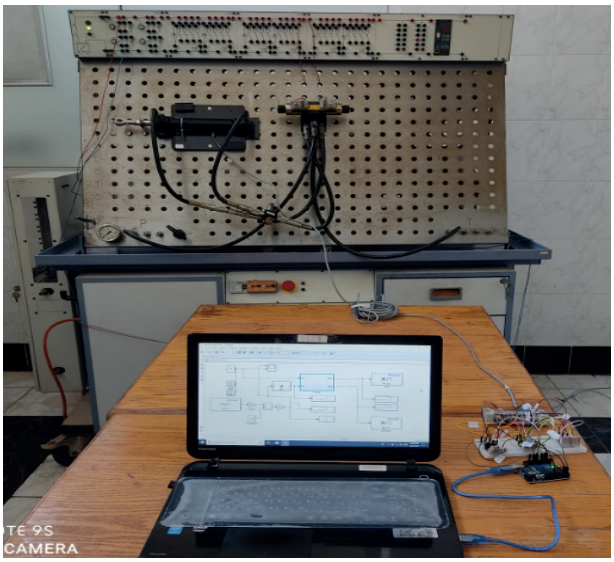


Figure 5 *Electrohydraulic test rig*

to facilitate the study of the fluid behavior through the hydraulic circuit and a controller is designed by the aim of Simulink tool, as well.

Figure 4 shows the simulation code of the system on Matlab-Simulink.

The system equations are represented in the code with different input signals.

The system is also represented by a transfer function, by using the system identification tool of the program and it gives the following transfer function:

$$\frac{8.468S + 11.05}{S^2 + 8.522S + 11.11}. \tag{13}$$

The controller of the model can be selected, by the transfer function which is the PID controller that is used to adjust and resolve the error of the system.

It controls the system by evaluating the feedback and compensating the system error. The mathematical equation of the PID controller is:

$$u(t) = K_p e(t) + K_i \int_0^t e(t)dt + K_d \frac{de(t)}{dt}, \tag{14}$$

where:

$u(t)$ is the controller output,

$e(t)$ is the system error,

K_p, K_i and K_d are the controller constants were: K_p = 0.428, K_i = 5.58 and K_d = 0

4 Experimental work

The experimental work was done by using the same components configuration as mentioned in section (3), which is the same as the mathematical model configurations.

Figure 5 shows the test rig used in this study.

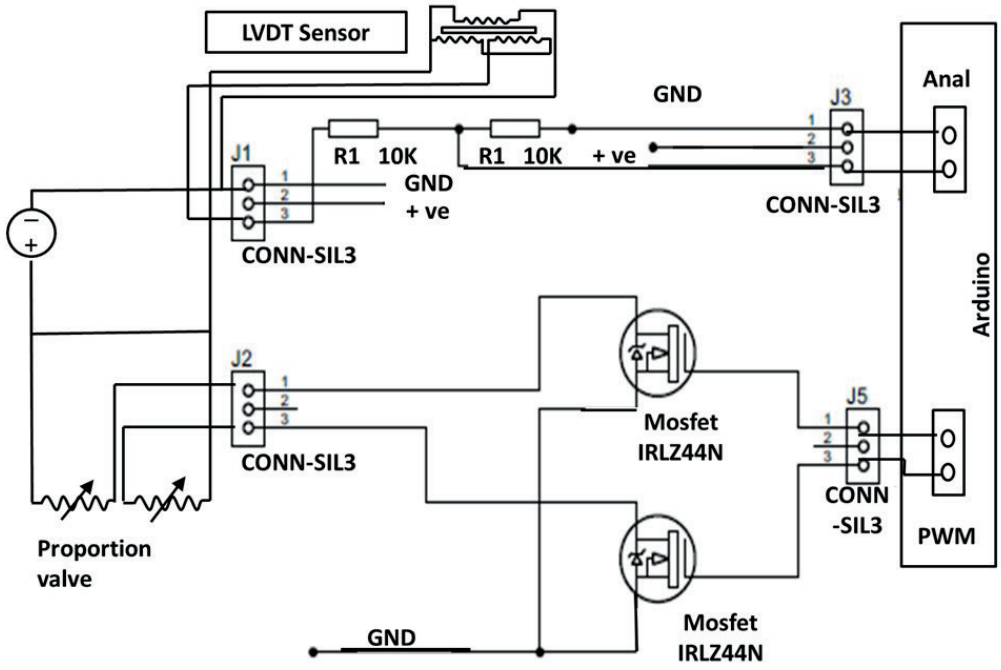


Figure 6 *Electric circuit for controlling the system*

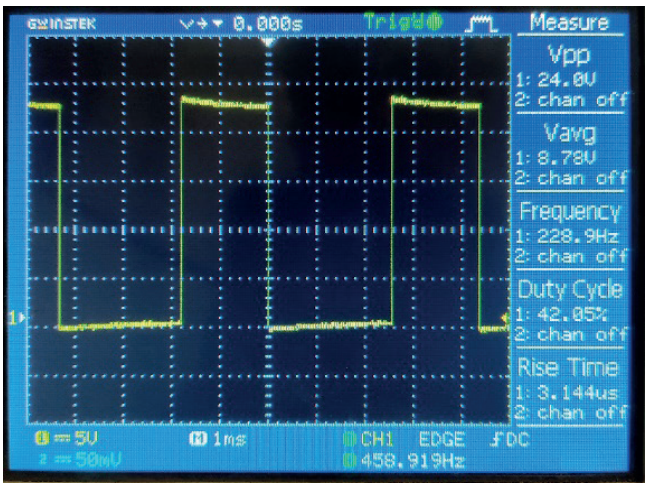


Figure 7 *Pulse width modulation input signal 180*

Figure 6 shows the electrical circuit used in controlling and monitoring the position tracking of the actuator.

The input signal is transferred from the Matlab-Simulink to the control card (Arduino mega 2560) and then delivered to the two coils of the (EHPV) through an electric circuit.

The two coils receive the signal from the Arduino (limit voltage 5 V DC) and boost this signal to (24 V DC) by the aim of MOSFET transistor (IRLZ44).

The feedback position is delivered to the Arduino by displacement sensor (LVDT).

The output from the sensor is up to (10 V DC), while, as mentioned, the Arduino limit voltage is 5 V DC.

There are a two 10 Ω resistors, used in series, to reduce the limitation of the signal voltage to 5V DC.

A new method of controlling the system is proposed in this study by experimentally testing the system by means of oscilloscope connecting to the two terminals of the proportional valve.

It has been found that the actuator response depends on changing the pulse width modulation (PWM).

Figure 7 shows the PWM input signal, which is detected by the oscilloscope with pulse width of 180, as an example of the input PWM signal.

Figure 8 shows the four PWM inputs to the system and its response on the actuator position with time.

As the pulse width increases, the speed of the actuator increases, as well.

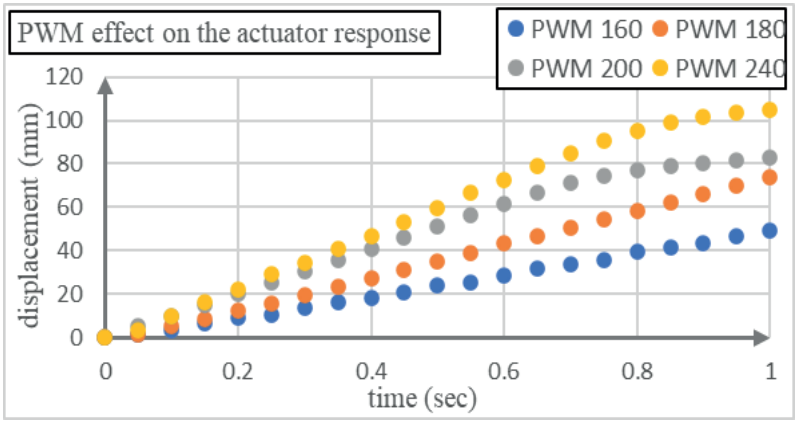


Figure 8 *Effect of the pulse width modulation on actuator speed*

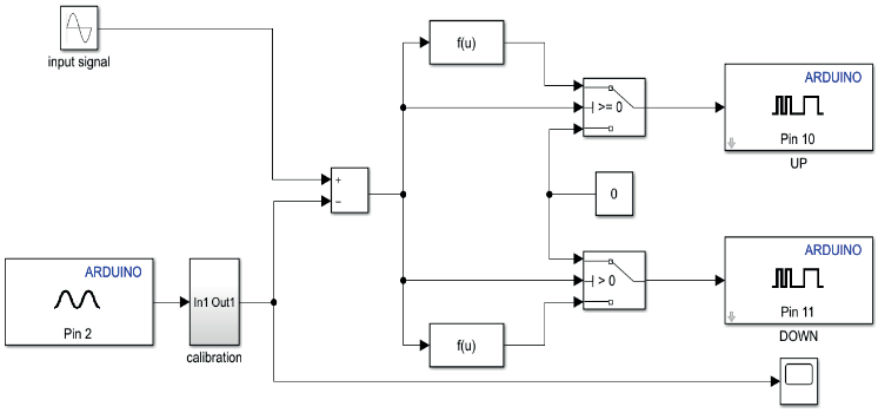


Figure 9 *The EHPS controlling code*

When the PWM is 160 the speed of the actuator reaches 50 mm/s and when the PWM reaches 180 the speed of the actuator reaches 74 mm/s.

The maximum actuator speed is reached when the PWM reaches 240 as the speed reaches 105 mm/sec and the inertia of the actuator increases, as well, which negatively affects the system control.

This experiment helps to produce a new method of electro-hydraulic proportional system control, by controlling the speed of the actuator to avoid the inertia of the actuator.

The following controller depends on adjusting the speed; when the actuator position is far from the target position the input PWM signal should be high to increase the speed of the actuator.

When the actuator approaches its target, the PWM signal should be reduced to avoid the actuator inertia.

Figure 9 shows the Matlab-Simulink code of this controller, which consists of:

- Arduino pin (2) block that receives the displacement of the actuator from Arduino, which receives it from the displacement sensor (LVDT).
- Arduino pin (10) and (11) blocks, which send the required (PWM) signal to the Arduino that delivered this signal to the two coils of the proportional valve.
- The two function blocks control the speed by calculating the difference between the input signal and the actuator position.

5 Results and discussion

The mathematical model is validated by the experimental work by varying the input signal with the following:

- Constant input 50 mm, step input 70 mm.
- Square signal 70 mm.
- Sinusoidal signal with amplitude 30 mm, bias 30 mm and frequency 0.5 rad/sec .08 Hz.

These results are shown in Figures 10 to 13, as they show that the model has a good agreement with the experimental results in the constant, step and square signal inputs, respectively

When applying a sinusoidal wave, the experimental result shows a relative delay compared to the mathematical model.

This delay is due to the controller, which reduces the actuator speed to avoid the actuator inertia that led to high overshooting; however, the mathematical model result is still in a good agreement with the experimental result.

The mathematical model helps in studying the fluid behavior inside the hydraulic circuit, which is calculated.

Figure 14 shows the pressure behavior in the hydraulic circuit by applying the constant input.

Figure 15 shows the pressure behavior by applying the sinusoidal wave, those results are serving for testing the system failure, when applying a high load or object to any component malfunction.

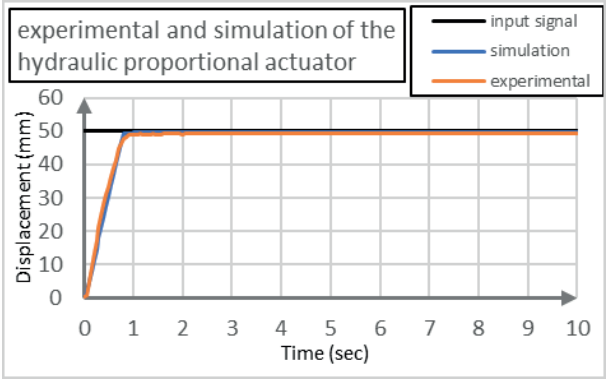


Figure 10 *Hydraulic actuator response by applying the constant input of 50 mm (experimental vs simulation)*

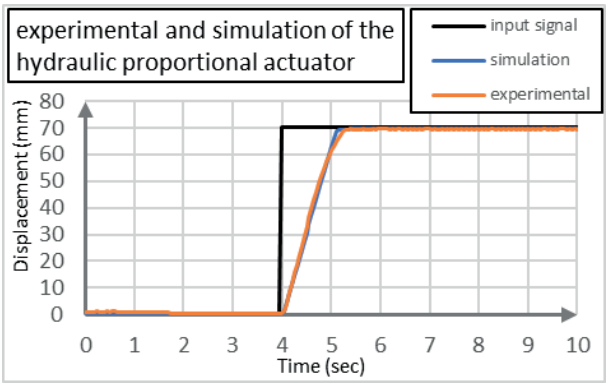


Figure 11 *Hydraulic actuator response by applying the step input of 70 mm (experimental vs simulation)*

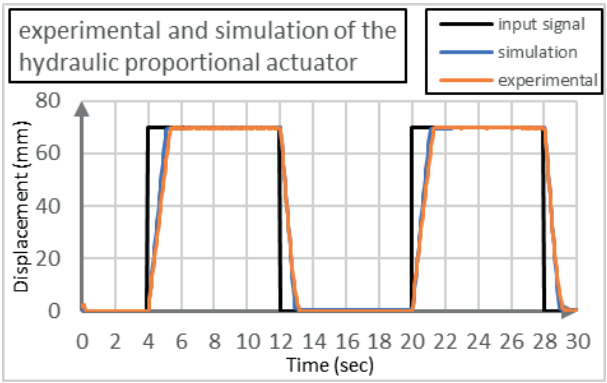


Figure 12 *Hydraulic actuator response by the applying square input of 70 mm (experimental vs simulation)*

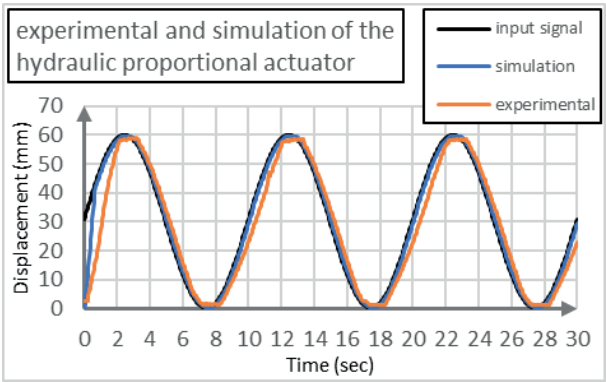


Figure 13 *Hydraulic actuator response by applying the sinusoidal wave input of 30 mm amplitude and 30 mm bias with frequency) 0.08 HZ (experimental vs simulation)*

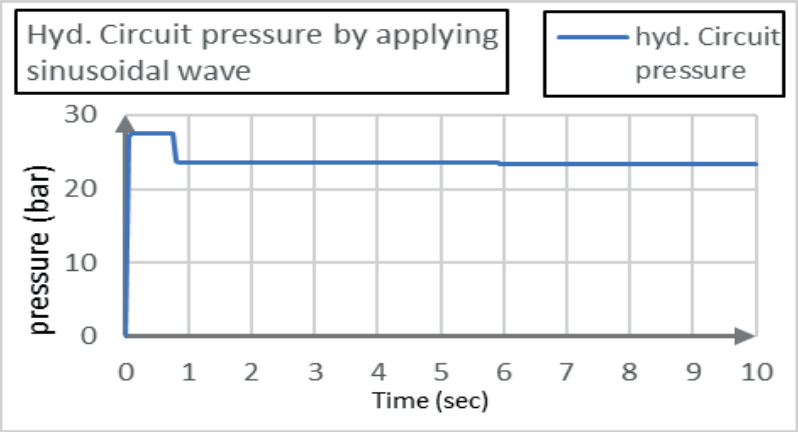


Figure 14 *Hydraulic circuit pressure behavior by applying the constant input of 50 mm*

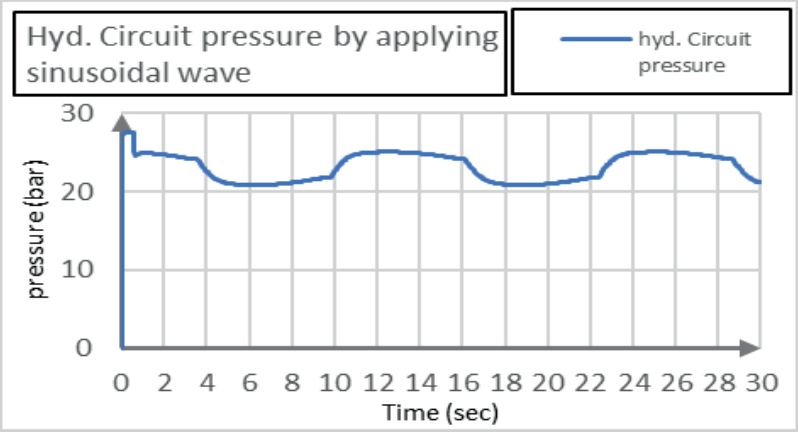


Figure 15 *Hydraulic circuit pressure behavior by applying the sinusoidal wave input of 30 mm amplitude and 30 mm bias with frequency) 0.08 HZ*

6 Conclusions

The study presented a new method for controlling the electro hydraulic proportional actuator by controlling the speed of the actuator.

This method is applied by controlling the pulse width modulation signal that operates the two coils of the proportional valve.

The proposed method of controlling the electro hydraulic proportional system is confirmed by good results with tracking different input signals.

The study presented a mathematical model of the system and its transfer function, and a controller of the model is done by the PID controller.

This study also facilitates studying the pressure behavior inside the hydraulic circuit.

References

[1] VAUGHAN, N. D., GAMBLE, J. B. The modeling and simulation of a proportional solenoid valve. *Journal of Dynamic Systems, Measurement and Control* [online]. 1996, **118**(1), p. 120-125. ISSN 0022-0434, eISSN 1528-9028. Available from: https://doi.org/10.1115/1.2801131

[2] CHEN, J., DIXON, W. E., WAGNER, J. R., DAWSON, D. M. Exponential tracking control of a hydraulic proportional directional valve and cylinder via integrator backstepping. In: ASME International Mechanical Engineering Congress and Exposition IMECE´02: proceedings. 2002. p. 895-906.

[3] RAHMAN, M. F., CHEUNG, N. C., LIM, K. W. Position estimation in solenoid actuators. *IEEE Transactions on Industry Applications*. 1996, **32**(3), p. 552-559. ISSN 0093-9994, eISSN 1939-9367. Available from: https://doi.org/10.1109/28.502166

[4] NIKSEFAT, N., SEPEHRI, N. Robust force controller design for an electro-hydraulic actuator based on nonlinear model. In: IEEE International Conference on Robotics and Automation: proceedings [online]. Vol. 1. IEEE, 1999. ISSN 1050-4729, ISBN 0-7803-5180-0, p. 200-206. Available from: https://doi.org/10.1109/robot.1999.769967

[5] ELMER, K. F., GENTLE, C. R. A parsimonious model for the proportional control valve. *Proceedings of the Institution of Mechanical Engineers, Part C: Journal of Mechanical Engineering Science* [online]. 2001, **215**(11), p. 1357-1363. ISSN 0954-4062, eISSN 2041-2983. Available from: https://doi.org/10.1243/0954406011524739
[6] DASGUPTA, K., WATTON, J. Dynamic analysis of proportional solenoid controlled piloted relief valve by bondgraph. *Simulation Modelling Practice and* Theory [online]. 2005, **13**(1), p. 21-38. ISSN 1569-190X. Available from: https://doi.org/10.1016/j.simpat.2004.08.002
[7] CHEN, K., HUANG, H., RONG, Z., LIU, G., LI, Y. Model-following controller based on neural network for variable displacement pump. In: 6th International Conference on Fluid Power Transmission and Control ICFP 2005: proceedings. 2005. ISBN 7506274027, p. 28-32.
[8] LIU, W., WEI, J., FANG, J., LI, S. Hydraulic-feedback proportional valve design for construction machinery. *Proceedings of the Institution of Mechanical Engineers, Part C: Journal of Mechanical Engineering Science* [online]. 2015, **229**(17), p. 3162-3178. ISSN 0954-4062, eISSN 2041-2983. Available from: https://doi.org/10.1177/0954406214568822
[9] AMIRANTE, R., DISTASO, E., TAMBURRANO, P. Sliding spool design for reducing the actuation forces in direct operated proportional directional valves: experimental validation. *Energy Conversion and Management* [online]. 2016, **119**, p. 399-410. ISSN 0196-8904. Available from: https://doi.org/10.1016/j.enconman.2016.04.068
[10] ACUNA-BRAVO, W., CANUTO, E., AGOSTANI, M., BONADEI, M. Control engineering practice proportional electro-hydraulic valves: an embedded model control solution. *Control Engineering Practice* [online]. 2017, **62**, p. 22-35, Available from: https://doi.org/10.1016/j.conengprac.2017.01.013

Annex - Nomenclature

nomenclature	meaning
a	area of cylinder rod side, m^2
A	area of cylinder piston side, m^2
A_a	throttle area a in directional proportional valve, m^2
A_b	throttle area b in directional proportional valve, m^2
A_c	throttle area c in directional proportional valve, m^2
A_d	throttle area d in directional proportional valve, m^2
A_p	poppet area of the relief valve, m^2
B	bulk modulus of elasticity of hydraulic oil, N/m^2
C_d	discharge coefficient
C	radial clearance, m
d	diameter of cylinder rod, m
D	diameter of cylinder piston, m
F_s	proportional solenoid force, N
f_r	damping coefficient of relief valve poppet, N.s/m
f_s	damping coefficient of directional proportional valve spool, N.s/m
F_s	proportional solenoid force, N
F_{seat}	seat reaction of the relief valve, N
k	stiffness of return spring in directional proportional valve, N/m
m_p	mass of poppet in the relief valve, g
m_s	mass of moving parts in the directional proportional valve, kg
p	pressure, bar
P_A	pressure at port A of the direction proportional valve, bar
P_B	pressure at port B of the direction proportional valve, bar
P_P	pressure at port P of the direction proportional valve, bar
P_t	tank pressure, bar
Q	flow rate, liter/min
Q_a	flow rate through opening area a at directional proportional valve block, liter/min
Q_{AR}	flow rate from port A to rod side chamber in the hydraulic cylinder, l/min

Q_b	flow rate through the opening area b at a directional proportional valve block, l/min
Q_c	flow rate through the opening area c at a directional proportional valve block, l/min
Q_d	flow rate through the opening area d at a directional proportional valve block, l/min
Q_{rv}	flow rate through the relief valve, l/min
V_R	volume actuator rod side
V_{ps}	volume actuator piston side
x	displacement of directional valve spool, m
y	displacement of cylinder rod, m
z	displacement of relief valve poppet, m

INVESTIGATION OF THE IMPACT STRENGTH OF THE EPOXY-POLYESTER MATERIAL FOR USING IN AGGRESSIVE ENVIRONMENTS IN THE WATER TRANSPORT

Serhii Yakushchenko[1,*], Mykola Brailo[1], Andriy Buketov[1], Anna Sapronova[1], Oleksandr Sapronov[1], Abdellah Menou[2]

[1]Kherson State Maritime Academy, Kherson, Ukraine
[2]International Academy of Civil Aviation, Casablanca, Morocco

*E-mail of corresponding author: yakushchenko.sv@gmail.com

Resume

The influence of the aggressive environments of river water, seawater, oil, petrol and sodium hydroxide on the impact strength of epoxy-polyester composite was investigated. Testing was conducted by two different methods. It was determined that the impact strength of specimens that were kept at air was $W' = 4.2$ kJ/m^2 (by the second method - $W'' = 7.0$ kJ/m^2). The energy spent on destruction of the control specimen was $E = 0.92$ J. The main regularities of the crack propagation process in the studied material were found and qualitatively described. The time of a crack propagation ($\tau = 0.16$ μs) was determined. The maximum load, which leads to destruction of the specimen was $P_{max} = 2.47$ kN. The comparative analysis of investigated specimens was conducted by the IR-spectroscopy method. It was found, that the biggest decrease in material properties was observed for the specimen that was kept in the petrol environment.

Article info

Received 21 February 2021
Accepted 21 April 2021
Online 17 September 2021

Keywords:

epoxy-polyester composite,
impact strength,
crack initiation,
main crack,
impact load,
IR-spectral analysis

Available online: https://doi.org/10.26552/com.C.2021.4.B346-B353

ISSN 1335-4205 (print version)
ISSN 2585-7878 (online version)

This is an open access article distributed under the terms of the Creative Commons Attribution 4.0 International License (CC BY 4.0), which permits use, distribution, and reproduction in any medium, provided the original publication is properly cited. No use, distribution or reproduction is permitted which does not comply with these terms.

1 Introduction

The technical readiness of a vessel to the accomplishment of its functions, reliability and economics of works, directly depends on its support in the satisfactory technical condition. The construction elements of a hull, mechanical plants, mechanisms, devices and systems are constantly exposed to the static and dynamic load. The vessel is a complex technical construction of high danger, all the life cycle of which passes in unfavourable conditions of operation (aggressive water environment, conditions of elevated temperatures, alternate and pulsed loads, excessive friction, trimming moments and etc.) [1]. Sea and river vessels are strategic industrial objects and, therefore, the ship owners put in claims of high demands for their long-term and reliable exploitation. Protective polymer coatings are used to protect the metal surfaces of parts and mechanisms of the vessel [2-6]. At the same time, the use of parts based on polymer composite materials (PCM) can significantly reduce their costs and overhaul time [7]. Such materials are characterized by increased physical and mechanical, thermophysical properties and wear resistance, which allow increasing of a service life of parts and mechanisms. In addition, it does not affect the increase in the costs of the vessel's repairing. Taking into account the influence of the aggressive environment on the working parts of such transport vehicles is important in this case. As it is known that physically and chemically active aggressive environments can have the same negative effect on the strength of composite materials (CM) and coatings on their basis (change of stiffness, cracking and complete destruction), but have different mechanism of influence [8]. Therefore, the development of the CM, resistant to impact of aggressive environments, is an actual practical task.

Based on previous studies of the polymer strength, it was found that the mechanism of the specimen destruction is associated with the process of growth and propagation of microcracks [9]. In accordance with the statistical theory, the fragile destruction of the specimen occurs gradually and not simultaneously by the entire surface of destruction. In this case, development of the destruction process of the specimen is investigated as a function of time. The fracture destruction is considered to be an irreversible time process of accumulation of structural damage in the volume of a deformed specimen [9]. The work, consumed for the specimen fracture, is one of the characteristics by which it is possible to estimate the strength of the material. It is attributed to the unit of the destruction surface (impact strength) [10]. The durability of the composite and the protective coating based on it, the resistance to statical and dynamical loading, can be estimated by its value [11]. In the works

[12-13], the impact strength of the CM of the different nature was investigated. Effective regimes of their forming and causes of structural degradation were determined. Processes of localization of deformations and destruction of the CM were investigated. The shock characteristics of the CM, modified by the energy and magnetic fields, ultraviolet irradiation, by addition of fillers of varying dispersion and nature were investigated by authors [14]. Literature analysis showed that most studies were conducted under normal conditions (pressure, temperature, humidity). At the same time, the study of the physically and chemically active aggressive environments influence on the shock properties of CM is insufficiently studied. Obtained results would allow predicting the behavior of the developed material in real conditions.

2 Materials and methods

The following components were used for the formation of the CM matrix:

a) Epoxy resin ED-20 (q = 100 wt%).
b) Orthophthalic dicyclopentadiene (DCPD) unsaturated pre-accelerated polyester resin ENYDYNE H 68372 TAE - q = 10 wt% (hereinafter are given per 100 weight parts of epoxy resin), which has an inhibitor to prevent instant polymerization (gel time from t = 20 to 24 min). It should be noted that, during the copolymerization reaction of the composition of unsaturated polyesters, with unsaturated monomer compounds in the presence of initiators, a significant amount of heat is released, therefore the reaction is exothermic.
c) The cold curing hardener polyethylene polyamine (PEPA) - q = 10 wt%.
d) The initiator for polyester resins Butanox-M50 - q = 1.5 mas.fr (the content is indicated on 100 weight parts of polyester resin), which is methyl ethyl ketone peroxide (MEKP) and contains a low amount of water and a minimum amount of polar compounds in comparison to ethylene glycol.
e) Modifier methylene diphenyl diisocyanate, widely known as MDI (4,4-MDI) - q = 0.25 wt%. Methylene diphenyl diisocyanate is aromatic diisocyanate, which is used for the three-dimensional cross-linking of polymers in the manufacture of polyurethane. Chemical formula: $CH_2(C_6H_4NCO)_2$, molar mass - 250 g/mol, density - 1180 kg/m^3.
f) Filler 1: Hexagonal boron nitride (h-BN) - 8-10 μm - q = 60 wt%
g) Filler 2: Mica 20-40 μm - q = 20 wt% (The fractionated micromica of series "Standard" (ISO 3262-12:2001, Extenders for Paints. Specifications and Methods of Test. Part 12. Muscovite-Type Mica) of the brand MC-20-80 with grains d = 20 - 40 μm. Mineral composition: mica-muscovite KAl_2 [$(OH, F)_2AlSi_3O_{10}$]. Chemical composition according to ISO 3262-12:2001: silicon oxide (SiO_2) - 44-50%, aluminium oxide (Al_2O_3) - 27-35%, iron oxide (Fe_2O_3) - less than 5%, magnesium oxide (MgO) - less than 2%, potassium oxide (K_2O) - more than 8%, water-soluble salts - less than 0.2%).

The composition without hardeners was modified by the ultraviolet irradiation for duration of 5 min before introducing of hardeners.

The specimens were solidified according to the following regime: the formation of specimens and their holding over time t = 12.0±0.1 h at a temperature T = 293 ± 2 K, heating at a rate of υ = 3 K/min to the temperature of T = 393 ± 2 K, keeping the specimens at a given temperature during the time t = 2.0 ± 0.05 h, slow cooling to the temperature of T = 293±2 K. For stabilization of the structural processes in the matrix, the specimens were kept during the time t = 24 h at air at the temperature of T = 293 ± 2 K, with subsequent experimental tests. Further, the formed specimens were kept in the following environments: oil, seawater, river water, petrol, sodium hydroxide (NaOH (50%)) during the 30 days. The control specimens were kept at air during that time.

The impact strength, relative mass change of specimens and activity of the surface of composite material were investigated by the IR-spectral analysis method.

The impact strength was determined by two methods.

The first method (W'). The impact strength was measured by pendulum copra according to Charpy method (ASTM D6110). The working angle of deviation of the pendulum after the destruction of the specimen, at a predefined initial corner of lifting of working body of installation, was determined. The investigation was conducted under the temperature of T = 298 ± 2 K and relative humidity of d = 50 ± 5%. The specimen dimensions were: $l \times b \times h$ = (63.5×12.7×12.7) ± 0.5 mm.

The second method (W''). The impact strength was measured with use of the notched specimens of sizes 10 × 15 × 75 mm (ASTM D6110). The tests were carried out with use of the impact pendulum machine RKP-300 under the high-rate loading (5.2 m/s). In doing so, the loading diagrams, "load-time" and "load-deflection", were registered. A total work of impact fracture E is composed of two components: i) crack initiation E_i and ii) crack propagation E_p.

The impact strength was determined as:

$$W = \frac{E}{bs}, \tag{1}$$

where E is the impact energy, consumed for the specimen fracture; b is the width of a specimen; s is the thickness of a specimen.

The impact loading diagram processing software "VUHI-CHARPY" was used to determine the fracture energy components by transforming the "loading - time" (P-t) dependence into the "loading - displacement" (P-s).

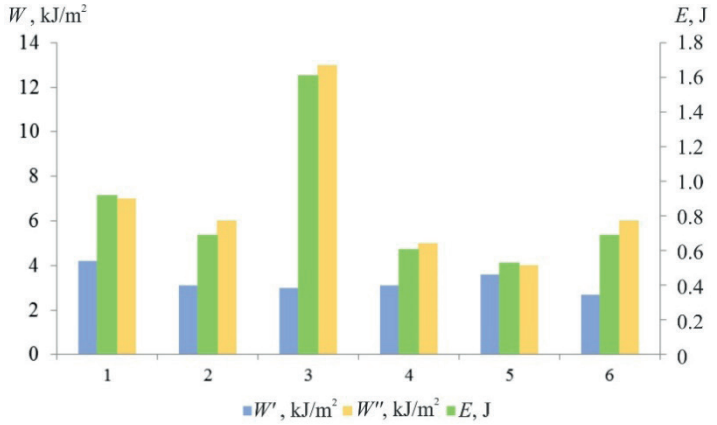


Figure 1 *Influence of aggressive environments on the impact strength (W' and W") and energy (E) spent on the destruction of material: 1) air (control specimen); 2) oil; 3) seawater; 4) river water; 5) petrol; 6) NaOH (50%)*

The mass of specimens was determined by weighing with analytical scales, with an accuracy of ± 0.001 g.

Deviation of values of impact strength and mass change was 4 - 6 % from nominal, during the study.

The chemical bonds on the composite surface were investigated with use of the IR-spectral analysis. The IR-spectra were registered with "IRAffinity-1" (Japan) spectrophotometer at the wave numbers range from ν = 400 to 4000 cm^{-1} by a single-beam method in the reflected light. The wavelength scanning at wave number $\lambda^{-1} = \nu$ was performed at diagrams within 225 mm, in the range of the above specified frequencies. The wave numbers (ν, cm^{-1}), absorption band intensity (T, %) and absorption band area (S, %) were determined by a computer program "IRsolution". The error of the wave number measurement was ν = ± 0.01 cm^{-1}, while the error of the peak location made ν = ± 0.125 cm^{-1}. The photometrical accuracy was ± 0.2% at software operated control of cracks and integration time t = 10 s. The integration step was $\Delta\nu$ = 4 cm^{-1}.

3 Results and discussion

At the first stage, the investigation of the impact strength of the material by two different methods was conducted after keeping specimens in different aggressive environments during the 30 days. The influence of physically and chemically active aggressive environments on the CM strength was studied. River water, seawater, oil environment, petrol were attributed as the physically active aggressive media and sodium hydroxide (50%) - as the chemically active (according to the classification of Zuyev, [9]). An influence of aggressive environments on the stability of composite materials to shock loads was analyzed. The investigation results are shown in Figure 1. It was found, that the impact strength of the control specimens was W' = 4.2 kJ/m^2 by the first method and W'' = 7.0 kJ/m^2 - by the second method. It should be noted, that the energy spent on the destruction of the control specimen was E = 0.92 J. Analysis of the experimental results allowed to determine the insignificant decrease of the impact strength of the specimens, which were kept in the aggressive environments (oil, seawater, river water). The impact strength values were W' = 3.0 - 3.1 kJ/m^2 (by the second method - W''= 5.0 - 6.0 kJ/m^2), except of for specimens, which were kept in seawater (by the second method W'' = 13.0 kJ/m^2). Hence, the energy, spent on destruction of specimens, decreased to the E = 0.61 - 0.69 J and for the specimen that was kept in seawater, the energy increased to E = 1.6 J. The impact strength of the specimens, which were kept in petrol was W' = 3.6 kJ/m^2 (by the second method - W'' = 4.0 kJ/m^2). Moreover, the energy, spent on destruction of the CM, decreased to E = 0.53 J (compared to the control specimens) (Figure 1). The impact strength of specimens that were kept in the alkaline environment, by the first method was - W' = 2.7 kJ/m^2 (by the second method - W''= 6.0 kJ/m^2). The energy spent on destruction of the specimen was E = 0.69 J.

In addition, it is important to determine the force that initiated the crack growth, since, at a shock load, the wave of stress passes through the specimen and destruction occurs when the critical stress is reached [15]. In turn, it would allow to determine the resistance to destruction of polymer materials and to evaluate the initiation and propagation of cracks after the impact loading. According to the second method, the investigation of the "load-time" (Figure 2, a) and "load-deflection" (Figure 2, b) dependences were carried out. During the analysis of the experimental data (Figure 2, Table 1), it was determined that the destruction of polymeric materials in a shock load occurs in several stages. It is known that behavior of the polymers on fatigue cracks is usually divided in three discrete phases: first - the threshold phase indicating the initiation of the crack (I); second - the phase of stable crack propagation (II); third - the phase of fast and unstable growth of cracks (III) (Figure 2, a) [16]. Analogous phases of the crack growth are indicated in works [14, 17], which allows to assert about the reliability of the obtained results.

Table 1 *The results of experimental investigation of polymer materials, which were kept in different environments*

environment	load at which initiated crack propagation, P_{max} (kN)	time of crack propagation, τ (μs)	the value of critical deformation, Δl (mm)
air	2.47	0.16	0.92
oil	2.20	0.14	0.86
seawater	1.24	0.07	0.44
river water	1.84	0.14	0.86
petrol	1.22	0.07	0.41
NaOH (50%)	1.73	0.14	0.84

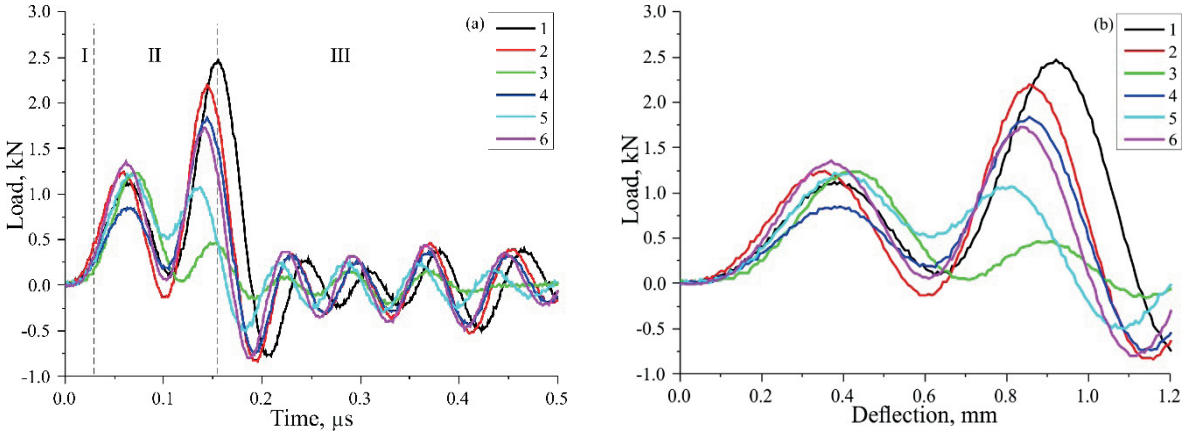


Figure 2 *Dependence of load on time (a) and deflection (b) of specimens, which were investigated in different environments: 1) air; 2) oil; 3) seawater; 4) river water; 5) petrol; 6) NaOH (50%)*

It was found, that the curves' shapes of the "load-time" at the beginning of the main crack growth (phases I and II, Figure 2a) are almost identical. This confirms that the initiation and growth of the crack for all specimens occurs at analogous phases. The load-deflection curves for all the specimens have a linear dependence with a sudden drop in load to zero at the time of initiation of the crack growth. Two peaks were found at the regime of the stable crack propagation. It was due to the "structural reorganization" of the specimens' material [18-19]. The time of macrocrack growth of the control specimen was τ = 0.16 μs (Figure 2 a, Table 1). At the same time, the maximal load was P_{max} = 2.47 kN. The critical deformation at this load was Δl = 0.92 mm (Figure 2 b). The expense of energy on the main cracks propagation for the specimens, which were kept in oil, river water and alkaline reached the maximum values at the same time interval τ = 0 - 0.14 μs. The crack growth initiation occurred with a slight decrease in load to P_{max} = 1.73 - 2.20 kN. At the same time, the value of the critical deformation for those materials was determined - Δl = 0.84 - 0.86 mm. Reducing resistance to the crack growth under shock loads is associated with a decrease in energy spending, which is characterized by the dispersive brittleness of the material. This is accompanied by a decrease in the maximum load at which the main crack arises.

In addition, at the second phase, the shift of the stress intensity range (in the direction of decrease) required for the initiation of the crack growth of specimens 3 and 5, was observed (Figure 2 a). Therefore, propagation of the main crack to reaching the maximum load occurred at: τ = 0.07 μs (Figure 2 a, Table 1). At the same time, the shape of curves 3 and 5 is typical for ductile failure throughout the studied range [20]. Taking into account this fact, it can be stated, that influence of aggressive environments on the impact properties of the developed materials is of a very slight degree.

At the stage of unstable cracks growth (Figure 2 a, III), processes of oscillations of small amplitude were observed. They are related to appearance of stripes of localization of deformations. These processes are associated with the heterogeneity of the material structure, the heterogeneous stress-strain state and the dynamic excitation of deformation processes due to the diffusion of the impact energy. The specimen material ceases to resist the crack propagation. Evidently, at this stage, the main crack increases until the complete destruction of the specimen. During the experimental data analysis, the time of the complete destruction of the specimens was determined (τ'). For the whole series of experiments, a time range of fracture was - τ' = 9.46 - 9.73 μs. This indirectly indicates an insignificant influence of the aggressive environment on the impact properties of the developed epoxy-polyester c omposite.

Study of the mass changes of specimens after the testing was performed in order to estimate the resistance of the developed CM for the influence of aggressive environments (Table 2). The relative mass

Table 2 *Influence of aggressive environments on the mass changes of specimens*

environment	mass changes (%)
air	0.12
oil	0.09
seawater	0.20
river water	0.23
petrol	0.11
NaOH (50%)	0.07

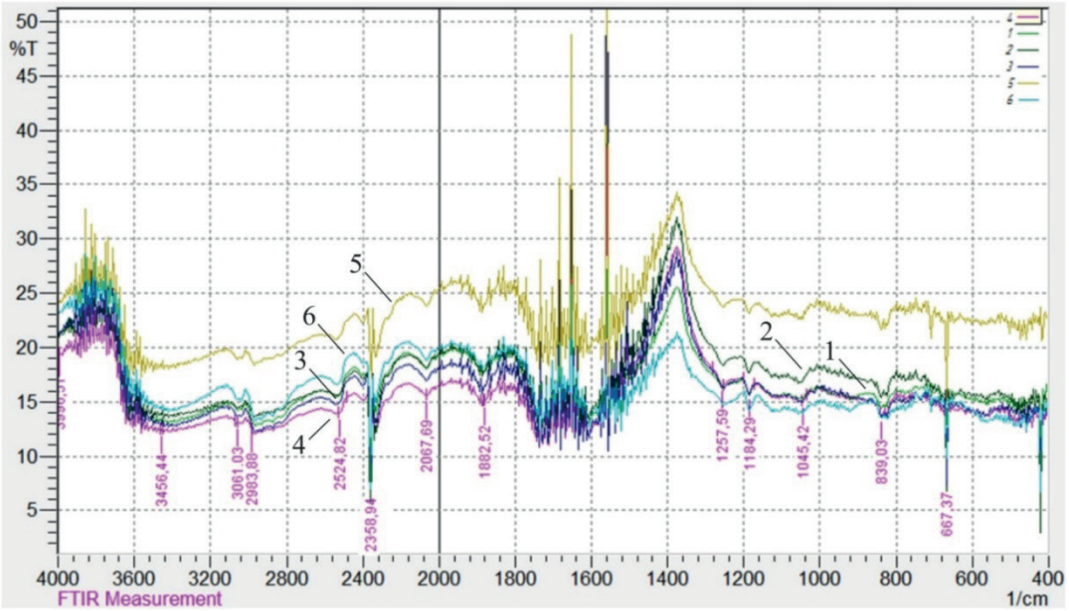


Figure 3 *IR-spectral analysis of CM, which were kept in the aggressive environment: 1 - air; 2 - oil; 3 - seawater; 4 - river water; 5 - petrol; 6 - NaOH (50%)*

change of specimens, which were kept in oil, seawater, river water, petrol, sodium hydroxide, was found.

The specimens, which were kept in oil, are characterized by the low mass change (compared to control the specimen). This is due to the high viscosity of the oil environment, which slows down the process of oil adsorption into the material. At the same time, material, which was kept in petrol, has a comparatively similar relative mass change compared to specimens, which were kept at air. It was believed, that a decrease in the mass change was due to the evaporation of petrol from the surface of the specimen during the drying. Thus, the maximum mass change was observed for specimens that were kept in sea and river water. It should be noted that the increase in the strength of the specimen, which was kept in seawater, at the moment of destruction (by the second method, Figure 1), can be due to increased flexibility of the macromolecular chains, which contributes to the alignment of stress in the polymer and facilitates the orientation of its molecules at stretching [9]. At the same time, seawater has positive affect on the composite properties (the presence of salt solution), because their water absorption decreases (compared to the river water). The chemical interaction of the aggressive alkaline environment with the specimen is in addition weakly expressed, since the reactivity of the material is limited by the slow diffusion of the environment into the material in the solid phase (in the presence of fillers).

The study results of the developed materials' resistance, to influence of the aggressive environment of physical and chemical nature, confirm the presence in the CM of spatial three-dimensional structure. As a result, the polymer loses the ability to dissolve in physically and chemically active environments [9]. The low values of water absorption of all the studied specimens can be explained by the presence of fillers (mica, hexagonal boron nitride), which are characterized by high modulus and low relaxation rate [14, 21-22]. Reducing of the impact strength and energy, spent on destruction of the specimen, which was kept in petrol, can be due to the wash-out of the low molecular weight fraction of the polymer [9].

The comparative IR-spectral analysis of physical and chemical processes on the CM surface, after keeping in aggressive environments, was conducted (Figure 3). The transmittance spectra allowed to determine the following parameters: absorption band intensity (T, %) and the absorption peak area (S, %), which characterize a different number of chemical bonds in polymer and,

Table 3 *Characteristic absorption bands and their intensity parameters according to the IR-spectral analysis*

band characteristics		IR-spectra of composite materials, which were kept in aggressive environments during 30 days											
group	v (cm^{-1})	No. 1		No. 2		No. 3		No. 4		No. 5		No. 6	
		T (%)	S (%)	T (%)	S (%)	T (%)	S (%)	T (%)	S (%)	T (%)	S (%)	T (%)	S (%)
-NH-, -CH- rocking vibrations, -C-C- stretching vibrations, primary amines: CH_2-NH_2, CH-NH_2, epoxy cycle	839.03	13.7	9.9	13.9	10.0	12.8	7.8	13.7	7.9	21.6	10.1	13.7	10.0
-C-C-, -C-N-, -C-O- stretching vibrations, secondary amines: CH_2-NH-CH_2, primary amines: CH_2-NH_2	1184.29	15.7	21.2	16.0	21.0	14.9	20.0	14.7	20.2	23.1	21.2	15.7	21.2
-OH- bending vibrations, -C-N-, -C-O- stretching vibrations; epoxy cycle, primary amines: -NH_2	1257.29	16.4	20.5	16.9	20.5	15.6	18.2	15.4	18.5	23.6	20.5	16.4	20.5
stretching vibrations of epoxy group	1882.52	14.9	14.8	16.0	14.8	14.1	14.0	14.1	14.2	23.2	14.2	16.2	14.8
-C ≡ N- stretching vibrations; alkyne group: -C ≡ C-H	2067.69	15.4	15.4	15.9	15.4	14.7	14.1	14.4	15.2	23.8	11.1	16.4	15.4
-C ≡ N- stretching vibrations	2524.82	13.9	7.1	14.1	7.1	11.0	6.0	13.2	6.1	20.7	6.6	14.9	7.1
-CH- stretching vibrations, methyl radical: CH_3-C, methylene -CH_2-	2983.88	12.4	10.3	13.2	10.3	11.7	10.0	11.4	10.1	18.4	9.7	13.4	10.3
-CH-, -OH, -NH - stretching vibrations, para-benzene	3061.03	12.9	10.2	13.3	10.2	11.0	10.0	12.9	10.2	8.9	9.4	13.8	10.2
-OH, -NH- stretching vibrations	3456.44	12.3	90.1	13.2	90.1	12.3	90.0	12.3	90.1	18.0	85.4	13.7	90.1

consequently, the cross-linking degree of the studied material.

The chemical activity of the surface of the developed material, which was kept in different environments, was conducted by the IR-spectral analysis (Figure 3). Defined adsorption bands correspond to the specific vibration of the molecular units of the epoxy-polyester composite (Table 3). The main difference between the spectra was observed in the region of the absorption bands corresponding to - OH stretching vibrations. These groups are centers that are characterized by increased adsorption and catalytic activity [9]. The activity of the specimen surface, after the action of aggressive environment, is possible to estimate by increasing of the hydroxyl groups, in the near-surface layer. An increase in the absorption band intensity at v = 3456.44 cm^{-1} from T = 12.3-13.7% to T = 18.0% appears only for specimen, which was kept in the aggressive environment of petrol. At the same time, decreasing in the absorption peak area (S, %), which is proportional to the number of active groups, was observed. It was considered that the matching of absorption peaks and absence of their displacement, for all the studied specimens, indicates stability of the material surface to chemical interaction with the aggressive environment and, as a result, does not lead to an increase of the sorption of the environment into the material. The comparative analysis allowed to determine the slight difference in intensity of the

absorption band and peak area for all specimens, except specimens kept in petrol.

Based on the conducted studies of the impact strength, mass change and IR-analysis, it was found that developed composite materials can be used in all the studied environments, except petrol, as protective coatings for ship hull superstructures and tanks. This is evidenced by a slight decrease in values of the impact strength of specimens, mass change and the data obtained in analysis of the IR-spectra. In particular, the results of the study suggest the ability of the developed CM to resist the aggressive environment in which the specimens were kept.

4 Conclusions

The impact strength of developed composite materials, which were kept in aggressive environments, was investigated by two methods. It was found that the aggressive environments of oil, seawater, river water, petrol and sodium hydroxide do not significantly affect the ability of polymeric materials to resist shock loads. The impact strength was W' = 2.7 - 4.2 kJ/m^2 by the first method (W''= 6.0 - 13.0 kJ/m^2 - by the second method). The energy spent on the specimen destruction varied at E = 0.8 - 1.0 J. The phases of growth of the main crack: the initiation of the crack growth, stable crack propagation and unstable growth of the crack were determined on the "load-time" and "load-deflection" curves. The time of the macrocrack growth initiation, for all the specimens, was τ = 0.07 - 0.16 μs. The maximum load that leads to destruction of a specimen was observed for the control specimen - P_{max} = 2.47 kN. The critical deformation at this load was l = 0.92 mm.

The relative mass change of specimens that were kept in different aggressive environments was found. It was determined that the composite material at the content q = 60 wt% of hexagonal boron nitride and q = 20 wt% of mica is characterized by a decrease in adsorption of environment on the material's surface.

The obtained results were confirmed by the IR-spectroscopy. It was found that the studied composite material is characterized by the same bonds after keeping in different environments. The increase in the intensity of the hydroxyl groups and hence the activity of the material surface, was found for the specimen, which was kept in an environment of petrol.

The results of investigation of the impact strength, mass changes of specimens and IR-spectral analysis, suggest the ability of the developed CM to resist the aggressive environment in which the specimens were kept. Consequently, this confirms the expediency of using the composite material and coating on its basis for the protection of parts and mechanisms of sea and river transport.

References

[1] ZAYED, A., GARBATOV, Y., SOARES, C. G. Reliability of ship hulls subjected to corrosion and maintenance. *Structural Safety* [online]. 2013, **43**, p. 1-11. ISSN 0167-4730. Available from: https://doi.org/10.1016/j.strusafe.2013.01.001

[2] YOUNGBLOOD, J. P., ANDRUZZI, L., OBER, CH. K., HEXEMER, A., KRAMER, E. J., CALLOW, J. A., FINLAY, J. A., CALLOW, M. E. coatings based on side-chain ether-linked poly(ethylene glycol) and fluorocarbon polymers for the control of marine biofouling. *Biofouling* [online]. 2003, **19**(1), p. 91-98. ISSN 0892-7014, eISSN 1029-2454. Available from: https://doi.org/10.1080/0892701021000053381

[3] ANDERSON, C., ATLAR, M., CALLOW, M., CANDRIES, M., MILNE, A., TOWNSIN, R. The development of foul-release coatings for seagoing vessels. *Proceedings of the Institute of Marine Engineering, Science and Technology Part B: Journal of Marine Design and Operations*. 2003, **B4**, p. 11-23. ISSN 1476-1556.

[4] CHAMBERS, L. D., STOKES, K. R., WALSH, F. C., WOOD, R. J. K. Modern approaches to marine antifouling coatings. *Surface and Coatings Technology* [online]. 2006, **201**(6), p. 3642-3652. ISSN 0257-8972. Available from: https://doi.org/10.1016/j.surfcoat.2006.08.129

[5] BUKETOV, A. V. V., BRAILO, M. V. V., YAKUSHCHENKO, S. V. V., SAPRONOV, O. O. O., SMETANKIN, S. O. O. The formulation of epoxy-polyester matrix with improved physical and mechanical properties for restoration of means of sea and river transport. *Journal of Marine Engineering and Technology* [online]. 2020, **19**(3), p. 109-114. ISSN 2046-4177, eISSN 2056-8487. Available from: https://doi.org/10.1080/20464177.2018.1530171

[6] BUKETOV, A. V., SAPRONOV, O. O., BRAILO, M. V., MARUSCHAK, P. O., YAKUSHCHENKO, S. V., PANIN, S. V., NIGALATIY, V. D. Dynamics of destruction of epoxy composites filled with ultra-dispersed diamond under impact conditions. *Mechanics of Advanced Materials and Structures* [online]. 2020, **27**(9), p. 725-733. ISSN 1537-6494, eISSN 1537-6532. Available from: https://doi.org/10.1080/15376494.2018.1495788

[7] HUSSAIN, F., HOJJATI, M., OKAMOTO, M., GORGA, R. E. Review article: Polymer-matrix nanocomposites, processing, manufacturing and application: an overview. *Journal of Composite Materials* [online]. 2006, **40**(17), p. 1511-1575. ISSN 0021-9983, eISSN 1530-793X. Available from: https://doi.org/10.1177/0021998306067321

[8] BARTENEV, G. M., ZUYEV, Y. S. *Strength and failure of visco-elastic materials* [online]. Elsevier, 1968. ISBN 9780080031101. Available from: https://doi.org/10.1016/C2013-0-05219-X

[9] ZUYEV, Y. S. *Destruction of polymers under the influence of aggressive media* / *Razrusheniye polimerov pod deystviyem agressivnykh sred* (in Russian). Khimiya, 1972. (in Russian)

[10] FU, J., SHI, L., YUAN, S., ZHONG, Q.-D., ZHANG, D.-S., CHEN, Y., WU, J. Morphology, toughness mechanism and thermal properties of hyperbranched epoxy modified diglycidyl ether of bisphenol A (DGEBA) interpenetrating polymer networks. *Polymers for Advanced Technologies* [online]. 2008, **19**(11), p. 1597-1607. eISSN 1099-1581. Available from: https://doi.org/10.1002/pat.1175

[11] WANG, Y., CAO, R., WANG, M., LIU, X., ZHAO, X., LU, Y., FENG, A., ZHANG, L. Design and synthesis of phenyl silicone rubber with functional epoxy groups through anionic copolymerization and subsequent epoxidation. *Polymer* [online]. 2020, **186**, p. 122077. ISSN 0032-3861. Available from: https://doi.org/10.1016/j.polymer.2019.122077

[12] CHEN, L. Y., FU, J. F., YU, W. Q., HUANG, L., YIN, J. T., DONG, X., ZONG, P. S., LU, Q., SHANG, D. P., SHI, L. Y. Enhanced thermal and mechanical properties of epoxy composites by spherical silica with different size. *Key Engineering Materials* [online]. 2017, **727**, p. 519-526. ISSN 1662-9795. Available from: https://doi.org/10.4028/www.scientific.net/KEM.727.519

[13] GARCIA-MORENO, I., CAMINERO, M., RODRIGUEZ, G., LOPEZ-CELA, J. Effect of thermal ageing on the impact and flexural damage behaviour of carbon fibre-reinforced epoxy laminates. *Polymers* [online]. 2019, **11**(1), p. 80. ISSN 0032-3861. Available from: https://doi.org/10.3390/polym11010080

[14] BUKETOV, A., STUKHLYAK, P., MARUSCHAK, P., PANIN, S. V., MENOU, A. Regularities of impact failure of epoxy composites with Al2O3 microfiller and their analysis on the basis of external surface layer concept. *Key Engineering Materials* [online]. 2016, **712**, p. 149-154. ISSN 1662-9795. Available from: https://doi.org/10.4028/www.scientific.net/KEM.712.149

[15] VISSER, H. A., CAIMMI, F., PAVAN, A. Characterising the fracture toughness of polymers at moderately high rates of loading with the use of instrumented tensile impact testing. *Engineering Fracture Mechanics* [online]. 2013, **101**, p. 67-79. ISSN 0013-7944. Available from: https://doi.org/10.1016/j.engfracmech.2012.09.024

[16] KOTHMANN, M. H., ZEILER, R., RIOS DE ANDA, A., BRUCKNER, A., ALTSTADT, V. Fatigue crack propagation behaviour of epoxy resins modified with silica-nanoparticles. *Polymer* [online]. 2015, **60**, p. 157-163. ISSN 0032-3861. Available from: https://doi.org/10.1016/j.polymer.2015.01.036

[17] PATIL S, TRIVEDI, M. K. Influence of biofield treatment on physical, structural and spectral properties of boron nitride. *Journal of Material Science and Engin*eering [online]. 2015, **04**, 04. ISSN 2169-0022. Available from: https://doi.org/10.4172/2169-0022.1000181

[18] PASCAL, T., BONNEAU, J. L., BIOLLEY, N., MERCIER, R., SILLION, B. Approach to improving the toughness of TGMDA/DDS epoxy resin by blending with thermoplastic polymer powders. *Polymers for Advanced Technologies* [online]. 1995, **6**(4), p. 219-229. eISSN 1099-1581. Available from: https://doi.org/10.1002/pat.1995.220060401

[19] LIU, H.-Y., WANG, G., MAI, Y.-W. Cyclic fatigue crack propagation of nanoparticle modified epoxy. *Composites Science and Technology* [online]. 2012, **72**(13), p. 1530-1538. ISSN 0266-3538. Available from: https://doi.org/10.1016/j.compscitech.2012.05.025

[20] STUKHLYAK, P. D., BUKETOV, A. V., PANIN, S. V., MARUSCHAK, P. O., MOROZ, K., KINLOCH, A. J., LEE, S. H., TAYLOR, A. C. Improving the fracture toughness and the cyclic-fatigue resistance of epoxy-polymer blends. *Polymer* [online]. 2014, **55**(24), p. 6325-6334. ISSN 0032-3861. Available from: https://doi.org/10.1016/j.polymer.2014.10.018

[21] M., POLTARANIN, M. A., VUKHERER, T., KORNIENKO, L. A., LYUKSHIN, B. A. Structural fracture scales in shock-loaded epoxy composites. *Physical Mesomechanics* [online]. 2015, **18**(1), p. 58-74. ISSN 1029-9599, eISSN 1990-5424. Available from: https://doi.org/10.1134/S1029959915010075

[22] BISHOP, J. L., LANE, M. D., DYAR, M. D., BROWN, A. J. Reflectance and emission spectroscopy study of four groups of phyllosilicates: smectites, kaolinite-serpentines, chlorites and micas. *Clay Minerals* [online]. 2008, **43**(1), p. 35-54. ISSN 0009-8558, eISSN 1471-8030. Available from: https://doi.org/10.1180/claymin.2008.043.1.03

UNIVERSITY
OF ŽILINA

In its over 65 years of successful existence, the University of Žilina (UNIZA) has become one of the top universities in Slovakia.



SURFINT 2021

Progress in Applied Surface, Interface and Thin Film Science

CONFERENCE DESCRIPTION

The main goal of the conference is to contribute to new knowledge in surface, interface, ultra-thin films and very-thin films science of inorganic and organic materials by the most rapid interactive manner - by direct communication among scientists of corresponding research fields.

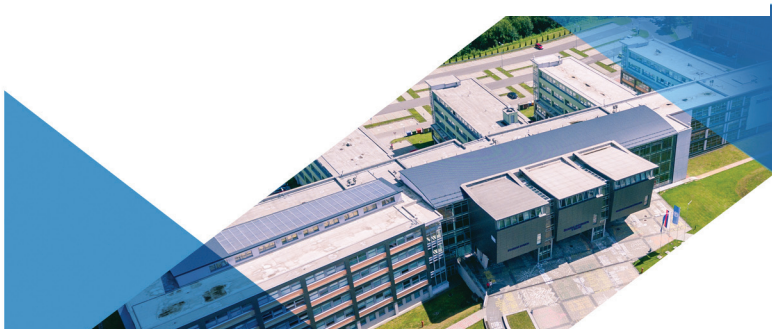
CONFERENCE TOPICS OF INTEREST:

- Atomically clean surfaces
- Interfaces
- Ultra-thin and very-thin layers
- Multilayers
- Interaction of low temperature plasma and low energy beams with surfaces of organic and inorganic substrates
- Interaction of liquids with surfaces of organic and inorganic substrates
- Defects of surfaces, interfaces and thin films
- Porous materials from view of surfaces and interfaces
- Passivation of defect states
- New approaches in experimental preparation and treatment of organic and inorganic surfaces, thin films, and interfaces
- Advanced mathematical data processings applied during/or after measurements of physical and chemical properties of unique types of surfaces, thin films, and interfaces
- New approaches in theoretical physics and chemistry of surfaces, thin films, and interfaces
- Sensors based on unique properties of surfaces, thin films, and interfaces

VENUE & DATE

22. 11. -25. 11. 2021
Smolenice Castle, Slovakia
https://lm.uniza.sk/~jurecka/SURFINT2021-Smolenice/

CONTACT:
UNIVERSITY OF ŽILINA
Institute of Aurel Stodola
Faculty of Electrical Engineering and Information Technology
Univerzitná 8215/1, 010 26 Žilina, Slovakia
e-mail: stanislav.jurecka@uniza.sk



SIMULATION VERIFICATION OF BALANCING SYSTEM BASED ON NUMBER OF CELLS

Marek Šimčák*, Matúš Danko

Department of Mechatronics and Electronics, Faculty of Electrical Engineering and Information Technology, University of Zilina, Zilina, Slovakia

*E-mail of corresponding author: marek.simcak@feit.uniza.sk

Resume

This paper deals with the simulation verification of balancing systems with different numbers of batteries. There is a simulation model of the battery with adjustable inputs and a simulation model of flyback converter. These components are interconnected and controlled externally to ensure balancing of individual cells. The batteries are connected in series and a flyback converter is connected to each battery. The outputs of these inverters are connected to the output of all the batteries. So, one can say that this balancing system is designed to lighten the charger. The results of the simulations show the voltage, current and State of Charge (SoC) of the batteries. Simulation models are presented in diagrams. These models were created in the PLECS environment.

Article info

Received 23 November 2020
Accepted 23 December 2020
Online 23 June 2021

Keywords:

battery management system,
LiFePO4,
R2C2 battery model,
battery,
flyback converter,
flyback topology,
balancing system

Available online: https://doi.org/10.26552/com.C.2021.4.C83-C89

ISSN 1335-4205 (print version)
ISSN 2585-7878 (online version)

This is an open access article distributed under the terms of the Creative Commons Attribution 4.0 International License (CC BY 4.0), which permits use, distribution, and reproduction in any medium, provided the original publication is properly cited. No use, distribution or reproduction is permitted which does not comply with these terms.

1 Introduction

This article is motivated by researching the battery systems and improving battery performance. Capacity, durability and efficiency are essential features, not only of battery systems but of many electronic systems, as well. This article discusses how to manage and protect the energy stored in the battery. The high-voltage batteries often suffer from being connected in series to achieve the higher voltage. This connection causes a disproportionate capacity in the batteries. This capacity difference results in overcharging and over-discharging the individual battery cells. These inequalities arise during the production of those cells. Based on this knowledge, the battery management system is being examined. This battery management has three basic features: monitoring part, protective part and communication part. The monitoring part is designed to measure voltages, currents and temperature. Based on these measured values, the balancing system is controlled. The balancing system has the task of balancing the voltage levels of the individual cells. This avoids overcharging and overdischrging of the individual battery cells. The balancing is divided to two basic topologies: active balancing and passive balancing. The passive balancing system consists of converting the excess energy of the individual cells into heat, which is generated by the transfer of electric current through the shunt resistance. This method is inefficient and is only used for the low-capacity batteries and lead-acid batteries without control. An active balancing system consists of transferring the power from the overcharged cell to the entire battery pack or from the battery pack to the weakest cell. These methods may be CELL-TO-PACK, PACK-TO-CELL or CELL-TO-PACK-TO-CELL. The passive method has the CELL-TO-ZERO topology. The active balancing systems are divided according to the energy transfer and storage element used. They are divided into capacitor topologies, inductor topologies or DC/DC converter topologies. The protective part provides protection against overcharging, overdischarging or other unwanted conditions. The communication part provides communication between other control units, for example in an electric vehicle. This communication can be, for example, via CAN-BUS or other buses. All this is ensured by the battery management system. With increasing demands on batteries, this research is therefore potential in terms of research and the selection of a suitable topology for an active balancing system [1-4].

2 The battery model

The simulated model of the selected battery is shown in Figure 1. The model considers dynamics during the battery charging or discharging [1]. The individual RC components of the battery equivalent

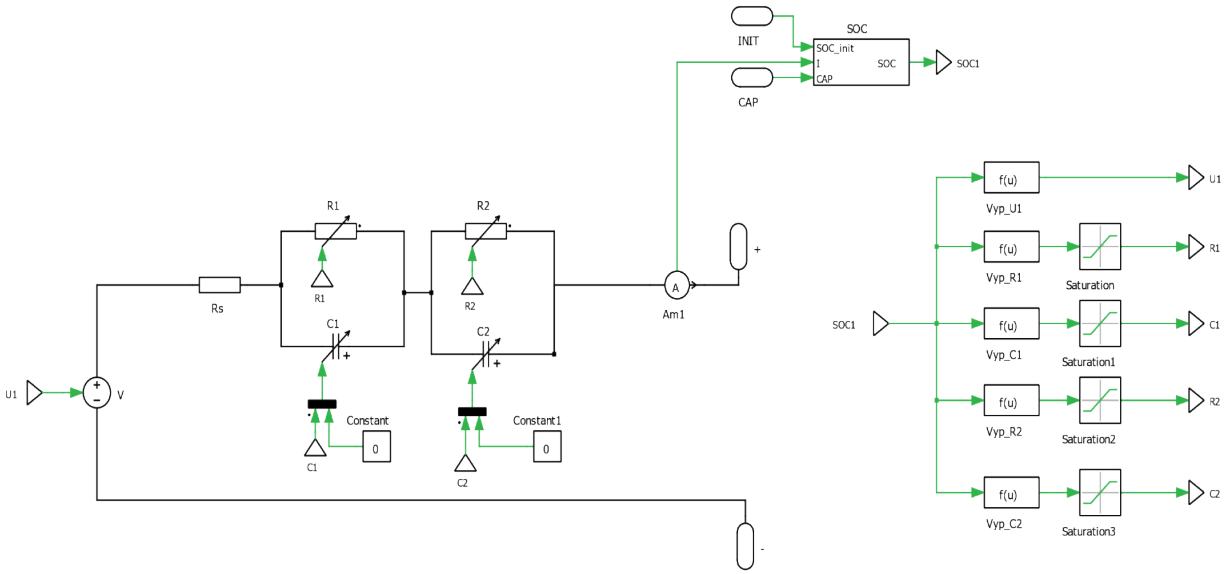


Figure 1 *Equivalent battery scheme*

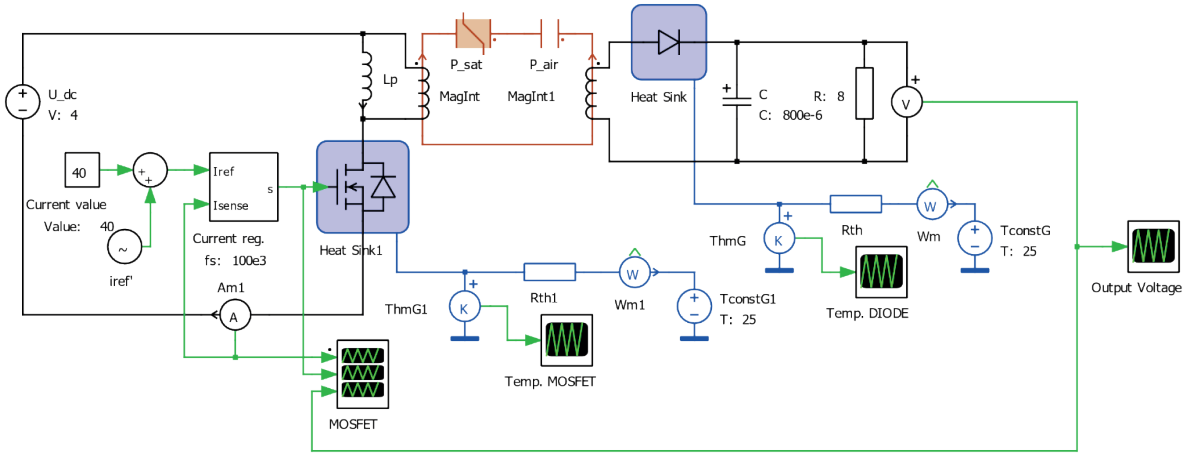


Figure 2 *Model of the flyback converter controlled by the primary side current*

circuit were determined from the results of laboratory battery measurements [1-4]. This battery simulation model can calculate the SoC by the Coulomb counting method. This is R2C2 equivalent battery model [5-10].

Functions blocks consist of calculation functions identified based on [11-13]:

$$U_1 = -1.031e^{-35u} + 3.685 + 0.2156u - 0.1178u^3\,, \quad (1)$$

$$R_1 = 0.3208e^{-29.14u} + 0.0745\,, \quad (2)$$

$$C_1 = -752.9e^{-13.51u} + 703.6\,, \quad (3)$$

$$R_2 = 6.603e^{-155u} + 0.4984\,, \quad (4)$$

$$C_2 = -6.056e^{-27.12u} + 4475\,. \quad (5)$$

3 The flyback converter

The topologies best suited for battery applications include the flyback converter topology. This is determined by its main advantages, one of which is galvanic isolation of input and output. Another advantage is that this flyback converter can be both an up and down converter. Based on these properties, a flyback converter was selected for simulation purposes. In the first case it was a flyback converter controlled by the input current (Figure 2) and in the second case a flyback converter controlled by the voltage of the secondary side of the high-frequency transformer (Figure 3). The disadvantage of this topology are the high losses in the transformer. These losses are compounded by the fact that this application is the low voltage one. The flyback converter has three base circuits: the primary side with the high frequency MOSFET or GaN transistor; the secondary side with the power diode or rectifier, while the third circuit is the magnetic circuit of the high-frequency transformer that provides the power transfer from the primary side to the secondary side of the high-frequency transformer. The flyback converter works blocking, i.e. when the transistor is turned on, energy is stored in the transformer core and when the transistor is turned off, this energy passes from the transformer core to the

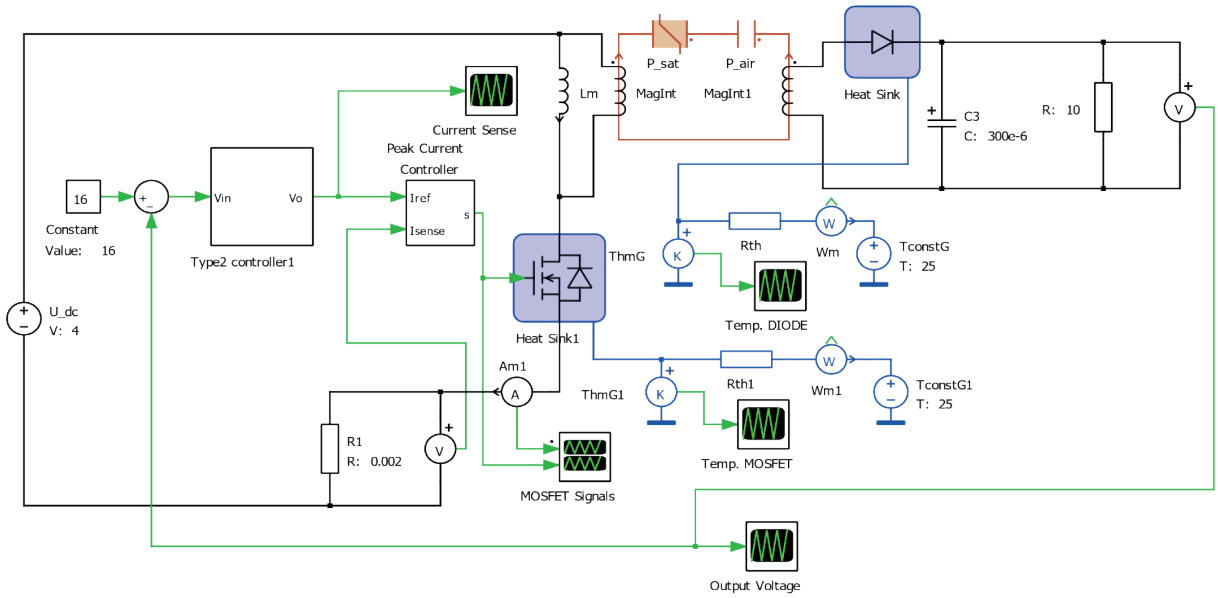


Figure 3 *Model of thef lyback converter controlled by the secondary side voltage*

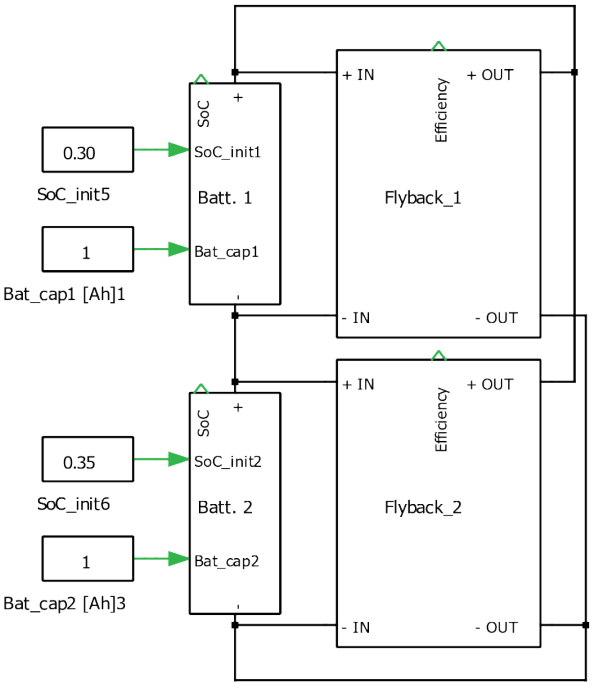


Figure 4 *Simulation model of the BMS with 2 cells*

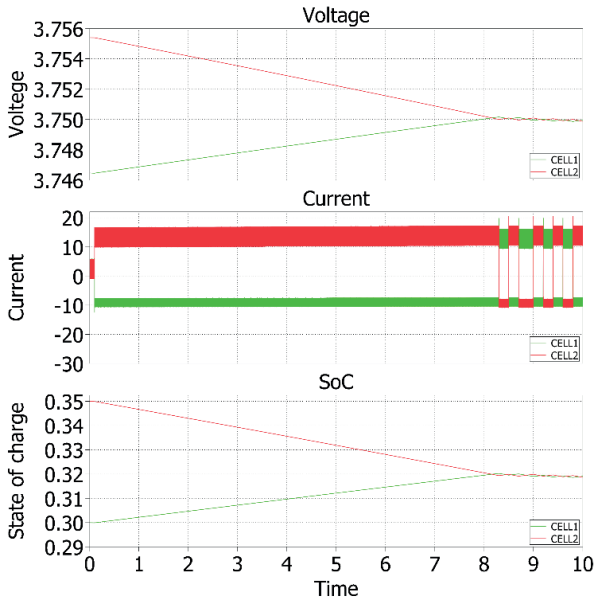


Figure 5 *Waveforms of voltage [V], current [A] and state of charge [-] in terms of time [s]*

secondary side of the transformer and to the output. This is especially true for high-frequency transformer of the flyback converter. Therefore, this topology has the great transformer requirements, mainly core saturation or thermal management [14-17].

In the PLECS environment, two simulation models of the flyback converter were created. One flyback converter is controlled by the primary side current value (Figure 2) and the other flyback converter is controlled by the secondary side voltage value (Figure 3). This model considers a replacement battery model at the primary side input. This is a voltage of 3-4 V DC. The output voltage is set by the transformer ratio. For the two-cell balancing system, this is a (3/15) ratio, while for the four-cell balancing system, the ratio is (2/21). Those ratios take into account the switching frequency of the MOSFET transistor and the saturation of the transformer core. Those values were calculated according to [18]. Thus, the output voltage in the balancing system will be twice the maximum voltage of one cell. Similarly, in a 4-cell balancing system, the output voltage will be four times the maximum cell voltage. Thermal power (blue) and magnetic circuit (brown) are simulated in this model, as well. Since it was intended to ensure the realistic behavior of simulation experiments, those flyback converters were implemented in a single block of the balancing system for the simple representation of the simulation block diagram. [19-20]

Table 1 *The flyback converter parameters for the 2-cell balancing system*

parameter	value
input voltage range	3 - 4 V
output voltage	8 V
output nominal current	9 A
output nominal power	75 W
switching frequency	100 kHz
required efficiency	80 %

4 Balancing system with two cells

As shown in Figure 4, the two-cell balancing system consists of the two battery models, two flyback converters and an evaluation circuit. Two constants enter the batteries: the battery capacity and the initial State of Charge (SoC). The flyback converters are connected by the primary side to a single cell and by the secondary side to the entire battery. Therefore, the secondary voltage value is twice as high for a two-cell balancing system. The evaluation section simply compares where the SoC value is greater and, based on that evaluation, a flyback converter is triggered for the cell where the SoC value is greater. In this way, the excess energy passes from the cell to the entire battery. This is the CELL-TO-PACK topology. The flyback converter parameters for the 2-cell balancing systems are shown in Table 1 [21].

The results of the described balancing method are shown in the graph in Figure 5. This graph shows the three values that are the most important for monitoring the balancing systems. Those values are the state of charge, voltage and current (Figure 5) of each cell. For the high simulation requirements, especially for time, battery capacity values are only 1 Ah. This value is a fraction of the real value of the battery capacity. This was done to ensure that the simulation time is not an unnecessarily long. The monitored values would have the same courses, but they would be simulated faster [20-21].

Figure 5 shows the SoC balancing waveform. Here one can see that the initial SoC CELL1 is 30 % and the SoC CELL2 is 25 %. In this course, one can see how the energy from CELL1 recharges CELL2. This works for up to 8.2 seconds. At 8.2 seconds, the SoC values get to a similar value. This ensures that the SoC values are kept at the same value. Thus, the balancing system has proven to work properly. However, one can see that the SoC value has a slight decrease. This decrease is caused by the efficiency of the flyback converters. This efficiency at such a low voltage is proportional to the size of the flyback converter current. From the given results one can say that there is no condition after which an unwanted condition may occur, such as under-voltage or over-voltage.

Figure 5 also shows the waveforms of balancing currents that compensate for the differences in the SoC on the cells. Here one can see how the CELL1 discharges via the flyback, thus charging both CELL1 and CELL2. After 8.2 seconds, the SoC reaches the same values and both flyback converters begin to switch. In this graph one can also see that one current is positive and one negative. This is caused by the current flow direction from and to the individual cells. When the current is positive, the cell discharges and when it is negative, the cell charges.

5 Balancing system with four cells

In contrast to the previous case, this system has the double number of batteries, as well as the double number of the flyback converters. This is a 4-battery system. As in the previous case, the flyback input of the inverters is connected to individual batteries and the output is connected to the entire battery. This determines that the inverter output must be four times the maximum voltage value of one battery. As in the previous case, the flyback block contains a trigger input, which is signaled by the evaluation part. This evaluation section aims to determine which cell has the highest SoC value. It determines which flyback converter will be started accordingly. This flyback converter transfers power from the strongest cell to the entire battery. This balancing system topology is CELL-TO-PACK. The flyback converter parameters for the 4-cell balancing systems are shown in Table 2 [21].

In the first experiment with a 4-cell balancing system (Figure 6), the flyback converters were used that were correct according to the input current value. Initially, the SoC values of the batteries were around 25-40 %. Figure 7 shows the SoC waveforms, voltage and current of each cell in the flyback controlled to the input current value (Figure 2). This value can be seen in the current waveform, where the current is in the 40 A range. This is exactly the value to which these flyback converters are regulated. This value means that the course of the SoC and voltage balancing is constant. In 34 seconds, all the cells are balanced. Another feature that is needed to design a balancing system is efficiency. This value can be seen in the decrease in the SoC value after all the cells are balanced. At a current control value of 40 A, one can see in Figures 7 and 8 that both the cell is discharged and charged at the same time, so the value of 40 A, to which the flyback converter is set, this value will be lower by the secondary current

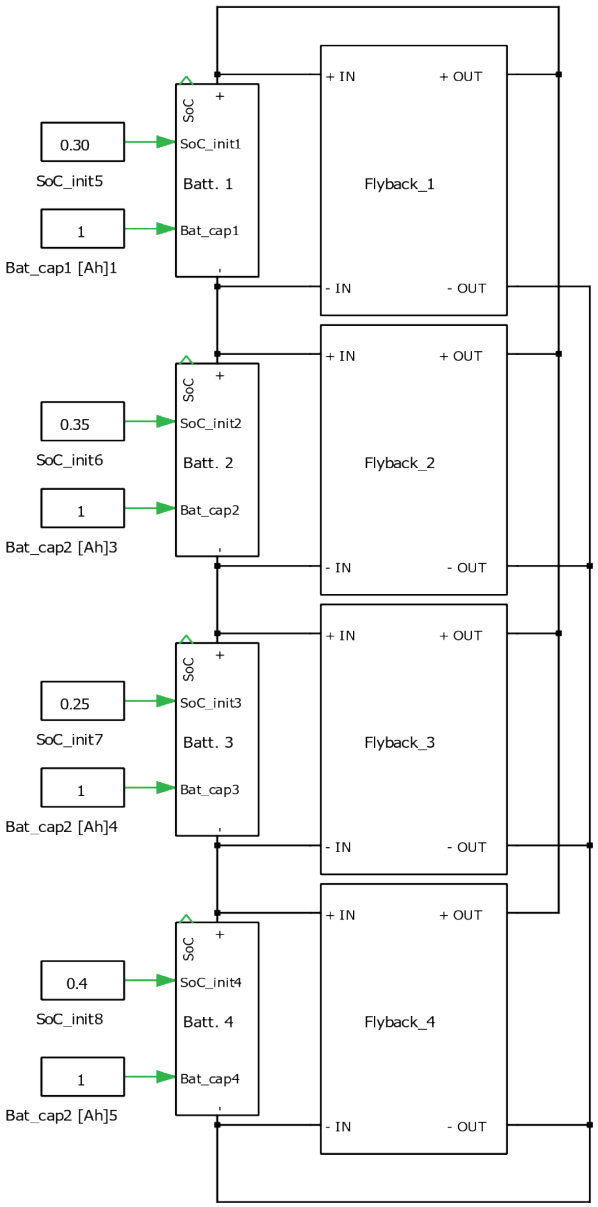


Figure 6 *Simulation model of the BMS system with 4 cells*

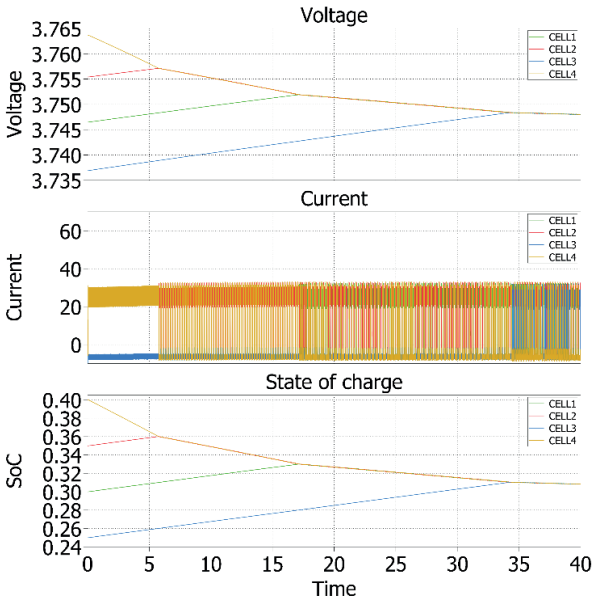


Figure 7 *Voltage [V], current [A], state of charge [-] balancing waveform for the 4 cell battery system in terms of time [s]*

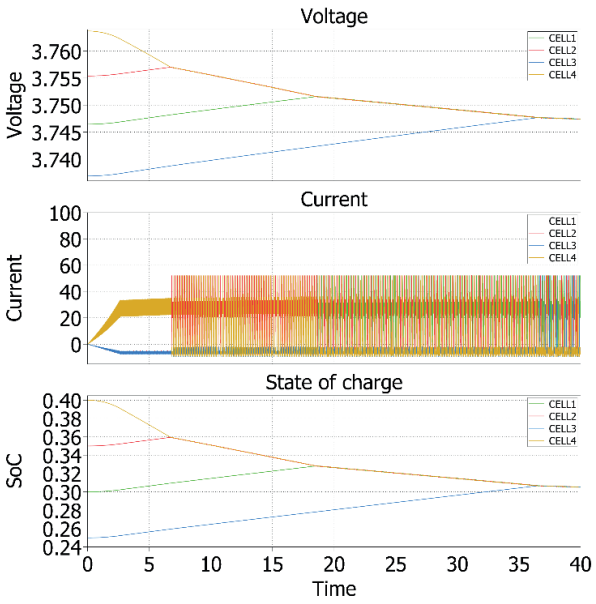


Figure 8 *Voltage [V], current [A], state of charge [-] balancing waveform for the 4 cell battery system in time [s]*

of the flyback converter, which charges the entire battery. Therefore, the current range on the graphs is 40 A. If one increases this value, the efficiency would drop rapidly at this low voltage. Therefore, it is very important to select the value to which these flyback converters will be regulated, in this input current control method. This is a disadvantage of the flyback converter application [11].

The basis of the balancing system and its control is also the same as in the previous 4-cell balancing system. The difference is in the control of the flyback converter. The flyback converters are controlled according to the output voltage value (Figure 3). Figure 8 shows the simulation results and SoC waveforms, voltages and currents of individual cells. Here one can see that all the cells are balanced in as little as 36 seconds. This is mainly due to the magnitude of the current, which reaches a peak value of nearly 50 A and the RMS value of nearly 35 A [11].

6 Conclusions

The balancing systems were simulated in this paper. In the first case, the 2 cells were balanced, which had capacities of 1 Ah and SoC of 25 % and 30 % respectively. The capacity was so small only for simulation requirements that the simulation was not so high in the real time. As

Table 2 *The flyback converter parameters for the 4-cell balancing system*

parameter	value
input voltage range	3 - 4 V
output voltage	16 V
output nominal current	7 A
output nominal power	120 W
switching frequency	100 kHz
required efficiency	70 %

one see in the results of this simulation, the balancing system works.

In the second case, 4 cells were balanced. However, the cell capacities were 1 Ah and SoC at 25-40% SoC. The resulting times are therefore as low as these cell capacities were also low. This was set due to the simulation requirements. The main difference in the balancing time of the 4-cell system is in the way of management. In the first case, when the flyback was controlled to the value of the input current, the balancing system immediately took an input current of 30 A. In the second case, when the flyback was controlled to the value of the output voltage, the flyback regulators of the converter had a longer response. As one can see in Figure 8, the current value reaches 30 A in up to 3 seconds. As a result, this mode is 2 seconds slower than in the case of a flyback converter controlled to the value of the input current.

This method of control consists of finding the maximum value of the SoC. As a result, the more cells are determined on a similar SoC value, the longer it takes to balance the next cell. Therefore, this balancing method is not very suitable for batteries with 8 or more cells.

These simulations were performed due to the skew control of the balancing system and the course of the measured values. Here, it was found that this control is appropriately chosen for both cases. Simulation courses prove it. Further, one can say that the characteristics of the battery replacement scheme and the flyback converter are similar to those of the real applications.

Acknowledgment

This publication was realized with support of Operational Program Integrated Infrastructure 2014 - 2020 of the project: Innovative Solutions for Propulsion, Power and Safety Components of Transport Vehicles, code ITMS 313011V334, co-financed by the European Regional Development Fund.

References

[1] Battery university [online]. Available from: https://batteryuniversity.com/.

[2] PAVELEK, M., SPANIK, P., FRIVALDSKY, M. Voltage stress reduction on compensation capacitors of wireless charging systems for transport and industrial infrastructure. *Communications - Scientific Letters of the University of Zilina* [online]. 2019, **21**(2), p. 50-57. ISSN 1335-4205, eISSN 2585-7878. Available from: https://doi.org/10.26552/com.C.2019.2.50-57

[3] DAOWD, M., OMAR, N., VAN DEN BOSSCHE, P., VAN MIERLO, J. Passive and active battery balancing comparison based on MATLAB simulation. In: 2011 IEEE Vehicle Power and Propulsion Conference: proceedings [online]. IEEE, 2011. ISSN 1938-8756. ISBN 978-1-61284-247-9. Available from: https://doi.org/10.1109/VPPC.2011.6043010

[4] ADAMEC, J. Research into the possibility of increasing the reliability and safety of energy storage in electric vehicles / Vyskum moznosti zvysovania spolahlivosti a bezpecnosti zasobnikov energie v elektromobiloch (in Slovak). PhD dissertation thesis. Zilina: FEIT-UNIZA, 2019.

[5] BOUKHAL, M. A., LAGRAT, I., ELBANNAY, O. Implementation of a lithium-ion battery state of charge estimation algorithm for BMS on the real time target NI myRio. In: 2019 International Conference on Wireless Technologies, Embedded and Intelligent Systems WITS 2019: proceedings [online]. 2019. p. 1-5. Available from: https://doi.org/10.1109/WITS.2019.8723849

[6] SEN, C., KAR, N. C. Battery pack modeling for the analysis of battery management system of a hybrid electric vehicle. In: IEEE Vehicle Power and Propulsion Conference VPPC'09: proceedings. IEEE, 2009. ISBN 9781424426003, p. 207- 212.

[7] MOGHADDAM, A. F., VAN DEN BOSSCHE, A. An active cell equalization technique for lithium ion batteries based on inductor balancing. In: 9th IEEE International Conference on Mechanical and Aerospace Engineering ICMAE 2018: proceedings [online]. IEEE, 2018. ISBN 978-1-5386-7229-7, p. 274-278. Available from: http://hdl.handle.net/1854/LU-8572445

[8] CACCIATO, M., NOBILE, G., SCARCELLA, G., SCELBA, G., SCIACCA, A. G. Energy management optimization in stand-alone power supplies using online estimation of battery SOC. In: 18th European Conference on Power Electronics and Applications EPE'16 ECCE Europe: proceedings [online]. 2016. p. 1-10. Available from: https://doi.org/10.1109/EPE.2016.7695559

[9] FARZAN MOGHADDAM, A., VAN DEN BOSSCHE, A. Flyback converter balancing technique for lithium based batteries. In: 8th International Conference on Modern Circuits and Systems Technologies MOCAST 2019: proceedings. 2019. p. 1-4. Available from: https://doi.org/10.1109/MOCAST.2019.8741893

[10] AIELLO, G., CACCIATO, M., MESSINA, S., TORRISI, M. A High efficiency interleaved PFC front - end converter for EV battery charger. *Communications - Scientific Letters of the University of Zilina* [online]. 2018, **20**(1), p. 86-91. ISSN 1335-4205, eISSN 2585-7878. Available from: http://komunikacie.uniza.sk/index.php/communications/article/view/52

[11] WANG, Z., LAI, X., WU, Q. A PSR CC/CV flyback converter with accurate CC control and optimized CV regulation strategy. *IEEE Transactions on Power Electronics* [online]. 2016, 32(9), p. 7045-7055. ISSN 0885-8993. Available from: https://doi.org/10.1109/TPEL.2016.2629846

[12] GALAD, M., SPANIK, P., CACCIATO, M., NOBILE, G., Comparison of common and combined state of charge estimation methods for VRLA batteries. In: 11th International Conference ELEKTRO 2016: proceedings [online]. 2016.p.220 225. Available from: https://dolorg/10.1109/ELEKTRO.2016.7512069

[13] CACCIATO, M., NOBILE, G., SCARCELLA, G., SCELBA, G. Real-time model-based estimation of SOC and SOH for energy storage systems. *IEEE Transactions on Power Electronics* [online]. 2017, **32**(1), p. 794-803. ISSN 0885-8993. Available from: https://doi.org/10.1109/TPEL.2016.2535321

[14] FRIVALDSKY, M., CUNTALA, J., SPANIK, P., KANOVSKY, A. Investigation of thermal effects and lifetime estimation of electrolytic double layer capacitors during repeated charge and discharge cycles in dedicated application. *Electrical Engineering* [online]. 2018, **100**(1), p. 11-25. ISSN 0948-7921, eISSN 1432-0487. Available from: https://doi.org/10.1007/s00202-016-0482-2

[15] KOSCELNIK, J., FRIVALDSKY, M., PRAZENICA, M., MAZGUT, R. A review of multi-elements resonant converters topologies. In: 10th International Conference ELEKTRO 2014: proceedings. 2014. ISBN 9781479937219.

[16] SPANIK, P., CUNTALA, J., FRIVALDSKY, M., DRGONA, P. Investigation of heat transfer of electronic system through utilization of novel computation algorithms. *Elektronika Ir Elektrotechnika* [online]. 2012, **123**(7), p. 31-36. ISSN 1392-1215, eISSN 2029-5731. Available from: https://doi.org/10.5755/j01.eee.123.7.2371

[17] FRIVALDSKY, M., DOBRUCKY, B., SCELBA, G., SPANIK, P., DRGONA, P. Bidirectional step-up/step-down DC-DC converter with magnetically coupled coils. *Communications - Scientific Letters of the University of Zilina* [online]. 2013, **15**(3), p. 21-25. ISSN 1335-4205, eISSN 2585-7878. Available from: http://komunikacie.uniza.sk/index.php/communications/article/view/682

[18] SPANIK, P., SUL, R., FRIVALDSKY, M. Performance investigation of dynamic characteristics of power semiconductor diodes. *Elektronika Ir Elektrotechnika* [online]. 2010, **99**(3), p. 3-6. ISSN 1392-1215, eISSN 2029-5731. Available from: https://eejournal.ktu.lt/index.php/elt/article/view/9894

[19] DRGONA, P., PRIKOPOVA, A., FRIVALDSKY, M., PRIECINSKY, M. Simulation based method for design and application of digital control system. *Communications - Scientific Letters of the University of Zilina* [online]. 2011, **13**(2A), p. 32-37. ISSN 1335-4205, eISSN 2585-7878. Available from: http://komunikacie.uniza.sk/index.php/communications/article/view/839

[20] SPANIK, P., FRIVALDSKY, M., DRGONA, P., KANDRAC, J. Efficiency increase of switched mode power supply through optimization of transistor's commutation mode. *Elektronika Ir Elektrotechnika* [online]. 2010, **105**(9), p. 49-52. ISSN 1392-1215, eISSN 2029-5731. Available from: https://eejournal.ktu.lt/index.php/elt/article/view/9168

[21] D'ANGELO, V., CANNAVACCIUOLO, S., LECCE, S., BENDOTTI, V., PENNISI, O. Enhanced hotplug protection in BMS applications. Part I: Theoretical aspects and practical issues. In: 2019 AEIT International Conference of Electrical and Electronic Technologies for Automotive AEIT Automotive 2019: proceedings [online]. 2019. p. 1-5. Available from: https://doi.org/10.23919/EETA.2019.8804513

COMPARATIVE LIFE CYCLE ANALYSIS OF HYBRID AND CONVENTIONAL DRIVE VEHICLES IN VARIOUS DRIVING CONDITIONS

Emilia M. Szumska

Department of Automotive Engineering and Transport, Kielce University of Technology, Kielce, Poland

*E-mail of corresponding author: eszumska@tu.kielce.pl

Resume

Growing environmental concern prompts vehicle users to search for cleaner and ecological transport modes. Many consumers and organizations have decided to replace conventional diesel or gasoline powered vehicles with alternative drive or alternative-powered vehicles. Operating conditions may have a heavy influence on the operating parameters of vehicles, such as: air-pollution emission, energy consumption and fuel consumption. This paper presents a comparative analysis of the life cycle of conventional and hybrid drive vehicles in various driving conditions. The presented LCA results show that replacing a conventional diesel or gasoline vehicle with a hybrid electric drive vehicle results in approximately 40% lower total lifetime air-pollutant emissions than those of conventional drive vehicles in urban driving conditions.

Article info

Received 17 September 2020
Accepted 25 October 2020
Online 8 July 2021

Keywords:

hybrid electric vehicles,
Life Cycle Assessment,
emission

Available online: https://doi.org/10.26552/com.C.2021.4.D34-D41

ISSN 1335-4205 (print version)
ISSN 2585-7878 (online version)

This is an open access article distributed under the terms of the Creative Commons Attribution 4.0 International License (CC BY 4.0), which permits use, distribution, and reproduction in any medium, provided the original publication is properly cited. No use, distribution or reproduction is permitted which does not comply with these terms.

1 Introduction

Transport activities bring substantial socioeconomic benefits and support increasing demands for passengers and cargo mobility, but on the other hand, have an unfavorable impact on environmental systems. Among all economic activities, transport is recognized to be one of the major sources of the greenhouse gases emissions. In 2017 the greenhouse gases emissions emitted by transport were 25% of the total GHGs emissions of the European Union economy (Figure 1). Road transport generated the highest air-pollutant emissions of all the transport modes (Figure 2).

The authors of study [3] distinguished transport impacts within three categories:

- direct impacts - represent the immediate consequences of transport activities for the environment. They are easily identified and have direct harmful effects, such as: noise and carbon monoxide emissions;
- indirect impacts - are defined as the secondary (or tertiary) effects of transport activities on environmental systems. They are more difficult to establish and have more serious consequences than the direct impacts; for example, particulate matters that are indirectly associated with human respiratory and cardiovascular problems;
- cumulative impacts - are the additive, multiplicative or synergetic consequences of transport activities, including the varied effects of direct and indirect impacts on an ecosystem, which are often unpredictable, such as climate change.

The negative effect of the road transport manifests itself through: climatic changes caused by the greenhouse gas emissions and loss of biological diversity by occupation of land by newly build roads and technical infrastructure vehicles. The growing network of roads has dramatically altered the landscape and can impact wildlife in a number of deleterious ways [4]. Pollution by harmful substances, caused by movement of motor vehicles, as well as light and noise pollution from roads, can be detrimental to wild animals [5-6]. Many studies, focused on sustainable transport efficiency, consider air-pollutants as an undesirable output, the examples of which are found in papers [7-8].

The impact of road transport is especially noticeable in cities. According to results presented in papers [9-11] traffic and congestion can increase air-pollutant emission by as much as 80%. Local emissions of air and noise pollutants caused by movement of motor vehicles negatively influence human health. According to WHO studies, transport-generated urban air pollution causes: cardiovascular and pulmonary diseases, ischemic heart disease, cancers, asthma and strokes. Outdoor air pollution alone is responsible for 4.2 million deaths annually [12-13]. To reduce air pollutants many cities have decided to adopt activities to support sustainable development. These actions entail reduction of parking

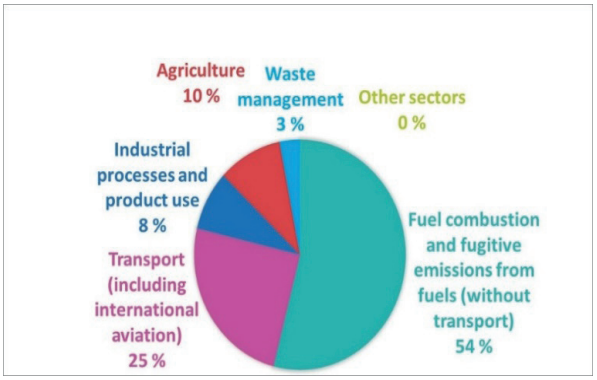


Figure 1 *Greenhouse gases emissions, by source sector in EU-28 in 2017 [1]*

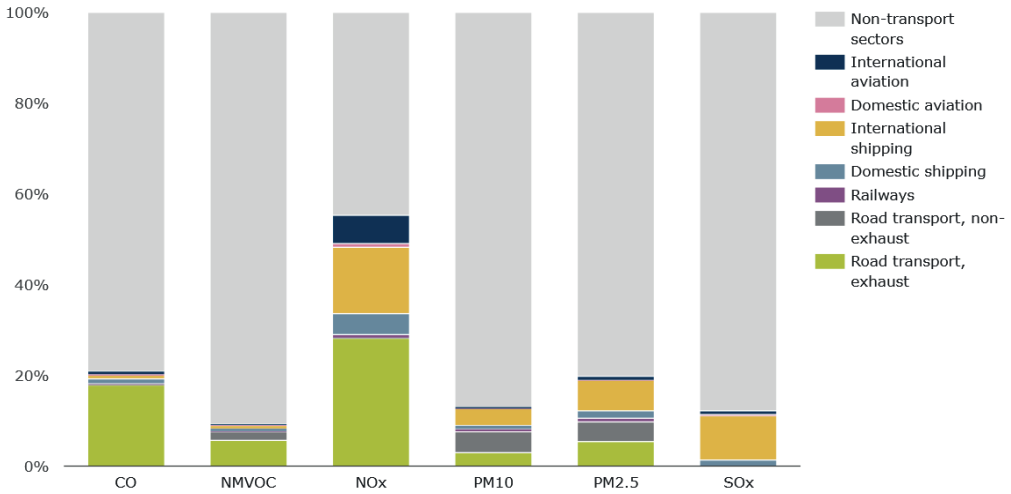


Figure 2 *Contribution of the transport sector to total emissions of the main air-pollutants [2]*

zones, increasing parking fees in the city center, site greening, encouraging the use of public transport and creating new cycle paths - these being but a select few of such actions in cities [14].

To reduce this negative aspect of driving, car manufacturers have begun producing vehicles that are more environmentally friendly. At present, the largest majority of cars are equipped with systems ensuring low emissions. Some of the solutions that have been developed include engine improvements (such as variable charge motion in-cylinder, cylinder deactivation and GDI - gasoline direct injection), exhaust gas recirculation, turbo chargers, three-way converters and particulate - matter filters. In addition, the number of low-emission automobiles on the roads is growing. Vehicles equipped with alternative drives (electric, hybrid) and powered by alternative fuels (CNG, LPG, biofuels) are a commonplace sight. Operating conditions may heavily influence vehicle operating parameters, such as air-polluting emissions, energy and fuel consumption. The aim of this paper is to provide a comparative air-pollutant analysis of vehicles equipped with conventional drives and those equipped with hybrid drives. Therefore, the Life Cycle Assessment method was used to examine the lifetime air-pollutant emissions for the hybrid and conventional drives vehicles in various driving conditions.

2 LCA - Life Cycle Assessment

The Life Cycle Assessment (LCA) is focused on estimation and assessment of environmental impacts consequences on individual stages of a vehicle life cycle. Those include e consumption of the raw materials and energy and their emission of harmful gases and substances, starting with the vehicle production phase through the production of materials to the assembly phase and to e usage of a vehicle along with the necessary f production of fuel or electrical energy and the level of fuel consumption and terminating with the end of the life cycle and the attendant costs of recycling and utilization. The LCA is commonly used to assess different vehicle technologies from various points in their life cycle. It should be noted that economic criteria are not taken into account in the LCA method [15]. Studies [16-17] identified, quantified and assessed the environmental impacts by the entire LC of vehicles equipped with alternative and conventional drives using the LCA methodology. Many studies have been devoted to the Life Cycle Assessment for city buses equipped with various types of propulsion systems. Papers [18-19] present comparison analyses of lifetime vehicle emission values of the manufacture, use, maintenance and



Figure 3 *Scheme of the GREET software tool [26]*

infrastructure phases of diesel, hybrid and battery electric buses.

The LCA method can be used to assess the environmental impacts of a specific vehicle component's life cycle. For example, papers [20-21] present the analyses of greenhouse gas emissions of every stage of the lithium-ion battery life-cycle. Studies [22-23] present the estimation of the environmental impacts of recycling during the vehicle's end-of-life.

The LCA results could be used for the estimation of Life Cycle Cost. Emissions values of harmful compounds assessed using the LCA method are presented in the form of costs. Therefore, the costs of emissions are the constituent element of the total life cycle costs of a vehicle. Examples are found in papers [24-25].

3 Methodology

The presented LCA analysis was carried out for passenger cars fitted with conventional power drives and hybrid electric power drives. The total mileage was assumed as 300 000 km and the operation time was 10 years. The LCA analysis was conducted for three types of driving conditions: driving in urban conditions, driving in areas entirely outside the city and conditions where driving was done in a combination of urban and non-urban, in half of shares each (50-50).

The Life Cycle Assessment (LCA) was carried out using the GREET program (Greenhouse gases, Regulated Emissions and Energy use in Transportation Model), developed by the Argonne National Laboratory (ANL) as a part of a project ran by the US Department of Energy. The GREET program enables estimating the impact of individual phases of the life cycle of vehicles equipped with conventional and alternative propulsion systems on the natural environment. The program uses data provided by studies undertaken by the EPA (Environmental Protection Agency), an US Government agency dealing with the protection of human health and the environment [26]. The GREET provides the opportunity to estimate energy consumption and emissions of harmful compounds caused by production and distribution of fuel and by all the phases of a vehicle's life cycle. The program scheme is presented in Figure 3.

The model of a vehicle's life cycle includes the submodels: "the fuel cycle" and "the vehicle cycle". The fuel cycle includes raw material extraction, raw material transport, refining and purification, distribution and consumption of fuel during the vehicle operation. In the vehicle cycle model the following stages are identified: sourcing of raw materials, production and processing of raw materials, production of components, assembly of a vehicle , operation of a vehicle and its decommissioning. The results of calculations are:

- the amount of energy coming from the combustion of the fossil fuels (oil, gasoline, gas, coal) or from renewable sources (biomass, wind, solar rays, water);
- the level of greenhouse gas emissions (CO_2, CH_4, N_2O) of harmful compounds contained in the exhaust gases (CO, NO_x, PM_x, SO_x, aliphatic and aromatic hydrocarbons);
- water creation.

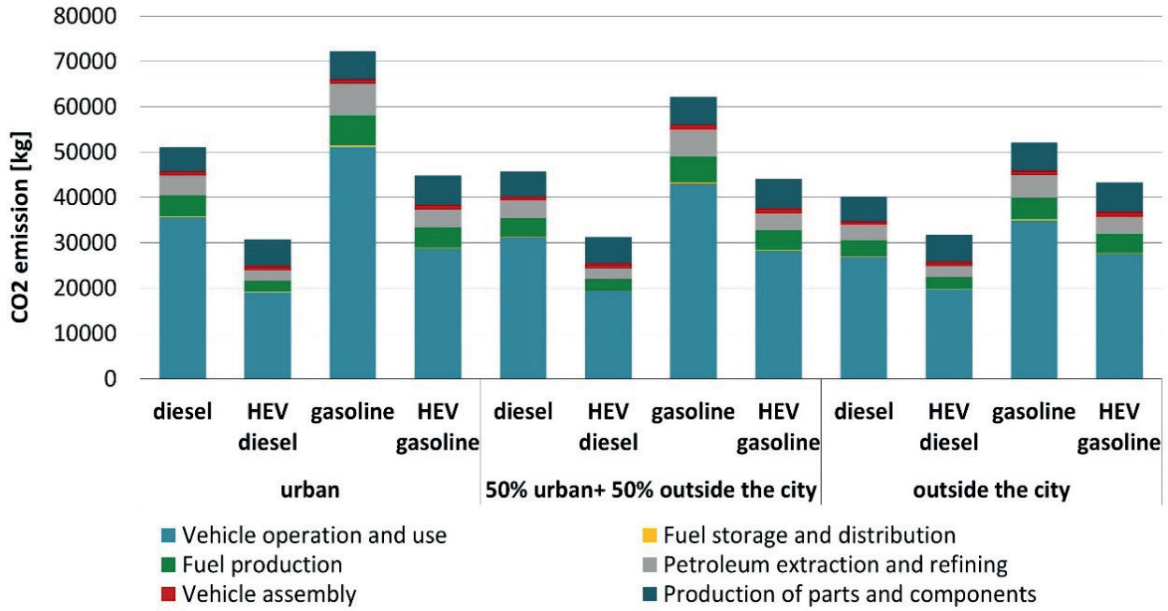


Figure 4 *CO_2 emissions over the vehicle life cycle*

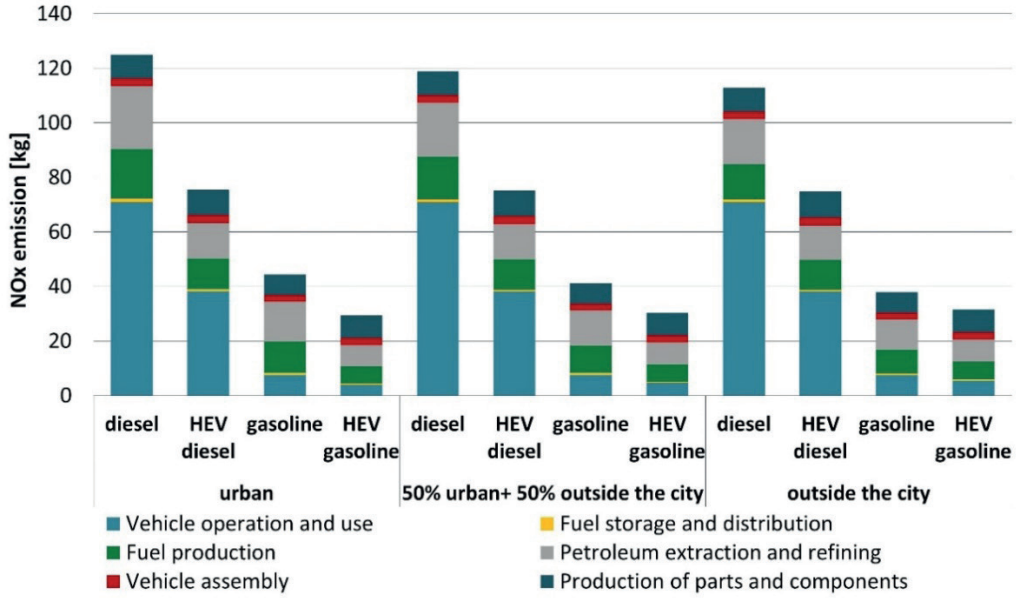


Figure 5 *NO_x emissions over the vehicle life cycle*

4 Results

The LCA analysis provided shows the levels of emissions of carbon dioxide (CO_2), nitrogen oxides (NO_x), particulate matter (PM_x) and volatile organic compounds (VOC) for the environmental life cycle of the examined passenger cars. The life cycle of the vehicles selected for investigation is divided into the following phases: fuel production (petroleum extraction and refining, production of fuel, distribution and storage), production of a vehicle (production of parts and components and vehicle assembly) and the vehicle operation and use. Figure 4 shows the CO_2 emission level of the above mentioned compounds for the life cycle of cars with conventional drives and cars with hybrid drives.

It can be seen that the vehicles equipped with gasoline engines demonstrate the highest level of the lifetime CO_2 emission. For urban driving conditions the vehicles equipped with a hybrid drive show a level of life cycle carbon dioxide emissions approximately 40 % lower than those of the conventional cars. For the combined driving conditions (urban and outside the urban area), the CO_2 life cycle emissions emitted by the hybrids are 30 % less than those of the conventional drive vehicles. In driving conditions outside the urban area, the cars equipped with gasoline- and diesel-powered engines exhibit 20 % higher CO_2 emissions than the hybrid vehicles.

The highest share in the lifetime CO_2 emissions value falls on the phase of vehicle operation and use, approximately 70 % of the total CO_2 life cycle emissions. The nitrogen oxides (NO_x) emissions

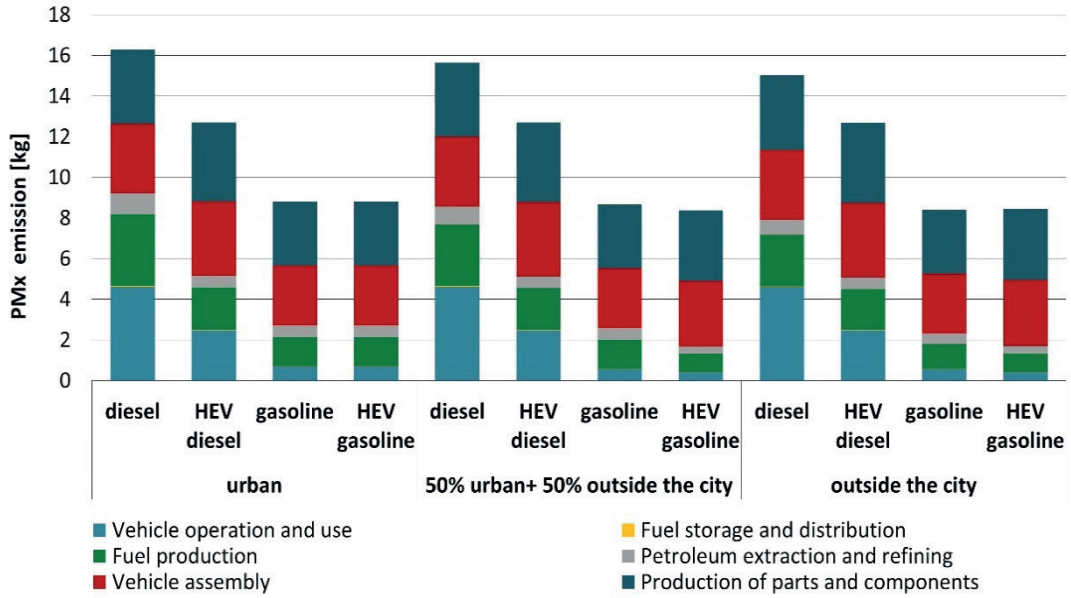


Figure 6 *PM_x emissions over the vehicle life cycle*

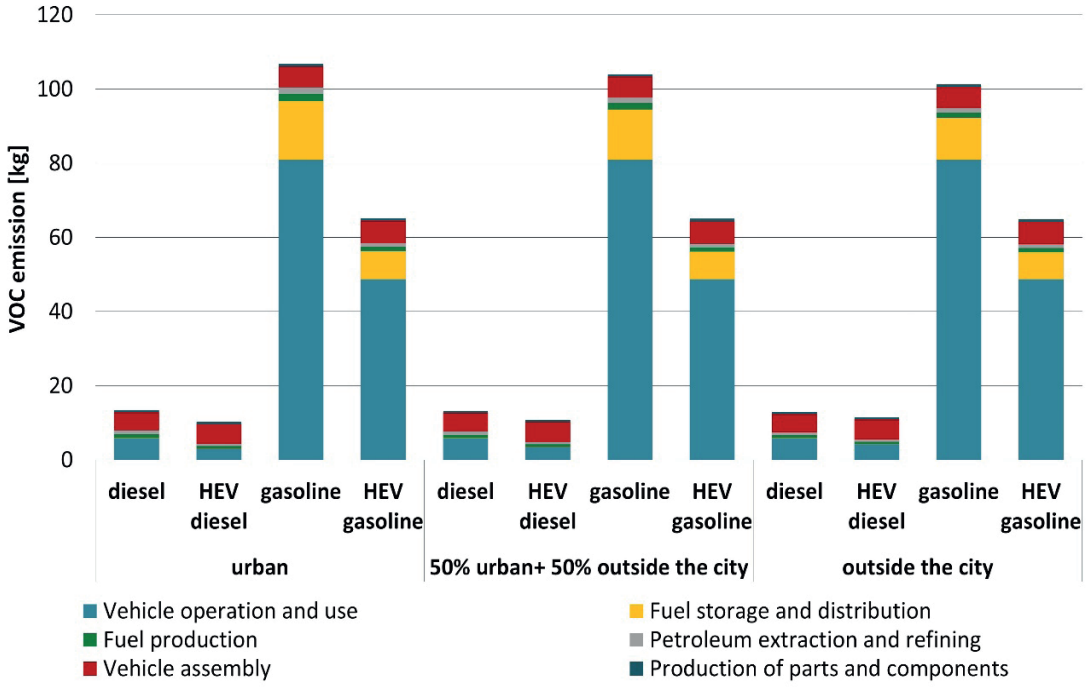


Figure 7 *VOC emissions over the vehicle life cycle*

levels for the life cycles of the analysed vehicles are presented in Figure 5.

The vehicle operation and use stage is the largest contributor to the life cycle NO_x emissions for vehicles fitted with diesel engines, accounting for 51 %-62 % of total NO_x emissions. It is found that for the examined driving conditions, the lifetime NO_x emissions estimate by diesel hybrid is approximately 40 % lower than those of conventional diesel car. In conditions both urban combined in-city and outside the urban area driving, the total life cycle NO_x emissions emitted by gasoline hybrid car are approximately 30 % less than those of the conventional gasoline vehicle. In conditions excluding city driving the difference is 17 %. The greatest share of the lifetime NO_x emissions of vehicles fitted with gasoline engines falls on phases of production, distribution and storage of fuel, approximately 60 % of the total. Figure 6 shows the level of particulate matter (PM_x) emissions during the life cycles of the analysed vehicles.

The particulate matter emissions level for a hybrid diesel car are about 20 % lower compared to a conventional diesel vehicle. The differences in PM_x emissions emitted by hybrid and conventional vehicles equipped with a gasoline engine are negligible, at most 3 %. The largest part of lifetime particulates emissions falls on the phases related to the production of ae vehicle, that is to say, production

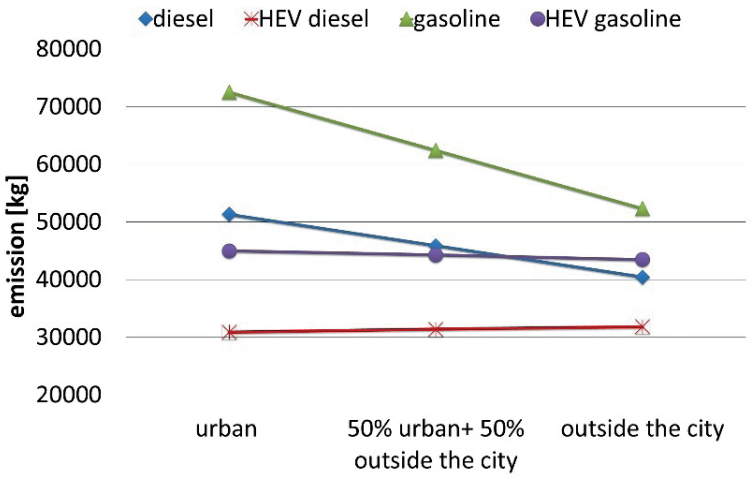


Figure 8 *Air pollutant emissions over the vehicle life cycle*

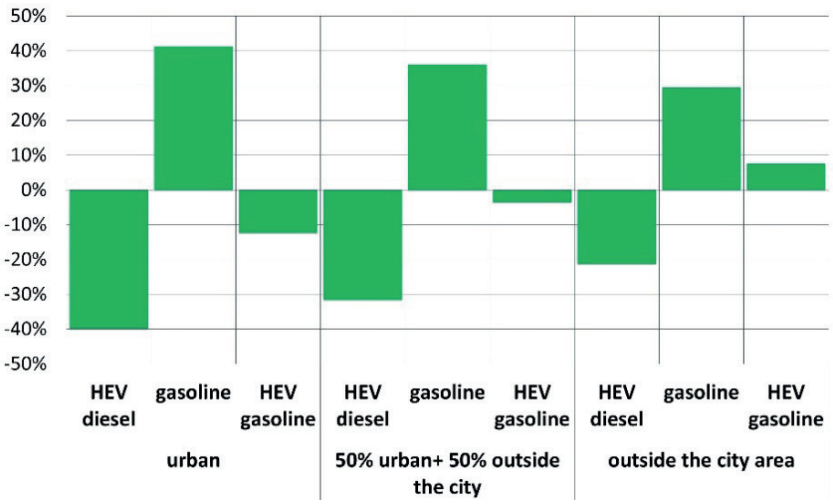


Figure 9 *Percentage difference of lifetime air-pollutant emissions related to conventional diesel vehicle (diesel emission =100 %)*

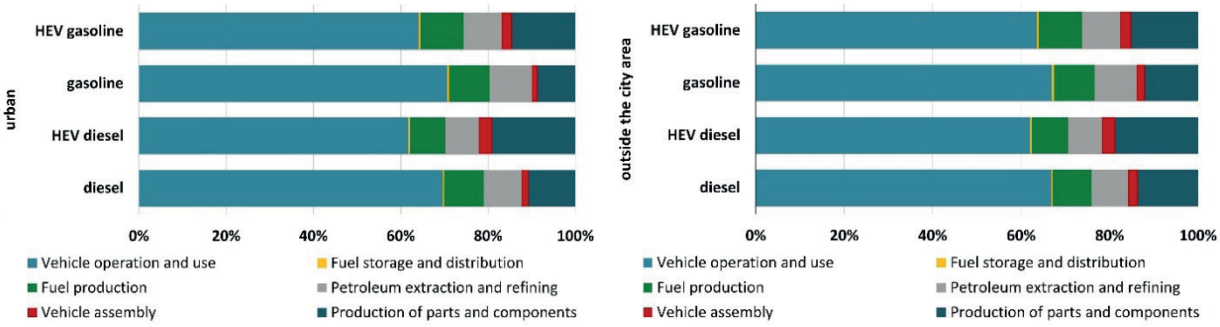


Figure 10 *Percentage of lifetime air pollutant emissions during different life cycle stages*

of parts and components and assembly of a vehicle. In addition, it can be seen that the high percentage of air pollutant emission emitted by diesel-powered cars, falls on the operation stage, accounting for 20 %-30 % of the total. The levels of volatile organic compounds (VOC) for the life cycles of the analysed vehicles are shown in Figure 7.

Volatile organic compounds contain aliphatic hydrocarbons (decane, octane, hexane), aromatic hydrocarbons (toluene, xylene, benzene), benzene alkyl derivatives, aldehydes, ketones, amines, alcohols, esters, terpenes and others. The highest share of the VOC life time emissions occurs in the vehicle operation stage. The vehicles fitted with gasoline-powered engines demonstrate higher VOC emissions values than the diesel-powered cars. Figure 8 shows values for air pollutant emissions during the life cycle stages of the examined vehicles.

In urban driving conditions, the vehicles equipped with hybrid drives have 40 % lower life cycle air pollutant emissions than do the conventional cars (Figure 9). Smaller differences occur in driving condition outside

the urban area, where the hybrids achieve approximately 20 % lower air pollutant emissions in comparison to the conventional vehicles. Compared to the conventional vehicles fitted with a diesel-powered engine, in all the examined driving conditions the conventional gasoline vehicle exhibits higher values of the lifetime air-polluting emissions. As mentioned above, the gasoline vehicles show the lowest NO_x and PM_x emissions, but they indicate higher emissions of CO_x and VOC than do the diesel vehicles. Figure 10 shows the percentage contribution of different life cycle stages.

It can be seen that the vehicle operation and use stage is the largest contributor to total air pollutant emissions during the lifetime of a vehicle, accounting for 62 %-71 % of total air pollutant emissions (Figure 10). The high percentage of air pollutant emission falls to production of a vehicle (production of parts and components, vehicle assembly). It is found that air-pollutants emitted during the vehicle production constitute 12 %-16 % of the total emissions of conventional vehicles, 17 % of the total emissions of gasoline hybrid vehicles and 22 % of the total emissions of diesel hybrid vehicles.

5 Conclusion

Typically, vehicle air pollutants emissions exhibit values during their operation. To estimate the average operation emissions, a number of driving cycles have been developed. These cycles reflect the vehicle driving conditions typical for a particular city, town, or region. The test cycles are used in vehicle approval tests to estimate carbon dioxide emissions and average fuel consumption. In the EU, the NEDC had been used to test passenger vehicles and light duty vehicles and it is now using the Worldwide Harmonized Light Vehicles Test Procedure, or WLTP for short. For buses, the International Association of Public Transport introduced the SORT cycles. However, standardized tests have a disadvantage. They do not fully reflect the real conditions of a vehicle operation. Therefore, in many works and projects are found the driving cycles developed for the traffic conditions of a particular city or region. Driving conditions have a significant influence on values for emissions and fuel consumption. Traffic conditions in the city are characterized by the low driving speeds, together with frequent acceleration, frequent braking and frequent stops. The non-urban driving conditions imply the higher speeds with less braking and fewer stops.

In order to assess the total emissions of a vehicle from production to end-of-life, the impact of the operation phase should be taken into account, as well as the emissions related to the manufacture of components, the assembly of a vehicle and production of fuel. The LCA method can be used for these purposes. It shows the influence of the different stages of the vehicle on the total emissions during the life of the vehicle. LCA can be used to make comparisons between the conventional and alternative vehicles and to facilitate purchasing decisions.

The paper shows the comparative life cycle analysis of conventional and hybrid drive vehicles with respect to various driving conditions. The presented results show that replacing a conventionally powered vehicle (diesel, gasoline) with a hybrid results in significant reduction of the lifetime air-pollutant emissions. In comparison to conventional cars, hybrids emitted 40 % fewer air-pollutant lifetime emissions in urban driving condition, approximately 30 % fewer life cycle air-pollutant emissions in combined urban and non-urban area conditions and around 20 % fewer air-pollutant lifetime emissions in driving conditions excluding the urban areas. The major vehicle contributor to total air pollutant emissions for vehicles lifetime is the operation and use stage.

References

[1] Greenhouse gas emission statistics - Eurostat [online] [accessed 2019-12-16]. Available from: https://appsso.eurostat.ec.europa.eu/nui/show.do?dataset=env_air_gge&lang=en

[2] Emissions of air pollutants from transport - European Environment Agency (EEA) [online]. Available from: https://www.eea.europa.eu/data-and-maps/indicators/transport-emissions-of-air-pollutants-8/transport-emissions-of-air-pollutants-8

[3] RODRIGUE, J. P. *The geography of transport systems*. 4. ed. Routledge, 2016. ISBN 1138669571.

[4] CHAPMAN, L. Transport and climate change: a review. *Journal of Transport Geography* [online]. 2007, **15**(5), p. 354-367. ISSN 0966-6923. Available from: https://doi.org/10.1016/j.jtrangeo.2006.11.008

[5] SEILER, A., HELLDIN, J. O. Mortality in wildlife due to transportation. *The Ecology of Transportation: Managing Mobility for the Environment* [online]. 2006, **10**, p. 165-189. ISBN 978-1-4020-4503-5. Available from: https://doi.org/10.1007/1-4020-4504-2_8

[6] RYTWINSKI, T., FAHRIG, L. The impacts of roads and traffic on terrestrial animal populations. In: *Handbook of road ecology* [online]. UK: John Wiley & Sons Ltd, 2015. ISBN 9781118568187, eISBN 9781118568170, p. 237-246. Available from: https://doi.org/10.1002/9781118568170.ch28

[7] PARK, Y. S., LIM, S. H., EGILMEZ, G., SZMEREKOVSKY, J. Environmental efficiency assessment of U.S. transport sector: a slack-based data envelopment analysis approach. *Transportation Research Part D: Transport*

and Environment [online]. 2018, **61**, p. 152-164. ISSN 1361-9209. Available from: https://doi.org/10.1016/j.trd.2016.09.009

[8] LUOMA, J., SIVAK, M. Interactions of environmental and safety measures for sustainable road transportation. *European Transport Research Review* [online]. 2012, **4**(4), p. 189-199. ISSN 1867-0717. Available from: https://doi.org/10.1007/s12544-012-0078-5

[9] SZUMSKA, E., JURECKI, R., PAWELCZYK, M. Evaluation of the use of hybrid electric powertrain system in urban traffic conditions. *Eksploatacja i Niezawodnosc - Maintenance and Reliability* [online]. 2020, **22**(1), p. 154-160. Available from: http://ein.org.pl/sites/default/files/2020-01-18.pdf

[10] BHARADWAJ, S., BALLARE, S., ROHIT, CHANDEL, M. K. Impact of congestion on greenhouse gas emissions for road transport in Mumbai metropolitan region. *Transportation Research Procedia* [online]. 2017, **25**, p. 3538-3551. ISSN 2352-1465. Available from: https://doi.org/10.1016/j.trpro.2017.05.282

[11] ZHANG, K., BATTERMAN, S., DION, F. Vehicle emissions in congestion: comparison of work zone, rush hour and free-flow conditions. *Atmospheric Environment* [online]. 2011, **45**(11), p. 1929-1939. ISSN 1352-2310. Available from: https://doi.org/10.1016/j.atmosenv.2011.01.030

[12] KRZYZANOWSKI, M., KUNA-DIBBERT, B., SCHNEIDER, J. Health effects of transport-related air pollution [online]. World Health Organization, 2005. ISBN 9289013737. Available from: http://www.euro.who.int/en/publications/abstracts/health-effects-of-transport-related-air-pollution

[13] Health risk assessment of air pollution. General principles [online]. World Health Organization, 2016. ISBN 9789289051316. Available from: http://www.euro.who.int/en/publications/abstracts/health-risk-assessment-of-air-pollution.-general-principles-2016

[14] BĄK, I., SZCZECINSKA, B., CHEBA, K. The impact of transport on the quality of the environment in cities of Poland - a statistical analysis. *Transportation Research Procedia* [online]. 2019, **39**, p. 24-33. ISSN 2352-1465. Available from: https://doi.org/10.1016/j.trpro.2019.06.004

[15] FINKBEINER, M. *Special types of life cycle assessment*. Springer, 2016. ISBN 978-94-017-7610-3.

[16] DEL PERO, F., DELOGU, M., PIERINI, M. Life cycle assessment in the automotive sector: a comparative case study of internal combustion engine (ICE) and electric car. *Procedia Structural Integrity* [online]. 2018, **12**, p. 521-537. ISSN 2452-3216. Available from: https://doi.org/10.1016/j.prostr.2018.11.066

[17] FOLEGA, P., BURCHART-KOROL, D. Environmental assessment of road transport in a passenger car using the life cycle approach. *Transport Problems* [online]. 2017, **12**(2), p. 147-53. ISSN 1896-0596. Available from: https://www.exeley.com/transport_problems/doi/10.20858/tp.2017.12.2.14

[18] BICER Y., DINCER I., Life cycle environmental impact assessment and comparison of alternative fuel for clean vehicles. *Resources, Conservation and Recycling* [online]. 2018, **132**, p. 141-157. ISSN 0921-3449. Available from: https://doi.org/10.1016/j.resconrec.2018.01.036

[19] KLIUCININKAS, L., MATULEVICIUS, J., MARTUZEVICIUS, D. The life cycle assessment of alternative chains for urban buses and trolleybuses. *Journal of Environmental Management* [online]. 2012, **99**, p. 98-103. ISSN 0301-4797. Available from: https://doi.org/10.1016/j.jenvman.2012.01.012

[20] JWA, K., LIM, O. Comparative life cycle assessment lithium-ion battery electric bus and diesel bus from well-to-wheel. *Energy Procedia* [online]. 2018, **145**, p. 223-227. ISSN 1876-6102. Available from: https://doi.org/10.1016/j.egypro.2018.04.039

[21] DAI, Q., KELLY, J.C., GAINES, L., WANG, M. Life cycle analysis of lithium-ion batteries for automotive applications. *Batteries* [online]. 2019, **5**(2;48), p. 1-12. eISSN 2313-0105. Available from: https://doi.org/10.3390/batteries5020048

[22] SOO, V. K., COMPSTON, P., DOOLAN, M. Interaction between new car design and recycling impact of life cycle assessment. *Procedia CIRP* [online]. 2015, **29**, p. 426-431. ISSN 2212-8271. Available from: https://doi.org/10.1016/j.procir.2015.02.055

[23] SOO, V. K., PEETERS, J., COMPSTON, P., DOOLAN, M., DUFLOU, J. R. Comparative study of end-of-life vehicle recycling in Australia and Belgium, *Procedia CIRP* [online]. 2017, **61**, p. 269-274. ISSN 2212-8271. Available from: https://doi.org/10.1016/j.procir.2016.11.222

[24] SZUMSKA, E., PAWELCZYK, M., PISTEK, V. Evaluation of the life cycle costs for urban buses equipped with conventional and hybrid drive trains. *The Archives of Automotive Engineering - Archiwum Motoryzacji* [online]. 2019, **83**(1), p. 73-86. eISSN 2084-476X. Available from: https://doi.org/10.14669/AM.VOL83.ART5

[25] KARA, S., LI, W., SADJIVA, N. Life cycle cost analysis of electrical vehicles in Australia. *Procedia CIRP* [online]. 2017, **61**, p. 767-772. ISSN 2212-8271. Available from: https://doi.org/10.1016/j.procir.2016.11.179

[26] GREET life-cycle model. User guide. Center for Transportation Research Energy Systems Division, Argonne National Laboratory, 2016.

OPTIMIZATION OF ENERGY MANAGEMENT IN A CITY BUS POWERED BY THE HYDROGEN FUEL CELLS

Arkadiusz Malek[1,*], Rodolfo Taccani[2], Dariusz Kasperek[3], Jacek Hunicz[4]

[1]University of Economics and Innovation, Lublin, Poland
[2]University of Trieste, Trieste, Italy
[3]Ursus Bus, Lublin, Poland
[4]Faculty of Mechanical Engineering, Lublin University of Technology, Lublin, Poland

*E-mail of corresponding author: arkadiusz.malek@wsei.lublin.pl

Resume

The article describes the design and optimization of operation of an electric bus powered by the hydrogen fuel cells. At the beginning, an approach to design of a 12-meter urban bus, powered by hydrogen, is presented, as well as examples of components for its construction. Next, the problem of selecting the size of traction batteries and stacks of the Proton Exchange Membrane (PEM) hydrogen fuel cells was discussed. These are the key components affecting the price of the bus and should be subject to optimization. The results of optimization of the size of traction batteries and the fuel cell system for a bus traveling in inter-city traffic are presented. The optimization was based on data from the literature and data from the monitoring system of actual hydrogen powered buses located on the Internet platform. The main purpose of the research, which was to determine the total costs of ownership (TCO), is presented as well.

Article info

Received 17 September 2020
Accepted 22 March 2021
Online 23 August 2021

Keywords:

hydrogen,
fuel cell,
fuel cell bus,
control strategy,
total costs of ownership,
energy management

Available online: https://doi.org/10.26552/com.C.2021.4.E56-E67

ISSN 1335-4205 (print version)
ISSN 2585-7878 (online version)

This is an open access article distributed under the terms of the Creative Commons Attribution 4.0 International License (CC BY 4.0), which permits use, distribution, and reproduction in any medium, provided the original publication is properly cited. No use, distribution or reproduction is permitted which does not comply with these terms.

1 Introduction

The constant pursuit of improving air quality in cities has given rise to the need for new solutions aimed at reducing CO_2 emissions. This includes the urban transport sector [1]. The use of alternative fuels and propulsion systems based on electricity and hydrogen is an important activity in this respect [2]. Alternative fuels, characterized by the low CO_2 emissions, are an important factor in the gradual reduction of transport emissions, which is the basic goal of the Europe 2020 strategy. The strategy includes development of sustainable transport for the first half of the 21st century regarding a 60% reduction in CO_2 emissions by 2050 in transport. The use of such fuels will also have a beneficial effect on the ability of urban areas to meet the EU air quality commitments, this includes the elimination of conventional vehicles by 2050. Both city authorities [3], municipal transport companies and bus manufacturers are involved in pursuing this goal [4]. Buses fleet electrification is possible by production of the new models or conversion existing vehicles [5-6]. It is noteworthy that the zero emissions of electric and electric-hydrogen buses at their place of use is just one of their many advantages. Other benefits include a lack of noise [7], vibrations and a high level of driving dynamics resulting from characteristics of electric motors [8].

For the city and intercity buses, the area of energy management is very wide. Many research works, carried out in the last 10 years, are concerned with the optimal use of energy from several decentralized sources, most of which use renewable energy sources. Hydrogen and fuel cells are seen as an indispensable component of both stationary and mobile electricity generators [9-10]. Very often energy production and its consumption on board vehicles are considered separately. Fuel consumption prediction is very helpful in planning a hydrogen vehicle route [11].

Entire hydrogen-powered fleets are being increasingly implemented in selected European cities. Such investments are long-term investments and, in addition to the vehicles themselves, require the construction of infrastructure for hydrogen production and refuelling [12]. Increasingly, hydrogen to power vehicles comes from the electrolysis of water using electricity from renewable energy sources. Such hydrogen is characterized by very high purity and does not contain any harmful components that can poison hydrogen fuel cells. In the case of long-term investments, the time of correct operation of both hydrogen cells and hydrogen fuel cells is of a great importance [13]. For the latter, the expected working time is from 20,000 to 30,000 hours and the guaranteed time is 15,000 hours. The entire vehicle fleet should be able to be monitored online, which

allows for preventive maintenance and optimization of all the application functions. Online and offline analyses allow to calculate the actual costs of using vehicles. They can be used to calculate the payback time and to compare the costs of different solutions to each other.

When it comes to energy management on board vehicles, it can be seen that it is more convenient to separate the two problems according to the time horizon. In the long term, energy management can be based on criteria depending on forecasts, investment and infrastructure costs, and the size of optimization steps. The real-time energy management is, however, required to achieve optimal power distribution on board the vehicle subject to power restrictions using given powertrain architecture components [14].

In the case of the hybrid bus traction system, the power demand must be met. Full optimization is possible with knowledge of the power flow characteristics and route profile. The total optimum is achieved provided that the energy consumption is minimized over the entire known route [15].

Previous articles explored different approaches to managing energy distribution for the same type of traction chain and increasing autonomy, minimizing fuel consumption by the main power source [16]. Among these approaches, dynamic programming, used offline when the route profile is known, is undoubtedly the most cited in the literature. This method, based on the Bellman principle, based on the discretization of the energy space of the storage system, reveals some weaknesses associated with the choice of the size of the discretization step, which significantly affects the time of calculations and the quality of decisions. Another method often cited in this area is the Optimal Control approach based on the Pontryagin minimum principle and calculation of derivatives of the Hamilton function or reporting of consumption of all the sources in an equivalent space in which the optimal control is carried out. Energy management methods on board hydrogen buses are still being developed with using a combinatorial optimisation approach to energy management [17]. Very promising is a real-time optimization [14], hierarchical approximate global optimization [18] and multi-mode prediction of the energy consumption, both in the stationary and mobile applications [19]. Control strategies for fuel saving in the hydrogen fuel cell vehicles should be still developed and promptly applied to existing and new produced vehicles [20-21].

City and intercity buses are usually built in hybrid systems. Most of them are specially designed to achieve the low total costs of ownership for heavy duty applications. The element, contributing to the low total cost of ownership, is selection of the key components with long life and high performance [22]. The power of hydrogen fuel cells and the energy capacity of traction batteries determine not only the production costs of a hydrogen bus, but its performance and operating costs, as well.

The authors propose a comprehensive approach to design of a hydrogen bus taking into account its exact purpose. This approach has used all the latest components on the market for hydrogen bus construction and control techniques. All the stages that take into account the simulation should then be validated under real conditions [23].

2 Components of the electric and hydrogen city bus

During the last 10 years, electric drive systems dominated with increasingly larger traction batteries in order to obtain a greater range. This took place both for the drive of passenger vehicles and buses. However, many companies conducted parallel research and development related to use of hydrogen as fuel. Stacks of fuel cells and hydrogen tanks capable of powering city buses have been developed. Hydrogen technologies have the special advantage of faster hydrogen refuelling than charging vehicle traction batteries with fast DC chargers. Development of the hydrogen refuelling infrastructure for vehicles at 350 and 700 bar was also observed. These are favourable conditions for dissemination of the hydrogen-using drives in both passenger cars and buses.

In the 21st century, many components became available to build an electric bus drive system. The most important of them include: an electric motor and traction batteries and in the case of hydrogen propulsion, a fuel cell stack and hydrogen tanks. The appropriate selection of each component determines the suitability of the bus for a specific application (urban, intercity) and its price. In addition to the correct selection of components, it is also important to integrate them in order to obtain the trouble-free operation with high efficiency [24].

2.1 Electric motor and drive axle

The task of the electric drive system is to efficiently transfer power to the road wheels in all the bus operating conditions [25]. One of the most important components is the electric motor whose parameters determine its suitability for bus propulsion. According to global and European trends, in production of both passenger cars and buses, a Permanent Magnet Synchronous Motor (PMSM) is the most popular choice.

Three drive concepts, central-motor, electric portal axle and in wheel hub drive, fitted in a 12 metre electric bus with a daily mileage of 200 km based on a usage period of 340 days a year, were compared by a bus manufacturer (see Figure 1). The bus was equipped according to the current standard of the respective manufacturers and the selected driving cycle SORT2. In order to ensure comparability, the tyre pressure and the total/overall vehicle weight (m 14,410 kg) were adjusted accordingly [26].

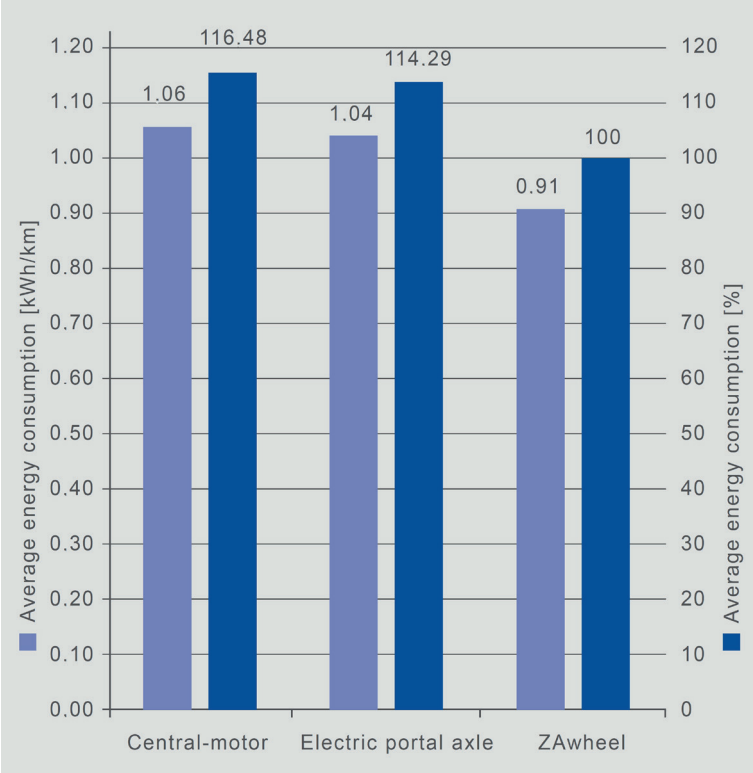


Figure 1 *Comparison of different drive concepts [26]*

The results were unambiguous. The direct costs benefits of a wheel hub drive include:

- Reduction of initial costs due to smaller battery pack (approx. 30 kWh lower)
- Reduction of annual operational costs due to low energy consumption (approx. 8,840 - 10,200 kWh less)

Further benefits of the wheel hub drive:

- Minimal installation space requirements
- Weight reduction
- Low maintenance
- Minimal noise characteristics (< 70 dBA at 80 km/h)

2.2 Traction battery

Traction batteries are another key component of the electric bus drive system. The most common technology used in the automotive industry is lithium-ion batteries, which are available in many varieties [27]. According to the authors, the NMC-type lithium-ion batteries (lithium nickel manganese cobalt oxide battery - LiNiMnCoO2 or NMC) should be used to build a low-costs, but highly reliable energy storage system. Lithium-titanium (LTO) batteries are increasingly used in the construction of electric buses [28]. They are characterized by a tolerance to very high currents during the charging process, which significantly reduces the charging time. Supercapacitors are used for the short-term storage of electrical energy recovered during the braking [29]. However, due to their high price and limited use, they have not been fitted in many road vehicles as yet [30]. The charging process of the batteries should be included in any discussion about traction batteries. The optimal solution, due to infrastructure costs and the time required to fully charge the battery, is charging with direct current using external chargers. The CCS Combo 2 charging system can charge with up to 150 kW of power. It is worthwhile for every electric bus to have an on-board charger with a power output of at least 20 kW, which may be supplied from a three-phase 400 V socket. The expansion of the charging infrastructure should be developed along with an increase in the number of electric buses [31].

2.3 Fuel cell system

The type of fuel cell that best meets contemporary automotive requirements is the PEM (Proton Exchange Membrane) cell. This assertion has been confirmed by the trends among leaders in this field. The PEM fuel cells have been used to build many working prototypes and commercial vehicles.

The choice of the LTPEM (Low Temperature Proton Exchange Membrane) or High Temperature HTPEM (High Temperature Proton Exchange Membrane) system has a significant impact on the control strategies used for the entire power generation system under various operating conditions and this translates into some challenges related to their operation. The LTPEM functions normally at temperatures of up to 85 °C while the HTPEM operates normally up to 200 °C.

Table 1 *Comparison of parameters of different hydrogen buses*

bus name or project title	electric motor type and power (kW)	battery type and energy capacity (kWh)	fuel cell system type and power (kW)	hydrogen tanks capacity (kg)	additional systems
Ursus bus hydrogen bus	wheel-hub 2x110	2x37.8	2x30	33	
Van Hool CHIC		100	150	35	break resistors
EVO bus CHIC	wheel-hub	250	2x60	35	
Wrightbus		0	75	33	break resistors, supercapacitor 240 kW
Solaris Urbino 12	wheel-hub 2x125	120	60	36.8	

The HTPEM systems, despite several disadvantages, have numerous advantages over the LTPEM systems, as well. The first of these concerns the lack of a need to moisten the membrane and use of a complicated and expensive humidifier. Further advantages with the simple construction of the entire HTPEM system are associated with the greater efficiency of the entire system, which compensates for the 10% lower voltage performance of the cell itself [32]. Greater CO tolerance by the HTPEM systems translates into the possibility of using hydrogen from steam reforming of hydrocarbon fuels to supply them.

In the case of use of the hydrogen, originating from hydrolysis or reforming characterized by a purity of 99.999%, the cheapest solution would be to use LTPEM type cells.

2.4 Hydrogen storage

There are many ways to accumulate hydrogen. It can be collected in a compressed or cryogenic version. The latter method allows for accumulation of large amounts of hydrogen in a small volume. However, this is very expensive due to the need to maintain very low temperatures at the level of production, distribution and transport of hydrogen. There are also hybrid tanks available with cryogenic and additionally compressed hydrogen (cryo-compressed tanks) [33]. Hydrogen can also be collected in metal hydrides. They are very straightforward to use and efficient, but they have one drawback - they are excessively heavy. One of the newest methods of hydrogen accumulation is use of tanks made from carbon nanotubes [34]. However, metal or composite high pressure tanks are most often used to accumulate hydrogen on board vehicles. Several European and global manufacturers produce tanks with international approval.

3 Overview of solutions in existing projects

Continuous striving to improve air quality in cities necessitates the search for new solutions aimed at reducing CO_2 emissions in the urban transport sector. An important activity in this area is use of alternative fuels and drives. Currently, they include electricity and hydrogen. Polish and European urban bus manufacturers are introducing new generations of eco-friendly city buses [1].

Electric-hydrogen bus projects are most often implemented by consortia of bus manufacturers, universities, research institutes and science and technology parks. It is often the case that specialized start-ups with software and firmware programming skills in the newest programming languages are included in these groups. Table 1 gathers data from several ongoing projects that aim to build an electric-hydrogen bus at the TRL9 standard (Technology Readiness Level).

4 Research aim - Ursus demo hydrogen bus

A practical example of a performance design and production costs optimization is the Ursus Demo Hydrogen Bus. The vehicle uses two 30 kW LTPEM cell modules (total power 60 kW), compatible with a set of NMC lithium-ion batteries with an energy capacity of 70 kWh. More specifically, it is an electric bus with a hydrogen range extender [35]. This is due to impossibility of the supplying the electric motor directly from the fuel cell system. The motors are powered by traction batteries and the hydrogen system recharges them constantly.

Hydrogen is stored on board in a compressed form under a pressure of 35 MPa, which is the European standard in this area. The vehicle range is approximately 450 km and is expected to increase. The service life assumed by the manufacturer is 20 000 working hours, which corresponds to a mileage of 700 000 km.

The drive system consists of electric motors located in the wheel hubs, roof-mounted traction batteries and 2 hydrogen fuel cell modules located at the back of the bus, as shown in Figure 2.

The electric bus with a hydrogen range extender has many advantages, which include [36]:

- traction properties exceeding those of typical electric buses - the vehicle's range without charging the

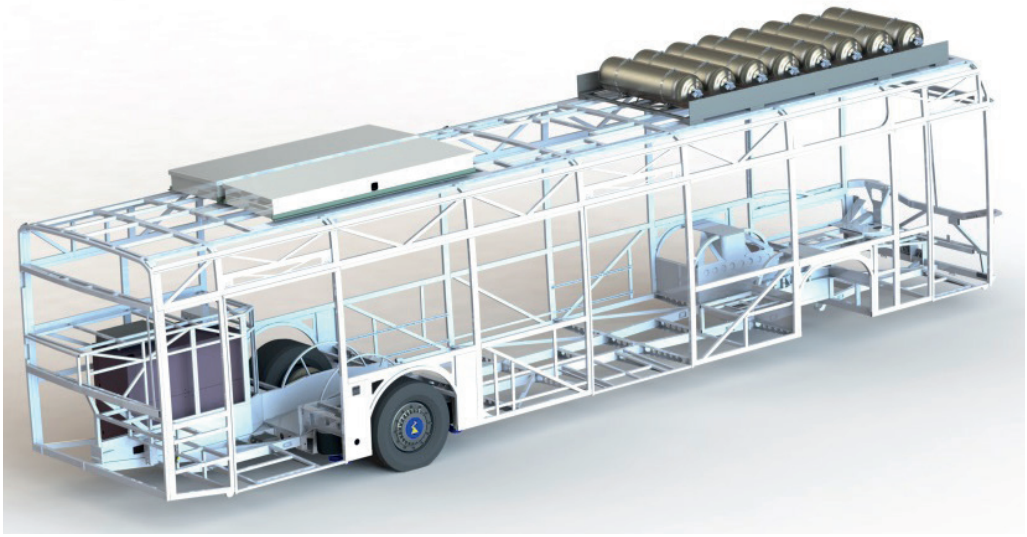


Figure 2 *Arrangement of components in the bus*

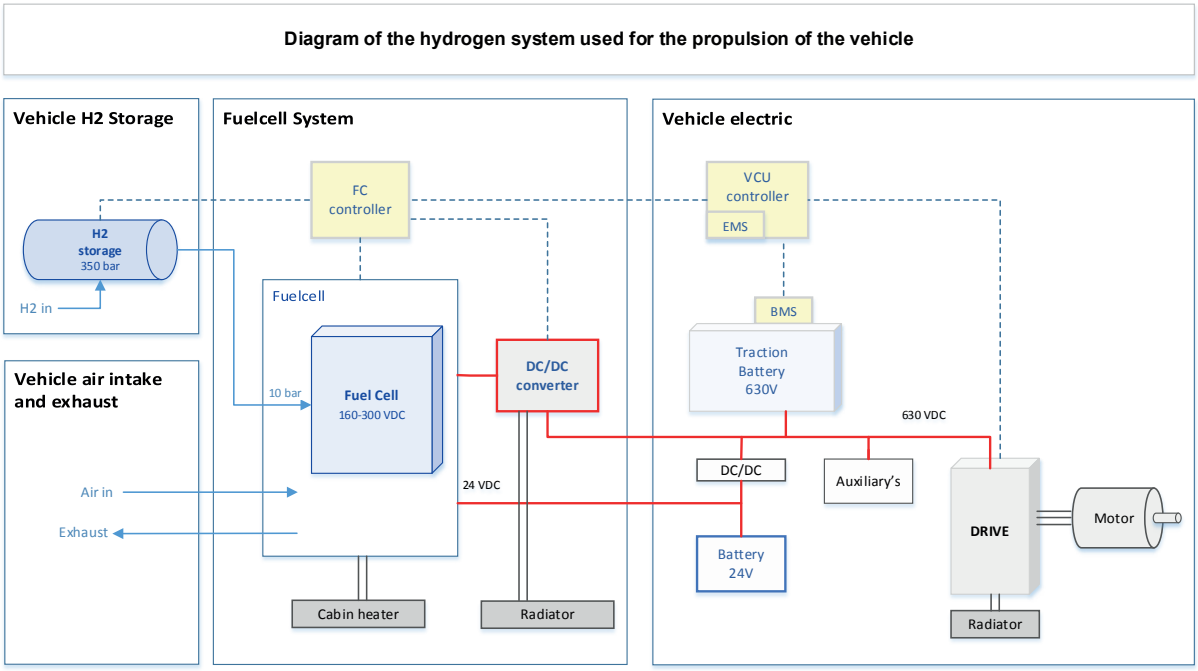


Figure 3 *Diagram of the propulsion system of the hydrogen bus*

battery is approximately 450 km;

- the option of travelling on intercity communication lines;
- quick refuelling of hydrogen to on-board tanks, the process lasts approximately 15 min;
- high travel comfort - "smooth ride", no noise or vibration.

The Ursus FCEB (Fuel Cell Electric Bus) passed all of the relevant tests and was approved in the M3 category [1].

This article considers the special structure of a hybrid electric vehicle with two power sources: a fuel cell and traction batteries. A detailed diagram of the bus drive system is shown in Figure 3.

5 Bus monitoring using an online platform

Effective structural optimization in the scope of component selection and costs reduction in the area of the costs of constructing and operating electric-hydrogen buses cannot be based solely on a literature analysis. All the issues, subjected to theoretical analysis, should be validated under real conditions. In order to make this feasible, the bus must have the facilities of a mobile laboratory capable of making advanced measurements of selected parameters. In addition, it must be able to collect large amounts of measurement data and transmit them by various methods of wired and wireless transmission. The next challenge is their processing and

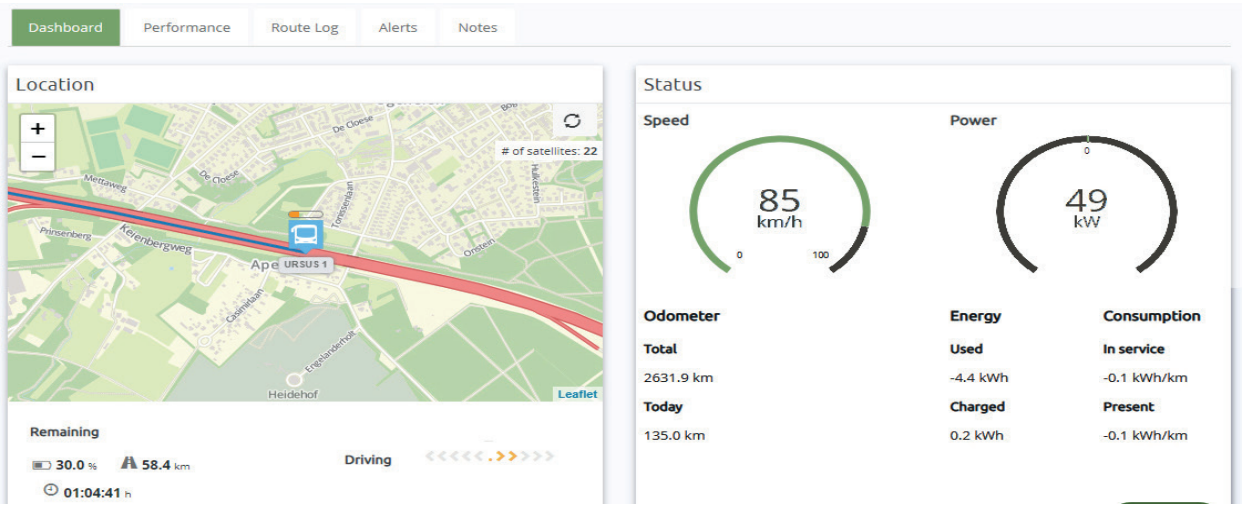


Figure 4 *Internet platform window [37]*

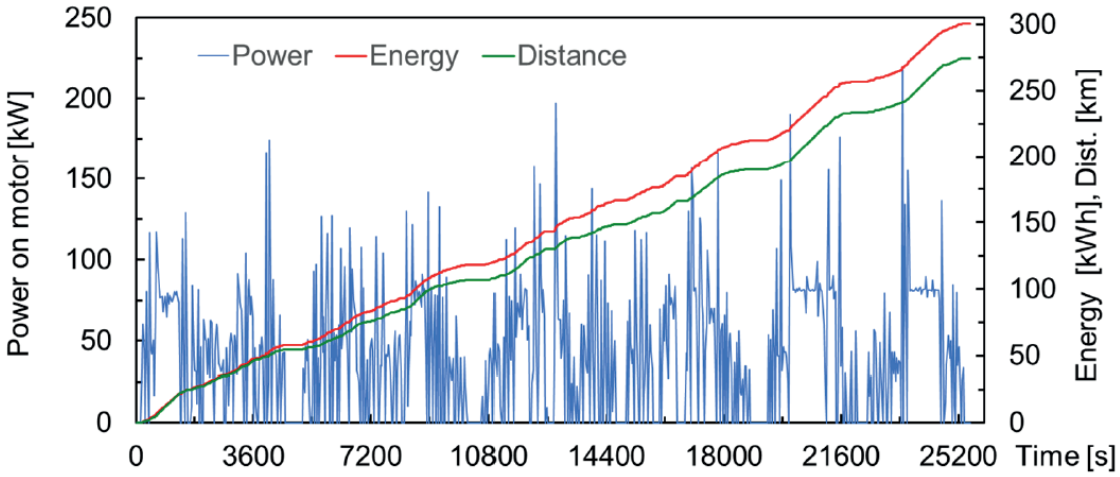


Figure 5 *Results of dynamic models testing*

careful analysis. In recent times, advanced systems have been acquired, for transmitting and visualizing data from vehicles. An example is shown in Figure 4.

The platform allows for the on-line reading of selected parameters and their off-line analysis [37]. It is a very useful tool for monitoring the correctness of work, error diagnostics and the optimization of electric-hydrogen propulsion systems.

6 Simulation testing

Based on the real data from driving an electric-hydrogen bus, dynamic models of electricity and hydrogen consumption were constructed on board the bus [38]. The model of the electric-hydrogen drive system takes into account the power of the fuel cell module, its efficiency and the efficiency of the air compressor [39]. Results of testing dynamic models are presented in Figure 5.

After that, a representative inter-city route of 275 km was chosen, which the vehicle covered at an average speed of 38.6 km/h (Figure 6). This distance is too great for a conventional electric bus to travel, especially at such a high speed. Energy of 300 kWh is required to complete the entire journey. It is therefore necessary to use an electric-hydrogen drive. The task of the simulation tests is to determine which components are capable of accumulating electricity (traction batteries) and generating energy (hydrogen fuel cells) on board the vehicle.

Intelligent offline energy management is critical to meeting the requirements of an electric motor, while complying with various restrictions of hybrid vehicles related to system operation, safety conditions and power source designs. Various fuel cell systems and energy split control algorithms [40] have been tested taking into account fuzzy logic/proportional and adaptive [41-42].

Based on simulation tests, the total amount of energy needed to cover a representative route was determined. This energy comes primarily from hydrogen accumulated in the tanks. Only a small part of it comes from the vehicle's traction battery. Based on the exact amounts of hydrogen consumed and the electricity taken to charge the traction batteries, one can calculate the costs of the vehicle's driving along a representative route.

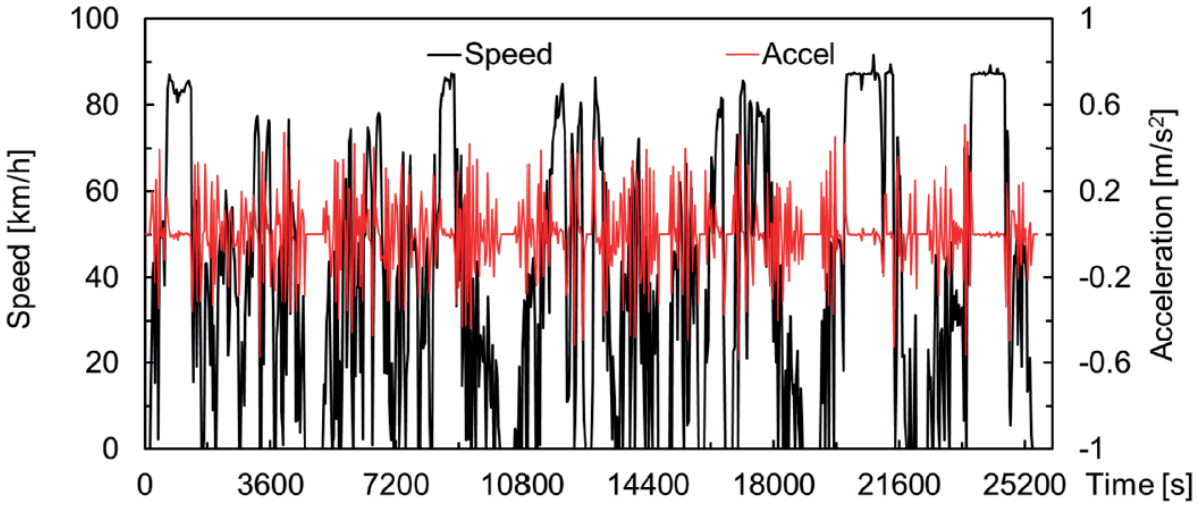


Figure 6 *Representative inter-city route*

7 Total costs of ownership calculations

The main purpose of the research was to determine the total costs of ownership (TCO) resulting from the construction and operation of a hydrogen bus at a given time and with a certain intensity. The costs of building a hydrogen bus were determined based on the component's configuration presented in Section 3. The calculation was made for many variants of sizes of the hydrogen fuel cells and traction batteries. The costs of operating a hydrogen bus on a selected route were calculated based on the simulation tests presented in Section 5. Compared to ICE buses, electric and fuel cell buses have less maintenance costs due to simpler mechanics of its electric motor. Based on the data contained in the report [43], the costs of maintaining a hydrogen bus in European conditions amount to USD 7.02/100 km. USD to EUR exchange rate is 0.82.

The following assumptions were used during the simulation tests:

- the price of a basic bus (called C_{BUS}) with 33 kg hydrogen tanks is 280,000 €
- the size of the lithium-ion battery packs is 33.33 kWh and is scalable to a maximum energy capacity of 233.33 kWh
- the power of the hydrogen fuel cell systems is 30 kW and it is scalable to a maximum power of 210 kW
- the prices of the lithium-ion battery packs (called C_{BAT}) are the average value of 3 offers received from various manufacturers in 2018 and amount to 27,906.98 €
- the prices of the hydrogen fuel cell systems (called C_{FC}) are the average value of 3 offers received from various manufacturers in 2018 and amount to 58,139.53 €
- the hydrogen price is 6 €/kg
- the price of electricity is 0.2 €/kWh
- the vehicle starts its journey with 100 % charged (SOC) traction batteries
- the traction batteries are not charged from external sources while driving
- the vehicle recovers energy during braking [44]
- no hydrogen refuelling takes place while driving
- the vehicle travels along a representative route 340 days a year over a period of 8 years of operation
- the total costs of ownership include the costs of buying a bus in a given configuration and the costs of fuel (electricity and hydrogen) and costs of maintenance

The bottom-up approach is taken for the TCO analysis across the Europe, across a 8-year timespan. The presented approach takes into account the modular construction of an electric-hydrogen bus from any number of hydrogen fuel cell modules and traction battery packs. This approach looks not only at detailed build costs for a Fuel Cell Bus, down to the drivetrain, fuel system and others, but also at operational costs such as fuel, maintenance and so forth. In authors' opinion this approach is not only unique in the marketplace, but also offers the readers a perspective that can be applied to almost any operational business model.

Equation for calculation of the costs of building a Fuel Cell Bus (TC_{FCB}), in various battery and fuel cell configurations, was determined as:

$$TC_{FCB} = C_{BUS} + C_{FC} \times n_{FC} + C_{BAT} \times n_{BAT}, \quad (1)$$

where:
C_{BUS} - Costs of Basic Bus,
C_{FC} - Costs of Fuel Cell Module,
n_{FC} - number of Fuel Cell Modules,
C_{BAT} - Costs of Battery Pack,
n_{BAT} - number of Battery Packs.

As a result of simulation tests the following was determined:

- total costs of building an electric-hydrogen bus in various battery and fuel cell configurations (Table 2)

Table 2 *Costs of the basic bus, battery packs and fuel cell systems in different configurations*

cost of basic bus + battery packs + fuel cell systems (€)								
		fuel cells power (kW)						
		30	60	90	120	150	180	210
battery capacity (kWh)	33.33	366 047	424 186	482 326	540 465	598 605	656 744	714 884
	66.66	393 953	452 093	510 233	568 372	626 512	684 651	742 791
	100	421 860	480 000	538 140	596 279	654 419	712 558	770 698
	133.33	449 767	507 907	566 047	624 186	682 326	740 465	798 605
	166.66	477 674	535 814	593 953	652 093	710 233	768 372	826 512
	200	505 581	563 721	621 860	680 000	738 140	796 279	854 419
	233.3	533 488	591 628	649 767	707 907	766 047	824 186	882 326

- the amount of hydrogen (Table 3) and electricity consumed (Table 4)
- fuel costs (electricity + hydrogen)
- TCO (Table 5)

Total costs of building an electric-hydrogen bus in various battery and fuel cell configurations is presented in Table 2. The costs of the electric-hydrogen bus include the costs of the base bus and the number of individual fuel cell modules and traction battery packs. The cheapest version of the base bus with one fuel cell module and one battery pack costs € 366,047. Buses are manufactured in a modular design and any number of fuel cell modules and battery packs can be installed on board. Of course, there are some limitations to the weight of the battery packs and the volume of the fuel cell modules. The greater number of components of the electric-hydrogen drive system reduces the weight and volume of the transported cargo, i.e. passengers. Due to these requirements, the number of fuel cell modules and battery packs is limited to seven. The fuel cell modules are more expensive than battery packs of comparable power. Therefore, a bus with more fuel cell modules than the battery packs will be more expensive.

An important component of the TCO is the costs associated with use of the hydrogen bus. The equation for calculation of the operational costs (C_{OP}) was determined as:

$$C_{OP}=C_{H2}+C_{EL}+C_{MAINT}, \quad (2)$$

where:
C_{H2} - Hydrogen Costs,
C_{EL} - Electricity Costs,
C_{MAINT} - Maintenance Costs.

Operating costs of the selected costs items (hydrogen costs, electricity costs, maintenance costs) were set by the following:

- Fuel costs (hydrogen) were calculated based on the specific hydrogen consumption to cover representative route, assumed distance travel (Σkm) and actual hydrogen price.
- Electricity costs were calculated based on the specific energy consumption from batteries to cover representative route, assumed travel distance (Σkm) and actual electricity price.
- Determination of operating costs also required calculation of other costs. Other costs were defined as a planned repair and maintenance (washing, disinfection, standard repairs), vehicle technical control (1-year intervals) and regular vehicle service control at a mileage of 10 000 km. The average costs of maintaining a hydrogen bus in European conditions, as mentioned before, amount to USD 7.02 / 100 km.

The first component of operating costs are the hydrogen costs, which depend on its consumption. Simulations results of the hydrogen consumption necessary to cover a representative route is presented in Table 3. Hydrogen consumption was calculated using the dynamic model described in Section 5. Hydrogen consumption was calculated for each constructional configuration of an electric-hydrogen bus. The calculated hydrogen consumption takes into account the total power and efficiency of the fuel cell modules, as well as the power and efficiency of the air compressor. Buses with smaller number of fuel cell modules will run with a higher load of the fuel cell stacks. Such operating points are characterized by higher efficiency and lower hydrogen consumption. However, they need larger traction battery packs to cover the power requirements of the traction motors.

Due to the consumption of hydrogen, there are certain limitations in the construction of an electric-hydrogen bus. Hypothetical cases are highlighted in various colours in Table 3:

- insufficient energy capacity of traction batteries (*)
- battery discharge current too high ($^{+}$)
- excessive hydrogen consumption (‡).

For a bus consisting of one fuel cell module and several battery packs, the amount of energy stored and produced in them may not be sufficient to cover the representative route (yellow). For a bus configuration with a small number of battery packs and a large number of fuel cell modules, the hydrogen consumption may be so high that it will not fit into the existing 33 kg hydrogen tanks. This case is marked in blue.

Table 3 *Hydrogen consumption necessary to cover a representative route*

		hydrogen consumption (kg)						
		fuel cells power (kW)						
		30	60	90	120	150	180	210
battery capacity (kWh)	33.33	15.94*	28.48	35.97‡	38.22‡	44.87‡	56.35‡	70.30‡
	66.66	14.52*	26.03	33.28‡	35.14‡	40.72‡	51.22‡	62.88‡
	100	12.85*	23.67	29.77	32.66	37.58‡	46.59‡	56.83‡
	133.33	11.59*	21.44	27.55	30.09	34.23‡	42.15‡	51.01‡
	166.66	10.54*	19.62	24.91	27.87	31.41	38.75‡	46.66‡
	200	8.78+	16.98	21.52	24.31	27.30	33.10‡	38.94‡
	233.3	7.55+	14.88	19.08	22.11	24.75	29.84	34.67‡

Table 4 *Electricity consumption necessary to cover a representative route*

		electrical energy consumption (kWh)						
		30	60	90	120	150	180	210
battery capacity (kWh)	33.33	109.32*	20.09	17.53	17.62	17.95	18.29	18.46
	66.66	120.85*	36.27	33.97	34.07	34.39	34.77	34.95
	100	140.85*	52.72	50.46	50.57	50.87	51.27	51.45
	133.33	157.09*	69.21	66.96	67.17	67.38	67.77	67.95
	166.66	170.44*	85.70	83.46	83.67	83.90	84.27	84.45
	200	192.78+	102.21	99.96	100.06	100.40	100.77	100.95
	233.3	208.54+	119.23	116.46	116.67	116.91	117.27	117.44

Table 5 *TCOs for different bus configurations*

		total costs of ownership (€)						
		fuel cells power (kW)						
		30	60	90	120	150	180	210
battery capacity (kWh)	33.33	729 801*	944 077	1 122 983‡	1 217 998‡	1 384 831‡	1 630 458‡	1 916 388‡
	66.66	740 839*	940 828	1 116 086‡	1 204 605‡	1 353 913‡	1 583 591‡	1 832 101‡
	100	752 384*	939 119#	1 095 585	1 200 895	1 339 551‡	1 544 983‡	1 770 323‡
	133.33	768 598*	939 664	1 096 181	1 195 964	1 321 803‡	1 509 425‡	1 712 161‡
	166.66	786 600*	946 851	1 090 010	1 196 558	1 312 596	1 490 783‡	1 678 163‡
	200	797 925+	940 535	1 071 580	1 175 415	1 282 384	1 435 422‡	1 588 955‡
	233.3	814 251+	943 438	1 068 667	1 176 345	1 277 693	1 419 073	1 556 167‡

Simulations results of the electricity consumption, necessary to cover a representative route, is presented in Table 4. The amount of electricity stored in seven lithium-ion battery packs alone is not sufficient to cover the demand for a representative route of 275 km. An electric / hydrogen bus must be equipped with at least one hydrogen fuel cell module. In this case, however, there is another limitation related to the excessive battery discharge current (yellow). The research shows that an electric-hydrogen bus should consist of at least two fuel cell modules and any number of traction battery packs.

The TCO are therefore the sum of the total costs of Fuel Cell Bus TC_{FCB} in various battery and fuel cell configurations, Equation (1) and operational costs C_{OP}, Equation (2) as presented below:

$$TCO=TC_{FCB}+C_{OP}. \quad (3)$$

Assumed travel distance (Σkm) is based on the length of the representative route (275 km). The vehicle travels along a representative route 340 days a year over a period of 8 years of operation. The results of the simulation tests of TCO are shown in Table 5.

For the TCO, there is an optimum - minimum (#) that corresponds to a bus configuration consisting of a 60 kW fuel cell system and traction batteries with an energy capacity of 100 kWh. For a specific representative route, any other configuration of the number of fuel cell modules and lithium ion battery packs will be less economical. Increasing the number of fuel cell modules will only cause them to work with less efficiency, which will contribute to an increase in hydrogen consumption.

Increasing the number of battery packs will increase the costs of purchasing the bus and increase its weight.

Additional economic and ecological benefits can be obtained by producing electricity and hydrogen from renewable energy sources [45].

8 Summary and conclusions

The construction of a structurally and costs-optimized electric-hydrogen bus is not straightforward, but it is feasible. A scientific approach should be used. Firstly. a review of the current state of the relevant science and technology in selected areas is required. These areas are associated with the relevant components needed to construct such a bus. An analysis of the state of the art would enable the selection of the most common and reliable components. This would allow for costs optimization. For the TCO, there is an optimum - minimum that corresponds to a bus configuration consisting of a 60 kW fuel cell system and traction batteries with an energy capacity of 100 kWh. An analysis of the relevant research areas is even more important since it allows for the sourcing of innovative components that will deliver a competitive advantage.

The approach proposed by the authors is universal. It should be carried out at the stage of developing design assumptions for each electric-hydrogen bus. This approach takes into account the purpose of the bus to cover the assumed routes. A different representative route is selected for urban, intercity or mixed travel. Based on that, the basic design assumptions of the electric-hydrogen drive system can be made and the consumption of hydrogen and electricity stored in battery packets can be determined.

Due to the great interest in production of buses powered by hydrogen fuel cells in Poland. the authors plan further research in this area. The dynamic model of the electric-hydrogen drive system can be freely modified as a result of development of components with better performance. Various control algorithms can be used to calculate the energy consumption of the bus needed to travel the representative route. Therefore. the presented approach can be used to make all kinds of comparisons of the system performance and economic costs.

References

[1] BERGER, R. Fuel cell electric buses - potential for sustainable public transport in Europe. A Study for the fuel cells and hydrogen joint undertaking [online] [accessed 2020-03-13]. 2015. Available from: http://www.fch.europa.eu/sites/default/files/150909_FINAL_Bus_Study_Report_OUT_0.PDF

[2] CHANG, C. C., LIAO, Y. T., CHANG, Y. W. Life cycle assessment of alternative energy types - including hydrogen - for public city buses in Taiwan. *International Journal of Hydrogen Energy* [online]. 2019, **44**(33), p. 18472-18482. ISSN 0360-3199. Available from: https://doi.org/10.1016/j.ijhydene.2019.05.073

[3] LANE, B., SHAFFER, B., SAMUELSEN, G. S. Plug-in fuel cell electric vehicles: a California case study. *International Journal of Hydrogen Energy* [online]. 2017, **42**(20), p. 14294-14300. ISSN 0360-3199. Available from: https://doi.org/10.1016/j.ijhydene.2017.03.035

[4] LEE, D. Y., ELGOWAINY, A., VIJAYAGOPAL, R. Well-to-wheel environmental implications of fuel economy targets for hydrogen fuel cell electric buses in the United States. *Energy Policy* [online]. 2019, **128**, p. 565-583. ISSN 0301-4215. Available from: https://doi.org/10.1016/j.enpol.2019.01.021

[5] GABSALIKHOVA, L., SADYGOVA, G., ALMETOVA, Z. Activities to convert the public transport fleet to electric buses. *Transportation Research Procedia* [online]. 2018, **36**, p. 669-675. ISSN 2352-1465. Available from: https://doi.org/10.1016/j.trpro.2018.12.127

[6] MELO, P., RIBAU, J., SILVA, C. Urban bus fleet conversion to hybrid fuel cell optimal powertrains. *Procedia - Social and Behavioral Sciences* [online]. 2014, **111**, p. 692-701. ISSN 1877-0428. Available from: https://doi.org/10.1016/j.sbspro.2014.01.103

[7] LAIB, F., BRAUN, A., RID, W. Modelling noise reductions using electric buses in urban traffic. a case study from Stuttgart, Germany. *Transportation Research Procedia* [online]. 2019, **37**, p. 377-384. ISSN 2352-1465. Available from: https://doi.org/10.1016/j.trpro.2018.12.206

[8] CORREA, G., MUNOZ, P., FALAGUERRA, T., RODRIGUEZ, C. R. Performance comparison of conventional, hybrid, hydrogen and electric urban buses using well to wheel analysis. *Energy* [online]. 2017, **141**, p. 537-549. ISSN 0360-5442. Available from: https://doi.org/10.1016/j.energy.2017.09.066

[9] FUNEZ GUERRA, C., JAEN CAPARROS, M., NIETO CALDERON, B., SENDARRUBIAS CARBONERO, V., NIETO GALLEGO, E., REYES-BOZO, L., GODOY-FAUNDEZ, A., CLEMENTE-JUL, C., VYHMEISTER, E. Viability analysis of centralized hydrogen generation plant for use in mobility sector. *International Journal of Hydrogen Energy* [online]. 2018, **43**(26), p. 11793-11802. ISSN 0360-3199. Available from: https://doi.org/10.1016/j.ijhydene.2018.04.178

[10] FUNEZ GUERRA, C., REYES-BOZO, L., VYHMEISTER, E., JAEN CAPARROS, M., SALAZAR, J. L., GODOY-FAUNDEZ, A., CLEMENTE-JUL, C., VERASTEGUI-RAYO, D. Viability analysis of underground mining

machinery using green hydrogen as a fuel. *International Journal of Hydrogen Energy* [online]. 2020, **45**(8), p. 5112-5121. ISSN 0360-3199. Available from: https://doi.org/10.1016/j.ijhydene.2019.07.250

[11] NIEOCZYM, A., CABAN, J., DUDZIAK, A., STOMA, M. Autonomous vans - the planning process of transport tasks. *Open Engineering* [online]. 2020, **10**(1), p. 18-25. ISSN 2391-5439. Available from: https://doi.org/10.1515/eng-2020-0006

[12] NAVAS-ANGUITA, Z., GARCIA-GUSANO, D., DUFOUR, J., IRIBARREN, D. Prospective techno-economic and environmental assessment of a national hydrogen production mix for road transport. *Applied Energy* [online]. 2020, **259**, e114121. ISSN 0306-2619. Available from: https://doi.org/10.1016/j.apenergy.2019.114121

[13] PEI, P., CHEN, D., WU, Z., REN, P. Nonlinear methods for evaluating and online predicting the lifetime of fuel cells. *Applied Energy* [online]. 2019, **254**, e113730. ISSN 0306-2619. Available from: https://doi.org/10.1016/j.apenergy.2019.113730

[14] BIZON, N. Real-time optimization strategies of fuel cell hybrid power systems based on load-following control: a new strategy and a comparative study of topologies and fuel economy obtained. *Applied Energy* [online]. 2019, **241**, p. 444-460. ISSN 0306-2619. Available from: https://doi.org/10.1016/j.apenergy.2019.03.026

[15] DAS, H. S., TAN, C. W., YATIM, A. H. M. Fuel cell hybrid electric vehicles: a review on power conditioning units and topologies. *Renewable and Sustainable Energy Reviews* [online]. 2017, **76**, p. 268-291. ISSN 1364-0321. Available from: https://doi.org/10.1016/j.rser.2017.03.056

[16] SULAIMAN, N., HANNAN, M. A., MOHAMED, A., MAJLAN, E. H., WANDAUD, W. R. A review on energy management system for fuel cell hybrid electric vehicle: issues and challenges. *Renewable and Sustainable Energy Reviews* [online]. 2015, **52**, p. 802-814. ISSN 1364-0321. Available from: https://doi.org/10.1016/j.rser.2015.07.132

[17] CAUX, S., GAOUA, Y., LOPEZ, P. A combinatorial optimisation approach to energy management strategy for a hybrid fuel cell vehicle. *Energy* [online]. 2017, **133**, p. 219-230. ISSN 0360-5442. Available from: https://doi.org/10.1016/j.energy.2017.05.109

[18] YUAN, J., YANG, L., CHEN, Q. Intelligent energy management strategy based on hierarchical approximate global optimization for plug-in fuel cell hybrid electric vehicles. *International Journal of Hydrogen Energy* [online]. 2018, **43**(16), p. 8063-8078. ISSN 0360-3199. Available from: https://doi.org/10.1016/j.ijhydene.2018.03.033

[19] ZHOU, Y., RAVEY, A., PERA, M. C. Multi-mode predictive energy management for fuel cell hybrid electric vehicles using Markov driving pattern recognizer. *Applied Energy* [online]. 2020, **258**, e114057. ISSN 0306-2619. Available from: https://doi.org/10.1016/j.apenergy.2019.114057

[20] FLETCHER, T., THRING, R., WATKINSON, M. An energy management strategy to concurrently optimise fuel consumption and PEM fuel cell lifetime in a hybrid vehicle. *International Journal of Hydrogen Energy* [online]. 2016, **41**(46), p. 21503-21515. ISSN 0360-3199. Available from: https://doi.org/10.1016/j.ijhydene.2016.08.157

[21] HAMES, Y., KAYA, K., BALTACIOGLU, E., TURKSOY, A. Analysis of the control strategies for fuel saving in the hydrogen fuel cell vehicles. *International Journal of Hydrogen Energy* [online]. 2018, **43**(23), p. 10810-10821. ISSN 0360-3199. Available from: https://doi.org/10.1016/j.ijhydene.2017.12.150

[22] ZHANG, H., LI, X., LIU, X., YAN, J. Enhancing fuel cell durability for fuel cell plug-in hybrid electric vehicles through strategic power management. *Applied Energy* [online]. 2019, **241**, p. 483-490. ISSN 0306-2619. Available from: https://doi.org/10.1016/j.apenergy.2019.02.040

[23] CIPOLLONE, R., DI BATTISTA, D., MARCHIONNI, M., VILLANTE, C. Model based design and optimization of a fuel cell electric vehicle. *Energy Procedia* [online]. 2014, **45**, p. 71-80. ISSN 1876-6102. Available from: https://doi.org/10.1016/j.egypro.2014.01.009

[24] DE MIRANDA, P. E. V., CARREIRA, E. S., ICARDI, U. A., NUNES, G. S. Brazilian hybrid electric-hydrogen fuel cell bus: improved on-board energy management system. *International Journal of Hydrogen Energy* [online]. 2017, **42**(19), p. 13949-13959. ISSN 0360-3199. Available from: https://doi.org/10.1016/j.ijhydene.2016.12.155

[25] BIZON, N. Efficient fuel economy strategies for the fuel cell hybrid power systems under variable renewable/load power profile. *Applied Energy* [online]. 2019, **251**, e113400. ISSN 0306-2619. Available from: https://doi.org/10.1016/j.apenergy.2019.113400

[26] ZA wheel - energy savings lifeline - Ziehl-Abegg [online] [accessed 2020-03-13]. 2015. Available from: https://www.ziehl-abegg.com/gb/en/downloads/file/get/10917/

[27] JWA, K., LIM, O. Comparative life cycle assessment of lithium-ion battery electric bus and Diesel bus from well to wheel. *Energy Procedia* [online]. 2018, **145**, p. 223-227. ISSN 1876-6102. Available from: https://doi.org/10.1016/j.egypro.2018.04.039

[28] WANG, L., WANG, Z., JU, Q. Characteristic analysis of lithium titanate battery. *Energy Procedia* [online]. 2017, **105**, p. 4444-4449. ISSN 1876-6102. Available from: https://doi.org/10.1016/j.egypro.2017.03.942

[29] TONG, H. Y. Development of a driving cycle for a supercapacitor electric bus route in Hong Kong. *Sustainable Cities and Society* [online]. 2019, **48**, e101588. ISSN 2210-6707. Available from: https://doi.org/10.1016/j.scs.2019.101588

[30] ODEIM, F., ROES, J., HEINZEL, A. Power management optimization of an experimental fuel cell/battery/supercapacitor hybrid system. *Energies* [online]. 2015, **8**, p. 6302-6327. eISSN 1996-1073. Available from: https://doi.org/10.3390/en8076302

[31] XYLIA, M., SILVEIRA, S. The role of charging technologies in upscaling the use of electric buses in public transport: experiences from demonstration projects. *Transportation Research Part A: Policy and Practice* [online]. 2018, **118**, 399-415. ISSN 0965-8564. Available from: https://doi.org/10.1016/j.tra.2018.09.011

[32] ZULIANI, N., TACCANI, R. Micro-cogeneration system based on HTPEM fuel cell fuelled with natural gas: performance analysis. *Applied Energy* [online]. 2012, **97**, p. 802-808. ISSN 0306-2619. Available from: https://doi.org/10.1016/j.apenergy.2011.12.089

[33] AHLUWALIA, R. K., PENG, J., ROH, H. S., HUA, T. Q., JAMES, B. D. Supercritical cryo-compressed hydrogen storage for fuel cell electric buses. *International Journal of Hydrogen Energy* [online]. 2018, **43**(22), p. 10215-10231. ISSN 0360-3199. Available from: https://doi.org/10.1016/j.ijhydene.2018.04.113

[34] FAZLE KIBRIAA, A. K. M., MOA, Y. H., PARKA, K. S., NAHMA, K. S., YUN, M. H. Electrochemical hydrogen storage behaviors of CVD, AD and LA grown carbon nanotubes in KOH medium. *International Journal of Hydrogen Energy* [online]. 2001, **26**(8)**,** p. 823-829. ISSN 0360-3199. Available from: https://doi.org/10.1016/S0360-3199(01)00007-6

[35] GENG, C., JIN, X., ZHANG, X. Simulation research on a novel control strategy for fuel cell extended-range vehicles. *International Journal of Hydrogen Energy* [online]. 2019, **44**(1), p. 408-420. ISSN 0360-3199. Available from: https://doi.org/10.1016/j.ijhydene.2018.04.038

[36] ALVAREZ FERNANDEZA, R., CORBERA CARABALLO, S., BELTRAN CILLERUELO, F., LOZANO, J. A. Fuel optimization strategy for hydrogen fuel cell range extender vehicles applying genetic algorithms. *Renewable and Sustainable Energy Reviews* [online]. 2018, **81**(1), p. 655-668. ISSN 1364-0321. Available from: http://dx.doi.org/10.1016/j.rser.2017.08.047

[37] Viriciti Internet Platform [online] [accessed 2020-03-30]. Available from: https://dashboard.viriciti.com

[38] VEPSALAINEN, J., OTTO, K., LAJUNEN, A., TAMMI, K. Computationally efficient model for energy demand prediction of electric city bus in varying operating conditions. *Energy* [online]. 2019, **169**, p. 433-443. ISSN 0360-5442. Available from: https://doi.org/10.1016/j.energy.2018.12.064

[39] HUNICZ, J., KASPEREK, D., MALEK, A., SMIETANKA, M. Real-time monitoring and energy split optimization of a hybrid fuel-cell-battery city bus. In: 2nd International Conference on Science and Technology Research ICSTR: proceedings. 2019.

[40] CAI, Y., OUYANG, M. G., YANG, F. Impact of power split configurations on fuel consumption and battery degradation in plug-in hybrid electric city buses. *Applied Energy* [online]. 2017, **188**, p. 257-269. ISSN 0306-2619. Available from: https://doi.org/10.1016/j.apenergy.2016.11.126

[41] ZHANG, S., HU, X., XIE, S., SONG, Z., HOU, C. Adaptively coordinated optimization of battery aging and energy management in plug-in hybrid electric buses. *Applied Energy* [online]. 2019, **256**, e113891. ISSN 0306-2619. Available from: https://doi.org/10.1016/j.apenergy.2019.113891

[42] ETTIHIR, K., HIGUITA CANO, M., BOULON, L., AGBOSSOU, K. Design of an adaptive EMS for fuel cell vehicles. *International Journal of Hydrogen Energy* [online]. 2017, **42**(2), p. 1481-1489. ISSN 0360-3199. Available from: https://doi.org/10.1016/j.ijhydene.2016.07.211

[43] Fuelling the future of mobility hydrogen and fuel cell solutions for transportation - Deloitte Financial Advisory, Deloitte, China [online]. 2020. Available from: https://www2.deloitte.com/content/dam/Deloitte/cn/Documents/finance/deloitte-cn-fueling-the-future-of-mobility-en-200101.pdf

[44] CABAN, J., ZARAJCZYK, J., MALEK, A. Possibilities of using electric drives in city buses. In: 23rd International Scientific Conference Transport Means: proceedings. 2019. p. 543-547.

[45] MALEK, A., CABAN, J., WOJCIECHOWSKI, L. Charging electric cars as a way to increase the use of energy produced from RES. *Open Engineering* [online]. 2020, **10**(1), p. 98-104. ISSN 2391-5439. Available from: https://doi.org/10.1515/eng-2020-0009

TWO OBJECTIVE PUBLIC SERVICE SYSTEM DESIGN PROBLEM

Jaroslav Janáček, Michal Kohání, Dobroslav Grygar*, René Fabricius

Faculty of Management Science and Informatics, University of Zilina, Zilina, Slovakia

*E-mail of corresponding author: dobroslav.grygar@fri.uniza.sk

Resume

The public service system serves population spread over a geographical area from a given number of service centers. One of the possible approaches to the problem with two or more simultaneously applied contradicting objectives is determination of the so-called Pareto front, i.e. set of all the feasible non-dominated solutions. The Pareto front determination represents a crucial computational deal, when a large public service system is designed using an exact method. This process complexity evoked an idea to use an evolutionary metaheuristic, which can build up a set of non-dominated solution continuously in the form of an elite set. Nevertheless, the latter approach does not assure that the resulting set of solutions represents the true Pareto front of the multi-objective problem solutions. Within this paper, authors deal with both approaches to evaluate the difference between the exact and heuristic approaches.

Article info

Received 17 December 2020
Accepted 15 February 2021
Online 21 September 2021

Keywords:

service system,
multi-objective,
Pareto front,
exact approach,
genetic algorithm

Available online: https://doi.org/10.26552/com.C.2021.4.E68-E75

ISSN 1335-4205 (print version)
ISSN 2585-7878 (online version)

This is an open access article distributed under the terms of the Creative Commons Attribution 4.0 International License (CC BY 4.0), which permits use, distribution, and reproduction in any medium, provided the original publication is properly cited. No use, distribution or reproduction is permitted which does not comply with these terms.

1 Introduction

The public service system design problem is usually formulated as a task of selection of p-center locations from a finite set of possible center location so that a given objective, based on user's distances to the nearest service center, is minimal. According to applied objective, the design problem can be formulated in several ways. The most usual one is the way that prefers the solution with minimal average user's distances to the service center. This objective is called the min-sum or system objective and it has been used by many authors in emergency system designing. In this case, the problem is often presented as the weighted p-median problem [1-4]. This min-sum problem consists of determination of the p-center locations so that the sum of user's distances to the nearest service center, weighted by an expected number of the user demands, is minimal [5-6].

In contrast to the min-sum formulations, users of a public service system share cost of the system by paying tax, which approves them to claim the equal or fair access to the provided service. A plethora of fairness schemes was studied in connection with public service system design. The most known one is the min-max objective, where the maximal distance from a user to the nearest service center should be minimal. This formulation of the public service design is called the p - center problem. The strongest fairness scheme, applicable in the public service system design, is the so-called lexicographic min-max criterion [7]. When solving a fair public system design problem as the lexicographical min-max fair design, a sequential process of optimization is used. The nearest distance to the service center of the worst situated user is minimized first, followed by the minimizing of the distance of the second-worst situated users and so on, unless the minimal reached distance of the previously processed users is worsened.

All the above-mentioned formulations of public service system design have only one objective function and can be efficiently solved by the so-called radial approach in the case of the min-sum formulation [4, 8-10]. The min-max fair public service system design problem proved to be easily solvable using the radial formulation [11]. The radial formulation has been also successfully applied to the lexicographical min-max fair design [12].

When consequences of the fairness schemes were studied, it was found that the fair and system objectives contradict. It means that if a fair objective is minimized, then the system objective takes bigger, i.e. worse, value, what usually means that the fairer solution is paid by worsening of the average distance between a user and the service center [13-14]. The similar relationship can be observed between the sum of fixed charges and the cost of users' demand satisfaction [15]. The next case of the objective contradiction can be found in the field of fuzzy set theory applied to the public service system design in the situations, when traversing times in a transportation network are uncertain [16]. In such a case, the level of satisfaction contradicts to the min-sum objective function value [17].

All the mentioned cases represent a mathematically unsolvable situation because there exists a set of feasible solutions with different values of the objective functions and it is impossible to decide on the best one without an additional comparative rule. A possible approach to the public service system design with two or more contradicting objectives consists in producing Pareto front, or a set of non-dominated solutions. This output of the designing process enables to put the final decision on a supervising manager's board.

The real Pareto front is a set of all the non-dominated solutions, what means that each other solution, is outperformed by a solution of the front in each of the applied objectives. As the most of the public service system design problems have finite domains of objective functions, the real Pareto front can be obtained by a finite sequence of runs of an exact mathematical programming method. This approach represents a crucial computational deal, especially when a large public service system is designed using an exact mathematical programming method. It is necessary to consider that each run of the sequence represents solving of a hard and large combinatorial problem, which solution is obtained by time demanding inspection of a vast searching tree. To avoid this computational burden, professionals prefer a heuristic approach based on imitating the biological processes [18-19]. To obtain a good set of the non-dominated feasible solutions, an evolutionary metaheuristic seems to be a convenient tool, because an evolutionary metaheuristic is able to build up a set of the non-dominated solutions continuously in the form of an elite set [20]. Nevertheless, it must be taken into account that the latter approach does not assure that the resulting set of solutions represents the true Pareto front of the multi-objective problem solutions.

Within this paper, authors studied both approaches and compared them from the points of computational time and quality of the resulting set of non-dominated solutions. The solved cases of the public service system design will dispose of with min-sum and min-max objectives.

The remainder of the paper is organized as follows: Section 2 is devoted to the radial formulation of the min-sum problem with limited min-max criterion. The exact approach to Pareto front determination is described in Section 3 and metaheuristic approach is explained in Section 4. The associated numerical experiments are reported in Section 5. The results and findings are summarized in Section 6.

2 Radial formulation of the min-sum problem with the limited distance

The studied public service system is designed to satisfy demands for service of the system users, which are in the serviced area at finite set J of user locations. The demand of a user $j \in J$ is expressed by an expected frequency b_j of visits performed by a servicing vehicle. It is assumed that the vehicles start their servicing route from a service center and they return back to their center after a user's demand has been satisfied. The public service system design consists of locating of the p service centers at the possible service center locations, which form a finite set I. The further defined objectives are based on integer network distances, where symbol d_{ij} denotes the network distance from location $i \in I$ to the location $j \in J$ for any pair of locations from I and J. The min-sum objective function value $f^{mS}(I_1)$ for a given set I_1 of located service centers can be defined by:

$$f^{mS}(I_1) = \sum_{j \in J} b_j \min\{d_{ij} : i \in I_1\}. \tag{1}$$

The min-max objective function value $f^{mM}(I_1)$ of the same design I_1 of the public service system is given by:

$$f^{mM}(I_1) = \max\{\min\{d_{ij} : i \in I_1\} : j \in J\}. \tag{2}$$

The public service system design problem, with the min-sum objective and with limit h of any distance between a user and the associated service center, can be modelled by the combinatorial model in Equation (3).

$$\min\{f^{mS}(I_1) : I_1 \subset I, |I_1| = p, f^{mM}(I_1) \le h\}. \tag{3}$$

The problem in Equation (3) can be rewritten into a linear programming form in several ways and then the problem can be solved by any integer programing solver. Based on our previous experiences, we describe the problem by a radial model, which proved to be more easily solvable than the other models.

Let m denote the maximal relevant distance between a possible service center location and a user location. Then the following three-dimensional matrix $\{a_{ijs}\}$ can be defined by Equation (4) for each $i \in I$, $j \in J$ and s= 0, …, m-1.

$$if\ d_{ij} \le s\ then\ a_{ijs} = 1, else\ a_{ijs} = 0. \tag{4}$$

To complete the model, the decision variables $y_i \in \{0,1\}$ for $i \in I$ are introduced. The variable y_i models the decision on service center location at place $i \in I$. The variable takes the value of 1 if a service center is located at i and it takes the value of 0 otherwise. Further, the auxiliary zero-one variables x_{js} for $j \in J$ and s = 0, …, h-1 are introduced. The variable x_{js} takes the value of 1, if the distance from a user located at $j \in J$ to the nearest located center is greater than s and it takes the value of 0 otherwise. Then, the problem in Equation (3) can be formulated as follows.

$$Minimize \sum_{j \in J} b_j \sum_{s=0}^{h-1} x_{js}. \tag{5}$$

$$Subject\ to:\ x_{js} + \sum_{i \in I} a_{ijs} y_i \ge 1 \quad for\ j \in J, s = 0, \ldots, h-1 \tag{6}$$

$$\sum_{i \in I} y_i = p \tag{7}$$

$$\sum_{i \in I} a_{ijh} y_i \geq 1 \ \ for \ \ j \in J \tag{8}$$

$$y_i \in \{0,1\} \ \ for \ \ i \in I \tag{9}$$

$$x_{js} \geq 0 \ \ \ for \ \ j \in J, \ s = 0,1,\ldots,h-1 \, . \tag{10}$$

In this model, the objective function in Equation (5) represents the total travel distance necessary for satisfaction of all the users' demands, as the expression $x_{j0} + x_{j1} + x_{j2} + \ldots + x_{jh\text{-}1}$ constitutes the distance to user location j from the nearest located service.

The constraints in Equation (6) ensure that the variables x_{js} can take the value of 0, if there is at least one center located in radius s from the user location j and constraint in Equation (7) limits the number of located centers by p. The constraints in Equation (8) ensure that each user has a service center in the radius h.

Let $I_R(h)$ denote the resulting set of service center locations $\{i \in I: \ y_i^*=1\}$ obtained from optimal solution $(\boldsymbol{y}^*, \boldsymbol{x}^*)$ of the problem in Equations (5)-(10) for a given integer value h.

3 The Pareto front determination using the exact approach

Quality of any feasible solution I_1, of the above-mentioned public service design problem, can be evaluated according to each of the two contradicting objectives, $f^{mS}(I_1)$ and $f^{mM}(I_1)$, described by (1) and (2), respectively. A solution I_1^* is called the non-dominated if there exists no feasible solution I_1 such that $f^{mS}(I_1) \leq f^{mS}(I_1^*)$ and $f^{mM}(I_1) \leq f^{mM}(I_1^*)$ and, in addition, if it holds either $f^{mS}(I_1) < f^{mS}(I_1^*)$ or $f^{mM}(I_1) < f^{mM}(I_1^*)$. The real Pareto front is a set of all the non-dominated solutions. As the set of all the feasible solutions is finite, the Pareto front of the studied problem must be also finite and it can be obtained by the process described below.

Let the function $f^{mS}(I_R(h))$ be generalized so that it gives the value bigger than a penalty Q, when the problem has no feasible solution for given h. It is asserted that the Pareto front solutions can be selected from the sequence of solutions $I_R(h)$ for $h=h_0, \ldots, m$, where h_0 is the lowest integer, for which $f^{mS}(I_R(h_0))<Q$ holds, i.e. $I_R(h_0)$ is a feasible solution of the problem in Equation (3).

Obviously, the solution $I_R(h_0)$, evaluated by a pair of the two objective values $[f^{mS}(I_R(h_0)), \ f^{mM}(I_R(h_0))]$, is a non-dominated solution of the public service system design problem from the following reasons. In this case, the equality $h_0=f^{mM}(I_R(h_0))$ holds, since no feasible solution exists for $h < h_0$ and thus $f^{mM}(I_R(h_0)) \leq f^{mM}(I_1)$ holds for each feasible solution I_1. As $I_R(h_0)$ is optimal solution of Equation (3) for $h_0=f^{mM}(I_R(h_0))$, then each feasible solution I_1 satisfying $h_0=f^{mM}(I_1)$ also satisfies the following inequality $f^{mS}(I_1) \geq f^{mS}(I_R(h_0))$.

Further, the elements of the sequence $\{I_R(h) : h=h_0, \ldots, m\}$ must generally satisfy Equation:

$$\begin{aligned} &f^{mS}(I_R(h)) \geq f^{mS}(I_R(h+1)) \ and \\ &f^{mM}(I_R(h)) \leq f^{mM}(I_R(h+1)) \ for \\ &h = h_0, \ldots, m-1. \end{aligned} \tag{11}$$

It is noted that if $f^{mS}(I_R(h)) = f^{mS}(I_R(h+1))$, then $I_R(h+1)$ cannot be the new non-dominated solution, because it is either dominated by $I_R(h)$ or it has the same evaluation in both objective functions.

One can also prove that the implication in Equation (12) holds for the sequence $\{I_R(h) : h=h_0, \ldots, m\}$.

$$\begin{aligned} &if \ \ f^{mS}(I_R(h)) > f^{mS}(I_R(h+1)), then \, also \\ &f^{mM}(I_R(h)) < f^{mM}(I_R(h+1)) \ \ for \\ &h = h_0, \ldots, m-1. \end{aligned} \tag{12}$$

The implication can be proved by contradiction. Let it be supposed that the assumption holds and that $f^{mM}(I_R(h)) = f^{mM}(I_R(h+1))$. It means that the increase of h does not impact the optimal solution of Equation (3), i.e. no distance from a user to the nearest service center exceeds $f^{mM}(I_R(h))$. It follows that $f^{mS}(I_R(h)) = f^{mS}(I_R(h+1))$, what contradicts the assumption.

Now, one can claim that if $f^{mS}(I_R(h)) > f^{mS}(I_R(h+1))$, then $I_R(h+1)$ represents a new element of the Pareto front. The claim follows from the facts that $I_R(k)$ for $k<h+1$ does not dominate $I_R(h+1)$ and no solution $I_R(k)$ for $k>h+1$ can dominate $I_R(h+1)$ due to Equation (12).

Based on the above reasons, one can apply the following algorithm to establish the Pareto front for the solved problem.

0. Determine h_0 and insert $I_R(h_0)$ into the Pareto front. Set $h=h_0+1$.
1. While $h \leq m$ repeat step 2.
2. Compute $I_R(h)$.
   If $f^{mS}(I_R(h)) < f^{mS}(I_R(h\text{-}1))$, then insert $I_R(h)$ into the Pareto front.
   Set $h=h+1$.

4 The genetic algorithm for the set of non-dominated solutions

The genetic algorithm (GA) became popular in solving large combinatorial optimization problems. The main idea comes from the theory of evolution. In nature, populations exchanges are performed by transition and exchange of genetic information between members of a current population. This process is modelled using algorithmic operations of crossovers and mutations. The GA is suitable for solving problems where a solution can be represented by vector $\mathbf{y}$ with 0-1 components. A solution can be also called a member of a population or individual. This vector can be called chromosome and its components are called genes. Chromosomes modelled in this way are changed by implemented operations of

```
Choose an initial population of chromosomes (population size)
Select elite set from population (elite set size ratio)
while running time not elapse do
    copy elite set to next population
    while next population is not completed
        select two parents by tournament selection (tournament size ratio)
        perform crossover
        perform mutation (mutation probability, maximal mutation counts per offspring)
        perform offspring optimization (offspring optimization probability)
        insert new chromosomes to population
    end-while
    perform diversity test (mutation step, acceptable difference in the population, count of the population
    diversity controls)
end-while
```

Figure 1 *Used template of genetic algorithm with important parameters [21]*

mutation and crossover, like the natural process. The mutation changes the value of one or more components in chromosome with some probability. Crossover is the process of generating two offspring from two-parent chromosomes [21]. The set of newly created individuals represents a pool of candidates for the next population. The new population is formed using the approach where members of the elite set from the old population are transited to the new population and new population is created by selection of individuals from the pool.

In authors' previous research, the genetic algorithm was implemented as metaheuristic for the given problem. As mentioned above, the set of good solutions is evaluated by the two partially conflicting criteria in the problem. As a result, a collection of good solutions is preferred rather than the single best solution. That implementation yields the semi-Pareto front as the output of an optimization run. The semi-Pareto front, obtained by the heuristic, approximates the exact Pareto front. The semi Pareto front is a part of the elite set. Adjustment of this algorithm to the goal of obtaining the good semi-Pareto front is based on testing if the obtained solution should be added to the current semi-Pareto front. here is briefly introduced The basic structure of the implemented genetic algorithm, is here briefly introduced, in the form of a template shown in Figure 1 [21].

For the better explanation of the implemented algorithm the specific modifications, performed in the introduced steps of the template, are described. It is decided to represent a solution using a list of the p-locations instead of 0-1 vector. The 0-1 vector can be obtained by a simple conversion if necessary. The initial population is generated randomly. For this implementation, the special crossover and mutation were developed r to preserve the admissibility of the created solutions. That implementation of the crossover takes advantage of the fact that the number of differing genes in the two selected solutions is always even. Genes (possible located centres) that are the same in both parents are preserved in both offspring. For the set of differing genes, the associated portion of units is distributed randomly over the offspring so that each offspring gets the same number of units. This approach ensures that the offspring are also feasible solutions. Mutation process is also implemented with regarding the offspring feasibility. The mutation is a swap between one selected gene and the non-selected one.

One iteration of the population change works as follows. Individuals from the old elite set remain as individuals of the new population. To complete the new generation, the next individuals are obtained by crossover and selection from the previous population.

Pairs of individuals are selected from the previous generation by the random process called the tournament. It consists of random selection of individuals based on their fitness. This process is repeated until the population is complete. After that, the semi-Pareto front and elite set are updated in the following way. Each new member of the population is tested whether it belongs to the semi-Pareto front. If yes, it is inserted in it, dominated ones are removed. Then the process continues with the next iteration.

Tuning of the GA parameters is an important part of this study. Information on the GA parameters are given in the next Section.

5 Computational study

The multiple tests were performed to compare the metaheuristic approach with the exact results. All the heuristic tests were done on the following hardware: Processor Intel Core i5-4460 3.2 GHz, with 8 GB of DDR3 memory; the genetic algorithm was developed in the Java programming language; to obtain the exact results for the benchmarks described in the previous sections, the optimization software FICO Xpress 7.9 (64-bit, release 2015) was used and the experiments were run on a mobile workstation equipped with a processor

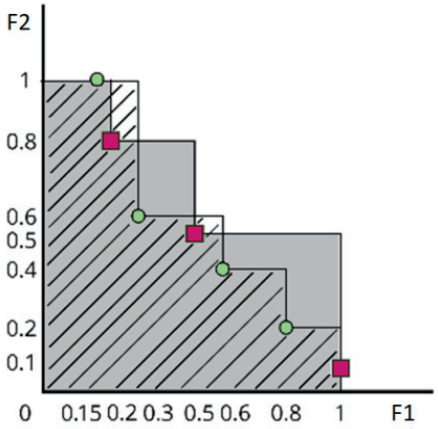


Figure 2 *Example of the two compared Pareto fronts, the first surface area of the Pareto front (area: 0.6) is marked in hatched, the second (area: 0.69) in grey; it is assumed, that the lower value is better, so the first front is the better one [20]*

Table 1 *Comparation of areas under normalized exact and approximate Pareto-fronts*

	exact result	heuristic GA - one by one		heuristic GA - each by each	
		average	best result	average	best result
BA	0.15854043	0.346925	0.20727	0.336714	0.233965
BB	0.060582	0.557023	0.382774	0.549060	0.360898
KE	0.069284634	0.367419	0.218435	0.365578	0.200383
NR	0.1614823	0.454372	0.329542	0.437669	0.304113
PO	0.045180031	0.543496	0.396628	0.4419	0.34113
TN	0.058402242	0.401947	0.298893	0.379348	0.224277
TT	0.043653727	0.441135	0.132829	0.518205	0.294873
ZA	0.054469734	0.605164	0.446484	0.592686	0.419366

Intel Core i5-7200U 2.5 GHz and 16 GB of DDR4 RAM.

Eight regions of the Slovak Republic were used as the benchmarks. For each self-governing region, i.e. Bratislava (BA), Banska Bystrica (BB), Kosice (KE), Nitra (NR), Presov (PO), Trencin (TN), Trnava (TT) and Zilina (ZA), all cities and villages were taken into account, as the set of possible locations. The cardinalities of these sets vary from 87 to 664 according to the considered region.

It was necessary to use an effective way how to compare two solutions (or more), which are represented by the semi-Pareto fronts. Both compared fronts needed to be normalized, so that all the solutions in the front have both objective functions ranging from 0 to 1. Comparison of more than two fronts can be also done using this approach. After the mentioned transformation one can calculate the area restricted by the axes and curve of Pareto front. The points of the individual Pareto front and semi Pareto front are connected by the line as in Figure 2. Both areas under the connector were calculated. The better approximation of the Pareto front corresponds to one with the smaller area [20].

For each of the eight regions, the parameter settings, according to two approaches, were obtained. The time-consuming heuristic run was performed, where 40 different semi-Pareto fronts were obtained for each region and each parameter combination.

The exact results were compared to the two heuristic approaches with initial parameters obtained in different ways. “One by one” and “Each by each” are the parameter tuning approaches.

The first parameter tuning approach, called “One by one” parameter, consists of the following steps. Firstly, the set of r parameters is ordered into a sequence p_1, p_2, …, p_r and subscript t of the current parameter is set to 1. The parameters are set at some initial values from their ranges. Then, in the t-th step, one has to find the best value of parameter p. The set of permissible values is given for each parameter. The best option is selected according to the results of the test run. The best value of the parameter is assigned to p_t for the next step. Finally, if t is less than r, the t is increased by one and the process continues. Otherwise, the tuning process terminates.

The second tuning process is called “Each by each” and consists of a performed time-consuming enumeration of all the combinations of individual parameters.

The following parameters were tuned: population size, elite set size ratio, mutation probability and tournament size ratio. The other used parameters with

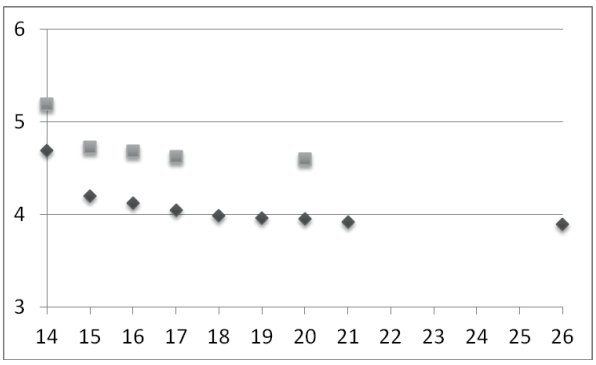


Figure 3 *Exact Pareto front (rhombus) compared to heuristic one (squares) for the Banska Bystrica region*

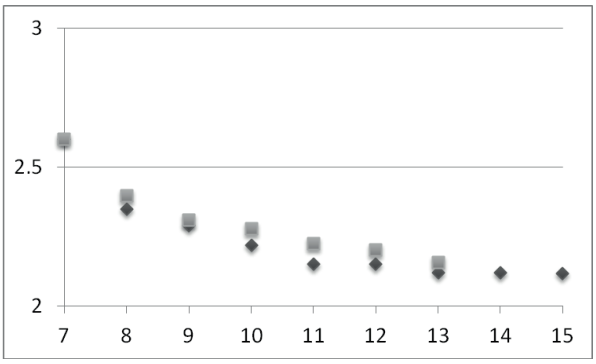


Figure 4 *Exact Pareto front (rhombus) compared to heuristic one (squares) for the Bratislava region*

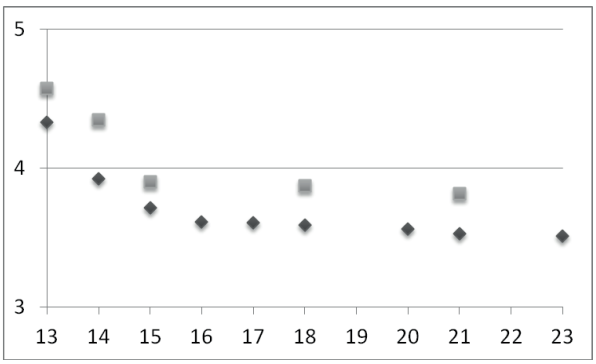


Figure 5 *Exact Pareto front (rhombus) compared to heuristic one (squares) for the Kosice region*

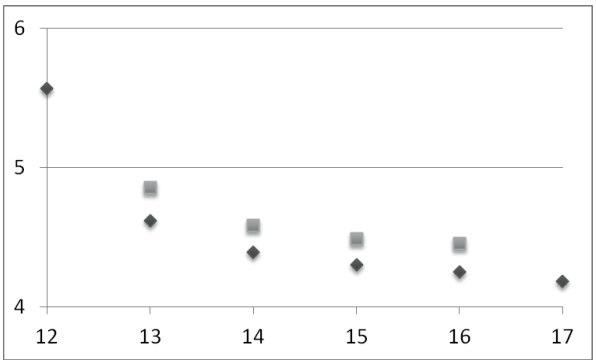


Figure 6 *Exact Pareto front (rhombus) compared to heuristic one (squares) for the Nitra region*

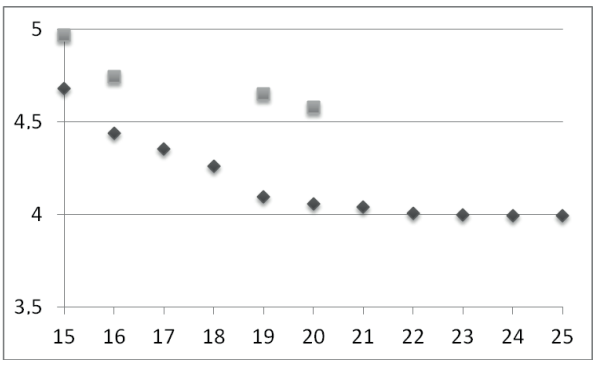


Figure 7 *Exact Pareto front (rhombus) compared to heuristic one (squares) for the Presov region*

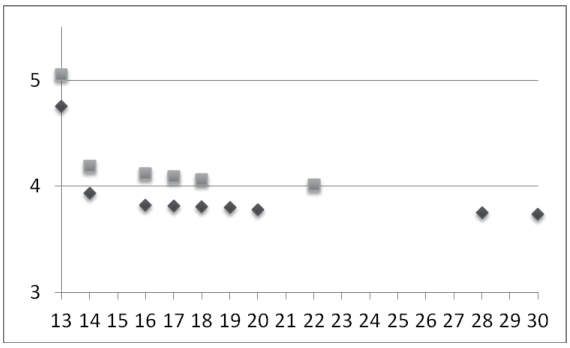


Figure 8 *Exact Pareto front (rhombus) compared to heuristic one (squares) for the Trencin region*

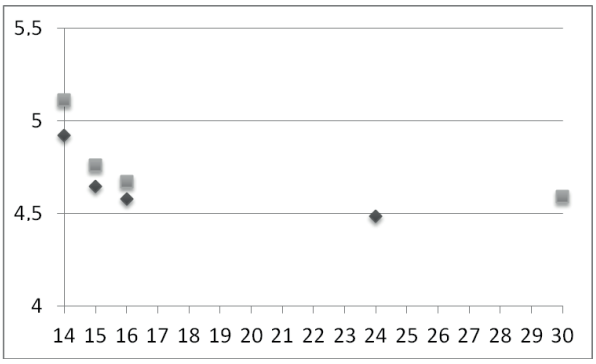


Figure 9 *Exact Pareto front (rhombus) compared to heuristic one (squares) for the Trnava region*

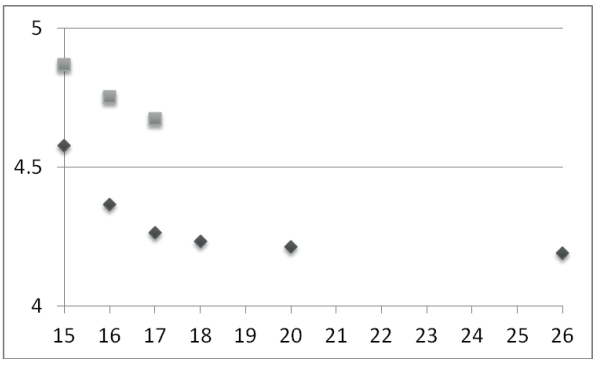


Figure 10 *Exact Pareto front (rhombus) compared to heuristic one (squares) for the Zilina region*

fixed values: Mutation step, maximal mutation count per offspring, offspring optimization probability, the acceptable difference in the population and final count of the population diversity controls.

The hypothesis that mean values for both sets of heuristic results are the same as the optimal result was tested. The hypotheses were tested using the Student t-test. To use this test, it was necessary to verify that the results obtained had a normal distribution. The Kolmogorov-Smirnov test for normality was used for that purpose. As it is shown in Table 1, the heuristic results were compared to the exact ones. After performing the above-mentioned test, the hypotheses that mean values of a heuristic run are the same as an exact result at 5% significance level for all the datasets, were rejected.

Comparison of the best-found approximation of the Pareto fronts and exact Pareto fronts, for each self-governing region, can be found in Figures 3 - 10. The horizontal axis depicts the min-max values in km and the vertical axis contains average min-sum values in km of resulting Pareto fronts.

According to the presented results in Figures 3-10 and Table 1, the genetic algorithm can be used for approximation of the Pareto front. One can see that in Bratislava, Kosice, Nitra, Trencin and Trnava (Figures 4, 5, 8 and 9) relatively good approximation of the exact results was obtained, which means that this approach can be permissible while solving large problems. However, in general comparison to the exact results, one can see that more numerous Pareto front members were found using the exact approach.

6 Conclusions

This research was devoted to inspection of the genetic algorithm ability in obtaining an approximation of the Pareto front of the p-location problem solutions. For this purpose, two conflicting criteria were considered. The first min-sum objective was to minimize an average distance between a user and the nearest service center and the other min-max objective was to minimize the maximal distance from a user to the nearest service center. To be able to perform proper analysis of the approximate results, the exact Pareto front were determined for each benchmark, by an exact optimization method and comparing it to the Pareto front approximation, authors came to the following findings. The genetic algorithm can be used to find an approximation of the Pareto front of the non-dominated public service system designs with conflicting criteria, but the approximation may be a bit biased in the case when a bigger instance of the problem is solved. A future research in this field will be aimed at methods, which can enable to direct the evolutionary process at a refinement of the Pareto front approximation.

Acknowledgement

This work was supported by the Slovak Research and Development Agency under the Contract no. APVV-19-0441 and by the by the research grant VEGA 1/0216/21 “Design of emergency systems with conflicting criteria using artificial intelligence tools”.

References

[1] BROTCORNE, L., LAPORTE, G., SEMET, F. Ambulance location and relocation models. *European Journal of Operational Research* [online]. 2003, **147**(3), p. 451-463. ISSN 0377-2217. Available from: https://doi.org/10.1016/S0377-2217(02)00364-8

[2] DOERNER, K. F., GUTJAHR, W. J., HARTL, R. F., KARALL, M., REIMANN, M. Heuristic Solution of an Extended Double-Coverage Ambulance Location Problem for Austria. *Central European Journal of Operations Research*. 2005, **13**(4), p. 325-340. ISSN 1435-246X, eISSN 1613-9178.

[3] JANOSIKOVA, L. Emergency medical service planning. *Communications - Scientific Letters of the University of Zilina* [online]. 2007, **9**(2), p. 64-68. ISSN 1335-4205, eISSN 2585-7878. Available from: http://komunikacie.uniza.sk/index.php/communications/article/view/1133

[4] GARCIA, S., LABBE, M., MARIN, A. Solving large p-median problems with a radius formulation. *INFORMS Journal on Computing* [online]. 2011, **23**(4), p. 546-556. ISSN 1091-9856, eISSN 1526-5528. Available from: https://doi.org/10.1287/ijoc.1100.0418

[5] KVET, M. Computational study of radial approach to public service system design with generalized utility. In: 10th International IEEE Conference Digital Technologies 2014: proceedings. 2014. p. 198-208.

[6] KVET, M. Advanced radial approach to resource location problems. In: *Studies in computational intelligence: developments and advances in intelligent systems and applications* [online]. ROCHA, A., REIS, L. P. (eds.). Springer, 2018. ISBN 978-3-319-58965-7, eISBN 978-3-319-58965-7, p. 29-48. Available from: https://doi.org/10.1007/978-3-319-58965-7

[7] OGRYCZAK, W., SLIWINSKI, T. On direct methods for lexicographic min-max optimization. In: International Conference on Computational Science and Its Applications ICCSA 2006: proceedings [online]. Lecture Notes in Computer Science. Vol. 3982. Berlin, Heidelberg: Springer, 2006. ISBN 978-3-540-34075-1, eISBN 978-3-540-34076-8, p. 802-811. Available from: https://doi.org/10.1007/11751595_85

[8] JANACEK, J., KVET, M. Public service system design with disutility relevance estimation. In: International Conference on Mathematical Methods in Economics 2013: proceedings. 2013. p. 332-337.

[9] ELLOUMI, S., LABBE, M., POCHET, Y. A new formulation and resolution method for the p-center problem. *INFORMS Journal on Computing* [online]. 2004, **16**, p. 84-94. ISSN 1091-9856, eISSN 1526-5528. Available from: https://doi.org/10.1287/ijoc.1030.0028

[10] SAYAH, D., IRNICH, S. A new compact formulation for the discrete p-dispersion problem. *European Journal of Operational Research* [online]. 2016, **256**(1), p. 62-67. ISSN 0377-2217. Available from: https://doi.org/10.1016/j.ejor.2016.06.036

[11] KVET, M., JANACEK, J. Price of fairness in public service system design. In: International Conference on Mathematical Methods in Economics 2014: proceedings. 2014. p. 554-559.

[12] KVET, M., JANACEK, J. Lexicographic fair design of robust emergency service system. In: International Conference on Mathematical Methods in Economics 2016: proceedings. 2016. p. 495-500

[13] BERTSIMAS, D., FARIAS, V. F., TRICHAKIS, N. The price of fairness. *Operations Research* [online]. 2011, **59**(1), p. 17-31. ISSN 0030-364X, eISSN 1526-5463. Available from: https://doi.org/10.1287/opre.1100.0865

[14] JANOSIKOVA, L., GABRISOVA, L., JEZEK, B., Load balancing location of emergency medical service stations. *E+M Ekonomie a Management / E+M Economics and Management* [online]. 2015, **18**(3), p. 30-40. ISSN 1212-3609, eISSN 2336-5064. Available from: http://dx.doi.org/10.15240/tul/001/2015-3-003

[15] ARROYO, J. E. C., DOS SANTOS, P. M., SOARES, M. S., SANTOS, A, G. A multi-objective genetic algorithm with path relinking for the p-median problem. In: Ibero-American Conference on Artificial Intelligence IBERAMIA 2010: proceedings [online]. Lecture Notes in Computer Science. Vol. 6433. Berlin, Heidelberg: Springer, 2010. ISBN 978-3-642-16951-9, eISBN 978-3-642-16952-6, p. 70 - 79. Available from: https://doi.org/10.1007/978-3-642-16952-6_8

[16] JANACEK, J. Public service system design with fuzzy parameters of perceived utility. In: *Central European Journal of Operations Research* [online]. 2015, **23**(3), p. 595-606. ISSN 1435-246X, eISSN 1613-9178. Available from: https://doi.org/10.1007/s10100-014-0370-7

[17] KVET, M., JANACEK, J. Iterative approaches to design of robust emergency system. In: *2017 IEEE International Conference on Service Operations and Logistics and Informatics SOLI: proceedings*. 2017. ISBN 978-1-5386-0949-1, p. 13-16.

[18] RYBICKOVA, A., BURKETOVA, A., MOCKOVA, D. Solution to the location-routing problem using a genetic algorithm. In: 2016 Smart Cities Symposium Prague SCSP: proceedings [online]. IEEE. 2016. ISBN 978-1-5090-1116-2, p. 1-6. Available from: https://doi.org/10.1109/SCSP.2016.7501016

[19] RYBICKOVA, A., MOCKOVA, D., TEICHMANN, D. Genetic algorithm for the continuous location-routing problem. *Neural Network World* [online]. 2019, **29**, p. 173-187. ISSN 1210-0552, eISSN 2336-4335. Available from: https://doi.org/10.14311/NNW.2019.29.012

[20] GRYGAR, D., FABRICIUS, R. An efficient adjustment of genetic algorithm for pareto front determination. *Transportation Research Procedia* [online]. 2019, **40**, p. 1335-1342. ISSN 2352-1465. Available from: https://doi.org/10.1016/j.trpro.2019.07.185

[21] REEVES, C. R. Genetic algorithms. In: *Handbook of Metaheuristics*. 2. ed. GENDREAU, M., POTVIN, J. Y. (eds.). New York, Dordrecht, Heidelberg, London: Springer, 2010. ISBN 978-3-319-91086-4.

UNIVERSITY
OF ŽILINA

In its over 65 years of successful existence, the University of Žilina (UNIZA) has become one of the top universities in Slovakia.



Development of Euroregion Beskydy XV

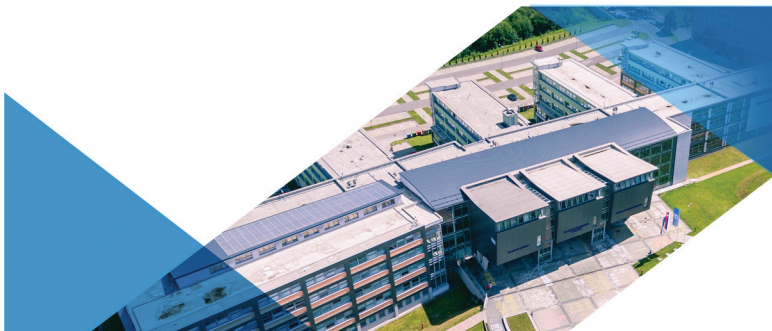
CONFERENCE DESCRIPTION

Diagnosis of socio-economic conditions in the region. Strategic management of the region taking into account various aspects of sustainable development. New trends in the management of the network entrepreneurship in a knowledge economics in the era of globalization. Innovative approaches in the development of territorial self-government in terms of knowledge-based economy in the background of globalization and economic recession. Indicators of quality of life and sustainable development. Options to increase the security of citizens and their property in the regions. The experience from using of EU projects in the border regions.

VENUE & DATE

5. 11. 2021
Virtual Event
http:// www.uniza.sk

CONTACT:
UNIVERSITY OF ŽILINA
Department of Communications
Faculty of Operation and Economics of Transport and Communications
Univerzitná 8215/1, 010 26 Žilina, Slovakia
e-mail: anna.padourova@fpedas.uniza.sk



FATHERS' PREDOMINANCE IN TRANSPORT ARRANGEMENTS FOR FAMILY TOURISM: E-CHAID-BASED PROFILING IN EAST ASIA

Yi-Fang Lan[1], Che-Jen Su[2,*]

[1]Graduate School of Tourism, Wakayama University, Wakayama City, Japan
[2]Department of Restaurant, Hotel and Institutional Management, Fu Jen Catholic University, New Taipei City, Taiwan

*E-mail of corresponding author: 040084@mail.fju.edu.tw

Resume

In decisions about transportation for family vacations, the distribution of the decision-making role between fathers and other family members is subject to characteristics of the society, the travel and the household. Therefore, the purpose of this study is to present a data-mining model that identifies the relative importance of those determining characteristics in predicting the probability of the father's predominance in transportation decisions for family vacations. By investigating cases across four East Asian societies and using exhaustive chi-square automatic identification detector analysis, it was found that the primary source of the family's income was the strongest predictor of the father-determined likelihood of decisions about vacation transportation. The results also suggested that the decision tree method is appropriate for targeting the father-predominant market of transportation in cross-societal contexts.

Article info

Received 9 November 2020
Accepted 22 January 2021
Online 8 June 2021

Keywords:

decision tree,
East Asia,
Exhaustive Chi-square Automatic Identification Detector (E-CHAID),
family tourism,
Father-Determined Likelihood (FDL)

Available online: https://doi.org/10.26552/com.C.2021.4.G13-G24

ISSN 1335-4205 (print version)
ISSN 2585-7878 (online version)

1 Introduction

Transportation is considered to be an indispensable aspect of family tourism because participants' perceived risk of transport arrangements strongly affects their regard for travel information [1]. An important topic in family tourism research is the family's decision-making style for decisions about means of transport [2], but the extant research on the father's role in decision-making about the means of transportation for family vacations has produced contradictory results. For instance, Wang et al. [3] study in Taiwan found that the father and mother decided the means of transportation for family tours jointly, which agrees with the findings of a recent study in Spain [4] and Croatia [5]. Similar additional research results have supported a general argument that family vacation decisions are made jointly by the father and mother [6-8]. However, Kim et al. [9] from evidence in South Korea concluded that the father usually acted as the main decision-maker of transportation-related activities, thus supporting the general style of the family tourism decision-making in South Korea [10]. Their findings represent a broader contention that the father predominates in the decisions of transportation arrangements for family vacations in East Asia. A recent study by Cheng et al. [2] confirmed that fathers' predomination in determining the means of transportation for the family vacations prevailed across 25 societies. These various contradictory findings can be attributed to the choice of different respondents within the families accessed by the studies. Extant evidence on the roles that fathers play in the decision-making about the means of transportation for family vacations is rarely based on the data obtained from adolescent children [2], who, in fact, do possess the cognitive competence necessary to describe how the vacation decision roles are distributed within the family [11-14]. Perception bias can plague conclusions that are based on use of the traditional couple-reporting method to describe the distribution of roles in family vacation decision-making.

Indeed, the father's role in family vacations has rarely been studied [15]. A call has emerged for more exploration into fatherhood-related factors that will elaborate on family tourism from various perspectives, such as gender differentiation, dyadic consensus and parental style [16]. To address these issues in a general framework, it is advisable to conduct multilevel research that incorporates cultural and socioeconomic backgrounds at the societal level and travel-household-related characteristics at the individual level in the family decision-making processes for choosing tourist products [2, 7-8, 14, 17]. However, no study to date has examined the predictive ability of variables at macro and micro levels regarding the father-determined

This is an open access article distributed under the terms of the Creative Commons Attribution 4.0 International License (CC BY 4.0), which permits use, distribution, and reproduction in any medium, provided the original publication is properly cited. No use, distribution or reproduction is permitted which does not comply with these terms.

likelihood (FDL) of family vacation decisions, such as transportation means, based on data mining across other societal contexts, such as East Asian societies. Thus, this study sought to apply the decision tree technique to develop a data-mining model of societal, travel and household attributes that could predict adolescents' perceptions of the FDL of decisions about transport means, using the binary categories of "yes" (i.e., by the father alone) or "no" (i.e., not (just) the father) for family travel. By investigating cases collected in China, Japan, South Korea and Taiwan, the overall cases of family vacation were segmented, from the rules generated by the model. In so doing, the relative importance of the predictor variables for the FDL of transport means was identified.

2 Crossvergence across East Asia and family vacation decisions

The concept of East Asia is also termed interchangeably as Confucian Asia in cross-societal studies, because societies of this cluster share Confucianism as a primary source of sociocultural influence on the formation of values [18]. Harmony is the underlying value of the Confucian family, school and workplace. To maintain harmony, family norms stress the division of roles in the husband–wife relationship, filial piety in the parent–child relationship and unequal priority between siblings [19-20]. Regardless of the value system that has evolved across the East Asian societies, through distinctive historical backgrounds and societal ideology, Confucianism has been widely used in analytical frameworks for research on issues of the Asian family [20-21], including family vacation decision-making [10, 22]. According to Confucian tradition, which emphasizes family-based interpersonal relationships in terms of communication and behavioural norms, clearly defined roles emerge for individuals in the family decision-making process.

At the societal level, individuals' behavioural variations across societal contexts can be explained by society's common value system, which is influenced by the two different categories of antecedents: culture and ideology. The two kinds of factors are advocated by *convergence* and *divergence* theories, respectively [23-24]. Societal-convergence theory contests that a society's values are conditioned entirely by an ideological drive, such as the use of technology, the governance system, or the developmental orientation and that ideological drive furnishes a shared logic with which to shape similar norms. Conversely, the societal-divergence theory argues that individual-level values with respect to culture are preserved over time, regardless of changes in economy and technology [25-28]. Recently, the perspective of multilevel crossvergence, which entails societal-level divergence by culture and convergence by ideology and individual-level characteristics [29], has been introduced in an elaboration of family purchase decision-making under down-to-earth circumstances [21, 30]. The multilevel crossvergence perspective was developed from the crossvergence theory [23, 31] and forms the foundation for reference frameworks in cross-societal-context research. In response to that trend, it is worthwhile to extend the crossvergence perspective into family purchase decisions in order to take into account a multilevel theoretical foundation of societal backgrounds, such as sociocultural and ideological influences and individuals' features, on the formation of the family vacation decision-making.

The focus of this study is on four Eastern Asian societies: those of China, Japan, South Korea and Taiwan. These four societies share similar historical, geopolitical and geographical features but differ in their cultures and their development ideologies [10, 18-19, 21, 32]. In fact, their sociocultural and ideological differences could lead to significant variations in their FDL of decisions about family vacation transportation. Furthermore, it is argued against an assumption that all the East Asian consumers operate from shared similarities. Cultural and socioeconomic characteristics should be taken into consideration with travel- and household-related characteristics when one is trying to understand the roles that fathers play in deciding transport means for family vacations. Indeed, authors believe that the region's diversity is well represented by the four societies that were selected to represent East Asia. This study is innovative and should serve as groundwork for further studies on the FDL of transportation decisions for family travels in East Asia.

3 Application of the decision tree methods in tourism studies

A decision tree is a powerful data-mining approach for classification, prediction, interpretation and data manipulation and it has been used widely in behavioural research. For research designs, the application of a decision tree has two advantages that address the interpretability of results and the quality of data [33-34]. First, decision tree models simplify complex dependence relationships by dividing cases into distinctive subgroups, thus providing outputs that are clear to interpret. Second, a decision tree is a nonparametric approach without distributional assumptions. It needs no imputation to react to missing values and no transformation to respond to heavily skewed data. In addition, a decision tree is robust to outliers. The commonly used algorithms of a decision tree that are available in software are the Chi-square Automatic Interaction Detector (CHAID), the Classification and Regression Tree (CART) and the Quick, Unbiased, Efficient Statistical Tree (QUEST). In sum, these algorithms are distinctive in terms of their variable type, node splitting, tree pruning and splitting rules [33-34].

Table 1 *Factors conditioning the FDL of transportation means for family vacations*

label and source	description	category
sociocultural/ideological characteristics		
SOC (Cheng et al., 2019; Yen et al., 2020)	society	(1)China, (2) Japan, (3) South Korea, (4) Taiwan
travel characteristics		
STA (Nanda et al., 2007)	status of travel	(1) domestic vacation,(2) foreign vacation
DUR (Nanda et al., 2007)	duration of the trip, in days	(1) 1~2, (2) 3, (3) 4 or more
GS (Kang et al., 2003; Nanda et al., 2007)	travel group size	(1) 2~3, (2) 4, (3) 5 or more
household characteristics		
CN (Bronner & de Hoog, 2008; Filiatrault & Ritchie, 1980; Koc 2004; Nanda et al., 2007; Spiers, 2017)	number of children in family	(1) 1, (2) 2, (3) 3 or more
INC (Koc 2004; Filiatrault & Ritchie, 1980; Nanda et al., 2007)	main source of income for family	(1)both parents, (2) father, (3) mother, (4) others

In general, empirical comparisons have suggested that the CHAID-based models have been evaluated to be stably preferable to CART and QUEST [33, 35-37]. Moreover, the CHAID algorithm has been widely used to explore favourable segments of tourism market [38], profiles of tourist choice behaviours [39-40], tourist satisfaction [41]. The basic CHAID algorithm has also been modified as the Exhaustive CHAID (E-CHAID), which performs a more thorough merging and testing of the predictor variables. The remedies make E-CHAID an advantageous technique for tourism research. Even the use of CHAID-based algorithms contributes to tourist behaviour research, but no empirical study has heretofore attempted to use the decision tree analyses to explore the FDL of family vacation issues. Moreover, typical decision-tree research on tourist or travel behaviours rarely incorporates cultural factors into the model. Rules resulting from a single society tend to lack generalizable implications [42].

4 Research significance

This study's methodology extended and refined the use of decision tree analyses to examine decision-making about the means of transport in family tourism. First, rather than querying the fathers or mothers [43], the families' decision-making experiences were collected from adolescent family members, thus guaranteeing a more neutral approach than a lateral report from either of the parents would provide. In so doing, the risk of perception bias in the participants' descriptions of how family roles were distributed in vacation decision-making was greatly limited [2, 44]. Previous research also accepted that in addition to the parents, other family members who possess the cognitive competence are able to describe how decision roles are distributed in the family travel decision-making [11-13]. Furthermore, here cases were confined to families with adolescent(s) and in so doing the parent couples interacting with other family member(s) in a decision-making group was completely documented, [8, 12, 15, 45-48]. Third, these cases were drawn from four East Asian societies that have similarities yet are diverse in their sociocultural and ideological backgrounds and the sample size accommodated the conditions for applying a decision tree model. That sampling approach, with its cross-societal evidence, ensured that the results would have greater validity. Fourth, by using the E-CHAID technique, the East Asian tourist market of transportation for family travel in terms of fathers' predominance in making transport arrangements, was segmented according to the simultaneous predictive factors of society, travel and household. Therefore, this study clarifies the relative importance of condition variables at both the macro and micro levels in predicting whether the father alone is the decision maker about the means of transport for the family travel. It extends the application of decision tree analyses in tourist market segmentation to situations of cross-societal contexts, which have been highly emphasized for aiding the r understanding of the growing market of family tourism in East Asia [44].

5 Methods

5.1 Measures

The dependent variable, the FDL of transportation means, was measured by rating it on a binary scale: 1 = yes (i.e., by the father alone), 2 = no (i.e., not (just) the father). Table 1 summarizes the condition variables suggested by the literature review, with three types of conditions used for the E-CHAID analysis and their description and corresponding categories. They are (a) sociocultural/ideological characteristics—society (with SOC categorizing each case into *China, Japan, South Korea* and *Taiwan*); (b) travel characteristics—status of travel (with STA categorizing each case into *domestic vacation* or *foreign vacation*), duration of the trip, by number of days (with DUR categorizing each case into *1~2 days*, *3 days*, or *4 or more days*) and travel group size

(with GS categorizing cases into *2~3 group members*, *4 group members*, or *5 or more group members*); and (c) household characteristics—the number of children in the family (with CN categorizing each case into *1*, *2*, or *3 or more children*) and the family's primary source of income (with INC categorizing each case into *both parents*, *the father*, *the mother*, or *others*). In addition, the respondents' demographics was investigated (i.e., gender, age, current stage of the family's life cycle, the highest educational level of the head of the household and the occupation of the head of the household). The authors' original questionnaire was produced in English and then the standard back-translation procedures were used to convert the questionnaire into each surveyed society's official language.

5.2 Sample and procedures

Total of 1,016 usable responses were collected from adolescents at campuses of senior high schools (i.e. the equivalent of grades 10 through 12 in the U.S. school system), from the four East Asia societies: China (n = 201), Japan (n = 262), South Korea (n = 268) and Taiwan (n = 285). An E-CHAID model was analyzed, consisting of six predictors, with the sample size of 1,016 and that yielded a sample size–to–condition variable ratio of 169.3, which exceeded the minimum ratio of 150 [40]. The sampling criteria confined the age range of the participants (mean = 16.43 years, s.d. = 0.91) and thus attempted to avoid any significant variations in the family experience that the adolescent respondents' age-related transitions in decision-making competence would explain [8]. The participants were asked to recall a family decision that had included them and that had been about vacation during the past year. They were then asked to report the father-versus-other distribution in decisions about transportation for the vacation in their cohabiting family. Seventy percent of the participating adolescents were female, most (87.4%) were currently living with both parents and a majority (68.6%) came from a double-income family. Most respondents (47.5%) came from families with two children. A majority (45.2%) came from a family whose head of household was working in business or industry and a majority (59.2%) came from a family in which the head of household was 35 years old or older and the youngest child was 0-17 year(s) old. The majority of the travel cases (82.7%) were domestic and 66.9% of the vacations ranged from one to three days in duration. Overall, the vacations' means of transportation was determined by the father alone (58.2 %).

5.3 Data analysis

To induce rules that explained the FDL based on the condition variables, the IBM SPSS Decision Trees 20 program was used to analyse the data. The SOC was forced as the first predictor, to split the overall sample, because this research was cross-society oriented. The stopping criteria for FDL were set at 60 cases before and 30 cases after the division of the (sub)sample [41], at a significance level of 0.05 for predictor eligibility. The splitting process continued until either the split did not help to improve the predictive accuracy or a node contained fewer cases than the specified size.

6 Results

6.1 Algorithm

The decision tree structure that we constructed using the E-CHAID algorithm is shown in Figure 1. The top square of the tree diagram shows the distribution of the cases over the dependent variable, the categories of "yes" and "no." Below each of the squares are the predictor variables with the statistics for the split; the p-value, the Chi-square statistic and the degrees of freedom. The number and percentage of cases per category are given for each (group of) predictor category(ies). The model exhibited six layers of characteristics and ultimately led to eight end nodes that represented the final subgroups of the tree. The tree began with the top decision node (Node 0), with all 1,016 cases of the data set and the entire data set was then divided into two distinctive groups based on society: Node 1 (*China*) was dominated by "no" (59.2%) and Node 2 (*Japan, South Korea, Taiwan*) was dominated by "yes' (62.5 %). Node 1 was further divided into two groups based on status of travel: Node 3 (*domestic vacation*) was dominated by "no" (51.9%) and Node 4 (*foreign vacation*) was dominated by "no" (73.5 %). Node 3 was split into two groups, determined by the duration of the trip: Node 7 (*3 days or fewer*) was dominated by "yes" (69.6%) and Node 8 (*4 or more days*) was dominated by "no" (63.2 %). In the same vein, the node at the right (Node 2) was broken into two groups by the family's main source of income: Node 5 (*father, both parents, others*) was dominated by "yes" (65.8%) and Node 6 (*mother*) was dominated by "no" (83.6 %). Then, Node 5 was divided into two groups based on status of travel: Node 9 (*domestic vacation*) was dominated by "yes" (69.3%) and Node 10 (*foreign vacation*) was dominated by "no" (56.3 %). In addition, Node 9 was divided into two groups based on travel group size: Node 11 (*2~3 group members*) was dominated by "yes" (51.8%) and Node 12 (*more than 3 members*) was dominated by "yes" (72.8 %). At the bottom of the tree, Node 11 was split into two groups on the basis of the number of children in the family: Node 13 (*1 child*) was dominated by "yes" (71.7%) and Node 14 (*more than one child*) was dominated by "no" (66.7 %). The dendrogram shows that the rankings of predictors according to their ability to explain the variances of the FDL were INC (χ^2 = 53.43, Bonferroni adjusted p < .001),

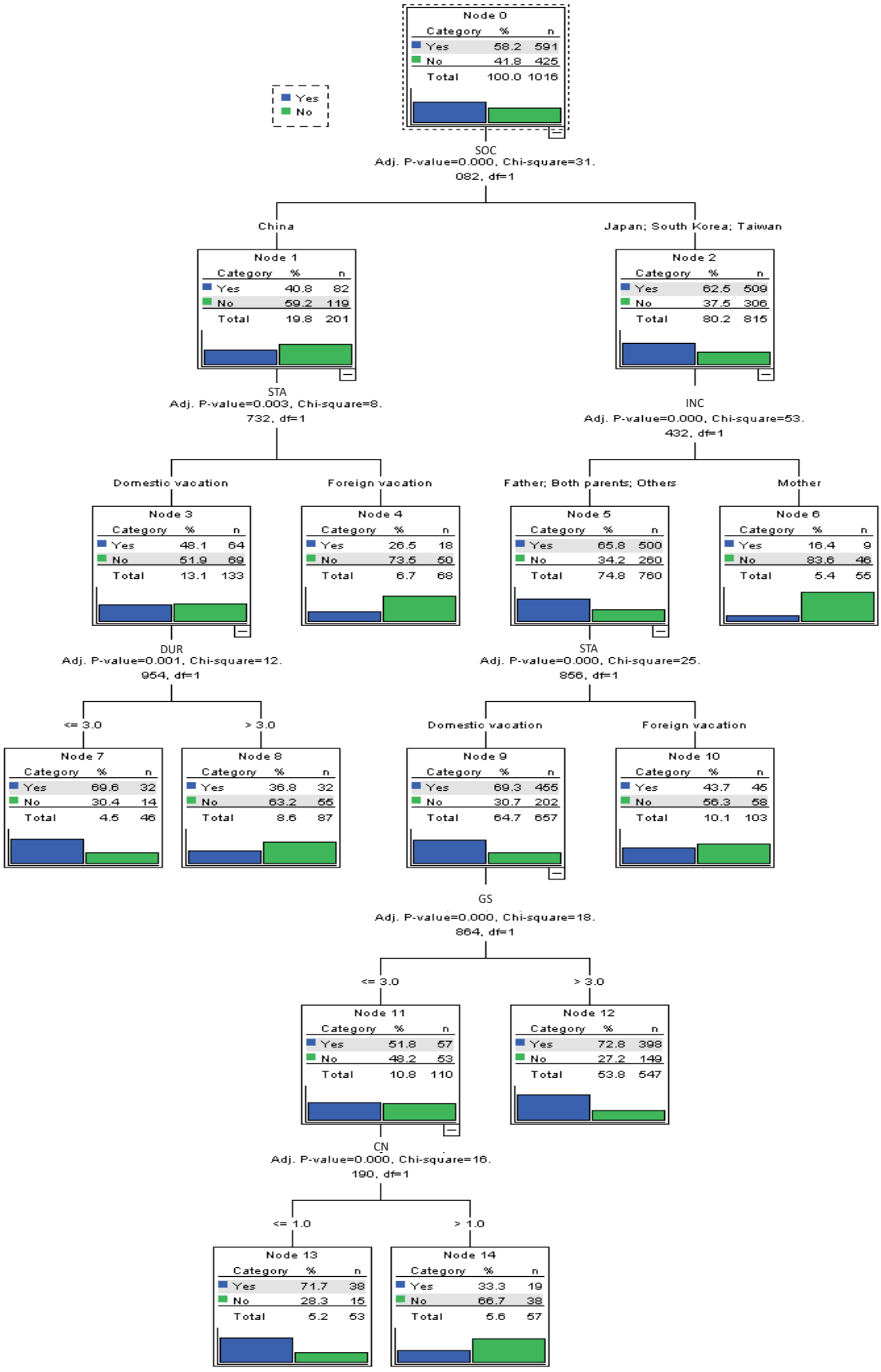


Figure 1 *The E-CHAID dendrogram*

Table 2 *FDL classification rules generated by the E-CHAID decision tree*

FDL	node	rule
yes	7	IF SOC = "China" and STA = "domestic vacation" and DUR = "1~2" or "3" THEN FDL ="yes"
	13	IF SOC = "Japan" or "South Korea" or "Taiwan" and INC = "both parents" or "father" or "others" and STA = "domestic vacation" and GS = "2~3" and CN = "1" THEN FDL ="yes"
	12	IF SOC = "Japan" or "South Korea" or "Taiwan" and INC = "both parents" or "father" or "others" and STA = "domestic vacation" and GS = "4" or "5 or more" THEN FDL ="yes"
no	8	IF SOC = "China" and STA = "domestic vacation" and DUR = "4 or more" THEN FDL ="no"
	4	IF SOC = "China" and STA = "foreign vacation" THEN FDL ="no"
	14	IF SOC = "Japan" or "South Korea" or "Taiwan" and INC = "both parents" or "father" or "others" and STA = "domestic vacation" and GS = "2~3" and CN = "2" or "3 or more" THEN FDL ="no"
	10	IF SOC = "Japan" or "South Korea" or "Taiwan" and INC = "both parents" or "father" or "others" and STA = "foreign vacation" THEN FDL ="no"
	6	IF SOC = "Japan" or "South Korea" or "Taiwan" and INC = "mother" THEN FDL ="no"

Table 3 *Gains for the end nodes and the end nodes' index scores and ranking*

node	segment size (% of overall sample size)	number of 'yes' respondents (% of all 'yes' respondents)	% of 'yes' respondents to the segment	index score
12	547 (53.8)	398 (67.3)	72.8	125
13	53 (5.2)	38 (6.4)	71.7	123
7	46 (4.5)	32 (5.4)	69.6	120
10	103 (10.1)	45 (7.6)	43.7	75
8	87 (8.6)	32 (5.4)	36.8	63
14	57 (5.6)	19 (3.2)	33.3	57
4	68 (6.7)	18 (3.0)	26.5	46
6	55 (5.4)	9 (1.5)	16.4	28

SOC (χ^2 = 31.08, Bonferroni adjusted $p < .001$), STA (χ^2 = 25.86, Bonferroni adjusted $p < .001$), GS (χ^2 = 18.87, Bonferroni adjusted $p < .001$), CN (χ^2 = 16.19, Bonferroni adjusted $p < .001$) and DUR (χ^2 = 12.95, Bonferroni adjusted $p < .001$).

The classification rules generated by the decision tree are summarized in Table 2, following the path from each end node to the root node. The relationships between the condition variables and the percentage of the FDL associated with each variable were therefore determined.

Table 3 presents the gains for the end nodes and ranks the end nodes according to their index scores, which refer to the FDL rate of each segment relative to the overall FDL rate of 58.2%. An index score exceeding 100 suggests that the corresponding end node had an above-average probability of predicting the FDL. By that criterion, three end nodes met the threshold. Node 12 had the highest index score, 125 (72.8 %/58.2 %), thus reflecting it having the highest probability of predicting FDL (72.8%). Next were Node 13, with an index score of 123 (71.7 %/58.2%) and Node 7 with an index score of 120 (69.6 %/58.2 %). In contrast, an index score below 100 suggests that the corresponding end node had a below-average probability of predicting the FDL. Five end nodes were in that category that appeared to have a low probability of predicting the FDL. Node 6 scored the lowest, with 28 (16.4 %/58.2 %), thus reflecting its having the lowest probability of predicting the FDL (16.4 %). Next, also with low probabilities of predicting the FDL and each shown in comparison with the overall rate of 58.2%, were Node 4 (46 = 26.5 %/58.2 %), Node 14 (57 = 33.3 %/58.2 %), Node 8 (63 = 36.8 %/58.2%) and Node 10 (75 = 43.7 %/58.2 %).

6.2 Model performance

The cumulative gain chart was used to evaluate the model's performance (see Figure 2). The horizontal axis plots the percentages, sorted based on the probability, from high to low and denotes the percentages of the test data set. The vertical axis records the percentages of the actual predicted values on the curved line. As Figure 2 shows, the line was an upward curve that rose steeply and then levelled off, thus suggesting that the tree model was acceptable for predicting the FDL.

The cumulative index chart was also used to check whether the tree model was appropriate for predicting the FDL. As is shown in Figure 3, the line started above 100%, remained on a high plateau as it extended to the right and then gradually descended toward 100%, thus confirming that the model was appropriate for predicting our target category of "yes."

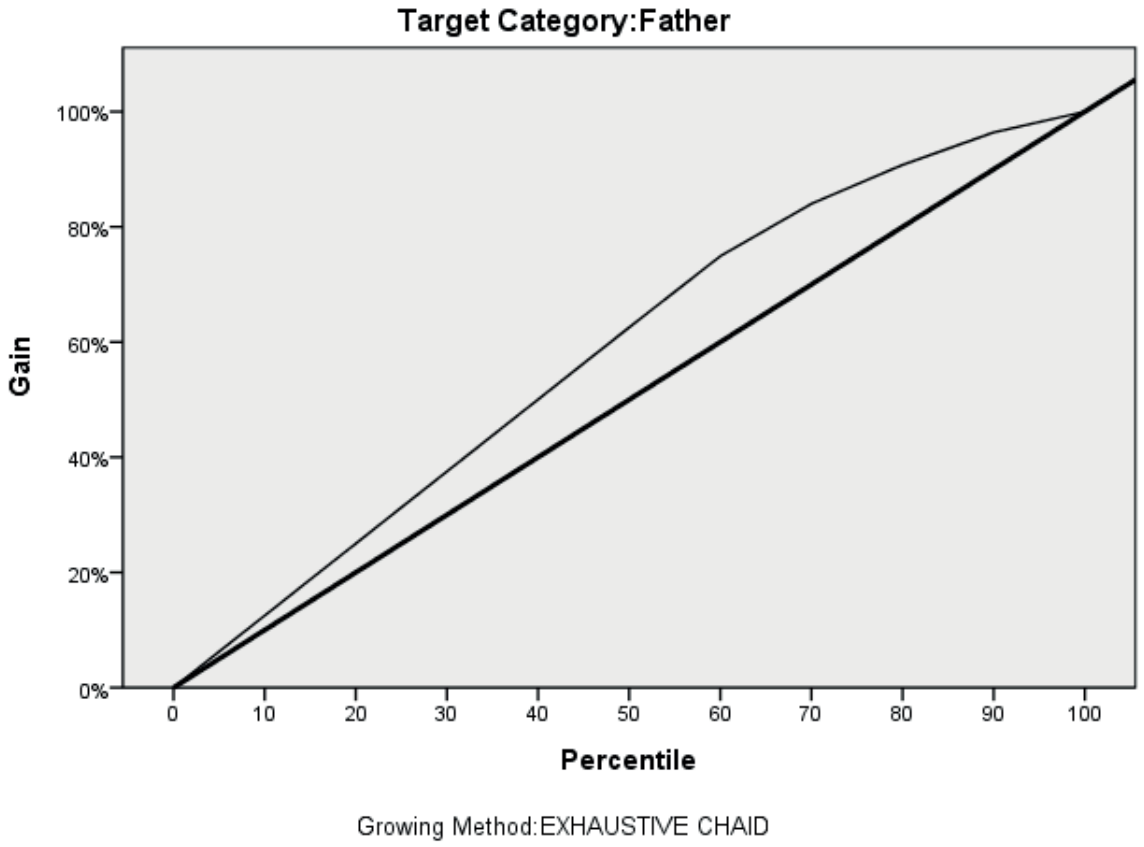


Figure 2 *Gain chart for the "Yes" category of FDL*

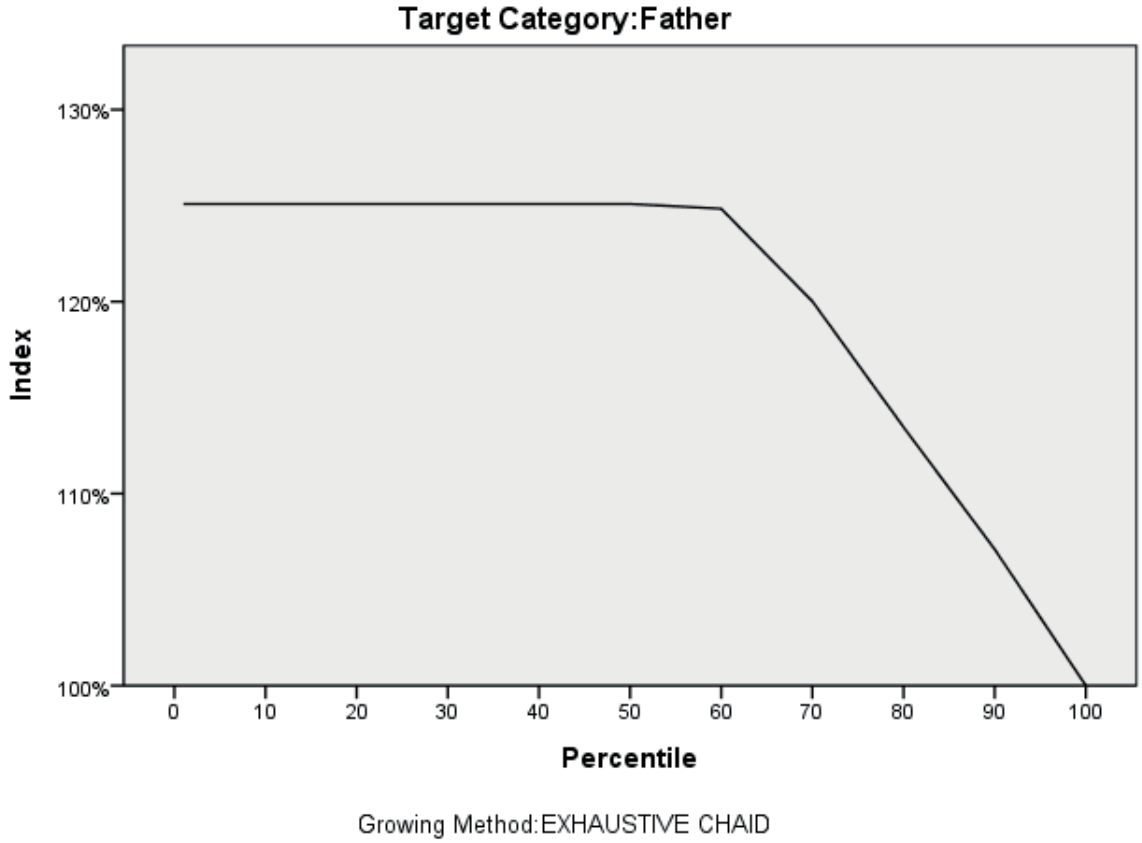


Figure 3 *Index chart for the "Yes" category of FDL*

Table 4 *Confusion matrix and classification accuracy*

actual	predicted		
	yes	no	% correct
yes	468	123	79.2
no	178	247	58.1
overall %	63.6	36.4	70.4

Risk estimate = .296; std. error = .014

The confusion matrix presented in Table 4 shows that the recall was 79.2% for predicting "yes" and was 58.1% for predicting "no," thus yielding a prediction accuracy of 70.4%. In sum, our E-CHAID–generated model performed satisfactorily in elaborating on the condition variables of FDL.

7 Discussion

7.1 Summary

The presented study used the E-CHAID approach and the findings contribute to the relatively limited literature on the predominant role that fathers play in deciding the transportation means for the family travel. The results, derived from the 1,016 original cases from four societies in East Asia, provide a dendrogram that illustrates a set of rules based on the importance of various condition variables in predicting the FDL of decisions about transportation means for the family travel. Through following those rules, the study presents a profile of a viable set of segments, with distinctive sociocultural, ideological, travel and household characteristics, that are based on family tourism and can be used by the transportation market in East Asia. The decision tree model identified the rankings of several predictor variables for the FDL, according to the magnitude of the variables' effects and by using those predictor variables the model identified eight distinctive segments of cases of family travel.

7.2 Contributions to theory

Presented results align with the assertion that fathers tend to be powerful decision-makers about the transportation arrangements for family vacations and travel [2, 6, 9]. The evidence of fathers' predominance also adds to the rationale behind why the means of transportation is the least discussed by family members of all the sub-decisions for a family vacation [49]. For East Asian cases of family travel in general, transportation arrangements were most often determined by the father alone. That result echoes the understanding that the family role distribution for deciding aspects of family travel depends on the family members' relative involvement and their relative involvement in turn is shaped by their respective perceptions of knowledge of the issues and of relevant information [4, 8, 21, 30, 50] and by the gender-role division of responsibilities between spouses within the family [51]. In general, in families in East Asia, fathers are likely to take more responsibility for choosing the transportation means for family travel than mothers and children do, because of the fathers' personal interests and their opportunities to access information regarding transportation and their conformity to social expectations about the husband's role in the family, as well. However, the first decision tree splits showed that the Chinese group had more cases of "no", thus suggesting that China is distinctive in having a societal culture or development ideology that decreases fathers' predominance in deciding the means of transport for family travel, compared to Japan, South Korea and Taiwan, considered as a whole. This study confirms the advantage of having a synergetic perspective on values formation and evolution in cross-societal studies on the family travel decision-making [23, 31, 52]. The use of composites of culture and societal effectiveness as predictors takes into account the similarities and differences of macro-level backgrounds across societies. Such an approach is expected to help refine the research methods and to explain family travel behaviour with greater validity [2, 14].

It is noteworthy that overall, regardless of the diversity of values formation and evolution across the four East Asian societies studied, the main source of household income, rather than the society, appeared to be the most important predictor of the fathers' predominance in vacation transportation decisions. This finding confirms that the primary source of the family's income determines the distribution of the decision-making power in planning family vacations [7-8, 48]. Taking the cases of Japan, South Korea and Taiwan as a group, in particular, showed that when mothers were the main source of family income, the fathers were not the predominant decision-maker, thus suggesting that the structure of economic power and reliance within the family, more than sociocultural or ideological forces, may shape the father-versus-other dominance style in decisions about transportation for family travel. Research also has shown that individuals' power over family purchase decisions decreases as their dependence on their family increases [21, 30]. This concept of dependence refers to the extent to which the individuals rely on the family to achieve their goals [53], such as financial reliance derived from their relationship with the family [54-55]. That economic support usually

derives from the main income source for the family. The results suggested that for a Confucian region, such as East Asia [18], where male-oriented values underlie spousal roles in the family vacation decisions [10], the economic-reliance relationship appears to change the typical role distribution in spite of societal norms. In addition, it is found that fathers were a greater decision-maker about transport means for domestic vacations than for the foreign ones (Node 3 vs Node 4; Node 9 vs Node 10); for medium-short vacations than for the long ones (Node 7 vs Node 8); and for one-child families than for families with two or more children (Node 13 vs Node 14). These findings confirm the speculation that family vacations that have high expenditures, long distances to the destination and long durations match the joint decision-making style between spouses [8]. Taken altogether, the presented model not only integrated multilevel variables in the segmentation and targeting of the family travel products market, but it elucidated the interactions among the multiple facets of family vacation market segmentation, as well. These findings offer East Asian evidence for application of an expanded crossvergence theory and demonstrate the theory's value in multilevel analyses of family vacation decisions.

7.3 Managerial implications

For marketing measures of family vacation products in East Asia, the results discussed above highlight the managerial implication that marketers, who wish to initiate a father-focused promotional strategy for entering the market of transportation for the family travel, should consider targeting Nodes 7, 12 and 13, rather than other segments, in their efforts to access and persuade fathers, because overall those three segments carried above-average likelihoods of father predominance in travel decision-making. It also implies that marketers need to take the significant condition variables into account in designing family vacation products and customizing communications programs that support fathers' decision-making about the means of transportation for the family vacations and prevent audience misunderstandings across societies. In addition, marketers could periodically update the database and amend the model to classify and predict the favourability of new cases expeditiously and identify additional contributing factors to the FDL of the means of transportation for the family vacation travels in East Asia. Such outputs could serve as references for examining the implementation of marketing strategies and revising them properly.

7.4 Conclusions

Results obtained in this study relate findings from other recent research [2, 56] to strongly suggest that although a general knowledge of history and culture is very important, such knowledge by itself is not sufficient to predict familial interpersonal dynamics. Further research is needed that will apply a multilevel-crossvergence perspective of regional, societal and individual influences to extend the understanding of the family decision-making about vacations. Such an approach will guide researchers to elaborate systematically on the effects that multilevel factors exert on the decision-making process about family vacations. Therefore, continuing the survey used in this study could be worthwhile in providing data on the decision-making roles of other issues, such as the family vacation's destination choice, so that further comparisons can be made. In addition, Confucianism-based norms of behaviour incorporate the distribution of roles of multiple generations within families [10, 16, 22]. Thus, the future endeavours would do well to expand vacation cases from the nuclear family to the multigenerational family, thereby considering grandparents and other seniors [57], so that one can capture a complete overview of the family tourism market in East Asia. Finally, this study focused on "means of transportation" decision that is a general description rather than on each mode of transportation (e.g., rented vehicle versus private vehicle or energy-efficient mode versus eco-efficient mode) [5, 58-60]. Authors recommend that the future studies explore how fathers' predominance in arraying the modes of transportation is ruled by the condition variables.

References

[1] MASER, B., WEIERMAIR, K. Travel decision-making: from the vantage point of perceived risk and information preferences. *Journal of Travel and Tourism Marketing* [online]. 1998, **7**(4), p. 107-121. ISSN 1054-8408, eISSN 1540-7306. Available from: https://doi.org/10.1300/J073v07n04_06

[2] CHENG, I. F., SU, C. J., LIAO, H. H., LORGNIER, N., LEBRUN, A. M., YEN, W. S., LAN, Y. F., HUANG, Y. Adolescents' perceptions of mother-father dominance in family vacation decisions: a 25-society study. *Service Business* [online]. 2019, **13**(4), p. 755-778. ISSN 1862-8516, eISSN 1862-8508. Available from: https://doi.org/10.1007/s11628-019-00404-6

[3] WANG, K. C., HSIEH, A. T., YEH, Y. C., TSAI, C. W. Who is the decision-maker: The parents or the child in group package tours? *Tourism Management* [online]. 2004, **25**(2), p. 183-194. ISSN 0261-5177. Available from: https://doi.org/10.1016/S0261-5177(03)00093-1

[4] ROJAS-DE-GRACIA, M. M., ALARCON-URBISTONDO, P. Couple roles in sub-decisions on family vacations. *Cornell Hospitality Quarterly* [online]. 2018, **59**(2), p. 160-173. ISSN 1938-9655, eISSN 1938-9663. Available from: https://doi.org/10.1177%2F1938965517734941

[5] SRNEC, T., LONCARIC, D., PRODAN, M. P. Family vacation decision making process: evidence from Croatia. In: Faculty of Tourism and Hospitality Management in Opatija. Biennial International Congress Tourism & Hospitality Industry 2016: proceedings. 2016. p. 432-445.

[6] JENKINS, R. L. Family vacation decision-making. *Journal of Travel Research* [online]. 1978, **16**(4), p. 2-7. ISSN 0047-2875, eISSN 1552-6763. Available from: https://doi.org/10.1177%2F004728757801600401

[7] KOC, E. The role of family members in the family holiday purchase decision-making process. *International Journal of Hospitality & Tourism Administration* [online]. 2004, **5**(2), p. 85-102. ISSN 1525-6480, eISSN 1525-6499. Available from: https://doi.org/10.1300/J149v05n02_05

[8] NANDA, D., HU, C., BAI, B. Exploring family roles in purchasing decisions during vacation planning: Review and discussions for future research. *Journal of Travel and Tourism Marketing* [online]. 2007, **20**(3-4), p. 107-125. ISSN 1054-8408, eISSN 1540-7306. Available from: https://doi.org/10.1300/J073v20n03_08

[9] KIM, S. S., CHOI, S., AGRUSA, J., WANG, K. C., KIM, Y. The role of family decision makers in festival tourism. *International Journal of Hospitality Management* [online]. 2010, **29**(2), p. 308-318. ISSN 0278-4319. Available from: https://doi.org/10.1016/j.ijhm.2009.10.004

[10] YANG, M. J. H., KHOO-LATTIMORE, C., YANG, E. C. L. Three generations on a holiday: Exploring the influence of Neo-Confucian values on Korean multigenerational family vacation decision making. *Tourism Management* [online]. 2020, **78**, 104076. ISSN 0261-5177. Available from: https://doi.org/10.1016/j.tourman.2020.104076

[11] KOZAK, M., KARADAG, L. Who influences aspects of family decision making? *International Journal of Culture, Tourism and Hospitality Research* [online]. 2012, **6**(1), p. 8-20. ISSN 1750-6182. Available from: https://doi.org/10.1108/17506181211206216

[12] SPIERS, M. *Families with adolescents: vacation decision making* [online]. PhD thesis. Melbourne, Australia: Victoria University, 2017. Available from: http://vuir.vu.edu.au/id/eprint/33206

[13] SU, C. J., LIAO, H. H., LORGNIER, N., YEN, W. S., BOUCHET, P., HIROOKA, Y., JALLOULI, R., ROBERTS-LOMBARD, M., LAN, Y. F. Measuring adolescent influence tactics with parents in family vacation decisions: A comparable scale across 19 societies. *SAGE Open* [online]. 2019, **9**(1), 209. ISSN 2158-2440, eISSN 2158-2440. Available from: https://doi.org/10.1177/21582 44019835950

[14] YEN, W. S., SU, C. J., LAN, Y. F., MAZUREK, M., KOSMACZEWSKA, J., SVAGZDIENE, B., CHERENKOV, V. Adolescents' use of influence tactics with parents in family travel decision making: a cross-societal comparison in Eastern Europe. *The Social Science Journal* [online]. 2020, in press. ISSN 0362-3319, eISSN 1873-5355. Available from: https://doi.org/10.1080/03623319.2020.1745519

[15] SCHANZEL, H. The inclusion of fathers, children and the whole family group in tourism research on families. In: *Family tourism: multidisciplinary perspectives*. SCHANZEL, H., YEOMAN, I., BACKER, E. (eds.). Bristol, UK: Channel View Publications, 2012. ISBN 9781845413262, p. 67-80.

[16] LI, M., LEHTO, X., LI, H. 40 years of family tourism research: Bibliometric analysis and remaining issues. *Journal of China Tourism Research* [online]. 2020, **16**(1), p. 1-22. ISSN 1938-8160, eISSN 1938-8179. Available from: https://doi.org/10.1080/19388160.2020.1733337

[17] THERKELSEN, A. Deciding on family holidays: Role distribution and strategies in use. *Journal of Travel and Tourism Marketing* [online]. 2010, **27**(8), p. 765-779. ISSN 1054-8408, eISSN 1540-7306. Available from: https://doi.org/10.1080/10548408.2010.526895

[18] GUPTA, V., HANGES, P. J., DORFMAN, P. Cultural clusters: Methodology and findings. *Journal of World Business* [online]. 2002, **37**(1), p. 11-15. ISSN 1090-9516. Available from: https://doi.org/10.1016/S1090-9516(01)00070-0

[19] HOFSTEDE, G., HOFSTEDE, G. J., MINKOV, M. *Cultures and organizations, software of the mind. Intercultural cooperation and its importance for survival*. 3. ed. NY, New York: McGraw-Hill, 2010. ISBN 978-0-07-177015-6.

[20] PARK, M., CHESLA, C. Revisiting Confucianism as a conceptual framework for Asian family study. *Journal of Family Nursing* [online]. 2007, **13**(3), p. 293-311. ISSN 1074-8407, eISSN 1552-549X. Available from: https://doi.org/10.1177%2F1074840707304400

[21] SU, C. J., WANG, S. A cross-cultural study of East Asian adolescents' influence in family purchase decisions. *Journal of Global Business and Technology* [online]. 2010, **6**(1), p. 52-67. ISSN 1553-5495, eISSN 2616-2733.

[22] WU, M. Y., WALL, G. Chinese research on family tourism: Review and research implications. *Journal of China Tourism Research* [online]. 2016, **12**(3-4), p. 274-290. ISSN 1938-8160, eISSN 1938-8179. Available from: https://doi.org/10.1080/19388160.2016.1276873

[23] RALSTON, D. A. The crossvergence perspective: Reflections and projections. *Journal of International Business Studies* [online]. 2008, **39**(1), p. 27-40. ISSN 0047-2506, eISSN 1478-6990. Available from: https://doi.org/10.1057/palgrave.jibs.8400333

[24] REISINGER, Y., CROTTS, J. C. Applying Hofstede's national culture measures in tourism research: illuminating issues of divergence and convergence. *Journal of Travel Research* [online]. 2010, **49**(2), p. 153-164. ISSN 0047-2875, eISSN 1552-6763. Available from: https://doi.org/10.1177%2F0047287509336473

[25] BUDHWAR, P. S., VARMA, A., PATEL, C. Convergence-divergence of HRM in the Asia-Pacific: Context-specific analysis and future research agenda. *Human Resource Management Review* [online]. 2016, **26**(4), p. 311-326. ISSN 1053-4822. Available from: https://doi.org/10.1016/j.hrmr.2016.04.004

[26] DUNPHY, D. Convergence/divergence: a temporal review of the Japanese enterprise and its management. *Academy of Management Review* [online]. 1987, **12**(3), p. 445-459. ISSN 0363-7425, eISSN 1930-3807. Available from: https://doi.org/10.5465/amr.1987.4306560

[27] GUO, C. Cultural convergence, divergence and crossvergence. Vol. 6: International management [online]. In: *Wiley encyclopaedia of management*. COOPER, C. L., VODOSEK, M., HARTOG, D. N., MCNETT, J. M. (eds.). Hoboken, NJ: John Wiley & Sons, 2015. ISBN 9781118785317. Available from: https://doi.org/10.1002/9781118785317.weom060049

[28] RICKS, D. A., TOYNE, B., MARTINEZ, Z. Recent developments in international management research. *Journal of Management* [online]. 1990, **16**(2), p. 219-253. ISSN 0149-2063, eISSN 1557-1211. Available from: https://doi.org/10.1177%2F014920639001600202

[29] RALSTON, D. A., EGRI, C. P., CASADO, T., FU, P., WANGENHEIM, F. The impact of life stage and societal culture on subordinate influence ethics: a study of Brazil, China, Germany and the US. *Journal of International Management* [online]. 2009, **15**(4), p. 374-386. ISSN 1075-4253. Available from: https://doi.org/10.1016/j.intman.2009.02.004

[30] SU, C. J. The moderating role of composites of cultural values in predicting adolescents' influence on family purchase decisions: A study of Asian cases. *African Journal of Business Management* [online]. 2011, **5**(15), p. 6058-6071. ISSN 1993-8233. Available from: https://doi.10.5897/AJBM10.225

[31] RALSTON, D. A., GUSTAFSON, D. J., CHEUNG, F. M., TERPSTRA, R. H. Differences in managerial values: A study of US, Hong Kong and PRC managers. *Journal of International Business Studies* [online]. 1993, **24**(2), p. 249-275. ISSN 0047-2506, eISSN 1478-6990. Available from: https://doi.org/10.1057/palgrave.jibs.8490232

[32] XU, X., SONG, L. Export similarity and the pattern of East Asian development. In: *China in the global economy*. LLOYD, P. J., ZHANG, X. (eds.), Cheltenham, UK: Edward Elgar Publishing, 2000. ISBN 9781840642902, p. 145-164.

[33] LIN, C. L., FAN, C. L. Evaluation of CART, CHAID and QUEST algorithms: A case study of construction defects in Taiwan. *Journal of Asian Architecture and Building Engineering* [online]. 2019, **18**(6), p. 539-553. ISSN 1346-7581, eISSN 1347-2852. Available from: https://doi.org/10.1080/13467581.2019.1696203

[34] SONG, Y. Y., LU, Y. Decision tree methods: applications for classification and prediction. *Shanghai Archives of Psychiatry* [online]. 2015, **27**(2), p. 130-135. ISSN 1002-0829. Available from: https://doi.org/ 10.11919/j.issn.1002-0829.215044

[35] CHOU, J. S. Comparison of multi-label classification models to forecast project dispute resolutions. *Expert Systems with Applications* [online]. 2012, **39**(11), p. 10202-10211. ISSN 0957-4174. Available from: https://doi.org/10.1016/j.eswa.2012.02.103

[36] JAN, C. L. An effective financial statements fraud detection model for the sustainable development of financial markets: Evidence from Taiwan. *Sustainability* [online]. 2018, **10**(2), 513. eISSN 2071-1050. Available from: https://doi.org/10.3390/su10020513

[37] SUT, N., SIMSEK, O. Comparison of regression tree data mining methods for prediction of mortality in head injury. *Expert Systems with Applications* [online]. 2011, **38**(12), p. 15534-15539. ISSN 0957-4174. Available from: https://doi.org/10.1016/j.eswa.2011.06.006

[38] HSU, C. H., KANG, S. K. CHAID-based segmentation: international visitors' trip characteristics and perceptions. *Journal of Travel Research* [online]. 2007, **46**(2), p. 207-216. ISSN 0047-2875, eISSN 1552-6763. Available from: https://doi.org/10.1177%2F0047287507299571

[39] BARGEMAN, A., JOH, C. H., TIMMERMANS, H., VAN DER WAERDEN, P. Correlates of tourist vacation behavior: a combination of CHAID and loglinear logit analysis. *Tourism Analysis*. 1999, **4**(2), p. 83-93. ISSN 1083-5423, eISSN 1943-3999.

[40] VAN MIDDELKOOP, M., BORGERS, A., TIMMERMANS, H. Inducing heuristic principles of tourist choice of travel mode: A rule-based approach. *Journal of Travel Research* [online]. 2003, **42**(1), p. 75-83. ISSN 0047-2875, eISSN 1552-6763. Available from: https://doi.org/10.1177%2F0047287503254116

[41] ROJAS-DE-GRACIA, M. M., ALARCON-URBISTONDO, P. Couple's decision-making process and their satisfaction with the tourist destination. *Journal of Travel Research* [online]. 2019, **58**(5), p. 824-836. ISSN 0047-2875, eISSN 1552-6763. Available from: https://doi.org/10.1177%2F0047287518785052

[42] RAMASWAMI, M., BHASKARAN, R. A CHAID based performance prediction model in educational data mining. *International Journal of Computer Science Issues*. 2010, **7**(1), p. 10-18. ISSN 1694-0814, eISSN 1694-0784.

[43] ZALATAN, A. Wives involvement in tourism decision processes. *Annals of Tourism Research* [online]. 1998, **25**(4), p. 890-903. ISSN 0160-7383. Available from: https://doi.org/10.1016/S0160-7383(98)00038-3

[44] KHOO-LATTIMORE, C., PRAYAG, G., CHEAH, B. L. Kids on board: Exploring the choice process and vacation needs of Asian parents with young children in resort hotels. *Journal of Hospitality Marketing and Management* [online]. 2015, **24**(5), p. 511-531. ISSN 1936-8623, eISSN 1936-8631. Available from: https://doi.org/10.1080/19368623.2014.914862

[45] CHAUDHARY, M. Family decision - making in emerging economies. International *Journal of Business and Globalisation* [online]. 2015, **14**(3), p. 310-320. ISSN 1753-3627, eISSN 1753-3635. Available from: https://doi.org/10.1504/IJBG.2015.068630

[46] CHAUDHARY, M., GUPTA, A. Children's influence in family buying process in India. *Young Consumers* [online]. 2012, **13**(2), p. 161-175. ISSN 1747-3616. Available from: https://doi.org/10.1108/17473611211233512

[47] GHOUSE, S. M., CHAUDHARY, M., DURRAH, O. Socialization and the buying behaviour of the Arab child consumers: insights from Oman. *Journal of Islamic Marketing* [online]. 2019, **11**(2), p. 461-478. ISSN 1759-0833. Available from: https://doi.org/10.1108/JIMA-09-2018-0176

[48] FILIATRAULT, P., RITCHIE, J. R. B. Joint purchasing decisions: A comparison of influence structure in family and couple decision making units. *Journal of Consumer Research* [online]. 1980, **7**(2), p. 131-140. ISSN 0093-5301, eISSN 1537-5277. Available from: https://doi.org/10.1086/208802

[49] BRONNER, F., DE HOOG, R. A new perspective on tourist information search: discussion in couples as the context. *International Journal of Culture, Tourism and Hospitality Research* [online]. 2011, **5**(2), p. 128-143. ISSN 750-6182. Available from: http://dx.doi.org/10.1108/17506181111139555

[50] LIEN, N. H., WESTBERG, K., STAVROS, C., ROBINSON, L. J. Family decision-making in an emerging market: Tensions with tradition. *Journal of Business Research* [online]. 2018, **86**(C), p. 479-489. ISSN 0148-2963. Available from: https://doi.org/10.1016/j.jbusres.2017.09.003

[51] PENZ, E., KIRCHLER, E. Sex-role specialization in a transforming market: Empirical evidence from Vietnamese middle-class households. *Journal of Macromarketing* [online]. 2012, **32**(1), p. 61-73. ISSN 0276-1467, eISSN 1552-6534. Available from: https://doi.org/10.1177%2F0276146711421787

[52] RALSTON, D. A., HOLT, D. H., TERPSTRA, R. H., KAI-CHENG, Y. The impact of natural culture and economic ideology on managerial work values: A study of the United States, Russia, Japan and China. *Journal of International Business Studies* [online]. 1997, **28**(1), p. 177-208. ISSN 0047-2506, eISSN 1478-6990. Available from: https://doi.org/10.1057/palgrave.jibs.8490097

[53] KEITH, J. E., JACKSON JR, D. W., CROSBY, L. A. Effects of alternative types of influence strategies under different channel dependence structures. *Journal of Marketing* [online]. 1990, **54**(3), p. 30-41. ISSN 0022-2429, eISSN 1547-7185. Available from: https://doi.org/10.1177%2F002224299005400303

[54] BEATTY, S. E., TALPADE, S. Adolescent influence in family decision making: A replication with extension. *Journal of Consumer Research* [online]. 1994, **21**(2), p. 332-341. ISSN 0093-5301, eISSN 1537-5277. Available from: https://doi.org/10.1086/209401

[55] FOXMAN, E. R., TANSUHAJ, P. S., EKSTROM, K. M. Adolescents' influence in family purchase decisions: A socialization perspective. *Journal of Business Research* [online]. 1989, **18**(2), p. 159-172. ISSN 0148-2963. Available from: https://doi.org/10.1016/0148-2963(89)90033-7

[56] RALSTON, D. A., EGRI, C. P., KARAM, C. M., LI, Y., FU, P. P. Changes in work values across the regions of China. *Asia Pacific Journal of Management* [online]. 2018, **35**(1), p. 145-179. ISSN 0217-4561, eISSN 1572-9958. Available from: https://doi.org/10.1007/s10490-017-9519-y

[57] WANG, K. C., CHEN, J. S., CHOU, S. H. Senior tourists' purchasing decisions in group package tour. *Anatolia* [online]. 2007, **18**(1), p. 23-42. ISSN 1303-2917, eISSN 2156-6909. Available from: https://doi.org/10.1080/13032917.2007.9687034

[58] KANTAWATEERA, K., NAIPINIT, A., SAKOLNAKORN, T. P. N., KROEKSAKUL, P. Tourist transportation problems and guidelines for developing the tourism industry in Khon Kaen, Thailand. *Asian Social Science* [online]. 2015, **11**(2), p. 89-95. ISSN 1911-2017, eISSN 1911-2025. Available from: http://dx.doi.org/10.5539/ass.v11n2p89

[59] REILLY, J., WILLIAMS, P., HAIDER, W. Moving towards more eco-efficient tourist transportation to a resort destination: The case of Whistler, British Columbia. *Research in Transportation Economics* [online]. 2010, **26**(1), p. 66-73. ISSN 0739-8859. Available from: https://doi.org/10.1016/j.retrec.2009.10.009

[60] SUNG, H. H., MORRISON, A. M., HONG, G. S., O'LEARY, J. T. The effects of household and trip characteristics on trip types: A consumer behavioral approach for segmenting the US domestic leisure travel market. *Journal of Hospitality & Tourism Research* [online]. 2001, **25**(1), p. 46-68. ISSN 1096-3480, eISSN 1557-7554. Available from: https://doi.org/10.1177%2F109634800102500105

CREATIVE CITIES AND KNOWLEDGE MANAGEMENT APPROACH TO CULTURE-BASED URBAN REGENERATION IN SLOVAKIA: A MODEL

Mária Tajtáková*, Mária Olejárová

School of Management / City University of Seattle Programs, Bratislava, Slovakia

*E-mail of corresponding author: mtajtakova@vsm.sk

Resume

The term "Creative City" emerged in the 90s of the 20th century reflecting the trend of transforming post-industrial cities into new creative urban centres - bases for knowledge intensive firms, highly-skilled workers and major cultural assets. The concept of culture-based urban regeneration describes a scheme where culture is purposely employed as a vehicle for an overall urban and social revitalization. The paper addresses innovative processes within culture-based urban regeneration projects in three Slovak cities - Bratislava, Zilina and Kosice - under the concept of creative city. The focus is on the implementation of a tailor-made multi-factor knowledge management model with the aim of exploring the knowledge management practices in urban development projects dealing with the adaptive re-use of industrial and cultural heritage based on the non-profit bottom-up initiatives.

Article info

Received 5 September 2020
Accepted 18 January 2021
Online 25 June 2021

Keywords:

creative city,
culture-based urban regeneration,
adaptive re-use,
knowledge management,
model

Available online: https://doi.org/10.26552/com.C.2021.4.G25-G37

ISSN 1335-4205 (print version)
ISSN 2585-7878 (online version)

This is an open access article distributed under the terms of the Creative Commons Attribution 4.0 International License (CC BY 4.0), which permits use, distribution, and reproduction in any medium, provided the original publication is properly cited. No use, distribution or reproduction is permitted which does not comply with these terms.

1 Introduction

In the last decades knowledge has been increasingly recognized as the core factor of a new socio-economic model called the "Knowledge Economy". Within this paradigm the knowledge is considered to be the main source of economic progress in a nowadays society. It generates innovation, which enhances the creation of new socio-economic values and further development [1]. Sousa [2] emphasizes the recognition of knowledge as the fundamental driver of sustainable competitive and collaborative advantage and a major breakthrough in management thinking. In addition, Florida [3] advocates knowledge networks and highly skilled labour forces in creative industries as key factors driving the economic and urban growth and highlights the birth of a parallel socio-economic phenomenon - the "Creative Economy".

The creative economy is based on creative industries recognizing creative labour as a vital force for the future development. Levickaite and Reimeris [4] summarized major concepts of this new phenomenon: (1) *Creative industries* - based on John Howkins' creative economy [5] encompassing 15 sectors such as advertising, architecture, art, crafts, design, designer fashion, film/video, music, performing arts, publishing, scientific research and technology, software, toys/games, TV/radio and computer games; (2) *Creative class* - defined by Florida [3] as people working in the creative industries; (3) *Economic properties* - suggested by Caves [6] as a new logic of economic behaviour taking into account intrinsic factors like personal fulfilment, the variability of skills and talents and unpredictability; (4) *Creative identities* - described by Hartley [7] as vanishing borders between the creator, the vendor and the user of creative services; and (5) *Creative cities* - introduced by Landry and Bianchini [8] as a model of urban development based on culture and creative industries.

As emphasized by Renz [9], creativity, in the sense of Florida [3] and Landry and Bianchini [8], is not reserved to artists, but is a feature of all the occupations that are representing an ideas-driven knowledge economy. In this respect, the report entitled *Culture, the heart of the knowledge-based economy*, prepared by the European Cultural Parliament Lisbon Agenda Research Group [10], highlighted the strategic use of culture that goes beyond the arts and heritage and creates a new driving force for change and innovation in different domains of society. The culture has a potential to inject new ideas into business and the economy, it inspires communities to promote new ways of participation, responsibility and cohesion and re-energizes education. Furthermore, the communication of the European Commission named *Unlocking the Potential of Cultural and Creative Industries (CCI)* [11], recognised the CCI as one of Europe's most dynamic sectors catalyzing the spill-over effects on a wide range of economic and social contexts.

It is assumed that knowledge and creative economy are the two major forces that influence current economic and social development showing important intersections and possessing a significant potential of achieving a synergic effect. The paper addresses concurrent influences of knowledge and creative economy on innovative processes within the culture-based urban regeneration projects in Slovakia under the concept of creative city. Although cities are bases for knowledge-intensive activities, as well as centres of major cultural assets, only a limited attention [12-15] has been paid to the knowledge transfer within the culture-based urban regeneration projects. The focus here is on the implementation of a tailor-made multi-factor knowledge management model within the urban revitalization initiatives in three Slovak cities - Bratislava, Zilina and Kosice. Authors' aim is to explore the knowledge transfer and related managerial practices in urban development projects, dealing with the adaptive re-use of industrial and cultural heritage, based on non-profit bottom-up initiatives.

2 Creative cities and knowledge management: conceptual framework

The concept of the "Creative City" emerged in the 90s of the 20th century thanks to publications such as *The creative city* by Landry and Bianchini [8], *The cultural economy of cities* by Scott [16] and later on, *Cities and creative class* by Florida [17]. These works introduced a new way of thinking about the interrelationship between culture and a place. Culture has been understood as a "way of doing", which is typical for a particular location and thus determines its comparative advantage in the production of specialised goods and services [18].

The new perspective highlights a city as a place of opportunities suggesting that people living in it can respond to challenges of urban life with their creativity, as long as, the city provides conditions allowing them to do so [8]. Florida [17] emphasizes the economic value of human creativity in the city and proposes a three Ts concept for the economic growth - technology, talent and tolerance - stressing the important role of cities in bringing these three factors together.

Rodrigues and Franco [19] synthetized definition of creative cities as those that "advocate socio-cultural, economic and political changes and are characterized by diversity, openness, tolerance, the presence of a creative class and high cultural dynamism"'. Power and Scott [20] claimed that the creative cities show an intelligent strategy by joining their economic and urban strategies with culture. In view of the knowledge economy, cities being bases for knowledge intensive firms and institutions (such as universities, research centres or the cultural industries) possess a new strategic importance [8]. It is estimated that 54 % of the world population (3.7 billion people) live in urban areas and this percentage is expected to grow up to 73 % (5 billion) by 2030 [21].

From the development perspective, cities have been defined as dynamic systems, which flourish, stagnate and decline as a result of the interactions between the main actors in the urban arena: households, firms and the government [22]. According to Borg and Russo [18], the dynamism of the system is determined by technological progress, by changes in regulations and regimes (e.g. liberalisation of world markets and European integration) and by evolution in socio-economic factors, such as taste, education and demographics. In this regard, Scott [16] highlights a particular role of local culture in shaping the nature of intra-urban economic activity, which becomes a dynamic element of the culture-generation and innovative capacities of given places.

Stern [23] points out that places with high concentrations of cultural organizations and/or access to arts activities are more likely to undergo economic revitalization and to overcome barriers relating to class and ethnicity. Similarly, Shang-Ying Chen [24] argues that the more concerns on culture/creative industry and cultural tourism, the more concrete interactions between culture, economic and development occur.

Culture is seen as an eminent city industry and a typical urban phenomenon [18]. However, according to Stasilius [25] most of the nowadays cities live in their transitory periods caused by the vitality of renewed globalization leading to a new urban model in which an added value of cities does not depend on what is produced but on the intellectual capital applied to processes and services. This suggests growing impact of the knowledge economy on current urban transitions.

The process of transformation of an "industrial city" into the so-called "creative city" works under the concept of culture-based urban regeneration, respectively culture-led urban development. It describes a scheme where the culture is purposely employed as a vehicle for economic grow, local community enhancement, social inclusion and cultural tourism development leading to an overall urban and social revitalization. Pastak and Kahrik [26] highlight a substantial effect of the culture-based urban regeneration on improving the physical quality of public spaces by creating arenas for social interaction and educational activities. Borg and Russo [18] identify three main impact areas of culture on urban development: (1) direct and indirect economic impacts (employment, value creation, etc.), (2) induced effects of cultural activities on the quality of a place and (3) "creative inputs" accruing to the local networks of production and creative class development.

Actually, the concept of culture-based urban development is not really new. According to Scott [16], the interpenetration of culture and economy in given places was already highlighted by Alfred Marshall in his *Principles of Economics* (1920) who referred to the beneficial effects of "atmosphere" on the workings of 19th

century industrial districts. Scott [16] argues that in the present context, atmosphere refers more than anything else to a conglomeration of cultural synergies and semiotic fields rooted in the life, work and institutional infrastructures of particular cities. On a practical level, Landry [27] encourages urban planners to change their thinking from an urban engineering approach to a creative city making agenda where good atmosphere is the priority.

The nowadays perception of culture-based urban regeneration is basically twofold: On one hand, it is regarded as a mean for improving the quality of life for local residents and social inclusion [28-31]. On the other hand, it is seen as a way of enhancing the economic status and competitive position of cities including the cultural tourism development [17, 32-33]. However, Miles and Paddison [34] argue that achieving social cohesion and economic competitiveness have been increasingly considered as parallel and interrelated goals.

The culture-based urban development and the concept of creative city have been increasingly important for the global institutional and political agenda, as well. Since 2004, the *Creative Cities Network* has been developed by UNESCO with the aim of promoting cooperation with and among cities that have identified creativity as a strategic factor for sustainable urban development. Up to date the network comprises 246 cities from all over the world. The only Slovak city - Kosice - was included into the UNESCO *Creative Cities Network* in 2017 [35]. The network offers a key forum for brainstorming the role of creativity as a driver and an enabler for sustainable urban development and a platform for action and innovation towards implementing the 2030 Agenda for Sustainable Development at the city level [36].

In 2015, the European Commission established *The Cultural and Creative Cities Monitor* (CCC) as a tool for promoting mutual exchanges and learning between cities to boost culture-led development. It is designed to help cities to identify their strengths and opportunities, benchmark their performance and push for policies that boost their cultural, creative and innovation potential. In 2020, the second edition (mapping the year 2019) of the Cultural and Creative Cities Monitor was released showing how well 190 selected cities in 30 European countries (the EU-28 with Norway and Switzerland) perform compared to their peers. It provides evidence of the value of cultural investment and illuminates the importance of culture and creativity for cities increasingly competing on a global scale [37].

Creative cities have been selected based on their demonstrable engagement in promoting culture and creativity, from about 1 000 cities in Eurostat's Urban Audit. Therefore, the cities featured in the Monitor are already top performers. Four Slovak cities - Bratislava, Nitra, Kosice and Presov - have been included into the annual evaluation by the CCC Monitor. In total, 29 indicators and their organisation into nine dimensions, three sub-indices "Cultural Vibrancy", "Creative Economy" and "Enabling Environment" and an overall index "The Cultural and Creative Cities - C3 Index" is evaluated using both quantitative and qualitative data on a yearly basis. Up to date the CCC Monitor encompasses [37]:

- 98 cities, which have been or will be European Capitals of Culture (ECoCs) up to 2019, or which have been shortlisted to become an ECoC up to 2023;
- 59 UNESCO Creative Cities (including the most recent winners in 2015) - excluding overlap with the ECoC;
- 33 cities hosting at least two regular international cultural festivals running until at least 2015.

In 2020, the European Commission [38] launched a project named *Cultural Heritage in Action* as a part of the *European Framework for Action on Cultural Heritage* aimed at empowering cities and regions to strengthen their cultural heritage policies and initiatives as well as develop innovative solutions to preserve cultural heritage assets. One of the three key topics of the project is the adaptive re-use of heritage buildings that shall give a new use to obsolete, underused or misused buildings. In the adaptive reuse approach, rather than continuing the building's existing use through upgrades or restoring it to a specific time period, the new use is defined and adapted to the building while preserving and respecting its value and significance.

Authors assume that the crucial factor determining the success of culture-led urban development within the concept of creative city - and the factor interconnecting all three Borg and Russo's areas [18] - is the effective knowledge management. Yet, as pointed out by Porumb and Ivanova [12], knowledge distribution can be the most sensitive aspect of the knowledge management practice. Appelyard [39] emphasizes the need of understanding the mechanisms and determinants of knowledge flows in the organizational environment highlighting diverse knowledge sharing practices. The knowledge sharing is a critical element due to its role in converting individual tacit knowledge into the organization knowledge. In, addition, Martini [40] points out that knowledge sharing is becoming more essential for areas or industries that mostly depend on innovation as a competitive advantage, such as creative industries.

Therefore, a multi-factor knowledge management model is proposed, based on the SECI model to be implemented within the process of culture-led urban regeneration. The purpose of the model is to map and systematize crucial factors influencing the knowledge transfer within this particular environment and identify the most effective knowledge management practices. Authors believe that the expected economic effects, community inclusion and cultural sustainability within culture-based urban development can only be achieved in the repeated cycles of knowledge creation, externalization and sharing, storing and critical assessment.

Table 1 *Revitalization projects included into the study*

	project	city	original use	new use	revitalization period
1	KC Dunaj	Bratislava	department store	independent cultural centre	2010 - ongoing
2	Stara trznica	Bratislava	market city hall	market city hall & cultural centre	2013 - ongoing
3	Stanica Zariecie	Zilina	local train station	local train station & independent cultural centre	2003 - ongoing
4	Nova synagoga	Zilina	Jewish synagogue	cultural & community centre	2011 - ongoing
5	IC Culture Train Vysne Opatske	Kosice	suburb community centre	independent contemporary art centre	2005 - 2008
6	Tabacka Kulturfabrik	Kosice	tobacco factory	creative cultural factory & co-working incubator	2009 - ongoing

3 Methodology

3.1 The scope of the study

The study consisted of six culture-based urban regeneration projects carried out in different parts of Slovakia (Table 1). All the projects represented culture-led urban regeneration activities with a common aim of transforming unused and dilapidated buildings with diverse types of original use into new cultural venues. The regeneration processes started between the years 2003 and 2013 and are partly still in progress, although the major revitalization effort has already been accomplished.

The analysed projects were located in three different cities in Slovakia representing also three different regions: Bratislava - Cultural Centre Danube (Kulturne centrum - KC Dunaj) and Market City Hall (Stara trznica); Zilina - Local Train Station Zilina-Zariecie (Stanica Zilina-Zariecie) and New Synagogue (Nova synagoga); and Kosice - IC Culture Train (Vysne Opatske) and Tobacco Cultural Factory (Tabacka Kulturfabrik).

3.2 Data and methods

Both primary and secondary data were collected to map the knowledge management processes in the culture-led urban regeneration projects in three Slovak cities. Primary data were gathered via exploratory qualitative research using the method of semi-structured in-depth interviews. Repeated interviews with the main representatives of six culture-based urban regeneration initiatives were conducted in order to capture the larger process of knowledge conversion and transfer. Interviewees were initially approached by e-mail and further interviewed personally and by phone. After establishing the initial contacts, on-going revitalization processes were continuously monitored by phone, e-mail and media in the time span of five years between 2015 and 2020. The average number of repeated contacts with one interviewee represented nine interactions. In total, seven persons from six revitalization projects were interviewed. They encompassed executive managers, innovative leaders, founders/co-founders of not-for-profit organizations responsible for regeneration processes, networkers and other creative and knowledge workers representing the so-called bottom-up initiatives. The average length of practice in urban revitalization endeavours among the interviewees was eight years (in 2020). Several interviewees were involved in more than one project from the sample and acted as knowledge brokers.

In addition, primary observatory data was gathered in the form of notes and audio-visual recordings from visited events related to the revitalization projects. In total, almost hundred events organized by explored organizations, mostly in Bratislava, but also in Zilina and Kosice, were personally visited during the study. A very valuable addition was a participation in conferences, workshops and various events organized by local, regional and international institutions such as city councils, Slovak government, chambers of commerce and EU structures. The intention was to analyse, compare and summarize best practices in using knowledge tools, knowledge transfer and knowledge management within urban regeneration initiatives implementation. The secondary research, comprising the analysis of available printed and electronic documents related to the revitalization projects and official public reports (Ministry of Culture of the Slovak republic), was used in order to complement the primary research. This included also regular monitoring of the revitalization projects' web pages, local and national newspapers such as Trend, Profit, Forbes, Hospodárske noviny, SME, The Slovak Spectator, Journal SaB - Stavebníctvo a bývanie, CE.ZA.AR prize and others.

Table 2 *Codes for processing textual data*

	categories/codes	specification
1	actors & activities	presentation of main actors involved in the regeneration process (leaders and their teams) and activities connected with the revitalization effort
2	history & revitalization of the building	identification of the original purpose of the buildings, their history and the type of revitalization processes
3	adaptive re-use	transformation of the buildings' original purpose into new usage alternatives after the accomplished regeneration
4	programming	the structure and frequency of offered events and activities in the revitalized venues after their adaptive re-use
5	target group(s)	identification of target group(s) of the revitalized venues based the proposed activities and program
6	knowledge management	types of knowledge transfer, internal and external communication channels, involved actors, formalized and informal knowledge management processes
7	financing	sources of funding used for the regeneration, financial structure, financial vs. non-financial inputs, budgeting
8	stakeholders' feedback	opinions and reactions of stakeholders to the performance of the revitalized urban venues after their regeneration

Table 3 *Factors influencing the knowledge management in the sample*

organization type	organization size	management style	environment type	program offer	knowledge type	knowledge processes
civil organizations, urban cultural centres	small (up to 15 workers)	informal, low bureaucracy, low power distance, high trust	learning organization, middle degree of uncertainty, volunteering	multi-genre, stable, ad hoc	tacit, explicit	leadership, routines, acquiring, capturing, sharing

3.3 Data processing

A manual coding was applied in order to process the textual data from the in-depth interviews transcripts and gathered documents. Prior to the interviewing process, a coding scheme was developed by standardizing the units of text. These units represented also the final structure of interviews (Table 2): Actors and activities; history and revitalization of the building; adaptive re-use; programming; target group(s); knowledge management; financing; and stakeholders' feedback.

Nevertheless, the large amount of data and demanding conversion processes required a complex and systematic approach in data selection, analysis and comparison of the examined phenomena. The data processing involved detailed analysis and comparison of selected categories in all the examined projects, identifying similar and different characteristics. It was assumed that only an integrated framework and unified criteria could lead to design of the intended knowledge management model as an effective tool for mapping the knowledge transfers within the culture-based urban regeneration initiatives.

After processing all the gathered information, a multi-factor knowledge management model for the culture-based urban regeneration was developed. During this process, diverse factors influencing the knowledge management practices in the sample were summarized (Table 3).

4 The multi-factor knowledge management model

The tailor-made multi-factor knowledge management model [13-14] was developed for a specific purpose - the culture-led urban regeneration of unused buildings or venues - with the aim of mapping the knowledge transfer within this particular environment. The model is grounded in Nonaka and Takeuchi's SECI model (Socialization-Externalization-Combination-Internalization) suggesting that knowledge sharing can support creation of a new knowledge since it can transfer both tacit knowledge and explicit knowledge into the organizational knowledge [41]. The SECI model was selected as the most suitable one for application in the environment of urban revitalization after having researched and analysed several types of available knowledge management models. It highlights the need of assessing all the consecutive phases of knowledge conversion in order to achieve a desired goal: the efficient and effective knowledge management and communication between all the actors (team leaders, team members and stakeholders).

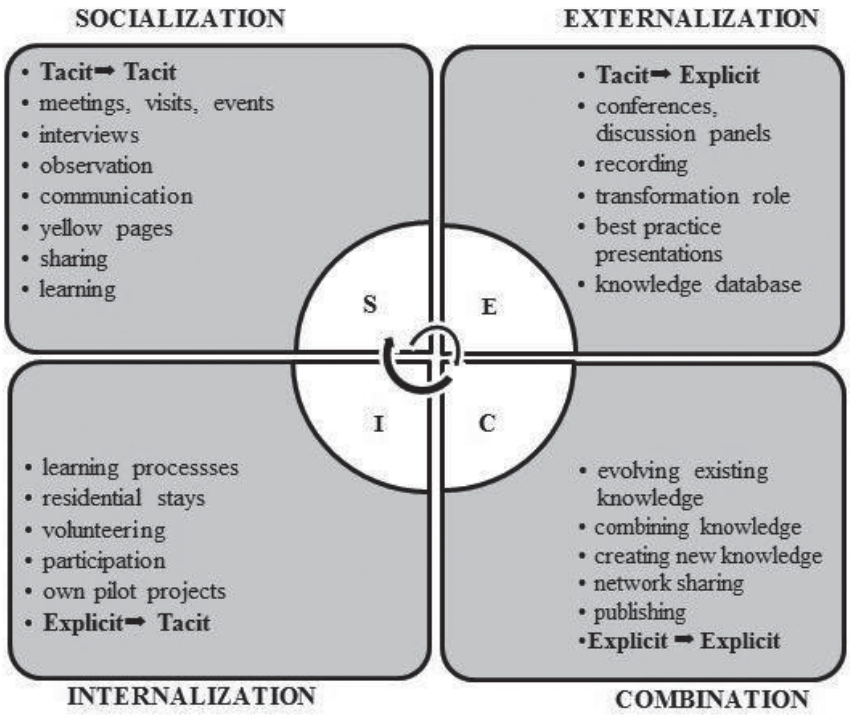


Figure 1 *Adjusted SECI model for application within the culture-based urban regeneration, based on Nonaka and Takeuchi's SECI model, [41]*

In the first stage, different phases of the SECI model were applied to the knowledge management processes implemented within the examined projects of the culture-based urban regeneration (Figure 1). While individual stages of the SECI model stayed identical, specific elements within them were modified or newly defined based on this research.

- **Socialization**

The initial phase of the SECI model runs within the context of culture-based regeneration projects at several levels:

1. Among the team members involved in regeneration projects (internally) and all stakeholders (externally) on the local and regional level.
2. Among the teams of non-profit organizations registered in the Slovak network of independent cultural centers ANTENA (Network of cultural centres and organisations operating in the field of independent arts and culture in Slovakia) on the national level.
3. Among the members of the international network T.E.H. - Trans Europe Halles (International network for grassroots cultural centres focused on repurposing abandoned buildings for arts, culture and activism), as the oldest and largest organization assisting in sharing experiences among European independent cultural centers on the international level.

The most effective and frequently used tools were visits, meetings, stays and presentations focused on identifying, learning and sharing the best practices experineced within diverse revitalization projects.

- **Externalization**

The phase of externalization includes organization of meetings, workshops, conferences and panel discussions with the use of explicit visual forms of knowledge management as pictures, videos, photographs, data presentations, statistics and reviews of visitors, or even documentaries from the reconstruction phases of the revitalized venues. Since most of the urban regeneration projects are run by the non-profit organizations supported via public funding schemes, the externalized knowledge is mandatory available on their websites, as well, as a tool for ensuring the transparent operations within the subsidized projects.

- **Combination**

Authors assume that the potential of the combination phase lies in implementation of information and knowledge exchange platforms, inspiration, adoption of successful ideas and creation of the new ones. However, it is important to be aware that the universal rules do not always work and specific local or regional differences should be considered. Therefore, it is recommended to achieve a high diversity and flexibility in activities such as program offers, entire dramaturgy, seasonal character, stakeholders' input and volunteers' involvement.

- **Internalization**

The final phase of the SECI model - internalization - appears to be an opportunity for creating a certain added value to all the previous stages. Within this phase it is expected to implement the skills and knowledges developed during the effective learning processes

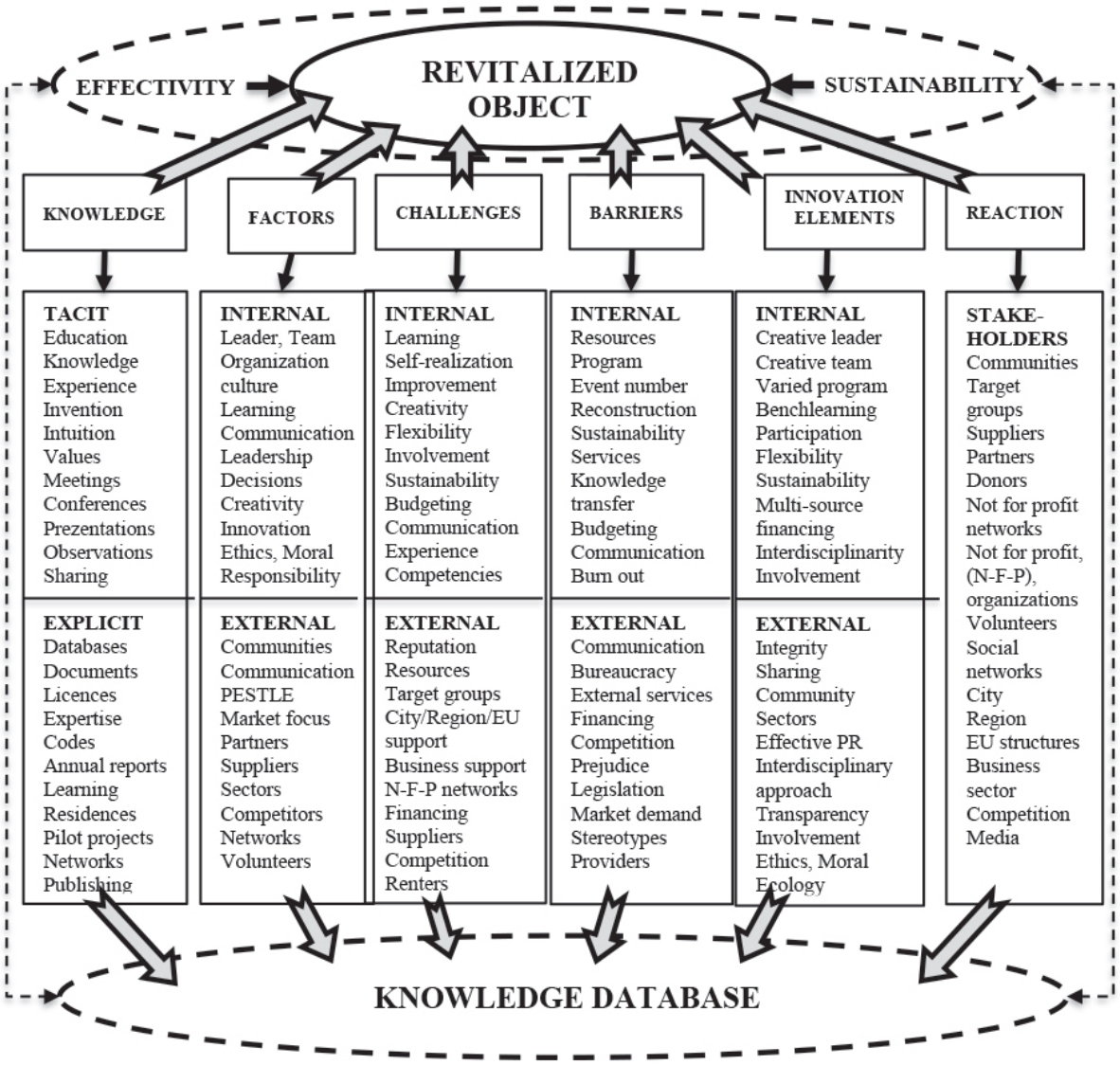


Figure 2 *The multi-factor knowledge management model for the culture-based urban regeneration*

in previous stages, active participation or creative and innovative approach. Through such activities as workshops, residential stays, visits, volunteering and regular communication, the project teams should succeed in developing and managing their own revitalization projects, with all the signs of transparency, effectiveness and sustainability.

In the second stage, the original spiral SECI model was enlarged for the purpose of this particular research by adding eight specific elements: Revitalized object, knowledge database, knowledge, factors, challenges, barriers, innovative elements and reaction. Its modification required a careful selection of processes and tools, which reflect the particular urban context of the examined organizations involved in the culture-based urban regeneration projects (Figure 2).

- **Revitalized object**

Revitalized object represents unused buildings or venues, which undergo a revitalization process. It should be noted that most of the urban regeneration projects are carried out as non-profit and bottom-up initiatives based on creative ideas and social innovation. The knowledge sharing from one project to another is a common modus operandi in this field. The main objective of the regeneration process is to bring unused buildings and venues back to life. In most cases the revitalization process involves a change of the original use of buildings into the new usage alternatives. The focus here was on those projects whose new purpose is linked to culture.

- **Knowledge database**

The knowledge database represents a generator of human knowledge coming from different sources, disciplines and areas. It is a bank of data, contacts, procedures, proposals, processes and solutions related to cases and issues that are treated or have been treated in the past. The knowledge database is an effective tool

especially in view of sustainability. Once the revitalization project is accomplished, the creative leaders may not present anymore, yet the needed knowledge remains available to other team members. However, the essential condition for the effective performance of knowledge database is its on-going maintenance. The data has to be gathered, sorted and stored in order to be available when needed. In addition, it requires the ability of all the involved workers to correctly identify the data, find, implement and share them.

- **Knowledge**

According to Wiig [42], knowledge - as a unique and very valuable source owned by an organization - is tightly connected to creation of an outstanding competitive advantage. Bures [43] highlights the unique value and character of knowledge as it possesses such attributes which are absent in other resources. However, its specific character of being unstable, unquantifiable, intangible and inseparable of its bearer makes it vulnerable at the same time. Therefore, the key factor of knowledge exploitation is its transfer and implementation. In the context of this study the focus was on transmission of both the tacit and explicit knowledge among team members, as well as from the previous regeneration projects to the new ones.

- **Factors**

In order to achieve desired outcomes in any type of organization, it is necessary to define and analyse both internal and external factors influencing the organizational performance. Several specific factors have to be considered in the case of urban regeneration projects, in particular the effective team management, creativity, innovation, learning environment and organizational culture. It is also necessary to highlight the importance of brave visions, complex and conceptual thinking, ethics, as well as open and effective communication with all the stakeholders: communities, municipality, regional and state institutions, businesses, media, European Union institutions, foundations, networks, etc.

- **Challenges**

Managers of the culture-based urban regeneration projects face several particular challenges given by the specific nature of this type of endeavours. Their ambition and mission are to contribute to the management of public matters, enhancement of the bottom-up activities, changes in stereotypes and replacement of the non-functional usage solutions with innovative and creative alternatives with inclusive and environmental emphasis. Expected results include goodwill, successful inter-sectoral cooperation and the attraction of diverse target groups and volunteers.

- **Barriers**

Barriers within the process of culture-led urban regeneration involve mainly administrative and functional obstacles, constraints, risks and limits. Basically, they can be split into two categories: internal barriers (lacking personal, insufficient material and financial resources, limitations in program offers or frequency of events) and external barriers (communication with stakeholders, competition on the market, low institutional support, biases). The impact of both has an equal importance and deserves attention in the urban revitalization processes in order to avoid the risk of failure.

- **Innovation elements**

Defining and implementing innovative elements within the culture-led urban regeneration processes appears to be a crucial activity for achieving demanding conversions of the venues, as well as for ensuring their sustainability. The innovative elements are often results of the bottom-up initiatives proposed by visionary leaders. Their common features are interdisciplinarity, holistic perspective, team learning, transparency, multi-source financing, synergy and tight public links.

- **Reaction**

Reaction within the model stands for the feedbacks received from all stakeholders. The ambition of most urban-regeneration projects lies in offering a unique vision, innovative added value and the meaningful transformation of unused buildings and venues into vibrant cultural and creative centres. Such an ambition addresses diverse publics including municipalities, regional and state institutions, not-for-profit organizations, businesses, artists, citizens, tourists and possibly others. It is important to monitor the reactions of all the concerned groups in order to ensure the acceptance and sustainability of the new purpose of revitalized industrial and cultural heritage.

As depicted at the scheme, the revitalized object and knowledge database represent two poles of the multi-factor knowledge management model. They interfere with the remaining elements within repeated knowledge transfers. The ultimate aim of the model is to achieve effectivity and sustainability of urban regeneration endeavours by ensuring the adequate knowledge transfer.

5 Findings

Provided that the focus was on urban regeneration, the regional capitals - Bratislava, Zilina and Kosice - from western, central and eastern part of Slovakia were included into the study. Two of the cities from our sample - Bratislava and Kosice - have already been recognized as “Creative Cities” and monitored within the *Cultural and Creative Cities Index* (CCC) established by the European Commission in 2015 (Table 4).

Bratislava registers the highest score in Slovakia within the C3 overall index and ranks 9th among the

Table 4 *Cultural and Creative Cities Index 2019 of the Slovak cities in the sample*

creative city	C3 index (overall)	cultural vibrancy	creative economy	enabling environment	group of cities	cities / group
Bratislava	31.9 (9th)	25.7 (12th)	44.4 (1st)	19.3 (33rd)	L*	40
Kosice	13.2(76th)	16.1 (71st)	9.6 (72nd)	14.9 (66th)	S-M**	79

* L group: 250 000 - 500 000 inhabitants

** S-M group: 50 000 - 250 000 inhabitants

based on [44]

40 ranked European cities with 250 000 to 500 000 inhabitants. Bratislava gets the top spot on "Creative Economy" in its group thanks to its leading position on *New Jobs in Creative Sector* and its good performance on *Creative & Knowledge-based Jobs* (8th). It also performs well on "Cultural Vibrancy" reaching the 12th position in the group.

Among the other ranked Slovak cities, all with fewer than 250 000 inhabitants, Kosice reaches the overall 76th position and performs best on "Enabling Environment", ranking the 66th among the 79 ranked European cities in the smallest population group. As in other European countries, capitals generally lead on "Creative Economy" but non-capitals, mostly medium-sized, do better on "Cultural Vibrancy" [44-45]. Being the only Slovak member of the UNESCO *Creative Cities Network*, Kosice becomes a hotspot for media arts thanks to its strong position in the ICT sector and a young vibrant creative community [35].

Most of the culture-based urban regeneration projects, included into the sample, represented cases where the original purpose of the venue was transformed into a new one, with a partial exception of Stara trznica (City Market Hall) in Bratislava and Zilina-Zariecie (Local Train Station) in Zilina. Diverse original purposes of the examined venues shifted into new creative urban centres satisfying the needs of various target groups: young people, families, seniors, creative artists, students and tourists. Moreover, those centres were expected not only to provide multi-genre cultural events and additional services, but also to preserve the historical value of the revitalized industrial and cultural heritage (buildings and its facilities).

Five of the six examined urban revitalization projects have been able to sustain their original intention and keep serving for cultural purposes. However, one project - IC Culture Train (Vysne Opatske) in Kosice did manage to revitalize the unused building but did not succeed in maintaining its cultural usage. As a result, the revitalized building serves as a grocery store today. Generally, the examined revitalization initiatives represented a continuous regeneration effort performed in several consecutive stages. The regeneration stages were carried out as follows:

(1) KC Dunaj: 2010 - 2012 Main reconstruction, 2013 - 2016 Interior revitalization and gallery, 2019 Interior remodelling.
(2) Stara Trznica: 2013 - 2015 Main Reconstruction with parallel Saturday markets in 2015, 2016 - 2019 Interior remodelling, 2017 Exterior square revitalization, 2018 - ongoing vivid square revitalization project.
(3) Stanica Zilina-Zariecie: 2003 - 2009 Main reconstruction, 2019 Remodelling after the fire.
(4) Nova Synagoga: 2011 - 2017 Main reconstruction with parallel cultural events, 2018 ongoing contemporary constructions upon exhibitions and events.
(5) IC Culture Train: 2005 - 2008 accomplished regeneration. The cultural purpose was not sustained.
(6) Tabacka Kulturfabrik: 2009 - 2015 Main reconstruction, 2020 Art garden revitalization.

The results of the research are very consistent within the whole sample in terms of the performance across the eight examined categories (textual codes). All the revitalized buildings possessed a historical value and were the property either of the municipality, region, state or church. The revitalization process involved the adaptive re-use of industrial or cultural heritage that gave a new use to obsolete, underused or misused buildings. The new purpose of the revitalized buildings was ensured via written agreements on their future usage alternatives between their owners and new operators. This approach is in line with Landry's [27] vision of the "Creative City", understood as a method of strategic urban planning where urban innovators are requested to reinvent the city as a lively centre of creativity laying the foundations for improving quality of life of the citizens.

Another common feature of all the analysed cases was implementation of the transparent multi-source financing models, perceived as a guarantee of the projects sustainability. In addition, the permanent effort to monitor stakeholders' and visitors' feedback, together with open and effective communication and long-term cooperation with municipalities and the business sector, helped in fulfilling the innovative and creative visions of the revitalization projects. In particular, the long lasting collaboration with municipalities in developing creative cities has been pointed out by Landry [27] who emphasizes the need of ensuring the facilitating factors that propel the creativity of creative people. These factors include infrastructure, research capacity, venture capital investment or clusters of producers.

Table 5 *Comparison and summary of the examined categories in the revitalized venues*

	categories	comparison and summary
1	actors & activities	Creative, innovative and interdisciplinary individuals, educated professionals with experiences and skills. They worked in organizations with strong culture and vision and used a conceptual thinking leading to the effective performance and sustainability.
2	history & building revitalization	Each of the regenerated venues had a distinct original purpose and historical value, though, after the reconstruction and conversion they all served as cultural, creative and community centres.
3	adaptive re-use	Buildings conversion was directed towards community cultural centres, independent culture, social events, markets and creative industries including creative hubs or labs.
4	programming	After the conversion, all the revitalized objects were characterized by multi-genre programming, regular markets, creative and innovative workshops, charity events, various services as shops, bars and cafes.
5	target group(s)	Target groups encompassed broad age and interest spectrum, social categories, locals and visitors and the representatives of all sectors.
6	knowledge management	Several types of knowledge transfer were identified: external knowledge transfer between different revitalization projects across Europe (based on networking), internal knowledge transfer via people working on more than one project and intra-team knowledge transfer via the transmission of individual knowledge into organizational knowledge. The project leaders shared their knowledge in managing the urban revitalization with their teams and also with other urban regeneration projects.
7	financing	Multi-source transparent financing models aimed at achieving sustainability of the revitalization projects were implemented.
8	stakeholders' feedback	Declared continual support, long-term visions, best practices status, awards for development, community involvement, effective communication, transparency and sustainability.

In spite of the fact that the revitalized venues were located in different cities and regions of Slovakia (considering possible demographic and economic deviations), the summarized findings indicate a prevailing compliance visible in all the analysed projects. Table 5 summarizes the outputs gained after the assessment and comparison of all the urban regeneration projects included into the sample.

In view of the knowledge transfer, it was crucial that the organizations implementing the revitalization projects were active members of several national and international platforms/networks for sharing knowledge and experiences related to urban regeneration initiatives, e.g. ANTENA (Network of cultural centres and organisations operating in the field of independent arts and culture in Slovakia) and T.E.H. (Trans Europe Halls - International network for grassroots cultural centres focused on repurposing abandoned buildings for arts, culture and activism). This was particularly important in view of the external knowledge transfer (both explicit and tacit) between different revitalization projects and cases. In addition, an internal knowledge transfer was identified and ensured via people who worked on more than one project (usually two projects) and transferred their knowledge gained in one project to the other one. Finally, an intra-team knowledge transfer was identified in the form of the transmission of individual tacit knowledge into organizational knowledge. Especially, the transfer of tacit knowledge from different sources was significant for succeeding in urban regeneration effort.

As a result, knowledge managers, together with their teams and other stakeholders, underwent the processes of gradual reconstruction and regeneration of dilapidated and unused heritage buildings and actively anticipated their adaptive re-use as vivid cultural urban centres. These successful urban transformations, encompassing innovative learning processes and effective knowledge management, caught the attention of public, as well as experts and resulted in attributing several Slovak and foreign awards.

6 Conclusions

Common success factors for an effective and efficient knowledge management were identified within the culture-based urban regeneration under the concept of a creative city. All the projects included into the study showed almost identical characteristics in the examined categories. Their primary intention was to convert dilapidated and unused buildings into vibrant cultural centres offering a rich multi-genre program for diverse target groups. This research confirmed that creative and innovative approach within knowledge management enables overcoming barriers and obstacles in the revitalization of urban industrial and cultural heritage, based on the bottom-up initiatives and effective knowledge creating-sharing cycle. It recognized that the effective knowledge transfer is a key element for achieving a successful urban regeneration, based on the adaptive re-use of unused venues with the aim of developing creative quarters and cities. Considering the fact that knowledge management involves a significant multidisciplinary character, a complex and holistic approach is suggested for an effective

knowledge management within the culture-based urban regeneration initiatives.

The proposed multi-factor knowledge management model served to map knowledge management processes in culture-based urban regeneration projects in three Slovak cities. Nevertheless, the model can be applied to all the cases of revitalization of unused, respectively inappropriately used urban buildings and their adaptive re-use for cultural purposes. It highlights and recommends the correct usage of knowledge management tools for teams and organizations involved in the culture-led urban revitalization. The knowledge that is not well managed and shared evaporates easily, especially the tacit knowledge that resides in the minds of people and is accumulated over time, which must be shared. Hence, the knowledge sharing is considered to be the crucial element for an effective knowledge management.

The attention should be paid especially to the knowledge database (serving as a basis of human knowledge, procedures, data and solutions from various disciplines and fields), which constitutes the indispensable ground for knowledge utilization, as well as the knowledge transfer. The authors are convinced that only permanent creation, distribution, storing and sharing of knowledge, among creative knowledge workers and other involved participants, ensure that the knowledge management becomes an effective tool for achieving a successful culture-based urban revitalization. Project leaders together with their teams demonstrated the ability to learn and share valuable knowledge and experiences coming not only from their previous activities but from experiences of their Slovak or foreign peers, as well.

The authors believe that the creative, innovative and interdisciplinary approach, together with the bottom-up activities, focused on the multi-functional usage of revitalized venues contributed to strengthening their genius loci while serving a new cultural purpose. In addition, it is believed that the adaptive re-use of obsolete, underused or misused heritage buildings enhances the potential of urban areas for becoming vivid creative quarters and fosters regional development based on the creative economy.

The limitations of this study consist in lacking comparison of knowledge management practices in similar culture-based urban revitalization projects under the concept of creative city. This is due mainly to the limited research carried out in the concerned area. Therefore, a further research is needed in order to confirm or debate these findings.

References

[1] TAJTAKOVA, M. The arts and culture in the knowledge era. In: 7th International Workshop on Knowledge Management: proceedings. 2012. ISBN 978-8089-306-183, p. 1-7.

[2] SOUSA, M. Open innovation models and the role of knowledge brokers. ARK Knowledge Management Insight. 2008, p. 18-22 [online] [accessed 2018-9-12]. Available from: http://citeseerx.ist.psu.edu/viewdoc/download?doi=10.1.1.457.2055&rep=rep1&type=pdf

[3] FLORIDA, R. *The rise of the creative class: and how it's transforming work, leisure, community and everyday life*. New York: Basic Books, 2002. ISBN 978-0465024773.

[4] LEVICKAITE, R., REIMERIS, R. A pentagon of creative economy / Kurybos ekonomikos penkiakampis (in Lithuanian). *Coactivity: Philosophy, Communication / Santalka: Filosofija, Komunikacija* [online]. 2011, **19**(1), p. 83-91. ISSN 2029-6320, eISSN 2029-6339. Available from: https://doi.org/10.3846/coactivity.2011.09

[5] HOWKINS, J. *The creative economy: how people make money from idea.* 2. ed. London: Penguin Business, 2013. ISBN 9780713994032.

[6] CAVES, R. *Creative industries: contracts between arts and commerce.* Cambridge: Harvard University Press, 2002. ISBN 978-0674008083.

[7] HARTLEY, J. *Creative industries.* Wiley-Blackwell Publishing, 2005. ISBN 978-1-405-10147-9.

[8] LANDRY, C., BIANCHINI, F. *The creative city.* Paper no. 12. London: Demos in association with Comedia, 1995. ISBN 1898309167.

[9] RENZ, E. Business models and the creative city: Amsterdam's knowledge mile in the limelight. Hogeschool van Amsterdam, Media, Creatie en Informatie, CREATE-IT Applied Research, Research Group Crossmedia, Supervisor VAN VLIET, H., 2015 [online] [accessed 2020-10-12]. Available from: https://www.hva.nl/create-it/gedeelde-content/publicaties/ publicaties-algemeen/crossmedia/paper-erich-renz.html

[10] EUROPEAN CULTURAL PARLIAMENT. Lisbon Agenda Research Group. Culture, the heart of the knowledge-based economy. The strategic use of culture in the European project. Tuscany, 2006 [online] [accessed 2020-10-12]. Available from: http://www.kulturparlament.com/wp-content/uploads/2011/05/ECP-EU-strategic-use-of-culture-030906-final.pdf

[11] EUROPEAN COMMISSION. Unlocking the potential of cultural and creative industries. Green paper. Brussels, 27.4.2010 COM(2010) 183 final [online] [accessed 2020-10-12]. Available from: https://eur-lex.europa.eu/legal-content/EN/TXT/PDF/?uri=CELEX: 52010DC0183&from=EN

[12] PORUMB, E. M., IVANOVA, N. V. Development through knowledge economy: Cluj-Napoca - European smart city. *Management Dynamics in the Knowledge Economy.* 2014, **2**(3), p. 453-461. ISSN 2286-2668.
[13] OLEJAROVA, M. Knowledge management and learning in urban revitalization processes of selected non-profit cultural organizations in Slovakia. In: 20th International Conference on Interactive Collaborative Learning and 46th International Conference on Engineering Pedagogy ICL 2017: proceedings. 2017.
[14] OLEJAROVA, M., TAJTAKOVA, M. Knowledge management within culture-based urban regeneration projects in Slovakia. In: 13th International Workshop on Knowledge Management "Knowledge: Measurement, Evaluation and Interpretation": proceedings. 2018. ISBN 978-80-89306-37-4, p. 98-108.
[15] TAJTAKOVA, M., OLEJAROVA, M. The role of knowledge brokers in culture-led urban revitalization. In: 14th International Workshop on Knowledge Management "*Knowledge Workers in the Knowledge Era*": proceedings. 2018. ISBN 978-80-89306-41-1, p. 133-139.
[16] SCOTT, J. A. The cultural economy of cities. *International Journal of Urban and Regional Research* [online]. 1997, **21**(2), p. 323-339. eISSN 1468-2427. Available from: https://doi.org/10.1111/1468-2427.00075
[17] FLORIDA, R. *Cities and the creative class*. London: Routledge, 2005. ISBN 0-415-94887-8.
[18] VAN DER BORG, J., RUSSO, A. P. *The impact of culture on the economic development of cities.* Rotterdam: European Institute for Comparative Urban Research, Erasmus University Rotterdam, 2005.
[19] RODRIGUES, M., FRANCO, M. Measuring the performance in creative cities: proposal of a multidimensional model. *Sustainability* [online]. 2018, **10***(11),* 4023. eISSN 2071-1050. Available from: https://doi.org/10.3390/su10114023
[20] POWER, A. J., SCOTT, D. Culture, creativity and urban development. In: *Handbook of local and regional development*. PIKE, J., RODRIGUEZ-POSE, A., TOMANEY, A. (eds.). Routledge: Abingdon-on-Thames, UK, 2011. ISBN 9780415548311, p. 162-171.
[21] UNESCO. Creative cities of UNESCO for sustainable development. 2018 [online] [accessed 2020-7-12]. Available from: https://en.unesco.org/creative-cities/sites/creative-cities/files/unesco_uccn_en_180530_final.pdf
[22] VAN DEN BERG, L. *Urban systems in a dynamic society*. Aldershot: Gower Pub Co, 1987. ISBN 978-0566052514.
[23] STERN, M. Testimony of Mark J. Stern. Social impact of the arts project. 2000 [online] [accessed 2018-09-12]. Available from: http://www.ssw.upenn.edu/SIAP
[24] SHANG-YING, CH. Constructing cultural indicator system of Kaohsiung City, Taiwan. In: 9th International Conference of Arts and Cultural Management A.I.M.A.C.: proceedings. 2007.
[25] STASIULIS, N. The idea of the creative society and the development of creative industries. *Economics and Sociology* [online]. 2017, **10**(2), p. 217-226 [accessed 2020-7-12]. ISSN 2071-789X. Available from: https://doi.org/10.14254/2071-789X.2017/10-2/16
[26] PASTAK, I., KAHRIK, A. The impacts of culture-led flagship projects on local communities in the context of post-socialist Tallinn. *Sociologicky Casopis / Czech Sociological Review* [online]. 2016, **52**(6), p. 963-990 [accessed 2018-09-12]. ISSN 0038-0288, eISSN 2336-128X. Available from: https://doi.org/10.13060/00380288.2016.52.6.292
[27] LANDRY, C. *The creative city. a toolkit for urban innovators* [online] [accessed 2020-10-12]. London: Earthscan, 2008. ISBN 1-85383-613-3. Available from: https://doi.org/10.1080/23311975. 2015.1127744
[28] TUROK, I. Property-led urban regeneration: panacea or placebo? *Environment and Planning* [online]. 1992, **24**(2), p. 361-379 [accessed 2020-7-12]. ISSN 0308-518X, eISSN 1472-3409. Available from: https://doi.org/10.1068/a240361
[29] JAYNE, M. Culture that works? Creative industries development in a working class city. *Capital and Class* [online]. 2004, **84**, p. 199-210 [accessed 2018-09-12]. ISSN 0309-8168, eISSN 2041-0980. Available from: https://doi.org/10.1177/030981680408400119
[30] EVANS, G. Measure for measure: evaluating the evidence of culture's contribution to regeneration. *Urban Studies* [online]. 2005, **42**, p. 959-983 [accessed 2018-09-12]. ISSN 0042-0980, eISSN 1360-063X. Available from: https://doi.org/10.1080/00420980500107102
[31] SAGAN, I., GRABKOWSKA, M. Urban regeneration in Gdansk, Poland: local regimes and tensions between top-down strategies and endogenous renewal. *European Planning Studies* [online]. 2012, **20**(7), p. 1135-1154 [accessed 2018-09-12]. ISSN 0965-4313, eISSN 1469-5944. Available from: https://doi.org/10.1080/09654313.2012.674347
[32] TEMELOVA, J. Flagship developments and the physical upgrading of the postsocialist inner city: the Golden Angel project in Prague. *Geografiska Annaler: Series B - Human Geography* [online]. 2007, **89B**(2), p. 169-181. eISSN 1468-0467. Available from: https://doi.org/10.1111/j.1468-0467.2007.00246.x
[33] PRATT, A. C. Creative cities: the cultural industries and the creative class. *Geografiska Annaler: Series B - Human geography* [online]. 2008, **90**(2), p. 107-117 [accessed 2018-09-12]. eISSN 1468-0467. Available from: https://doi.org/10.1111/j.1468-0467.2008.00281.x

[34] MILES, S., PADDISON, R. Introduction: the rise and rise of culture-led urban regeneration. *Urban Studies* [online]. 2005, **42**, p. 833-839 [accessed 2018-09-12]. ISSN 0042-0980, eISSN 1360-063X. Available from: https://doi.org/10.1080/00420980500107508

[35] UNESCO. Creative cities network [online] [accessed 2020-08-02]. Available from: https://en.unesco.org/creative-cities/

[36] UNESCO. Voices of the city. UNESCO creative cities moving towards the 2030 Agenda for Sustainable Development. 2019 [online] [accessed 2020-08-02]. Available from: https://en.unesco.org/creative-cities/sites/creative-cities/files/16_pages_villes_creatives_ uk_bd.pdf

[37] MONTALTO, V., TACAO MOURA, C., PANELLA, F., ALBERTI, V., BECKER, W., SAISANA, M. *The cultural and creative cities monitor: 2019 edition* [online] [accessed 2020-08-02]. Luxembourg: Publications Office of the European Union, 2019. ISBN 978-92-76-08807-3. Available from: https://doi.org/10.2760/257371.

[38] EUROPEAN COMMISSION. Cultural Heritage in Action. European Framework for Action on Cultural Heritage. 2020. [online] [accessed 2020-08-02]. Available from: http://www.cultureforcitiesandregions.eu/culture/project

[39] APPLEYARD, M. How does knowledge flow? Interfirm patterns in the semiconductor industry. *Strategic Management Journal, Special Issue: Knowledge and the Firm*. 1996, **17**(2), p. 137-154 [online] [accessed 2020-10-12]. Available from: https://doi.org/10.1002/smj.4250171112

[40] MARTINI, L. Knowledge sharing in a creative city. In: International Conference on Knowledge Management ICKM 2016: proceedings [online] [accessed 2020-10-12]. 2016. p. 79-90. Available from: http://doi:10.1016/j.procs.2016.09.102

[41] NONAKA, I., TAKEUCHI, H. The knowledge-creating company? How Japanese create the dynamics of innovation. *Long Range Planning* [online]. 1996, **29**(4), p. 592. ISSN 0024-6301. Available from: https://doi.org/10.1016/0024-6301(96)81509-3

[42] WIIG, K. Knowledge management: an emerging discipline rooted in a long history. *Journal of Knowledge Management* [online]. 1999, **1**(4), p. 269-274 [accessed 2020-08-02]. ISSN 1367-3270. Available from: http://www.krii.com/ downloads/km_emerg_discipl.pdf

[43] BURES, V. Conceptual perspective of knowledge management. *E and M: Economics and Management* / *E a M: Ekonomie a Management*. 2009, **12**(2), p. 84-96. ISSN 1212-3609.

[44] EUROPEAN COMMISSION. The Cultural and Creative Cities Monitor 2019. Country fact sheets 2019 - Slovakia [online] [accessed 2020-08-02]. Available from: https://publications.jrc.ec.europa.eu/repository/bitstream/JRC117336/sk.pdf

[45] EUROPEAN COMMISSION. Cultural and creative cities monitor. Composite indicators [online] [accessed 2020-08-02]. Available from: https://composite-indicators.jrc.ec.europa.eu/cultural-creative-cities-monitor/performance-map

INCREASED INTEREST IN MILITARY TOURISM ON SELECTED EXAMPLES FROM THE AREA OF NORTHERN AND NORTHEASTERN POLAND

Aleksandra Zienkiewicz[1], Tomasz Podciborski[2], Rafal Kaźmierczak[2,*]

[1]Institute of Socio-Economic Geography and Tourism, Pomeranian University in Slupsk, Slupsk, Poland
[2]Department of Spatial Analysis and Real Estate Market, Faculty of Geoengineering, University of Warmia and Mazury in Olsztyn, Olsztyn, Poland

*E-mail of corresponding author: rafal.kazmierczak@uwm.edu.pl

Resume
Military tourism is one of the forms of tourism that is not sufficiently researched throughout Poland. It is only in recent years, after the period of political transformation, that interest in this phenomenon has been growing every year. This research has aimed to indicate the possibilities of military tourism development in northern and northeastern Poland. It includes an analysis of data concerning the Naval Museum in Gdynia, the "Wolf's Lair" Fortress in Gierloz and an example of a military event - an air show, which took place on the premises of the 44th Airborne Museum in Gdynia. Results of the analysis of the military tourism development in northern and north-eastern Poland indicate that military sites and military-themed events attract considerable tourist traffic and play an important role in the overall development of tourism.

Article info
Received 31 January 2021
Accepted 29 March 2021
Online 13 September 2021

Keywords:
military tourism,
former military sites,
the attractiveness of tourist destinations,
northern Poland,
north-eastern Poland

Available online: https://doi.org/10.26552/com.C.2021.4.G38-G50

ISSN 1335-4205 (print version)
ISSN 2585-7878 (online version)

1 Introduction

In the period before the Pandemic COVID19 in 2019, 959 museums and museum branches were active in Poland. This was 1.5% more museums than in 2018, with a total of 40.2 million visitors to all facilities. Museums organized 2.7 thousand regular exhibitions and 5.0 thousand temporary exhibitions in Poland. The number of visitors to museums per 1000 people amounted to 1048 people. Among all the museums in Poland, 77.1% belong to the public sector and they are managed by local self-governments. The characteristics of museums in Poland are presented in Figure 1 [1].

Many countries are actively pursuing tourism-oriented policies to boost their economic growth [2]. Tourism means different things to different people [3]. The military tourist institutions have a significant capacity regarding both room and board services and non-accommodation services at their disposal what makes an important factor relevant to any adequate positioning in both domestic and foreign tourist market [4]. Military tourism is a segment of the tourism industry that has been attracting increasing interest in Poland and throughout the world in recent years. The growing popularity of military tourism can be attributed not only to a large number of historic military sites, in particular in northern and north-eastern Poland but also to the military-themed events and shows that attract crowds of spectators each year [5]. This term can also be analyzed in a broader context because military tourism enthusiasts have an interest in a wide variety of military objects, fortification lines, museums, exhibitions, military collections, historic military trails, cultural heritage trails and battlefields. For this reason, this form of tourism sometimes also refers to military tourism as military culture tourism, war tourism, battlefield tourism, or armament tourism [6-10]. This phenomenon was also noticed by Hrusovsky and Noeres, who claim that one can distinguish tourism products that focus on use of military equipment and products that focus on products related to historical events [11].

This study aimed to identify the opportunities for development of military tourism on the example of former military sites and structures in northern and north-eastern Poland that have been transformed into tourist destinations and recreational areas. The study focuses on two geographic areas: the South Baltic Littoral Region and the East Baltic Lakelands [12]. Military tourism was discussed on the example of the Naval Museum in Gdynia, the Wolf's Lair in Gierloz and the 44th Naval Air Base in Siemirowice. The sites and events selected for this study are located in northern

This is an open access article distributed under the terms of the Creative Commons Attribution 4.0 International License (CC BY 4.0), which permits use, distribution, and reproduction in any medium, provided the original publication is properly cited. No use, distribution or reproduction is permitted which does not comply with these terms.

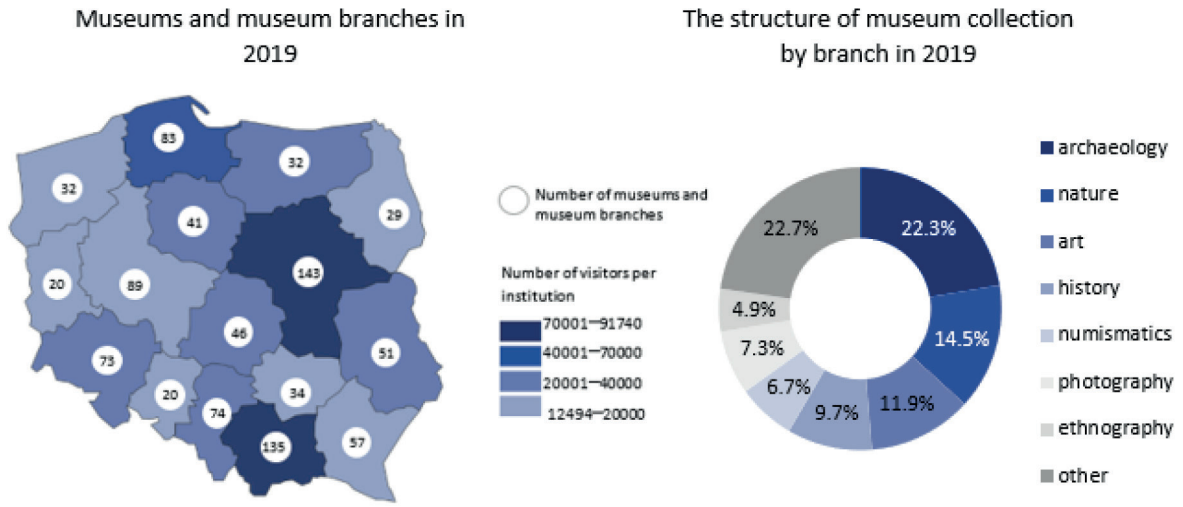


Figure 1 *Museums and museum branches in 2019 [1]*

and north-eastern Poland, which abounds in military attractions on account of its rich history and strategic location. Throughout centuries, the Polish borders have been shaped by foreign powers. Numerous battles were fought and defensive structures were built in these Polish regions. The examples of military sites and objects presented in the article are nowadays used as tourist and recreation areas, as well.

The current state of research on military tourism in Poland is still insufficient, therefore this study aimed to indicate the possibilities of development of military tourism in northern and north-eastern Poland, inter alia, through analysis of tourist traffic in selected objects related to military heritage and on the example of a selected outdoor event. An important aspect of the research was also an attempt to answer questions about the current position of military tourism among other forms of tourism and whether maintaining the current trend of interest in military tourism would provide a chance for its development in Poland. The findings obtained as a result of the analyses would allow an assessment of the current functioning of the facilities and should indicate the desired direction of promotion and creation of appropriate tourist offers.

As a part of this study, research on the tourism movement of military facilities was carried out to indicate the further development of a relatively new form of tourism, which is military tourism.

2 Literature review

Military tourism is an atypical and relatively new form of tourism, which is also referred to as military culture tourism, war tourism, battlefield tourism and armament tourism [13-14]. Generally, one can define "military tourism" as a typical recreational and tourist program of visual, cultural and material consumption [15]. The definitions of tourism proposed in the Polish literature emphasize the cultural value of tourist destinations, which cater to the demand of visitors who have a specific interest in the military history of a given region. According to Jedrysiak and Mikos von Rohrscheidt [16], military culture tourism involves travel undertaken for self-education and personal experience, where visits to defensive structures and historic sites related to military conflict, the armed forces, weapons and military equipment are an important part of the tour program. Tourists visit fortifications, historic battlefields, areas connected with famous military leaders, military factories, museums, military shelters, bunkers and other defensive structures and they attend military-themed events and shows [17].

Tourists also have a growing interest in facilities and centers that plan military operations, former military factories, current and former military training areas, areas connected with famous military leaders, battlefields and military cemeteries. Lawin and Stasiak [18] identified the following categories of military-themed attractions: defensive structures, battlefields, military museums, other museums with large collections of military artefacts, battle memorials, monuments commemorating historic events, areas connected with famous military leaders, war graves, military cemeteries and military events. Examples of military sites and objects presented in the article are nowadays also used as tourist and recreation areas.

According to Kowalczyk [13, 19], heritage tourism and military tourism have the following functions: historical, educational, martyrological, political, ideological, cultural, entertainment, recreation, sports and adventure. The cited author also classified military tourism attractions into those that are and are not directly related to a specific geographic location (and involve objects of material and non-material culture). Kowalczyk defined historic military tourism as all the forms of tourist activities that are undertaken - as the primary or secondary goal - to visit historic sites

and locations connected with military activity and the military culture [20].

According to Lawin and Stasiak [18], military tourists have an interest in defensive structures such as strongholds, fortresses, citadels, bunkers, fortification lines (accessible or not accessible to tourists), battlefields, military museums, battle memorials, war graves and military cemeteries. Tourists also attend military-themed events, such as military picnics, military fan conventions and reenactments of historical battles.

Interestingly, the concept of military tourism emerged in Polish literature only towards the end of the first decade of the 21st century. In their monograph, Lijewski, Mikulowski and Wyjrzykowski [21] referred to local history tourism, exploratory tourism, as well as man-made attractions such as historic and military sites and monuments, but they did not identify military tourism as a separate category of tourism. The cited authors remarked that one of the objectives of local history tourism is to provide visitors with an opportunity to experience sites associated with patriotic events. The Polish history and landscape abound in national memorials and areas where battles for independence were fought. These sites became widely available to the public only after the end of the Communist regime in the early 1990s. They can be expected to become important destinations for exploratory tourism shortly. Poczta [22] reported on the growing popularity of individual tourism, including adventure tourism. The above study also revealed an increase in the demand for active tourism, which enables visitors to experience pristine nature and unspoiled landscapes. Military tourism is an unconventional form of active tourism. In Poland, research into military tourism was also conducted by Chylinska [23], Cynarski [24], Stach [25], Stach et al. [26] and Zglobicki [27].

In foreign literature, the first studies on military heritage tourism were undertaken in the early 21st century [28]. Military heritage tourism was defined as a subset of heritage tourism that enables individuals to experience feelings of appreciation, awe, nostalgia and emotional attachment through contact with past events, culture and shared history. The growing popularity of military heritage sites worldwide was highlighted in a paper entitled "Commercial tourist attraction" [29]. Lemelin, Whyte et al. [30] analyzed military tourism from the indigenous perspective in areas where colonial conquest took place (Battles of Isandlwana, Rorke's Drift and Blood River). Logan and Reeves [15] remarked on the growing popularity of heritage sites related to dark events and traumatic memories, both at the national and international level. Military tourists have an interest in places and institutions that represent the legacy of painful periods in history, such as massacre and genocide sites, former prisons, places of military internment and battlefields.

Military heritage tourism was explored by Huh [11] and Chhabra et al. [31], whereas the experiences related to blood tourism and dark tourism were described by Biran and Hyde [32]. Raine [33] listed several factors that motivate individuals to visit military heritage sites. Magee and Gilmore [34] identified three categories of tourists who travel to military sites:

- visitors for whom military heritage sites have personal and emotional significance and carry a feeling of being connected to their heritage,
- ordinary tourists who do not have personal links to military heritage sites and view them merely as a leisure activity. These types of tourists primarily seek education and knowledge,
- ambivalent tourists who visit military heritage sites to "see it to believe it" [35].

Publications exploring the historical background of military events, such as Military Pomerania between the 12th and the 21st century [36] and Military Artefacts of Pomerania [37] play an important role in the literature on military tourism in northern and north-eastern Poland. Other notable publications in this field of research include "Squandered Opportunities" by Pradzynski [38], Military Artefacts of Polish Military Formations and the Polish Army from 1914-1922 [39], Military Museology [40-41], Underwater Military Vehicles and Artefacts in the Gulf of Gdansk [42], as well as articles by Piatek [43], Jurga [44], Lamparska and Malik [36] and Jarosz [37]. Encyclopedia of Military Technology [5] and Military Artefacts of Pomerania from the 19th to the 20th century by Drzewiecki and Rozycki [45] also make valuable contributions to the literature on military heritage.

Although military tourism is slowly gaining popularity all over the world, as evidenced by quite a rich literature on the subject, in Poland it is still niche tourism. Even though there are quite a lot of studies on military heritage sites, so far there has not been enough research on the state of tourism in these sites. Most of the research includes historical or architectural analyses. Bearing in mind the above-mentioned premises, the authors hope that this article will expand the knowledge on possibilities of growth and possible development of tourism in tourist facilities of military importance, or even greater interest in the participation of tourists in military outdoor events.

3 Materials and methods

Research methods and techniques for this study had to be carefully selected to address the unique character of the research problem and the relevant scarcity of data sources. The research methodology of this study included several stages:

1) Research project and case selection (objects, events)

In the first stage of the research, the objects and events related to the military heritage located in northern and north-eastern Poland were analyzed. An important determinant was the availability of tourist

traffic statistics in the above-mentioned objects and the possibility to visit these places in person.

2) Review of literature in the light of the state of development of research on military tourism

To determine the research subject matter of the presented article, an analysis of the literature was undertaken in terms of issues related to military tourism. This allowed for the initial systematization of knowledge describing phenomena related to this type of tourism.

3) Collection and analysis of source data

A very big challenge is to obtain information on museum resources and statistical data for monitoring the volume of tourist traffic. There is no unified system for managing museums and historical events. Obtaining information relies on direct contact with museum directors. There are no standards for storing and making tourist data available. This causes very high difficulties in managing the tourism sector.

In the presented study on the issue of military tourism, methods based on the secondary information contained in lists and registers provided by the institutions were used: Naval Museum in Gdynia, Centre for Historical and Natural Education "Wilczy Szaniec" of Srokowo Forest District and data of Gdynia Naval Aviation Brigade. The scope of collected and analyzed statistical data included information on the volume of tourist traffic in the years 1996-2019 (in the case of "Wilczy Szaniec" only the period 2017-2019, which is related to the change of ownership of the facility and the lack of data for earlier years) and in the months January-February 2018 in the case of the Naval Museum in Gdynia.

Observations, interviews and photographs were highly valuable sources of primary information. Due to considerable variations in behavior of individual tourists and the general scarcity of statistical data, field observations and interviews conducted during the military-themed events, such as the Open Day at the 44th Naval Air Base in Siemirowice, provided highly valuable insights. The observations and an interview with the press officer of the Gdynia Navy Airborne Brigade on 1.06.2018 allowed authors to determine what properties of the objects and events proposed for research are of interest to military tourists. Designed in the research and then placed in the study photographs of selected objects and phenomena are intended to show, on the one hand, the diversity and attractiveness of the above-mentioned places and, on the other hand, help to quickly estimate the number of tourists located in the area. They also prove the interest of the audience in particular elements of shows/exhibitions/buildings. Of course, due to lack of space, this article contains only a few illustrations showing only selected cases.

The authors also relied on the Google Trends website to analyze the popularity of search queries for the Wolf's Lair in Gierloz across geographic locations. The second advantage of this method was the possibility to estimate the amount of general interest in the selected tourist attraction on a global scale.

4 Results

4.1 Development of military tourism on the example of the Naval Museum in Gdynia

According to Jedrysiak and Mikos von Rohrsscheidt [16], attractive museums exert a direct impact on the way visitors perceive reality and influence tourist traffic. Museum visits have become a popular pastime for millions of people. Military museums play a very important role in a civic society by creating a direct link to the past, acting as repositories of knowledge and by preserving historical resources and memories of



Figure 2 *ORP Blyskawica in Gdynia*

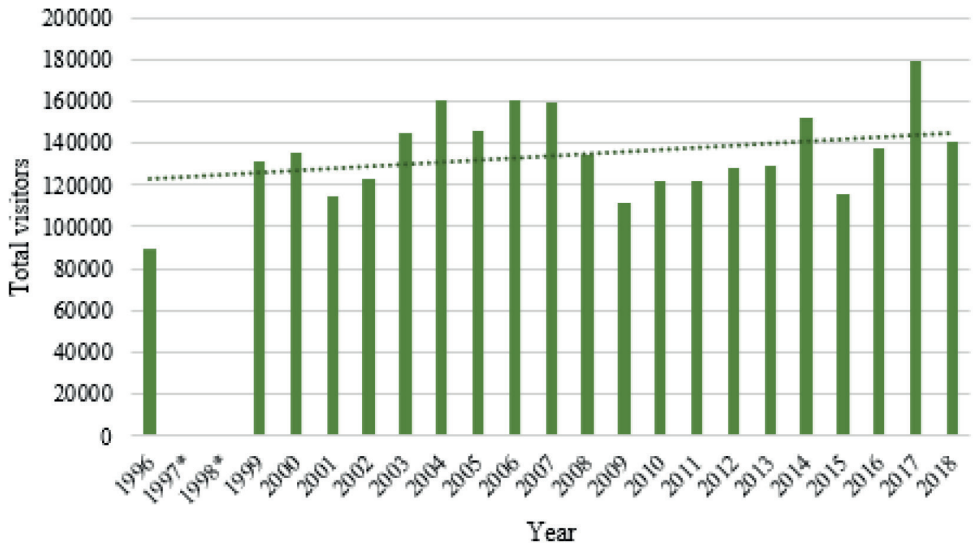


Figure 3 *The number of visitors to the Naval Museum in Gdynia in 1996-2018, based on data from the Register of the Naval Museum in Gdynia*

the past for future generations [27]. Military museums amass collections of armor and weapons spanning many centuries, where some collections are dedicated to specific battles fought in the remote past [15 ,42]. According to Jedrysiak [17] and Rottermund [46], museums play a special role in social life due to their continued existence, as well as the fact that the esthetic and educational value of the displayed objects has been scientifically substantiated [14, 16]. The Naval Museum in Gdansk is one of such facilities. Its collection consists of around 50,000 objects divided into several categories, including military artefacts, models, memorabilia, art, ship equipment, archives and photographs. Ship models, flags, streamers, vessel names and symbols on ship hulls, ship bells and other naval objects are among the museum's greatest attractions. One of the most highly prized objects in the museum's collection is ORP Blyskawica (Lightning), a destroyer ship that served in the Polish Navy during World War II. The ship was converted into a museum in 1976 and it is open to the public in the Kosciuszki Square in Gdynia (Figure 2). The ship boasts a vast collection of military equipment and memorabilia linked to crew and history during World War II. ORP Blyskawica serves representative functions during the national ceremonies and conferences [16].

Tourist traffic and seasonal changes in tourism demand are the key indicators of tourism development, including military tourism [10, 47-48]. An analysis of tourist traffic in the Naval Museum in Gdynia revealed that the number of visitors has increased considerably from 89,000 in 1996 to nearly 140,400 in 2018 (Figure 3). Tourist traffic peaked in 2017 when the number of visitors was approximately 180,000. These data indicate that the popularity of military tourism continues to increase each year in Poland.

Seasonal demand for tourism is an important measure of visitors' interest in a given region or tourist attraction. These data influence development of various types of tourism and the growth of tourism in general. Analyses of the seasonal distribution of tourist traffic provide valuable insights for tourism operators, for example by identifying the most profitable months for organizing mass events such as military-themed shows.

The data presented in Figure 4 indicate that the Naval Museum in Gdynia and ORP Blyskawica attract the highest number of visitors between May and September. Considerable differences in the volume of tourist traffic can be observed between months with the lowest and highest numbers of visitors. In 2018, monthly tourist traffic ranged from around 500 visitors in February (0.9% of annual traffic) to around 14,000 in July (28.4%) in the Naval Museum in Gdynia and from 0 visitors in February-April to around 15,800 in July (28.3%) in ORP Blyskawica. Combined tourist traffic in both sites was the lowest in February (500 visitors, 0.3% of annual traffic) and the highest in July (39,800 visitors, 28.3%).

The study also revealed that ORP Blyskawica attracted more visitors (by 42,500) than the Naval Museum in 2018. This difference could be explained by the ship's convenient location along the main promenade in the Gdynia harbor, as well as the novel experience of touring an authentic warship.

4.2 Military tourism in the Wolf's Lair Bunker in Gierloz

The Wolf's Lair in Gierloz is unquestionably one of the greatest tourist attractions in the Mazury and Suwalki Lakeland in northern Poland [49]. The bunker served as one of Adolf Hitler's first military headquarters on the Eastern Front. It was built near the village of Gierloz, 9 km away from the East Prussian town of Rastenburg (Ketrzyn), on the territory of present-day Poland. The Wolf's Lair is one of the best-

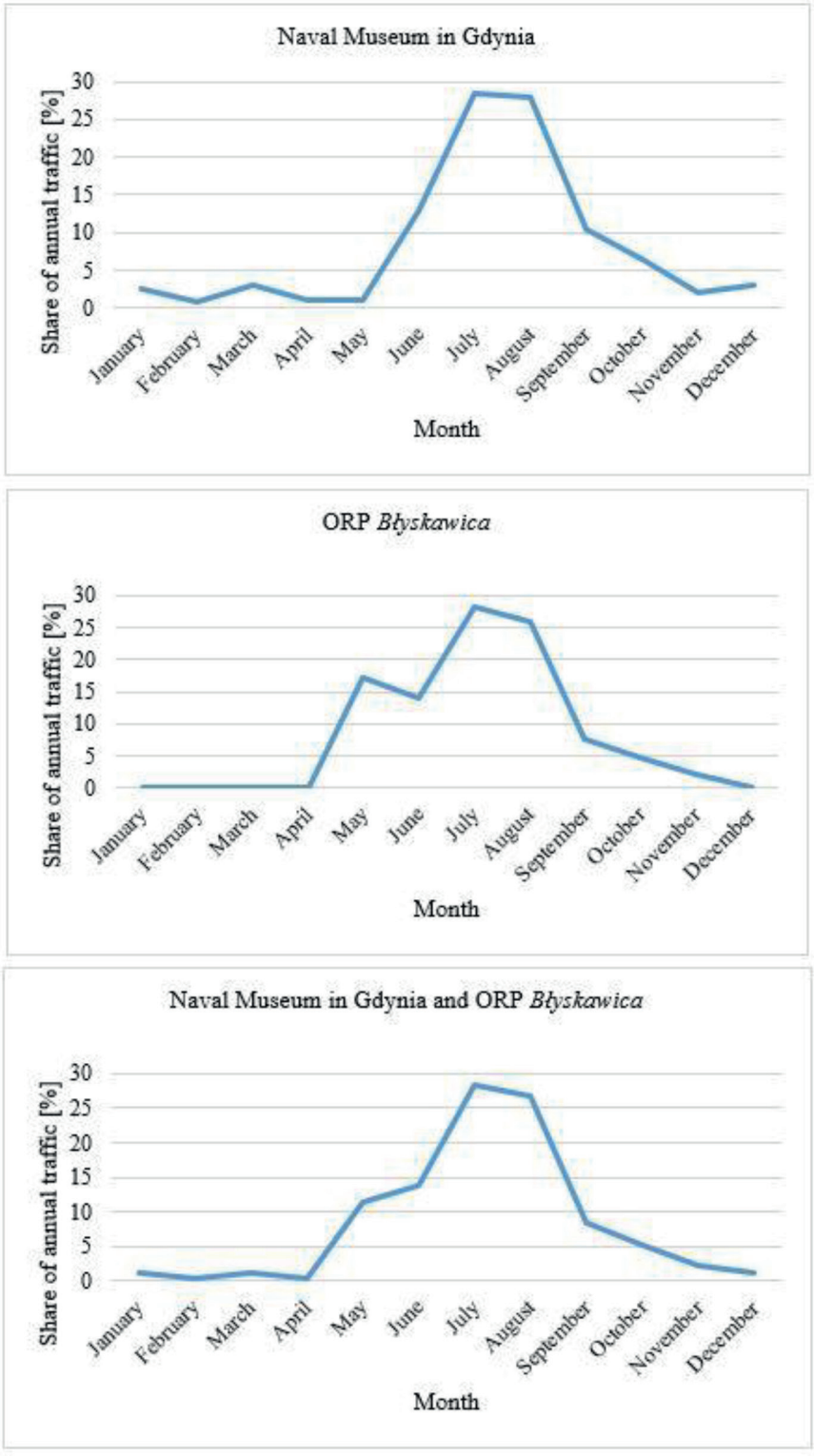


Figure 4 *Seasonal distribution of tourist traffic in the Naval Museum in Gdynia in 2018, based on data from the Register of the Naval Museum in Gdynia*

known high-security historic military sites in Europe. It was originally composed of nearly 200 buildings, including security bunkers, residential bunkers, air-raid shelters, military barracks, two airfields, a power plant and a railway siding. The entire complex had access to main water, heating and ventilation systems. Other military command centers and headquarters of German military institutions were built in the vicinity [44]. In 2017, the Wolf's Lair was transformed into the Historical and National Education Center of the Srokowo Forest District.

An analysis of the site's tourism attractiveness revealed that Wolf's Lair is characterized by considerable functional cohesion due to the presence of nearly twenty

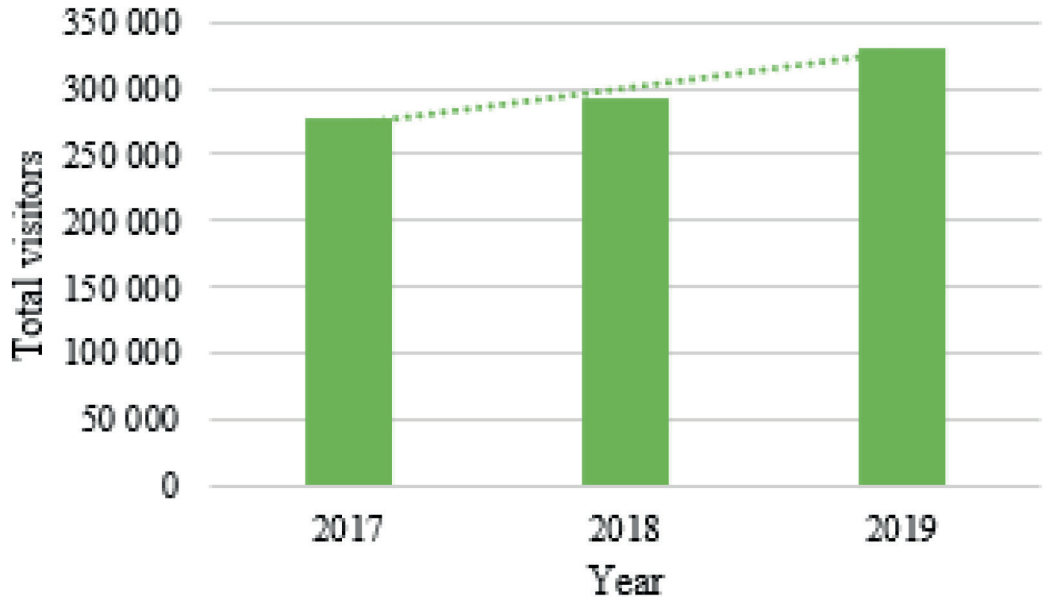


Figure 5 *The number of visitors to the Wolf's Lair in Gierloz in 2017-2019, based on the data of the Wolf's Lair Historical and Natural Education Center of the Srokowo Forest District*



Figure 6 *Geographic distribution of queries containing the words "Wolf's Lair (historic site in Gierloz)" in Google Trends between 1 January 2010 and 1 January 2020, [50]*

attractions, extensive access to tourist information, guided tours, restaurants and a car park [10]. The Wolf's Lair enjoys growing popularity among tourists (Figure 5). In 2017, it was listed by The Telegraph as one of the 25 most popular tourist destinations in Eastern Europe. Nearly 276,300 tourists visited the site in 2017 and the number of visitors increased by more than 50,000 to nearly 330,000 by the end of 2019.

According to Srokowo Forest District data, nearly 40% of visitors attended guided tours of the Wolf's Lair and a total of 11,000 guided tours have been held since 2017. The remaining visitors toured the site individually with use of a mobile guide application, printed guides and maps that can be purchased on the site. The main buildings and attractions are very well signposted, which facilitates tourist movement. The Wolf's Lair attracts visitors from various regions of the world and according to Srokowo Forest District data, foreign tourists, mostly from Germany, generated a third of tourist traffic on the site. The number of Google searches related to the Wolf's Lair also testifies to the site's considerable popularity (Figure 6).

An analysis of Google Trends queries containing the words "Wolf's Lair (historic site in Gierloz)" between 1 January 2010 and 1 January 2020 revealed that this military site attracted the interest of Internet users



Figure 7 *Orlik Aerobatic Team flying PZL-130 turboprop trainer aircraft during the Open Day of the 44th Naval Air Base in Siemirowice on 16 July 2016*



Figure 8 *Exhibition of naval aircraft during the Open Day of the 44th Naval Air Base in Siemirowice on 16 July 2016*

from 60 countries around the world. The highest number of searches in the analyzed period was made in Poland, Lithuania, Latvia, Germany, Estonia, Czechia, Austria, Finland, Slovakia, Luxembourg, Sweden, Denmark and Switzerland.

4.3 Open Day in the 44th Naval Air Brigade in Siemirowice

Field events and shows are among the greatest attractions for tourists with a special interest in military heritage. The Open Day and Air Show in the 44th Naval Air Base in Siemirowice was one of such events in 2016.

The 44th Kaszuby-Darlowo Naval Air Base was established on 1 January 2011 when the 29th Darlowo Air Force Squadron and the 30th Kaszuby Air Force Squadron were incorporated into the 44th Naval Air Base. The naval base comprises the Kaszuby Aviation Group in Siemirowice, which operates An-28B1R and An-28B1RM Bis patrol and reconnaissance aircraft and An-28E environmental monitoring aircraft and the Darlowo Aviation Group, which operates Mi-14PL anti-submarine helicopters, Mi-14PL/R and W-3RM rescue helicopters and Mi-2 helicopters. The main tasks of the 44th Naval Air Base include maritime reconnaissance; recognition and indication of targets to marine units; search, tracking and destruction of submarine warfare; search and rescue missions; and environmental monitoring of the Polish Exclusive Economic Zone of the Baltic Sea. In the naval air bases in Siemirowice and Darlowo, patrol aircraft and rescue helicopters are on round-the-clock duty as a part of the national surveillance system, the NATO reconnaissance system and the national marine and aviation rescue system. The base can be visited by members of the public on open days and military-themed events and shows are held every five years to celebrate milestone anniversaries.

The Open Day at the 44th Naval Air Base in Siemirowice, held on 16 July 2016 between 9:30 a.m. and 4:30 p.m., attracted more than 10,000 visitors, most enthusiasts of military technology, military aircraft and vehicles. The event was organized to celebrate the 60th anniversary of the first aircraft landing in Siemirowice and the 96th birthday of the Polish Navy. The air show (Figure 7) involved presentations of naval aircraft such as Mi-14PL anti-submarine helicopter, W-3RM Anakonda rescue helicopter, MiG-29 and F-16 jet fighter aircrafts and Mi-24 attack helicopter. The aerobatic

maneuvers performed by the two Su-22 fighter-bomber aircrafts and performance of the Orlik Aerobatics Team involving seven PZL-130 turboprop trainer aircrafts also attracted considerable interest.

The event also involved an exhibition of military equipment, including the Blenda anti-aircraft artillery system, armored vehicles of the 1st Mechanized Battalion in Lebork and state-of-the-art weapons of the Naval Missile Unit (Figure 8).

Open days are usually held every five years, but the Naval Air Base in Siemirowice does not keep statistical records of these events, which is why the number of spectators cannot be accurately defined. However, according to the press officer of the Naval Air Brigade in Gdynia, the popularity of military-themed events and air shows in Siemirowice continues to increase steadily.

4.4 Transport accessibility of selected sites

The most important role of transport in the tourism sector is to provide access for tourists to the places they visit. Transport is one of the key elements influencing the attractiveness of a given area in terms of possibilities for development of tourism [21, 51]. The basis for appropriate functioning of transport is a sufficiently developed network of railways and motorways, as well as its good technical conditions and appropriate frequency of bus and railway connections between particular locations. Nowadays, access to airports and seaports is also becoming increasingly important [13, 52-53]. A very important aspect in the light of the present research is therefore the indication of the communication accessibility of the selected ones of military importance.

The Museum of the Navy, located in Gdynia, has relatively good communication accessibility. From the research conducted into the location of tourist attractions in the geographical space of Pomorskie Voivodeship, it can be concluded that the convenience of communication, in this case, lies in the proximity of transport corridors and hubs of regional, supra-regional and international significance. The communication accessibility of the above-mentioned museum is largely based on the existence of corridors of European importance (Baltic-Adriatic Corridor, Northern Corridor/ Northern Seaside Corridor) and the existence of the national Lakeland Corridor (based on national road No. 22 and railway line No. 203). European conditions also include connections within the Trans-European Transport Networks (TEN-T) running through the Pomeranian Region, including priority lines, i.e.: the E65 railway line (Gdansk - Warsaw - Brno/ Bratislava - Vienna), A1 motorway (Gdansk - Brno/ Bratislava - Vienna), motorways of the sea in the Baltic Sea, "Galileo" satellite navigation and positioning system. Short sea shipping and small harbors and ports are in the immediate vicinity. The TEN-T network priorities also include waterways, i.e. the E-40 (Vistula - Bug - Dniester) and E-70 (Hohensaaten lock - Oder - Warta - Notec - Bydgoski Canal - Brda - the Vistula - Nogat - Vistula Lagoon - Baltic Sea). Another possibility is to reach the above-mentioned museum with the partial use of the sea transport (port in Gdynia and Gdansk). In Gdansk's Matarnia district there is the Lech Walensa Airport, which was opened in 1974 and occupied an area of 240 ha. It plays the role of a TEN-T network node of both national and international importance [10].

Transport accessibility of "Wilczy Szaniec" Fortress in Gierloz, located in Warminsko-Mazurskie voivodeship, Ketrzyn poviat, Ketrzyn commune, is less developed.



Figure 9 *Overview map with the transport network*

The main reason for this situation is the peripheral location of the province itself, as well as poorly developed internal and external communication. Undoubtedly, the following factors are responsible for this situation: natural environment requiring protection, rather low population density, dispersed settlement network and low investment attractiveness of the region [48]. One of the problems of the voivodship is also the existence of numerous objects and post-military areas, which require reclamation and introduction of new functions. Direct access to "Wilczy Szaniec" is very difficult. The site was intentionally built in a place that is difficult to access - it is situated far from main communication routes, in a forest area that provides natural protection for military facilities. The Great Masurian Lakes located to the east of the forest are also a significant barrier.

The 44th Naval Air Base, on the other hand, was built in Siemirowice, in the Pomeranian Voivodeship, Lebork County, in the municipality of Cewice. The military facility, where air shows were organized in 2016, is generally characterized by good communications, although it is approximately 11.8 km from the national road S6/international route E28. Siemirowice is furthermore located approximately 45 km from the nearest airport and seaport. Furthermore, the 44th Naval Air Base is located close to the same transport corridors of national and international importance as the Naval Museum in Gdynia.

In terms of accessibility to particular sites of military significance, the general population potential is also of considerable importance, as is the presence of adequate tourist infrastructure (e.g. hotels, restaurants and other facilities) in the vicinity of the listed tourist attractions. Figure 9 shows an overview map with the location of the studied objects with the transport network.

5 Discussion

The problem related to the management of, inter alia, museum resources and information on the increase in use of the results of socio-economic research in shaping national and regional development policies until 2028 was noted by the Ministry of Culture and National Heritage in Poland. Among other things, the lack of statistical data on tourism and tourism resources causes difficulties in creating development plans. Examples of museums, discussed in the article, represent regions that base their functioning, among other things, on tourism. To solve this problem of access to information, the National Centre for Research and Development has announced an ordered project (GOSPOSTRATEG V), which includes digital cultural heritage. The project envisages the creation of a "National aggregator of data on digital cultural heritage". A diagnosis concerning the resources of Polish culture will facilitate its management on a national scale. All the development works should begin with an inventory of resources. Therefore, it is, as the first of all, planned to carry out a comprehensive survey on the condition of digital cultural resources in Poland, which are in possession of the state and self-government cultural institutions, scientific units and other entities collecting digital cultural resources. The second task will be to estimate the resources that should be digitized. As a result of this work, an IT platform will be created that will make it possible to create compilations and analyses of the resources held. The analyses carried out on selected museums confirmed the lack of a uniform system for making data and information available [54].

The three discussed examples confirm that narrow thematic specialization in the case of museums and thematic events can attract a very large crowd Managers of museums and historical events should use publicly available IT tools (e.g. google trends) to monitor in which regions and countries a given event or museum attracts the most interest. This will allow choosing the right promotional strategies. At the same time, taking into account the very high potential of military tourism, it would be advisable to set up a consortium or cluster to improve recognition and increase the effectiveness of reaching tourists. Global trends show that such a cooperation improves possible audience reach.

6 Conclusions

Historic military sites and tourist destinations in Poland, featuring unique military artefacts and weapons, including objects that are related to the history of World War II, should drive the development of military tourism. The presented examples of military heritage sites in northern and north-eastern Poland indicate that military tourism is a rapidly growing segment of the tourist industry.

The main objective of the research was to indicate the possibilities of military tourism development in north and north-eastern Poland. The conducted studies in this area included an analysis of tourist traffic in selected objects related to military heritage and on the example of an outdoor event. This made it possible to indicate the current trends of interest in this form of tourism.

Military museums, including the Naval Museum in Gdynia, historic military sites such as the Wolf's Lair in Gierloz, military-themed events and open day shows organized by military bases and former military facilities are important sources of historical knowledge.

The research conducted in the objects selected for analysis shows that currently there is an increase in interest in military tourism, which is manifested in the increased tourist traffic.

An analysis of the tourist traffic in military heritage sites and military-themed tourist destinations points to the steady growth of military tourism in Poland. Military

bases and historic sites attract growing numbers of visitors who have an interest in history and the armed forces. These tourist destinations are often linked with acts of heroism and they promote patriotic values.

This study revealed an increase in tourist traffic in the analyzed tourist destinations. The number of visitors to the Naval Museum in Gdynia increased from 89,000 in 1996 to nearly 140,400 in 2018. In the Wolf's Lair Historical and Natural Education Center of the Srokowo Forest District, tourist traffic increased from 276,300 in 2017 to nearly 330,000 in 2019. The air-show during the Open Day at the 44th Naval Air Base in Siemirowice in 2016 also enjoyed immense popularity and attracted more than 10,000 spectators.

Another aspect of the research was also an attempt to answer the question of what place military tourism currently occupies among other forms of tourism in Poland and whether maintaining the current trend in the volume of tourism would be an opportunity for its further development. Taking into account the statistics presented above, the authors of the article agree that there is a high probability that military tourism may occupy a very important place in the structure of tourism forms in Poland because it combines the advantages of cultural tourism with other forms of tourism and often concerns important aspects related to history. It is also possible to further increase interest in this form of tourism, which may lead to a situation where it will become one of the most popular forms. Unfortunately, the current epidemiological situation in Poland and the world also imposes restrictions on museum objects in terms of limiting their activity. Therefore, the present research needs to be thoroughly deepened regarding further qualitative and quantitative studies of tourist traffic and research on the impact of the SARS-CoV-2 coronavirus epidemic on the volume of this traffic.

The authors hope that this article will expand the knowledge on possibilities of growth and possible development of tourism in military heritage sites and will contribute to the even greater interest of tourists in military outdoor events.

References

[1] Statistical office in Krakow. Activity of museums in 2019 [online] [accessed 2021-03-29]. Available from: https://stat.gov.pl/en/topics/culture-tourism-sport/culture/activity-of-museums-in-2019,8,2.html

[2] NADEEM, M. A., LIU, Z., XU, Y., NAWAZ, K., MALIK, M. Y., YOUNIS, A. Impacts of terrorism, governance structure, military expenditures and infrastructures upon tourism: empirical evidence from an emerging economy. *Eurasian Bus Review* [online]. 2020, **10**, p. 185-206. eISSN 2147-4281. Available from: https://doi.org/10.1007/s40821-020-00152-y

[3] MCKERCHER, B. Differences between tourism and recreation in parks. *Annals of Tourism Research* [online]. 1996, **23**(3), p. 563-575. ISSN 0160-7383. Available from: https://doi.org/10.1016/0160-7383(96)00002-3

[4] VENTER, D. Examining military heritage tourism as a niche tourism market in the South African context. *African Journal of Hospitality, Tourism and Leisure*. 2017, **6**(1), p. 1-19. ISSN 2223-814X.

[5] Encyclopedia of military technology / Encyklopedia techniki wojskowej (in Polish). Warszawa: Wydawictwo Ministerstwa Obrony Narodowej, 1987.

[6] FINNEY, P. Miniature: finding the Fuhrer bunker. *Rethinking History* [online]. 2007, 11(2), p. 287-291. ISSN 1364-2529, eISSN 1470-1154. Available from: https://doi.org/10.1080/13642520701270526

[7] WALSH, K. *The representation of the past: museums and heritage in the post-modern world*. London: Routledge, 1992. ISBN 9780415079440.

[8] RANISAVLJEVIC, M., TESANOVIC, B., NIKEZIC, S. Military tourist institutions within the tourist offers of Serbia. *International Journal of Economics and Law* [online]. 2017, **7**, p. 133-146. ISSN 2217-5504.

[9] SADOWSKI, P. Battlefields of 1939 Campaign in southern Lesser Poland as destinations of military cultural tourism. In: *Tourism role in the regional economy*. Vol. 7. WYRZYKOWSKI, J., MARAK, J., DROZDOWSKA, M. (eds.). Wroclaw: University of Business in Wroclaw, 2016. p. 213-226.

[10] ZIENKIEWICZ, A., PODCIBORSKI, T. The assessment of attractiveness and accessibility of historic military facilities utilized for the needs of tourism. *Acta Scientiarum Polonorum-Administratio Locorum* [online]. 2019, **18**(3), p. 335-343. ISSN 1644-0749, eISSN 2450-0771. Available from: https://doi.org/10.31648/aspal.4186

[11] HUH, J. *Tourist satisfaction with cultural/heritage sites: the Virginia historic triangle*. (Master's Thesis). Blacksburg: Virginia Polytechnic Institute and State University, 2002.

[12] KONDRACKI, J. *Regional geography of Poland / Geografia regionalna Polski* (in Polish). Warszawa, 2002. ISBN 9788301160227.

[13] KOWALCZYK, A. Contenporary cultural tourism / Wspolczesna turystyka kulturowa (in Polish). In: *Cultural tourism. Geographic view / Turystyka kulturowa. Spojrzenie geograficzne*. KOWALCZYK, A. (ed.). Warszawa: Uniwersytet Warszawski, 2008.

[14] Military Pomerania XIIth-XXIth centuries / Pomorze militarne XII-XXI wiek (in Polish). In: Materials from the scientific session November 27, 2003 in the Pomeranian Dukes' Castle, Szczecin "Borderland" Society, Faculty of

Humanities of the University of Szczecin, State Archives in Szczecin, Sczecin, 2004 KOZLOWSKI, K., RYMAR, E. (eds.)

[15] LOGAN, W., REEVES, K. *Places of pain and shame. Dealing with difficult heritage*. Oxon: Routledge, 2009. ISBN 9780415454506.

[16] JEDRYSIAK, T., VON ROHRSCHEIDT, A. M. *Military cultural tourism / Militarna turystyka kulturowa* (in Polish). Warszawa: Polskie Wydawnictwo Ekonomiczne, 2011. ISBN 978-83-208-1952-6.

[17] JEDRYSIAK, T. *Cultural tourism / Turystyka kulturowa* (in Polish). Warszawa: Polskie Wydawnictwo Ekonomiczne, 2008. ISBN 978-83-208-1759-1.

[18] LAWIN, M., STASIAK, A. Historical and military facilities / Obiekty historyczno-wojskowe (in Polish). In*: The geography of Polish tourism. A guide to sightseeing exercises*. STASIAK, A. (ed.). Warszawa: PWE, 2009. EAN 9788320817690, p. 129-130.

[19] KOWALCZYK, A. Historical and military tourism / Turystyka historyczno-militarna (in Polish). In: *Contenporaryforms of cultural tourism / Wspolczesne formy turystyki kulturowej.* Vol. 1. BUCZKOWSKA, K., VON ROHRSCHEIDT, A. M. (eds.). Poznan: Akademia Wychowania Fizycznego im. Eugeniusza Piaseckiego w Poznaniu, 2009. ISBN 9788361414179, p. 286-312.

[20] KOWALCZYK, A. Content and form of maps used in historical and military tourism / Tresc i forma map wykorzystywanych w turystyce historyczno-militarnej (in Polish). *Turystyka Kulturowa*. 2018, **1**, p. 95-143. ISSN 1689-4642.

[21] LIJEWSKI, T., MIKULOWSKI, B., WYRZYKOWSKI, J. *The geography of Polish tourism / Geografia turstyki Polski* (in Polish). Warszawa: Polskie Wydawnictwo Ekonomiczne, 2002. ISBN 978-83-208-1763-8.

[22] POCZTA, J., FIZYCZNEGO, A. W. Military tourism as a manifestation of a new form of tourism activity in Poland / Turystyka militarna jako przejaw nowej formy aktywnosci turystycznej w Polsce (in Polish). *Militaria (Poligon, Bunkry, Fortyfikacje)*. 2008, **58**, 18.

[23] CHYLINSKA, D. Modern permanent fortifications - selected problems of tourist development / Nowozytne fortyfikacje stale - wybrane problemy (in Polish). *Turystyka i rekreacja*. 2006, **2**, p. 52-63. ISSN 1895-3700.

[24] CYNARSKI, W. Castles as the heritage of Polish fortification art and as a tourist attraction. *IDO Movement for Culture. Journal of Martial Arts Anthropology*. 2012, **12**(4), p. 44-55. ISSN 2084-3763.

[25] STACH, E. The current use of military facilities and sites in Poland in the aspect of military cultural tourism / Aktualne wykorzystanie obiektow i miejsc militarnych w Polsce w aspekcie militarnej turystyki kulturowej (in Polish). In: *New fortifications in Poland: research, realization, projects and development for modern functions / Fortyfikacje nowozytne w Polsce: badania, realizacje, projekty i zagospodarowanie do wspolczesnych funkcji*. NAREBSKI, L. (ed.). Torun: UM Wojewodztwa Kujawsko-Pomorskiego, 2013. p. 213-223. ISBN 978-83-937545-2-6.

[26] STACH, E., PAWLOWSKA, A., MATOGA, L. Development of tourism in military-historical facilities and sites - a case study of the Rise project complexes in Gory Sowie / Rozwoj turystyki w obiektach i miejscach militarno-historycznych - studium przypadku kompleksow projektu Riese w Gorach Sowich (in Polish). *Polish Journal of Sport and Tourism*. 2014, **21**, p. 36-47. ISSN 1899-1998, eISSN 2082-8799.

[27] ZGLOBICKI, W. Evaluation of the offer of selected military facilities in Poland for the needs of children and youth tourism / Ocena oferty wybranych obiektow militarnych na obszarze Polski dla potrzeb turystyki dzieci i mlodziezy (in Polish). *Turystyka Kulturowa*. 2016, **2**, p. 116-134. ISSN 1689-4642.

[28] ZAWADZKI, W. Polish military museums / Polskie muzea wojskowe (in Polish). Bydgoszcz: Przedsiebiorstwo Marketingowe "LOGO", 2002 .

[29] Commercial tourist attraction. Darwin, on Stokes Hill Wharf, Australia, Northern Territory. 2015.

[30] LEMELIN, R. H., WHYTE, K. P., JOHANSEN, K., DESBIOLLES, F. H., WILSON, C., HEMMING, S. Conflicts, battlefields, indigenous peoples and tourism: addressing dissonant heritage in warfare tourism in Australia and North America in the twenty-first century. *International Journal of Culture, Tourism and Hospitality Research* [online]. 2013, **7**(3), p. 257-271. ISSN 1750-6182. Available from: https://doi.org/10.1108/IJCTHR-05-2012-0038

[31] CHHABRA, D., HEALY, R., SILLS, E. Staged authenticity and heritage tourism. *Annals of Tourism Research* [online]. 2003, **30**(3), p. 702-719. ISSN 0160-738. Available from: https://doi.org/10.1016/S0160-7383(03)00044-6

[32] BIRAN, A., Hyde, K. F. New perspectives on dark tourism. *International Journal of Culture, Tourism and Hospitality Research* [online]. 2013, **7**(3), p. 191-198 [accessed 2020-02-13]. ISSN 1750-6182. Available from: http://dx.doi.org/10.1108/IJCTHR-05-2013-0032

[33] RAINE, R. A dark tourist spectrum. *International Journal of Culture, Tourism and Hospitality Research* [online]. 2013, **7**(3), p. 242-256 [accessed 2020-02-23]. ISSN 1750-6182. Available from: http://dx.doi.org/10.1108/IJCTHR-05-2012-0037

[34] MAGEE, R., GILMORE, A. Heritage site management: from dark tourism to transformative service experience? *The Service Industries Journal* [online]. 2015, **35**(15-16), p. 898-917. ISSN 0264-2069, eISSN 1743-9507. Available from: https://doi.org/10.1080/02642069.2015.1090980

[35] Wolf's Lair / Wilczy Szaniec (in Polish) [online] [accessed 2020-02-23]. Available from: http://www.wilczyszaniec.olsztyn.lasy.gov.pl/aktualnosci/
[36] LAMPARSKA, J., MALIK, A. *Castles / Zamki* (in Polish). Warszawa: Multico Oficyna Wydawnicza, 2011.
[37] JAROSZ, J. *Coastal artillery of the Polish coast. Compendium and* guide / *Artyleria nadbrzezna polskiego wybrzeza. Kompendium i przewodnik* (in Polish). Gdynia: Wydawnictwo Region, 2018. ISBN 9788375916249.
[38] PRADZYNSKI, I. *Field fortification / Umocnienie polowe* (in Polish). Polscy Teoretycy Wojskowi, Wojskowy Instytut Historyczny im. Wandy Wasilewskiej. Warszawa: Wydawnictwo Ministerstwa Obrony Narodowej,1985.
[39] Polish formations and the Polish Army from 1914-1922 / Militaria polskich formacji i Wojska Polskiego z lat 1914-1922 (in Polish). Old Weapons and Colors Lovers Association, Staleczny Branch Major Franciszek Pukacki / Stowarzyszenie Milosnikow Dawnej Broni i Barwy Oddzial Stoleczny im. mjr Franciszka Pukackiego. Warszawa: Stoleczna Pracownia Dokumentacji Dobr Kultury, 1989. TIN TOO913310.
[40] Muzealnictwo wojskowe (in Polish). Muzeum Wojska Polskiego . Vol. 3. Warszawa: Wydawnictwo Ministerstwa Obrony Narodowej, 1985.
[41] Polish Army Museum. Military museums / Muzealnictwo wojskowe (in Polish) [online]. Vol. 10. Warszawa: Wydawnictwo Ministerstwa Obrony Narodowej, 2017. Available from: http://polona.pl/item/38336198
[42] Underwaterfacilities and military in the Bay of Gdansk / Obiekty podwodne i militaria Zatoki Gdanskiej (in Polish). KOMOROWSKI, A. (ed.). Gdynia: Impuls Plus Consulting, 2001. ISBN 83-7322-223-5.
[43] PIATEK, J. J. Tools of war and their modern development (selected aspects for the 20th century / Narzedzia wojny i ich wspolczesny rozwoj (wybrane aspekty dla XX wieku) (in Polish). Torun: Wydawnictwo Adam Marszalek, 2009. ISBN 9788376112671
[44] JURGA, R. M. *Fortifications of the Third Reich in spatial drawings / Fortyfikacje III Rzeszy w rysunkach przestrzennych* (in Polish). Czerwonak: Bialostockie Zaklady Graficzne, 2013. EAN 9788377311462.
[45] DRZEWIECKI, A., ROZYCKI, L. *Pomeranian military (19th-20th century). History - education - tourism / Militaria pomorskie (XIX-XX wiek). Historia - edukacja - turystyka* (in Polish). Gdansk - Oswiecim: Wydawnictwo Napoleon V, 2014.
[46] ROTTERMUND, A. Museums and Tourism / Muzea i turystyka (in Polish). In: Materials of the international conference. International Cultural Center, 1999, p. 41.
[47] Gdynska brigade of naval aviation / Gdynska brygada lotnictwa marynarki wojennej (in Polish) [online] [accessed 2018-06-01]. Available from: http://blmw.wp.mil.pl/pl/1_288.html
[48] GIETKOWSKI, M., NADOLSKI, L. Pomeranian military. Collection of studies / Militaria pomorskie. Zbior studiow (in Polish). Vol. 11. Bydgoszcz: Muzeum Wojsk Ladowych w Bydgoszczy, 2017. ISBN 978-83-64130-14-4.
[49] Muzeum Bunkier V-3 [online] [accessed 2018-06-01]. Available from: http://www.bunkierv3.pl/mapy.html
[50] Google Trends, https://trends.google.com/trends/?geo=US, accessed on 20 March 2020
[51] PODCIBORSKI, T. The method of assessing the tourist and recreational attractiveness of Warmian villages / Metoda oceny atrakcyjnosci turystyczno-rekreacyjnej wsi warminskich (in Polish). Zeszyty Naukowe Wyzszej Szkoly Ekonomiczno-Spolecznej w Ostrolece. 2016, 20, p. 22-31. ISSN 2391-9167.
[52] ZIENKIEWICZ, A. Development of the tourist function in the Kartuzy districct / Rozwoj funkcji turystycznej w powiecie kartuskim (in Polish). Warszawa: Wydzial Geografii i Studiow Regionalnych, Uniwersytet Warszawski, 2016.
[53] ZIENKIEWICZ, A. Transport infrastructure as a factor in the development of tourism in the Kartuzy district / Infrastruktura komunikacyjna jako czynnik rozwoju turystyki powiatu kartuskiego (in Polish). Slupskie Prace Geograficzne. 2017, 14, p. 281-300. ISSN 1641-8468.
[54] Gospostrateg V [online] [accessed 2021-03-20]. Available from: https://www.gov.pl/web/ncbr/gospostrateg-v

komunikácie
COMMUNICATIONS

VEDECKÉ LISTY ŽILINSKEJ UNIVERZITY
SCIENTIFIC LETTERS OF THE UNIVERSITY OF ZILINA

VOLUME 23 Number 4

https://doi.org/10.26552/com.J.2021.4

October 2021

Editor-in-Chief:
Branislav HADZIMA - SK

Associate Editor:
Jakub SOVIAR - SK

Executive Editor:
Sylvia DUNDEKOVA - SK

Language Editor:
Ruzica NIKOLIC - SK

Graphical Editor:
Juraj ZBYNOVEC - SK

Honorary Members:
Otakar BOKUVKA - SK
Jan COREJ - SK (in memoriam)
Milan DADO - SK
Pavel POLEDNAK - CZ

Scientific Editorial Board:
Greg BAKER - NZ
Abdelhamid BOUCHAIR - FR
Pavel BRANDSTETTER - CZ
Mario CACCIATO - IT
Jan CELKO - SK
Andrew COLLINS - GB
Samo DROBNE - SI
Erdogan H. EKIZ - MA
Michal FRIVALDSKY - SK
Juraj GERLICI - SK
Vladimir N. GLAZKOV - RU
Ivan GLESK - GB
Mario GUAGLIANO - IT
Andrzej CHUDZIKIEWICZ - PL
Jaroslav JANACEK - SK
Zdenek KALA - CZ
Antonin KAZDA - SK
Michal KOHANI - SK
Jozef KOMACKA - SK
Matyas KONIORCZYK - HU
Tomas LOVECEK - SK
Frank MARKERT - DK
Jaroslav MAZUREK - SK
Marica MAZUREKOVA - SK
Vladimir MOZER - CZ
Jorge Carvalho PAIS - PT
Peter POCTA - SK
Maria Angeles Martin PRATS - ES
Pavol RAFAJDUS - SK
Che-Jen SU - TW
Giacomo SCELBA - IT
Janka SESTAKOVA - SK
Eva SVENTEKOVA - SK
Eva TILLOVA - SK
Anna TOMOVA - SK
Franco Bernelli ZAZZERA - IT

Executive Editorial Board:
Michal BALLAY - SK
Martin BOROS - SK
Kristian CULIK - SK
Jan DIZO - SK
Lukas FALAT - SK
Filip GAGO - SK
Lubica GAJANOVA - SK
Stefan HARDON - SK
Martin HOLUBCIK - SK
Maros JANOVEC - SK
Matus KOZEL - SK
Lenka KUCHARIKOVA - SK
Matus MATERNA - SK
Daniela MICHALKOVA - SK
Eva NEDELIAKOVA - SK
Pavol PECHO - SK
Jozef PROKOP - SK
Marek PRUDOVIC - SK
Michal SAJGALIK - SK
Anna SIEKELOVA - SK
Simona SKRIVANEK KUBIKOVA - SK
Michal TITKO - SK
Vladislav ZITRICKY - SK

Address of the Editorial Office:
University of Zilina
EDIS - Publishing House
Univerzitna 8215/1
010 26 Zilina, Slovakia

E-mail: komunikacie@uniza.sk

Individual issues of the journal can be found on: http://komunikacie.uniza.sk

Each paper was reviewed by two reviewers.

Journal is excerpted in SCOPUS and EBSCO host.

Published quarterly by University of Zilina in EDIS - Publishing House of the University of Zilina.

Registered No: EV 3672/09

ISSN (print version) 1335-4205
ISSN (online version) 2585-7878

ICO 00397 563

The full author quidelines are available at: http://komunikacie.uniza.sk/index.php/communications/guidelines